e-ISSN : 2320-0847
p-ISSN : 2320-0936

American Journal of Engineering Research (AJER)

Volume 5 Issue 2– February 2016

www.ajer.org ajer.research@gmail.com

Editorial Board

American Journal of Engineering Research (AJER)

Volume-5 Issue-2

American Journal of Engineering Research (AJER) 2016
American Journal of Engineering Research (AJER)
e-ISSN: 2320-0847 p-ISSN : 2320-0936
Volume-5, Issue-2, pp-01-09
www.ajer.org
Research Paper Open Access

Influence of Chlorine Induced Corrosion and Temperature of Exothermic Reaction on Failure of Methyl Isocyanate (MIC) Storage Tanks

Chennakesava R Alavala
(Department of Mechanical Engineering, JNT University, Hyderabad, India)

ABSTRACT : *The aim of the present work was to know the facts of Methyl Isocyanate (MIC) gas leakage and burst of its storage tank. The failure of the tank was evaluated based on the Tresca, von Mises criteria, Weibull criteria. The significance of chlorine induced corrosion and temperature derating factor were recognized using Taguchi techniques. The bursting pressure of the storage tank was highly dependent on the temperature derating factor and the crack depth. The reasons for the failure of experimental storage tanks used in the present work would satisfy the causes for the leakage of Methyl isocyanate gas and failure of the storage tank during the Bhopal gas disaster.*

Keywords : *Methyl Isocyanate, stainless steel, temperature degrading factor, crack depth, bursting pressure, Tresca criterion, von Mises criterion.*

I. INTRODUCTION

Methyl isocyanate (CH_3NCO) is utilized to produce carbamate pesticides. It reacts exothermically with water through an evolution of heat (325 calories per gram of CH_3NCO). Methyl isocyanate vapors are explosive when exposed to heat, flame or sparks. When it is decomposed in the presence of water, the solvent chloroform generates chlorine ions. Chlorine ions can corrode the stainless steel tank used for storage of CH_3NCO. Due to the exothermic reaction, the temperature and pressure in the tank increase causing the burst of storage tank. This was the main cause for Bhopal gas tragedy (Fig. 1) which occurred on the night of 2–3 December 1984 at the Union Carbide India Limited (UCIL) pesticide plant in Bhopal, Madhya Pradesh [1]. The government of Madhya Pradesh established a total of 3,787 deaths associated with the Bhopal gas tragedy [2]. A government affidavit in 2006 confirmed that the leak caused 558,125 injuries, together with 38,478 short-term injuries and about 3,900 severely and permanently disabling injuries [3].

An initial investigation by UCC showed that a large volume of water had been transported into the methyl isocyanate (MIC) tank. On account of exothermic reaction of MIC in the presence of water, hydrogen chloride was generated. The hydrogen chloride dissolved iron from stainless steel of the tank.

The reaction was accelerated by the presence of iron from corroding non-stainless steel pipelines [4]. The exothermic reaction increased the temperature inside the tank to over 200 °C and raised the pressure. This forced the emergency venting of pressure from the MIC holding tank, releasing a large volume of toxic gases. Also, the material of the storage tank lost due to chlorine initiated corrosion; the tank '610' was burst with lack of material's strength to withstand 42 tons of MIC. Based on several investigations, the safety systems in place could not have prevented a chemical reaction of this magnitude from causing a leak. The causalities of Bhopal gas tragedy are illustrated in Fig. 2. Not only ladies, gents, children, but also birds, dogs and cattle lay dead on the streets of Bhopal. The extremely hazardous gas had also left the surrounding land, lake and vegetation polluted with a toxic cocktail of chemicals. It is not just the aged but the young also put up with the plague of the toxic leak even today. According to the activists and organizations working for the welfare of the Bhopal gas tragedy victims, the rationale at the rear the birth of children with defects (Fig. 3) is due to exposure of their families to toxic chemicals that poisoned the entire area and contaminated groundwater.

The passive layer on stainless steel can be exposed to the chloride ion (Cl^-). With hydrochloric acid, the passive layer on stainless steel may be attacked depending on concentration and temperature and the metal loss is made available over the entire surface of the steel (Fig. 4). Stress corrosion cracking (SCC) is also possible owing to the specific combination of tensile stress, temperature and chloride ions. If the carbon level in the stainless steel is too high, intergranular corrosion is probably on account of reaction between chromium with carbon to form chromium carbide.

Fig. 1 Bhopal gas tragedy.

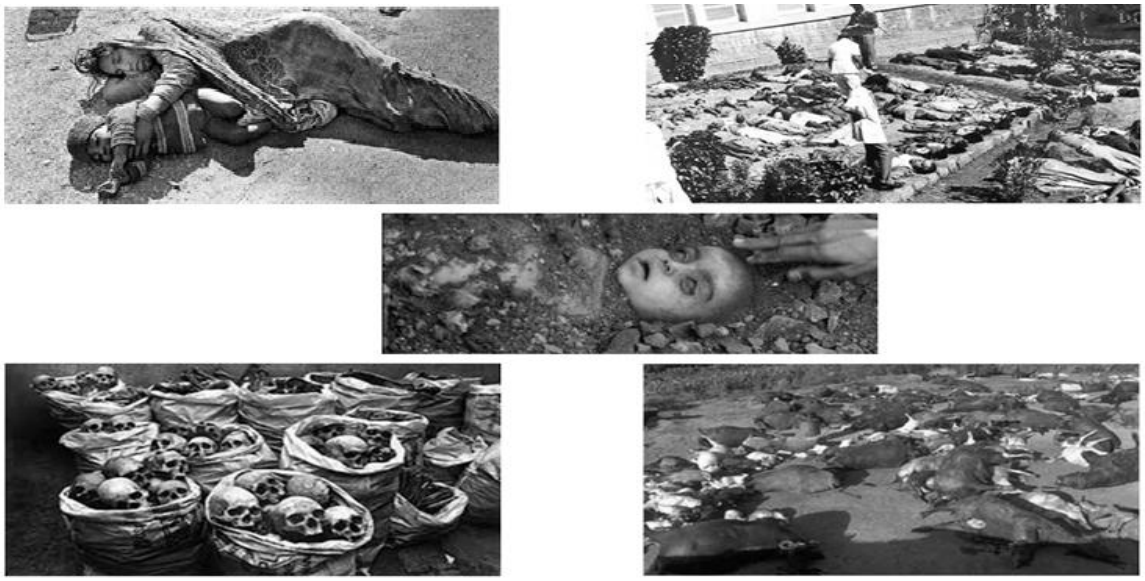

Fig. 2 Causalities of the Bhopal gas disaster.

Fig. 3 Birth defects

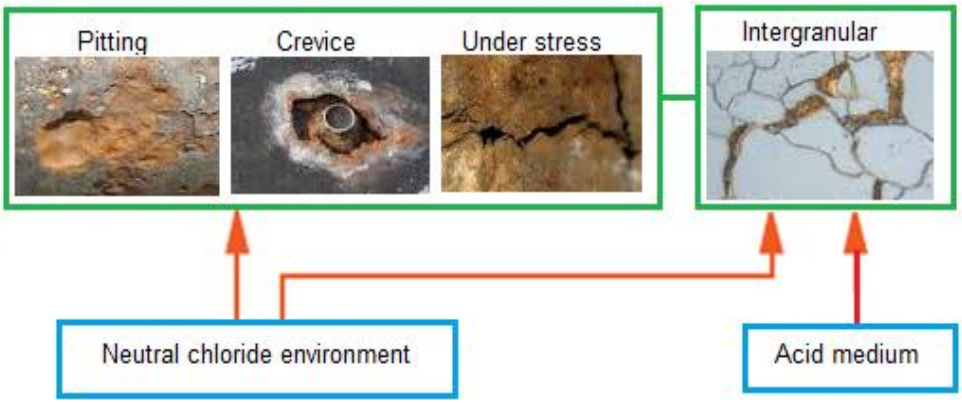

Fig. 4 Corrosion of stainless steel.

Most popular failure pressure methods for pressurized vessels with active corrosion defects are ASME B31G [5, 6] and modified ASME B31G [5, 7], DNV-RP-F101 [8, 9], SHELL-92 [10, 11], RSTRENG [12, 13], PCORRC [14, 15], LG-18 [16, 17], Fitnet FSS [18, 19] and Choi criteria [20, 21].

The present work was tantamount to predict the failure of MIC storage tanks due to chlorine induced corrosion and temperature developed in exothermic reaction of MIC with water. The failure analysis was investigated using modified ASME B31G criterion based on Taguchi design of experimentation [22]. The results were further cross-checked with those computed from ASME B31G, DNV-RP-F101, SHELL-92, PCORRC, LG-18, RSTRENG, Fitnet FSS and Choi criteria.

II. MATERIAL AND METHODS

The material of pipes was stainless steel. In the present study, the dimensions of the test tank were 200 mm outer diameter and 6000 mm length. The chosen control parameters are shown in table 1. The control factors were assigned to the various columns of an orthogonal array (OA), L9 is given in table 2. The corrosion pits were modeled as a single crack (because of their near proximity) as given in table 3. The dimensions of crack are given in Fig. 5.

Table 1. Control factors and their levels

Factor	Symbol	Level–1	Level–2	Level–3
Temperature derating factor	A	0.6	0.8	1.0
Length of crack, mm	B	200	250	300
Depth of crack	C	40%t	50%t	60%t
Type of steel	D	AISI 304	SAE J405	A516 G 70

where t is pipe thickness.

Table 2. Orthogonal Array (L9) and control factors

Treat No.	A	B	C	D
1	1	1	1	1
2	1	2	2	2
3	1	3	3	3
4	2	1	2	3
5	2	2	3	1
6	2	3	1	2
7	3	1	3	2
8	3	2	1	3
9	3	3	2	1

Table 3: Interaction criterion of cracks

Interaction criterion	Dimensions of crack after interaction
$c_1 + c_2 \geq d$	$2c = 2c_1 + 2c_2 + d$
	A = max[a_1, a_2]

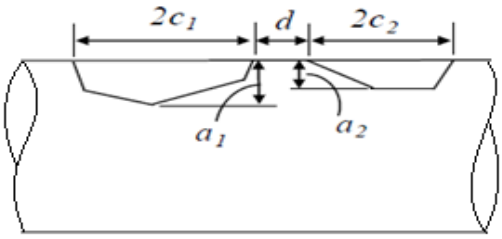

Fig. 5 The crack dimensions.

The Tresca and von Mises criteria were applied to investigate the failure analysis. In principal stress space (σ_1, σ_2, σ_3), the Tresca criterion can be expressed as

$$\tau_{max} = \max\left(\frac{|\sigma_1-\sigma_2|}{2}, \frac{|\sigma_2-\sigma_3|}{2}, \frac{|\sigma_1-\sigma_3|}{2}\right) = \frac{\sigma_{YS}}{2} \quad (1)$$

where τ_{max} is the maximum shear stress and σ_{ys} is the yield strength in tension.

The von Mises criterion can be expressed by the principal stresses in the form:

$$\tau_{vm} = \sqrt{\frac{1}{6}[(\sigma_1 - \sigma_2)^2 + (\sigma_2 - \sigma_3)^2 + (\sigma_3 - \sigma_1)^2]} = \frac{\sigma_{YS}}{\sqrt{3}} \quad (2)$$

where τ_{vm} is the von Mises effective shear stress.

Chloride pitting initiated on tank inner diameter (ID) surfaces was observed (Fig. 6). Acidification was made by adding hydrochloric acid at different temperatures. The test period was 72 hours depending on the standard. A critical value of pH exists, under which the corrosion rate sharply increases. Of the steel Cr18Ni9, the critical pH value is 1.5 [23]. The temperature rise is mitigated through heat transfer from the gas to the cylinder walls. The depth of corroded pits was measured using pit depth gage (Fig. 7). Corroded pits in a sample coupon are shown in Fig. 8.

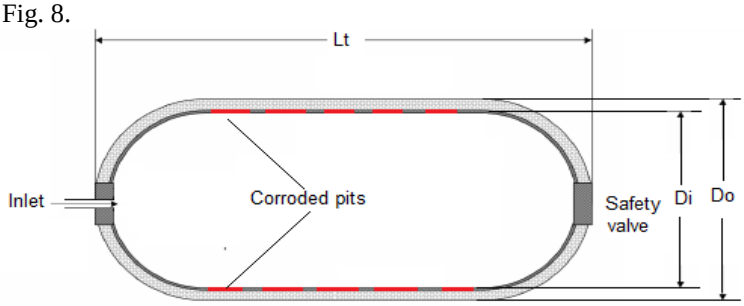

Fig. 6 The storage tank for experimentation.

Fig. 7 The pit depth gage.

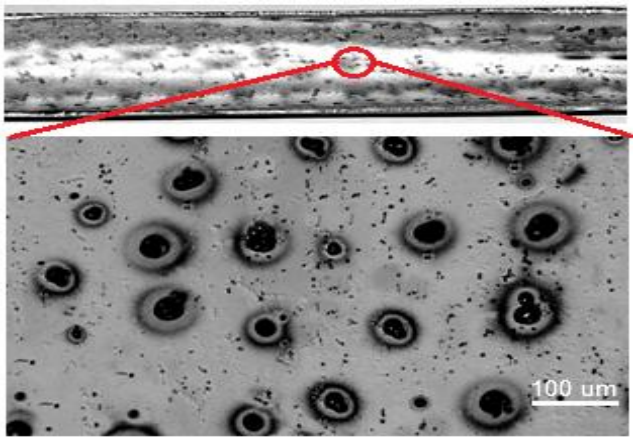

Fig. 8 Corrosion pits in the test specimen.

III. RESULTS AND DISCUSSION

The bursting pressures were computed from PCORRC, ASME B31G, modified ASME B31G, DNV-RP-F101, SHELL-92, RSTRENG, Fitnet FSS, LG-18 and Choi criteria are given in Fig. 9. The lower limit represents the results computed from ASME 31G criterion and the upper limit stands for the results calculated from RESTRENG criterion.

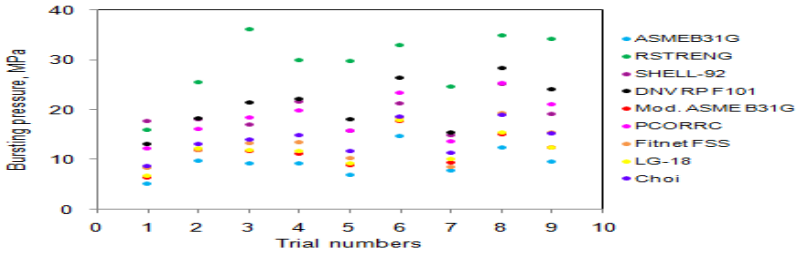

Fig. 9 Bursting pressures computed from different methods.

3.1 Influence of temperature degrading factor, crack dimensions and tube material on bursting strength

Table 4 gives the ANOVA (analysis of variation) summary of bursting pressure. All the process parameters could satisfy the Fisher's test at 90% confidence level. The temperature degradation factor (A), all by itself contributed to a two-third of the total variation observed. Crack length (B), crack depth (C) and type of steels (D) shared, respectively, 4.01%, 19.56% and 15.62% of the total variation in the bursting pressure.

Table 4: ANOVA summary of the bursting pressure based on modified ASME 31G criterion.

Source	Sum 1	Sum 2	Sum 3	SS	v	V	F	P
A	22.44	33.34	40.99	57.93	1	57.93	13984.72	60.82
B	29.49	33.68	33.59	3.82	1	3.82	922.18	4.01
C	37.39	32.54	26.83	18.63	1	18.63	4497.42	19.56
D	26.80	406.20	96.76	14.88	1	14.88	3592.14	15.62
e				0.0166	4	0.0041	1.00	-0.01
T	116.12	505.76	198.17	95.24	8			100

Note: SS is the sum of square, v is the degrees of freedom, V is the variance, F is the Fisher's ratio, P is the percentage of contribution and T is the sum squares due to total variation.

Figure 10a shows in the dependence of bursting pressure on the temperature degrading factor. As the degrading factor de-creased the pressure needed to burst the pipe would also de-crease. Degrading factor is temperature dependent. It decreases with the increase of temperature. The temperature would build up over the exothermic reaction of MIC in the presence of water. The storage tank with no leakage contains a fixed mass. For a fixed mass of gas in the storage tank, at a constant volume, the pressure (P) is directly proportional to the absolute temperature (T). The gas pressure increases by the collision of the moving gas particles with each other and against the walls of the storage tank. The effect of crack length was very slight on the bursting pressure (figure 10b). This implies that the interaction effect of corrosion pits was very low on the bursting pressure. If the crack depth increased, the pipe could fail even at low bursting pressure (figure 10c). In presence of chloride ions, pits grow by an autocatalytic mechanism. Pitting corrosion of stainless steel is illustrated in the figure 11. AISI 304 failed at low bursting pressure while SAE J405 and ASTM A516 grade 70 required high bursting pressure to fracture (figure 10d).

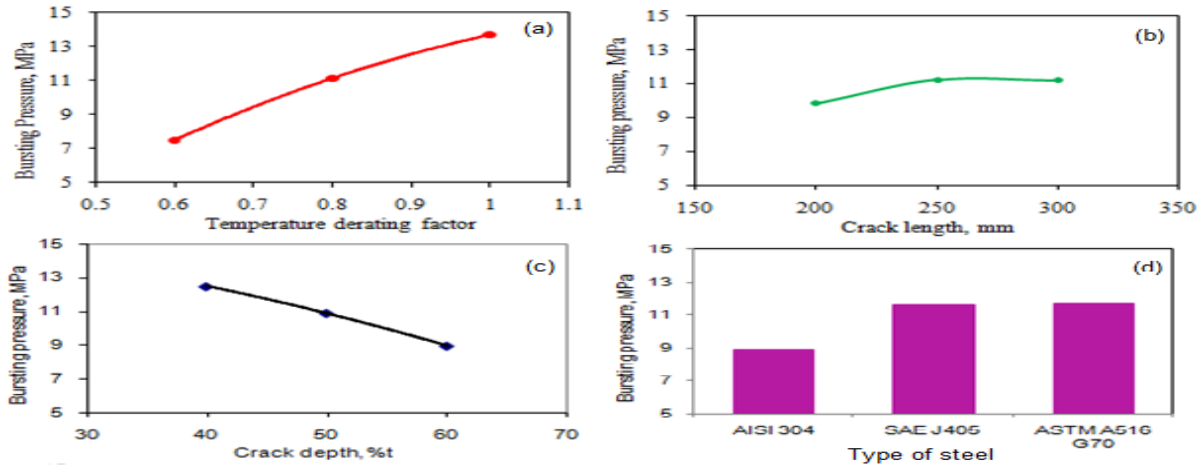

Fig. 10 Effect of process variables on bursting pressure.

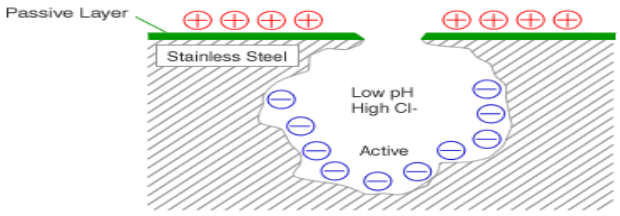

Fig. 11 Pitting corrosion mechanism.

Table 5: ANOVA summary of the Tresca criterion

Source	Sum 1	Sum 2	Sum 3	SS	v	V	F	P
A	147.02	199.29	244.93	1600.27	1	1600.27	1760779.5	55.02
B	190.30	201.54	199.40	23.74	1	23.74	26121.2	0.82
C	237.09	194.27	159.88	997.49	1	997.49	1097539.8	34.3
D	173.13	14531.00	591.24	286.85	1	286.85	315621.5	9.86
e				0.00364	4	0.00091	1.00	0
T	747.54	15126.09	1195.45	2908.35	8			100

3.2 Failure criteria

Table 5 and 6 give the ANOVA summary of the Tresca criterion and von Mises criterion respectively. Even though all the process parameters could assure the Fisher's test at 90% confidence level, only temperature degrading factor and crack depth had leading roles in the total variation of Tresca and von Mises criteria. The degrading factor (A) and crack depth (C) contributed, respectively, nearly 55.02% and 34.30% of the total variation in the Tresca and von Mises criteria. The type of stainless steel (D) put in 9.86% of the total variation in the Tresca and von Mises criteria. The crack length was insignificant in the variation of Tresca and von Mises criteria.

Table 6: ANOVA summary of the von Mises criterion

Source	Sum 1	Sum 2	Sum 3	SS	v	V	F	P
A	254.64	345.18	424.23	4800.81	1	4800.81	21193252	55.02
B	329.61	349.07	345.37	71.2	1	71.2	314314	0.82
C	410.65	336.48	276.92	2992.47	1	2992.47	13210306	34.3
D	299.87	43593.01	1024.05	860.55	1	860.55	3798912	9.86
e				0.00091	4	0.00023	1.00	0
T	1294.8	44623.74	2070.58	8725.03	8			100

The maximum shear stress as a function of temperature de-grading factor is shown in figure 12a. The maximum shear stress at failure decreased with decrease of degrading factor (or increase of temperature). The crack length (or integration of corrosion pits) did not influence much on the failure shear stress (figure 12b). The failure shear stress decreased with increase of crack depth (or depth of corrosion pits) as revealed in figure 12c. The failure shear stress induced in the AISI 304 was smaller than those of AE J405 and ASTM A516 grade 70 steels (figure 12d).

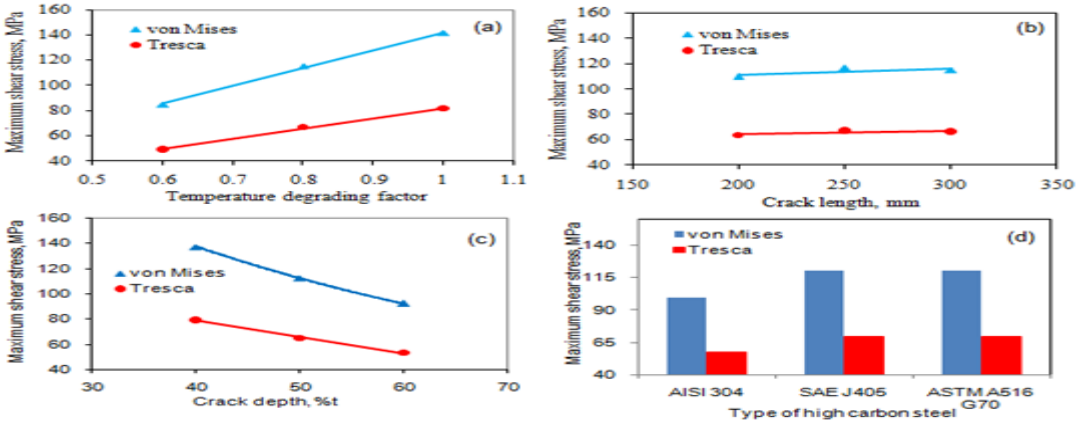

Fig. 12 Effect of process variables on failure criteria.

The stainless steel 304 alloy contains 18% Cr, 8% Ni and 2% Mn. This alloy has an austenitic structure. The stainless steel 405 alloy contains 13% Cr, and 1% Mn. This alloy has a martensitic structure. The steel ASTM A516 grade 70 contains 0.2%C, 1.05% Mn and 0.32% Si. The depths of corroded pits of all trials tested experimentally are presented in figure 13. The average of three maximum depths (green continuous line) was used in the present investigation to estimate the bursting strengths. Fig. 14a depicts the corroded pit induced in AISI 304 stainless steel subjected to testing conditions of trial 9. Fig.14b represents the corroded pit developed in SAE J405 stainless steel subjected to testing conditions of trial 6. Fig. 14c reveals the corroded pit produced in ASTM A516 grade 70 steel subjected to testing conditions of trial 8. For trials 6, 8 and 9, the average maximum depths of corroded pits were, respectively, 2.43 mm, 2.54 mm and 3.11 mm. Fig. 15 shows the interaction among local corrosion pits forming chainlike flaws.

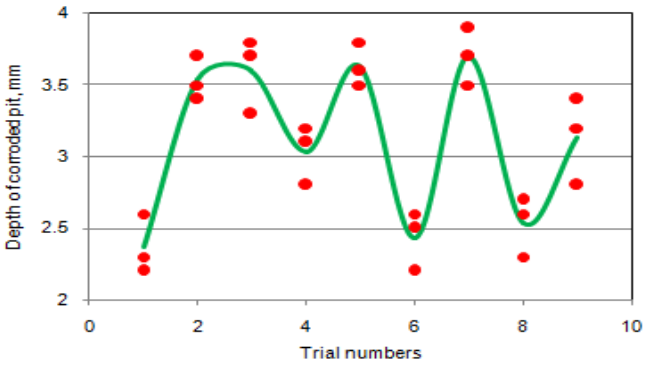

Fig. 13 Depths of corroded pits.

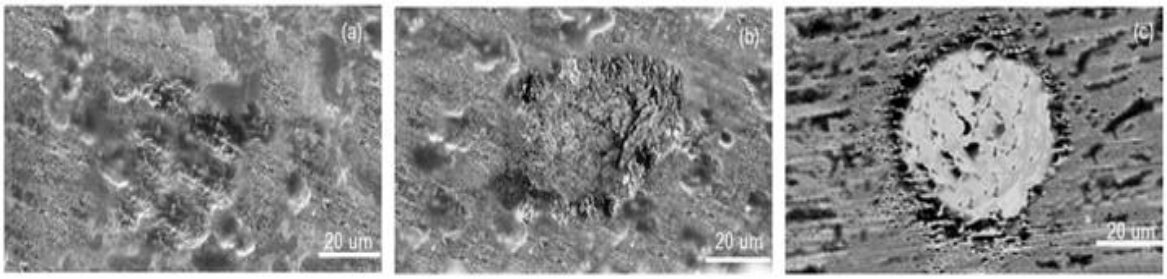

Fig. 14 SEM images of corrosion pits: (a) AISI 304, (b) SAE J405 and (c) ASTM A516 G70 steels.

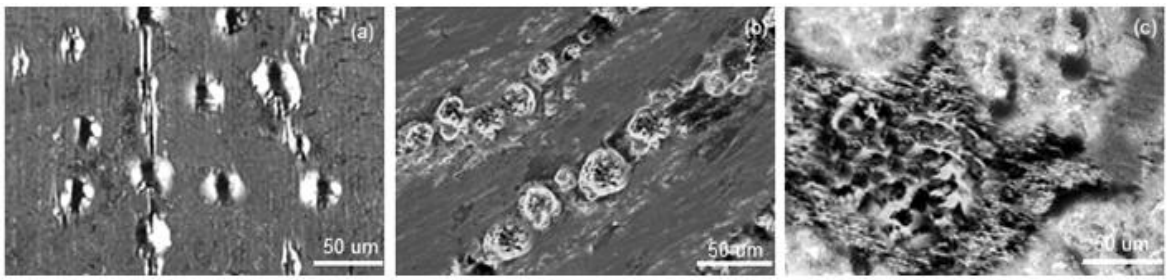

Fig. 15 Interaction of local corrosion pits: (a) AISI 304, (b) SAE J405 and (c) ASTM A516 G70 steels.

As observed from F. 16a, only pipes 6, 8 and 9 were burst under von Mises failure criterion even though all the pipes were found safe under the Tresca criterion (Fig. 16b). The Wei-bull criterion was utilized to predict the reliability of all the tanks. The least reliable criterion was ASME 31G and the most dependable criterion was RESTRENG (Fig. 17). For 80% of reliability the maximum bursting pressures were, respectively, 5.52 MPa and 19.77 MPa for ASME 31G and RESTRENG criteria. For test conditions 6, 8 and 9 bursting pressures were 14.16 MPa, 16.78 MPa and 12.39 MPa at danger level of reliabilities of 0.063, 0.013 and 0.145 according ASME B31G criterion.

The reasons for the failure of tanks were due to:

- decreased temperature derating factor (i.e., increase of temperature due to exothermic reaction and consequently increase of pressure in the tank),
- increased depths of corroded pits (the depth of corroded pits depends upon the resistance to chlorine induced corrosion).

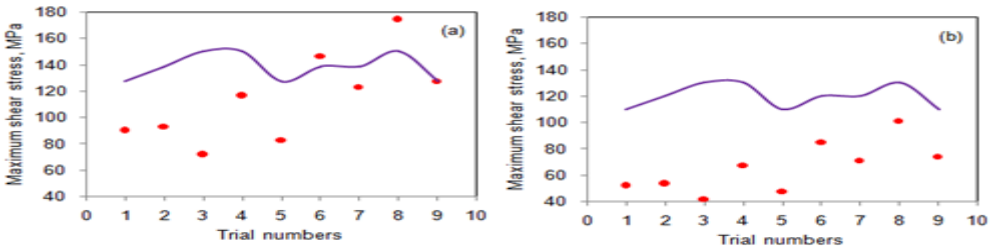

Fig. 16 Failure criterion of all pipes: (a) von Mises and (b) Tresca.

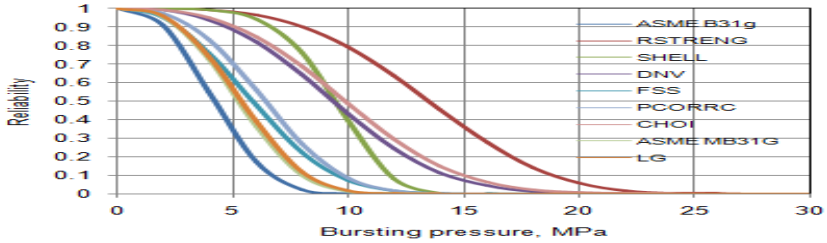

Fig. 17 Weibull failure criterion of all pipes.

It is better to understand the exothermic reaction, rise of temperature and pressure and corrosion mechanism. Methyl isocyanate is prepared by the reaction of monomethylamine and phosgene as follows:

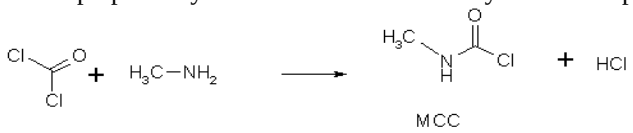

A mixture of methyl isocyanate and two moles of hydrogen chloride are formed.

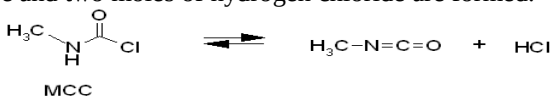

Methyl isocyanate reacts exothermically with water and forms 1,3-dimethylurea and carbon dioxide with the evolution of heat (325 calories per gram of MIC):

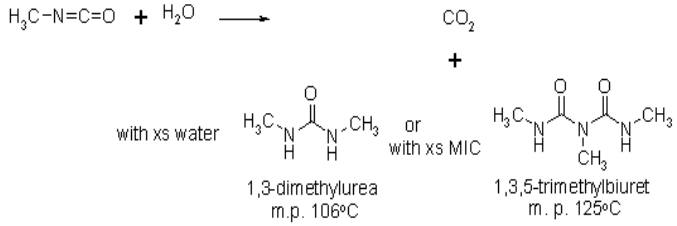

Half of Methyl isocyanate is consumed in 9 min At 25 °C, in excess water [24]. Methyl isocyanate boils rapidly if the heat is not efficiently removed. Methyl isocyanate also reacts with itself to form a trimer.

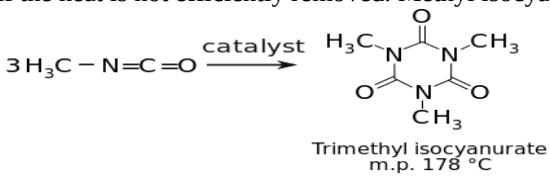

The penetration of chloride ions is the main contributing factor for inducing corrosion of the steel. The conditions for the occurrence of corrosion are elevated chloride concentration, presence of moisture and oxygen and electrical conductivity. If the pH is greater than 12.5, the steel gets corroded. The corrosion mechanism is as follows (figure 10):

Decomposition of passivity layer: $Fe^{2+} + 2Cl^- \rightarrow FeCl_2$

Corrosion of steel: $Fe \rightarrow Fe^{2+} + 2e^-_2$ (reduction)

$$\frac{1}{2}O_2 + H_2O + 2e^- \rightarrow 2OH^- \quad \text{(oxidation)}$$

Formation of rust: $Fe^{2+} + 2OH^- \rightarrow Fe(OH)_2$

$$2Fe(OH)_2 + \frac{1}{2}O_2 + H_2O \rightarrow Fe_2O_3.3H_2O \quad \text{(rust)}$$

The oxidation of iron atoms in steel reduces of steel cross section owing to the "rusting away" which may lead to inadequate areas of steel necessary for carrying pressure on the inner walls of the tank.

AISI 304, SAE J405 and ASTM A516 G70 steels are subjected to crevice corrosion and pitting corrosion. They make a range of incubation times. AISI 304 stainless steel can perform well where chloride levels are small. When chloride levels are high, the performance of AISI 304 stainless steel is poor. For SAE J405 and ASTM A516 G70 steels, the incubation time for non-uniform attack in chloride containing environments is very short, often only hours or a few days. Tanks made of SAE J405 and ASTM A516 G70 steels were failed due to corrosion even though they have good strength. Yield strengths of SAE J405 and ASTM A516 G70 steels are, respectively, 276 MPa and 260 MPa. The test conditions 6 and 8 represents SAE J405 and ASTM A516 G70 steels respectively. Even though AISI 304 stainless steel has yield strength of 215 MPa, the corrosion rate was slower as those of SAE J405 and ASTM A516 G70 steels.

The causalities of Bhopal gas disaster might be caused by toxic characteristic of Methyl isocyanate. The threshold limit value of MIC set by the American Conference on Government Industrial Hygienists is 0.02 ppm. Over 12 ppm level of expo-sure, MIC can result in pulmonary or lung edema, emphysema and hemorrhages, bronchial pneumonia and death [25].

IV. CONCLUSIONS

The bursting pressure of the storage tank was highly dependent on the temperature derating factor and the crack depth. The bursting pressure is decreased with the increase of crack depth and the decrease of degrading factor (or increase of temperature). The rise of temperature in the storage was caused by exothermic reaction MIC with water. The rise in temperature increased the pressure in the storage tank. The von Mises criterion was very near the failure pattern of the tanks. The failure criteria would satisfy the reliability results obtained from the Weibull criterion and ASME 31G criterion used for the estimation of the bursting strength. The reasons for the failure of experimental storage tanks used in the present work would satisfy the causes for the leakage of Methyl isocyanate gas and failure of the storage tank during the Bhopal gas disaster.

REFERENCES

[1] Bhopal trial: Eight convicted over India gas disaster,. BBC News. 7 June 2010.
[2] Madhya Pradesh Government : Bhopal Gas Tragedy Relief and Rehabilitation Department, Bhopal,. www.Mp.gov.in.
[3] A.K. Dubey, Bhopal Gas Tragedy: 92% injuries termed "minor", 21 June 2010 .
[4] The Bhopal Saga-Causes and Consequences of the World's Largest Industrial Disaster. India: Universities Press: doi:10.13140/2.1.3457.5364.
[5] American National Standards Institute (ANSI) / American Society of Mechanical Engineers (ASME), Manual for determining the remaining strength of corroded pipelines, ASME B31G, 1991.
[6] A. C. Reddy, Prediction of bursting pressure of thin walled 316 stainless steel pipes based on ASME B31G criterion, National Conference on Advances in Design Approaches and Production Technologies (ADAPT-2005), Hyderabad, 22-23rd August 2005, 225-228.
[7] A. C. Reddy, Decent prophecy of bursting strength of natural gas pipelines based on modified ASME B31G criterion, National Conference on Excellence in Manufacturing and Service Organizations: The Six Sigma Way, Hyderabad, 26-27 August 2010, 112-115.
[8] Anon, DNV-RP-F101, Corroded Pipelines, Det Norske Veritas, 1999.
[9] A. C. Reddy, Estimation of bursting pressure of thin walled 304 stainless steel pipes based on DNV RP F101criterion, National Conference on Advances in Design Approaches and Production Technologies (ADAPT-2005), Hyderabad, 22-23rd August 2005, 229-231.
[10] D. Ritchie and S. Last, Burst Criteria of Corroded Pipelines - Defect Acceptance Criteria, Proceedings of the EPRG/PRC 10th Biennial Joint Technical Meeting on Line Pipe Research, Cambridge, UK, 18-21 April 1995, 32-1 - 32-11.
[11] A. C. Reddy, Reliability assessment of corrosion cracks in cold rolled 302 stainless steel pipes based on SHELL-92 criterion, National Conference on Advances in Design Approaches and Production Technologies (ADAPT-2005), Hyderabad, 22-23rd August 2005, 232-234.
[12] J. F. Kiefner and P. H. Vieth, A Modified Criterion for Evaluating the Strength of Corroded Pipe, Final Report for Project PR 3-805 to the Pipeline Supervisory Committee of the American Gas Association, Battelle, Ohio, 1989.
[13] A. C. Reddy, Trustworthiness judgment of corrosion cracks in cold rolled 305 stainless steel pipes based on RSTRENG criterion, National Conference on Advances in Design Approaches and Production Technologies (ADAPT-2005), Hyderabad, 22-23rd August 2005, 235-237.
[14] D.R. Stephens and B.N. Leis, Development of an Alternative Criterion for Residual Strength of Corrosion Defects in Moderate- to High-Toughness Pipe, Proceedings of the Third International Pipeline Conference (IPC 2000), Calgary, Alberta, Canada, American Society of Mechanical Engineers, 1-5 October 2000, 781-792.
[15] A. C. Reddy, Consistency prediction of bursting strength of 317 stainless steel pipes based on PCORSS (Batelle) criterion, National Conference on Excellence in Manufacturing and Service Organizations: The Six Sigma Way, Hyderabad, 26-27th August 2010, 105-108.
[16] A. Cosham, P. Hopkins, P. and K. A. Macdonald, Best Practice for the Assessment of Defects in Pipelines-Corrosions, Engineering Failure Analysis, 14, , 2007, 1245-1265.
[17] A. C. Reddy, Reliable forecasting of remaining strength of petroleum pipelines based on LG-18 criterion, National Conference on Excellence in Manufacturing and Service Organizations: The Six Sigma Way, Hyderabad, 26-27 August 2010, 109-111.
[18] GTC1 – 2001 – 43049, FITNET, European Fitness for Service Network.
[19] A. C. Reddy, Trustworthy prediction of bursting strength of ductile iron pipes based on Fitnet FSS criterion, International Journal of Research in Engineering and Technology, 4(12), 2015, 48-53.
[20] J. B. Choi, B.K. Goo, J.C. Kim, Y.J. Kim and W.S. Kim, Development of limit load solutions for corroded gas pipelines, International Journal of Pressure Vessels and Piping, 80, 2003, 121-128.
[21] A. C. Reddy, Reliability computation of bursting strength of ammonia pipelines based on Choi's criterion, International Journal of Innovative Research in Science, Engineering and Technology, 5(1), 2016, 28-36.
[22] A. C. Reddy and V.M. Shamraj, Reduction of cracks in the cylinder liners choosing right process variables by Taguchi method, Foundry Journal, 10(4), 1998, pp.47-50.
[23] J. M. Zhao, Y. Zuo, The effects of molybdate and dichromate anions on pit propagation of mild steel in bicarbanate solution containing Cl^-, Corrosion Science, 44, 2002, 2119-2130.
[24] E. A. Castro, R.B. Moodie, P.J. Sansom, The kinetics of hydrolysis of methyl and phenyl isocyanates, Journal of the Chemical Society, Perkin Transactions ,2(5), 1985, 737–742.
[25] G. Kimmerle, A. Eben, Zur Toxizität von Methylisocyanat und dessen quantitativer Bestimmung in der Luft, Archiv für Toxikologie, 20 (4), 1964, 235–241.

American Journal of Engineering Research (AJER) 2016
American Journal of Engineering Research (AJER)
e-ISSN: 2320-0847 p-ISSN : 2320-0936
Volume-5, Issue-2, pp-10-20
www.ajer.org
Research Paper Open Access

Assessment of groundwater vulnerability and sensitivity to pollution in Berrechid plain, using drastic model

M. Aboulouafa[*1], H. Taouil[*1], S.Ibn Ahmed[*1]
**1:Faculté des Sciences Université IBN Tofail kénitra Morocco*

Abstract: *The Groundwater protection and management is vital for human evolution, socio-economic development and ecological diversity, because it is one of the most valuable natural resources. Agricultural and industrial activities, more and more intensive and significant population growth, have contributed to the degradation of Berrechid Groundwater quality. The present study aimed to assess the vulnerability of Berrechid aquifer using the DRASTIC models. The application of the methodology developed has needed the establishment of a Geographical Information System synthesizing a considerable mass of data (geological, hydrogeological, geophysical, etc.), constitutes a real tool to aid in the decision for the managers of water resources in the region of Chaouia. The results show that three classes of vulnerability are observed in the study area: the higher drastic indices appear at the areas with low groundwater table depth and the areas which are not protected by the clays, and the areas less vulnerable are located in areas where the water is deeper and the clays recovery is important.*

Keywords*: Groundwater vulnerability / DRASTIC / Berrechid plain.*

I. Introduction

The Berrechid plain extends to the south of Casablanca on an area of 1600 km2. It is at the surface as a pit of subsidence, limited to the south by the limestone of the Cretaceous, and elsewhere by primary formations consisting of shales and quartzites. The land of filling is formed of marine sandstone dune and the Pliocene **[1] (Fig.1),** its main aquifer is located between 5 and 30 m depth **[2].**

This groundwater has an underground hydraulic potential which represents the sole and unique water resource in the region; it is the source of the drinking water supply of a large part of the rural areas of the province and a part of Settat city.

Berrechid City of has known these past fifteen years a development of industrial and agricultural activities with a use of more and more exaggerated chemical fertilizers. To which is added the pressure of Demographic growth. This is reflected by the growing risks of groundwater pollution.

Berrechid groundwater is generally of a very bad quality for the whole of the sampling points. This state of quality is due: to the strong mineralization, elevated chloride and nitrate [**3].**

The prevention of groundwater pollution is an important step, to which scientists must deploy more effort, including the discovery of the groundwater vulnerability.

The main objective of this study is the assessment of the vulnerability of the Aquifer using the DRASTIC model **[4]** and the combination of the data of the hydrogeological layers in the GIS.

Seven parameters are taken into account: the depth of the water, the annual recharge of the Aquifer effective, aquifer lithology, the type of soil, topography, the impact of the unsaturated zone and the hydraulic conductivity of the aquifer.

II. Presentation of the study area

The Berrechid groundwater: Located in the south of the city Casablanca, it is characterized by the importance of its extent around 1500km^2. It fits in the quadrangle formed by the cities of Settat, El Gara, Mediouana and the center of Bousakoura. This groundwater is developed in formations sandstones of age plio-Quaternary, under a silty Coverage with average thickness of 20m. Geologicaly, this plain is composed of sedimentary rocks formed Cretaceous limestone (Cenomanian) with intercalations of clays and marls and sedimentary rocks formed of calcareous sandstone to cemented conglomerates toward the base .The whole is surmounted by a coverage of clayey silts of the quaternary recent. This part of the low Chaouia, receives of the upstream elements of varied erosion from the high Chaouia (Plateau of Settat - Ben Ahmed) from which it is separated by the flexure of Settat **[1]**.

The recharge of the aquifer is mainly done in the marginal areas. The deposits are covered by location of clays whose thickness can reach approximately 50 m; clays that form the more important accumulations of Quaternary deposits offering a natural protection to the Pliocene aquifers. The areas where the thickness of sediment is more low (less than 5 m) or the sectors where the Quaternary deposits are mainly trained of sands would constitute the areas most vulnerable to infiltration of pollutants. **[5]**.

The Berrechid Groundwater is limited: in South and Southeast: by the Settat plateau who plunges in the plain through flexures and defects and forming the bedrock Eocene; in the north-east: the valley of the Oued El Mellah; in the north: the plain of the Chaouia which is the natural extension of plain of Berrechid and to the west and to the north-west by the primary outcrops **(Fig.1),**.

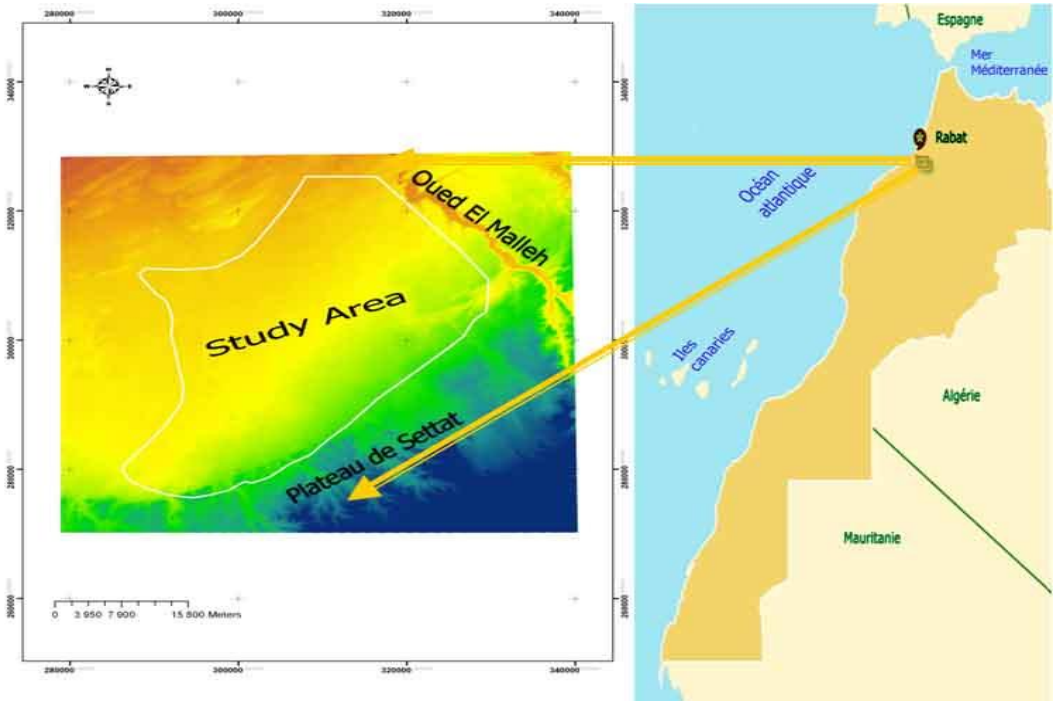

Fig. 1: The study area location

III. Data and Methodology

The DRASTIC model was developed in USA for the purpose of protecting the groundwater resources; it is an empirical groundwater model that estimates groundwater contamination vulnerability of aquifer systems based on the hydrogeological settings of that area **[1]**. The DRASTIC method is based on a weighting and indexing system of parameters **[4],** based on ratings and weights given to the criteria chosen to study, classify and represent in the horizontal plane; the protective role of the interface between water resources of the source of pollution **[6].**

The DRASTIC hydrogeologic vulnerability ranking method uses a set of seven hydrogeologic parameters to classify the vulnerability or pollution potential of an aquifer. The parameters are: **[7]**

- **Depth of groundwater (D):** is subdivided into seven vulnerability classes. More depth to the top of the table, the less the area is vulnerable;
- **Recharge rate (R):** is expressed as depth of water seeped into the water table over a year. It is divided into 5 classes. More charging, the higher the vulnerability is too. The assumption made here is that the importance of charging is a factor aggravating the pollution as it pushes into the system. This assumption does not take into account that most charging is more important pollution is diluted;
- **The Aquifer media (A)** is established according to ten major lithological units as massive limestones, karstified limestone, metamorphic rocks, moraines, sandstone ... Each type of lithology is assigned varying degrees of vulnerability which is defined by the expert according to the reactivity of the aquifer, its fracturing and sorption phenomena which may occur therein;
- **The Soil media (S)** are subdivided into eleven classes according to their composition, their texture and structure. More soils are permeable, more they are considered vulnerable because they promote the infiltration

of pollution. The possibility that the water flows on impermeable soils and contaminants then infiltrating in a concentrated way downstream ,is not considered in this approach;

- **Topography (T)** or more exactly the percentage of slope is divided into five classes. The assumption made here is that more the slope is steeper, more there is infiltration and the area is vulnerable. As for the "soil" parameter, the issue of re-infiltration of water into slope foot area is not addressed. As the issue of soil erosion favored by the slope and transporting fine solids in the resulting aquifer;
- **The Impact of the vadose zone (I)** is divided into eleven classes according to the lithologies within it. As for the criterion "geology of the aquifer rock", each lithology has varying degrees of vulnerability which are defined by the expert based on his knowledge of the system. Generally, lithology wherein the water circulates rapidly is considered more vulnerable than lithology wherein the water flows slowly. This classification does not consider the superposition of different lithologies, such as, for example, the plating on karst moraine;
- **The hydraulic Conductivity of the aquifer (C)** is divided into six different classes. More it is higher, more the medium is considered vulnerable because the mechanisms to mitigate pollution have less time to occur. This criterion is closely related to the geology of the aquifer rock.

Table 1 Drastic parameters assigned weights [4]

Factor	Weight
D Depth to top the of the Aquifer	5
R Net Recharge	4
A Aquifer Media	3
S Soil Media	2
T Topography	1
I Impact of the Vadose Zone	5
C Hydraulic Conductivity of the Aquifer	3

Drastic sensitivity index was computed based on the following formula.

Drastic index =(Dr×Dw)+(Rr×Rw)+(Ar×Aw)+(Sr×Sw)+(Tr×Tw)+(Ir×Iw)+(Cr×Cw) (1)

Where letters indicate the name of the layer, the sub-letter *w* indicates the weight of the layer, sub-letter *r* indicates the ranking number as weighting factor based on sensitivity of parameters.
The vulnerability degree is assessed on the basis of the DRASTIC index classes. The vulnerability is even more important than the calculated index is high**. [8]**

Table 2. (a) Classes and notes used for Depth of water (D); (b) Classes and notes used for net recharge (R); (c) Classes and notes used for aquifer lithology (A); (d) Classes and notes used for soil (S); (e) Classes and notes used for topography (T); (f) Classes and notes used for unsaturated zone (I); (g) Classes and notes used for permeability (C).

Class(m)	Note
0 -1.5	10
1.5 - 4.5	9
4.5 - 9	7
9.0 -15.0	5
15 – 23	3
23 – 30	2
>30	1
(a)	

Class(mm)	Note
0 – 50	1
50 - 100	3
100 – 175	6
175 - 225	8
>225	9
(b)	

Class	Typical Note
Massive shale	2
Metamorphic	3
Metamorphic altered-Sandstone	6
Limestone massive	8
Sandstone	6
Sand and gravel	8
Basalt	9
Limestone	10

(c)

Class	Note
Thin or absent	10
Gravel	10
Sands	9
Sandy loam	6
Silts	4
Silty loam	3
Clays	1

(d)

Range of slope (in degrees)	Note
0 - 2	10
2 – 6	9
6 – 12	5
12 – 18	3
> 18	1

(e)

Lithological Nature	Typical Note
Silt and clay	3
Shale	3
Limestone	3
Sandstone	6
Sand and gravel with silt and clay pass	6
Sand and gravel	8
Basalt	9
Limestone karst	10

(f)

Range of permeability (m/s)	Note
$1.5* 10^{-7} – 5*10^{-5}$	1
$5*10^{-5} – 15*10^{-5}$	2
$15*10^{-5} – 33*10^{-5}$	4
$33*10^{-5} – 5*10^{-4}$	6
$5*10^{-4} – 9.5*10^{-4}$	8
$>9.5*10^{-4}$	10

IV. Results and Discussions

a. Drastic settings and the aquifer vulnerability

- **Depth of groundwater (D):** has been developed by the interpolation of data on the water level **[9].** The interpolation is performed by the ordinary kriging method **(Fig. 2a).**
- **Recharge rate:** The values of this parameter are acquired by the application of the Thiessen polygons on the data of effective rainfall **(Fig. 2b).**
- **The Aquifer media:** The development of the matrix Card “aquifer media” has been based, essentially, on the interpretation and the correlation between drilling in the study area **(Fig. 2c).**
- **The Soil media**: The study area map “Soil media” has been developed by the digitalisation of the card national soil, conducted by the Department of Agriculture and the Agricultural Development. This map shows a dominance of Clay textures and loam-Clay **(Fig. 2d).**
- **Topography**: The matrix slope map is carried out from the digital model of terrain SRTM (Ftp://e0srp01u.ecs.nasa.gov) **(Fig. 2e).**
- **The Impact of the vadose zone**: The evaluation process of the impact parameter of the vadose zone is based on the interpretation of the lithological drilling slices. The correlation shows that the unsaturated zone is constituted essentially by the clayey facies , sand and gravel **(Fig. 2F).**
- **The hydraulic Conductivity of the aquifer**: This card has been developed by the digitalisation of the hydraulic conductivity map of (ABHBC, 20012) **(Fig. 2g).**

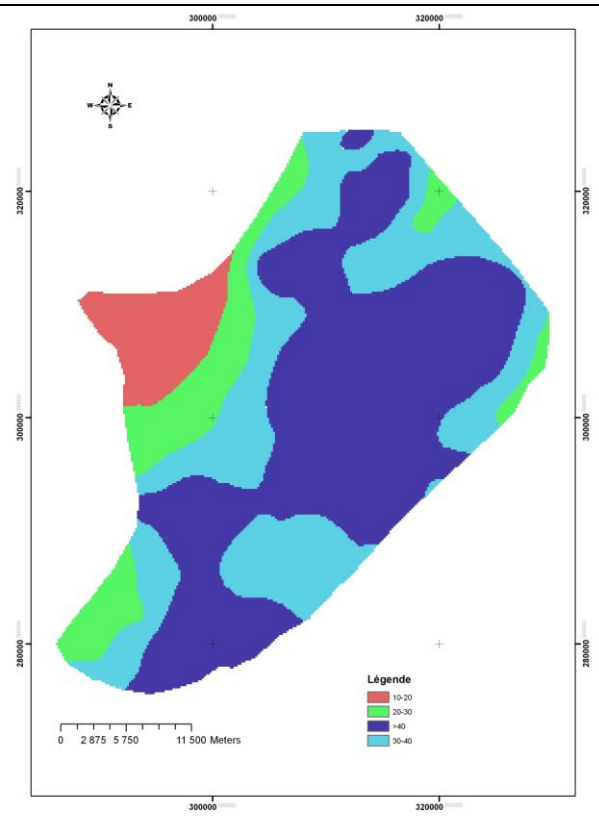

Fig. 2a : Map of groundwater depth (D)

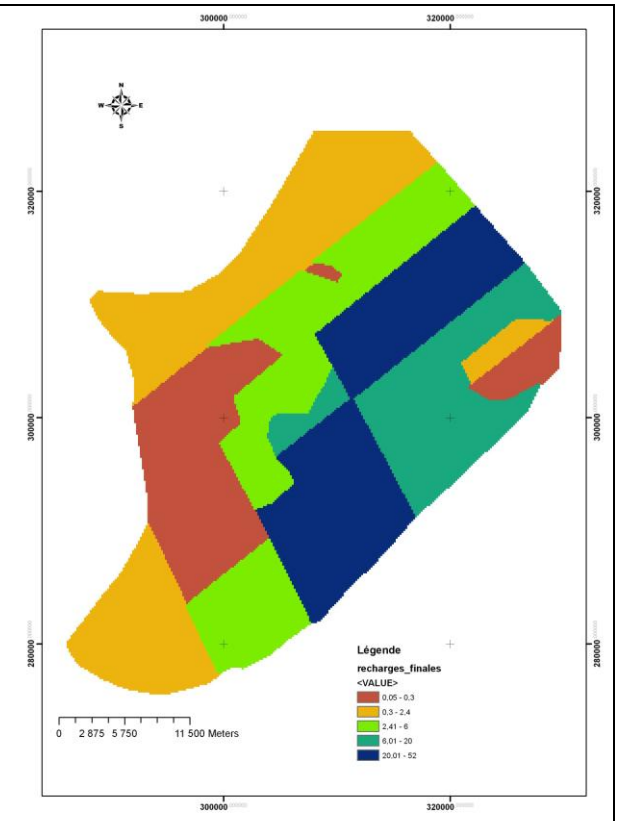

Fig. 2b: Map of groundwater net recharge (R).

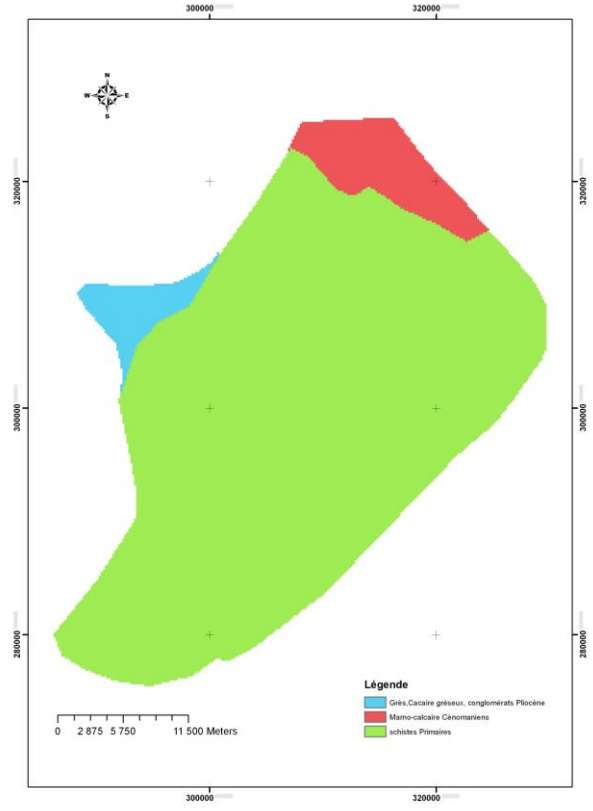

Fig. 2c: Map of aquifer lithology (A).

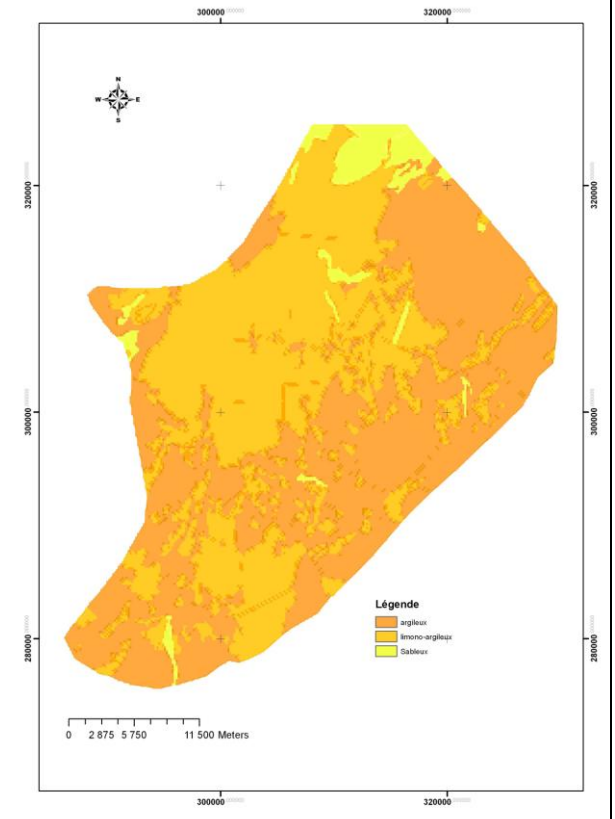

Fig. 2d : Map of groundwater pedology (S)

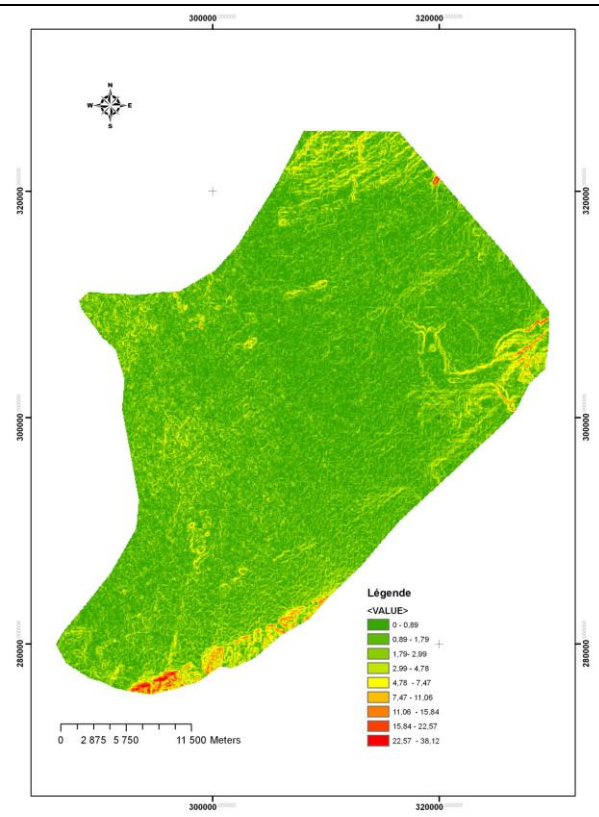

Fig. 2e: Map of aquifer topography (T).

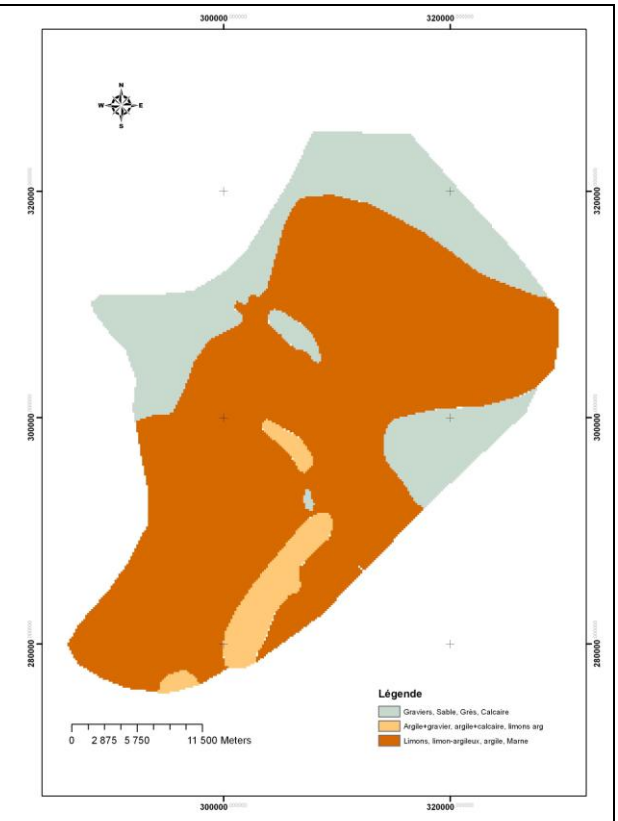

Fig. 2f: Map of groundwater unsaturated zone (I).

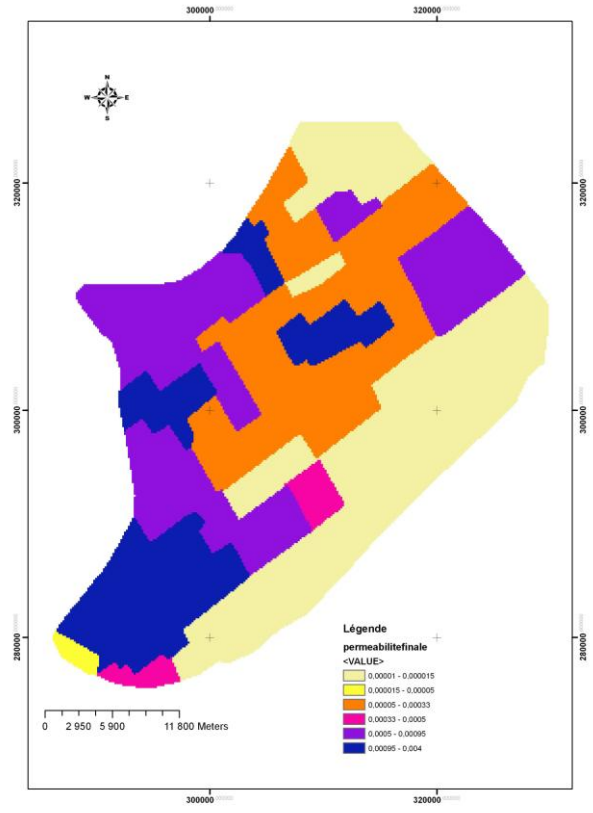

Fig. 2g: Map of ground water permeability (C).

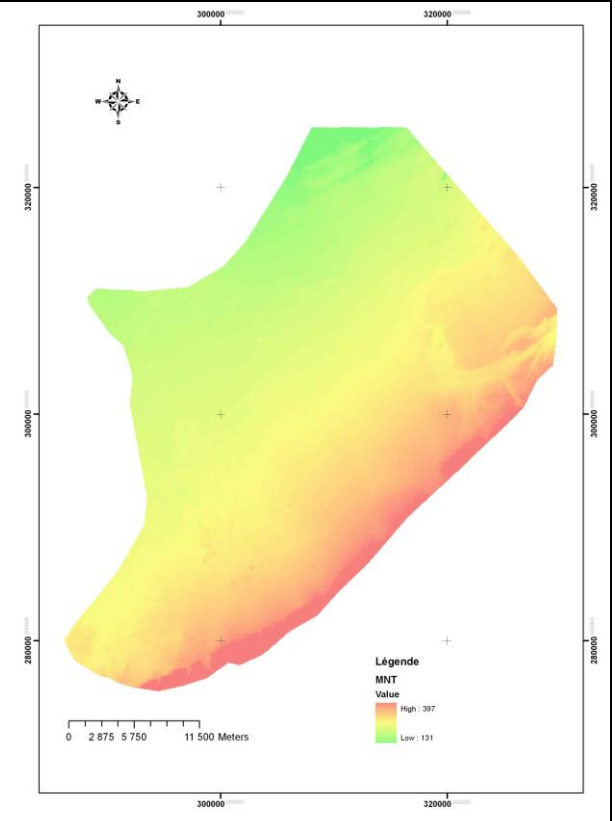

Fig. 2h : MNT of the study area

Fig 2: Maps used for the development of the vulnerability map (drastic).

All the maps of the figure 2 are classified; depending on the rating system of the DRASTIC method (Table 2). The figure 3 represents the classified maps.

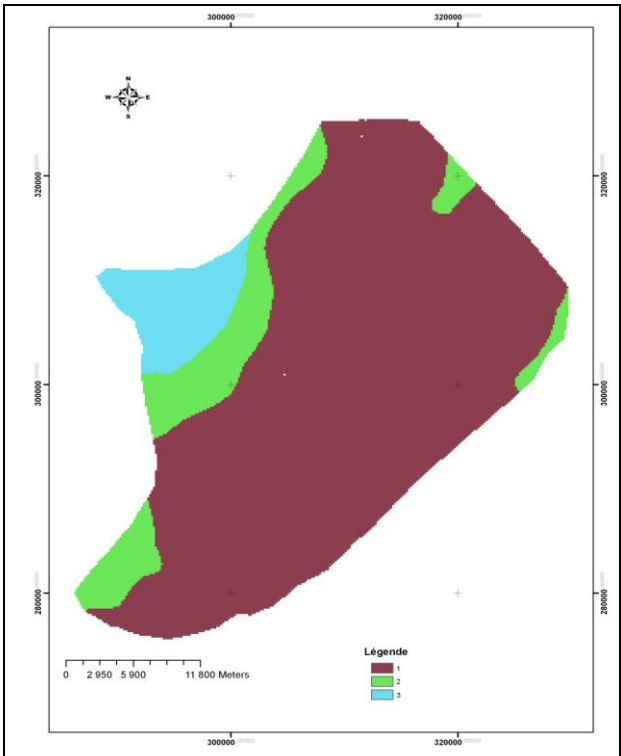

Fig. 3a : Map of groundwater depth after reclass

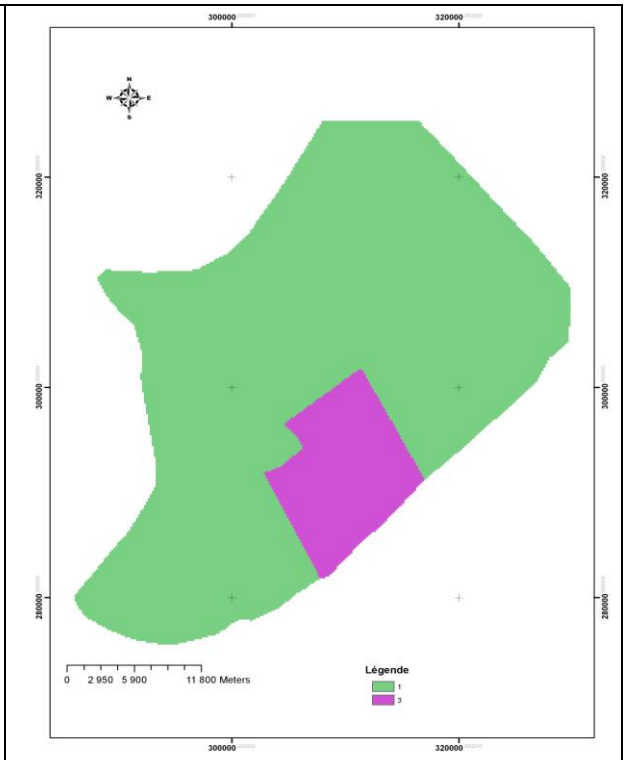

Fig. 3b: Map of groundwater net recharge after reclass.

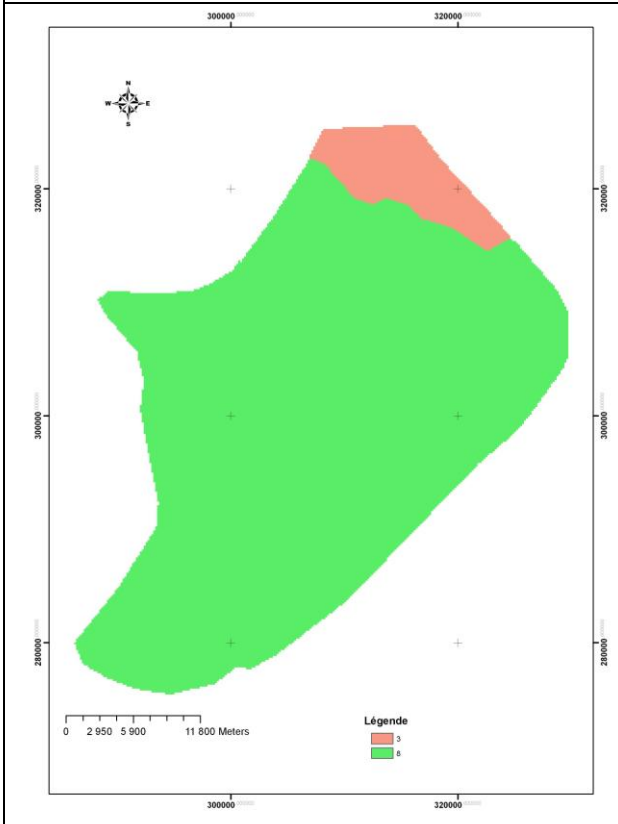

Fig. 3c: Map of aquifer lithology after reclass.

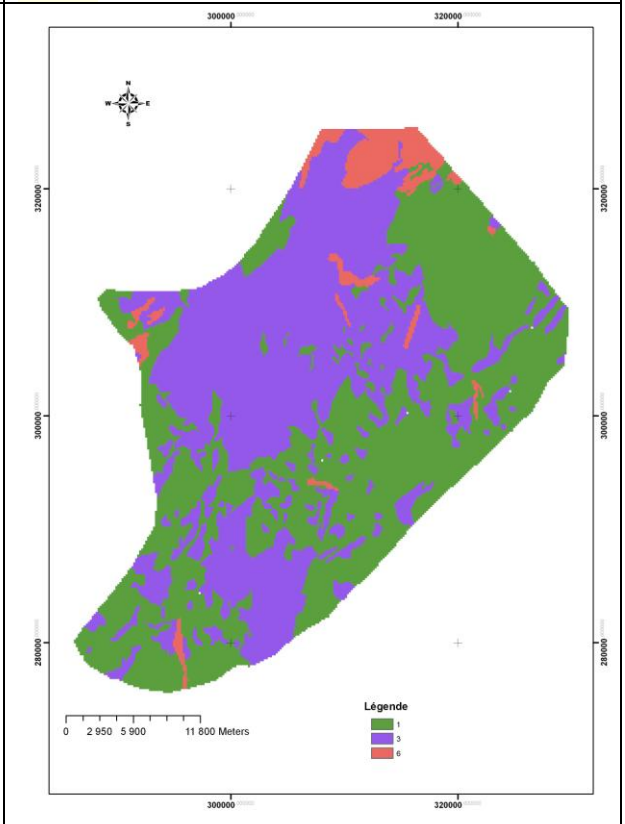

Fig. 3d: Map of groundwater pedology after reclass.

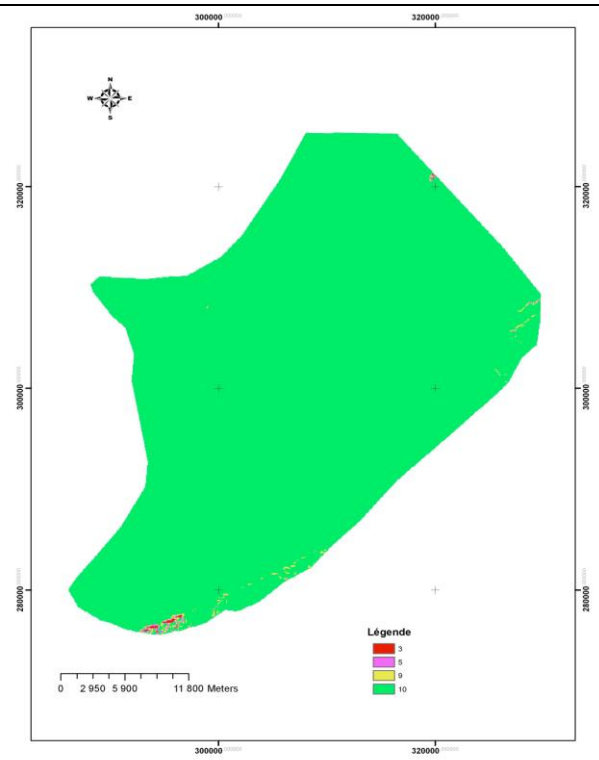

Fig. 3 e : Map of aquifer topography after reclass

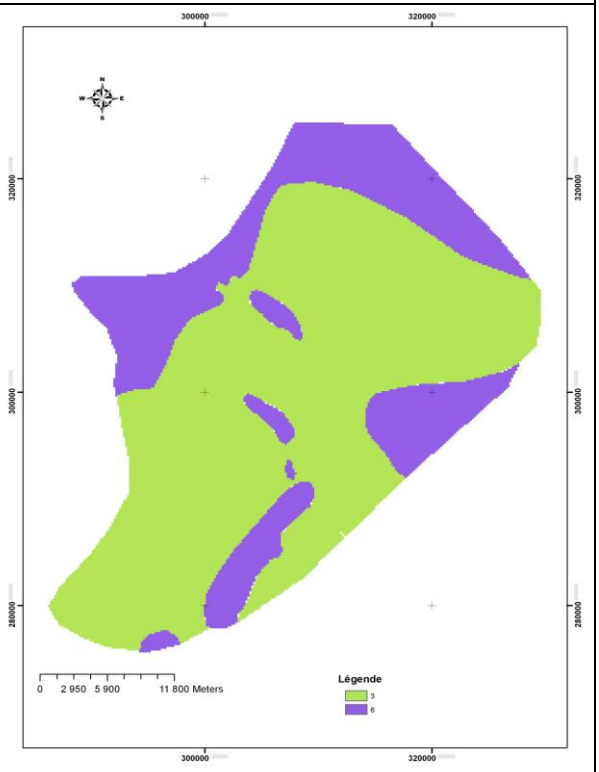

Fig. 3f : Map of groundwater unsaturated zone after reclass

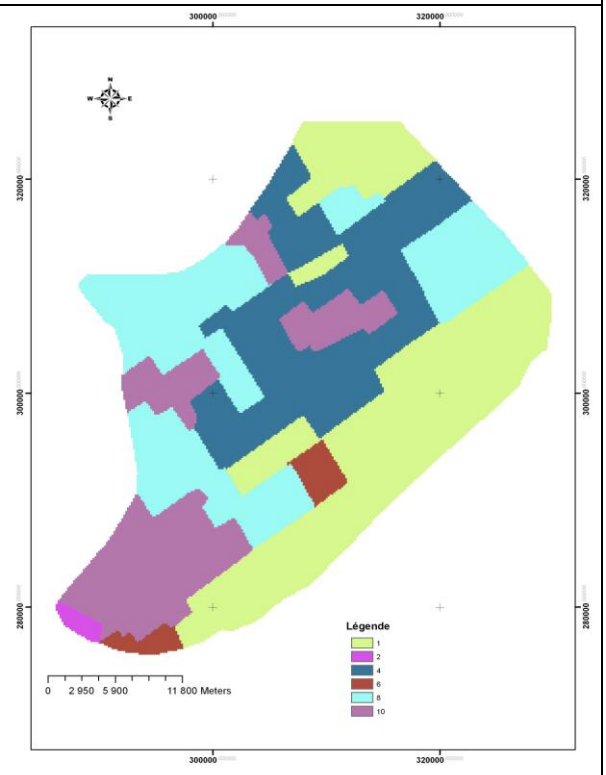

Fig. 3g: Map of ground water permeability after reclass

Fig 3: Maps used for the development of the vulnerability map (drastic) after reclass.

The vulnerability map of Berrechid plain (Drastic) thus obtained by the Formula 1 is the following **(Fig. 4)**

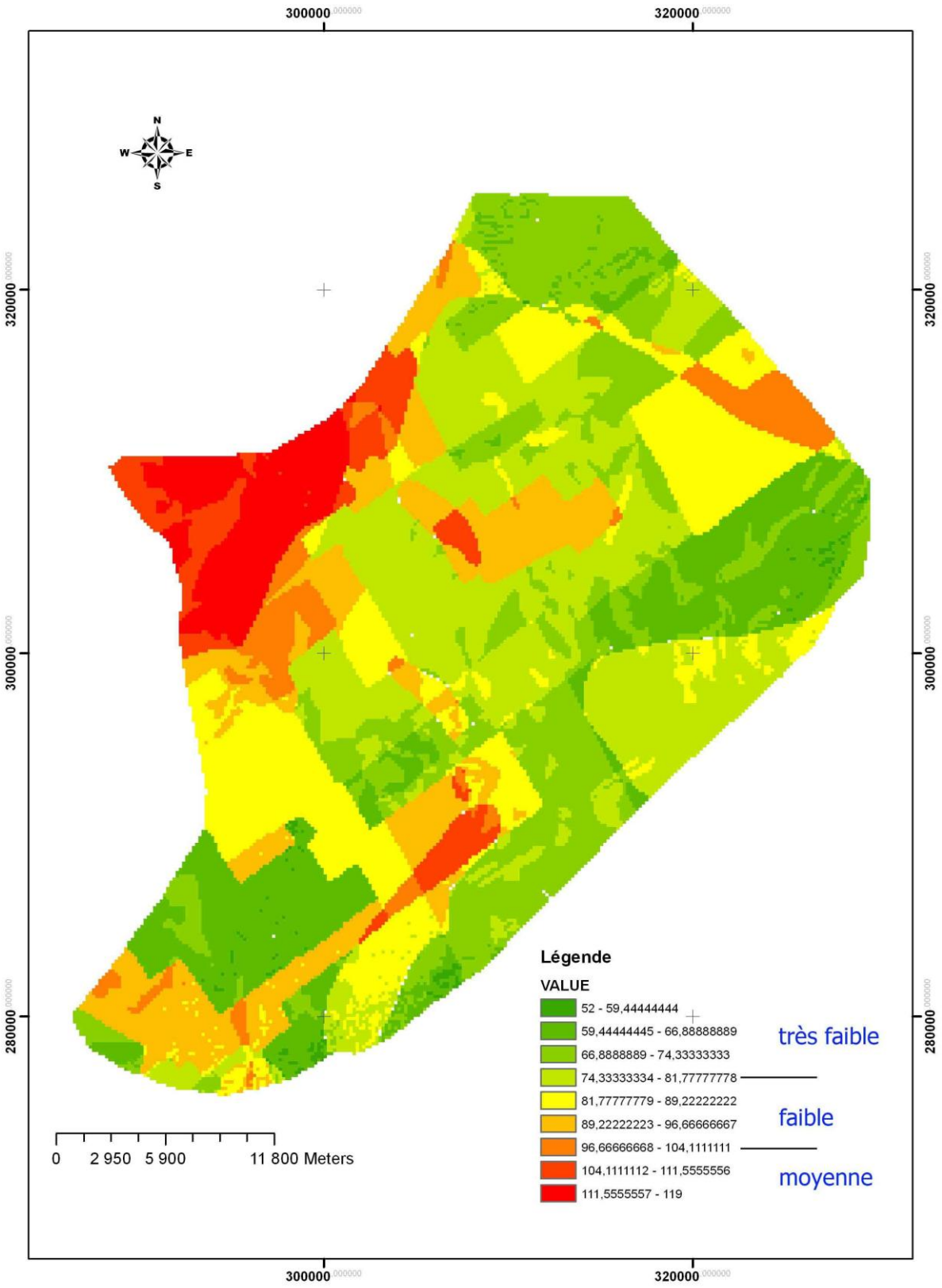

Fig. 4: Map of vulnerability of Berrechid groundwater (DRASTIC)

Any vulnerability map developed is tested and validated by the measurement and analysis of chemical data of groundwater [10 -12].

The validity of the vulnerability assessment to pollution by drastic methods in the case of this study has been tested by the pollution by nitrates in the water. So we compare the distribution of nitrate in groundwater and the distribution of vulnerability classes. The Figure 5 shows the map of the nitrate distribution in Berrechid groundwater [9]

We note that the area NW with high drastic index shows elevated levels of nitrates.

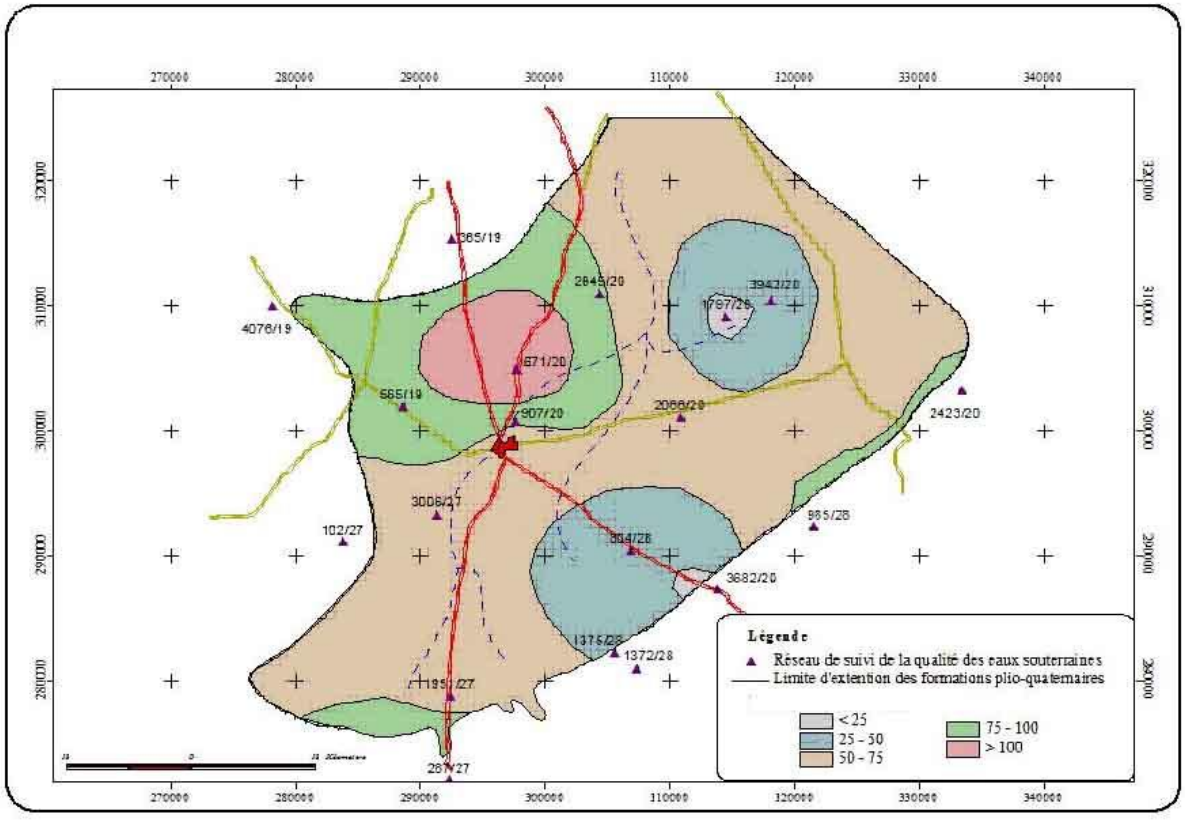

Fig. 5 Map of distribution of nitrates in Berrechid groundwater (ABHCB)

The analysis of the drastic card allows you to distinguish 3 classes of vulnerabilities: very low, low and average.

The spatial distribution of vulnerability classes of Berrechid groundwater is generally low to medium vulnerability with a drastic index between 52 and 119.

The highest drastic indices are located mainly in areas n and NW of Berrechid city. These areas are characterized by low slopes, low depth of the Plan of water and the nature of the rock formations permeable.

While the areas with vulnerability very low occupy the borders NE and E of the study area. These areas are characterized by a low permeability and the nature lithological little permeable "clay", offering to the aquifer a natural protection.

b. Sensitivity of the drastic Model

Table 3 shows the summary data statistics of the seven parameters used to calculate the index drastic in the Berrechid plain. The analysis of the medium sized shows that the greatest risk of groundwater contamination of the plain of Berrechid is favored by the parameters "**topography**, **Aquifer media and hydraulic conductivity**" (whose averages are respectively: 9.87, 7.64 and 5.04). However the parameters "**unsaturated zone and soil**" participates with a moderate risk (averages is 3.89 and 2.14), and the parameters **Depth of groundwater and** recharge promotes a low risk (medium: 1.27 and 1.24).

The coefficient of variation shows that the great contribution to variations in the index of vulnerability is due to the parameter "**hydraulic conductivity**" (CV: 68.45%). The parameters **"soil, unsaturated zone, recharge, depth of the groundwater and unsaturated zone"** show an average contribution (CV: 60.28%, 52.42%, 45.67% and 35.22%) however **the aquifer and topography** represent a contribution to the variation of the index of vulnerability medium to low (CV: 16.75 and 5.98).

Table 3. The summary statistics of drastic parameters

	D	*R*	*A*	*S*	*T*	*I*	*C*
Min	***1***	***1***	***3***	***1***	***3***	***3***	***1***
Max	***3***	***3***	***8***	***6***	***10***	***6***	***10***
Moy	***1,27***	***1,24***	***7,64***	***2,14***	***9,87***	***3,89***	***5,04***
SD	***0,58***	***0,65***	***1,28***	***1,29***	***0,59***	***1,37***	***3,45***
CV	***45,67***	***52,42***	***16,75***	***60,28***	***5,98***	***35,22***	***68,45***

V. Conclusion

In this study, we have attempted to assess the vulnerability of the ribbon cable for Berrechid and to identify and classify the vulnerable and the areas not vulnerable to contamination of groundwater in order to provide the zoning in the protection of the groundwater table and the implementation of effective strategies for the management of groundwater. We used for this objective, the GIS through the DRASTIC method. In effect, the SIG has provided an effective environment for analyzes and a strong capacity of handling of large quantities of spatial data. The Seven Parameters of the model have been built, classified and coded using the GIS tool and its features. The vulnerability index was easily calculated. The Berrechid groundwater is polluted with high values of nitrates due to several phenomena: the discharge of solid and liquid wastes of the industry, domestic, and also by the use of large quantities of fertilizers in agriculture. This study has produced a very important tool for the management and development, because it gives full details on the vulnerability of groundwater, it is now high time that the stakeholders in the water sector, the environment and the local authorities, use this approach to the vulnerability as a tool to aid decision making, and reflect on solutions and facilities promoting a sustainable protection of this resource.

References

[1] R. Hazan and L. Mouillard, « Notice hydrogéologique de la plaine de Berrechid ».
[2] Ruhard, J.P. (1975). Chaouia et plaine de Berrechid. Ressources en eau du Maroc. Serve. Géol. Rabat. Maroc. II, N° 231.
[3] L'Agence du Bassin Hydraulique du Bouregreg et de la Chaouia (ABHBC) Etat de la qualité des ressources en eau 2015.
[4] L. Aller, T. Bennet, J.H. Lehr, R. Petty and G. Hackett, DRASTIC: Standardized system to evaluate ground water pollution potential using hydrogeologic settings, (U.S Epa-600/2-87-035, 1987).
[5] Aït Sliman (2009) utilisation des systèmes d'information géographique et du modèle drastique pour l'évaluation de la vulnérabilité des eaux souterraines dans la plaine de berrechid, Maroc.
[6] M.A. Ahmed (2012) Assessment of Intrinsic Vulnerability to Contamination for the Alluvial Aquifer in El-Fayoum Depression Using the DRASTIC Method.
[7] L. Thüler(2014) Estimation et cartographie de la vulnérabilité des aquifères en milieu forestier.
[8] R. Bouchnan (2014) Dynamic Vulnerability: Application to the Bou-Areg Aquifer (Morocco)
[9] L'Agence du Bassin Hydraulique du Bouregreg et de la Chaouia (ABHBC) contrat de la nappe(2013).
[10] H .Elfarrak (2014) Development of Vulnerability through the DRASTIC Method and Geographic Information System (GIS) (Case Groundwater of Berrchid), Morocco.
[11] J. P. Jourda, K. J. Kouamé, M. G. Adja, S. K. Deh, A. T. Anani, A. T. Effini and J. Biémi, "Evaluation du Degré de Protection des Eaux Souterraines: Vulnérabilité à la Pollution de la Nappe de Bonoua (Sud-est de la Côte d'Ivoire) par la méthode DRASTIC," Par la Méthode DRASTIC. Session Environnement/Eau, 2007,11 p.
[12] M. H. Hamza, A. Added, R. Rodriguez, S. Abdeljaoued and A. Ben Mammou, "A GISbased DRASTIC Vulnerability and Net Recharge Reassessment in an Aquifer of a Semiaridregion (Metline-Ras Jebel-Raf Raf Aquifer, Northern Tunisia," Journal of Environmental Management, Vol. 84, No. 1, 2007, pp. 12-19.

American Journal of Engineering Research (AJER) 2016
American Journal of Engineering Research (AJER)
e-ISSN: 2320-0847 p-ISSN : 2320-0936
Volume-5, Issue-2, pp-21-26
www.ajer.org
Research Paper Open Access

Application of Fuzzy Algebra in Automata theory

Kharatti Lal
Dept. of Applied Science – Mathematics Govt. Millennium polytechnic College Chamba Himachal Pradesh – 176310 (INDIA)

ABSTRACT: *In our first application we consider strings of fuzzy singletons as input to a fuzzy finite state machine. The notion of fuzzy automata was introduced in [58]. There has been considerable growth in the area [18]. In this section present a theory of free fuzzy monoids and apply the results to the area of fuzzy automata. In fuzzy automata, the set of strings of input symbols can be considered to be a free monoid. We introduced the motion of fuzzy strings of input symbols, where the fuzzy strings from free fuzzy submonoids of the free monoids of input strings. We show that fuzzy automata with fuzzy input are equivalent to fuzzy automata with crisp input. Hence the result of fuzzy automata theory can be immediately applied to those of fuzzy automata theory with fuzzy input. The result are taken from [7] and [34].*

Key Words: *Fuzzy strings, Pattern recognition, Membership function, Homomorphism semigroup, inferred fuzzy automata,*

I. INTRODUCTION

The basic idea is that the class of non-fuzzy system, that are approximately equivalent to a given type of system from the point of view of their behaviours is a fuzzy class of systems. For instances the class of system that are approximately linear .This idea of fuzzy classification of system was first hinted at by Zadeh 1965. Saridis 1975 applied it to the classification of nonlinear systems according to their nonlinearies, pattern recognition methods are first used to build crisp classes. Generally, this approach does not answer the question of complete identification of the nonlinearlies involved within one class. To distinguish between the nonlinearlies belonging to a single class, membership value in this class are defined for each nonlinearly one of thee considered as a references with a membership value 1.The membership value of each nonlinearity is calculated by comparing the coefficients of its polynomial series expansion to that of the reference nonlinearlity. This technique of classification is similar to those used in fuzzy pattern classification.We now mention some other way $\Rightarrow$ fuzzy abstract algebra has been applied. The paper [35] deals with the classification of knowledge when they are endowed with some fuzzy algebraic structure. By using the quotient group of symmetric knowledge as algebraic method is given in [35] to classify them also the anti fuzzy sub groups construction used to classify knowledge.

In the paper [20] fuzzy points are regarded as data and fuzzy objects are constructed from the set of given data on an arbitrary group. Using the method of least square, optimal fuzzy subgroups are defined for the set of data and it is shown that one of them is obtained as f fuzzy subgroup by a set of some modified data.In [55], a decomposition of an valued set given a family of characteristic functions which can be considered as a binary block code. Conditions are given under which an arbitrary block code corresponds to L-valued fuzzy set. An explicit description of the Hamming distance, as well as of any code distance is also given all in lattice-theoretic terms. A necessary and sufficient conditions is given for a linear code to correspond to an L-valued fuzzy set.

Lemma1: $\Phi_1 < \Phi_2 < \ldots\ldots \Phi_n < 1$. As the asymmetric between code words on which fuzzy codes will be based become large, there is only a small increase in the measurable distance between codewords. For unidirectional errors, the case is that the space of the code will effect the distance between the fuzzy code words. These issues must be taken into account in designing fuzzy codes.

Lemma 2: $\Gamma_1 < \Gamma_2 < \ldots \Gamma_n > 2$.

Proof: If instead of using the Hamming distance between two fuzzy codes, we used the asymmetric distance, so that

$$D_a(\tilde{A}_u, \tilde{A}_u) = \left(\sum_{w \in F^n} \left(\tilde{A}_u(w) - \tilde{A}_u(w)\right) V \sum_{w \in F^n} \left(\tilde{A}_v(w) - \tilde{A}_u(w)\right) V \right)$$

Then the following theorem holds.

Corollary 1: A fuzzy column vectors $h^1 \in A^n$ is independent of a set of fuzzy column vectors $\{\tilde{h}_1, \ldots, \tilde{h}_n\}$. If S (i) = φ for any i ∈ {1,……, m}.

Proof: We give the algorithm for checking if a non-null column x_k in the Sub semimodule F is linearly dependent on a set of fuzzy vectors at the end of this section. In a set of the column vectors $\tilde{g}_i$, i = 1, ...n, is given a complete set of independent fuzzy vectors $\tilde{f}_i$, i = 1, ...i, can be selected such that subsemimodule generated by $\{\tilde{f}_i, \ldots, \tilde{f}_m\}$ contains the $\tilde{g}_i$ s the procedure is shown in the form of the flow chart.

We now consider a positive sample set R^+ = 0.8ab, 0.8aa,bb, 0.3ab, 0.2bc, 0.99bbc. The finite submatrix of the fuzzy Hankel matrix H(r) is shown.

Using the algorithm DEPENDENCE the independent columns of the fuzzy Hankel matrix have been indicated as F_1, F_2, F_5, F_6, F_7.

The finite submatrix of the fuzzy Hankel matrix H $(r)^2$.

$$\mu(a) = \begin{array}{c} \\ S_1 \\ S_2 \\ S_3 \\ S_4 \\ S_5 \\ S_6 \\ S_7 \end{array} \begin{array}{c} \begin{array}{ccccccc} S_1 & S_2 & S_3 & S_4 & S_5 & S_6 & S_7 \end{array} \\ \begin{bmatrix} 0 & 0 & 0 & 0 & 0 & 0 & 0 \\ 0 & 0 & .03 & 0 & 1 & 0 & .08 \\ 0 & 0 & 0 & 0 & 0 & 0 & 0 \\ 0 & 0 & 0 & 0 & 0 & 0 & 0 \\ 0 & 0 & 0 & 0 & 0 & .08 & 0 \\ 0 & 0 & 0 & 0 & 0 & 0 & 0 \\ 0 & 0 & 0 & 0 & 0 & 0 & 0 \end{bmatrix} \end{array}$$

$$\mu(b) = \begin{array}{c} \\ S_1 \\ S_2 \\ S_3 \\ S_4 \\ S_5 \\ S_6 \\ S_7 \end{array} \begin{array}{c} \begin{array}{ccccccc} S_1 & S_2 & S_3 & S_4 & S_5 & S_6 & S_7 \end{array} \\ \begin{bmatrix} 0 & 0 & 0 & 0 & 0 & 0 & 0 \\ 0 & 0 & 0 & 0 & 0 & 0 & 0 \\ 0 & 0 & 0 & 1 & 0 & 0 & 0 \\ 0 & 0 & 0 & 0 & 0 & 0 & 0 \\ 0 & 0 & 1 & 0 & 0 & 0 & 0 \\ 0 & 0 & 0 & 0 & 0 & 0 & 1 \\ 1 & 0 & 0 & 0 & 0 & 0 & 0 \end{bmatrix} \end{array}$$

$$\mu(c) = \begin{array}{c} \\ S_1 \\ S_2 \\ S_3 \\ S_4 \\ S_5 \\ S_6 \\ S_7 \end{array} \begin{array}{c} \begin{array}{ccccccc} S_1 & S_2 & S_3 & S_4 & S_5 & S_6 & S_7 \end{array} \\ \begin{bmatrix} 0 & 0 & 0 & 0 & 0 & 0 & 0 \\ 0 & 0 & 0 & 0 & 0 & 0 & 0 \\ 0 & 0 & 0 & 0 & 0 & 0 & 0 \\ 1 & 0 & 0 & 0 & 0 & 0 & 0 \\ 0 & 0 & 0 & 0 & 0 & 0 & 0 \\ 0 & 0 & 0 & 0 & 0 & 0 & 0 \\ 0 & 0 & 0 & 0 & 0 & 0 & 0 \end{bmatrix} \end{array}$$

$$\mu(c) = \begin{array}{c} \\ \lambda \\ a \\ ab \\ abc \\ bc \\ abb \\ abbc \\ aa \\ aab \\ aabb \\ \\ \end{array} \begin{array}{c} \begin{array}{ccccccccccc} \lambda & ab & a & abc & bc & c & abbc & bbc & aabb & abb & bb \end{array} \\ \begin{bmatrix} 0 & .8 & 0 & .3 & .2 & 0 & .9 & 0 & .8 & 0 & 0 \\ 0 & 0 & .8 & 0 & .3 & 0 & 0 & .9 & 0 & .8 & 0 \\ .8 & 0 & 0 & 0 & .9 & .3 & 0 & 0 & 0 & 0 & 0 \\ .3 & 0 & 0 & 0 & 0 & 0 & 0 & 0 & 0 & 0 & 0 \\ .2 & 0 & 0 & 0 & 0 & 0 & 0 & 0 & 0 & 0 & 0 \\ 0 & 0 & 0 & 0 & 0 & .9 & 0 & 0 & 0 & 0 & 0 \\ .9 & 0 & 0 & 0 & 0 & 0 & 0 & 0 & 0 & 0 & 0 \\ 0 & 0 & 0 & 0 & 0 & 0 & 0 & 0 & 0 & 0 & 0 \\ 0 & 0 & .8 & 0 & 0 & 0 & 0 & 0 & 0 & 0 & 0 \\ .8 & 0 & 0 & 0 & 0 & 0 & 0 & 0 & 0 & 0 & 0 \end{bmatrix} \\ \begin{array}{ccccccccccc} F_1 & & F_7 & & F_3 & F_4 & F_2 & F_5 & & & F_6 \end{array} \end{array}$$

The algorithm depends also identifies column if any column vector $\tilde{h}(j)$ is dependent on the set of generator $H \cup (m) = H \cup (m) = \{\hat{f}_1, \ldots, \hat{f}_m\}$ of the Hankel matrix as constructed intable.It also identifies the coefficient S_i, using the procedure ARRANGE CS(i), N, CARD(i) and the procedure COMPARESO(k), SO(K – 1).

Once the independent set of the column vectors are extracted, the next steps is to find out mathematic's $\mu(x)$, $x \in V_T$. In order to determine the matrices $\mu(x)$, $x \in v$ the expression x F has to be computed for x = a, b, c and i = 1, ...,7, the matrices $\mu(a)$, $\mu(b)$ and $\mu(c)$ given in table. The x_i's can be computed from the relationship $\alpha = F_1(\lambda), \ldots, F_m(\lambda))$, where the vector corresponds to the entries in the set of independent columns $F_1, \ldots, F_m$ for the row in H(r) labelled by λ thus

$\alpha = (0\ 0\ 0.90\ 0.2\ 0\ 0\ 0)$

The vector $\beta = (10\ 0\ 0\ 0\ 0\ 0)$ because the column F_1 is an independent column. Once α, β and $\mu(a)$, $\mu(b)$ and $\mu(c)$ have been determined the fuzzy automation can be constructed by the method described. The fuzzy automation that accepts the strings is shown

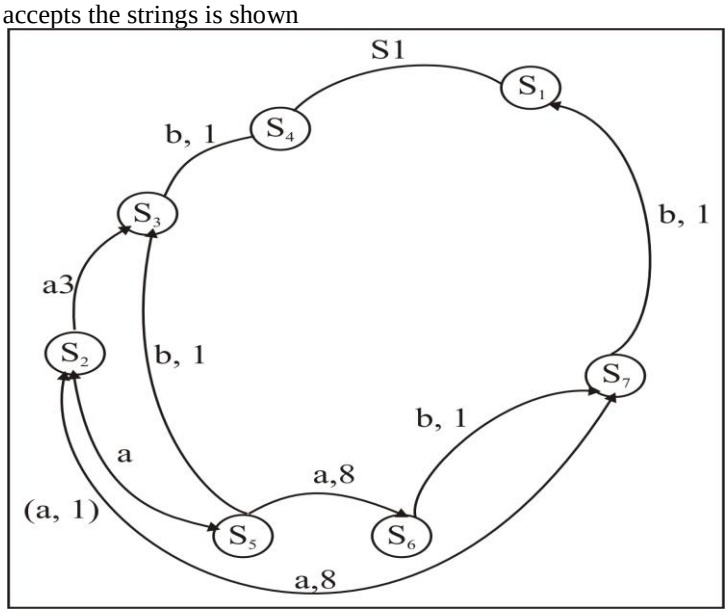

Fig 2: Inferred Fuzzy Automata

PROCEDURE DEPENDENFE

Step 1 i = 1 from S (i) such that

$S(i) = \{v_j \mid h_{ji} \geq h_i\}$

Find card (S (i))

Step 2: If card (S (i) = 0 go to step 12 Else do

Step 3: If card (S (i)) = 1 and S (i) = $\{j_k\}$.

$\delta_{f_1} = \delta_{j_u} = h_i$ for $j = f_k$,

for any other $j \neq j_k$, $\delta_{j_1} = 1$ go to step 5. Else do

Step4: If (S(i)) > 1

$\delta_{j_1} = 0$ and $\delta_{j_u} = h_i$ for all $j = j_k$

for any other $j \neq j_k = \delta_{j_1} = 0$, $\delta_{j_u} = 1$

Step 5: i = i + 1 repeat the procedure until i = m.

Step 6: j = 1 find $v = \{\delta_{j_{kl}}\}$ and $\{\delta_{j_{kl}}\}$, k = 1, ...,n if $v = \{j_{jki}\} > \Lambda\{\delta_{jku}\}$ go to step 12. Else do

Step 7: Select a δ_j such that

$\delta_{jkl} / Max < \delta_j < \delta_{jku} / min$ and set $R_j = \theta$

Step 8: From $R_j = R_j V i$ (i ∈ 1, ... , n) such that
$h_i = \delta_j \Lambda h j i)$

Step 9: j = j + 1 if j < n, go to step 6

Step 10: Check if R_j converse all i ∈ {1, ...n} if $R_j = \{1, ...n\}$ go to step 11.

Step 11: Else do go to step 12.

$\hat{h}$ is dependent, point the value of δ_{ji}.

Step 12: $\hat{h}$ is independent.

Theorem 1.1: Kleen – Schutzenberger for the free monoid $V_T^\star$.The set $A^{rec}[[V_T^\star]]$ and $A^{rat}[[V_T^\star]]$ conicide. We now define the Hankel matrices. They can be used to characterize rational power series.

Definition: The Hankel matrix of r ∈ A $[[V_T^\star]]$ is a doubly infinite matrix H(r) whose rows and columns are indexed by the word $sV_T^\star$ and whose elements with the indices 4 are equal to (r, x_v)

A formal power series r∈A $[[V_T^\star]]$ is a function from, $V_T^\star$ to A, we denote the set of all function from $V_T^\star$ to A by $AV_T^\star$. The set $AV_T^\star$ also provides a convenient way to visualize the column of H(r) as element in $AV_T^\star$ we note that with the column H(r) corresponding to the word v ∈$V_T^\star$. We may associate the function $f_u \in AV_T^\star$ as follows

$\Rightarrow F_u(u) = (r, u v), \forall u \in V_T^\star$

Definition 1.1: A code C over the alphabet A is called a prefix (suffix) code if it satisfies $CA^+ \cap C = \Theta$ ($A^+ C \cap C = \Theta$). C is called a biprefix code of it is a prefix and a suffix code. A submonoid M of any monoid N. Satisfying of proposition.$CA^+ \cap C = \Theta$ is called the left unitary in N. M is called right unitary in N if it is satisfies the dual of $\forall x \in A^\star$, $Mw \cap M \neq \theta$ implies w ∈ M namely $A^+ C \cap C = \Theta$.

Let M be a submonoid of a free monoid $A^\star$ and c its base then the following conditions are equivalent:

(i) $\forall w \in A^\star$, $Mw \cap M \neq \Theta$ implies w ∈ M

(ii) $CA^+ \cap C = \Theta$

By the condition (ii) in this proposition no word of C is a proper left factor of another word of C define the relation $\leq \ell$ on A^* by $\forall x, v \in A^*$, $x \leq \ell v$ if v is the left factor of u. Then ≤ 1 is a partial ordering of $A^\star$. In the diagram to follow we display the top part of $A^\star$ partially ordered $\leq \ell$ when A = {a, b} and when A = {a, b, c}

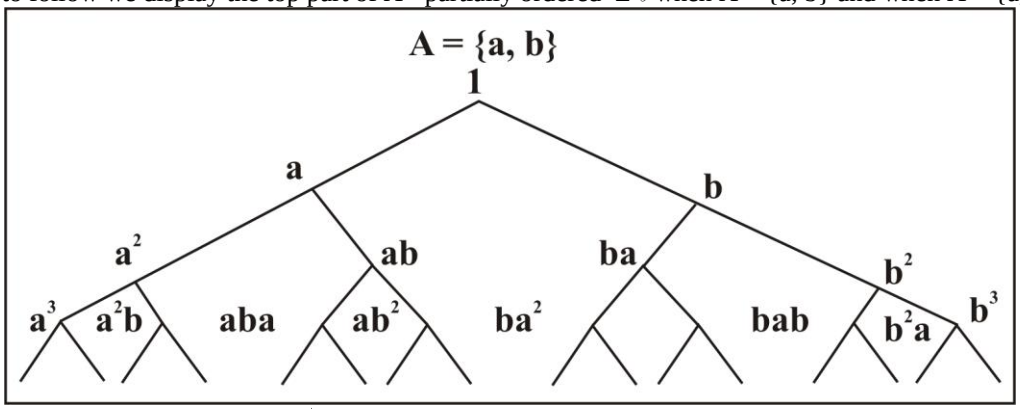

$A^\star$ partially ordered ≤ (when A = {a, b}

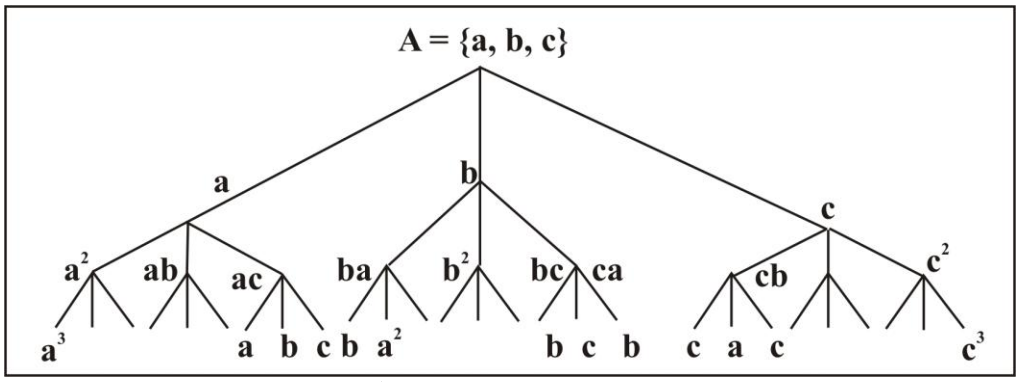

$A^{\star}$ partially ordered by $\leq \ell$

When A = {a, b, c}

A necessary and sufficient condition for a subset C i of $A^{\star}$ to be prefix code is that6 for every $c \in C$, $w \in A^{\star}$, $w \leq n\ \ell$, c and $w \neq c$ implies $w \notin C$. This to obtain example of prefix codes, it suffices to select subsets C of $A^{\star}$ that will be end points for $\leq \ell$. For **Example:** The trees displayed below give the prefix codes. C_1 = {a^2,aba, ab^2, b} over {a, b} and c_2 = {a^2, ab, ac, ba, b^2, cb,c^2} over {a, b, c}. The set

〈 B = {a^nb | n∈ □} is an example falling tree with end points a^nb, n ∈ □

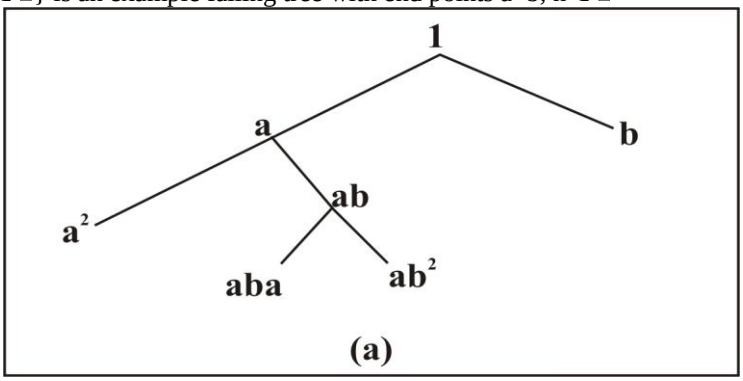

Prefix codes over {a, b}

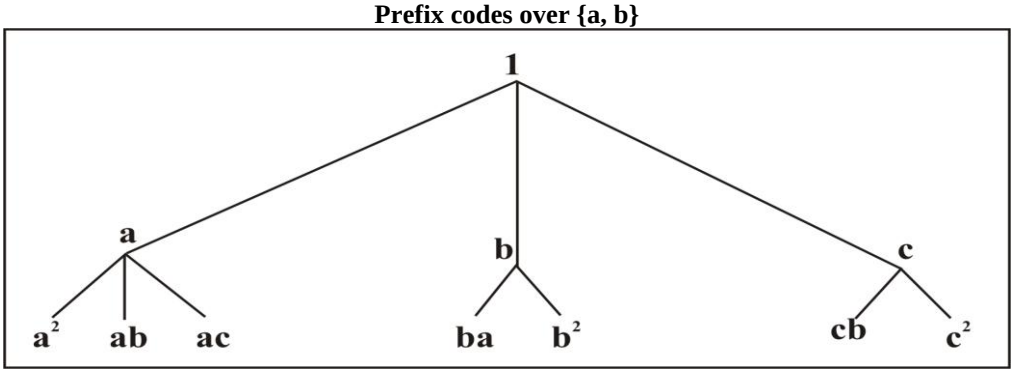

Prefix over code {a, b, c}

This is no simple characterization general codes analogous to condition. The proposition is to for prefix codes.

Proposition 1.1: Let $A^{\star}$ be a free monoid and C be a subset of $A^{\star}$. Define the subset D_i of $A^{\star}$ recursively by D_0 = C and $D_i = \{w \in A^{\star} \mid D_{i-1}w \cap c \neq 0$ or C w $\cap$ $D_{i-1} \neq \Theta\}$, i = 1, 2, ... Then c is a code over A if and only if $C \cap D_i = \Theta$ for i = 1, 2, ...

Suppose e is a finite then the length of the word in C. Hence there is only a finite number of distinct D_i and this proposition gives an algorithm for deciding whether or c is a code.

Proposition 1.2: Let S be a semigroup C a column system for S and ga homomorphism of B^+ into S. Then the function $\tilde{A} : B^+ \to C$ defined by $\forall\ x \in B^+\ \tilde{A}(x) = \langle g(x) \rangle$b a c - sub-semigroup of B^+. If $\forall$ x, y ∈ B^+ if $\forall$ xy ∈ B^+

(i) $x \in \langle y\,x,\ xy,\ y \rangle$

(ii) $x \in \langle y\,x,\ xy \rangle$

(iii) $x \in \langle x^n \rangle\ \forall\ n \in$ □

(iv) $x \in \langle y\, x, y\rangle$
(v) $x \in \langle xy, y\rangle$
(vi) $x \in y\, x, y > \cap \langle xy, y\rangle$

then $\tilde{A}$ is free, pure, every pure, left unitary, right unitary, or unitary, respectively. Moreover, $\tilde{A}\, X = g^{-1}(X)$ for every $X \in C$.

Example 1.1:

(i) For $e = \{c = a, a^3b, aba\}$
We have $D_0 = C$, $D_1 = \{a^2b, ba\}$
$D_2 = \{ab\}$ and $D_3 = \{a, b\}$
Since $C\, AD_3 \neq \Theta$, C is not a code

(ii) $C = \{a, a^2b, bab, b^2\}$ we have $D_0 = C$,
$D_1 = \{ab\}$, $D_2 = \{b\}$ and $D_i = \{ab, b\}$
For $i = 3, 4$, ... Since $C \cap D_i = \theta$
For $i = 1, 2$, ... C is a code.

Therefore we now consider the construction of codes using fuzzy subsemigroups. Let L is the partially ordered set L is called a Λ - semi lattice if $\forall$ x, y $\in$ L x: x and y have a greatest lower bound least upper bound, say $x \cap y$ ($x \vee y$. AΛ - semilattice is called complete if for every subset of L has a greatest lower bound in L. Let $\left\{\tilde{A} \mid \tilde{A} : B^+ \to L\right\}$ is a semi lattice whose elements are L-subsets of the free semigroup B^+. An L-subset $\tilde{A}$ of B^+ is an L-subsemigroup of B^+ if for it $t \in L$, the level set

$\tilde{A}^+ = \left\{x \in B^+ \mid \tilde{A}(x) \geq t\right\}$ is a subsemigroup of B^+. Then $\tilde{A}$ is a L-sub-semigroup of B^+ if $\forall$ x, y $\in B^+$

$$\tilde{A}(xy) \geq \tilde{A}(x) \cap \tilde{A}(y)$$

The search for suitable codes for communication theory is known. It was proposed by Garla-that-L-semi-group theory be used. To this end free, pure, very pure, left unitary, right unitary, unitary such L-submsemigroup there is a family of codes associated with it. An L-subsemigroup of a free semigroup if free, one are, pure, very pure, left unitary right unitary respectively.Thus any method used to construct an L-=subsemigroup of a free semigroup of one of these types yields a family of semigroups of the same types. Namely the level sets of the L - subsemigroup.

V. CONCLUSION

We have assumed that error in the transmitted of words across a noisy channel were symmetric in nature i.e., the probability of $1 \Rightarrow 0$ and $0 \Rightarrow 1$ cross over failures were equally likely. However error in VSLI circuit and many computer memories are on a undirectional nature [8] A undirectional error model assumes that both $1 \Rightarrow 0 \Rightarrow 1$cross overs can occur, but only are type of error occurs in a particular data word. This has provided the basis for a new direction in coding theory and fault tolerance computing. Also the failure of the memory cells of some of the LSI transistor cell memories and NMOS memories are most likely caused by leakage of charge. If we represent the presence of charge in a cell by 1 and the absence of charge by 0, then the errors in those type of memories can be modeled as $1 \Rightarrow 0$ type symmetric errors, [8].The result in the remainder of this section are from [15]. Once again F denotes the field of integers module 2 and F^n the vector space of n - tuples over F, we let p denotes the transmitted 1 will be received as a1 and a transmitted 0 will be received as a 0, Let q = 1–p. Then q is the probability that there is an error in transmission in an arbitrary bit.

REFERENCE

[1] Malik D.S. Mordeson J.N. and Sen M.K. Free fuzzy submonoids and fuzzy automata. Bull. Cal. Math. Soc. 88: 145-150, 1996.
[2] Mordeson J.N. Fuzzy algebraic varieties II advance in fuzzy theory and technology Vol. 1: 9-21 edited by Paul Wang 1994.
[3] Gerla, G, Code theory and fuzzy subrings-semigroup. J. Math. Anal, and Appl. 128: 362-369, 1987.
[4] Kandel A, "Fuzzy Mathematical technology" with application. Addison-Wasely Pub. Co. 1986.
[5] Fuzzy Automata and Decession Process M.M. Gupta, G.N. Saridis, and B.R. Gaines, Eds, pp-77-88, North Holand Publ. Amsterdam.
[6] Bourbaki, Elements of mathematics' commutative algebra, Springer Verlag, New York, 1989.
[7] Gerla, G, '' Code theory and fuzzy subrings- semigroup ''. J. Math. Anal, and Appl. 128: 362-369, 1987.

American Journal of Engineering Research (AJER) 2016
American Journal of Engineering Research (AJER)
e-ISSN: 2320-0847 p-ISSN : 2320-0936
Volume-5, Issue-2, pp-27-34
www.ajer.org
Research Paper Open Access

Irrigation-yield response factor of processing potato for different phonological growth stages

Afrin Jahan Mila[1], Md. Hossain Ali[2]
[1]*Irrigation and Water Management Division, Banglsdeah Agricultural Research Institute (BARI), Gazipur-1701, Bangladesh*
[2]*Agricultural Engineering Division, Bangladesh Institute of Nuclear Agriculture (BINA), Mymensingh-2202, Bangladesh*

ABSTRACT: *The yield response factor of processing potato (variety: BARI Alu-25 and BARI Alu-28) was determined from field experimental data conducted during two consecutive years (2013 and 2014) at Bangladesh Agricultural Research Institute, Gazipur. There were six irrigation treatments including full irrigation at three growth stages (stolonization, tuberization and bulking stages), single irrigation at each growth stage, irrigations at stolonization and bulking stage, and irrigation at tuberization and bulking stage. Results reveal that the crop yield response factor (k_y) and sensitivity index (λ_i) increased with the increase of intensity of water deficit at different phonological growth stages. Non-significant difference was found in paired t-test at 5% level of significant. On an average, the k_y for tuberization + bulking, stolonization + bulking, stolonization + tuberization, tuberization and stolonization was 0.23, 0.24, 0.28, 0.03, and 0.006 for BARI Alu-25, while 0.23, 0.24, 0.27, 0.04, and 0.007 for BARI Alu-28, respectively. According to the value of yield response factor, the most critical growth stages were in the order: stolonization + tuberization>stolonization + bulking>tuberization + bulking>tuberization>stolonization. For the entire growing season, the k_y values were 0.76, 0.86, 1.07, 0.71 and 0.07 for tuberization + bulking, stolonization + bulking, stolonization + tuberization, tuberization and stolonization for BARI Alu-25, while 0.98, 1.13, 1.86, 0.77 and 0.08 for BARI Alu-28, respectively. The $\lambda_i$fortuberization + bulking, stolonization + bulking, stolonization + tuberization, tuberization and stolonization stage was 0.12, 0.13, 0.19, 0.01, and 0.002 for BARI Alu-25, while 0.13, 0.15, 0.17, 0.01 and 0.003 for BARI Alu-28, respectively. A more sensitive growth stage has a higher value of lamda i, and therefore water supply is more important at stolonization + tuberization stage.*

Keywords *-Processing potato, yield response factor, sensitivity index, deficit irrigation*

I. INTRODUCTION

Availability of water is decreasing day by day due to climate change, rapid growth of population, excessive use of irrigation water and management practices (Hanjra and Qureshi, 2010;Kundzewiczet al. 2008; Rosegrant et al. 2002; Vorosmarty et al. 2000). To cope with this we have to depend on utilization of minimum water which will give optimum yield with maximum water productivity instead of maximum yield. This technique is called deficit irrigation and efficient utilization of water is possible. In addition to, this technique can save irrigation cost with negligible yield reduction consequently net farm income increase (Ali et al. 2007). When water deficit occurred in a crop at different growth stages, climatically occurred crop stress will differ. Orgezet al.(1992) reported that yield hampered by deficit irrigation is the effect of both the intensity and timing of water deficit. The term crop yield response factor is an important tool which helps to make irrigation scheduling under water deficit condition. Its value exceeds one indicate more stress and water must be available at that stage to get optimum yield. Also, the stage, which is most vulnerable to water, is called critical or sensitive growth stage. From the value of yield response factor sensitive growth stage can be determined. As a result, accurate irrigation scheduling under water scarce situation can be obtained.

For practical application in the field, Doorenbos and Kassem (1979) developed a reliable method which permits the quantification of crop yield response to water under full and deficit water supplies. This method expresses a quantitative relationship between relative yield decrease and relative evapotranspiration deficit. Therefore, this method can form an outline by providing directive for optimum crop production and water productivity for the rational planning of water management (Ali 2009). By using this method many scientists determined crop yield response factor for different crops throughout the growing season as well as individual growth stages (Ayas and Korukcu, 2010;Istanbulluoglu et al. 2010;Ali 2009;Moutonnet P. 2002;Kirdaet al.1999).

Ayas and Korukcu (2010) found crop yield response factor (k_y) of potato was 0.909 for the entire growth period in Yenisehir, Bursa. Doorenbos and Kassam (1979) reported the k_y value of 1.10 for whole growing season and the k_y value of 0.45, 0.80, 0.70 and 0.20 for early vegetative, late vegetative, yield formation and ripening stage. International Atomic Energy Agency (IAEA) estimated k_y values of 0.40, 0.33, and 0.46 for vegetative, flowering, and yield formation stage. Ayas (2013) did experiment on potato crop by using five pan co-efficient of 100%, 75%, 50%, 25% and 0%. He found the k_y value of 1.13 for total growing period. He also found the k_y values of 0.00, 0.94, 1.16, 1.19, and 1.11 for 100%, 75%, 50%, 25% and 0%, respectively. Darwish et al. (2006) found the k_y values of processing potato was 0.80 for entire growing period.

Though there is a few study occurred on this topic of processing potato crop, now its importance is increasing due to prevailing water crisis. From the above studies, it is clear that the value of response factor varies from location to location (depending on weather and soil), variety to variety, crop to crop, season to season and also for individual growth stages to entire growing season what Ali (2009) discussed in determining response factor of winter wheat in Bangladesh. Therefore, it is argent to determine location specific as well as variety specific response factor for efficient utilization of water. Processing potato is a winter loving and short durated tuber crop which can easily substitute Boro rice in Bangladesh as water is dwindling. Therefore, this study has been undertaken to quantify the effect of water deficit on processing potato (yield response factor or sensitivity factor) and to find out critical growth stages, which could be used for proper water management to minimize yield losses under situations of water deficit.

II. MATERIALS AND METHOD

Field experiment was undertaken during 2013 and 2014 growing season at the research fields of Bangladesh Agricultural Research Institute, Gazipur (latitude: 23°99´´N, longitude: 90°41´´E). The soil texture was sandy clay. The soil was alkaline pH (6.45), low in organic matter (0.94 %), and with basic infiltration rate of 5.42 $mmhr^{-1}$. The upper and lower limits of available water were 0.30 and 0.14 m^3m^{-3}.

The local climate is subtropical monsoon, with average annual rainfall of about 1898 mm and 1895 mm, respectively. The processing potato–growing period, November to March, is characterized by dry winter with 14 mm rainfall in the year 2014 (Fig.1). There was no recorded rainfall in the year 2013 during the growing season. At the initial stage reference ET_0 was higher and decreased at the mid-stage and again rose at the late stage (Fig.1).

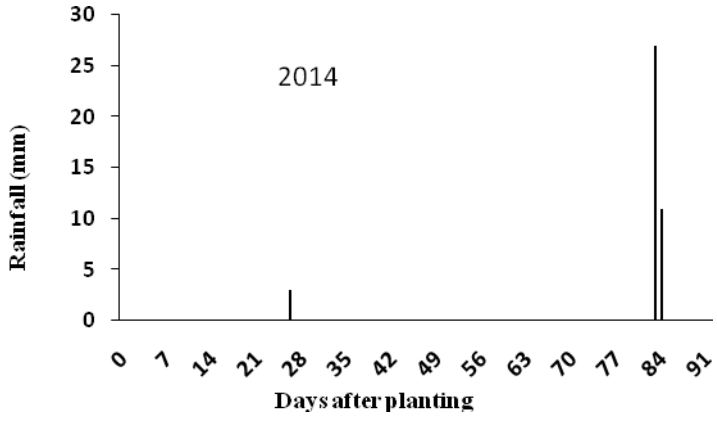

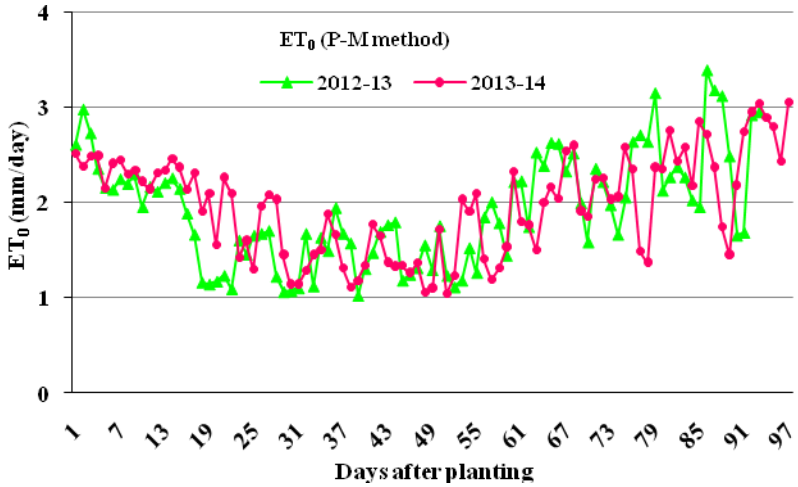

Figure 1:Rainfall and reference evapotranspiration (ET_0, Penman-Monteith method) during the study period

Two processing potato varieties of BARI Alu-25 and BARI Alu-28 is characterized by high specific gravity and dry matter content, and high yield potential (average 25 - 30 tha^{-1}) (ATHB 2014). Total growing period of this crop is 90-96 days depending on cultivar, climatic condition and management practices etc. The water deficit of different degrees was imposed at different phonological stages with the treatments. There are three phonological stages which are stolonization, tuberization and bulking stage. Irrigation treatments were arranged as full irrigation through the growing season; single irrigation at different stages and two irrigations at different growth stages (Table 1). Deficit irrigation was imposed according to the design of the treatments. Irrigation will be applied up to field capacity to meet the effective root zone depth of 60 cm where 80% of the root is concentrated. The layout of the experiments was completely randomized block design with three replications. The plot size and spacing were 4.2 m × 3 m and 60 cm× 25 cm, respectively. The crop was harvested manually and yield data was taken.

Table1 Definition of irrigation treatments corresponding to plant growth phases (with different DC)

Treatments	Irrigation at 3 plant growth phases with DC		
T_1	1	0	0
T_2	0	1	0
T_3	0	0	1
T_4	1	0	1
T_5	0	1	1
T_6	1	1	1

Note: DC =1 means irrigating 100% of the root zone deficit (i.e. FC – Mc) (that is, no deficit).

Crop sensitivity to water deficit was evaluated by Stewart (Stewart et al. 1977) model for the whole growing season as well as individual growth stages, while Jensen (Jensen 1968) model was used to calculate individual growth stages.

1.1 Calculation of crop response factor from Stewart model

Stewart model fits well in conditions where sensitivity differs significantly according to phonological growth stages. This model was derived from the relationship between relative yield decreases with relative evapotranspiration deficit in considering all production factors at their optimum level. The water deficit factor, determined as the ratio of actual to potential evapotranspiration (ET/ET_m) that control the final yield. The equation can be written as:

$$Y/Y_m = \prod_{n=1}^{m} [1-k_{y(n)}(1-ET/ET_m)_n] \quad \ldots\ldots\ldots\ldots\ldots\ldots (1)$$

where Y is the actual yield, Y_m is the maximum yield with no water deficit during the growing season, ET is the actual evapotranspiration and ET_m is the maximum evapotranspiration, n is generic/total growth stage,

m is the number of growth stage considered, and k_y is the yield response factor. In this equation Stewart used different coefficient for each growth stage. Therefore, k_y was determined by following the procedure given by (Doorenbos and Kassam, 1979). Maximum yield (Y_m) of processing potato was determined which dictated by climate, in considering water, fertilizer, pests and diseases do not restrict yield. Maximum evapotranspiration (ET_m) was calculated when crop water requirement is equal to available water supply. Actual evapotranspiration (ET_a) was calculated depending on factors relating to available water supply to the crop. Finally, actual yield (Y_a) under water deficit condition was determined by the relationship between relative yield decrease and relative ET deficit.

$$1 - Y_a/Y_m = k_y(1 - ET_a/ET_m) \quad \text{..... (2)}$$

or,

$$k_y(i) = \frac{1 - \frac{Y_a(i)}{Y_m(i)}}{1 - \frac{ET_a(i)}{ET_m(i)}} \quad \text{..... (3)}$$

Previously, the above two equations were used by many researchers (Ayas and Korukcu, 2010;Istanbulluoglu et al. 2010; Ali 2009;Damir et al. 2006; FAO 2002;Moutonnet P. 2002;Kirdaet al.1999) across the world for calculating crop response factor for different crops. For more detailed information, please refer to (Doorenbos and Kassam, 1979). Doorenbos and Kassam (Doorenbos and Kassam, 1979) estimatedk_y values for each phonological periods and also for whole growing period, for different crops. The k_y value for whole growing period was estimated on the effect of seasonal water used under water stress by using equation (2). On the other hand, stage specific $k_y$value was estimated on the effect of water stress for each growth period (i) by using equation (3). The k_y is a crop yield response factor that varies according to different species, variety, irrigation method and management practices, and different growth stages when deficit evapotranspiration is imposed (Kirda 2002). The value of k_y represents an indication of whether the crop is tolerant to water stress.

1.2 Calculation of Crop sensitivity index from Jensen model

Jensen model (Jensen 1968) was used to calculate crop sensitivity to water deficit at different growth stages and the equation was as follows

$$\frac{Y}{Y_m} = \prod_{i=1}^{n} \left(\frac{ET_i}{ET_m}\right)^{\lambda_i} \quad \text{..... (4)}$$

where, Y is tuber yield under water deficit condition, Y_m is the maximum yield when maximum evapotranspiration (ET_m) occurred under no water deficit during the whole crop growing period, ET_i is the actual evapotranspiration during the growth stage *i*, λ_I is the sensitivity index of crop to water deficit at *i*-th stage, and *i* the individual growth stage (for processing potato it was 3).

For easy application of irrigation practice, Tsakiris (Tsakiris 1982) proposed a modified method from Jensen model. He illustrated the procedure of this model using data for grain sorghum. However, crop sensitivity index,λ_i, was determine the procedure derived by Tsakiris (1982). Therefore, the equation (4) can be written as:

$$\frac{Yi}{Y_m} = \prod_{i=1}^{m} (\omega_i)^{\lambda_i} \qquad 0 < \omega_i < 1 \qquad \text{..... (5)}$$

Where ω_i is the relative evapotranspiration ($= \frac{ET_i}{ET_m}$).

If water deficit is imposed to a certain growth stage, assume, i-th stage, then, ω_i =1 for all growth stages except that stage. Hence, the equation (5) can be written as:

$$\frac{Yi}{Y_m} = \omega_i^{\lambda_i}$$

or,

$$\log\left(\frac{Yi}{Y_m}\right) = \lambda_i \log \omega_i \quad \text{..... (6)}$$

Therefore, λ_i for individual growth stages can be calculated with the ratio of $\log\left(\frac{Yi}{Y_m}\right)$ and $\log \omega_i$.

1.3 Uniformity coefficient for the k_y and λ_i values

The uniformity coefficient (UC) of the yearly k_y and λ_i values were determined by following (Devittet al. 1992) as

$$UC = 1 - (\text{standard deviation} / \text{mean}) \quad \text{..... (7)}$$

III. RESULTS AND DISCUSSION

1.1 Yield response factor for individual growth stage

Yield response (k_y) factor for individual growth stages is presented in Table 2. This value varies depending on season, location and intensity of water deficit. Among two varieties and treatments, paired t-test and uniformity coefficient was done and no statistical difference between two years data was found. During 2013, the highest yield response factor was found at stolonization + tuberization stage, followed by stolonization + bulking stages. The lowest was found in stolonization stage. This trend was consistent during the year 2014.

On an average, the yield response factor of 0.28 and 0.27 was found at stolonization + tuberization stage for V_1 and V_2. For V_1, the water stress at tuberization + bulking, stolonization + bulking, tuberization and stolonization stage exerted 17.86 %, 14.29%, 89.29 %, and 97.86% less stress than most stressed treatment (T_3), while 14.81%, 11.11%, 85.19% and 97.41% for V_2. Very little variation was found between two varieties in terms of k_y values. Martyniak (2008) reported that drought tolerance varies strongly between growth stages for many crops.Therefore, the order of water deficit for individual growth stages can be written as: stolonization + tuberization>stolonization + bulking >tuberization + bulking >tuberization>stolonization. Hence, it can be said that the stolonization + tuberization stage was the critical stage for processing potato cultivation.

Doorenbos and Kassam (1979) reported the k_y value for early vegetative, late vegetative, yield formation and ripening stage was 0.45, 0.80, 0.70 and 0.20, while International Atomic Energy Agency (IAEA) estimated k_y values of 0.40, 0.33, and 0.46 for vegetative, flowering, and yield formation stage, respectively. Ayas (2013) did experiment on potato crop by using five pan co-efficient of 100%, 75%, 50%, 25% and 0%. He found the k_y value for growing season was 0.00, 0.94, 1.16, 1.19, and 1.11 for 100%, 75%, 50%, 25% and 0%, respectively.

Table 2 The yield response factors (k_y) for individual growth stages

Treatments	Growth stages	k_y for individual growth stages		Mean	Standard deviation (SD)	Uniformity coefficient (UC)	Coefficient of variance (CV)
		2013	2014				
V_1							
T_1	Tuberization + bulking	0.24	0.22	0.23	0.014	0.94	0.06
T_2	Stolonization + bulking	0.24	0.23	0.24	0.0071	0.97	0.029
T_3	Stolonization + tuberization	0.27	0.29	0.28	0.014	0.95	0.51
T_4	Tuberization	0.03	0.03	0.03	0	1	0
T_5	Stolonization	0.006	0.006	0.006	0	1	0
V_2							
T_1	Tuberization + bulking	0.23	0.23	0.23	0	1	0
T_2	Stolonization + bulking	0.24	0.24	0.24	0	1	0
T_3	Stolonization + tuberization	0.27	0.26	0.27	0.0071	0.97	0.026
T_4	Tuberization	0.04	0.03	0.04	0.0071	0.82	0.18

T_5	Stolonization	0.007	0.006	0.007	0.00071	0.90	0.10

Table 3 Tuber yield (t ha^{-1}) under different treatments

Treatments[a]	Tuber yield (t ha^{-1})		
	2013	2014	Mean
V_1			
T_1	30.81G[b]	30.91G	30.86
T_2	30.70H	30.85G	30.78
T_3	30.19I	30.28H	30.24
T_4	36.76C	36.88C	36.82
T_5	37.71B	37.80B	37.76
T_6	37.92A	38.02A	37.97
V_2			
T_1	29.41J	29.51I	29.46
T_2	29.28K	29.39J	29.34
T_3	28.91L	29.00K	28.96
T_4	34.78F	34.90F	34.84
T_5	35.67E	35.76E	35.72
T_6	33.90D	35.98D	35.94
LSD (5%)	0.076	0.1134	-
CV	0.136	0.202	-

[a]T_1, T_2, T_3, irrigation at stolonization, tuberization, and bulking stage; T_4, irrigation at stolonization and bulking stage; T_5, irrigation at tuberization and bulking stage; T_6, irrigation at stolonization, tuberization and bulking stage. V_1= BARI Alu-25, V_2= BARI Alu-28.
[b]Mean values followed by different letter within columns differ significantly at $P<0.05$ according to Duncan's range test.

1.2 Yield response factor for whole growing period

Yield response factor (k_y) for entire growing season are represented in Table 4. The different values of response factor were observed for individual treatments during total crop period. This was increased according to the intensity of imposing water deficit. Paired t-test was done at 5% level of significant and no significant difference was observed between two years data. In addition to, uniformity coefficient range from 0.63 to 0.90 for V_1, whereas 0.43 to 0.80 for V_2, respectively. The highest value was observed in treatment T_3 where irrigation was applied 100% of the root zone deficit at bulking stage consequently; yield decreased (Table-3). The lowest was observed in treatment T_5 where irrigation was applied 100% of the root zone deficit at tuberization + bulking stage. In V_1, compare with most stressed treatment, treatment T_1, T_2, T_4 and T_5 exerted 28.97%, 19.63%, 33.64% and 93.46% less stress than thatof treatment T_3, while 47.31%, 39.25%, 58.60% and 95.70% for V_2. Also, it was found that V_2 experienced little bit more stress than that of V_1during the year 2013. This was due to the effect of rainfall in the year 2014 (Fig-1). On an average, the relative sensitivity to water deficit (k_y) for entire cropping period decreased followed by the order of water deficit treatment: $T_3>T_2>T_1>T_4>T_5$ for V_1 and V_2.

Ayas and Korukcu (2010) reported that the seasonal crop yield factor (k_y) of potato was 0.909. Doorenbos and Kassam (1979) reported the k_y value of 1.1 for whole growing season. Ayas (2013) estimated seasonal yield response factor of 1.13 for total growing period. Darwish et al. (2006) found the k_y values of processing potato was 0.80 for entire growing period.

Table 4 The yield response factors (k_y) for the total growth period of processing potato

Treatment	Growth stages	k_y for total growth period		Mean	Standard deviation (SD)	Uniformity coefficient (UC)	Coefficient of variance (CV)
		2013	2014				
V_1							
T_1	Tuberization + bulking	0.81	0.70	0.76	0.078	0.90	0.10
T_2	Stolonization + bulking	0.97	0.75	0.86	0.156	0.82	0.18
T_3	Stolonization + tuberization	1.24	0.89	1.07	0.247	0.77	0.23
T_4	Tuberization	0.89	0.52	0.71	0.262	0.63	0.37
T_5	Stolonization	0.08	0.05	0.07	0.021	0.70	0.30
V_2							
T_1	Tuberization + bulking	1.13	0.82	0.98	0.2192	0.78	0.22
T_2	Stolonization + bulking	1.46	0.77	1.13	0.4879	0.57	0.43
T_3	Stolonization + tuberization	2.6	1.11	1.86	1.504	0.43	0.57
T_4	Tuberization	0.88	0.66	0.77	0.156	0.80	0.20
T_5	Stolonization	0.10	0.05	0.08	0.035	0.56	0.44

1.3 Sensitivity index of Jensen model

The drought sensitivity index (lambda i, λ_i) of processing potato for three growth stages according to the treatment is represents in Table 5. This value was dictated by timing and amount of water stress. Non-significant variation was found in paired t-test at 5% level of significant within two years data. Besides, uniformity coefficients value was very close to one. Therefore, it can be reported that there was no statistical difference between two years data. The λ_i values among three growth stages with different degrees of water deficit were varied during two years but the trend was similar. During 2013, the highest sensitivity index (λ_i) was found at stolonization + tuberization stage and the lowest was observed at stolonization stage for both the variety. This was also similar for the year 2014. For V_1, the mean crop sensitivity to water deficit at tuberization + bulking, stolonization + bulking, tuberization and stolonization stage was 36.84%, 31.58%, 94.74% and 98.95% less than stolonization + tuberization stage (T_3), while 23.53%, 11.76%, 94.12% and 98.24% for V_2. Therefore, the order can be written as: stolonization + tuberization>stolonization + bulking>tuberization + bulking>tuberization>stolonization. Hence, it can be reported that stolonization + tuberization stage was the critical stage to irrigation for processing potato cultivation. This result was similar with the result obtained from yield response factor (k_y) for individual growth stages.

Table 5 Sensitivity index (λ_i, of Jensen model) of processing potato yield to water deficit at different growth stages

Treatment	Growth stages	λ_i – during different years		Mean	Standard deviation (SD)	Uniformity coefficient (UC)	Coefficient of variance (CV)
		2013	2014				
V_1							
T_1	Tuberization + bulking	0.12	0.12	0.12	0	1	0
T_2	Stolonization + bulking	0.14	0.12	0.13	0.014	0.89	0.11
T_3	Stolonization + tuberization	0.17	0.20	0.19	0.021	0.89	0.11
T_4	Tuberization	0.01	0.01	0.01	0	1	0
T_5	Stolonization	0.002	0.002	0.002	0	1	0
V_2							
T_1	Tuberization + bulking	0.12	0.13	0.13	0.0071	0.95	0.054
T_2	Stolonization + bulking	0.15	0.14	0.15	0.0071	0.95	0.047
T_3	Stolonization + tuberization	0.18	0.16	0.17	0.014	0.92	0.083

T_4	Tuberization	0.01	0.01	0.01	0	1	0
T_5	Stolonization	0.003	0.002	0.003	0.00071	0.76	0.24

IV. CONCLUSION

Yield response factor and sensitivity index of processing potato differs according to location, weather, variety, severity of water deficit and growth stages. For individual growth stages, the yield response factor $k_y$followed the order of sensitive growth stages to water deficit were stolonization + tuberization, stolonization + bulking, tuberization + bulking, tuberization, and stolonization for both variety. The sensitivity index (λ_i) for individual growth stages followed the same order like crop yield response factor for individual growth stages for BARI Alu- 25 and BARI Alu-28. The response factor for whole growth period was followed the order of sensitive growth stages to water deficit were stolonization + tuberization, stolonization + bulking, tuberization + bulking, tuberization and stolonization. Some water must be ensured at stolonization + tuberization stage for water scarce region to avoid severe yield loss.

REFERENCES

[1] M.A.Hanjra, and M.E. Qureshi, Global water crisis and future food security in an era of climate change, *Food Policy, 35,* 2010, 365–377.

[2] Z.W. Kundzewicz, L.J. Mata, N.W. Arnell, P. Doll, B. Jimenez, K. Miller, T. Oki, Z. Sen, and I. Shiklomanov, The implications of projected climate change for freshwater resources and their management, *Hydrological Sciences–Journal–des Sciences Hydrologiques, 53(1),* 2008, 3-10.

[3] M.W. Rosegrant, X. Cai, and S.A. Cline, World water and food to 2025: dealing with scarcity, Intl Food Policy Res Inst. 2002.

[4] C.J. Vorosmarty, P. Green, J. Salisbury, and R.B. Lammers, Global water resources: vulnerability from climate change and population growth,*Science, 289(5477),* 2000, 284-288.

[5] M.H. Ali, M.R. Hoque, A.A. Hassan, and M.A. Khair, Effects of deficit irrigation on wheat yield, water productivity and economic return,*Agricultural Water Management, 92, 2007,*151- 161.

[6] F. Orgez, L. Mateos, and E. Fereres, Season length and cultivar determine the optimum ET deficit in cotton,*Agronomy Journal, 84, 1992,* 700 –706.

[7] J. Doorenbos, and A.H. Kassam, Yield response to water, FAO Irrigation and Drainage Paper No. 33, FAO Rome, 1979.

[8] M.H. Ali, Irrigation – yield response factor of winter wheat for different growth stages,*Journal of Agrometeorology, 11(1), 2009,* 9 – 14.

[9] S. Ayas, and A. Korukcu, Water-Yield Relationships in Deficit Irrigated Potato, *Journal of Agricultural Faculty of Uludag University, 24(2), 2010,* 23-36.

[10] A. Istanbulluoglu, B. Arslan, E. Gocmen, E. Gezer, and C. Pasa, Effects of deficit irrigation regimes on the yield and growth of oilseed rape (*Brassica napus L.*), *Biosystems Engineering,*105, *2010,* 388-394.

[11] P. Moutonnet, Yield response factors of field crops to deficit irrigation. In. Deficit Irrigation Practices. Water Reports 22, FAO, Rome, 2002, 11-15.

[12] C. Kirda, R. Kanber, K. Tulucu, and H. Gungor, Yield response of cotton, maize, soybean, sugar beet, sunflower and wheat to deficit irrigation. In: Kirda, C., Moutonnet, P., Hera, C., Nielsen, D.R. (Eds.), Crop Yield Response to Deficit Irrigation. Kluwer Academic Publishers, Dordrecht, Boston, London, 1999, 21–38.

[13] S. Ayas, The effects of different regimes on Potato (SolanumTuberosumL. Hermes) yield and quality characteristics under unheated greenhouse conditions. *Bulgarian Journal of Agricultural Science, 19 (1), 2013,* 87-95.

[14] T.M. Darwish, T.W. Atallah, S. Hajhasan, and A. Haidar, Nitrogen and water use efficiency of fertigated processing potato. *Agricultural Water Management, 85, 2006,* 95–104.

[15] ATHB, Agricultural Technology Handbook, Part-1 (6th Edition), Bangladesh Agricultural Research Institute, Joydebpur, Gazipur, 2014, 307-310.

[16] J.I. Stewart, R.H. Cuenca, W.O. Pruitt, R.M. Hagan, and J. Tosso, Determination and Utilization of water production functions for principal California crops. W-67 Calif. Contrib. Proj. Rep. University of California, Davis, 1977.

[17] M.E. Jensen, Water consumption by agricultural plants. In: Kozlowski (edit.), Water deficit and plant growth, 2 (New York: Academic press, 1968) 1-22.

[18] A.O. Demir, A.T. Goksoy, H. Buyukcangar, Z.M. Turan, and E.S. Koksal, Deficit irrigation of sunflower (Helianthus annuus L.) in a sub-humid climate,*Irrigation Science, 24, 2006,* 279–289.

[19] FAO. Deficit irrigation practices, Water Reports. FAO, Rome, Italy. 2002.

[20] C. Kirda, Deficit irrigation scheduling based on plant growth stages showing water stress tolerance. In. Deficit Irrigation Practices. Water Reports 22, FAO, Rome, 2002, 102.

[21] G.P. Tsakiris, A method for applying crop sensitivity factor in irrigation scheduling,*Agricultural Water Management, 5, 1982,* 335–343.

[22] D.A. Devitt, R.L. Moris, and D.C. Bowman, Evapotranspiration, crop coefficients, and leaching of irrigated desert turfgrass systems, *Agronomy Journal, 84, 1992,* 717 – 723.

[23] L. Martyniak, Response of spring cereals to a deficit of atmospheric precipitation in the particular stages of plant growth and development,*Agricultural Water Management,* 95, *2008,* 171–178.

American Journal of Engineering Research (AJER) 2016
American Journal of Engineering Research (AJER)
e-ISSN: 2320-0847 p-ISSN : 2320-0936
Volume-5, Issue-2, pp-35-41
www.ajer.org
Research Paper Open Access

Optimum design of phase opposition disposition pulse width modulation logic circuit for switching seven level cascaded half bridge inverter

Nentawe Y. Goshwe, Douglas T. Kureve and Samuel T. Awuhe
(*Department of Electrical and Electronics Engineering,*
Federal University of Agriculture, Makurdi, Nigeria.)

ABSTRACT: *Theevolution of multilevel inverters (MLIs) has made it possible to extract power from direct current (DC) sources to alternating current (AC) power. This paper presents the design of a novel phase opposition disposition pulse width modulation scheme (PODPWM) logic circuit for a conventional single phase seven level cascaded H-Bridge (CHB) inverter using Matlab/Simulink. The minimum switching logic circuit for the single phase seven level CHB inverter was obtained by modeling the logic equations that could be used with any number of levels depending on the number of modulating and carrier signals involved. The reduction in total harmonic distortion (THD) of the output voltage for the MLI using low switching frequency at different modulation indixes is also investigated. The logic equations have made it easier to design a PODPWM circuit for any CHB inverter and the logic gates designed gave an optimum THD value of 16.73 % at modulation index of 0.20.*

Keywords-*CHB, Matlab, MLI, PODPWM, THD*

I. Introduction

The increase in energy production from fossil fuel sources is to meet the ever increasing demand for power. But there is enormous pressure to reduce global warming which is one of the demerits of fossil fuel energy production. Thus, the use of inverter technology to exploit renewable energy sources has been introduced. However, conventional inverters have limitations at high power and high voltage applications [1]. This has made multilevel inverter (MLI) more popular for high power and high voltage applications due their increased number of levels at the output. As the number of level increases, the harmonics are reduced and output voltage tends to be more pure [2].
Multilevel inverters have switching regulators which could be Bipolar Junction Transistors (BJTs), MOSFETs or Insulated Gate Bipolar Transistor (IGBT) through which the output voltage levels can be controlled. Pulse width modulation techniques are normally employed for switching MLIs.

The aim of this paper is to design a logic circuit that uses phase opposition disposition (POD) strategy to control a single phase seven level cascaded H-bridge inverter. The paper establishes equations for the design of logic modulation circuit for any number of levels for a cascaded H-bridge inverter using PODPWM and also investigates the best amplitude modulation index at which significant reduction in total harmonic distortion could be achieved.

II. Principle of Operation

The conventional seven level cascaded H-bridge inverter comprises twelve switches which form three half bridges (H bridges). The three half bridges have cascaded connection. Each H- bridge has a separate DC voltage source with three levels (+Vdc, 0,-Vdc), so the output voltage levels in the seven level CHB inverter are (+3Vdc, +2Vdc, +Vdc, 0,-Vdc,-2Vdc,-3Vdc) [3]. In this paper, the signals to the switches of the single phase seven level MLI are modulated using PODPWM. The modulation technique involves the sampling of six carrier signals to produce the seven output voltage levels. The modulating or the reference signal has the frequency $f_m$and an amplitude A_m while the carrier signal has the frequency f_c and an amplitude A_c. At each instant, the carrier signals are compared with the reference signal to give the desired output.

III. Basic Seven Level CHB Inverter

The modulation strategy for an inverter involves two parameters called amplitude modulation index or ratio (m_a) and frequency modulation index or ratio (m_f).These indixes are obtained from the various parameters that contribute to the efficiency of the inverter [4].

For m-level cascaded H-bridge multilevel inverter, the amplitude modulation index and frequency modulation index [5] are given as:

$$m_a = \frac{A_m}{(m-1)A_c} (1)$$

$$m_f = \frac{f_c}{f_m} (2)$$

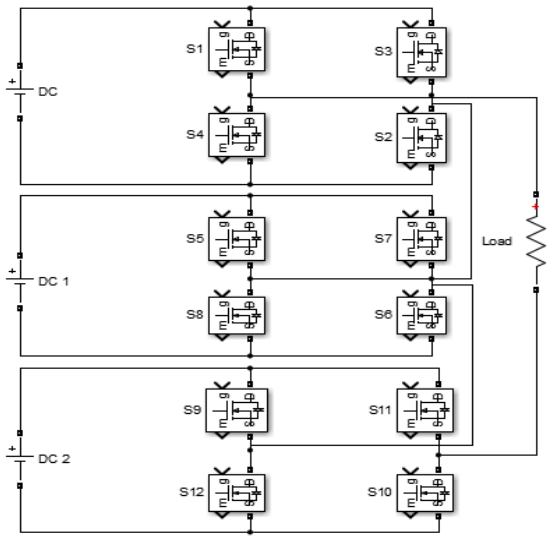

Figure 1.Conventional seven level CHB inverter

IV. Multicarrier Pulse Width Modulation

The carrier modulation schemes for MLIs are divided into two categories: phase-shifted and level-shifted multi carrier modulations [6]. Both modulation schemes can be applied to the cascaded H-bridge inverters. The THD value of phase-shifted modulation is higher than level-shifted modulation [7]. The level shifted multicarrier modulation scheme is categorized into four: phase opposition disposition (POD) method, alternate phase opposition disposition (APOD) method, phase disposition strategy (PD) and inverted phase disposition (IPD). In phase opposition disposition method, all the carrier waveforms above zero reference are in phase but they are 180° out of phase with the carrier signals below it. Alternative Phase Opposition Disposition (APOD) PWM has each carrier band shifted by 180° from the adjacent bands. Phase disposition (PD) PWM is similar to APOD except the carriers are in phase [8]. In inverted phase disposition scheme, all the carrier waveforms are inverted and intersected with the modulating waveform. When the modulating signal is higher than all the six carrier waveforms, pulses are generated in upper sequence and when the modulating wave is lower than all the six carrier signals, pulses are generated in the lower sequence [9]. Anuradha, Mohit and Suman [10] show that the THD of phase voltage of asymmetrical seven level cascaded multilevel inverter (CMLI) is studied under different modulation methods such as PD, POD and APOD and the least THD of 17.72 % is observed for APOD. Therefore, POD which has the highest THD value of 18.05 % is chosen for the inverter so that the THD value of the output voltage could be observed with the use of XOR and XNOR logic gates. The switching logic table for the MLI is shown in Table1.

Table 1. Table to Switch the Seven Level Inverter

S1	S2	S3	S4	S5	S6	S7	S8	S9	S10	S11	S12	Voltage level
1	1	0	0	1	1	0	0	1	1	0	0	+3vdc
1	1	0	0	1	1	0	0	1	1	1	1	+2vdc
1	1	0	0	1	1	1	1	1	1	0	0	2+vdc

1	1	1	1	1	1	0	0	1	1	0	0	+2vdc
1	1	0	0	0	0	0	0	0	0	0	0	+vdc
0	0	0	0	1	1	0	0	0	0	0	0	+vdc
0	0	0	0	0	0	0	0	1	1	0	0	+vdc
1	1	1	1	1	1	1	1	1	1	1	1	0
0	0	0	0	0	0	0	0	0	0	0	0	0
0	0	1	1	1	1	1	1	1	1	1	1	-vdc
1	1	1	1	0	0	1	1	1	1	1	1	-vdc
1	1	1	1	1	1	1	1	0	0	1	1	-vdc
0	0	1	1	0	0	1	1	1	1	1	1	-2vdc
0	0	1	1	1	1	1	1	0	0	1	1	-2vdc
1	1	1	1	0	0	1	1	0	0	1	1	-2vdc
0	0	1	1	0	0	1	1	0	0	1	1	-3vdc

V. MODELING OF SWITCHING LOGIC EQUATIONS

The operation of a traditional single-phase seven level cascaded H-bridge inverter requires six carrier signals and a modulating waveform which combine to produce pulses that switch the inverter using PODPWM. The switches of the CHB inverter are numbered from S_1 *to* S_{12}. The logic equations based on the analysis of the combination of the reference and the carrier signals are modeled but in order to reduce the propagation delay time and number of gates for implementation, De Morgan's laws are applied to the equations which give rise to the simplified equations below:

$$S_1 = A \oplus G \quad (15)$$

$$S_4 = \overline{A \oplus G} \quad (16)$$

$$S_5 = A_1 \oplus G \quad (17)$$

$$S_8 = \overline{A_1 \oplus G} \quad (18)$$

$$S_9 = A_2 \oplus G \quad (19)$$

$$S_{12} = \overline{A_2 \oplus G} \quad (20)$$

$$S_3 = B \oplus G \quad (21)$$

$$S_2 = \overline{B \oplus G} \quad (22)$$

$$S_7 = B_1 \oplus G \quad (23)$$

$$S_6 = \overline{B_1 \oplus G} \quad (24)$$

$$S_{11} = B_2 \oplus G \quad (25)$$

$$S_{10} = \overline{B_2 \oplus G} \quad (26)$$

Where A,A_1,A_2,B, B_1, $B_2$and G are signals that produce pulses for the inverter.

VI. Logic Gate Based PODPWM

The phase opposition disposition circuit is designed based on the switching pattern of the twelve switches in the conventional single phase seven level cascaded H-bridge inverter. The logic circuit is based on the modeled equations and it is made up of AND, OR, and NOT logic gates. But to simplify the circuit, XOR and XNOR logic gates are used for implementation.

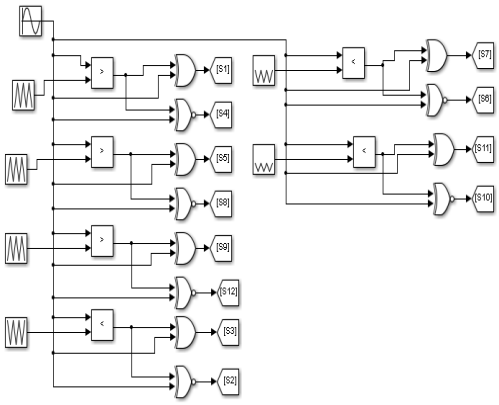

Figure 2. PODPWM logic circuit for seven level CHB inverter

VII. Simulation Results

Simulation of the gate-based PODPWM circuit for the traditional seven level CHB inverter is performed using Matlab software. The DC voltage used for each of the three half bridges of the inverter is 100V. The output voltage waveforms are generated at the carrier signal frequency of 5 KHz and at the frequency modulation index of 100.

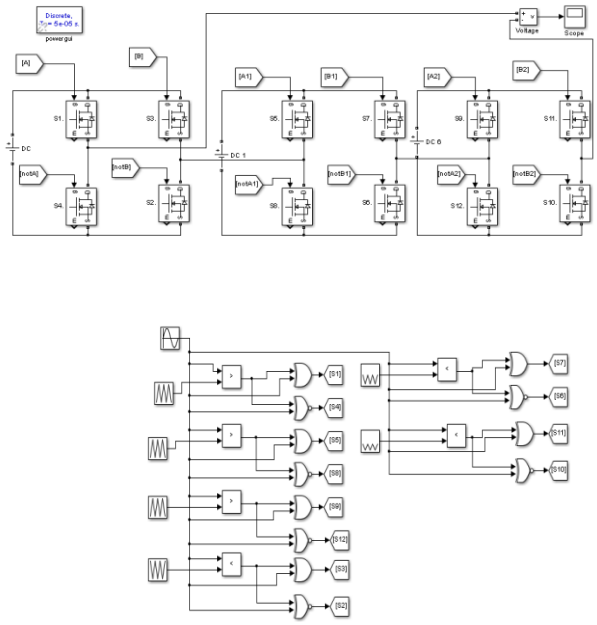

Figure 3. Seven level CHB inverter with logic gate circuit

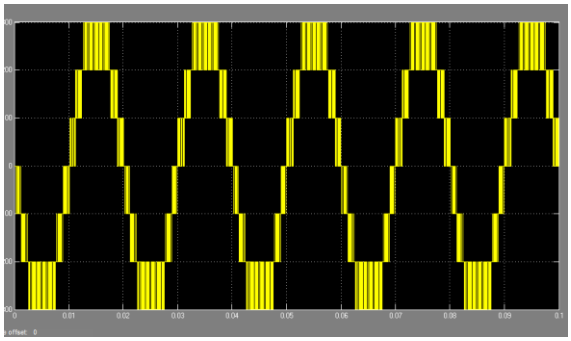

Figure 4. Output voltage waveforms of the inverter at m_f=100

The simulation is also done at amplitude modulation indices ranging from 0.10 to 0.24 at an interval of 0.02 to determine a relative decrease in THD value of output voltage around $\frac{1}{6}$ (≈ 0.17), which is a parameter value of amplitude modulation index when PODPWM is used for seven level inverter.

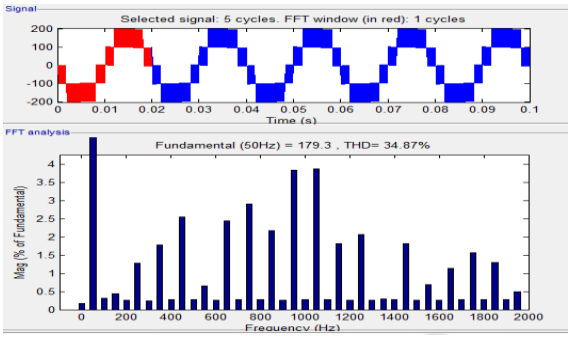

Figure 5. Output voltage waveform and THD spectrum at m_a=0.1

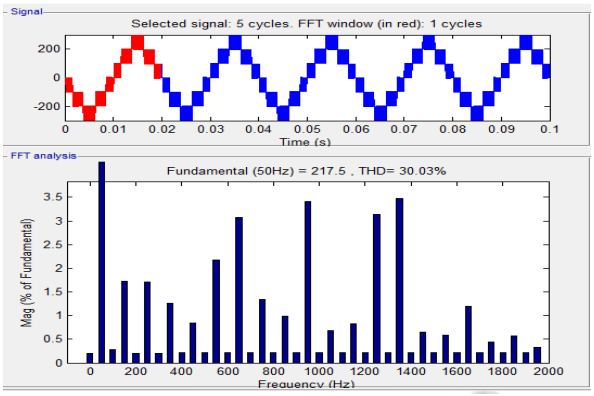

Figure 6. Output voltage waveform and THD spectrum at m_a=0.12

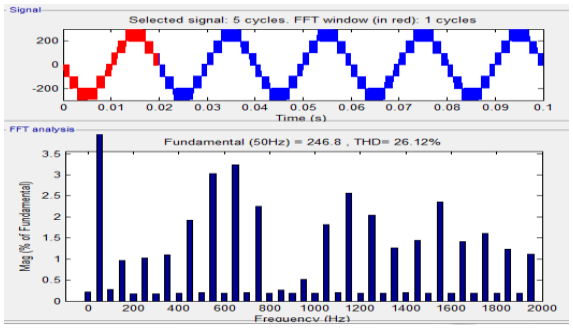

Figure 7. Output voltage waveform and THD spectrum at m_a=0.14

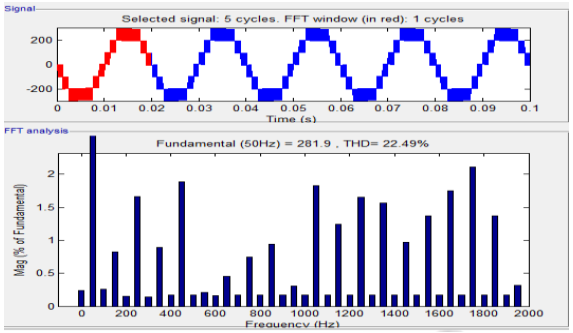

Figure 8. Output voltage waveform and THD spectrum at m_a=0.16

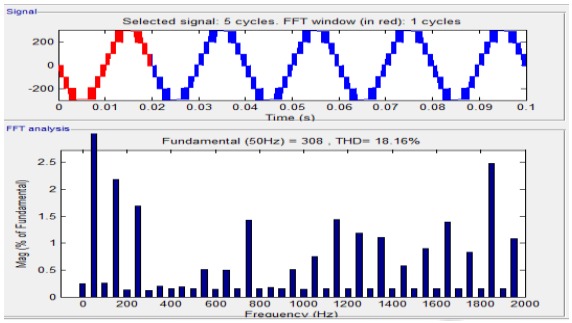

Figure 9. Output voltage waveform and THD spectrum at m_a=0.18

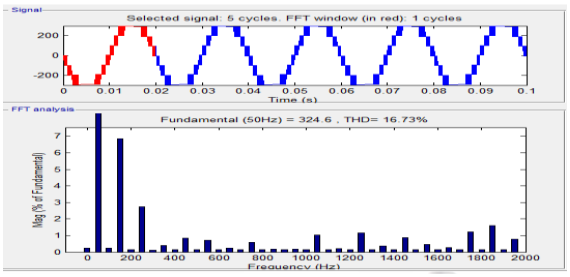

Figure 10. Output voltage waveform and THD spectrum at m_a=0.20

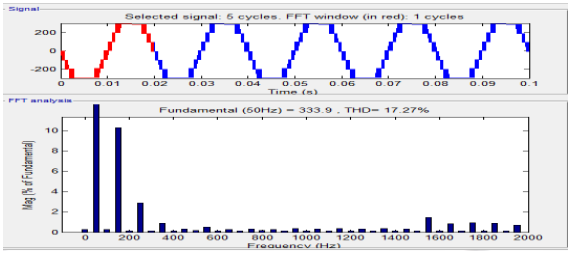

Figure 11. Output voltage waveform and THD spectrum at m_a=0.22

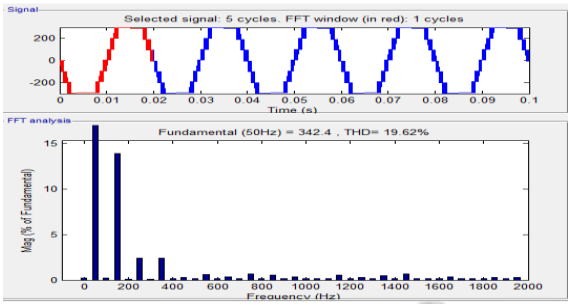

Figure 12. Output voltage waveform and THD spectrum at m_a=0.24

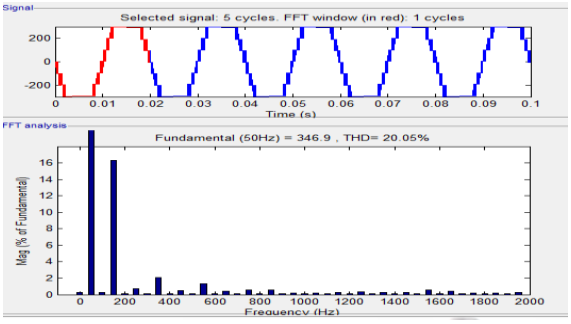

Figure 13. Output voltage waveform and THD spectrum at m_a=0.26

The THD values at different amplitude modulation indices are summarized in Table2.

Table 2. THD Values at Different Modulation Indices

Modulation Index	THD value (%)
0.10	38.87
0.12	30.03
0.14	26.12
0.16	22.49
0.18	18.16
0.20	16.73
0.22	17.27
0.24	19.62
0.26	20.05

VIII. Conclusions

The proposed PODPWM logic gate circuit uses six XOR and six XNOR gates based on the derived equations to produce pulses for the seven level MLI. The logic equations have made it easier to design a modulation circuit for a CHB inverter with any number of levels using PODPWM. The THD value of the output voltage for the proposed modulation circuit at the carrier frequency of 5 KHz around $\frac{1}{6}$ (≈ 0.17) amplitude modulation index is found to decrease steadily with increase in the modulation index from 0.10 to 0.20, where the least THD of 16.73 % is achieved without the use of a filter. However, the THD value increases gradually with increase in modulation index from 0.22 to 0.26. Therefore, the proposed logic circuit can be implemented at amplitude modulation index of 0.20 where the relative decrease in THD value is of prime importance.

REFERENCES

[1] S. Divya and R. Rasheed, Five Level Cascaded H-Bridge Multilevel Pulse Width Modulation Technique, *International Journal of Engineering and Innovative Technology*,*3(1)*,2013,438-441.

[2] S.A. Khadtare, S.P. Muley and B.S. Dani, Study of Three Phase Cascaded H-Bridge Multilevel Inverter for Asymmetrical Configuration, *International Journal of Engineering Research and Applications*,*3(2)*,2013,524-527.

[3] R. Kavitha, R. Thottungal and S. Agalya, Implementation of Seven Level Cascaded Multilevel Inverter in Closed Loop For Different Modulation Index, *International Journal of Emerging Technology and Advanced Engineering*, *4(3)*,2014,567-570

[4] A.K. Olusola and I.O. Olufemi, Gapped Alternate Phased Opposite Disposition pulse Width Modulation Control for Multilevel Inverters,*ARPN Journal of Engineering and Applied Sciences*,*9(4)*,2014,560-567.

[5] A. Venkadesan, P. Panda, P. Agrawal and V. Puli, Cascaded H-Bridge Multilevel Inverter for Induction Motor Drives, *International Journal of Research in Engineering and Technology*,*3(5)*,2014,260-266.

[6] C. Gomathi, Navyanagath, S.V. Purnima and S. Veerakumar, Comparism of PWM Methods for Multilevel Inverter, *International Journal of Advanced Research in Electrical, 2(12),* 2013,6106-6114.

[7] M. Kavitha, A. Arunkumar, N. Gokulnath, and S. Arun,New Cascaded H-Bridge Multilevel Inverter Topology with Reduced Number of Switches and Sources,*IOSR Journal of Electrical and Electronics Engineering*,*2(6)*,2012,26-36.

[8] E. Sambath, S.P. Natarajan and C.R. Balamurugan, Performance Evaluation of Multi Carrier Based PWM Techniques for Single Phase Five Level H-Bridge Type FCMLI, *IOSR Journal of Engineering*,*2(7)*,2012,82-90.

[9] P.M. Gnana, M. Balamurugan and S. Umashankar, A New Multilevel Inverter with Reduced Number of Switches, *International Journal of Power Electronics and Drive System*,*5(1)*,2014,63-70.

[10] S. Anuradha, J. Mohit and S. Suman, Analysis of THD and Output Voltage for Seven Level Asymmetrical Cascaded H-Bridge Multilevel Inverter Using LSCPWM Technique, *International Journal of Computer Applications*,*112(1)*,2015,1-5.

American Journal of Engineering Research (AJER) 2016
American Journal of Engineering Research (AJER)
e-ISSN: 2320-0847 p-ISSN : 2320-0936
Volume-5, Issue-2, pp-42-48
www.ajer.org
Research Paper Open Access

4D Collaborative Non-Local Means Based Diffusion MRI Denoising

Geng Chen, Yafeng Wu*
Data Processing Center, Northwestern Polytechnical University, Xi'an, China

ABSTRACT: *Noise is a major issue that reduces the quality of images acquired by diffusion MRI (dMRI). Recently, the non-local means (NLM) algorithm has been proposed and successfully applied in dMRI denoising. However, NLM relies on self-similarity information and tends to fails when recurrent image structures cannot be located. To address this issue, we introduce the improved collaborative NLM. Both inner-image and inter-image similarity information are used. Specifically, a group of co-denoising images are first registered to the target space. NLM-like block matching is then performed on both target noisy image and co-denoising images. This formulation can significantly increase the amount of similarity information and reduce the rare patch effect. Moreover, in order to adapt to the characteristics of dMRI, we present a complete denoising framework with multiple techniques including 4D image block, pseudo-residual-based noise standard deviation estimation, Rician bias correction, and block preselection. Extensive experiments on both synthetic and real data demonstrate that the proposed framework outperforms the classical NLM method.*

Keywords: *Block Matching, Denoising, Diffusion MRI, Non-Local Means, Kernel Regression.*

I. INTRODUCTION

Diffusion magnetic resonance imaging (dMRI) [1] is capable of measuring the diffusion process of water molecules in human brain non-invasively. Based on the diffusion properties obtained, tractography can then reconstruct white matter tracts [2,3]. Therefore, white matter integrity and degeneration can be effectively examined and brain connectome [4] can be further revealed among the development of nervous system [5] and a variety of neurological diseases such as Alzheimer's disease [6-10], autism [11,12], brain traumatic injury [13,14], and even genetics [15,16]. Since dMRI measures the signal attenuation caused by water diffusion, the images acquired tend to have low signal-to-noise ratio (SNR). Moreover, dMRI requires acquiring a large amount of images, which is very time consuming. To save the acquisition time, fast imaging protocol becomes necessary; however, it further decreases the SNR. The images with low SNR create significant difficulty for the following image analyses and may result in unreliable conclusions. Therefore, denoising plays an important role in the preprocessing of dMRI images.

Recently, the non-local means (NLM) [17] algorithm has been applied in dMRI studies and shown promising performance in denoising [18], super resolution [19] and voxel-based morphometry [20]. NLM estimates the true signals from the self-similarity information of image collected by block matching. However, the denoising performance is largely affected by the amount of self-similarity information. NLM fails when the matching features of certain unique structures cannot be located, which causes so-called "rare patch effect" [21]. To resolve this problem, Prime et al. [22] extended the NLM search volume to the symmetrical parts of human brain in order to increase the chance of locating matching structures. Although it improved the denoising performance, only doubling the search volume may not be sufficient. Chen et al. [23,24] introduced the inter-image similarity information by utilizing other co-denoising images. This formulation, named collaborative NLM (CNLM), significantly increases the amount of similarity information and thus reduces the influence of "rare patch effect" effectively. However, CNLM is designed only for structural MRI denoising, which may not be suitable based on the characteristics of dMRI.

To apply CNLM in dMRI, a major algorithm extension is to re-define the image blocks used in block matching. Diffusion images can be considered as vector-based or 4D images while all the volumes are stacked together. Hence, the 3D image block used in the original CNLM cannot be directly applied in dMRI. Yap et al. [18] constructed 4D image blocks from 3D image blocks extracted from a set of diffusion images and those 4D image blocks were then applied in block matching. It has been demonstrated that 4D image block is able to obtain more robust block matching performance than 3D image block. Another benefit for this formulation is high efficiency. When using 3D image blocks, we need to compute NLM weights in each individual image.

Therefore, the computation has to be performed multiple times to process the entire diffusion dataset. In contrast, 4D image block allows NLM weights to be computed only one time and diffusion images can be denoised jointly.

In this paper, we propose a complete framework in dMRI denoising with 4D CNLM, in which both inner and inter-image similarity information are used. 4D image blocks are applied to adapt the 4D characteristic of dMRI. Pseudo-residual [25] is used to get robust estimation of noise variance used in the calculation of NLM weights. Moreover, we utilize Rician bias correction [26] to adapt to the characteristics of dMRI noise and block preselection [25] to save the computational time. The proposed framework will be validated on both synthetic data and real human data to demonstrate its performance.

II. METHOD

2.1. Non-local means

Our method is based on the NLM algorithm. We first provide a quick review on the classical NLM algorithm. NLM has two major components, i.e., weighted average and block matching. Given a location $\mathbf{x}_i$, the first component takes the weighted average of all intensity values in the search volume to obtain the NLM recovered value $\mathrm{NL}(u)(\mathbf{x}_i)$, i.e.,

$$\mathrm{NL}(u)(\mathbf{x}_i) = \sum_{\mathbf{x}_j \in \mathcal{V}(\mathbf{x}_i)} w(\mathbf{x}_i, \mathbf{x}_j) u(\mathbf{x}_j), \tag{1}$$

where $\mathcal{V}(\mathbf{x}_i)$ is a cubic search volume centered at $\mathbf{x}_i$, and the size of $\mathcal{V}(\mathbf{x}_i)$ is $3(d+1)$. $u(\mathbf{x}_j)$ is the intensity value at $\mathbf{x}_j$. The second component compares two blocks and assigns a weight to indicate the similarity between two blocks. Let $\mathcal{N}_i$ be a cubic neighbor centered at $\mathbf{x}_i$, and the size of $\mathcal{N}_i$ is $3(m+1)$. We then define $u(\mathcal{N}_i)$ to be a vector containing all intensity values in $\mathcal{N}_i$. The weight $w(\mathbf{x}_i, \mathbf{x}_j)$ between $\mathbf{x}_i$ and $\mathbf{x}_j$ is then defined as a Gaussian function of the Euclidean distance between $u(\mathcal{N}_i)$ and $u(\mathcal{N}_i)$, i.e.,

$$w(\mathbf{x}_i, \mathbf{x}_j) = \frac{1}{Z_i} \exp\left\{ -\frac{\| u(\mathcal{N}_i) - u(\mathcal{N}_j) \|_2^2}{h_i^2} \right\}, \tag{2}$$

where h_i controls the attenuation of exponential equation; Z_i is a constant that guarantees that the sum of the weights equals one, i.e., $\sum_{\mathbf{x}_j \in \mathcal{V}(\mathbf{x}_i)} w(\mathbf{x}_i, \mathbf{x}_j) = 1$. The definition of Z_i then becomes

$$Z_i = \sum_{\mathbf{x}_j \in \mathcal{V}(\mathbf{x}_i)} \exp\left\{ -\frac{\| u(\mathcal{N}_i) - u(\mathcal{N}_j) \|_2^2}{h_i^2} \right\}. \tag{3}$$

We observe that $0 \leq w(\mathbf{x}_i, \mathbf{x}_j) \leq 1$. When $\mathbf{x}_i$ and $\mathbf{x}_j$ are the same, the weight will become one, which is too large in practice. Hence, we set $w(\mathbf{x}_i, \mathbf{x}_i) = \max(w(\mathbf{x}_i, \mathbf{x}_j)), \forall i \neq j$.

2.2. 4D Collaborative Non-local Means

4D CNLM introduces multiple co-denoising images to help denoise the target image. Specifically, co-denoising images are first warped to the target space. Then, block matching is not only performed in the search volume of the target image but also in those of co-denoising images. Hence, both inner-image and inter-image similarities can be captured in the weighted average and the performance is thus greatly improved. An overview of 4D CNLM is shown in Fig. 1.

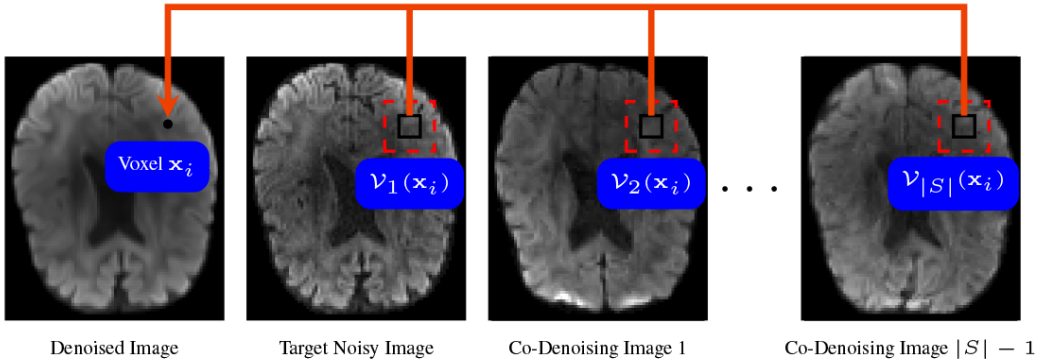

Fig. 1: An overview of 4D CNLM. The intensity value of the denoised target image voxel is decided based on those of the voxels in a set of search volumes located in both the target noisy image and the co-denoising images. Note that here all the diffusion image voxels are vector-valued or 4D.

Suppose we have an image group G, including one target noisy image and $|G|-1$ co-denosing images. The recovered diffusion signals given by 4D CNLM is:

$$\mathrm{NL}(\mathbf{u})(\mathbf{x}_i)=\frac{\sum_{k\in G}\sum_{\mathbf{x}_j\in\mathcal{V}_k(\mathbf{x}_i)}\hat{w}_k(\mathbf{x}_i,\mathbf{x}_j)\mathbf{u}(\mathbf{x}_j)}{\sum_{k\in G}\sum_{\mathbf{x}_j\in\mathcal{V}_k(\mathbf{x}_i)}\hat{w}_k(\mathbf{x}_i,\mathbf{x}_j)}, \tag{4}$$

where $\mathcal{V}_k(\mathbf{x}_i)$ is a search volume centered at $\mathbf{x}_i$ in image $k\in G$. $\hat{w}_k(\mathbf{x}_i,\mathbf{x}_j)$ is an un-normalized weight between $\mathbf{x}_i$ and $\mathbf{x}_j$. $\mathbf{u}(\mathbf{x}_j)$ is a vector containing all diffusion voxels in $\mathbf{x}_j$. Due to the 4D property of dMRI, instead of the 3D block defined in Eq.(2), we defined a 4D block $\mathcal{B}_i$ consisting of a group of 3D blocks, i.e., $\mathcal{B}_i=\{\mathcal{N}_i(\mathbf{q}_l)|l=1,\dots,L\}$. Each 3D block $\mathcal{N}_i(\mathbf{q}_l)$ represents a cubic neighborhood centered at $\mathbf{x}_i$ in the diffusion image acquired using gradient direction $\mathbf{q}_l$. The weight between two 4D blocks is then defined as

$$\hat{w}_k(\mathbf{x}_i,\mathbf{x}_j)=\exp\left\{-\frac{1}{L}\sum_{l=1}^{L}\frac{\|\mathbf{u}(\mathcal{N}_i(\mathbf{q}_l))-\mathbf{u}(\mathcal{N}_j(\mathbf{q}_l))\|_2^2}{h_i^2(\mathbf{q}_l)}\right\}, \tag{5}$$

NLM can then be regarded as a non-parametric kernel regression problem. Chen et al. [23,24] showed that increasing the sample size alone cannot reduce the estimation bias, and the corresponding bandwidth should be decreased accordingly. Hence, we define

$$h_i(\mathbf{q}_l)=\sqrt{2\beta(\hat{\sigma}_i(\mathbf{q}_l)|S|^{-\frac{1}{5}})^2|\mathcal{N}_i(\mathbf{q}_l)|}, \tag{6}$$

where β is a constant, and $\hat{\sigma}_i(\mathbf{q}_l)$ is the estimated noise standard deviation.

2.3. Noise Standard Deviation Estimation

The parameter $h_i(\mathbf{q}_l)$ controls the attenuation of exponential function. Based on Eq. (5), $h_i(\mathbf{q}_l)$ is further determined by the estimated local noise standard deviation $\hat{\sigma}_i(\mathbf{q}_l)$. The overestimated $\hat{\sigma}_i(\mathbf{q}_l)$ brings strong smoothness in deniosing, while the underestimated $\hat{\sigma}_i(\mathbf{q}_l)$ causes incomplete denoising. Hence, an accurate estimation of $\hat{\sigma}_i(\mathbf{q}_l)$ is the key to the successful denoising. We estimate $\hat{\sigma}_i(\mathbf{q}_l)$ using the robust pseudo-residual-based noise standard deviation estimation proposed in [25]. By leaving out $\mathbf{q}_l$ for the purpose of simplification (i.e., restricting the noise estimation in one single diffusion image), we first define pseudo-residual $\epsilon(\mathbf{x}_i)$ as

$$\epsilon(\mathbf{x}_j)=\sqrt{\frac{6}{7}}\left(u(\mathbf{x}_j)-\frac{1}{6}\sum_{\mathbf{x}_m\in\mathcal{P}(\mathbf{x}_j)}u(\mathbf{x}_m)\right), \tag{7}$$

where $\mathcal{P}(\mathbf{x}_j)$ is the six-neighbor of $\mathbf{x}_j$. $\hat{\sigma}_i$ is then estimated using

$$\hat{\sigma}_i=\sqrt{\frac{1}{|\mathcal{R}(\mathbf{x}_i)|}\sum_{\mathbf{x}_j\in\mathcal{R}(\mathbf{x}_i)}\epsilon^2(\mathbf{x}_j)}, \tag{8}$$

where $\mathcal{R}(\mathbf{x}_i)$ is a local volume centered at $\mathbf{x}_i$.

2.4. Adaption to Rican Noise

To apply the classical NLM in Rician noise removal, bias correction needs to be performed. The 2nd-order origin moment of Rician distribution follows

$$E(X^2)=\mu^2+2\sigma^2, \tag{9}$$

where μ is the true signal, and σ is a scale parameter to decide the level of Rician noise. Note that σ is not equal to the standard deviation of noise.

Based on Eq. (9), we then obtain the unbiased estimation using

$$\mathrm{NL}(u)(\mathbf{x}_i,\mathbf{q}_l)=\sqrt{\frac{\sum_{k\in G}\sum_{\mathbf{x}_j\in\mathcal{V}_k(\mathbf{x}_i)}\hat{w}_k(\mathbf{x}_i,\mathbf{x}_j)u^2(\mathbf{x}_j,\mathbf{q}_l)}{\sum_{k\in G}\sum_{\mathbf{x}_j\in\mathcal{V}_k(\mathbf{x}_i)}\hat{w}_k(\mathbf{x}_i,\mathbf{x}_j)}-2\hat{\sigma}}. \tag{10}$$

where $\hat{\sigma}$ is an estimate of σ and can be estimated from the image background using the method presented in [26].

2.5. Block Preselection

4D CNLM requires multiple search volumes in denoising, which causes astronomical computational burden. To make the algorithm efficient, a straightforward solution is to add a block preselection step.

Specifically, before the weight calculation, the search blocks far from the target block are discarded, and only some similar search blocks are kept. A preselection scheme based on block statistics [25] is shown below:

$$\hat{w}_k(\mathbf{x}_i,\mathbf{x}_j) = \exp\left\{-\frac{1}{L}\sum_{l=1}^{L}\frac{\| \mathbf{u}(\mathcal{N}_i(\mathbf{q}_l)) - \mathbf{u}(\mathcal{N}_j(\mathbf{q}_l)) \|_2^2}{h_i^2(\mathbf{q}_l)}\right\} \tag{11}$$

only if

$$\left(\mu_1 < \frac{\overline{\mathbf{u}(\mathcal{B}_i)}}{\overline{\mathbf{u}(\mathcal{B}_j)}} < \frac{1}{\mu_1} \vee \mu_1 < \frac{\mathrm{inv}(\overline{\mathbf{u}(\mathcal{B}_i)})}{\mathrm{inv}(\overline{\mathbf{u}(\mathcal{B}_j)})} < \frac{1}{\mu_1}\right) \wedge \sigma_1^2 < \frac{\mathrm{var}(\mathbf{u}(\mathcal{B}_i))}{\mathrm{var}(\mathbf{u}(\mathcal{B}_j))} < \frac{1}{\sigma_1^2}, \tag{12}$$

Otherwise, $\hat{w}_k(\mathbf{x}_i,\mathbf{x}_j) = 0$, where $\overline{\mathbf{u}(\mathcal{B}_i)}$, $\mathrm{inv}(\overline{\mathbf{u}(\mathcal{B}_i)})$ and $\mathrm{var}(\mathbf{u}(\mathcal{B}_i))$ are the mean, the inverted mean, and the variance of 4D block $\mathcal{B}_i$, respectively. The parameters $0 < \mu_1 < 1$ and $0 < \sigma_1 < 1$ are two thresholds. The inverted mean is defined as

$$\mathrm{inv}(\overline{\mathbf{u}(\mathcal{B}_i)}) = \max(\mathbf{u}(\mathcal{B}_i)) - \overline{\mathbf{u}(\mathcal{B}_i)}. \tag{13}$$

III. DATASETS

3.1. Synthetic Dataset

A set of synthetic spiral diffusion data was generated to evaluate the algorithm performance. Each fiber population was modeled by a tensor with $\lambda_1 = 1.7 \times 10^{-3}\mathrm{mm}^3/\mathrm{s}$, $\lambda_2 = \lambda_3 = 3 \times 10^{-4}\mathrm{mm}^3/\mathrm{s}$, and $b = 1000\ \mathrm{s/mm}^2$. The baseline signal without diffusion attenuation was set to 150. 30 diffusion directions consistent with the real data were applied in the simulation. The image was set to 128×128. To simulate the registration errors between images, 10 sets of rigid transformations were applied to the target ground truth image to generate the co-denoising images. The rigid transformation included random translations from −4mm to 4mm along each axis. Finally, four levels of Rician noise (3%, 6%, 9%, 12%) were added to the 11 ground truth images. The noise level $p\%$ indicated how much Gaussian noise (i.e., $\mathcal{N}(0, v*(p/100))$) was added in the complex domain of the signal, where v was the maximum signal value (150 in our case). The Rician noise was simulated using the method proposed in [25].

3.2. Real Human Dataset

The diffusion images from 11 subjects were acquired with a Siemens 3T TIM Trio MR scanner. The standard acquisition protocol is: 30 diffusion volumes with the diffusion directions uniformly distributed on a hemisphere with $b = 1000\ \mathrm{s/mm}^2$ and one volume with no diffusion weighting, image size 128×128, voxel size $2 \times 2 \times 2$ mm^3, TE=81ms, TR=7618ms, and 1 average. The diffusion images of one subject were used as the target images, while the rest were used as co-denoising images. Before performing 4D CNLM, we warped the co-denoising images to the target space using a large deformation diffeomorphic registration algorithm [27,28] designed for dMRI registration.

IV. RESULTS

For all experiments, we set d=1, m=2, β=1. Note that the resolution of dMRI is low, therefore, we did not use a large radius for the image block and search volume. $|G|$ was set to 11, including one target noisy image and 10 co-denoising images. In the experiments, we compared three methods including 4D CNLM, NLM and simple averaging. The methods were also evaluated in high order entities, i.e., orientation distribution function (ODF), and we used the method proposed in [29] to reconstruct ODFs.

Peak-to-signal-ratio (PSNR) was used for the quantitatively evaluation. The definition follows

$$\mathrm{PSNR} = 20\log_{10}\frac{\mathrm{MAX}}{\mathrm{RMSE}}, \tag{14}$$

where RMSE represents for root mean square error, MAX is the maximum intensity value of the input image (150 in our case).

3.1. Synthetic Data

The PSNR results of synthetic data are shown in Fig. 2. 4D CNLM gets the highest PSNR values at all noise levels. Compared to NLM, the largest improvement, 7.67 dB, happens at the noise level of 6%. The better PSNR value indicates the denoised image is closer to the ground truth. In contrast, simple averaging gives the lowest PSNR due to the simulated misalignment between images. NLM-based methods utilize robust block matching to correct inter-image misalignment and significantly improve the denoising performance. 4D CNLM utilizes a sufficient number of co-denoising images. From Fig. 3, we can observe that the PSNR value increases when more co-denoising images are used in denoising. The ODF reconstruction results, shown in Fig.4, demonstrate that 4D CNLM gives clean and coherent ODFs. Compared to other three methods, shown in (C), (D), and (F), the ODFs estimated with 4D CNLM is the closest to the ground truth.

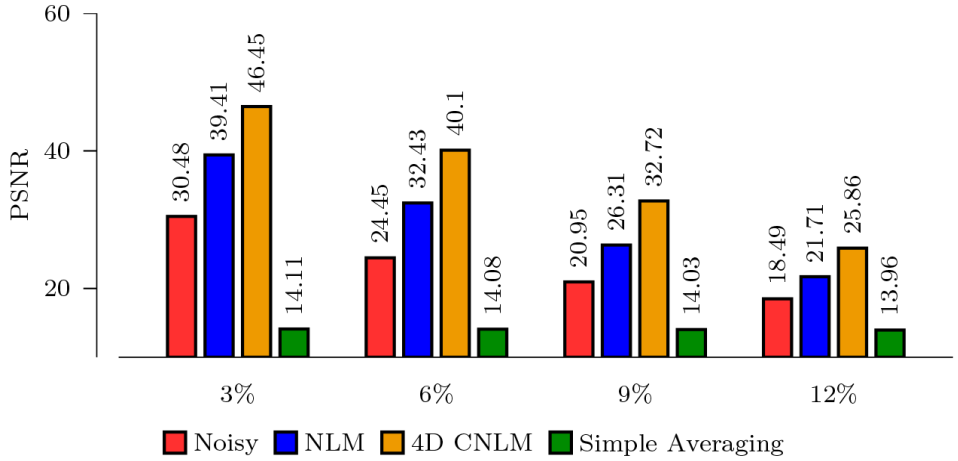

Fig. 2: PSNR comparisons between simple averaging, NLM, and 4D CNLM at different noise levels. Note that 10 co-denoising images are used in 4D CNLM and simple averaging.

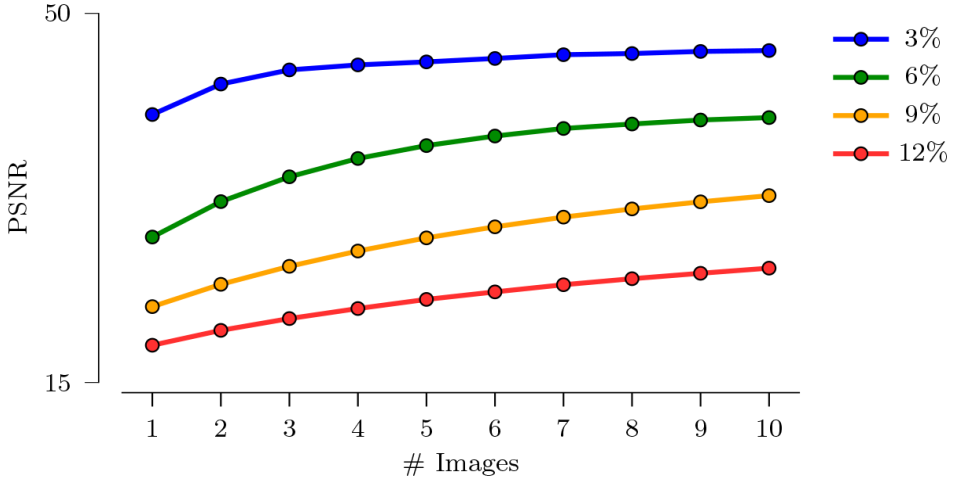

Fig. 3: The PSNR performance using different numbers of co-denoising images at different noise levels.

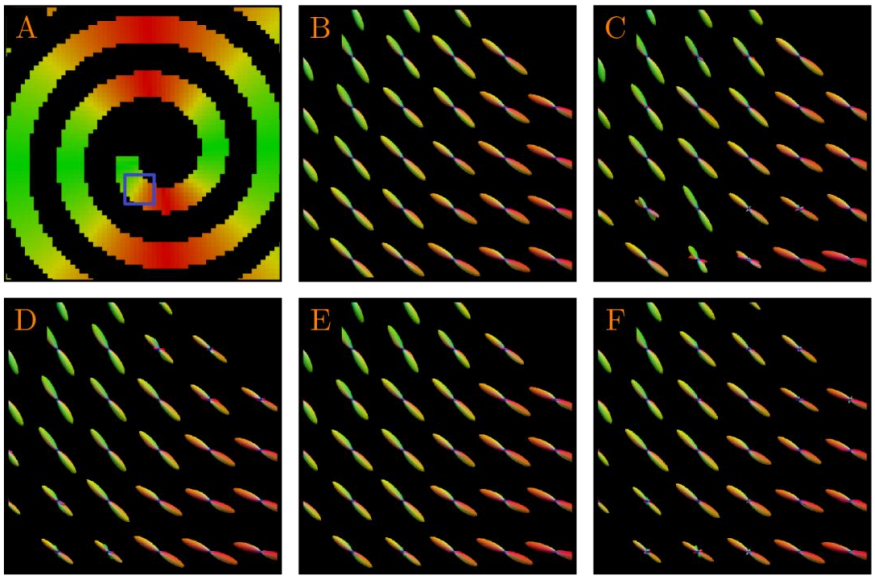

Fig. 4: Comparison of ODF visualization in synthetic data. (A) a direction-encoded color FA image for reference. The rest five images are the close-up views for the blue square in (A). (B) is the ground truth; (C) is a noisy version of (B); (D), (E) and (F) are the denoising versions using NLM, 4D CNLM and simple averaging, respectively. 10 co-denoising images are used in (E) and (F).

3.2. Real Human Data

From Fig. 5, we can observe that 4D CNLM is able to preserve important local subtle structures after denoising. The local subtle structures in grey matter area contain important information for disease diagnosis and are the basis of successful cortical surface extraction [30]. We also evaluated the influence of denoising in the ODF reconstruction. The ODF results, shown in Fig.6, indicate that 4D CNLM gives more coherent and clean ODFs. Plenty of spurious peaks can be seen in the ODFs reconstructed using the noisy data and NLM denoised data.

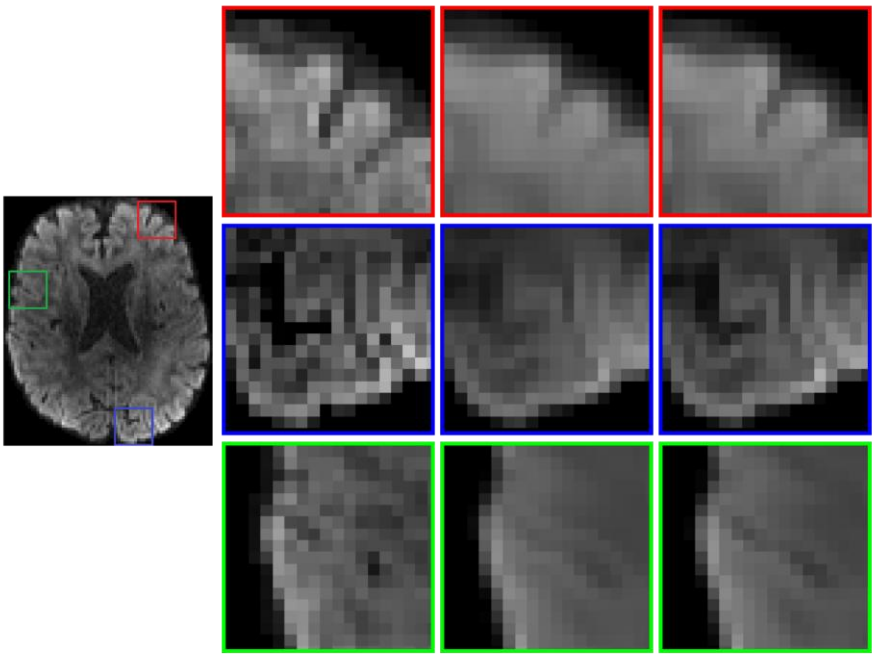

Fig. 5: Denoising of real data. (Far Left) Reference DW image. Regional close-up views for (Left) noisy DW image, (Middle) NLM denoised DW image, and (Right) 4D CNLM denoised DW image using 10 co-denoising images.

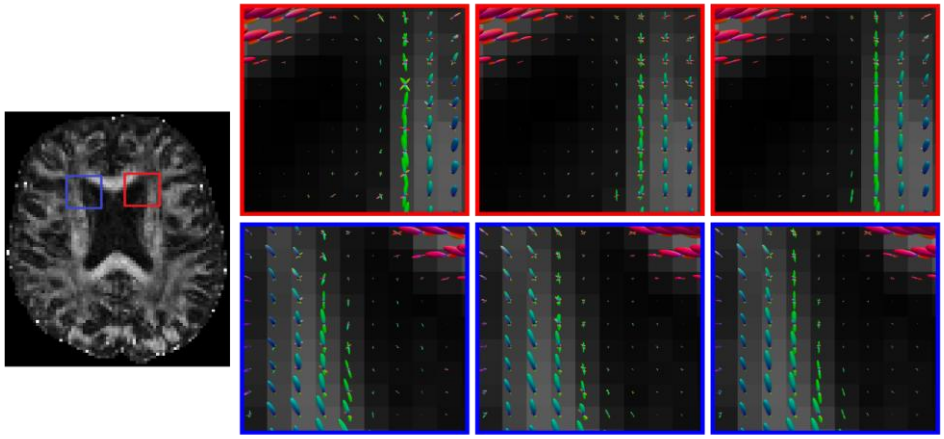

Fig 6: Comparison of ODFs in real human data. (Far Left) Reference FA image. ODFs estimated using (Left) noisy dMRI data, (Middle) NLM denoised dMRI data, and (Right) 4D CNLM dMRI data with 10 co-denoising images.

V. CONCLUSION

In this work, we propose a complete framework for dMRI denoising with 4D CNLM. 4D image block is used to adapt the characteristics of dMRI. Pseudo-residual is utilized to achieve robust noise standard deviation estimation. Ricain bias correction is considered to recover unbiased estimation. Finally, block perselection is added to reduce computational burden. Extensive experiments on synthetic data and real human data demonstrate that our method outperforms classical NLM algorithm. Further ODF results illustrate that the denoised images with our method can provide clean and coherent fiber orientations.

VI. Acknowledgements

The first author was supported by a scholarship from China Scholar Council (CSC).

REFERENCES

[1] H. Johansen-Berg and T. E. Behrens, Eds., Diffusion MRI - from quantitative measurement to in vivo neuroanatomy, *Academic Press*, 2009.

[2] Y. Jin and H. E. Cetingul, Tractography-embedded white matter stream clustering, *IEEE 12th international symposium on Biomedical imaging (ISBI)*, New York, USA, 2015, 432-435.

[3] Y. Jin, Y. Shi, L. Zhan, J. Li, G. I. de Zubicaray, K. L. McMahon, N. G. Martin, M. J. Wright, and P. M. Thompson, Automatic population HARDI white matter tract clustering by label fusion of multiple tract atlases, *Multimodal brain image analysis*, LNCS 7509, Nice, France, 2012, 147-156.

[4] P.-T. Yap, G. Wu, and D. Shen, Human brain connectomics: Networks, techniques, and applications, *IEEE Signal Processing Magazine*, 27(4), 2010, 131-134.

[5] P.-T. Yap, Y. Fan, Y. Chen, J. Gilmore, W. Lin, and D. Shen, Development trends of white matter connectivity in the first years of life, *PLoS ONE*, 6(9), 2011, e24678.

[6] C.-Y. Wee, P.-T. Yap, W. Li, K. Denny, J. N. Browndyke, G. G. Potter, K. A. Welsh-Bohmer, L. Wang, and D. Shen, Enriched white matter connectivity networks for accurate identification of MCI patients, *NeuroImage*, 54(3), 2011, 1812-1822.

[7] C.-Y. Wee, P.-T. Yap, D. Zhang, K. Denny, J. N. Browndyke, G. G. Potter, K. A. Welsh-Bohmer, L. Wang, and D. Shen, Identification of MCI individuals using structural and functional connectivity networks, *NeuroImage*, 59(3), 2012, 2045-2056.

[8] J. Li, Y. Jin, Y. Shi, I. D. Dinov, D. J. Wang, A. W. Toga, and P. M. Thompson, Voxelwise spectral diffusional connectivity and its applications to Alzheimer's disease and intelligence prediction, *Medical image computing and computer-assisted intervention (MICCAI)*, LNCS8149, Nagoya, Japan, 2013, 655-662.

[9] L. Zhan, J. Zhou, Y. Wang, Y. Jin, N. Jahanshad, G. Prasad, T. M. Nir, C. D. Leonardo, J. Ye, P. M. Thompson, and others, Comparison of nine tractography algorithms for detecting abnormal structural brain networks in Alzheimer's disease, *Frontiers in aging neuroscience*, 7:48, 2015. doi: 10.3389/fnagi.2015.00048.

[10] Y. Jin, Y. Shi, L. Zhan, and P. M. Thompson, Automated multi-atlas labeling of the fornix and its integrity in Alzheimer's disease, *IEEE 12th international symposium on Biomedical imaging (ISBI)*, New York, USA, 2015, 140-143.

[11] Y. Jin, C.-Y. Wee, F. Shi, K.-H. Thung, P.-T. Yap, D. Shen, and others, Identification of infants at risk for autism using multi-parameter hierarchical white matter connectomes, *Machine learning in medical imaging*, LNCS 9352, Munich, Germany, 2015, 170-177.

[12] Y. Jin, C.-Y. Wee, F. Shi, K.-H. Thung, D. Ni, P.-T. Yap, and D. Shen, Identification of infants at high-risk for autism spectrum disorder using multiparameter multiscale white matter connectivity networks, *Human Brain Mapping*, 36(12), 2015, 4880-4896.

[13] E. L. Dennis, Y. Jin, J. E. Villalon-Reina, L. Zhan, C. L. Kernan, T. Babikian, R. B. Mink, C. J. Babbitt, J. L. Johnson, C. C. Giza, P.M Thompson, and R.F Asarnow, White matter disruption in moderate/severe pediatric traumatic brain injury: Advanced tract-based analyses, *NeuroImage: Clinical*, 7, 2015, 493-505.

[14] E. L. Dennis, M. U. Ellis, S. D. Marion, Y. Jin, L. Moran, A. Olsen, C. Kernan, T. Babikian, R. Mink, C. Babbitt, J. Johnson, C.C. Giza, P.M Thompson, and R.F Asarnow, Callosal function in pediatric traumatic brain injury linked to disrupted white matter integrity, *The Journal of Neuroscience*, 35(28), 2015, 10202-10211.

[15] Y. Jin, Y. Shi, L. Zhan, G. I. De Zubicaray, K. L. McMahon, N. G. Martin, M. J. Wright, and P. M. Thompson, Labeling white matter tracts in HARDI by fusing multiple tract atlases with applications to genetics, *IEEE 10th international symposium on Biomedical imaging (ISBI)*,San Francisco, USA,2013, 512-515.

[16] Y. Jin, Y. Shi, L. Zhan, B. A. Gutman, G. I. de Zubicaray, K. L. McMahon, M. J. Wright, A. W. Toga, and P. M. Thompson, Automatic clustering of white matter fibers in brain diffusion MRI with an application to genetics, *NeuroImage*,100, 2014, 75-90.

[17] A. Buades, B. Coll, and J.-M. Morel, A review of image denoising algorithms, with a new one, *Multiscale Modeling & Simulation*, 4(2), 2005, 30.

[18] P.-T. Yap, H. An, Y. Chen, and D. Shen, Uncertainty estimation in diffusion MRI using the nonlocal bootstrap, *IEEE Transactions on Medical Imaging*, 33(8), 2014, 1627-1640.

[19] P. Coupé, J. V. Manjón, M. Chamberland, M. Descoteaux, and B. Hiba, Collaborative patch-based super-resolution for diffusion-weighted images, *NeuroImage*, 83, 2013, 245-261.

[20] G. Chen, P. Zhang, K. Li, C.-Y. Wee, Y. Wu, D. Shen, and P.-T. Yap, Block-based statistics for robust non-parametric morphometry, *Patch-based techniques in medical imaging*, LNCS9467, Munich, Germany, 2015, 62-70.

[21] J. Salmon and Y. Strozecki, Patch reprojections for non-local methods, *Signal Processing*, 92(2), 2012, 477-489.

[22] S. Prima and O. Commowick, Using bilateral symmetry to improve non-local means denoising of MR brain images, *International symposium on biomedical imaging (ISBI)*, San Francisco, USA,2013, 1231-1234.

[23] G. Chen, P. Zhang, Y. Wu, D. Shen, and P.-T. Yap, Collaborative non-local means denoising of magnetic resonance images, *IEEE 12th International symposium on biomedical imaging (ISBI)*, New York, USA, 2015, 564-567.

[24] G. Chen, P. Zhang, Y. Wu, D. Shen, and P.-T. Yap, Denoising magnetic resonance images using collaborative non-local means, *Neurocomputing*, 2015, in press.

[25] P. Coupé, P. Yger, S. Prima, P. Hellier, C. Kervrann, and C. Barillot, An optimized blockwise nonlocal means denoising filter for 3-D magnetic resonance images, *IEEE Transactions on Medical Imaging*, 27(4), 2008, 425-441.

[26] J. Manjón, J. Carbonell-Caballero, J. Lull, G. García-Martí, L. Martí-Bonmatí, and M. Robles, MRI denoising using non-local means, *Medical Image Analysis*, 12(4), 2008, 514-523.

[27] P. Zhang, M. Niethammer, D. Shen, and P.-T. Yap, Large deformation diffeomorphic registration of diffusion-weighted images with explicit orientation optimization, *Medical image computing and computer-assisted intervention (MICCAI)*, LNCS 8150, Nagoya, Japan, 2013.

[28] P. Zhang, M. Niethammer, D. Shen, and P.-T. Yap, Large deformation diffeomorphic registration of diffusion-weighted imaging data, *Medical Image Analysis*, 18(8), 2014, 1290-1298.

[29] P.-T. Yap, and D. Shen, Spatial transformation of DWI data using non-negative sparse representation, *IEEE transactions on medical imaging*, 31(11), 2012, 2035-2049.

[30] S. F. Eskildsen and L. R. Østergaard, Quantitative comparison of two cortical surface extraction methods using MRI phantoms, *Medical image computing and computer-assisted intervention (MICCAI)*, LNCS 4791, Brisbane, Australia, 2007, 409-416.

American Journal of Engineering Research (AJER) 2016
American Journal of Engineering Research (AJER)
e-ISSN: 2320-0847 p-ISSN : 2320-0936
Volume-5, Issue-2, pp-49-53
www.ajer.org
Research Paper Open Access

An Overview on Test Standards for Evaluation of Jute Agrotextiles

Prof. Swapan Kumar Ghosh[1], Mr. Satyaranjan Bairagi[2], Mr. Rajib Bhattacharyya[3], Mr. Murari Mohan Mondal[4]
[1](Professor, Department of Jute and Fibre Technology, Calcutta University, Kolkata, India)
[2,3,4](Senior Research Fellow, Department of Jute and Fibre Technology, Calcutta University, Kolkata, India)

Abstract: *The growth of the Indian Economy is significantly reliant on the success of the agriculture community. Traditional methods are limited in their ability to increase yields with the current constraints of restricted space and water supply. In this context, Agrotextiles have proved to be an effective alternative that delivers strong results despite the constraints. Some of the benefits of the usage of agrotextiles are enhancing freshness in fruits and vegetables, prevents soil from drying, protection from harmful pesticides, yield increase etc. However, due to the growing environmental concern across the globe, scientists, technologists and researchers are in search of natural agrotextile and jute agrotextile (JAT) seems to be the most potential candidate in responding to their search. JAT is highly effective in agri-horticulture and forestry for higher agricultural yield. Extensive research works and field study have been conducted with encouraging results. Now, there is a dire need for quality control in terms of testing and evaluation of JAT demanding formulation of new international standards for testing. The existing test standards for synthetic agrotextiles for evaluating different end use property parameters are not uniform globally i.e., these test standards vary from country to country. However, in the field of standardization for testing of different properties of JAT there is a paucity of data for formulation of specifications and quality control guidelines. Test standards for synthetic agrotextiles understandably do not exactly apply to JAT. While study is on to develop exclusive test and design standard for JAT, there is need to adopt any of the existing standards for synthetic agrotextiles that cater to the majority of requirements in the interim period. The paper suggests adoption of ASTM standards for testing JAT because of the wide range of test standards available and their credibility.*

Keywords:*ASTM standards, European Standards, Jute Agrotextile (JAT), Synthetic Agrotextiles, Technical Textile,*

I. Introduction

Agriculture forms the backbone of the Indian Economy and one cannot disregard the significant role that agriculture plays in the Indian Economy and in the daily life of its citizens. Yet, food security continues to be a pressing issue in India. In light of this major challenge, Agrotextile utilization has helped the agriculture community in attaining increased yield and enhanced quality in agriculture produce. Amongst its various benefits, agrotextiles protect produce from harmful external elements and assist in better soil management. These benefits provide farmers with enhanced productivity and increased yields resulting in further socio-economic development of the stake holders within the agriculture community. Agro processing sector has experienced expansion during the last five decades, starting with a handful of facilities which were mainly operating at domestic level [1]. The selection of Agrotextile product depends on crop needs. Selection of the agro textiles is also greatly influenced by the geographical location. But for any application and supervision quality control tests are an essential part. Again, proper testing of technical textiles meant for agriculture is critical to ensure their effective performance. The standards evolved for this purpose relate to synthetic agrotextiles only and are not uniform. Table 3 shows the existing BIS standards for the different synthetic agrotextiles used in different agriculture and horticulture applications. The design is based on rigorous empirical exercise carried out individually in each country. The site conditions are apt to vary and so also the approach to design. While some sort of uniformity in testing methods could be achieved in case of synthetic agrotextiles after 'synthesizing' the standards available, no such standards have drawn up so far for agrotextiles made of different natural fibres such as Jute Agrotextiles (JATs). In absence of testing standards for JAT, standards for synthetic agrotextiles are presently adopted for agrotextiles made of natural fibres. In view of the growing demand of JAT in particular, it is felt necessary to evolve exclusive application-wise standards for JAT.

The selection of JAT for a particular application in agriculture area necessarily depends on adequate and suitable fabric properties and specific functional characteristics in respect of end-use requirements. If these properties are technically inadequate for a particular application considering the limited durability of JAT and other natural Agrotextiles, distress/failure could be a distinct possibility. On the other hand, if these properties meet the desired specifications in excess of the actual requirement, the selection of the fabric will understandably prove uneconomical. As the physical features and mechanical properties of natural [2] and man-made fibres distinctly differ, we need to decide specifications of JAT carefully.

II. National Standards for Agrotextiles

There are reportedly 21 Bureau of Indian Standards (BIS) for the manufacture, testing, etc., of various types of synthetic agrotextiles [3] namely, IS 15351:2008 for Laminated high density polyethylene (HDPE) woven fabric (Geo-membrane) for water proof lining, IS 15907:2010 for Agro textiles - High Density Polyethylene (HDPE) Woven Beds for Vermiculture – Specification, IS 16008:2012 for Agro Textiles - Shade Nets for Agriculture and Horticulture Purposes – Specification, etc.

2.1 International Standards for Agrotextiles

Most of the countries of Western Europe (e.g. Belgium, France Germany, Italy, the Netherlands, Switzerland and the United Kingdom) have national standards [4] on the construction, testing and use of various types of synthetic agrotextiles. There is already a large volume of trade in agrotextiles among the countries of Western Europe but standard procedures for testing different parameters of agrotextiles of the producer country may differ with that of the user country creating ambiguity about the conformity of the test results of the different parameters of the product in particular JAT. European Economic Community (EEC) has a number of European Committees for Standardization (CENs) for various disciplines and product groups. The decision to use a particular agrotextile material in any agricultural process will depend, among other things, on whether it complies with the specifications indicated for that material by the specialist engineer in the design of the project. As already stated different countries have developed their own standards for use of agrotextiles which enable the specialist consulting engineers and other users to specify clearly the products they want; in addition, standardized testing methods make it possible to compare products and results.

2.2 Issues

The question is about the specifications and testing methods to be adopted in the intervening period till such time the application-wise specifications for JAT are finalized and testing methods specific for JAT are decided. Although there are a few BIS standards existing for agrotextiles, there is a dire need for international standards for the agrotextiles [2]. Whilst the national standards of different countries for test methods recommend a unified approach for testing, the way in which the test results are applied to specify an agrotextile for a particular application could hardly be uniform. As there is hardly any difference between JAT and synthetic agrotextiles functionally, the standards available for synthetic agrotextiles are applied for JAT. As the standard testing methods of agrotextile are not uniform in developed countries and are somewhat sporadic in developing countries, ASTM standard testing methods for testing of different types of synthetic agrotextiles as well as JAT in most of the cases are being followed for the sake of uniformity. In India, BIS standards are followed where such standards exist for testing of JAT.

III. Speciality of Jute Fibre

Jute is one of the most versatile natural fibres and is second only to cotton in availability and variety of uses among vegetable fibres. It is a long, soft, shiny vegetable fibre that can be spun into coarse, strong threads. It falls into the bast fibre category (fibre collected from bast or skin of the plant) along with kenaf, industrial hemp, flax (linen), and ramie. It is produced from plants in the genus Corchorus, which has been classified in the family Tiliaceae, or more recently in Malvaceae. Two species of Jute [5] which are commonly cultivated are Corchorus capsularis (White Jute) and Corchorus olitorius (Tossa Jute). The fibres are off-white to brown, and 1–4 metres (3–12 feet) long. Jute fibre is grown abundantly in Bengal (India) and adjoining areas of Indian subcontinent. Retted jute fibers have three principal chemical constituents, namely α-cellulose, hemicelluloses, and lignin. The hemicelluloses consist of polysaccharides of comparatively low molecular weight built up from hexoses, pentoses, and uronic acid residues. In jute, capsularis and olitorius have similar analyses, although small differences occur among different fiber samples. In addition to the three principal constituents, jute contains minor constituents such as fats and waxes inorganic matter, nitrogenous matter and traces of pigments [6]. The details of chemical composition [7, 8] of the jute fibre is given in Table – 1 and the fibre properties of most widely used fibres for producing Geotextiles like jute, polyester and polypropylene are depicted below in Table-2.

Table- 1: Average chemical composition (in percent of bone dry weight of the fibre) of jute [8] *C. Capsularis* (White Jute), *C. Olitorius* (Tossa Jute).

Constituent	***C. Capsularis* (White Jute)**	***C. Olitorius* (Tossa Jute)**
Cellulose*	60.0 – 63.0	58.0 – 59.0
Lignin	12.0 - 13.0	13.0 – 14.0
Hemicellulose**	21.0 - 24.0	22.0 - 25.0
Fats and waxes	0.4 - 1.0	0.4 - 0.9
Proteins or nitrogenous matter etc. (% nitrogen x 6.25)	0.8 - 1.87	0.8 - 1.56
Pectins	0.2 – 0.5	0.2 - 0.5
Mineral matter (Ash)	0.7 – 1.2	0.5 – 1.2
* Major constituents of jute-cellulose include glucosan (55.0 – 59.0%), xylan (1.8 – 3.0%) polyuronide (0.8 – 1.4%). **Major constituents of jute-hemicellulose include xylan or pentosan (15.5-16.5%), hexosan (2.0 – 4.0%), polyuronide (3.0 - 5.0%) and acetyl content (3.0-3.8%).		

Table- 2: Properties of jute fibre [9-18] in contrast with man-made fibre.

Sl. No.	**Properties**	**Jute**	**Polyester**	**Polypropylene**
01.	Specific gravity [21]	1.48	1.38	0.91
02.	Tenacity, g/d	3 to 5	2 to 9.2	2.5 to 5.5
03.	Breaking Elongation, %	0.8 to 2	10 to 14.5	14 to 100
04.	Elastic recovery, %	75 to 85	57 to 99	75 to 95
05.	Moisture regain [22], At 65% R.H. and 27^0C.	12.5 to 13.8	0.4 to 4.0	0.01
06.	Effect of heat	It does not melt. Up to 180^0C there is no major wt. loss and tenacity loss. However hemi cellulose degrades around 293^0C and other constituents at higher temperature.	Sticks at 180^0C and Melts at 230^0 – 240^0C	Softens at 143^0 – 154^0C, melts at 160^0C & decomposes at 288^0C
07.	Effect of acid /alkalis	Good resistant to dilute organic and mineral acids at room temperature but degrades in conc. mineral acids. Affected by hot alkali.	Good resistance at room temperature disintegrates in conc. hot alkali. Excellent resistance to acids.	Excellent resistance to conc. acid and alkalis.
08.	Effect of bleaches & solvents	Resistant to H_2O_2 bleaching conditions. Excellent resistant to organic solvents. However, affected by strong oxidizing agents.	Excellent resistance to bleaches & oxidizing agents.	Resistance to bleaches & solvents. Chlorinated Hydrocarbon cause swelling & dissolves at 160F and higher.

IV. BIS Standards Available

The following standards formulated for testing of synthetic Agrotextiles are given in Table – 3 below.

Table - 3: Standards [3] followed for Agrotextile Testing

AGROTECH		
SL. No.	BIS Standard	Description
1.	IS 15351:2008	Textiles- Laminated high density polyethylene (HDPE) woven fabric (Geo-membrane) for water proof lining (First revision)
2.	IS 15907:2010	Agro textiles - High Density Polyethylene (HDPE) Woven Beds for Vermiculture - Specification
3.	IS 4401:2006	Textiles-Twisted nylon fishnet twines (fifth revision)
4.	IS 4402:2005 /ISO 1107:2003	Textiles - Fishing nets - Netting - Basic terms and definitions (second revision)
5.	IS 4640:1993 /ISO 858:1973	Fishing nets - Designation of netting yarns in the tex system (first revision)
6.	IS 4641:2005 /ISO 1530:2003	Textiles - Fishing nets - Description and designation of knotted netting (second revision)
7.	IS 5815(Part 4):1993 /ISO 1805:1973	Fishing nets: Determination of breaking load and knot breaking load of netting yarns (first revision)
8.	IS 5815(Part 5):2005 /ISO 1806:2002	Textiles - Fishing nets - Determination of mesh breaking force of netting (second revision)
9.	IS 5815(Part 6):1993 / ISO 3090:1974	Netting yarns - Determination of change in length after immersion in water (first revision)
10.	IS 5815(Part 7):1993 / ISO 3790:1976	Fishing nets - Determination of elongation of netting yarns (first revision)
11.	IS 6348:1971	Basic terms for hanging of netting
12.	IS 6920:1993 /ISO 1532:1973	Fishing nets - Cutting knotted netting to shape ('Tapering')
13.	IS 8746:1993 /ISO 3660:1976	Fishing nets - Mounting and joining of netting - Terms and illustrations (first revision)

14.	IS 9945:1999	Fishing nets - Method for determination of taper ratio and cutting rate (first revision)
15.	IS 15788:2008	Fishing nets - Method of test for determination of mesh size - Opening of mesh
16.	IS 15789:2008	Fishing nets - Method of test for determination of mesh size - Length of mesh
17.	IS 5508 (Parts 1 to 24)	Guides for fishing gears
18.	IS 7533:2003	Polyamide monofilament line for fishing
19.	IS 14287:1995	PP Multifilament netting twine
20.	IS 6347:2003	PE Monofilament twine for fishing
21.	IS 16008:2012	Agro Textiles - Shade Nets for Agriculture and Horticulture Purposes – Specification *(Clubbed the specifications of 3 Shade net standards, i.e. Specifications for Shade net 50%, 75% and 90% for Agriculture Application. Thus, have 1 standard against 4 proposed standards)*

V. Problem of using the existing BIS Standards for Synthetic Agrotextiles in JAT

Growing market offers new possibilities for jute in technical textile sector [19, 20]. In order to meet the challenges in this area, JAT should conform to the stringent quality specifications. This may be achieved only by following the standards established specifically for JAT [21]. But as these specific standards for JAT are yet to be formulated and published, existing standards for synthetic agrotextiles are adopted which could be sometimes misleading for JAT. Separate specific standards are required for JAT as the different property parameters of JAT like physical, mechanical, and hydraulic and endurance properties are not similar to synthetic agrotextile. Apart from these, behavior of JAT on imposition of extraneous load and its withdrawal are different from synthetic agrotextiles. It is found that during straining, elongation at break for synthetic agrotextiles is much higher than that of JAT and their retractive behavior is different. In case of JAT properties for less than 50% are only applicable. Behavioral differences between JAT and synthetic agrotextiles demand formulation of separate standards for JAT for assessing of different property parameters in the laboratory for its acceptance globally. This will not only meet the technical requirements for assessing the property of JAT but also make successful marketing of JAT globally.

VI. Suitability of ASTM Standards as an interim option

There are different BIS standards available for synthetic agrotextiles. As there is no unified standard for JAT, BIS testing standards are considered the most preferred option for JAT testing till such time exclusive JAT standards are formulated and accepted. ASTM standards are accepted globally for its authenticity of all the existing standards. Testing parameters of JAT which are measured for finding its potential applications in different geotechnical applications are given in Table - 4.

Table-4: Properties of JAT [22]

	Erosion Control, & Afforestation				**Weed Management**	
	Woven				**Non-Woven**	
Criteria	**Conventional**	**Type-1**	**Type-2**	**Type-3**	**Type-1**	**Type-2**
Weight(g/m^2)	500	400	300	300	500	750
Thickness(mm)	5	3	3	2	6	8
Open Area (%)	60	40	60	70	0	0
Threads/dm Warp X Weft	6.5 × 4.5	34 × 15	17 × 4.6	11 × 12	-	-
Width(cm)	122	122	122	122	150	150
Length(m)	70	100	100	100	50	50
Water absorption capacity(%)	600	500	400	350	650	700
Tensile strength (kN/m) WarpX Weft	17.5 × 7.5	12 × 10	10 × 7.5	10 × 10	5 × 6	7 × 8
Elongation at Break (%) Warp X Weft	11 × 15	10 × 12	10 × 15	12 × 12	20 × 25	25 × 30

VII. Conclusions

Natural technical textile in the name of Jute Agrotextile (JAT) is highly effective in agri-horticulture and forestry for higher agricultural yield. Extensive R & D work and field study has been conducted by research Organizations in this field with encouraging results. Efficacy of the products have been established and documented. JAT helps faster growth of vegetation naturally. It is a natural fabric that helps retain soil humidity at conducive levels, arrests desiccation of soil and attenuates extremes of temperature due to its inherent capacity to absorb water/moisture to the tune of 5 times of its dry weight. Jute coalesces with soil after biodegradation, increases its permeability and supplementing its nutrient level. JAT fosters growth of plant in arid and semi- arid zones much faster than under control conditions without use of manures. Non- Woven JAT can suppress weed-growth effectively. JAT provides all these advantages without affecting eco-ambience

adversely at affordable and competitive cost. It has been envisaged that some of such products like, jute sleeve, nonwoven agro mulching sheet, fabric for plant wrapping etc. can be conveniently fabricated in rural areas with an ultimate impact on rural economy.

VIII. Acknowledgements

The authors convey their regards to the Honorable Vice Chancellor and Pro Vice Chancellor (academic), University of Calcutta, West Bengal, India for their kind consent to allow this review paper for publication in the scholarly journal and valuable guidance to carry out this paper.

References

[1] technotex.gov.in/Agrotextiles/Handbook%20for%20Agrotextiles.,2013
[2] T. K. Guha-Roy, A. K. Mukhopadhyay and A. K Mukherjee, Surface features of jute fiber using scanning electron microscopy,Textile Research Journal , 54(12), 1984, 874.
[3] Compendium on Standards in Technical Textiles sector, 2012
[4] M/107-Mandate to CEN/CENELEC concerning the execution of standardization work for harmonized standards on Geotextiles. European Commission. 1996.
[5] Bureau of Indian Standards. 1975. Indian standards, 271, New Delhi.
[6] Anon,Jute, Kenaf and Allied Fibres – Quarterly Statistics, Food and Agricultural Organisation of The United Nation,2002
[7] W. G. Macmillan, , Indian Textile Journal, 67, 1957, 338.
[8] A. Mazumdar, S.Samajpati, P.K.Ganguly, D.Sardarand, P. C. Dasgupta, Textile Research journal, 50, 1980, 575.
[9] E. R. Kaswell, Textile Fibres, Yarns and Fabrics (Reinhoid Publishing Corporation), 1953).
[10] B. C. Goswami, I. G. Martindale, and F. L Scardino, Textile Yarns; Technology, Structure and Applications, 1977.
[11] R. Meredith, The tensile behavior of raw cotton and other textile fibers, Journal of Textile Institute, 36, 1945, 107.
[12] P. W. Carlene, The moisture relations of textiles, Journal of Society dyers and Colourists, 60(9), 1944, 232.
[13] S. G. Barkar , The Moisture Relationships of Jute (IJMA , 1939).
[14] J. M. Preston, Modern Textile Microscopy (Emmot and Co. Ltd, 1933).
[15] J. M. Preston, and M. V. Nimkar, Measuring the Swelling of Fibers in Waters, Journal of Textile Institute, 40, 1949, 674.
[16] S. B. Bandyopadhyay, Frictional properties of jute and some other long vegetable fibers Part1: General study of characters, Textile research Journal, 21(9), 1951, 659.
[17] H. D. Smith, Textile Fibres: An Engineering Approach to Their Properties and Utilisation, A S T M Proc, 19th Edgar Marburg Lecture, 44, 1944, 543.
[18] A. K. Samanta, Effect of Chemical Texturising, Bleaching and Resin Finishing on Jute/polyester and Jute/cotton Blended Textile, 1995.
[19] T. P. Nevell, and S. H. Zeronian, Cellulose Chemistry and Its Application, Edited by (Ellis Harwood Ltd), 1985).
[20] Anon, Chemical processing of jute fabrics for decorative end use: part-I – Bleaching treatment for jute, 1977.
[21] P Ghosh, A.K. Samanta and D. Das, Effect of selective pretreatments and different resin post- treatments on jute-viscose upholstery fabric, Ind. J. Fibre & Text Res, 19(4), 1994, 227.
[22] P. K. Choudhury, J. Srinivasan, Jute agrotextiles- its properties and applications, Proc. All India Seminar on Technical Textiles in Civil Engineering: A tutorial review, WBSC, IE(I),Kolkata, 2007, 24-31

American Journal of Engineering Research (AJER) 2016
American Journal of Engineering Research (AJER)
e-ISSN: 2320-0847 p-ISSN : 2320-0936
Volume-5, Issue-2, pp-54-61
www.ajer.org
Research Paper Open Access

Effect of Tillage and Staking on the production of fluted Pumpkin

C.G Okeke[1], S.I. Oluka[1] and O. Oduma[2*]
[1]*Department of Agricultural and Bio-resources Engineering, Faculty of Engineering, Enugu State University of Science and Technology, Enugu,Nigeria*
[2]*Department of Agricultural and Bio-resources Engineering, College of Engineering and Engineering Technology, Michael Okpara University of Agriculture, Umudike, Nigeria*

ABSTRACT: *A field experiment was conducted using fluted pumpkin (telfairia occidentals) to determine the effect of 3 different tillage (zero, mound and flat) and 3 different staking (zero, individual and pyramid) on a sandy clay loam soil of the humid tropics at faculty research farm Esut, Enugu Southeastern Nigeria between June and December, 2008. The treatment consists of 3 levels of tillage and3 levels of staking as mentioned above. The experiment was a 3 x 3 factorial laid out in randomized complete block design (RCBD) with four replications and nine treatments. The results obtained revealed significant different of p 0.05 among some of the ç. treatments. The highest number of vine length and number of flower per plant of 196.16 and 36 were obtained from zero tillage / individual staking while the least were recorded for flat tillage/individual staking of 115.19 and zero tillage/pyramidal staking of 3 respectively. Average leaf yield ranged from 277.7 to 852.5 (g) were obtained. Based on their performance, treatment 5 (mound tillage/individual staking and treatment), 6(mound tillage/pyramidal staking) have the highest leaf yield.*

Keyword: *Fluted pumpkin, flat tillage, staking, mound, zero tillage*

I. INTRODUCTION

Fluted pumpkin, (terlfairia occidentals) is the most popular leafy vegetable crop belonging to the family (Cucurbitaccae) and the genus telfairai. It originated in East and West Africa. It is widely grown and consumed in Nigeria especially in Igbo land. It is also grown and consumed in mid-western area (Edo and Delta States) and to an appreciable degree in the south western states (Ondo, Ekiti Lagos, Ogun, Oyo) of Nigeria (Okoli and Mgbeogu, 1982). The crop is called ugu by the Igbos while Yorubas call it Ugwu. In Ghana, it is called Krobonko or oroko, it is called kobon in Cameroon but in Sierra Leone it is referred to as pondoko or gonugbe. It is a pot-herb (Akobundu1987), cultivated mainly for its succulent young leaves and shoots, which are used as vegetables.

Fluted pumpkin is a high climbing perennial plant with partial drought tolerance and perenting root system (Tindall, 1986). It is commonly cultivated as an annual crop because the leaves and young shoots dry at the end of growing season but as the starting of the rainy season, new shoots regenerate along the main branches, especially in female plant. The female plants can survive for about 4 years when their main stem must have reached a diameter of up to 10cm and its lianeous branches could be over 30cm long when found high up in trees. The male plants have short time of surviving than the female plants. Female plants withstand dry conditions better than the male plants. The male plants drop their leaves about 3 weeks earlier than the female plants.Fluted pumpkin has 3 to 5 lobes deeply divided leaves. The plants are dioeciously with protandrous flowering that is male and female flowers. The male flowers open before the female ones, and they open in the evening or at night and often shade their pollen soon afterwards. Female flowers open in the evening, but open wider from mid-morning until early afternoon. Male plants are borne in clusters while female plants are borne singly (Greensill, 1968). The male plants flower about 1-5 months from sowing while female flowers need extra 3 weeks before the first flowers is open.

Fluted pumpkin is a cross pollinated crop, but pollination by hand is more successful (Akoroda et al, 1989). The fruits mature about 9 – 10 weeks after pod setting. The fruits are green in colour, 60cm long in height and 30cm in diameter. When the crop is growing for it seeds, they produce about 3000-5000 fruits.

Seeds fail to germinate when they are kept dry (Thanpson, and Kelly, 1957). The seed quality is best when seeds inside the fruits are between 9 -12 weeks old. When seeds are left inside the fruit for too long, they

start germinating inside the pod (Schipper, 2000). The pods have bright yellow fibrous flesh and contain 50 — 100 which look like the colanut seed, and over 2.5cm in diameter (Asoegwu, 1987, Lrvine, 1969). The colour of the seed ranges from yellow to brown to dark — red.

Fluted pumpkin can be cultivated on a zero tilled land, tilled land and on mounds. Akoroda (1988) observed that telfairia occidentals are a common homestead garden crop in southern Nigeria,mostly cultivated by woman. In home gardens, they are grown close to fence or to a tree, wall, and structures on which the shoots are allowed to climb (Okoli and Mgbeogu, 1982). It can be allowed to creep on the ground or staked (Akoroda, 1988, Nihort, 1986). They grow on a wide range of soil including poor, sandy soils but perform better on sandy loam soils with internal drainage and are characterized as ultisols (Asiegwu;1985). They require a high temperature of above 25°C during the growing period and fairly low humidity. Fluted pumpkin is tolerant to slightly acidic soils (Stevels, 1999).

Tillage and staking are the 2 major cultural practices that are usually carried out in the production of the crop. Not much have been done on this crop, its literature is very scanty. There is the need to carry out more research work on the crop (telfairia occidentals). The objective ofthis work is to determine the effect of tillage and staking on the growth and yield of fluted pumpkin.

II. MATERIALS AND METHODS

2.1 Experimental Site

The experiment was carried out a the faculty research farm of Enugu State University of Science and Technology Enugu. The area is located within latitude 06° 25N and longitude 0.7°15E south west of derived agro ecological zone of Nigeria and on the soil classified as ultisols.

The research was carried outto determine the effect of tillage and stating on the performance of telfairiaoccidentalis (fluted pumpkin) in the agro ecological zone during 2008 cropping season.

2.2 Source of Material

The planting material (pod /fruit of telfairiaoccidentalis) that was use for the experiment was gotten from IITA Ibadan.

2.3 Soil Analysis

Soil sampling and analysis was carried out. Soil samples were collected from different parts of experimental site, to a depth of 0-20cm using soil auger and were bulked to produce a composite sample. The soil analysis was done to determine the soil naïve nutrient level and other soil properties. Soil properties analyzed for includes; clay, site, find sand, sand, pH value, organic matter %, exchangeable based(meg/bOg), CEC, Base salt, Exchangeable Acidity.

2.4 Field Method

The experimental site was cleared on the 27th day of May 2008 with the use of cutlass and hoe. After which, the plots were mapped out using measuring tape, pegs and ropes, to get a total land area of 161m2 (11.5m x 14m). The land area was divided into 12 plots. Each plot was divided into 3 sub-plot with total sub-plots of thirty six (36) which was used for the experiment.

The twelve (12) main plots were demarcated from each other with pegs and ropes and was spaced 1m x 1m square. Plots were cultivated on the 3rdday of June 2008, using 3 different methods of tillage via; zero mound and flat tillage. The fruit was plot open using matched and the seeds were extracted. The bright yellow fibrous pulps around the seeds were gently squeezed off the seeds. The seeds were later dried under the shade for two days before planting. They were planted on the 4th day of June 2008 at the rate of one seed per hole. Three seeds were planted in each subplot, nine (9) seeds per main plot and 27 seeds per block. According to the field layout model, 108 seeds / plants were planted in the project plot. The planting was done by opening the soil to a depth of 6cm and inserting the seeds after which the openings were covered with topsoil. Some of the vines were staked on the 16th day of June 2008 and some were left unstakedbased on the type of treatment.

2.5 Experiment Design

The experimental field layout was a 3 x 3 factorial in randomized complete block design (RCBD) with nine(9) treatments and four (4) replications.

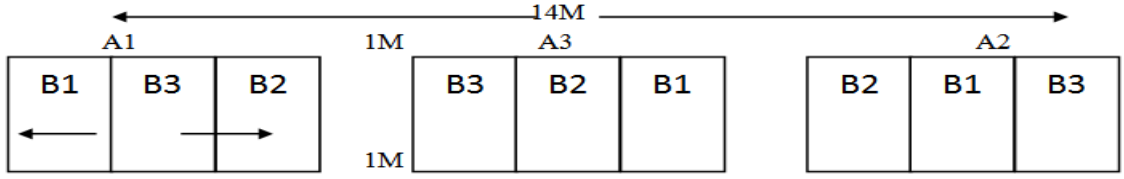

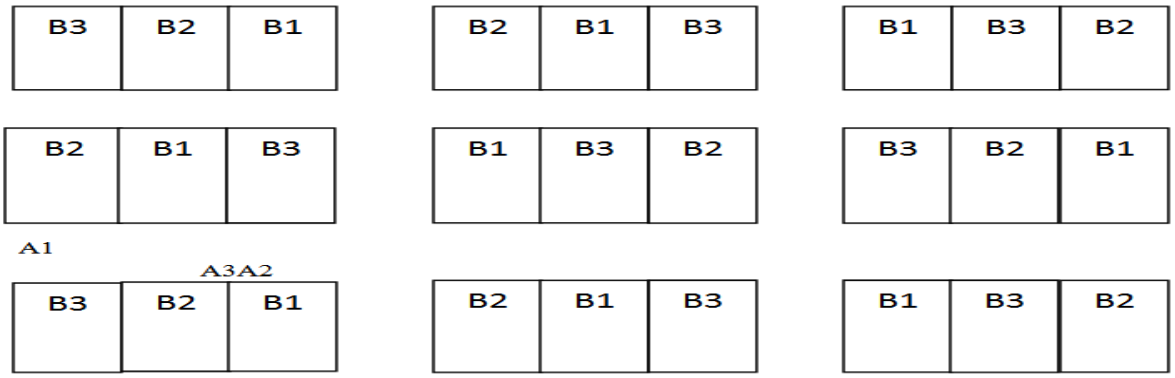

A1 = Zero Tillage B1 =Zero Staking
A2 = flat tillage B2 = individual staking
A3 = mound tillage B3 = pyramidal staking
9 treatments and 4 replications
Treatment 1 = zero tillage / unstaked; Treatment 2 = zero tillage / individual staked
Treatment 3 = zero tillage / pyramidal staked, Treatment 4 = mound tillage / unstaked
Treatment 5 mound tillage / individual staked, Treatment 6 = mound tillage / pyramidal staked, Treatment 7 = flat tillage / unstaked, Treatment 8 = flat tillage / individual staked, Treatment 9 = flat tillage / pyramidal staked

2.6 Cultural Practices

Adequate field maintenance was carried out to ensure that the crops perform well. Weeding was carried out twice in the field using traditional hoe. Poultrymanure was applied into the soil before the crops were planted. The fertilizer used was NPK 15:15:15. It was applied 23rd of June 2008 at equal rate of 0.0003267kg to each crop. Staking of vines was done on16th June 2008 with 3 different staking via: zero, individual and pyramidal staking.

2.7 Data Collection

The following agronomic data were collected:

i. Days to seed emergence:This was determined by counting the number of days it takes the plants to germinate. The plants did not germinate the same day. The germination started on 13th day of June 2008 that is 2 weeks after planting.

ii.Percentage emergence (%): This was determined visually by counting the total number of seedlings that emerged in each sub-plot after 2 weeks, over the total number of seeds planted on the sub-plot and the value expressed in percentage.

iii.Vine length (cm): This was measured as the distance from the baseof the plant to the tip of the vine. Vine length of 2plants! sub-plot were measured with a meter rule andthe mean taken. The measurement was made at 4weeks stage, 6 weeks, 8 weeks, 10 weeks and 12weeks.

iv. Leaf area index (LAI): This was determined by measuring the length and weight of the leaves with a meter rule. Two leaves per plant were measured. The result was calculated using the following formular:

$$LAI = \frac{\text{no of leaves x area of leaf x no of plant pr sub-plot}}{\text{Area covered (size of sub-plot)}} \quad (1)$$

v. Number of leave per plant: This was determined by counting the total number of leaves each plant produced.

vi. Number flower per plant: This was determined by counting the total number of flower produced by a plant.

vii. Number of aborted flowers:This was determined by counting the number of aborted flowers in each plant that produces flowers.

viii.Leaf yield per plant (g): This was obtained by weighing the leaf yield of telfairia per plant using a weighting balance and the mean taken.

2.8 Statistical Analysis

The analysis of variance (ANOVA) was carried out according to the procedure outlined by Steel and Torrie (1980), for a factorial experiment in randomized complete block design (RCBD), and separation of treatment means for significant effects was done using the least significant different (LSD) techniques.

III. RESULTS AND DISCUSSION

3.1 Results

The results of this research work are presented in Table 1-7

Table I: Soil Physico-chemical Properties of the Experimental Site

Properties	Contents
Particle size %	
Clay	29
Silt	21
Fine sand	28
Sand	22
pH value	4.1
H_2o	3.0
Kel	1.34
Organic matter %	
Carbon	
Organic matter	2.32
Total nitrogen	0.098
Exchangeable base ($cmol^1kg$)	2.6
Ca24	
Mg	2.6
K	0.18
Na	0.07
Cee	30.8
Exchangeable acidity	Trance
A1	
H	
	6.7
	5.60

Table II: Treatment Means of the Percentage Germination at Four (4) Weeks after Planting (WAP)

Treatment	% germination at 4 WAP
Zero tillage/unstaked	100
Zero tillage/individual staking	100
Zero tillage/pyramidal staking	100
Mound tillage / unstaked	100
Mound tillage / individual staking	100
Mount tillage / pyramidal staking	91.68
Flat tillage/individual staking	91;68
Flat tillage/pyramidal staking	100
Flat tillage/pyramidal staking	91.69
F-LSD (0.05)	Ns

Table III: Treatment Means of the Vine Length (Cm) at Four (4) and Six (6) Weeks after Planting (WAP)

Tr Treatment	Vine length at 4 WAP 6 WAP	
Zero tillage/unstaked	79.34	137.88
Zero tillage/individual staking	89.48	196.16
Zero tillage/pyramidal staking	89.32	158.06
Mound tillage / unstaked	90.03	173.58
Mound tillage / individual staking	89.74	152.39
Mount tillage / pyramidal staking	90.70	178.73
Flat tillage/individual staking	70.16	158.81
Flat tillage/pyramidal staking	71.45	115.19
Flat tillage/pyramidal staking	59.99	159.93
F-LSD (0.05)	33.21	ns

Table IV: Treatment Means of the Number of Leaves/Plant at Four (4) and Six (6) Weeks after Planting (WAP)

Treatment	Vine length at 4 WAP 6 WAP	
Zero tillage / unstaked	42	137
Zero tillage / individual staking	28	168
Zero tillage / pyramidal staking	43	134
Mound tillage / unstaked	37	157
Mound tillage / individual staking	33	100
Mound tillage / pyramidal staking	32	146
Flat tillage / unstaked	28	87
Flat tillage / individual staking	34	117
Flat tillage / pyramidal staking	24	112
F-LSD (0.05)	13.61	ns

Table V: Treatment Means of the Number of Flower Bud/Plant at Ten (10) and Twelve (12) Weeks after Planting (WAP)

Treatments	No of flower bud/plant at 10 WAP 12 WAP	
Zero tillage / unstaked	162	62
Zero tillage / individual staking	0	66
Zero tillage / pyramidal staking	15	109
Mound tillage / unstaked	0	60
Mound tillage / individual staking	99	100
Mound tillage / pyramidal staking	70	98
Flat tillage / unstaked	47	164
Flat tillage / individual staking	0	0
Flat tillage / pyramidal staking	0	0
F-LSD (0.05)	52.20	71.68

Table VI: Treatment means of the number of flower /plant, no. of aborted flower/plant and leaf yield/plant at twelve (1.2) weeks after planting (WAP**)**

Treatments No of F/plant, no of a.fl. leaf yield/plant (g) 12 WAP			
Zero tillage / unstaked	13	8	277.7
Zero tillage / individual staking	4	1	677.5
Zero tillage / pyramidal staking	3	3	477.5
Mound tillage / unstaked	30	0	658.75
Mound tillage / individual staking	36	16	852.5
Mound tillage / pyramidal staking	12	4	765
Flat tillage / unstaked	8	3	580
Flat tillage / individual staking	0	0	655
Flat tillage / pyramidal staking	0	0	622.5
F-LSD (0.05)	14.49	5.470	215.85

Table VII: Treatment Means of the Leaf Area Index (Lai) at Four (4), Six (6) and Eight (WAP) (8) Weeks after Planting

Treatments LAI at 4 WAP LAI at 6 WAP LAI at 8 WAP			
Zero tillage I unstaked	1.31	1.19	2.04
Zero tillage / individual staking	1.86	1.45	2.03
Zero tillage / pyramidal staking	1.45	1.43	1.98
Mound tillage / unstaked	1.53	1.79	1.79
Mound tillage / individual staking	1.82	1.57	2.35
Mound tillage I pyramidal staking	1.26	1.84	2.35
Flat tillage / unstaked	1.97	1.72	1.59
Flat tillage / individual staking	1.28	1.64	1.69
Flat tillage / pyramidal staking	1.80	2.44	2.15
F-LSD (0.05)	Ns	0.69	0.61

3.2 Discussion

3.2.1 Soil Characteristics of the Experimental Site

The soil analysis result shown in Table 1, indicates the chemical and physical properties at the experimental site. The soil was found to be acidic, pH 4.1 and 3.0 using H20 and KCL, as extractants respectively. It was found to contain 29% clay and 2% sand respectively.

The soil was clay in nature and low in organic matter content. But because of the lower content of organic matter of the soil, it was amended with NPK fertilizer. The result showed that application of urea increased shoot dry matter in telfairia. This is in line with Tsuna and Fujise (1984) and Stino (1953) when they reported that nitrogen increased dry matter production of sweet potato by increasing the leaf expansion. Nitrogen is usually associated with the building up of leaf tissue while potassium is essentially for meristematic and photosynthetic activities-factors important for crop growth and yield (Tsunaand Fujise, 1984).

3.2.2 Effect of Tillage and Staking on the Germination Percentage (%) of Fluted Pumpkin

The result presented in table 2 shows that there was no significant difference (p = 0.05) among the treatments with respect to generation. All the treatments had 100% germination except for treatment six (mound tillage / pyramidal staking), treatment 7 (flat tillage / unstaked) and treatment 9 (fIat tillage / pyramidal staking) that had approximately 90% germination.

The percentage growth rate of the telfairaoccidentalis seeds planted on the flat tilled plots was lower than others. The tillage practices affect the physical properties of the soil like the temperature, soil moisture, texture and structure (Lal, 1987). In the case of soil temperature, in south western and south eastern region, the maximum soil temperature on ridged / mound and ploughed plots were higher than on unploughed and straw mulch treatment.

It should then be agreed that high soil temperature causes excessive evaporation from the soil and may trigger planted seed into secondary dormancy.

In term of soil moisture, soil tillage can influence the water content of the upper soil and there by influence seed germination and seedling emergence (Hall and Cannel, 1979).

Loose open soil loses water more readily than firm soil with only small void because of mass air movement in large voids. It tends to become drier also because of poor contact with moist soil below and slower upward movement of water into the loose soil.

The seeds planted in zero tilled soil also found it slightly difficult to germinate because the area where they were planted was later compacted. This compaction was due to the effect of rain falling on the untilled soil, which causes the compaction and sealing of the partially tilled planting holes made before planting the seeds. The seeds planted on the zero tillage have the highest germination percentage followed by mound.This may be due to the lowering of the soil temperature and conservation of moisture in the soil. The seeds planted on the flat tilled plots have gradual germination starting from the first 2 weeks after planting.

3.2.3 Effect of Tillage and Staking on the Vine Length (cm) of Fluted Pumpkin

The result on vine length at 4 WAP shows a significant difference (p = 0.05) among some of the treatments as shown in table 2. Treatment 6 (mound tillage/pyramidal staking) had the highest vine length of 90.70 cm, which was significantly different from treatment 9 (flat tillage / pyramidal staking) with vine length of 69.99 cm. However, there was no significant difference among the vine length at 6 WAP as shown in Table 5. Treatment. 2 (zero tillage / individual staking) had the highest vine length of 196.16cm, which was statistically the same with vine lengths of treatment 3, 4, 6, and 9 (mound tillage / pyramidal staking).

The vine length of telfairiaoccidnetalis planted on flat tilled plots at 4 WAP and 6 WAP was not as high as other forms of tillage used. The telfairia planted on zero tilled plots were competing in terms of growth rate with those on mound — tilled plots.

It can then be asserted that if there are enough plant nutrients in the soil and proper management measure taken, telfairia can be grown on soil with moderate bulk density without tilling the soil. The problems that can be encountered in cultivating telfairiawith zero tillage are the poor infiltration rate of the soil and also high rate of erosion and weeds. Mulching or covering the soil with organic materials can solve these problems. Infiltration rate of telfairia that are allowed to creep on the ground can be improved when the leaves have fully covered the ground. It also helps to control erosion.

3.2.4 Effect of Tillage and Staking on the Number of Leaves I Plant of Fluted Pumpkin

The number of leaves/plant of talfairia obtained at 4 WAP shows a significant difference (p = 0.05) among some of the treatment as shown in table 2. Treatment 3 (zero tillage / pyramidal staking) had the highest number of treatment 9 (that tillage / phraamidal staking) with number of leaves of 24.5. At 6 WAP, there was no significant effect among the treatments. Treatment 2 (zero tillage / individual staking) had the highest number of leaves of 168.75, which is significantly the same with treatment 3, 5 and 9.

This experiment revealed that talfairia production could be highly enhanced by staking. According to Trenbath, (1976) staking exposes the leaves for effective light reception, as light is one of the factors needed by leafy vegetables. Staked plants produce the highest number of leaves and the longest vine length. Oyenuga, (1986) had earlier recommended staking as the leaves of telairiaspp are palatable and nutritious and are very much cherished by goats, while Akoroda et al, (1990) supported staking because it facilitates harvesting of the

leaves and pods. Talfairiaoccidentalis is not the only crop that is staked. Staking is practiced on crops like yam (Philips, 1964, Onwueme, 1979), bean (Vignaspp) (Akobundu, 1987), cucumber (Kwarteng and Twoler, 1994) and tomato. In yam; staking has encouraged the yield in clayed soils (Aams, 2002) while it reduced the incidence of blossom end rot and fruit crack in tomato (Anyanwu et al, 1979). However, Amah (1997) conclude that staking increased the loss of yam production by 30 — 35%. The availability of staked for staking tendering / climbing vines are diminishing at an alarming rate as the result of factors of urbanization, road construction, industrialization, bush fire and harvesting for fuel wood.

3.2.5 Effect of Tillage and Staking on the Number of Flower Bud I Plant of Fluted Pumpkin

The result presented in Table 4 shows that there was a significant difference (p = 0.05) for number of flower bud / plant at both 10 and 12 WAP. At 4 WAP, treatment 1 (zero tillage / unstaked) had the highest number of flower bud/plant of 162, which was statistically different from treatment 3 (zero tillage / pyramidal staking) with number of flower bud / plant of 15.At 12 WAP, treatment 7 (mound tillage / unstaked) had the highest number of flower bud I plant while treatment 2 (zero tillage / individual staking) had the least with number of flower bud I plant of 66. At 10 WAP and 12 WAP there was no flower bud / plant formation at treatment 8 and 9. The highest number of flower buds was recorded at the unstaked plants.

3.2.6 Effect of Tillage and Staking on the Number of Flower I Plant of Fluted Pumpkin

The number of flower / plant formation as showed in Table 5 has a significant different (p= 0.05) among the treatments except treatment 4 (mound tillage /unstaked) at 12 WAP. Treatment 5 (mound tillage /individual staking) had the highest flower / plant of 36,which was statistically different from number of flower /plant among other treatment. Treatments 8 and 9 have
no flower formation.

3.2.7 Effect of Tillage and Staking on the Number of Aborted Flowers I Plant of Fluted Pumpkin

The number of aborted flowers/plant presented in Table 5 shows a significant treatment different (p =0.05) among all the treatments that produced flower.Treatment 5 (mound tillage / individual staking) had thehighest number of aborted flowers of 16 while treatment3 and 7 have the least.

3.2.8 Effect of Tillage and Staking on the Leaf Yield I Plant (G) of Fluted Pumpkin

The result obtained from the leaf yield of talfairia at 12 WAP shows a significant different (p = 0.05) among some of the treatments as showed in table 7. Telfairiaplants on mound —tilled soil have the higher leaf yield than those planted on zero and flat tilled plots. Treatment 5 (mound tillage / individual staking) has the highest leaf yield of 852.2. Individual staked plots have the highest leaf yield followed by pyramidal staked plots while the unstaked plots have the least. The staked plots have the higher leaf yield than the unstaked plots, this may due to the exposure of the vines which obtained more photosynthesis than the unstaked once.

3.2.9 Effect of Tillage and Staking on the Leaf Area Index (Lai) of Fluted Pumpkin

The measurement of leaf area index LAI of telfairia leaves started at 4 WAP. Result shows that at 4 WAP there was no significant difference but at 6 and 8 WAP, there is significant difference (p = 0.05) among some of the treatments. At 6 WAP, the leaf area index (LAI) measured of talfairia varied significantly among all the treatment except treatment 3 (zero tillage / pyramidal staking). Treatment 9 (that tillage / pyramidal staking) had the highest leaf area index of 2.44. Significant treatment difference were found in the leaf area index of telfairia leaves at 8 WAP among treatment 6 (mound tillage / pyramidal staking), 7 (fIat tillage/unstaked) and 8 G (flat tillage / individuals staking).

IV. CONCLUSION AND RECOMMENDATION

The results obtained in this research work provethat planting telfairiaoccidentalis on mound and stakedwhen the vines come up will give the highest vine length and leaf yield.

The complete breakdown of the result of the research showed that the vine length of talfairia planted on mound and staked is greater than those planted on flat titled and staked, greater than those planted on flat tilled and unstaked it is also greater than those planted on zero, staked and unstaked. Also the yield followed the same trend.

It is recommend that further research should be conducted on the effect of tillage and staking on the performance of talfairiaoccidentalis to ascertain whether panting telfairia on mound and staking will give better performance.Plantingof telfairiaoccidnetalis on mound followed by individual staking is the best for the performance of the crop.

REFERENCES

[1] Adams, A. R. 2002, School Certificate Agriculture,Benin City: Moonrise Publishing House.
[2] Asoegwu S.N. 1985, Effect of seed size and sex identification of fluted pumpkin (telfairiaoccidencalis).
[3] Akobunda, I. O. 1987, Weed science in the tropies principles and practice. New York: John Wiley and Songs.
[4] Akoroda, M. 0. 1988, Ethno botany of telfairiaoccidentalis(cucurbitaccae) among Igbos of Nigeria", Economic Botany, 44 (1):29 — 39.
[5] Akoroda, M. O. and Adejero, M. A. 1990, Pattern of vegetative and sexual development of telfairaoccidentalis tropical agriculture,67(3):243-247.
[6] Akoroda, M. 0. Ogbechie, Odiaka, N. I. Adebayo, M. I. Ugoro and B.Fuwa1989),. Flowering, pollination and fruiting in fluted pumpkin.
[7] Amah, B. A. 1997, Root crop production in Nigeria. Agbor; Loner publishing limited.
[8] Asiegbu, J. E. 1985, Effect of method of harvest and interval between harvestson edible leaf yield in fluted pumpkin Scientia Horticultural 21:129-136.
[9] Greensill, T.M. 1968. Growing better vegetable: aguide for tropical gardeners (Evans 4th impression)1976. Pp 80.
[10] Hall and Cannel 1979. Agriculture in semi aridenvironment.
[11] Lruvine, F.R. (1969). West Africa Crops. OxfordUniversity press London, pp. 321-328.
[12] Kwarteng, J. A and Towler, M.J. 1994. West Africa Agriculture.A textbook for school and college. London Macmillan.
[13] Lal, R. 1987.Tropical ecology and physical edaphology.
[14] Okoli, B.E and C.M Mgbeogu1982." Fluted pumpkinTelfairiaoccidentaliswest Africa vegetable" EconomicBotany, 3 (7): 145 — 149.
[15] Onweme, I. C (1979). The tropical tuber crop. New York: john Willey and Sons limited.
[16] Onyenuga, V. A. 1986. Nigerians foods and feeding stuffs. Their chemistry nutritional value. Ibadan University press.
[17] Phillips, T. A. 1964. An Agriculture textbook.Lagos Longmans.
[18] Stell, and Torrie, J. 11 (1980). Principles and procedure of statistics.A biometrics approach, 2nd Eds. M.C. Gram Hill Book Company, Inc New York.Pp 481, 633.
[19] Stevels, J.M.C 1990. Legumes Traditional duCameroon, Unee'tudeAgrobataniqu. WageningenAgriculture University paper 90.
[20] Stiono, K.R. 1953. Effect of fertilizer on the yield and vegetative growth of sweet potato" proceeding of the America Society of Horticultural Science, 61:367-372.
[21] Thompson, H.O and Kally, W. C. 1957. Vegetable crops 5th Ed. M.C Graw Hill Book.New York London.
[22] Tindall, H. D. (1968). Commercial vegetable growing London Oxford University press.
[23] Trenbath, B. R. (1976). "Plant interaction in mixed communities multiple cropping." America Society of Agronomy, 27: 68 — 75.
[24] Tsuna, Y and K. Fujise (1984). Studies on the dry matter, production of sweet potato. The relation between dry matter production and the absorption of Mineral Nutrients. Proceedings of crop science Japan, 32:297-300.

American Journal of Engineering Research (AJER) 2016
American Journal of Engineering Research (AJER)
e-ISSN: 2320-0847 p-ISSN : 2320-0936
Volume-5, Issue-2, pp-62-70
www.ajer.org
Research Paper Open Access

Effect of Some Indigenous Legumes on Soil properties and Yield of Maize Crop in anultisol in South-Eastern Nigeria

C. G Okeke[1], S.I. Oluka[1] and O. Oduma[2*]
[1]*Department of Agricultural and Bio-resources Engineering, Faculty of Engineering, Enugu State University of Science and Technology, Enugu, Nigeria*
[2]*Department of Agricultural and Bio-resources Engineering, College of Engineering and Engineering Technology, Michael Okpara University of Agriculture, Umudike, Nigeria*

ABSTRACT: *The effects of some leguminous cover crops on soil properties and yield of maize grown on an ultisol in Enugu, Southeast Nigeria were evaluated. Five treatments comprising of Africa Yam bean, velvet bean, pigeon pea maize and bare soil were laid out in an RCB Design, replicated three times. At 90 DAP, plant height (cm) and leaf area index of maize were 187 (cm) and 39.1 cm. This was higher (P<0.05) compared to African yam bean by 54 and 86% respectively. African yam bean produced relatively higher nodule number (172) at 90 DAPS than pigeon pea which had 69. Result also indicated an increase in organic carbon% N-NH4% and N-N030% status between 30 — 90DAP in plots treated with legumes. At 90DAP, organic carbon and N-NH4, were low in bare plots (1.25 and 0.013%) when compare to plots treated with legumes. Bulk density mg/m^3 was higher (p.0.05) in maize plots at 90 DAP (1.35) than in Africa yam bean plots by 8%.Result of the study showed that average grain yield in African yam bean plots was higher 10.07 mg/ ha than in bare plots by 57%. Based on the above result, the African yam bean is highly recommended as an indigenous legumes species capable of improving fertility status of ultisols and yields of maize in South-Eastern Nigeria.*

Keywords: *Indigenous. Leguminous, soil properties, maize, ultisols.*

I. INTRODUCTION

Soil fertility decline is one of the factors limiting food production in the south-eastern part of Nigeria. Increased awareness by small holder farmers of the role of indigenous legumes as sources of food and fodder and for soil fertility improvement has stimulated research on the influence of herbaceous legumes in various soils and cropping system.Legumes have been extensively planted over the century mainly for food and for maintaining soil fertility (Anikwe, et al, 2003). As agriculture continues to develop in the tropics, soil fertility decline increase, thereby limiting food production. Smallholder framers in the study area have not been able to explore the new roles emerging for indigenous legumes in the new farming system. Such roles according to Anikwe et al (2003) include the continued expansion of pulse crops into infertile more stressful soils and exploration of new soil improving legumes which can retrieve lost nutrients from beyond the subsoil. Leguminous species achieve this by sourcing nitrogen (N) from the atmosphere through N_2 — fixation, nutrient pool and to capture available nutrients through their extensive root systems (Stanley et al, 2003).

One of the goals of sustainable agriculture lies in identifying a range of legumes that could be used in rotation with crops or inter-sown with them to improve the productivity of soil. Beckmann (2002) outlined some qualities which selected or identified soil improving legumes should possess and which make them adaptable and dependable in the farming system. The qualities include adaptability to local climate and soil type, quick establishment, ability to colonize an area and to cope with pests and disease in the local environment.

Farmers in Nigeria are experiencing lower maize yields due to a number of reasons viz, continuous cropping of maize, removal of field crop residue for feeding livestock, overgrazing and burning of stover in situ to ease ploughing which have resulted in the deterioration of both the physical and chemical properties of the soil (Onyango et al, 2001). According to Clement et al, (1998) legumes can be used in rotation with cereals or as green manures to compliment fertilizers particularly for subsistence farmers whose resources based are small. Some legume species (e.g. Mucuna spp) which have deep root systems help to alleviate compaction in intensively cultivated soils.

Rather than work on characterizing and selecting indigenous soil improving legumes for development and use in Africa, most effort are currently focused on introducing exotic varieties and use of fertilizers that have been proven in other environments. Exotic legumes find it difficult to persist in tropical environments. Thus, current research should be geared towards characterizing, selecting and using of soil improving legumes from a wide range of untapped genetic resources available in the tropics especially as this region holds one of the largest reserves of different kinds of legumes in the world (Anikwe et al, 2003).

The reason for carrying out this work is to enable farmers developed better practices on managing ultisols for optimal production using indigenous legumes. This will encourage the use of legumes as management strategy for replacement of fertilizers in soil fertility improvement. The objectives of this work was to study the effects of three indigenous soil improving legumes, maize and bar soil on soil properties and yield of subsequent maize crop in an ultisol in southeastern Nigerian.

II. MATERIALS AND METHODS

The study was carried out at the teaching and research farm of the federal college of agriculture Isagu. During two planting seasons the Teaching and Research Farm is located within Latitude 06°04 °N and longitude 08° 65° E southwest of the derived savannah zone of Nigeria. It has a pseudo — bimodal rainfall pattern from April to November, where July to August rainfall, which varies between 1700- 2060 mm, is received during April through the year. Humidity is quiet high, with the lowest levels (32%) during the dry season and the highest 80% in May- June as the rainy season begins. The soil is classified as a Tropaquept (Anikwe et al., 1999).

2.2 Field Methods

A total area of 137.75m^2 (14.5m by 9.5m) was mapped out for the experiment.

In the first season five treatments comprising three soil improving legumes, namely velvet bean (Mucuna Pruriens var cochinchensis), africa yam bean (Sphensostylis stenocarpa), and pigeon pea (Cajanue cajan); and maize (Zea mays L) and Bare Soil were laid out in the field using Randomized Complete Block Design (RCBD) with three replications. Each replication contained 5 plots, each plot measuring 2.5cm by 2.5m and demarcation by 0.5m wide pathway. The "Oba super 11" hybrid variety of maize was planted in the first planting season.

In the second planting seasons, maize was planted in all the plots using the "Oba supper 11" hybrid variety.

Maize, velvet beans, pigeon pea and African yam bean were planted manually at a spacing of 0.50m inter and intra row. Two seeds were planted per hole, which was later tinned down to one, two weeks after planting leaving each plot with 25 plants. Lost stands, were replanted within this period. 3 were weeded completely and left as 'bare soil' and no treatment applied on them throughout the first planning seasons.

The experimental area was kept relatively weed-free throughout the span of the experiment. Weeding was done at 3 weeks interval from planting date. 8.79 mg/ ha quantity of legume plant biomass was in corporated into the legume treated plots.

2.3 Data Collection.

The emergence count of all the crops were taken between 4-14 DAP (days after planting). Measurements for above ground biomass, leaf area index and plant height were recorded at 30, 60 x 90 DAP. Soil properties examined included bulk density; hydraulic conductivity, total porosity, organic carbon, ammonium nitrogen and nitrate nitrogen.

Since destructive sampling was employed, nodulation was checked at 30, 60 and 90 DAP. In the plots where legumes were planted, 3 plants were randomly selected and carefully lifted from the soil. The uprooted ones were cut at the base of their stems. Their roots saturated with water in a wash basin and the soil carefully and gradually washed, the roots were recovered in a wooden sieve, thereafter all the nodules were recovered, counted, even- dried and put in seed envelops.

2.4 Laboratory Methods

A composite soil sample (collected from 6 points in each plot) was analyzed in the laboratory. The physicochemical analyses of samples collected were carried out in the laboratory. However, Subsequent samples were collected from each plot at 30, 60, and DAP in the first planting season, which were analyzed in the laboratory for their organic carbon and nitrogen status. Total Nitrogen was determined using the procedure outlined by (Griffin, 1995). Particle size analysis was done by the Hydrometer method as described by (Gee and Bauder, 1986).

Ammonium was determined by the specific ion electrode method (Mulvaney, 1996). Organic carbon was determined by the Walkley and Black procedure described by (Nelson and Sommers, 1996). Available P, K, MgandPH were determined using the method described by (Eckert and Thomas 1995).

2.5 Data Analysis

Statistical analysis of data collected using analysis of Variance for a Randomized Complete Black Design (using F- LSD at P. 0.05) was carried out according to procedures outlined by Marray and Larry (1999).

III. RESULTS AND DISCUSSION

Table 1 Above Ground Biomass Yield (Mg Ha1) of three Soil Improving Legumes and Maize at 30, 60 And 90 DAP in the 2005 planting

Days after Planting	Above	Biomass	
Yield			
TREATMENT	30	60	90
Maize	2.7	4.0	5.3
Velvet bean	1.8	2.9	3.5
Pigeon pea	1.2	1.8	2.5
African Yam Bean	1.2	2.5	3.2
FLSD (p<0.05)	0.51	0.65	0.45

Table 2. Leaf area index of soil improving legumes and maize 2009 planting season.

TREATMENT	DAYS AFTER PLANTING		
	30	60	90
Maize	6.9	37.3	39.1
Velvet	3.8	15.9	19.9
Pigeon pea	1.25	10.9	11.1
African Yam bean	1.21	5.2	5.2
FLSD (p<0.05)	2.31	23.9	23.13

Table 3. Nodules numbers of three soil improving legumes (2009 plant season)

TREATMENT	DAYS AFTER PLANTING		
	30	60	90
Peagon pea	20	59	69
African	83	153	172
Velvet bean	42	102	105
FLSD (p<0.05)	32	41	48

Table 4: Effect of treatment on soil organic carbon, ammonium n and nitrate n (2009 cropping season).

	ORGANIC CARBON			N-NH_4 (%)			N-NO_3 (%)		
	30	60	90	30	60	90	30	60	90
Maize	1.27	1.23	1.25	0.015	0.012	0.15	0.012	0.019	0.012
Velvet bean	1.23	1.38	1.44	0.021	0.023	0.035	0.12	0.015	0.013
Pigeon pea	1.14	1.28	1.48	0.030	0.021	0.029	0.020	0.009	0.015
African yam bean	1.8	1.29	1.50	0.043	0.043	0.045	0.015	0.011	0.013
Bare soil	1.18	1.25	1.25	1.25	0.016	0.009	0.06	0.006	0.010
FLSD (P<0.05)	**0.05**	**0.07**	**0.06**	**0.04**	**0.019**	**0.009**	**0.019**	**0.007**	**0.017**

Table 5: Effect of treatments of soil bulk density, saturated hydraulic conductivity and total porosity (2009 planting season).

	BULK DENSITY (MG M^{-3})			HYDRAULIC CONDUCTIVITY			TOTAL POROSITY		
TREATMENT	30	60	90	30	60	90	30	60	90
Maize	1.22	1.26	1.30	54	41	23	54	53	51
Velvet bean	1.21	1.23	1.26	43	39	39	55	54	52
Pigeon pea	1.21	1.24	1.26	41	38	38	54	53	52
African yam bean	1.24	1.23	1.24	39	49	36	55	54	53
Bare soil	1.24	1.34	1.35	25	21	23	53	49	49
FLSD (P<0.05)	**0.02**	**0.03**	**9.16**	**8.5**	**9,54**	**Ns**	**3.5**	**3.2**	

Table 6. Plant height of maize (cm) (2010 planting season)

TREATMENT	**DAYS**	**AFTER**	**PLANTING**
	30	60	90
Maize	47.3	67.3	83.0
Velvet bean	88.3	151.0	184.3
Pigeon pea	80.0	104.0	122.0
African yam bean	105.0	192.3	212.0
Bare soil	45.0	65.0	96.0
FLSD (P<0.05)	14.8	14.04	8.19

Table 7 Leaf Area Index Of Maize At 30, 60 And 90 Dap In 2009

TREATMENT	**DAYS**	**AFTER**	**PLANTING**
	30	60	90
Maize	9.04	18.1	20.0
Velvet bean	22.0	38.4	38.3
Pigeon pea	22.4	37.4	40.0
African yam bean	39.0	67.0	75.0
Bare soil	6.7	16.3	17.0
FLSD (P<0.05)	**7.07**	**6.24**	**5.47**

Table 8 Seed of Maize (mg/ha) And Stover Weight At 90 DAP in 2006.)

Cob dry weight (Mg ha^{-1})	**Grain yield (Mg ha^{-1})**		**Stover weight (Mg ha^{-1})**
Maize	5.72	4.55	8.79
Velvet bean	7.84	6.25	9.59
Pigeon pea	6.57	5.3	9.32
African yam bean	10.81	10.07	12.91
Bare soil	5.3	4.24	2.36
FLSD (P<0.05)	**3.81**	**3.39**	**2.36**

4.1 ***Above Biomass Yield (mg/ ha) of Three Soil Improving Legumes and Maize at 30, 60 and 90 DAP in the 2005- Planting Season.***

Results of the study indicated differences (P < 0.05) in the above ground biomass production of three soil-improving legumes and maize at 30, 60 and 90 DAP (Table2).At 30 DAP, result showed that maize produced the highest (P< 0.05) above ground biomass with Mg ha'. maize plants biomass was significantly higher (P< 0.05) than velvet bean above ground biomass (1.8 Mg ha1). Similarly, the above biomass produced by maize was higher (P<0.05) than that produced by pigeon pea (1.2 Mg ha1) by 33%. Result also shown that the above ground biomass produced by maize was significantly higher (p< 0.05) than the above ground biomass produced by African yam bean (1.2 mg ha^{-1}) by 55%.

At 60 DAP; the results followed the same trend as for the 30 DAP. Maize crops produced the highest quantity (P< 0.05) of above biomass (4.0 Mg ha^{-1}) when compared with African yam bean, which had d2.5 Mg ha^{-1}. This was higher than that of velvet bean (2.9 Mg ha^{-1}) and pigeon pea (1.8 Mg ha^{-1}) by 27.5 and 50% respectively. Pigeon pea had the lowest above ground biomass of 1.8 Mg ha1.

At 90 DAP, the result of the study showed significant differences in the above ground biomass of the treatments. The result indicated significant increase in the above ground biomass produced by African yam bean (3.2 Mg ha^{-1}) and velvet bean (3.5 Mg ha^{-1}) when compared to the above biomass produced by both crops at 30

DAP. Maize produced 5.3 Mg ha^{-1} of above ground biomass at 90 DAP and was significantly higher ($p< 0.05$) compared to that produced by pigeon pea. Pigeon pea produced the lowest quantity of above ground biomass of 2.5Mg ha^{-1} 90 DAP.

This result indicated that maize, which usually is a row and erect crop established early and had more above ground biomass ay 30 DAP. This perhaps indicated the availability and utilization of N, which promotes rapid growth in maize crops. Velvet bean and African yam bean established more ground cover at 69 and 90 Dap. This perhaps indicated greater nutrient accumulation, retention and soil moisture conservation in legume treated plots. This increases in the above ground biomass of legume probably led to a reduction in the impact of sunshine, which causes scorching and N volatilization.

4.2 ***Leaf Area Index of Soil Improving Legumes And Maize (2009 Planting Season)***

The result of the significant difference ($p<0.05$) in the leaf area index (LAI) treatments.

At 30 DAP African yam bean had the lowest ($p<0.05$) leaf area index of 1.21 while pigeon pea velvet bean had higher values of (1.25) and (3.8) respectively. The result also indicated that maize plants had the highest ($p<0.05$) leaf area index than African yam bean (1.21) and pigeon pea (1.25) by 82% and 45% respectively.

The result indicated no significant difference in the leaf area index of African yam bean and pigeon pea. Similarly, the result shown a significant increase (68.2%) in the leaf area index of velvet bean compared to African yam bean which had leaf area index of 1.21.

Maize plants had the highest leaf area index of at 60 DAP 37.3 and this was significantly higher ($p<0.05$) than leaf area index of velvet bean (15.9) and pigeon pea (10.9) by 57.3 and 7l% respectively. African yam bean produced the smallest leaf area index of 5.2 when compared with maize and velvet bean this was significantly lower leaf area index of both maize (37.3) and velvet bean (15.9) by 59 and 80%. Africa yam bean plots had the lowest ($p<0.05$. leaf area index obtained from plots where maize were planted (39.1) by 88%. The result of the study also showed that velvet bean pea plots had plants which produced leaf area index of 19.9 and 11.1 and were significantly lower ($p<0.05$) than the leaf area index of maize (39.1) by 49 and 72% respectively.

No significant increase in the leaf area index of maize was found between 60 and 90 DAP was statistically the same and also, that there was no significant increase in the leaf area of pigeon bean between 60 and 90 DAP.

There was a significant increase in the leaf area index of maize and velvet bean between 30 and 90 Dap, leaf area index of maize increased from 6.9 at 30 DAP to 39.1 at 90 DAP, leaf area index of velvet bean increased from 3.8 at 30 DAP, to 19.9 at 90 DAP by 80 and 82% respectively.

The result of the study also showed significant increase in the leaf area index of pigeon pea between 30 and 90 DAP, (1.25 and 11.1) by 89%. The result also indicated that the leaf area index of African yam bean at 30 and 90 DAP were 1.21 and 5.2, indicating a significant difference of 77%.

The result of the study showed that the increase in the leaf area index of maize between 30 and 90 DAP more than the soil improving legumes was a result if increase of its growth parameters including leaf numbers, area height.

4.3 Nodule number of three soil improving legumes (2005 planting season).

Results of the study indicate significant differences the number of nodules produces by the three sc1 improving legumes at 30,60and 90 DAP, the result of the study indicate that low number of nodules were obtained from pigeon pea plots (20) and this was significantly lower ($p<0.05$) than that obtained from velvet bean plots (42). The result also showed that higher number of nodules were obtained from African yam bean plots (83). This was significantly higher ($p<0.05$). Than nodule number obtained from pigeon pea plots by 76%.

African yam bean produced higher number of nodules (153 nodules) at 60 DAP. The result also indicated that the total number of lower when compared to that produced by velvet bean which was on the medium range (102).

The smallest number of nodules were obtained at 90 DAP plots where pigeon pea were planted (69). The result followed a similar trend as velvet bean plots produced a total number of 105 nodules. The result also showed that the higher number of nodules was obtained from plots where plots where African yam bean were planted with a total number of 172 and when compared with velvet bean and pigeon pea, they differ by 39 and 60% respectively.

Significant treatment differences were indicated in the number of nodules obtained from each soil improving legume. The result indicated that African yam bean produced a total number of 408 nodules, velvet bean produced a total of 249 nodules and pigeon pea bad 148 nodules. These differ by ($p<O.05$) by 45 and 68% respectively.

Pigeon pea plots which produced 20 nodules increased to 69 nodules at 90 DAP. Velvet bean plots which produced 42 nodules at 30 DAP increased to 105 nodules at 90 DAP. The result also showed that at 30 DAP, African yam bean plots produced 83 nodules which increased to a total of 172 nodules at 90 DAP.

The variation in nodulation amongst the soil improving legumes may reflect their different capacities for growth under the same or varying edaphic and environmental conditions. The result show that if legumes are to be used as relay crops, species like sphenostylis stenocarpa and cajanus are selected for the benefit of subsequent crops.

4.4 Effect of treatment on soil organic carbon, ammonium and nitrate (2005 cropping season).

Result of the study indicated that the various treatments significantly affected the organic carbon contents of the study soil (table 4). At 30 DAP, the percentage organic carbon content was significantly higher (P<0.05) in maize plot (l.27%) when compared to plots planted with three soil improving legumes, velvet bean (l.23%), pigeon pea (1.14%) and African yam be (1.18%) by 3, 7 and l0% respectively.

Bare soil had organic carbon contents of l.l8%, this was lower than that in maize plots and velvet bean plots by 4 and 7% respectively.

The organic carbon level in bare plots increased to 1.25% at 60 DAP. The also showed a significant increase (P<0.05) in the organic carbon level in plots where African yam bean were planted (l.29%) when compared to the organic content at 30 DAP l.l8% and they differ by 8.5%. the result of the study also showed that the organic carbon content of maize plot was reduced by 3.l%. The result also showed that the organic carbon level in plots where velvet bean were planted increased, to l.38% and pigeon pea plots (1.28%) by 7.2%.

There was a significant difference in the organic carbon levels with treatments at 90 DAP. The highest organic carbon levels was obtained from plots where African yam bean were planted (l.50%), this wassignificantly higher (P<005) when compared with the organic carbon status obtained from bare plots (1.25%) by 16%. The result also indicated no significant in organic carbon content at 30 and 90 DAP in plots where maize as planted. The result of the study also showed increase organic carbon levels in plots with velvet bean and pigeon pea (1.44 and 1.40%).

Significant differences were recorded in ammonium nitrogen levels in all the plots (Table 4). The result showed that the ammonium nitrogen level obtained in African yam bean plots was 0.30% which was significantly higher (p<0.05) than ammonium nitrogen (N-NH4) status of bare plots (0.0l3%) by 95%. The result also indicated that the ammonium nitrate level in maize plots was 0.0l5%. However, no significance was found between ammonium nitrogen status of maize and bare soil spots. Results also indicated that the ammonium nitrogen levels of velvet bean and pigeon pea plots were 0.025% and 0.020% respectively. At 60 DAP, the result of the study followed a similar trend as the ammonium nitrogen level in African yam bean plots increased to 0.043%. this was significantly higher (P<0.05) that the percentage N — NH4 obtained from maize plots (O.0l2%) by 72%. The result atsc showed that the ammonium nitrogen level of bare plots was the same as that the ammonium nitrogen level of bare was the same as that obtained at 30 DAP and this was significantly lower (P<0.05) when compared with the ammonium nitrogen status of velvet bean and pigeon pea plots by 38 and 48% respectively. The result indicated no significant treatment difference between the ammonium nitrogen levels obtained from maize plots and bare plots.

There was significant difference (P<0.05) in ammonium nitrogen level of maize plots and bare plots at 90 DAP. The result showed that the ammonium nitrogen level of maize plot (0.0l5%) was significantly lower (P<0.05%) when compared to that in velvet bean and pigeon plots (0.035 and 0.029) by 14, 48 and 57% respectively.

Ammonium nitrogen (N — NH4) status was significantly higher in African yam bean plots (0.045%) when compared to other soil improving legumes. The result also indicated no significant increase in ammonium nitrogen status of maize plots between 30 and 90 DAP and also in bare plots between 30 and 90 DAP.

The result of the study indicated significant difference in the nitrate nitrogen (N — N03) levels of various plots (Table 4). Nitrate nitrogen status of plots which was left bare (bare soU) was O.0O9% at 30 DAP. This was significantly lower (P.<0.05) when compared with the level of nitrate nitrogen obtained from pigeon pea plots (0.020%) by 55%. The result also showed that the nitrate nitrogen contents of velvet bean and African yam bean plots were statistically comparable at 30 DAP.

Nitrate nitrogen level decreased in the bare plots (0.006%) at 60 DAP. It however, indicated that there was an increased (P<0.05) the nitrate nitrogen level in maize plots (O.Ol9%) when compared to its level at 30 DAP. On the contrary, there was a significant decrease in N - N03 level in pigeon pea plots (0.009). The result indicated no significant difference in the nitrate nitrogen levels of velvet bean Africa yam bean plots at 60 DAP.Nitrate nitrogen levels of velvet bean and African ya' bean plots were statistically comparable at 90 DAP. The result also indicated that the nitrate nitrogen level in maize plot (0.012%) was lower than its level at 60 DAP. Results also showed no significance difference between the nitrogen level of pigeon pea and velvet bean plots.

The three soil improving legumes were able to increase the contents of organic carbon, NH4 — N and N03 - N of the study soil, whereas maize crops depleted the contents of same properties. This considered most promising plant-bacteria association. This association can lead to an increase in yield of crops through biological Non fixation in the tropics (Onyangu et al 2001). The nutrient level in maize plots was low. This may be because of high utilization capacity of N by maize.

4.5 Effect of treatments on dary bulk density, saturated hydraulic conductivity and total porosity (2009 planting season).

The bulk density in plots which were left bare (1.24 Mg m^{-3}) was higher ($p<0.05$) than the bulk density in other plots. The result also showed that in maize an velvet beanplots, bulk density by 2 and 4% respectively. The result also indicated that the bulk density of African yam bean and pigeon pea plots were statistically comparable.

The bulk density of maize plants at 60 Dap (1.26Mg m^{-3}) increased relative to its density at 30 DAP. The result also indicated that bulk density in velvet bean (1.23Mg m^{-3}) were statistically comparable. Bare soil had the highest ($p<0.05$) bulk density of (1.34Mg^{-3}).

Maize and velvet bean plots each had bulk density of 1.30 and 1.26Mg^{-3} at 90 DAP respectively and they differ by 3.l%. The result also shown that African yam bean plots had the lowest ($p<0.05$) bulk density of 1.24Mgm^{-3} and also, bare soil had 1.35 Mg m^{-3} and they differ by 8%. Bulk density of maize and bare plots were marginally higher, this could be due to direct raindrop impact energy led soil compaction. Maize is also a row crop and may not relate achieve as much ground cover as legumes. Bulk density is treated with legumes were lower. This could be that the ground biomass of the legumes covered more soil surface helped to reduce raindrop impact energy and degree of ability which are factors that increase soil dry bulk density were all, 2003).

The hydraulic conductivity (Ksat cm^{-3}/h) in maize plots was 8cm/h at 30 DAP. Result also showed that the Ksat of velvet in (42.72cm^{-2}/h) and pigeon pea plots (41.03cm^{-3}/h) were statistically comparable. Result also showed that African yam bean is (38.96^{-3}/h) had higher ($p<0.05$) Ksat than bare plots (25.05cm) by 36%.

A decrease in the Ksat of most plots was recorded at 60 DAP receipt in African yam bean plots which had 48.52cm^{-3}/h. the result so showed that the lowest ($p<0.05$) Kast was recorded in bare plots (20.70cm^{-3}/h) and the highest Ksat was ($p<0.05$) in maize plots (10.52cm3/h) and they differ by 49%.

At 90 DAP, the Ksat (cm^{-3}/h) of maize plot decreased to 24.72cm^{-3}/h.

This suggests that the increase in Ksat in some plots at 30 and 60 DAP was due to more macro pore spaces usually determined by texture and structure. Soils with stable granular structure usually have higher saturated conductivities then those with unstable structural units,which break down upon being wetted (Brady and weil,1996).

Total porosity in maize plots was 53.9% at 30 DAP. This was higher than the total porosity in bare soil 53.2%. Result also showed that the highest ($p<0.05$) when compared to the total porosity of bare soil by 3%.

The highest ($p<0.05$) total porosity at 60 DAP obtained velvet bean (53.5%) and African yam bean (53.5%) plots which were statistically comparable. The result also showed that bare plots had 49.4% and maize plots 52.5% and they differ by 8 and 2% respectively when compared to the total porosity (%) in African yam bean plots.

The total porosity of velvet bean (52.4%) and pigeon pea (52.4%) at 90 DAP were also statistically comparable. The result also indicated that bare soil had the lowest ($p<0.05$) total porosity 49.l% and differs by 4% when compared to the total porosity obtained in maize plot (50.9%). African yam bean and pigeon pea plots had a porosity of 53.2 and 52.4% respectively.

Total porosity (%) which was high in some of the plots could have been due to low amount of ground covers and high saturated hydraulic conductivity in those plots. This perhaps led to increased infiltration and nutrient leaching. The soil macropores characteristically allow the ready movement of air and the drainage of water. High porosity depletes the soil of croups (Roldan et al 2003).

4.6 Plant Height of Maize (2006 Season).

The various treatment significantly affected plant height of maize at different number of days planting (Table 6).Tallest maize plants with plant height of 105 cm were found in plots with African yam bean (AYB) in the previous season. Maize plants in this plot were significantly taller than that found in plots without any treatment (bare soil) in the previous season which had plant height of 45cm (the lowest plant height). Similarly, maize plants in plots planted with African yam bean (AYB) in the previous season were taller ($p<0.05$) than those planted with velvet bean, pigeon pea and maize by 15,23, and 55% respectively.The result followed a similar trend as plots with African yam bean in the previous season with plant height of 192cm had maize plants that were significantly taller that plants with velvet bean (51cm), bare soil (56cm) representing 21,46,65 and

66% respectively. However no significant treatment differences in plant height of maize was found between plots left bare in the previous season and those planted with maize in the previous season.

Plots planted with African yam bean in the previous season were taller (P<O.05) than maize plants found on plots previously planted with velvet bean, pigeon pea and maize in the previous season by 13, 42, and 75% at the 90 DAP. Similarly. Result also show that maize plants in plots that were left bare in the previous season were no taller (P<0.05) than those where pigeon pea was planted in the previous season.

Maize plants in plots which were left bare in the previous season sere relatively shorter than maize plants in plots where the three soil improving legumes were planted previously. This can be attributed to low level accumulation of organic matter in the bare plots leading to poor performance of maize was plants therein. Similarly, maize plants in plots where maize was previously planted were shorter (P<0.05). This may also be attributed to the minimal levels of nutrients in the plots planted previously with maize. Maize is a heavy feeder and removes more nutrients from the soil (Caporali et al 2004).

This may be as a result of improvement made by these legumes on those plots by their legumes rhizobia symbiosis. Organic matter accumulation and increase in soil N may also have contributed to greater plant height of maize crops in legume treated plots.

4.7 Leaf Area Index (Lai) Of Maize (2006 Planting Season).

The leaf area index (LAI) of subsequent maize plants was affected significantly at different times after planting by the various treatments.At 30 DAP, the highest (P<0.05) leaf area index of maize plant (39.0) was recorded in plots where African yam bean was planted during the previous season.The leaf area index of maize plants in plots which were left bare during the previous season (2009) was not higher (P<0.05) than those where maize was planted in the previous season.

The result also followed a similar trend at 60 DAP as plots with African yam bean in the previous season (2009) had leaf area index of 67.0, this was significantly higher than the LAI of maize plants in plots where velvet bean (38.4), pigeon pea (37.4) and maize (18.1) were previously planted by 42, 44 and 72% respectively. Result also showed that the area indices of maize plants found in plots where African yam bean was previously differ by 76Io. However, no significant treatment difference in LAI of maize was found between plots previously left bare an those planted with maize in 2005.

Plots treated with African yam bean originally 2009 had higher (P<0.05) leaf area index (75.8) than maize plants found on plots previously planted with velvet bean (38.3), pigeon pea (40.0) and maize (20.0) by 47, 49 and 73% respectively. Similarly, results indicated that the LAI of maize plants in result which were left bare in 2009 was not higher (P<0.05) than the LAI of maize plants in plots previously planted with maize. The plots treated with African yam bean in 2009 produced subsequent maize plants with high leaf area indices. This may be ascribed to the fact that AYA improve the soil tremendously by increasing the levels, of organic matter ammonium nitrogen and nitrate nitrogen in those plots. Result also showed that plots left bare in 2009 and plots treated with maize in 2009 were statistically comparable. Both heights and their LAT were lower (P<0.05) compared with AYB, pigeon pea and velvet bean plots. This may be because decomposable organic carbon which would have been maize taken up by maize and because maize may have absorbed low LAI in 2006.

4.8 Seed Yield of Maize (Mg Hk1) And Stover Weight (mg/ha) at 90 DAP.

The result of the study showed that the different treatments significantly affected cob dry weight, seed yield and stover weight of maize at 90 DAP (Table 8).

The cob dry weight at 90 DAP was significantly higher (P< 0.05) in plots where african yam bean was previously planted. Dry cob weight of maize found in plots which were left bare in 2005 which had 5.3 mg/ha, (the lowest cob dry weight). Similarly, cob dry weight of maize plant in plots previously treated with african yam bean higher (P<0.05) than in plots where velvet bean (7.84), pigeon pea (6.57) and maize (5.72 Mg ha1) were previously planted by 22, 39 and 47% respectively. Results showed that dry weight of maize plants in plots left bare during the previous planting season (2005) were not higher (P<0.05) than that where maize was plant in the previous season (2005). Grain yield obtained from plots where African yam bean planted in the previous year was 10.07 (Mg/ ha). This was significantly higher than grain yield in plots where bean (6.25 mg/ ha1), pigeon pea (mg/ ha) and maize 55mg/ ha) were planted in the previous year by 37, 50 and 55% respectively.

The lowest quantity of grain yield was obtained in plots which were left bare in the previous season, (4.24 Mg ha1). The result showed that this significantly lower (P<0.05) than grain yield from plots which maize were planted in the previous season

The result followed a similar trend for stover weight (Mg ha1) as stover yield was higher (P<0.05) in plots were African yam were planted in 2005. Results showed that maize plants in AYB plots has stover weight of 17.91 Mg/ha, and this was significantly higher than stover weight in plots where velvet bean (9.59), pigeon pea (9.32) and maize (8.79) were planted in the previous season by 47, 50 and 91% respectively.

Stover weight in plots which were left bare during the first season were not higher ($P<0.05$) than those where maize was planted in the previous season. Indications from the results showed that plots treated the African yam bean during the previous season had higher stover weight than all other plots.

IV. CONCLUSION

In this study, the three indigenous legumes uses the experiment improved the soil fertility levels white maize depleted soil fertility. Fertility remained virtually stagnant in the plots left bare.

However, sphenostylis stenocrapa (African yam bean) improved some of the soil properties more than Mucuna cochinchinensis and Cajanus cajan. This led to an increase in both grain yield and stover weight (mg ha1) in plots where sphenostylis stenocarpa were planted in the previous planting season.

Growth parameters of subsequent maize crop were highly improved in plots where sphenostylis stenocarpa and Mucuna pruriens yarn cichinchinesis were planted previously. On the contrary, results showed that subsequent maize crops in plots found to have lower height, left area index (LAI) and yield.

It is therefore, highly recommended that indigenous legumes especially African yam bean (S. stenocarpa) and Velvet bean (M. pruriens Var. cochichinensis), in this order used by maize growers and mostly smallholder farmers in South- Eastern Nigeria area where predominant SHS ulitisols. It is also recommended that S stenocarpa d Velvet bean Var. cochinchinensis be used in relay cropping or incorporated as green manure in ultisols especially when maize or other cereal crops are to be planted subsequently.

REFERENCES

[1] Anikwe, M.A.N, Okonkwo, C.I., 2003. Nodulato Effectively, N Accumulation and Yield of Soyabean (Glycine max) in a Clayloam soil treated with Pre and pose- Emergence Herbicides. Trpcultura, 21, 22- 27.

[2] Anikwe, M.A.N., Okonkwo, C.I., and Aniekwe, N., 1999. Effect of changing land use on selected soil properties in Abakaliki agro- ecological zone of South- Eastern Nigeria. Environ. Edu. And Info. 18:79- 84.

[3] Beckamnn, R., 2002. Legumes offer a ray of hope in South Africa. Partners in Research for Development No.15. Australian Centre for internati-onal Agricultural Research, pp 114- 136.

[4] Caporali, E., Caporali F., Marcinelli R., 2004. Maize Performances as influenced by winter cover- crop. Green Manuring. Ital.J. Agron., 8,1,37-45.

[5] Clement, A., Jagdish, K., Ladha, Chalifour, F.P., 1998.Nitrogen dynamics of green manures, Species andrelationships to lowland rice production. Agron. J 90:149-154.

[6] Eckter, D., and Thomas. S.J., 1995. Recommended Soil pH and Lime Requirement tests. P.11-16. in J. Thomas Sims and Wolf A. (eds) Recommended Soil testing procedures for the Northeastern United State. Regional

[7] Bulletin H493. Agric. Exp. St. University of Delaware, Netwark DE.Elschler, M, 1997. Legume Green Manures in the management of maize-bean cropping systems in Eastern African with special references to crotobria (C. OcholenceG. Don.) PhD thesis No. 120.99 ETH. Swiss federal institute of Technology, Zurich.

[8] Gee, G.W., and Bauder, J.,W., 1986. Particle size analysisP. 383 — 411. in Kiute A.(ed). Methods of Soil analysispart. Physical and mineralogical methods. AgronomyMonograpy H9 (21c Edition). Amer. Sub

[9] Agron, MadisonWi.

[10] Griffin, C., 1995. recommended Soil Nitrate 1 testing procedures of the Northeastern United State Northeast N. Tests. P.P 17 — 24 in Thomas J. S Sims and Regional Bulletin H493. agric Expt, station, Wolf A. (eds) University of Delaware, Nermark, DE.

[11] Mulvany, R. L 1996. Nitrogen-inorganic in Sparks D. LMethods of soil Analysis, forms P. 1123-1200 part 3chemical methods. SSSA Book Series Number 5. am Soc ofAgron Madison W.I.

[12] Murray, R., and Larry, J. S. 1999. theory and Problems of statistics the McGraw- Hill Companies mc, USA.

[13] Nelson, D. W and sommers. LE 1996. Total Carbon organic carbon, and organic matter p. 961-1010 in sparks D. L (ed). Methods of soil Analysis, Part 3 chemical method, SSSA Book series No 5 an soc of Agron, amdison W.I.Onyango, M. A Nwangi, K., N' gency, M Luazalu,E., and Barkutwo, K. J 2003.

[14] effect of Relaying Green Manure Legumes on yields of intercropped maize in smallholder froms of trans Nzoia district Kenya. 7th eastern and southern African regional maize conference pp.330-334.

[15] Roldan, A., F., Caravaca, M/T! Hernandex, C., Gracia, C. Sanchex Brito, m.

[16] Velasquez and M. Tiscareno. 2003 Notillage, crop residue additions, and legume cover cropping effects on soil quality characteristics under maize inPatzcuaro watershed (Mexico), Soil Tillage Res. 72 pp. 67 - 73.

American Journal of Engineering Research (AJER) 2016
American Journal of Engineering Research (AJER)
e-ISSN: 2320-0847 p-ISSN : 2320-0936
Volume-5, Issue-2, pp-71-76
www.ajer.org
Research Paper Open Access

Design and Development of Mobile Phone Jammer

Oyediran Oyebode Olumide[1], Ogunwuyi Ogunmakinde Jimoh[2], Lawal Akeem Olaide[3]
[1]*Department of Computer Engineering, Osun State Polytechnic Iree, Osun State, Nigeria*
[2,3]*Department of Elect/Elect, Osun State Polytechnic Iree, Osun State, Nigeria*

Abstract: *This paper presents the design, implementation, and testing of a dual-band mobile-phone jammer. This jammer works at GSM 900 and GSM 1800 simultaneously and thus jams the four well-known carriers frequency in Nigeria (MTN, GLO, AITEL and ETISALAT). This paper went through two stages: Stage one: studying the GSM-system to find the best jamming technique, establishing the system design and selecting suitable components. Stage two: buying all the needed components, drawing the overall schematics, assembling the devices on a well known Veroboard, performing some measurements and finally testing the mobile jammer. The designed stage consist of voltage controlled oscillator, noise generator and Radio Frequency Amplification. MATBLAB Simulink 8.4 was used for the simulation of the frequency oscillator, On Running the simulation, and observing the output of the scope, a signal whose carrier repeatedly moves from 10.6927 to 10.9786 MHz was observed . We can see that the result was a signal at frequency RF covers the whole downlink The designed jammer was successful in jamming the four carriers in Nigeria operating on EDGE or 2G network*

Keywords: *GSM900, GSM1800, Jammer, Airtel, MTN, GLO, MATLAB, RF*

I. Introduction

Mobile jammers were originally developed for law enforcement and the military to interrupt communications by criminals and terrorists to foil the use of certain remotely detonated explosives. The civilian applications were apparent with growing public resentment over usage of mobile phones in public areas on the rise & reckless invasion of privacy. Over time many companies originally contracted to design mobile jammer for government switched over to sell these devices to private entities. As with other radio jamming, mobile jammer block mobile phone use by sending out radio waves along the same frequencies that mobile phones use. This causes enough interference with the communication between mobile phones and communicating towers to render the phones unusable. Upon activating mobile jammer, all mobile phones will indicate "NO NETWORK**".** Incoming calls are blocked as if the mobile phone were off. When the Mobile jammers are turned off, all mobile phones will automatically reestablish communications and provide full service. Mobile jammer's effect can vary widely based on factors such as proximity to towers, indoor and outdoor settings, presence of buildings and landscape, even temperature and humidity play a role. The choice of mobile jammers are based on the required range starting with the personal pocket mobile jammer that can be carried along with you to ensure undisrupted meeting with your client or a personal portable mobile jammer for your room or medium power mobile jammer or high power mobile jammer for your organization to very high power military jammers to jam a large campuses.

II. Related Works

The rapid proliferation of mobile phones at the beginning of the 21st century to near ubiquitous/ever present status eventually raised problems such as their potential use to invade privacy or contribute to rampant and egregious academic cheating. In addition public backlash was growing against the intrusive disruption cell phones introduced in daily life. While older analogue mobile phones often suffered from chronically poor reception and could even be disconnected by simple interference such as high frequency noise, increasingly sophisticated digital phones have led to more elaborate counters. Mobile phone jamming devices are an alternative to more expensive measures against mobile phones, such as Faraday cages, which are mostly suitable as built in protection for structures. They were originally developed for law enforcement and the military to interrupt communications by criminals and terrorists. Some were also designed to foil the use of certain remotely detonated explosives. The civilian applications were apparent, so over time many companies originally contracted to design jammers for government use switched over to sell these devices to private entities. Since then, there has been a slow but steady increase in their purchase and use, especially in major metropolitan areas.

2.1 **Mobile Telephone Service (1946- 1984):** This system was introduced on 17th of June, 1946. Also known as Mobile Radio-Telephone Service. This was the founding father of the mobile phone. This system required operator assistance in order to complete a call. These units do not have direct dial capabilities.

2.2 **Improved Mobile Telephone System (1964-present):** This system was introduced in 1969 to replace MTS. IMTS is best known for direct dial capabilities. A user was not required to connect to an operator to complete a call. IMTS units will have a keypad or dial similar to what you will find on a home phone.

2.3 **Advanced Mobile Phone System (1983-2010):** This system was introduced in 1983 by Bell Systems; the phone was introduced by Motorola in 1973 and released for public use in 1983 with the Motorola 8000. Advanced Mobile Phone System (AMPS) also known
as 1G is an improvement of IMTS.

2.4 Block diagram

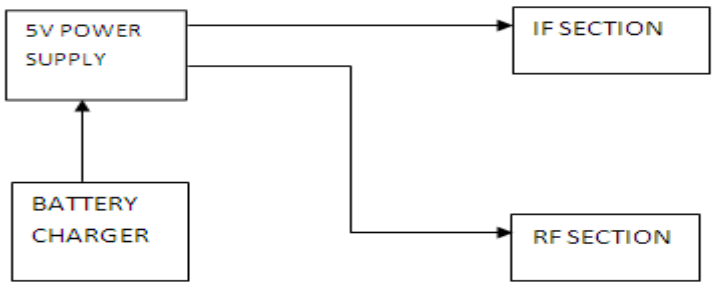

Figure 1: Block Diagram of Mobile Phone Jammer

2.5 Voltage Controlled Oscillator

A voltage controlled oscillator (VCXO) generates radio frequency (RF) signals that will interfere with the cellular phone signal. A VCXO uses an input voltage to determine its oscillation frequency. It can also receive a changing voltage to produce an oscillation with modulated frequency. VCXOs can be harmonic or relaxation types. Harmonic VCXOs produce sinusoidal waveforms; they have greater stability than relaxation VCXO over changes in noise, power supply and temperature. They also posses greater frequency control. Relaxation VCXOs produce triangular shaped waveforms.

At the heart of the RF jammer is a VCO, the device that generates the RF signal which will interfere with the cell phone, GPS receiver, etc. There are three selection criteria for selecting a VCO. Firstly, it should cover the bands that a user wants to jam.

a. Noise Generators

Noise Generator Circuit (NOISE): A noise generator is a circuit that produces electrical noise which is a random and non-deterministic signal. A lot of overlooked systems are noise sources; these include a rowdy room with everyone talking at different pitches (frequency), loudness (amplitude) and so on. A simple microphone as a transducer can be used to pick up such signals. In the field of electronics though, noise can be generated by different means. This includes a resistor exhibiting thermal noise (heated resistors), a Zener diode (exhibiting avalanche effect), temperature limited vacuum diodes, special circuits and gas discharge tubes. This project uses a zener diode in reverse bias, turning the zener diode to exhibit avalanche effect which is a noise generator and industrial (man-made) noise readily in the environment.

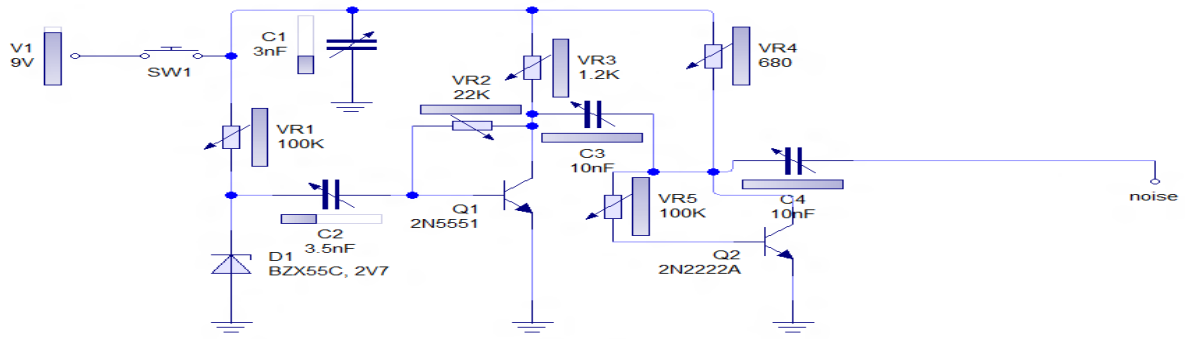

Figure 2: Noise circuit with zener diode in reverse bias.

III. Methodology

3.1 Power supply and Cooling Unit

Power system: The power system comprises of all subsystems working together to produce desired voltage levels which drive various circuit sections of the jammer. These include; Bridge rectifier, filter circuit, voltage regulators, and fuse.

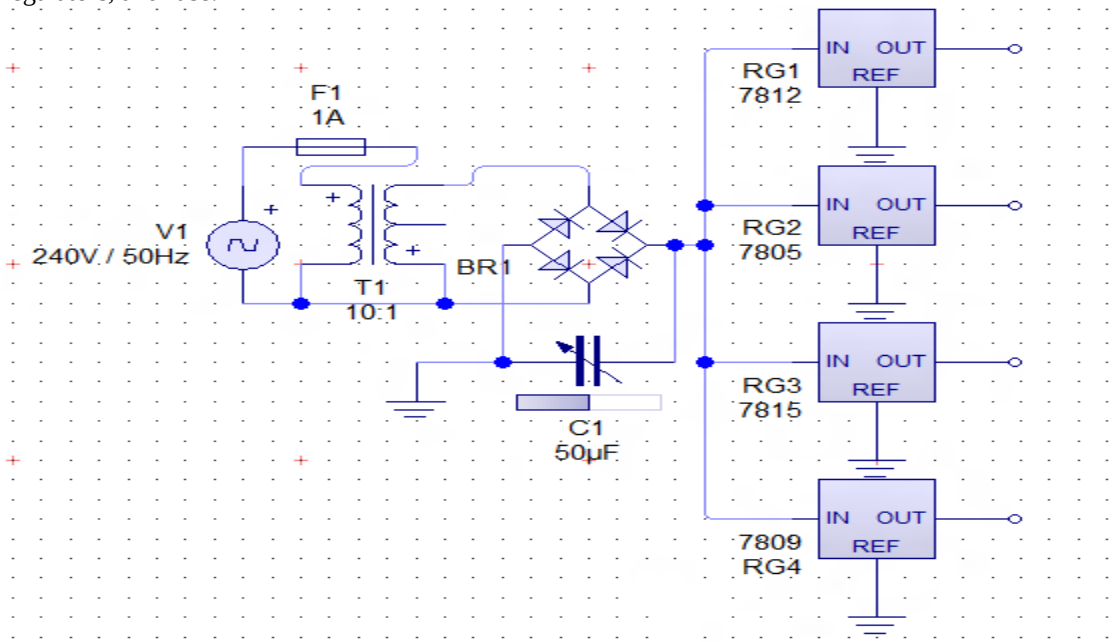

Figure 3: **Intermediate Frequency Unit**

The intermediate frequency which is a driving frequency for the radio frequency part consists of the following parts:

Common Emitter NPN-Transistor Amplifier (CE NPN): This circuit is the first processing stage of the noise signal. The NPN transistor in common emitter mode (CE) amplifies the weak noise generator signal.

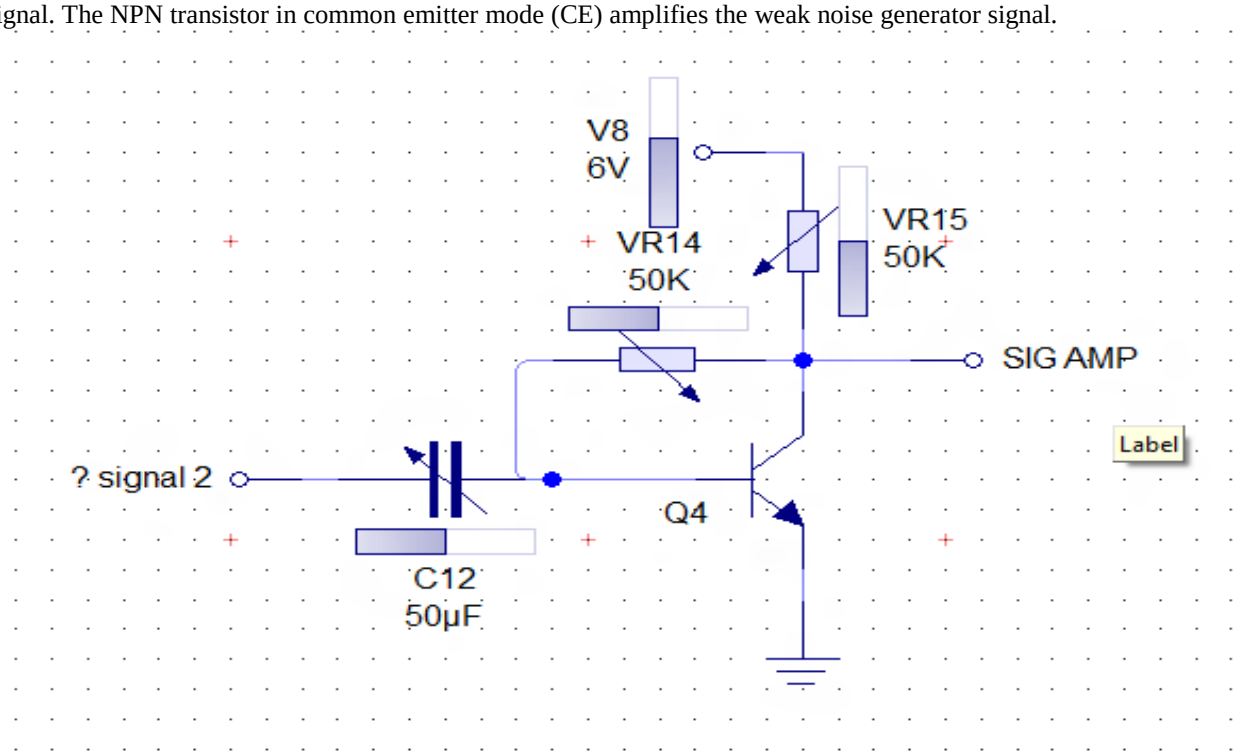

Figure 4: Common emitter signal amplifier

Low Voltage Power Amplifier (LVPA): This circuit is the second stage of the noise signal processing and increases the power level of the amplified noise (first stage). It utilizes an operational amplifier (LM386) which is a Low voltage power amplifier.

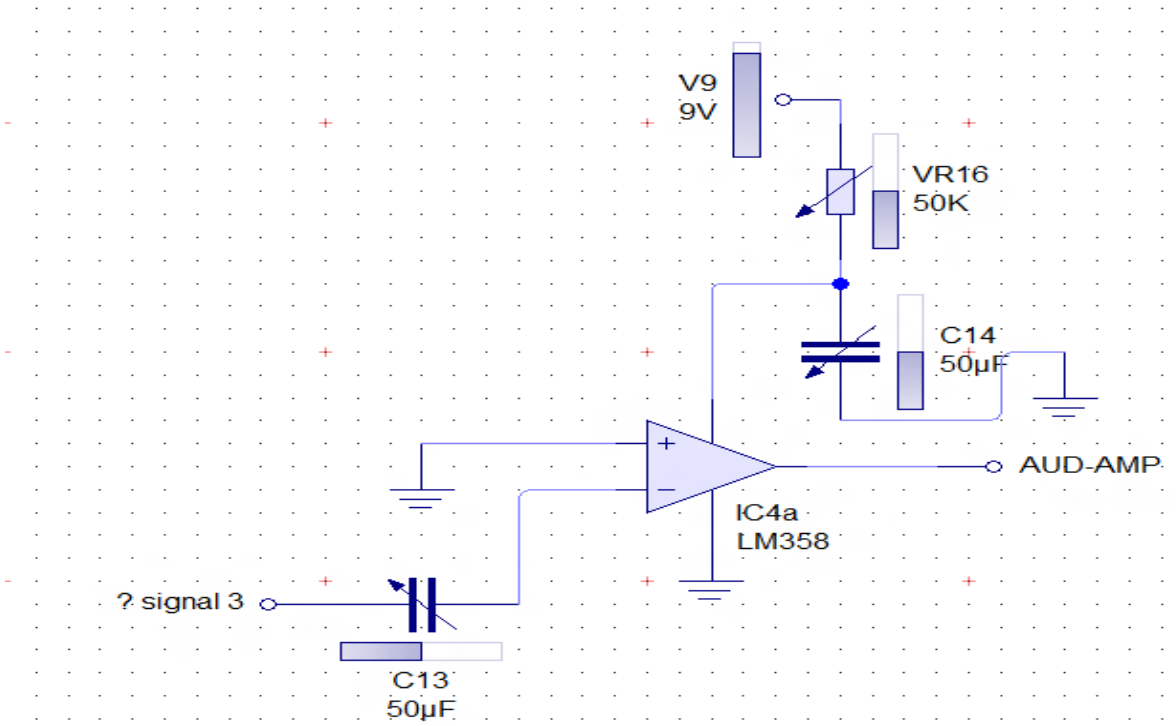

Figure 5: Audio amplifier using LM386 Opamp

Sweep Generator Circuit (SWP): A ramp signal is a linear increasing voltage waveform; it is used to modulate the VCXO so as to sweep jamming frequency over the entire band. The time period of the Ramp signal determines the rate at which the jammer sweeps the target band. The sweep generator is needed to tune the VCXO to the right frequencies at the right time. VCXOs are devices that produce RF signal which could be Triangular in nature (as in Relaxation types) or Sinusoidal (as in Harmonic types). The RF signal so produced is a function of the input voltage at the Voltage input pin of the VCXO. By creating a ramp or triangular waveform which is characterized by an increasing voltage with respect to time, it means it is possible to make the VCXO span wider range of frequencies. Since the VCXO is flexible in this sense, tuning circuit was designed to match its specifications with factors such as linearity, sensitivity and deviation put into consideration.

Summer Circuit (SC): A summer circuit is required to combine the signal waveforms produced by the sweep generator and the noise source in preparation to be fed into the VCXO. This project utilizes an operational amplifier, OP-AMP LM741 in summer mode configuration.

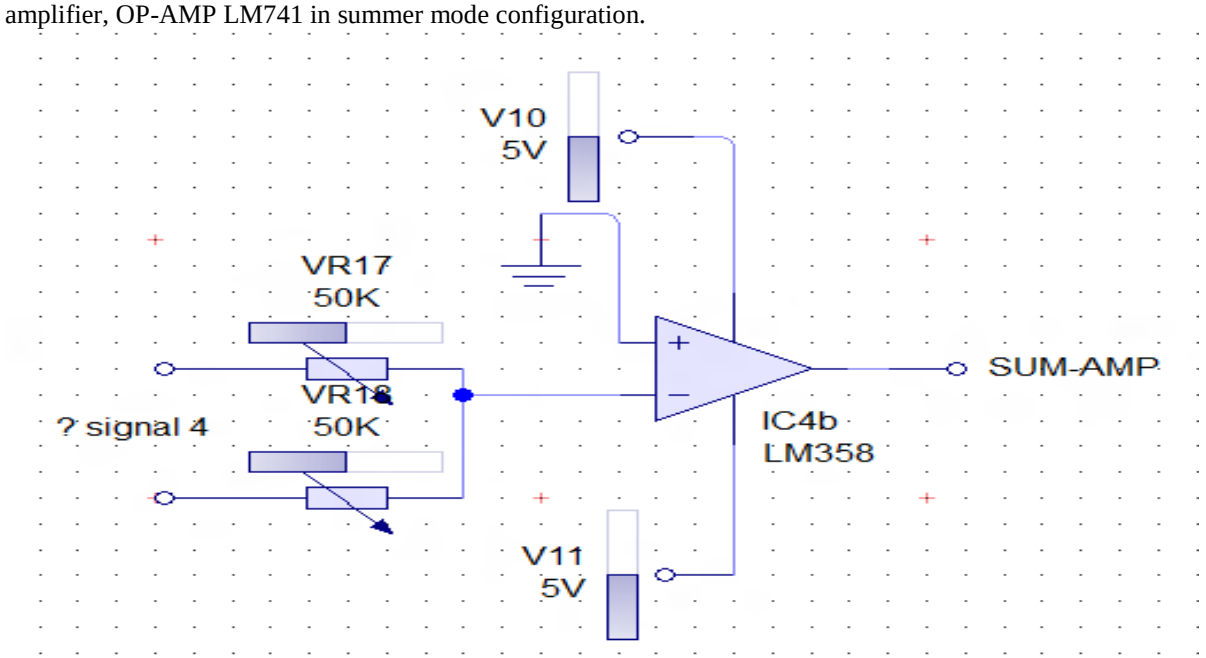

Figure 6: Summing amplifier

Clamper Circuit (CC): VCXO have specified input voltage levels below which the oscillator is OFF as specified by its datasheet. The aim of the clamper circuit is to raise the voltage to an acceptable level for the operation of the VCXO. The clamper circuit comprises of a Diode-Resistor-Capacitor and a voltage source to create an offset.

Clipper Circuit (CLC): The clipper circuit is necessary after the microphone stage to ensure that output levels of the microphone does not exceed certain limits to distort the normal frequency sweeping of the VCXO. This circuit consists of a diode, resistor and voltage source.

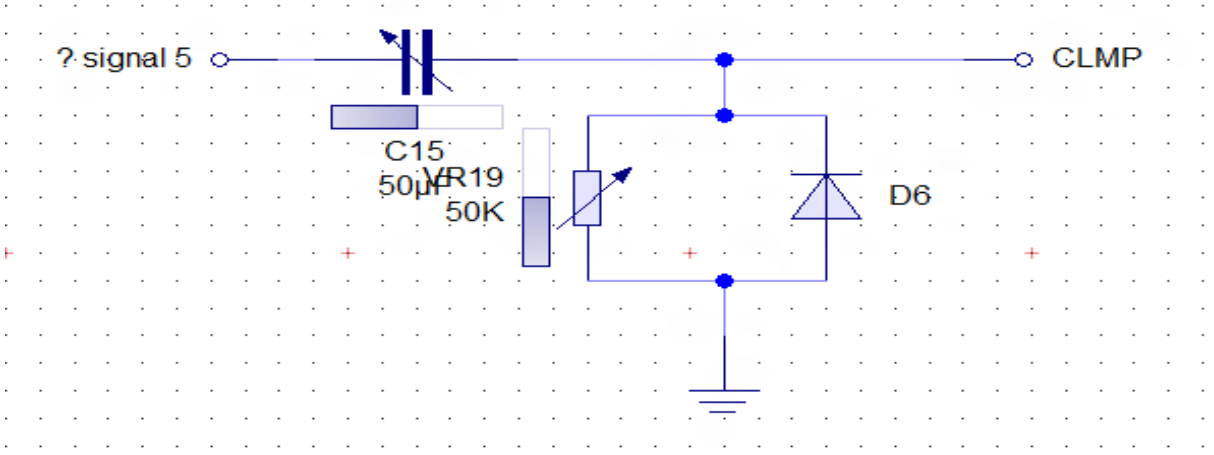

Figure 7: Signal clamper

3.4.4 Radio frequency Amplification

This requires the use of solid state power amplifiers to amplify jamming signal to levels that satisfy the jamming performance criteria.

RF Power Amplifier (RF-PA): The RF Power amplifier is an Integrated circuit (IC) which increases the power at its input to a finite value as designed for. The GSM jammer requires a maximum power output of 2W or 35dBm and as such, the RF-PA IC was purchased to work for the dual band frequencies and at the same time cater for the required power level.

3.4.5 Antenna Unit

Antenna Feed-line (FEED): Antenna Feed-line comprises of all components that makes the jamming signal arrive and radiate at the antenna efficiently and successfully. It is worthy of note that for maximum power transfer of any electrical system, the input impedance of such a system must match with its output impedance. A 50 ohm Micro-strip line performs impedance matching as the use of lumped elements and resistor networks is limited to low frequency applications. The impedance matching must be done to prevent an unacceptable VSWR (voltage standing wave ratio) which will create signal reflections and reduce the efficiency of the jammer or prevent it from functioning.

IV. Result and Discussions

4.1 SIMULATION

A Matlab/Simulink simulation to show the generation of fREF was carried out to illustrate the behavior of the oscillating generated signal. The block diagram modeling the oscillator is shown below. The simulation was done with Matlab /Simulink 2012.

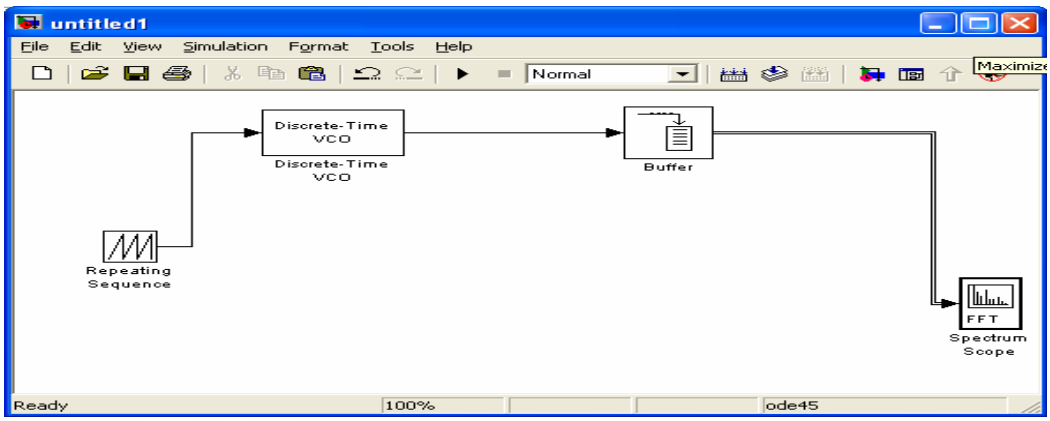

Figure 8: Block diagram of the varying frequency oscillator

where the repeating sequence block represents the periodic input signal to the VCO (more specifically the varying voltage at the pins of the variable capacitor) In the simulation it is considered to be a triangular signal but any periodic signal would lead to the same results. The signal was given a triangular variation from 0 - 5v and a period of 0.2885 msec1. The VCO which represents the oscillator formed by the varactor and an inductor, the range to be traversed by fREF is 285.9 KHz which corresponds to a 5v variation in the input signal and thus a sensitivity of 57.11 KHz/volt. A Discrete-time VCO was used to allow the use of the fast fourier transform to analyze the signal. The last part is the buffer and the FFT which help construct the frequency domain representation of the output signal achieved.

4.2 Results

On Running the simulation, and observing the output of the scope, a signal whose carrier repeatedly moves from 10.6927 to 10.9786 MHz . we can see that the result is a signal at frequency RF cover the whole downlink.

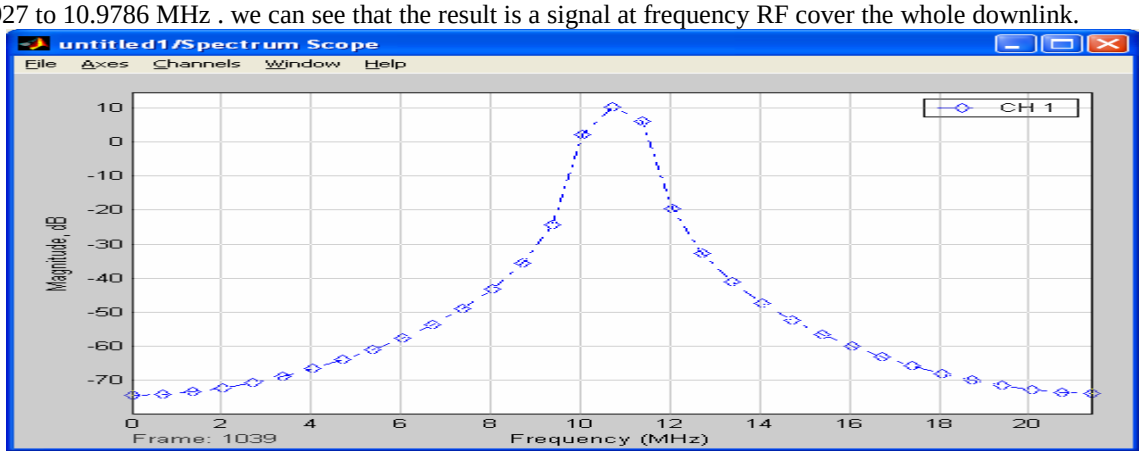

Figure 9: Simulation Result

V. Conclusion

The device was able to jam the four major cell phone carriers in Nigeria: MTN, GLOBACON, AIRTEL and ETISALAT. The effective jamming range was around 50 meters on AC and around 30metres on DC. From the research carried out on this paper, it was observed that as the distance between the cell phone and the base station increases, the effective jamming distance will increase. This is due to the fact that the amount of power reaching the cell phone from the base station decreases as the cell phone moves farther from the base station

This paper is effectively designed and tested working properly on 2G network. Hence, by designing this project GSM CDMA, 3G mobile phone signals are blocked within the given time

schedule i.e. a range of 850MHz to 2170MHz frequencies are blocked.

References

[1] Mika Ståhlberg, Radio Jamming Attacks Against Two Popular Mobile Networks(2000)
[2] Radio Advisory Board of Canada, Mobile and Personal Communications Committee's meeting (1999).
[3] Jyri Hämäläinen, Cellular Network Planning and Optimization (2008).
[4] Kosola, Jyri: Communications COTS and EPM. MSc Thesis, The Royal Military College of Science, Department of Aerospace, Power and Sensors, Shrivenham (1998), 108p.
[5] Syed A. Ahmed, Shah S. Zafar, Syed W. Jafri, GSM Jammer (2006)
[6] Australian communications authority ACA Report, Mobile phone jammers (2003).
[7] Erik Jan van Lieshout et al, Interference by new-generation mobile phones on critical care medical equipment (2007).
[8] Mobile & Personal Communications Committee of the Radio Advisory Board of Canada, "Use of jammer and disabler Devices for blocking PCS,Cellular & Related Services" available at: http://www.rabc.ottawa.on.ca/e/Files/01pub3.pdf
[9] Sage, C., "Microwave and Radio Frequency Exposure: A Growing Environmental Health Crisis" available at: www.sfms.org/sfm/sfm301h.htm
[10] Mouly M. and Pautet M.B., "The GSM System for Mobile Communications".
[11] Webtronics Website: http://www.webtronics.com/20wesdighard.html
[12] Rick Hartley, RF / Microwave PC Board Design and Layout, Avionics Systems.
[13] John Scourias, Overview of the Global System for Mobile Communications, University of Waterloo.
[14] Ahmed Jisrawi, "GSM 900 Mobile Jammer", undergrad project, JUST, 2006.
[15] Limor Fried, Social Defense Mechanisms: Tools for Reclaiming our Personal Space.
[16] Siwiak, K., Radio-wave propagation and Antennas for personal communication.
[17] Pozar, D., Microwave Engineering, John Wiley and Sons, 2005.
[18] FREQUENCY PLANNING AND FREQUENCY COORDINATION FOR THE GSM 900, GSM 1800, E-GSM and GSM-R LAND MOBILE SYSTEMS (Except direct mode operation (DMO) channels)" by Working Group Frequency Management" (WGFM).

American Journal of Engineering Research (AJER) 2016
American Journal of Engineering Research (AJER)
e-ISSN: 2320-0847 p-ISSN : 2320-0936
Volume-5, Issue-2, pp-77-81
www.ajer.org
Research Paper Open Access

Norms as The Formation of Boundary and Place in Madurase Dwellings of Madura-Indonesia

Lintu Tulistyantoro [1], Endang Titi Sunarti Bambang Darjosanjoto [2] ,Lintu Tulistyantoro [3]

[1](Department of Interior Design, petra Christian University, Indonesia; Department Architecture Institut Technologi of Sepuluh Nopember, Indonesia)
[2](Department of Architecture,Institute Technologi of Sepuluh Nopember, Indonesia)
[3](Department of Architecture,Institute Technologi of Sepuluh Nopember, Indonesia)

ABSTRACT: *This paper discusses the result of exploring the understanding of Madurese people live in the island of Madura, a part of East Java, Indonesia on the concept of place and boundary. The discussion was considered about spaces and practices that have been created, adopted, or invoked by the Madurese for their specific purposes.*

To understand the concept of place, must deal with the meaning of boundary. Boundary in Architecture means the distinguisher between an area with the other area. Boundary not only can separate place, but it can also communicate two different places. The form of boundary has many types; it can be visible or non-visible and physical or non-physical. An expression of boundary in shaping the place can actually be determined by the cultural factor. One example of boundary by the cultural factor is norm in culture.

The norms relating with dignity have boundary and place that are so powerful and clear. Boundary by the norms has a strong impact to the place shaping. Therefore, norms have become one element to shape a place. The norms can be non-physical but it has a very powerful boundary of place. The consequences of the norms are the boundary of the Madurese dwelling has a hierarchy, which is a very clear and strong boundary.

Keywords - *Norm, boundary, place, the madurese dwelling*

I. INTRODUCTION

A boundary in architectural terms may either be physical or non-physical [1][2][3]. A physical boundary can be in the form of a horizontal plane (floor and ceiling) or a vertical plane (wall). Meanwhile, a non-physical boundary may not be visually evident but it can be sensed. Through cultural perspectives, a boundary can also be formed as a result of a norm or an agreement between members of a particular society. The Madurese village of Somor Koneng, Bangkalan district in Indonesia has a unique conception of boundary between space and place. To the Madurese society, there are rules and criteria that determine a boundary. It may not be physically visible but it possesses a strong meaning because this type of boundary in this case is determined by norms.

These norms regulate the relationships between one another (particularly between the male and female). The term "outsider male" implies the that they do not have any blood relation with one another. The relationship between females and outside males in the Madurese Society regulate under a specific rule. It is difficult for outside males to meet the females without the latters' male partners. Certain boundaries are thus formed and these boundaries are a result of a mutual agreement. Although these boundaries are invisible, they are very significant in terms of authority.

II. RESEARCH METHODOLOGY

The research methodology used is qualitative research adopting the approach of Ethnography. This approach is used to discover respondent's insight to the roots. This research was performed under natural conditions with a complete setting and the human validation would be the main emphasis. Ethnographic research is truly related to anthropology. Today many ethnographic researches have been adopted from other research disciplines such as sociology, human geography, organizational studies, cultural studies and marketing. This method can be referred to the ethnographic applications by Linda Wong of the discipline of Architectural studies in Thailand [4].

This approach is performed holistically in the exploration, using detailed settings and complying with an unorganized system. Besides that, this method also focuses on a single case or small group, and the analysis of data emphasizes on the meaning and function of human actions. The author examined the opinions of a small group of society about a habitual pattern, custom or lifestyle that are reflected in daily life, in which an study of the daily activities of the specific group is performed as both a process and the result of this research.

> *"..An ethnography is a description and interpretation of a cultural or social group or system. The researcher examines the group's observable and learned patterns of behavior, customs, and ways of life.." (Harris, 1968 on Creswell, 1998).*

This research emphasizes on naturalistic behaviors. The data were collected through the participatory method in which the researcher involves himself into the life of the observed people to be able to examine and record the situation thoroughly [4]. The inductive technique is used to draw conclusions from the inside, meaning that the wide range of data acquired would be squeezed to obtain a summary of ideas. Meanwhile, the data would be processed trianggulationally, comparing between literature, expert's opinion and field surveys in order to obtain accurate conclusive data. From this research process, a conclusion of the society's view regarding boundaries and place whether according to norms or physical elements would be produced.

III. THE UNDERSTANDING OF BOUNDARY

The closest boundary is our personal boundary that could be in the form of a physical, emotional, mental or spiritual barrier. A boundary is defined as a separate condition from another. It is determined by its user, which means that every person identifies and determines his own boundaries, regulating how others would behave towards him. A physical boundary is one that relates to a sense of a personal, sexual or private space. An emotional and mental boundary involves emotions, beliefs, choices, responsibilities, priorities and relationships. Meanwhile, a spiritual boundary involves connections with the self, religion and spiritual practices. .

Boundaries are truly related to culture and every culture has different expressions from one another. [10] In Psychology, boundaries have been defined to be of many types from physical, emotional, spiritual, sexual and relational. In the field of architecture, boundaries has also been expressed physically and non-physically[2] A physical barrier can be felt, seen and touched. Meanwhile a non-physical boundary is one that cannot be seen but could be felt, frequently termed as illutional boundary.

Besides physical boundaries, non-physical boundaries that are invisible are applicable in a few tribal society in the world. In Indonesia, a boundary takes place in the form of a rock, plant, rice field, water or a natural condition as a result of an agreement between the users in the society. Non-symbolised boundaries or those that are not physically evident have also developed but these boundaries truly bind the people's life, are understood and significantly held by the users of the society. These boundaries are thus driven by norms and these norms do not only form boundaries but also acts as a place that possesses a certain character of privacy. This phenomenon is particularly related to culture and gender[15].

IV. THE RELATION BETWEEN SPACE AND PLACE

Space and place are terms that have a strong connection between one another. This perception cannot be detached as they are related to one another. Physically, space is formed as a result of what surrounds it[7]. The relationship between space and place is described as an inseparable entity in the following quote:

> '*Space and place cannot exist without each other-each summons up the other. If space is heat, fire, then place is fuel. We need both as basic elements of architecture: view a to the front and cover behind'*

In order to understand place, we would have to understand space the opposite applies. The two terms involves the interaction between human beings and their environment, and contains values that differentiate one from the other. Hertzberger[7] explained the elements that acts as differentiating entities between space and place. What transforms space to place is its contents that is marked by occasions that connect between what happens in the past and the present. Place connects emotions and contains memory, for instance, no matter how far birds fly away they will always return to their nest and so thus human beings who have memories of their home after an excursion. Hertzberger also described space as a place where humans actualize, a definite entity and brings comfort to its user. Place can be in the form of a dwelling, inside, house peace and place to rest. For example, balconies, a space to play, a house and others. Place can also be an idea of a closed space with a fixed identity and non-dynamic meaning[7].

Space, on the other hand, is a comfortable feeling that is realistic, implies outside, has a distance, is dynamic and open and is bounded. Space could be presented in order to create a meaning of place, both individually in a small scale as well as in a large scale. Apart from that, space is a result of an interaction between people and their environment that differentiates with its surroundings. Thus, place could be implied as something that is bounded for security and possessed a meaning as well as an interaction between humans and their environment.

The understanding of space then developed along with the arrival of cultural elements. Space emphasize on the presence of real and unreal dimensions. The real dimension is relative and can be shifted. The shift of this relative dimension occur as a result of a shift in the space's character. Foucoult [15] mentioned that perceiving space is not only bounded by visual boundaries but has to be viewed through its context and time at which the activity is happening. Thus, the boundary would not necessarily be limited to the physical but also the non-physical. In this perception, it is evident that space is not marked by physical boundaries and cultural elements become the support for this notion. In reality, this value is actually truly universal and every culture possesses signs, symbols and language that hare different from one another [15].

Space is viewed as open and abstract sheet of rug. Place is part of that space that is dwelt by human beings or things that contain meaning and value. This is an interaction between humans and their environment, producing differentiating character of the surrounding area. Place is the center of sensual value, a sense of safety and tranquility where biological needs are met. According to urban experts. Madanipour [8], place is a stationary point that is bounded by a definite identity and meaning that grants an opportunity as reduced dynamism. In this paper, space and place has been distinctly differentiated in which space emphasizes on the closed entity, contains a meaning and is an interaction with the environment [8].

Space contains abstract meanings while place is a physical space or place that has an added value or meaning. A person's experience will influence the concept of space and place and a human body provides an articulation or meaning of space. This added value relates to the posture of the human body and articulation of time. Thus, giving meaning to space can be articulated in the posture of the human body with the human himself as the center. In Tuan's perception, the focus is on something that is physical and that contains meaning [9].

Furthermore, it is metioned that the expression of place is connected to meaning in which the meaning is related to time. This understanding evidently reveals place to be part of space that brings the elements of accommodation, human, activities and meaning. This notion will be used as the mindset of this research.

V. FIELD DATA AND ANALYSIS OF SELF-VALUE IN MADURESE CULTURE

The people of Madura are fundamentally a matrilineal society in which married males would enter and live the female's family [9] [10]. The female is the rightful owner of the house[9]. Although this principle is becoming vague in the progress of time, the tradition of males entering the female's house is still evident even today, particularly in rural areas.

As in the general world as well as the traditional society, females play an important role and they are often differentiated in spatial consequences. For instance, the Greeks, North African and Latin Americans protect their females through private buildings structures. Rapoport[5] stated that females are important parts of the traditional family. Females are often connoted to reclusiveness. With an extreme method, the society protected females through a privacy that is made by this reclusiveness. This extreme value is truly distinct, abiding by strict rules in which males are made inaccessible to observe and meet the females. This expression is revealed through the articulation of space. Thus, females are often separated and positioned in a 'place' that is protected and reclusive yet still under the supervision of the male. The expression that is visually evident is the presence of a division of space between the male and the female.

Hillier (1993: 176-179), also discussed the issue of the female roles as an important aspect. Hiller stated that the practice of the consequence of space begins from a singular space to one that is more complex. Females are separated from the male and this boundary is very strict. This fact shows that females are truly a protected group of people.

Susan Kent[6], grouped categories according to the level of single space to a more complex one. In every category, the position of the female as a consequence of space occurs distinctly, starting from separation according to areas without physical boundary, simple boundaries to physical boundaries and the grouping of space orientation.

This study shows that the females, in the life of the traditional society, had a very specific position and this fact is truly revealed through spatial consequences. Physical boundaries can truly be seen, non-physical boundaries can also be grasped firmly and from this norm a boundary that cannot be crossed is revealed.

As mentioned by Kuntowijoyo[12], the different tribes of Indonesia also experience the same phenomenon. Males and females both possess truly distinct positions, including their spatial consequence. The Madurese females also play an important role in their society. Rifai[9] cited a Madurese quote about obedience as follws: "*bhu, pa', bhabbu', ghuru, rato"* which means mother, father, elders, teacher and king. This arrangement of obedience reveals that the priority of obedience begins from the mother, father, elders, teachers and then the government authorities. This means that the role of a mother is truly important as it is the first position of the line of obedience and respect. The next in the hierarchy are father, elders and authorities. This line of arrangement is truly important as it involves daily habits of interaction and communication. [8]. [13].

Apart from that, this rule also shows that the female position in matrilocal families is the first and most important position, in which females would be granted particular protection and attention both in the family and the larger society. This fact can be seen through the structure of the dwellings of the Madura people[14]. For instance, when leaving the house, the females are always accompanied by their husbands. When a couple rents a motorcycle, they will rent two motorcycles and the driver of one of the motorcycles would sit at the back with the other driver so that the other motorcycle could be used only for the couple. Furthermore, in terms of the human activities taking place in the house from dusk to dawn, the activities of the female dominate the space inside the house compared to the male.

In daily social interactions, the Madura people hold on to their ethics very firmly and this is evident in the spatial arrangement for the males and females. The outside males have a specific area that has been formed as a result of mutual agreements and this location is at the *langgar* or prayer house. This space is used for them to receive guests, dine, drink as well as sleep. This boundary is very clear through the norm that has been agreed upon. There will hardly be any violation or trespassing to the female areas of the *roma*, *dapor*, etc. Their norms are truly strict and cannot be violated. If there is any violation, the consequence would be grave. The activities inside the dwelling are dominated by the females. Meanwhile, males are given a spacious area outside the dwelling which is unlike the female's territorial space that is more privately situated. However, this custom does not apply for females who work as traders. They would have more authority over larger areas. Today, many females of this region perform trading activities. Others would only occasionally leave the house to perform transactions in markets that are far away from their home.

The activities of female children are also truly bounded in the interior space and usually in huts called *pondok*. Thus their mobility area is located inside the house like that of adult females. In normal conditions where there are no outside males, their mobility area would become very large, conquering the whole area of the house.

In conditions where there are no outside males, both males and females own a slightly similar area for the main family members (father, mother and children), whereas one single family has its own territorial area, particularly connected to *roma*, which is regarded a truly private area. Males of other building unit are not permitted to enter other *roma* as this would be considered impolite. Thus the boundary is truly clear and would not be trespassed. This pattern is reflected in the storage area of the daily household tools of the males which is located in the *langgar* and not the *roma*, where the female's tools are stored.

Family togetherness in one unit is truly strong and this is reflected in the authority over space. The kitchen area that is dominated by female activities is not bounded by any barrier between one main family to the other. Serving food is an activity done together. The eldest person the house takes responsibility in providing food for the family and is the key manager of the family's agricultural field and crops. This is evident in the observation that the eldest female would always provide food for her family members. Personal individual needs are determined by the husbands in the house who obtain money from outside through working, business, etc. This wealth and crop management system reveals that females conquer the living space as they are the owners of the house. The eldest female, in particular has the highest authority over the house. Thus, the general system of inheritance does not apply in in the Madurese family. Ownership that is passed down from generation to generation and managed communally is incapable of transferring rights over the land.

Problems arose when Indonesian Government adopted the land certificate system because according to the law, land ownership can only be given to one name. As a result, the house can only be owned by a single person when culturally, the land does not belong to one person but the whole family. The problems of land ownership are still an evident issue today. Many changes have also taken place because the tradition of following the female is also changing and thus in turn influences the rights over the house. However, authority over land in terms of function is still fundamentally given to the female as the manager of the house.

There are, however, exceptions in temporary cases such as during wedding rituals, regarding the authority over space, in which the male is permitted to enter deeper into the interior space until the permitted boundary, normally in the middle yard. This penetration occurs since there is a need for a larger space. The socialization area for outside males extends inside. Nevertheless, there is still a clear boundary of the female space in this case. Males would be served by males and femalaes by females. The boundary between the female and male is still very distinct as the society's norm separates one from the other and determines the boundary. Males own the area in the middle yard and *langgar* or prayer house while females own the kitchen area and *amper* (veranda). Although there is no physical boundary, males would not enter the kitchen and *amper*. Separation occurs for males with special cases in relation to the social status of the male, for instance a spiritual figure. Social positions such as the head of the village would be not be a problem. The spiritual status and those that are connected to it truly influences the spatial arrangement and division as well as the vertical separation of height, which is a very important issue.

In cases like this, elements supporting the ritual that are connected to worship activities are also given a very special space. They are located in the *langgar* together with the spiritual people.

Boundaries form because of function and function take place as a result of norms that separate males and females, between outside males an d inside females. Norms are thus the cause of the formations of invisible boundaries that would not be trespassed. Violation to these norms would result in prolonged conflicts and fatal issues. Violating ethical norms, for instance letting a male a female who are not legally married intermingle, would have devastating effects.

This type of case is truly avoided by the people as it is considered unethical and can trigger dangerous gossips. These would evolve into a big issue and would result in long conflicts. The Madurese society regard women as valuable beings who ought to be protected and this task is given to the males. When a female is injured, the male should be responsible for her. Disturbance to the female means disturbance to the whole family. This sort of issue has devastating effects. The male's pride is also a contributing factor in the emergence of conflicts. Emotional threats such as jealousy are truly hindered by the Madurese society to avoid conflicts. Their norms determine their social ethics that in turn trigger the formation of distinct boundaries and space for both the males and females, particularly in relation to the outside males.

VI. CONCLUSION

Boundaries, through the perception of the Madurese society, are not determined physically through walls and are not visually evident. They are formed as a result of norms that determine their social ethics between the male and the female. These boundaries, that are formed by norms, can be distinctly sensed and would result in grave consequences if they were trespassed. These norms have been passed down from generation to generation and though there is no written evidence, they have been strictly obeyed by the Madurese people for many centuries.

REFERENCES

Books:

[1] Pile, J. F. *Desain Interior*. (Pearson Education, Upper Saddle River, New Jersey, 2003).
[2] Ching, DK. *Architecture: Forn, Space and Order* (Van Nostrand Reinhold Company Inc, 1979).
[3] Rengel, R., *Shaping Interior Space* (Unitet State: Fairchild Publication, 2007).
[4] Groat, L., & Wang, D., *Architecture Research Method (*Canada: John Wiley and Son, 2002).
[5] Rapoport, A., *House, Form and Culture*. (Englewood Cliff, USA: Prentice Hall, Inc, 1969).
[6] Kent, S., *Domestic Architecture and The Use of Space* (Cambridge: Cambridge University Press, 1989).
[7] Heretzberger, H. *Space and The Architect.* (Rotterdam: 010 Publishers ,2000).
[8] Madanipour, A., *Design Of Urban Space* (England: John Weley and Son, 1996).
[9] Tuan, F. Y. (2001). *Space and Place.* Minnesota, USA: The University of Minnesota Press.
[10] Rifai, M. A., *Manusia Madura*.(Jogjakarta: Pilar Media , 2007).
[11] Kuntjaraningrat,
[12] Kuntowijoyo, *Perubahan Sosial dalam Masyarakat Agraris Madura 1850-1940* (Jogjakarta: Mata Bangsa , 2002).
[13] Mansurnoor, I. A., *Islam in An Indonesian World Ulama of Madura.* (Jogjakarta: Gadjah Mada Pres, 1990).
[14] Wiyata, A. L, *Mencari Madura.* (Jakarta: Bidik-Phronesis Publishing, 2013).

Chapters in Books:

[15] Foucault, M.. Of Other Spaces : Utopias and Heterotopias. In N. Leah, & N. Leah (Ed.), *Rethinking Architecture, A Reader in Cultural Theory* (London: Roudledge) 350-356.
[16] Rapoport, A., Culture and Built Form. In K. D. Moore, *Culture-Meaning-Architecture, Critical Reflections on The Work of Amos Rapoport* (England: Ash Gate Publishing Ltd, 2000) 175-216.

American Journal of Engineering Research (AJER) 2016
American Journal of Engineering Research (AJER)
e-ISSN: 2320-0847 p-ISSN : 2320-0936
Volume-5, Issue-2, pp-82-87
www.ajer.org
Research Paper Open Access

Survey on Techniques for Detecting Data Leakage

Bhosale Pranjali A. Gore Anita B. Pandit Sunita K. Prof. Amune Amruta C.
Department of CSE, G.H.Raisoni College of Engg. & Management, Ahmednagar, Savitribai Phule Pune University, India

ABSTRACT: *In current business scenario, critical data is to be shared and transferred by organizations to many stake holders in order to complete particular task. The critical data include intellectual copyright, patient information etc. The activities like sharing and transferring of such critical data includes threats like leakage of information, misuse of data, illegal access to data and/or alteration of data. It is necessary to deal with such problem efficiently and effectively, popular solutions to this problem are use of firewalls, data loss prevention tools and watermarking. But sometimes culprit succeeds in overcoming such security measures hence, if organizations becomes able to find out the guilty client responsible for leakage of particular data then risk of data leakage is reduced. For this many systems are proposed, this paper includes information about techniques discussed in some of such methodologies.*

Keywords: *Client/server, watermark, access right, authentication, encryption, decryption, data leakage, fake records.*

I. INTRODUCTION

A data distributor has given sensitive data to a set of supposedly trusted agents (Third parties) some of the data is leaked and found in an unauthorized place. This problem is known as data leakage problem. To identify the culprit who has leaked the critical organizational data is major challenge. This raises the risk of private data falling into unauthorized hand, whether caused by malicious intent, or an inadvertent mistake, by an insider or outsider, exposed sensitive information can seriously hurt an organization.

Traditionally, watermarking i.e. the process of embedding unique code in each distributed document is used to handle data leakage detection. If the watermarked copy is revealed in the hands of unauthorized party then such party will be declared as culprit. But every time it is not necessary that administration get to know about leakage or it can take time to server to know about the same after analysing such drawbacks of existing systems many researchers proposed different solutions for detection of data leakage.

II. RELATED WORK

2.1 TECHNIQUES FOR DATA LEAKAGE IDENTIFICATION:

2.1.1 Data leakage detection: A survey [1] by Sandip A. Kale C., Prof.S.V. Kulkarni C, 2012

The model proposed in this paper introduces unobtrusive technique for detecting leakage of a set of object or record [1]. This model is proposed for assessing guilt of agent.

The algorithms stated are as follows:

A. Evaluation of explicit data request algorithms:

This algorithm is used for identifying whether fake objects that improves the chances of detecting the culprit.

B. Evaluation of sample data request algorithms:

The distributor is "forced" to allocate certain objects to multiple agents only if the number of requested objects exceeds the number of requested objects in set T [1].

For successful identification of guilty agent 5 modules are declared in this paper, first of them is data allocation module which works for intelligently distributing the data by admin so as to improve probability of detecting the guilty client. Then the fake object module adds fake objects (objects generated by admin altering original document) to data this use of fake objects is inspired by the use of 'trace' records in mailing lists. The optimization module is the distributor's data allocation to agent which has constraints to satisfy agents request and objective is to recognize leakage. The data distributor model enables admin to view which file is leaking. The fifth model i.e. agent guilt module estimates probability of particular data guessed by target and improves the chances of indentifying guilty client.

2.2.2 Detection of guilty agents [2] by S.Umamaheswari, H.Arthi Geetha, 2011

The problem defined in this research work is "The distributor's data allocation to agents has one constraint and one objective. The distributor's constraint is to satisfy agents' requests, by providing them with the number of objects they request or with all available objects that satisfy their conditions. His objective is to be able to detect an agent who leaks any portion of his data.''

The two types of requests are used here:

Sample request Ri = SAMPLE (T; mi): Any subset of mi records from T can be given to Ui and Explicit request Ri = EXPLICIT (T; condi): Agent Ui receives all the T objects that satisfy condition, determined by user provides them data accordingly.

The modules described in this system are:

A. Database maintenance: Here details of agents and data requested by them are maintained.
B. Agent maintenance: In the first part i.e. registration the information about agent is collected and in second part i.e. history the entire details and transactions of users are maintained.
C. Detecting guilty agent: The goal of this module is to estimate the likelihood that the leaked data came from the agent as opposed to other sources, so that guilty agent cannot prove his self innocent.
D. Data allocation: Here, according to two requests handled (sample and explicit) and use of fake objects in data distribution four problem instances are generated and they are EF, EF, SF and SF.

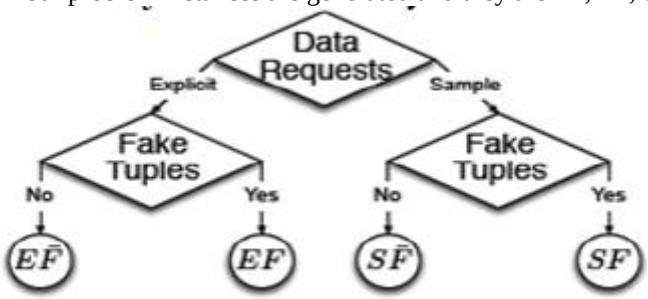

Fig 1. Leakage problem instances [3]

E. Adding fake objects: The addition of fake objects is done on data to be distributed so as to improve the effectiveness in identifying the culprit. The files with some modifications done by administrators are maintained these files are called as trace files which helps to identify improper use of data.
F. Database design: This module maintains all the records in particular manner.

The implementation of this system possible on Netbeans IDE, in input module login, registration etc form provided to user and user has to fill information accordingly then at output part identification and validation of user is done and also guilty agent is detected.

2.2.3 Data leakage and detection of guilty agent [3] by Rupesh Mishra and DK Chitre, 2012

There are lots of other works for avoiding data leakage like watermarking and mechanism that allow only authorized user's access sensitive data through various access control policies.

The system in this work has strict constraints where the distributor may deny to serve an agent and may not provide agents with perturbed versions of same objects and the objective is provided so as to maximize the chances of recognizing guilty agent. The data allocation strategies has given prime importance, because if the data is distributed properly then culprit can easily traced out also implicit and explicit request problem are handled in data allocation strategy.

A distributor owns a set T = {t1, t2, ..., tm) of valuable object and agent U1, U2, ... , Un. An agent Ui receives a subset of objects Ri subset T, either by sample request or by explicit request. The event that user Ui is culprit and leaked data s denoted by {Gi | S}, whereas Pr{Gi | S} is probability that agent Ui is culprit given evidence S. For the distribution the algorithm estimated is as follows:

Algorithm 1: Distribution Algorithm

1. **Assignment:** Assigning DID to data objects.
2. **Hashing:** H(AID)→ DID
3. **Fake record generation:** FID and Fake Record
4. **Mapping:** FID→ DID with P.K. of record
5. **Backup & Removal:** Store information and remove DID.

And once the object is distributed the guilty agent detection is performed by following algorithm:

Algorithm 2: Agent Detection

Set **S T** is obtained at unauthorized place

1. **Mapping DID**

2. **Agent Tracing**
    1. Distribution ID set
    2. Fake record
    3. Missing record
3. **Estimate guilt.**

2.2.4 Data leakage detection [4] by Sandip A. Kale, Prof. S.V. Kulkarni, 2012

This paper introduces 'unobtrusive' technique for detecting data leakage of set of object. The various techniques like watermarking are studied like embedding and extraction, secure spread spectrum, DCT based watermarking, spread spectrum, wavelet based watermarking, robust watermarking technique, invisible watermarking etc.

Data allocation module allows admin to send the files to authenticated client, the fake object module adds altered objects to database and they are distributed to increase the probability of detecting culprit. Optimization module has constraint to satisfy distributors request and objective to identify guilty client. According to experimental results of agent guilt module the probability that agent Ui is guilty is:

$$\Pr\{Gi \mid S\} = 1 - \prod_{te S \cap Ri} (1 - \frac{1-p}{|Vt|})$$

Eqn 3[4]

2.2.5 Detection of data leakage in cloud computing environment [5] by Neeraj Kumar, Vijay Katta, Himanshu Mishra, Hitendra Garg, 2014

The technique proposed focuses on how data leakage and data leakager is identified in cloud computing environment, also concentrates on how more proposed work uses the Bell-LaPadula model to analysis and design of secure computer system. The notion of "secure state" is defined and it is proven that each state transition preserve security by moving to other secure state, thereby inductively proving that system satisfies security objective of the model [5]. In the Bell-LaPadula model each subject S has a lattice of rights and access rights provided by it are reading down (NRU), writing up (NWD), simple security property, star property, read only, append only, execute only, read-write etc.

The first stage of the model described here is registration of client to server, after this server maintains database about the client which is called as server directory table and some fields of this table are client Id, SHA-512(hash) and (m, n). The next step is watermarking of secret message this technique is implemented using 2 steps in first the place where the watermarking should be done is calculated:

- Row positioning pixel, m = I (1; 1) + 2
- Column positioning pixel, n = I (1; 2) + 2

The secret message, encryption key K, AES-128 are used to calculate cipher text C, for placement of cipher C and authentication code M pixel value of image starting from (m, n) in original document is replaced by cipher C. Now the watermarked document is sent to client this process is shown in figure given below:

Fig 2. Sending watermarked document to client

To detect client id reverse process is applied i.e. first the placement of cipher C and authentication code M in document is pointed out for this server uses table where the point (m, n) is stored. Once the authentication code M is found the secret message IDc is calculated and verified for that AES- 128 decryption method is used.

2.2.6 Detecting Data Leakage in Cloud Computing Environment (A Case Study of General Hospital Software) [6] by Alex Ofori Karikari, Joseph Kobina Panford, James Ben Hayfron-Acquah, Frimpong Twum

For the development of system first analysis of old hospital system was conducted and the searching was that, the system does not have any transaction log so anything entered or deleted from the system could not be traced by administrator, and also analysing the existing system problem statement defined as the data leakages are a big concern to organisation as well as individuals and also costing huge sums of money to institutions.

The purpose of proposed methodology was to show how user accessibility and activity to a computing resource could be traced, monitored and audited to safeguard the integrity, accessibility and availability of data to authorized and authenticated users in cloud application. The proposed system has transaction log to monitor user activities, biometric verification system is used for client authentication purpose. Simulation test was done with the dual purpose how a wrongly configured network topology could grant access to both known and unknown user (data clerk) into the system to breach/leak data for instance [6]. This system allows administrators track down at least users in their system.

2.2.7 Data leakage analysis on cloud computing [7] by Bijayalaxmi Purohit, Pawan Prakash Singh, 2013

In this paper cloud describes the use of collection of services, applications, information, and infrastructure. Services like computation, network, and information storage. The major areas of focus are: - Information Protection, Virtual Desktop Security, Network Security, and Virtual Security. The need to protect such a key component of the organization cannot be over emphasized. Data Loss Prevention has been found to be one of the effective ways of preventing Data Loss. DLP solutions detect and prevent unauthorized attempts to copy or send sensitive data, either intentionally or unintentionally, without authorization, by people who have authorized access the sensitive information. Data loss, which means a loss of data that occur on any device that stores data. In this paper, we deal with both the terms data loss and data leakage in analyzing how the DLP technology helps minimizing the data loss/leakage problem? DLP technology minimizes the data loss problem in the organization. Data Loss/Leakage Prevention (DLP) is computer security which is used to finding, monitor, or protect data in use, data in motion, or data at rest. DLP is used to identify sensitive content by using deep information analysis to per inside files or with the use if network communications. DLP is mainly designed to protect information assets in minimal interference in the business processes. It also enforces protective controls to prevent unwanted incidents. DLP can be used to reduce risk and to improve data management practices and even lower compliance cost. Systems are designed to detect and prevent unauthorized use and transmission of confidential information.

2.2.7.1 Classification of Information Leakage:

In this paper information leakage into three levels which means a document containing confidential data can be classified as the unintentional leak, intentional leak, and malicious leak. Activities under unintentional Leak are:

1. Attach document
2. Zip and send
3. Copy & Paste

The unintentional leakage normally occurs when a user mistakenly sends a confidential data and information to third party or wrong recipient. This is done without any personal intention. For instance, if an employee sends an email attaching document mistakenly this contains confidential data to a wrong person.

Intentional Leak:

The intentional leakage normally occurs when user tries to send a confidential document without aware of company policy or finally sends anyhow. This is usually done when a user bypassing the security rules and regulations or devices without trying to gain personal benefits. For instance, when an employee renames a document folder and partially copies data from it. Intentional Leak can be performed using following activities:

1. Document renames
2. Document type change
3. Partial data copy
4. Remove keyword

Malicious Leak:

Malicious leakage usually caused when user deliberately trying to sneaks the confidential data past security rules. Malicious Leakage is done using:

1. Character encoding
2. Print screen
3. Password protected
4. Self extracted archive
5. Hide data
6. Policies or product.

For instance, when an employee sneaks a confidential data from enterprise system and sends them through email and even cause vulnerability to the system. In this paper, we do analysis of data leakage prevention. Why it can balance the data security and user convenience.

2.2.8 Detection of Data Leakage Using Unobtrusive Techniques [8] by Mr. Ajinkya S. Yadav, Mr. Ravindra P. Bachate, Prof. Shadab A. Pattekari, 2013.

Demanding market conditions encourage many companies to the outsource certain business processes (e.g. marketing, human resources) and associated activities to third party. This model is referred as Business Process Outsourcing (BPO) Security and business assurance are essential for the BPO.

In most cases, the service providers need access to a company's intellectual property or other confidential information to carry out their services. For example human resources BPO vendor may need access to the employee databases with sensitive information. The main security problem in BPO is that the service provider may not be fully trusted or may not be securely administered. Business agreements for BPO try to regulate how the data will be handled by service providers, but it is almost impossible to truly enforce or verify such policies across different administrative domains.

2.2.8.1 Unobtrusive Techniques:

In this develop a model for assessing the "guilt" of agents, also present algorithms for distributing objects to the agents, in a way that improves our chances of identifying a leaker. The distributor may be able to add fake objects to distributed data in order to improve his effectiveness in detecting guilty agents. However, fake objects may impact correctness of what agents do, so they may not always be allowable. Consider the option of adding "fake" objects to distributed set. Such objects do not correspond to real entities but appear realistic to agents. In a sense, the fake objects acts as a type of watermark for the entire set, without modifying the any individual members. If it turns out an agent was given one or more fake objects that were leaked, then distributor can be more confident that agent was guilty.

III. PERFORMANCE ANALYSIS

3.1 Accuracy for finding guilty agent:

The systems mentioned in this paper except "Detection of data leakage in cloud computing environment" does not provide much accuracy for finding guilty agent, hence we are preferring the technique of embedding the secret key in the data requested by client, as this key is unique for every data and client the accuracy and chances of indentifying culprit can be increased. For the encryption of key we prefer AES-128 algorithms.

The reason why AES-128 preferred over DES and RSA algorithm is given by following tables which was drawn after analysing [7],[8].

Sno	DES	AES	RSA	Data Size
1	3.0	1.6	7.3	153KB
2	3.2	1.7	10.0	118KB
3	2.0	1.7	8.5	196KB
4	4.0	2.0	8.2	868KB
5	3.0	1.8	7.8	312KB

Table1. Comparison of various packet sizes for DES, AES & RSA algorithm (Encryption Time) [5]

Sno	DES	AES	RSA	Data Size
1	1.0	1.1	4.9	153KB
2	1.2	1.2	5.0	118KB
3	1.4	1.24	5.9	196KB
4	1.8	1.2	5.1	868KB
5	1.6	1.3	5.1	312KB

Table 2: Comparison of various packet sizes for DES, AES & RSA algorithm (Decryption Time) [5]

Factor Analyzed	DES	AES	RSA
Development Years	1977	2000	1978
Key-Length (Bits)	56	128,192,256	$\leq$1024
Nature of Algorithms	Symmetric	Symmetric	Asymmetric
Encryption/Decryption(Speed)	Low	High	Medium
Nature of Security Attacks	Inadequate	Highly Secured	Highly Secured

Table 3: Analysis of various factors [5]

3.2 Watermarking techniques:

There are various watermarking systems are available like secure spread spectrum watermarking, wavelet based watermarking, robust watermarking, DCT-based watermarking etc. But we prefer "Invisible watermarking" for embedding the key because of its following features:

A. As watermarking is performed in most significant region of data, if culprit tries to remove or destroy the watermark it will degrade the appearance quality of data which helps to identify misuse of data.
B. The creation of watermark using input user watermark (logo) is allowed.
C. Preserves quality of host image.
D. Allows robust-insertion and extraction of watermark.
E. Ownership proof could be established under hostile attacks [4].

IV. CONCLUSION:

In this paper, we have studied different papers about data leakage that takes to conclusion that though there techniques like watermarking were available for securing data but these were inefficient, also the system stated are consists of fake records, explicit and implicit requests etc these can cause overhead to system so we are proposing a system which requires less memory and it will be affordable to low budget organisations also.

REFERENCES

[1] Sandip A. Kale C1, Prof.S.V. Kulkarni C "Data Leakage Detection: A Survey" IOSR Journal of Computer Engineering (IOSRJCE) Vol.1, Issue 6 (July-Aug 2012), PP 32-35.
[2] S.Umamaheswari, H.Arthi Geetha "Detection of Guilty Agents, Proceedings of National Conference on Innovations in Emerging Technology-2011.
[3] Rupesh Mishra and DK Chitre. "Data leakage and detection of guilty agent". International Journal of Scientific & Engineering Research, 3(6), 2012.
[4] Sandip A. Kale, Prof. S.V. Kulkarni" Data leakage detection" International Journal of Advanced Research in Computer and Communication Engineering Vol. 1, Issue 9, November 2012.
[5] Neeraj Kumar, Vijay Katta, Himanshu Mishra & Hitendra Garg, "Detection of Data Leakage in Cloud Computing Environment", in Sixth International Conference on Computational Intelligence and Communication Network, 2014.
[6] Alex Ofori Karikari, Joseph Kobina Panford, James Ben Hayfron-Acquah, Frimpong Twum "Detecting Data Leakage in Cloud Computing Environment (A Case Study of General Hospital Software)" International Journal of Scientific Engineering and Applied Science (IJSEAS) - Volume-1, Issue-3, June2015 ISSN: 2395-3470.
[7] Bijayalaxmi Purohit, Pawan Prakash Singh "Data leakage analysis on cloud computing" International Journal of Engineering Research and Applications (IJERA) Vol. 3, Issue 3, May-Jun 2013, pp.1311-1316.
[8] Mr. Ajinkya S. Yadav, Mr. Ravindra P. Bachate, Prof. Shadab A. Pattekari "Detection of Data Leakage Using Unobtrusive Techniques", IOSR Journal of Computer Engineering (IOSR-JCE) vol. 8, Issue 4 (Jan. - Feb. 2013), PP 79-84.
[9] NIST FIPS Pub. 197. Announcing the Advanced Encryption Standard (AES), 2001.
[10] Jakob Jonsson and Burt Kaliski. Public-key cryptography standards (pkcs)# 1: Rsa cryptography specifications version 2.1. 2003.

American Journal of Engineering Research (AJER) 2016
American Journal of Engineering Research (AJER)
e-ISSN: 2320-0847 p-ISSN : 2320-0936
Volume-5, Issue-2, pp-88-100
www.ajer.org
Research Paper Open Access

Municipal solid waste (MSW) management in Dhaka City, Bangladesh

[1]A.Z.A. Saifullah , [2]Md. Tasbirul Islam2
[1]*Professor & Chair Department of Mechanical Engineering IUBAT – International University of Business Agriculture and Technology, Dhaka 1230, Bangladesh.*
[2]*School of Mechanical Engineering, University Sains Malaysia (USM), Penang, Malaysia*

Abstract : *Dhaka is the capital city of Bangladesh, with the highest population density (129,501 people/square km) in the world. Municipal solid waste (MSW) generation in the city is 4634.52 tons/day. This study aims to explore current MSW management scenario which is found one of the most underestimated sectors of Dhaka City Corporation (DCC) – the responsible authority for MSW management. Overall operational and collection efficiency of DCC MSW management is 45% and 60%, respectively. Vehicle fleet for waste transport showed considerably low efficiency in terms of load carrying capacity and fuel consumption. Residential waste is found potential source of composting. At present, a 500 tons/day compost plant has been operating since September 1998. Worth of recoverable recyclable material is found US$ 82,428,449.9989. Open dumping is a pressing problem leading to groundwater pollution, environmental contamination and emission of greenhouse gases (GHGs). Each day, approximately, 1800 tons of MSW is dumped in the only official landfill site – Matuail. DCC spends 1.5% (601,350 Bangladesh Taka (BDT)/day) of the total budget for landfilling operation and management. Land required for disposal of MSW in Dhaka is estimated to be 110 ha per year. Clean Development Mechanism (CDM) projects in waste sector in Bangladesh are found promising. This study urge to prepare a detailed plan for sustainable MSW management in Dhaka for source separation, large scale investment on composting and Waste to Energy (WTE) projects, recycling, state of the art landfill development, and optimized reverse logistic operation*

Keywords: *MSW; Composting, Recycling; Electricity, GHGs, CDM, Dhaka, Bangladesh*

I. INTRODUCTION

Not only developing countries but also globally, municipal solid waste management (MSWM) is a critical and multifaceted problem (Barton et al., 2008, Chen et al., 2010, Manaf et al., 2009). Globally, municipal solid waste (MSW) generation was estimated about 1.6 billion tons in 2002 (Pappu et al., 2007), and it is predicted that, by year 2025 and 2050, solid waste generation will reach 2.2 and 4.2 billion tons/year, respectively; faster than rate of urbanization in large metropolis (Council, 2013). In recent years, developing countries started improving municipal solid waste management (MSWM) practices. Increasing urban solid waste is neither properly managed nor appropriately disposed. Major inhibitors for MSWM for developing countries, includes low level of technical know-how knowledge, financing MSW management, particularly in collection, transport and disposal mechanism, considering resource recovery (Henry et al., 2006, Imam et al., 2008, Shekdar, 2009). Several researchers from developing countries discussed improper MSWM in their respective cities (Alavi Moghadam et al., 2009, Henry et al., 2006, Manaf et al., 2009, Pokhrel and Viraraghavan, 2005, Sharholy et al., 2008, Troschinetz and Mihelcic, 2009, Zhen-Shan et al., 2009). Human health and biological degradation is affected by improper management of MSW that leads to socio-economic degradation (Abu Qdais, 2007, El-Fadel et al., 2002, Shekdar, 2009).

Dhaka is the capital city of Bangladesh, with a population over 7 million and the highest population density (129,501 people/square km) in the world. The city is located on latitude 23° 42′ 0″ north and longitude 90° 22′ 30″east. The population growth rate of Dhaka city in the last decade was 56.5% which is among the highest in the world (Hossain, 2008). With current pace of urbanization, waste generation is increasing exponentially. It is found that MSW generation in the city is 4634.52 tons/day (Alamgir and Ahsan, 2007a, Concern, 2009). Socio-economic condition, standard of living and rate of urbanization are some of the influencing factors for exponential growth of MSW, especially in the urban and semi-urban areas of developing countries (Rathi, 2006).

Dhaka City Corporation (DCC) – North and South is responsible for MSWM that is found ill-fated and malfunctioned for many years. However, it is now trying to improve the situation with the help of financial incentives from different donor agencies and development partners such as United Nation Development Programme (UNDP), Swiss Development Cooperation (SDC), United Nations Children's Fund (UNICEF) and non – government organizations (NGOs) and notable social business enterprise - Waste Concern (Zurbrügg et al., 2005).

This paper presents an overview of current MSWM in Dhaka city, and identifying constrains providing several recommendations for system improvement. Possible sustainable resource recovery technique through clean development mechanism (CDM) under Kyoto Protocol is also discussed. This study may be beneficial for municipal authorities and researchers to work towards redefining present MSWM system.

II. MATERIALS AND METHODS

Document analysis or desk research generally forms part of policy research (Ritchie and Spencer, 2002). Functional data were embedded through interviews based on the data found from the questionnaires distributed to city dwellers, urban planning officer, municipal authorities related to waste management. Secondary data were collected from various government and non-governmental reports, published articles, books, policy paper and conference proceedings. Study conducted by Japan International Cooperation Agency (JICA), and subsequent reporting of ‘’Clean Dhaka Master plan’’ is only up to date source that provided major part of the quantitative data for this article.

III. RESULTS AND DISCUSSION

In this section, current state of Dhaka city MSWM., its challenges and recommendations are discussed.

3.1 STATUS QUO OF DHAKA MSW MANAGEMENT

Several factors are involved in MSWM including waste generation, collection and handling, disposal, transport and transfer of waste (Kumar et al., 2009). In this section, the status quo of MSWM in Dhaka city is discussed.

3.1.1 MSW GENERATION AND CHARACTERISTICS

Waste generation in city areas is largely influenced by many of the factors such as geographical condition, waste collection frequency, stages of socio-economic development and climatic condition (Keser et al., 2012, Weng and Fujiwara, 2011). Quality generation is valuable information for future waste management planning (Beigl et al., 2008, Sharholy et al., 2007). Total MSW generation in DCC area is 4634.52 tons/day, with a per capita waste generation is 0.41kg/day (Concern, 2009). Among the other three metropolises of Bangladesh, waste generation varies from 172.83 tons/day to 1548.09 tons/day (Concern, 2009).

A percentage variation of the waste generation is shown in Table.1

Table 1: MSW composition (in %) at Dhaka between 1992 and 2005(Concern, 2009)

Sl no.	Parameters	1992 (in %)	2005 (in %)
1.	Glass/metal/Construction	6.38	8.17
2.	Plastics	1.74	4.1
3.	Textile	1.83	4.57
4.	Paper/cardboard	5.68	4.29
5.	Food waste (organic)	84.37	78.87

As shown, the percentage of organic food waste (FW) comprises as the highest in the MSW of Dhaka city. This generally happens due to lack of consumption of unprocessed foods. However, fraction of organic waste decreased from 84% in year 1992 to 78% in year 2005. The presence of large organic fraction in MSW is reported for many other developing countries such as India (40-60%) (Sharholy et al., 2008), Turkey (43-64%) (Keser et al., 2012), China (57-62%) (Chen et al., 2010), Nigeria (52-65%) , Nepal (60-70%) (Pokhrel and Viraraghavan, 2005). Physical and chemical composition of MSW in Dhaka is presented in Fig. 1 and Fig. 2. In recent times, percentage of plastics as packaging waste is changing due to large scale process food production in Bangladesh. Moreover, fast food culture that spreads widely throughout the city is making changes in food habit as well as the composition of waste items.

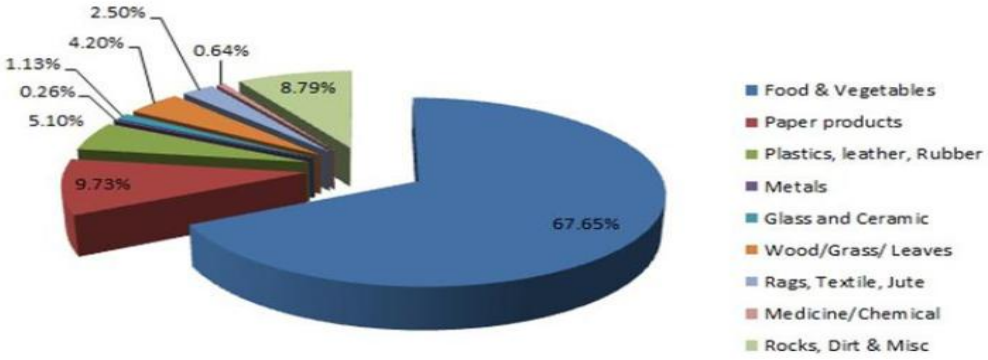

Fig. 1: Average Physical Composition of MSW in Dhaka (Concern, 2009)

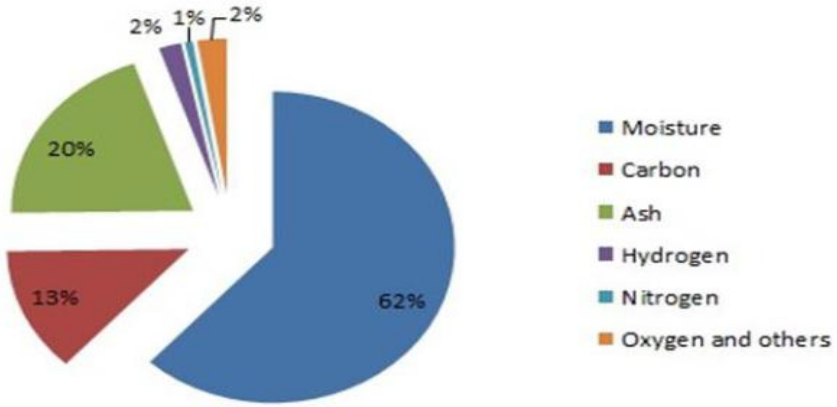

Fig. 2: Chemical composition in municipal solid waste in Dhaka city (Hamid Khan and Fayyaz Khan, 2009)

3.1.2 WASTE HANDLING AND PROCESSING IN DHAKA CITY

The method of waste handling and processing has direct effect on public health, collection efficiency, resource recovery of a MSWM system (Talyan et al., 2008). Like other developing countries, though unorganized and informal, MSW in Dhaka is generally handled and processed by large informal sector. Implementing source separation scheme at source is an important practice as part of sustainable MSW management and planning (Troschinetz and Mihelcic, 2009). However, there is no separation scheme is currently available in Dhaka city. Even, it is unfortunate that there is no hazardous waste collection and disposal scheme is present in Dhaka city. Separation of waste is an effective and sustainable practice from the view point of resource recovery and/or reuse of materials. Fig. 3. shows waste handling and processing flow, typically practiced in Dhaka

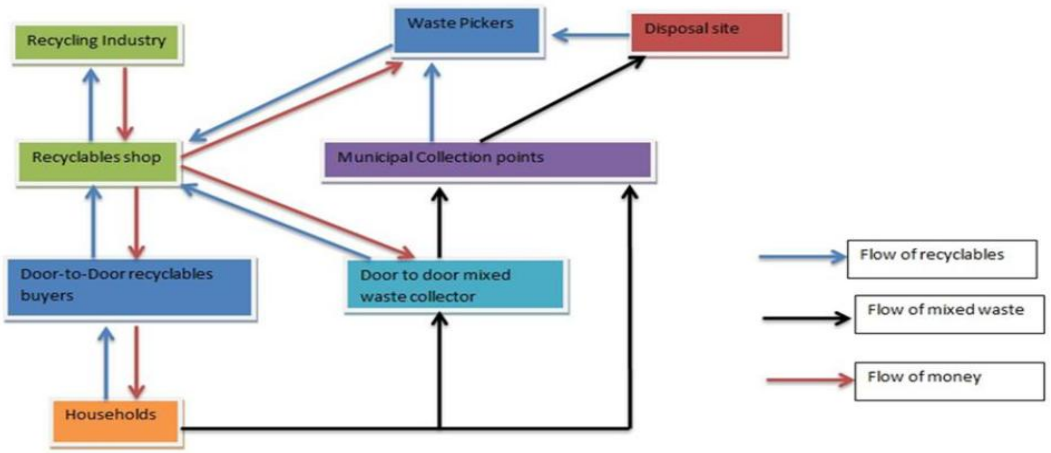

Fig. 3: Flow of waste, recyclables and money in MSW management in Dhaka (adopted from Matter et al. (2013))

3.1.3 COLLECTION OF SOLID WASTE

Collection, storage and transportation of large amount of generated MSW is a complex task that require attention considering contextual setting, constrain and opportunities (Ahsan et al., 2014). Organic fraction of the waste can degrade easily creating invasive odors, and leachate in open container those are placed haphazardly (even in the bus stop) beside the road sides may cause serious health impact on the city dwellers. In recent times, demountable containers are being used for onsite storage of MSW in some areas in Dhaka city. Numbers of containers for disposal are less. In Dhaka, 45% to 55% (2,200 ton/day) of the total waste is unmanaged and dumped in open space (SMS Rahman, 2009). However, The collection target for the year 2015 is about 3054 tons/day at present, which is higher than 218% as of 2004 (JICA, 2005). In Dhaka, DCC is primarily responsible for MSW collection and transport. Besides, there are total 47 non-government organizations (NGOs)/ Community based organizations (CBOs), currently working for household MSW collection. However, activities are limited to a small number of organizations (JICA, 2005). No community based participation has been developed and/or in action for MSWM, except small scale composting plant (A, 2000, Hai and Ali, 2005, TB, 1996). Manual waste collection method is generally practiced to collect household waste to transfer it to the containers. DCC waste collection vehicles collect the waste from open containers, transfer stations; and transport them to official landfilling site – Matuail. Each day, approximately, 1800 tons of MSW is dumped at the site (Yousuf and Rahman, 2007).

3.1.4 TRANSPORT AND TRANSFER

At present, transport system concerning MSW is managed both by private and city corporation vehicles – open trucks (OT), container carrier (CC) and Trailer trucks (TT) (JICA, 2005). Private organizations have three wheeler manual vans to collect household waste to disposal points/open container, situated at anonymous locations in different parts of the city, as primary collection point. Transfer station decreases operational cost of MSW transfer and handling (Alavi Moghadam et al., 2009). However, there are only 14 transfer stations in Dhaka (FE, 2014) . Collection and transportation has become a primary issue in MSWM in Dhaka city (JICA, 2009). Transport sector infrastructural development is found critical to achieve such target. As of 2009, DCC has 297 collection and transport vehicles that have carrying capacity of 1619 tons/day (JICA, 2009). It is clearly visible that collection efficiency (around 60%) with existing DCC vehicle fleet is very poor (JICA, 2005). Moreover, many of waste collection vehicles are too old and/or lack of repair and maintenance leading to vehicles malfunctioned

3.1.5 FINAL DISPOSAL

It is estimated that about 95% of MSW generated in the world is dumped either in land, rivers or even in sea without considering the subsequent environmental damages (Castaldi, 2014). Landfilling is found one of the most suitable options from the economic stand point for developing countries (Kumar and Sharma, 2014). Other popular methods of final disposal are incineration and composting. Even though, landfilling is cost effective, it is also responsible for ground water contamination (Peng et al., 2014). Like other developing countries, open dumping and landfilling, is the most common practice for MSW disposal in Dhaka. In several occasion, it was found that insinuation of leachate from open dumping cause contamination of land and ground water, and the surrounding environment (Aziz et al., 2014). Fig. 4. shows the MSW dumping at Matuail landfill site.

Fig. 4: Dumping of MSW at Matuail landfill site (Yousuf and Rahman, 2009)

Composting is found the most viable alternative option for disposal of MSW in Dhaka city. Typical organic waste contains high moisture about 62%. Decentralized composting projects found promising if composting plants are located at the proximity of waste generation. Low cost manual source separation, and adoptable technology along with socio-economic condition of the waste treatment workers is also vital implementing such

projects. Community based decentralized waste treatment, especially in case of composting, several developing countries, especially in the urban areas, showed tremendous success, mainly in the low income countries (i.e. Pakistan, Sri Lanka, India, Nepal, Bangladesh) (Zurbrugg, 2002). In Bangladesh, the first decentralized community based composting plant was established at Section-2, Mirpur, Dhaka, Bangladesh; by social business enterprise - Waste Concern in 1995. The capacity of the composting plant is about 3 tons/day, out of which maximum composting capacity is currently 2.52 tons/day (Zurbrügg et al., 2005). The plant is still continuing its operation and four more replications are about to proceed in other parts of the country.

Fig 5 shows the construction, installation and usage of barrel composting technology developed by Waste Concern with the technical and financial cooperation of United Nations International Children's Emergency Fund (UNICEF) and Department of Public Health Engineering (DPHE), Government of Bangladesh. The primary objective of such project is to encourage people to set up composting plant under private ownership and managing the waste by community participation (Concern, 2005a). Besides, barrel type composting; aerator and box type composting methods are also being used by waste concern (Iftekhar Enayetullah and Hashmi, 2006).

Fig. 5: Construction, installation and use of barrel composting developed by waste concern (Concern, 2005b)

3.2 RECYCLING OPPORTUNITIES FROM MSW IN BANGLADESH

Table 2 gives an overview of the availability of recyclable items from MSW generation in Bangladesh. Total market value of the recyclable items is 6396,975,262 BDT (US$ 82,428,449.9989). Inclusion of formal sector in reverse supply chain can also boost the overall operational performance of MSWM. Table 3 shows the recycling rate and overall waste reduction of major recyclable items in Dhaka city. It is found that recycling rate of glass, plastic and paper are considerably higher. But as the process food industry is growing in Bangladesh tremendously (Rasul et al., 2006), generation of packaging waste require more adoptable tools and technology for recycling.

Table 2: Market value of recoverable materials in MSW of Bangladesh (adopted from Alamgir and Ahsan (2007b))

Recyclable Items	weight (in ton)	Recoverable weight (in ton)	Market price (BDT/ton)	Total Market Value (in BDT)	Market value (BDT/kg)
Paper	288900	202410	20953.728	4241,244,084	20.9537
Plastic	110400	77280	13193.088	1019,561,841	13.193
Metal	53900	37730	23281.92	878,426,841.6	23.28192
Leather and rubber	34600	24220	8536.704	206,758,970.9	8.536704
Glass	21100	14770	2716.224	40,118,628.48	2.71622
Bone	5000	3500	3104.256	10,864,896	3.1042

1 USD (US$) = 77.6064 Bangladesh Taka (BDT)

Table 3: Estimated volume of recycled wastes in Dhaka city (JICA, 2005)

Material	Recycling rate (in %)	Contribution to waste reduction (in weight %)
Plastic	83	3.2
Paper	65	5.3
Glass	52	0.8
Metal	-	1.3
Compostable	0	0.2
Others	95	2.9
Total		13.6

3.3 THE PRESENT CHALLENGES OF SOLID WASTE MANAGEMENT IN DHAKA CITY

Like, other developing countries, a number of factors are responsible for the poor performance of MSWM in Dhaka which are summarized as below:

(a) Waste sector inventories in Bangladesh are very poor and/or inadequate. Time series database should be developed for future waste sector management planning.

(b) At present, there is no source/waste separation system exists in the DCC - north and south areas. Lack of policy implication leads to potential inhibitors for formalized recycling sector.

(c) Primary collection of MSW from households with rickshaw vans is not suitable because of its design constrains.

(d) The number of transfer stations is very limited. Transfer stations should be established within the proximity of primary collection route, as this operation is generally done by three wheeler manual rickshaw van. Several collection points remain in poor condition due to lack of awareness.

(e) Most of the open trucks and garbage containers are not properly and regularly washed after the disposal of MSW at landfills which eventually reduce the lifecycle of vehicles.

(f) Total units of vehicle are 343, and more than 60% are open trucks (OTs). Other vehicle includes 127 container carrier (CC) and 3 trailer trucks (TTs) (JICA, 2009). The duration required for maintenance and repair generally takes longer, generally handled by private workshops on contract basis. As of September 2004, out of 343 units of vehicles, 60 units were still under repair work. With the existing vehicle and transport facilities, operational efficiency of the DCC MSW management is about 45% (JICA, 2005) which is considerably low.

(g) The fuel consumption of the DCC operated open trucks is not monitored. Most of the DCC trucks are not even marked as a DCC trucks specially designated for waste collection. In this case, the open trucks are covered with hard plastics during its travel from disposal points to landfilling areas. As the trucks are old and under-maintained, high fuel consumption occurs due to limited parts repairing. According to Center for Clear Air Policy (CCAP), improved repairing and maintenance of waste collection vehicles can increase waste collection rate from 44% to 61% from year 2004 to 2015 (CCAP, 2014).

(h) Besides the only official landfilling site Matuail and 2 unofficial dumping sites at Uttara (5% of the total MSW disposed) and Berri Band (30% of the total MSW disposed) (JICA, 2009), a huge quantity of MSW is disposed of in open canals and drains, or dumped into low–lying areas instead being collected and transported to the official waste disposal site.

(i) A state of the art sanitary landfill must be developed with the collaboration of community participation and donor agencies coupled identifying strategic location of the landfills in Dhaka city. According to Department Environment (DOE) of government of Bangladesh (GOB), land requirements for landfilling site, considering existing capacity, and with 100% collection efficiency will be 141 acres and 273 acres respectively (DOE, 2010b). It is to be noted that the 90% of the Matuail landfill is already being filled up and within one year, it will be totally abandoned if no further expansion is made (Iftekhar Enayetullah and Hashmi, 2006). Furthermore, as the city is situated in low laying areas and under the active flood plain, suitable site selection for future landfilling site will also create problematic situation.

(j) Operational activities and management of Matuail, and other adjacent land filling site is uncontrolled and there is no specific leachate collection and treatment facility available for the sites.

(k) A limited number of environmental impact assessments are carried out concerning surrounding environmental pollution and ground water contamination, which must be monitored on a regular basis with latest available technology.

(l) Health hazard of waste pickers at the Matuail land filling site is very poor. Unhygienic as well as unorganized handling may possesses serious and long term impact on urban poor population whose income generation is largely dominated by waste picking from landfills and dump sites.

(m) Modernization of weighbridge data collection at landfill site is found limited (Yousuf and Rahman, 2007). Weight bridge database is suitable to identify cost minimization of expenditure head of the respective authority.

IV. CLEAN DEVELOPMENT MECHANISM (CDM) OPPORTUNITIES IN WASTE SECTOR IN BANGLADESH

It is estimated that 60% of the methane gas generated from MSW decomposition can be recovered by landfill gas (LFG) collection system when MSW collection efficiency is 50% (Chattopadhyay et al., 2009, Enayetullah et al., 2003). Current MSW collection efficiency is 60% in case of Dhaka (Concern, 2009). Landfill gas (LFG) is found one of the viable bio resource derived from MSW (Assamoi and Lawryshyn, 2012). According to United States environmental protection agency (USEPA), methane is generally considered as a major contributor (2nd place) of global warming potential which is even 20 times higher than carbon dioxide (CO2) considering over a 100 year period (USEPA, 2010). In case of USA scenario, CO2 emission is higher compared to methane, which is 20 tons/year; where Bangladesh is emitting only a fraction – 0.2 tons/capita/year, and this is also comparatively lower to other developing countries - 1.6 tons/year (Enayetullah et al., 2003).

However, Bangladesh is in better position to reduce the greenhouse gas emission especially methane and CO2 from waste sector. Under the current CDM projects in Bangladesh, it is expected that from year 2004 to year 2012, extraction and utilization of LFG from Matuail landfill will reduce 80,000 CO2 equivalents with the help of flaring and cogeneration technology (Visvanathan, 2006). Bangladesh is a good candidate for successful CDM projects including waste sector. Adopting existing technology for LFG collection, especially methane, 100% greenhouse gas (GHGs) emission reduction can be achieved (Enayetullah et al., 2003). CDM projects in Bangladesh should target optimum LFG collection to produce power generation. Electricity generation from LFG and incineration are the two promising and viable technology that reduce GHG reduction (Kofoworola, 2007). LFG recovery project conducted by Waste Concern estimated that a total of 501,473 tons of GHG can be reduced as well as 102,148 megawatt hour (MWh) of electricity can be produced through the recovery of methane with a 7 years project life time (Concern, 2014). In this case, the average dumping of MSW at Matuail landfill was estimated 1200 tons/day and total quantity of the MSW disposal will be 3,066,000 tons. Research conducted by Han et al. (2010) showed that 198,74 MWh of electricity can be generated from LFG which can reduce 1,386,081 tons of CO2 equivalent with a 21 years of operation. On the other hand, incineration which is comparatively superior in technology can produce 611,801 MWh of electricity with GHG emission reduction of 1,339,158 tons CO2 equivalent in just only 10 years' time with an electricity generation efficiency 10% (Han et al., 2010). Comparing these two scenarios, it is expected that CDM project duration of 7 to 20 years in Bangladesh has relatively high potential to be successful in terms of CO2 reduction and electricity generation. Fig. 6 shows the GHG emission potential from waste sector. MSW produced in Dhaka city can generate about 100 MW of electricity considering 40% plant efficiency and 24 hours plant operation (Hamid Khan and Fayyaz Khan, 2009). In such case it is found that plant running cost is one of the lowest compared to other fossil fuel (i.e. coal, gas and diesel) based power plants. This analysis can provide a useful insight for waste to energy (WTE) projects under Kyoto protocol and CDM. Bangladesh government should encourage CDM projects in both public and private sector to achieve CDM implementation concerning GHG emission target, especially to waste sector. Necessary financial, institutional support and infrastructural development should be carried out taking consent of all stakeholders (government authorities, donor agencies, local and international NGOs, civil society, small and medium enterprises (SMEs) in waste management sector.

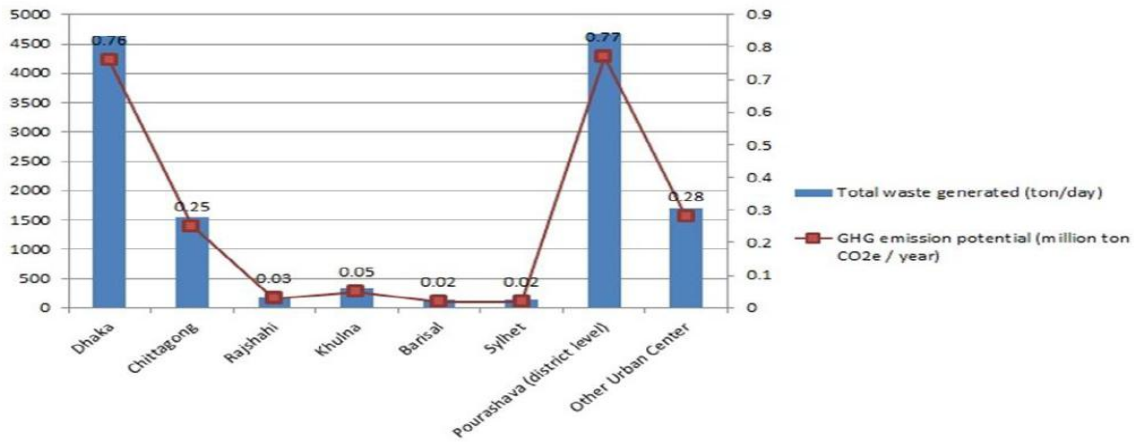

Fig. 6: Greenhouse gas emission potential from solid waste in Bangladesh (Concern, 2009)

A detailed techno-economic assessment of WTE plant and estimation of LFG generation from the landfills in Dhaka city should be carried out aiming to achieve socio-economic benefits (electricity generation, composting etc.) as well as opportunities for carbon trading under CDM. A generic flow diagram of electricity generation from LFG is shown in Fig 7.

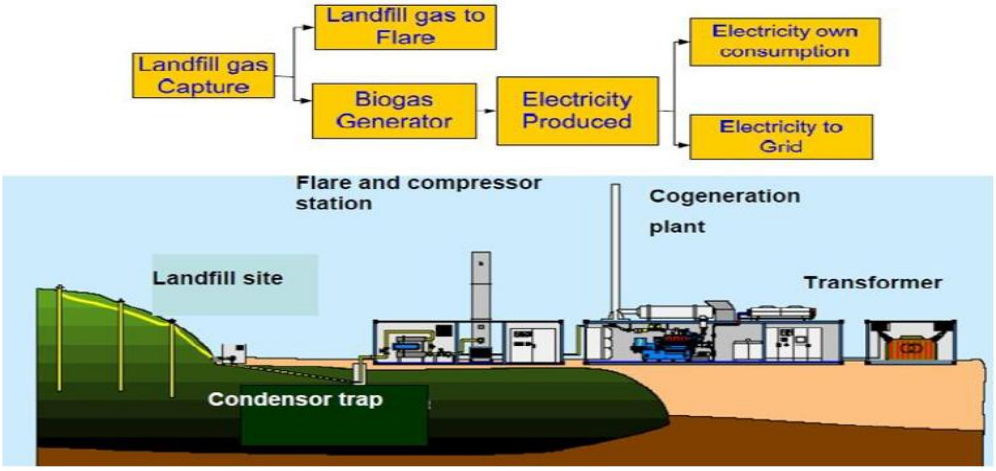

Fig. 7: Landfill gas utilization for electricity generation (Visvanathan, 2006)

4.1 OVERVIEW OF POTENTIAL WASTE TO ENERGY (WTE) PROJECTS IN DHAKA CITY

Incineration is found to one of the best possible WTE solutions in both developed and developing countries. According to Environmental Protection Department (EPD), Hong Kong, Integrated Waste Management Facilities (IWMF) aims to produce 480 million kilowatt-hours (kWh) of electricity from incineration plant which can supply electricity to 100,000 households using 3000 tons/day of MSW in Hong Kong (EPD, 2013). Council for Sustainable Development (CSD) of Hong Kong estimated that total cost for 10,000 tons/day waste incineration will cost about 10 to 15 billion Hong Kong dollar (HKD) (CSD, 2012). European Union (EU) Waste Incineration Directive 2000/76/EC is being followed to establish such large scale incineration plant which will also reduce 440,000 tons of greenhouse gas each year. Some of the countries found to be reluctant in establishing WTE incineration plant such as Australia due to political pressure (Chattopadhyay et al., 2009). From global perspective, importance of waste-to-energy is significantly growing. British glossary stores are utilizing waste food products to generate electricity by microbial anaerobic digestion. With this process, produced energy can be supplied to 200 homes for a year (SCIENCEALERT, 2014). However, major constrain of such project is significant initial capital investment. Fig. 8. shows that several developed countries possess higher degree of incineration options.

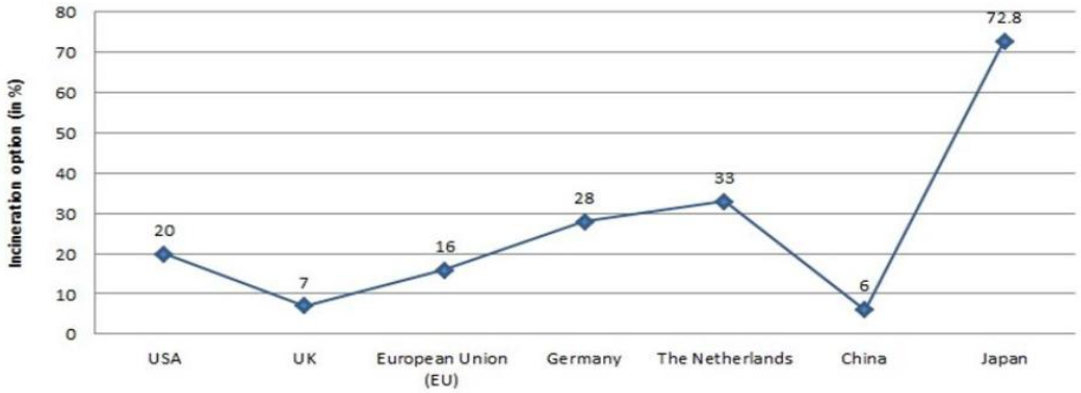

Fig. 8. Incineration option in different developed countries (Chattopadhyay et al., 2009, Hau et al., 2008)

In DCC there is no electricity generation plant from MSW (Sufian and Bala, 2006). Research conducted by JICA (2005) recommended that with a lower calorific value range from 2,303 to 3,559 kJ/kg is not suitable for combustion. However, it is estimated that current MSW generation and its growth projection up to year 2025, can contribute to 1,894,400 MWh of electricity that can meet 79% of electricity demand by 2025 in Dhaka city (Sufian and Bala, 2006). With the similar MSW composition Malaysia, an incineration plant can produce 640 kW of energy from 1500 tons of municipal solid waste (Kathirvale et al., 2004). Fig. 9. shows an incineration plant layout.

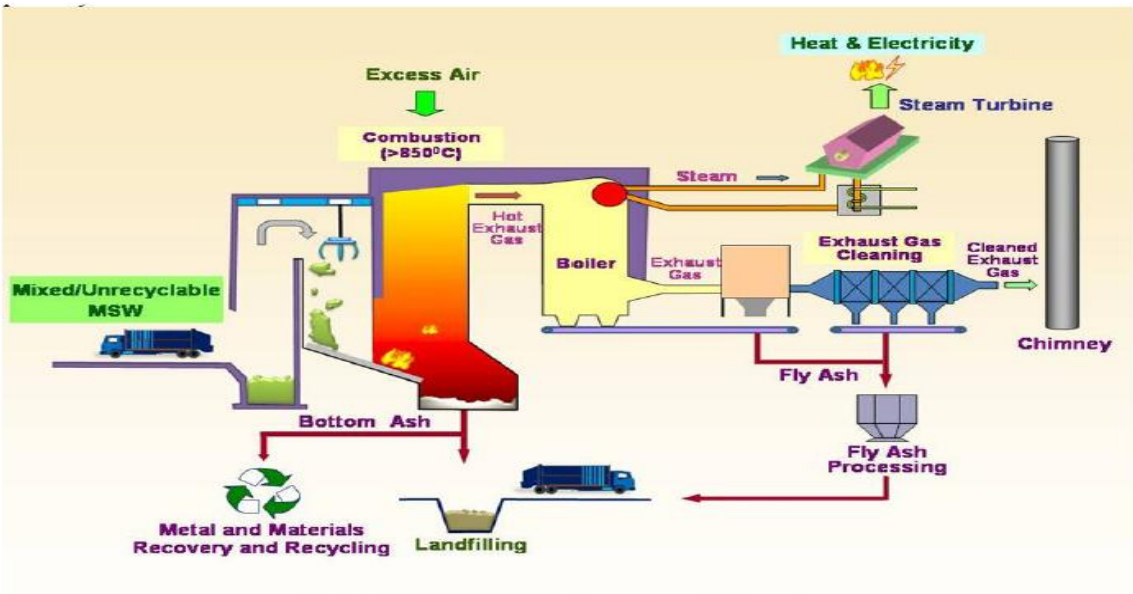

Fig. 9: Generalized incineration flow (EPD, 2009)

Bangladesh can adopt similar type of technology. However, initial capital investment for incineration plant is relatively higher. With the present chemical composition and organic content of MSW, mass burn technology is considered as the most viable solution in this regard compared to other available technology such as gasification, plasma, and pyrolysis. (Chattopadhyay et al., 2009, Islam and Saifullah, 2001, Sufian and Bala, 2006). WTE projects have potentials to mitigate the overwhelming waste management scenario, as well as taking opportunities of CDM (i.e. GHG reduction and carbon trading). A techno-socio-economic study should be conducted perspective and waste generation trend in Bangladesh especially in the Dhaka city.

V. HAZARDOUS, MEDICAL AND ELECTRONIC WASTE(E-WASTE) OVERVIEW

With the inventory study of Department Environment (DOE) of Government of Bangladesh (GOB) with the support of Asian Development Bank (ADB), it revealed that there are total 22 hazardous waste generating industries are currently situated at different parts of the country. Mainly, pharmaceuticals, dying and printing of textile industry, pesticides, paints and varnishes, plastics, industrial chemicals are responsible for generating hazardous waste in Bangladesh (DOE, 2010a). Among the divisional cities in Bangladesh, Dhaka and Chittagong have the highest concentration of hazardous waste. However, treatment facilities for the hazardous waste are not yet to be established, except some effluent treatment plant (ETP) in readymade garments (RMG) sector. Besides these typical waste streams, hospital and clinical waste become a major source of hazardous waste in Dhaka. Most of the medical waste is thrown untreated from the health care establishments (HCE). It is found that more than 22.6% of medical waste is generated in Dhaka with an average generation of 0.5kg/patient/day, and increasing at an alarming rate (Hassan et al., 2008). Fig. 10. shows medical waste management practice and material flow in some of the HCEs in Dhaka city.

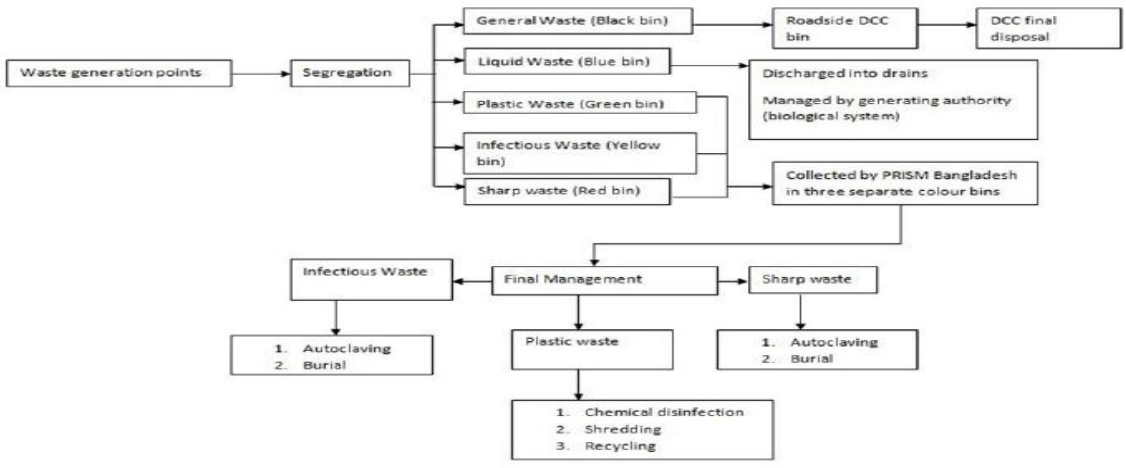

Fig. 10: Medical waste management flow in Bangladesh (Hassan et al., 2008)

Another emerging waste stream in Bangladesh is waste derived from waste electrical and electronics equipment (WEEE), or namely as e-waste. So far, no particular inventory has been developed on e-waste management (Ahmed, 2011, UDENRIGSMINISTERIET, 2014). However, most recent research conducted by Environment and Social Development Organization (ESDO), a total 2.81 million metric tons of e-waste are being generated in Bangladesh. Ship breaking industry is the highest contributor to current e-waste generation which is 2.5 million metric ton (MT)/year (ESDO, 2010). At present, total mobile subscriber in Bangladesh is 100 million with an annual growth rate of 10%. Among the whole population, mobile penetration is 66.36% (Islam, 2013). With current mobile phone penetration in Bangladesh market, it is expected that end-of-life (EOL) mobile phones will be considered as one of the major sources of e-waste in near future. Fig. 11. shows e-waste generation from other sources in Bangladesh. Like other developing countries, e-waste recycling is entirely controlled by large informal sector in Bangladesh. As Bangladesh is a signatory of Basel convention, trans-boundary movement of electronic waste is strongly prohibited (UDENRIGSMINISTERIET, 2014), which is still remained in paper work. E-waste contains several hazardous substances/components which are harmful for human health and can cause serious environmental impact, if not properly managed (Wei and Liu, 2012). GOB is preparing a draft named as Electrical and Electronic Waste (Management and Handling) Rules, 2011, which is still under preparation as priority concern under DOE jurisdiction (Ahmed, 2011). Government policy and regulation on e-waste management can take experience from EU's WEEE directives as well as lesson learnt from other developing countries.

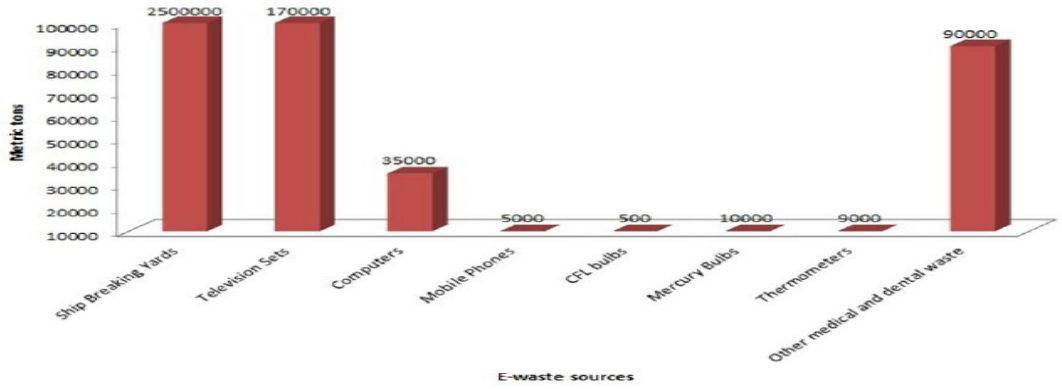

Fig. 11: E-waste generation in Bangladesh (ESDO, 2010)

5.1 REMOMMENDATION FOR HAZADOUS WASTE MANAGEMENT

Hazardous waste should be classified according to the following categories so that it would be convenient for further disposal and treatment.

(i) Wastes those are going to landfilling sites.

(ii) Wastes first needs to be stabilized and before transferring to landfills.

(iii) Establish appropriate and state of the art treatment facilities, especially for hazardous waste.

(iv) Wastes that require storage and further treatment should be considered as an economic and viable source of recycling and reuse.

(v) Some of the wastes may go for incineration process. This process will generate additional energy production that can be used in the other heating purpose.

VI. SUMMARY, RECOMMENDATION AND CONCLUSION

The generation of huge quantities of MSW in Dhaka has become a critical environmental issue. Local waste management authority – DCC found difficult to manage growing amount of waste in the Dhaka City for many reasons, among them lack of ordination among the urban planning authorities affects the most. Besides, there are a large number of open containers which are now generally being placed at the bus-stop causing serious nuisance and unbearable polluted air (bad odor). Closed container should be placed instead of open vats/container. Waste collection time from intermediate collection point to landfill must be maintained and monitored. Appropriate disposal points/transfer station should be established in DCC areas. Besides, in broaderscope, Geographical Information System (GIS) tool kit, weight bridge data and continuous monitoring unit should be used developing location of the collection points as well as in the landfill area - such as a Matuail landfill. In near future, government should implement online management information system (OMIS) to track records as part of development planning of waste management sector.

Transportation and collection vehicles should be modernized. Open trucks must be removed from the vehicle fleet and 5 tons compactor trucks should be introduced more, considering average fuel consumption and GHG emission potential. Vehicle repair time and maintenance schedule should be continuously followed.

Expenditure in landfill management must be increased, as this is the predominated part of MSW disposal in Dhaka. DCC spends on an average of 1.5% of total budget allocation. Planning for sanitary landfill should be established with possible local adoptable technology. In such way, pollution and ground order contamination will be mitigated and energy harness possibility can be developed. Mass burn technology could be implemented as an adoptable electricity generation technology from MSW. Besides, LFG can be converted into usable fuels for the waste collection vehicle to available technology.

Another issue, came out to this fact of mismanagement is the lack of waste segregation option. Collection efficiency can be much higher in separate bins for different types of wastes – glass, plastic, paper etc. School, colleges and universities can be primary separation points for MSW. Public awareness programs should be added more. Both government and non-government sector should come forward to make people understand environmental sustainability. Certain collection points with bins for different waste items should be placed. Community based waste management could be good solution. Recycling rate and urban poor employed can be mobilized through waste separation scheme project. Informal sector recycling should be considered as a starting point to become formalized by providing necessary technical support, awareness of health impact and know-how in required technical field. Non-government organization should come up more with the foreign donors investing in promoting the concept of ''Green Entrepreneurship'' – an implication of social business.

E-waste can be collected where information and communication technology (ICT) products are sold and repaired. As the e-waste products got resell value in Bangladesh, there should be one concrete policy framework collecting e-waste in formal way but keeping informal sector alive by providing financial and technical support adhering with the Basel Convention. A special technique should be adopted for e-waste coming from ship breaking industry. There are a number of child labours working in waste management cycle in Dhaka city as well as in whole Bangladesh. Environmental awareness among the street pickers should spread out. Human health impact can easily understandable in the battery recycling industry in Dhaka city, that employs a number of child labour. A formalized framework needs to be established mitigating current recycling practice and developing efficient formal recycling industry through the concept of social business enterprise in association with small and medium enterprises (SMEs). Composting is a good example in this regard.

Political influence is predominant in development works in Bangladesh. A clear and concise articulation of the waste management planning has to be made without politically biased decision or ―idea of not in my backward'' concept. Capacity building and improvement should be stressed out in a clear framework with existing waste management scenario.

REFERENCES

[1] Abu Qdais, H., 2007. Techno-economic assessment of municipal solid waste management in Jordan. Waste management 27, 1666-1672.

[2] Ahmed, F.R.S., 2011. E-waste Management waste Management Scenario in Bangladesh. Department of Environment, Government of Bangladesh, Dhaka, Bangladesh.

[3] Ahsan, A., Alamgir, M., El-Sergany, M., Shams, S., Rowshon, M.,Daud, N., 2014. Assessment of Municipal Solid Waste Management System in a Developing Country. Chinese Journal of Engineering 2014.

[4] Alamgir, M.,Ahsan, A., 2007a. Municipal solid waste and recovery potential: Bangladesh perspective. Iranian Journal of Environmental Health Science & Engineering 4.

[5] Alamgir, M.,Ahsan, A., 2007b. Municipal solid waste and recovery potential: Bangladesh perspective. Iranian Journal of Environmental Health Science & Engineering 4, 67-76.

[6] Alavi Moghadam, M., Mokhtarani, N.,Mokhtarani, B., 2009. Municipal solid waste management in Rasht City, Iran. Waste Management 29, 485-489.

[7] Assamoi, B.,Lawryshyn, Y., 2012. The environmental comparison of landfilling vs. incineration of MSW accounting for waste diversion. Waste management 32, 1019-1030.

[8] Aziz, S.Q., Aziz, H.A., Bashir, M.J.,Mojiri, A., 2014. Municipal Landfill Leachate Treatment Techniques: An Overview. Wastewater Engineering: Advanced Wastewater Treatment Systems, 208.

[9] Barton, J., Issaias, I.,Stentiford, E.I., 2008. Carbon–Making the right choice for waste management in developing countries. Waste Management 28, 690-698.

[10] Beigl, P., Lebersorger, S.,Salhofer, S., 2008. Modelling municipal solid waste generation: A review. Waste management 28, 200-214.

[11] Castaldi, M.J., 2014. Perspectives on sustainable waste management. Annual review of chemical and biomolecular engineering 5, 547.

[12] CCAP, 2014. Dhaka's Integrated Municipal Solid Waste Program. CENTER FOR CLEAN AIR POLICY, Washington, DC, USA.

[13] Chattopadhyay, S., Dutta, A.,Ray, S., 2009. Municipal solid waste management in Kolkata, India – A review. Waste Management 29, 1449-1458.

[14] Chen, X., Geng, Y.,Fujita, T., 2010. An overview of municipal solid waste management in China. Waste management 30, 716-724.

[15] Concern, W., 2005a. Community based composting, Slum based waste management and composting pilot program: Urban slum and suburb project. Waste Concern Dhaka.

[16] Concern, W., 2005b. Slum based waste management and composting pilot program: Urban slum and suburb project. GOB and UNICEF, Dhaka.

[17] Concern, W., 2009. Waste Data base of Bangladesh.

[18] Concern, W., 2014. Landfill gas recovery to produce energy, in: Group), W.W.R.G.W. (Ed.). Waste Concern.

[19] Council, W.E., 2013. World Energy Resources: Waste to Energy.
[20] CSD. 2012. *Incineration* [Online]. Council for Sustainable Development. Available: https://www.susdev.org.hk/susdevorg/archive2004/en/forum/message_list1914.html [Accessed 24/07/2014.
[21] DOE, 2010a. Hazardous waste management in Bangladesh: A country inventory, in: Department of Environment, M.o.E.a.F., Bangladesh (Ed.). Department of Enviornment, Dhaka, Bangladesh.
[22] DOE, 2010b. National 3R strategy for waste management. Department of Environment, Government of Bangladesh, Dhaka.
[23] El-Fadel, M., Bou-Zeid, E., Chahine, W.,Alayli, B., 2002. Temporal variation of leachate quality from pre-sorted and baled municipal solid waste with high organic and moisture content. Waste management 22, 269-282.
[24] Enayetullah, I., Hossain, I., Sinha, A.H.M.M.,Alam, M., 2003. CDM and its Opportunities in Bangladesh Capacity Development for Clean Development Mechanism in Bangladesh. WASTE CONCERN, Dhaka, Bangladesh
[25] EPD. 2009. *Advanced Incineration Technology* [Online]. Hong Kong, China: Environmental Protection Department, Hong Kong. Available: http://www.epd.gov.hk/epd/english/environmentinhk/waste/prob_solutions/WFdev_IWMFtech.html.
[26] EPD. 2013. *Integrated Waste Management Facilities* [Online]. Available: http://www.epd.gov.hk/epd/english/environmentinhk/waste/prob_solutions/WFdev_IWMF.html [Accessed 24/07/2014.
[27] ESDO, 2010. Study on E-waste: Bangladesh Situation. t Environment and Social
[28] Development Organization-ESDO, Dhaka, Bangladesh.
[29] FE. 2014. DNCC presents TK 20b budget for FY '15. *The Financial Express*, 9/07/2014.
[30] Hai, F.I.,Ali, M.A., 2005. A study on solid waste management system of Dhaka city corporation: effect of composting and landfill location.
[31] Hamid Khan, A.,Fayyaz Khan, M. Prospects of electricity generation from municipal solid waste of Dhaka city. Developments in Renewable Energy Technology (ICDRET), 2009 1st International Conference on the, 2009. IEEE, 1-4.
[32] Han, H., Long, J., Li, S.,Qian, G., 2010. Comparison of green-house gas emission reductions and landfill gas utilization between a landfill system and an incineration system. Waste Management & Research.
[33] Hassan, M.M., Ahmed, S.A., Rahman, K.A.,Biswas, T.K., 2008. Pattern of medical waste management: existing scenario in Dhaka City, Bangladesh. BMC Public Health 8, 36.
[34] Hau, J.L., Ray, R., Thorpe, R.B.,Azapagic∗, A., 2008. A Thermodynamic Model of the Outputs of Gasification of Solid Waste. INTERNATIONAL JOURNAL OF CHEMICAL REACTOR ENGINEERING 6.
[35] Henry, R.K., Yongsheng, Z.,Jun, D., 2006. Municipal solid waste management challenges in developing countries–Kenyan case study. Waste management 26, 92-100.
[36] Hossain, S., 2008. Rapid urban growth and poverty in Dhaka city. Bangladesh e-Journal of Sociology 5, 1-24.
[37] Iftekhar Enayetullah,Hashmi, Q.S.I. Community Based Solid Waste Management Through Public-Private-Community Partnerships: Experience of Waste Concern in Bangladesh. 3R Asia Conference, 2006 Tokyo, Japan.
[38] Imam, A., Mohammed, B., Wilson, D.C.,Cheeseman, C.R., 2008. Solid waste management in Abuja, Nigeria. Waste Management 28, 468-472.
[39] Islam, M.,Saifullah, A. olid waste and sugarcane bagasse—a renewable source of energy in Rajshahi City, Bangladesh. In: Proceedings of the fourth international conference on mechanical engineering,, 2001 Dhaka, Bangladesh. I33–36.
[40] Islam, M.Z. 2013. Bangladesh now has 100m mobile phone users. *Dhaka Tribune*, 28/05/2013.
[41] JICA, 2005. The study on the solid waste management in Dhaka city Clean Dhaka Master Plan. Japan Internal Cooperation Agency (JICA), Pacific Consultants International Yachiyo Engineering Co., Ltd., Dhaka.
[42] JICA, 2009. OUTLINE DESIGN STUDY ON THE PROGRAMME FOR IMPROVEMENT OF SOLID WASTE MANAGEMENT IN DHAKA CITY TOWARD THE LOW CARBON SOCIETY IN THE PEOPLE'S REPUBLIC OF BANGLADESH in: (JICA), J.I.C.A. (Ed.), FINAL REPORT JICA and Yachiyo Engineering Co., Ltd., Dhaka.
[43] Kathirvale, S., Muhd Yunus, M.N., Sopian, K.,Samsuddin, A.H., 2004. Energy potential from municipal solid waste in Malaysia. Renewable energy 29, 559-567.
[44] Keser, S., Duzgun, S.,Aksoy, A., 2012. Application of spatial and non-spatial data analysis in determination of the factors that impact municipal solid waste generation rates in Turkey. Waste management 32, 359-371.
[45] Kofoworola, O., 2007. Recovery and recycling practices in municipal solid waste management in Lagos, Nigeria. Waste management 27, 1139-1143.
[46] Kumar, A.,Sharma, M., 2014. Estimation of GHG emission and energy recovery potential from MSW landfill sites. Sustainable Energy Technologies and Assessments 5, 50-61.
[47] Kumar, S., Bhattacharyya, J., Vaidya, A., Chakrabarti, T., Devotta, S.,Akolkar, A., 2009. Assessment of the status of municipal solid waste management in metro cities, state capitals, class I cities, and class II towns in India: An insight. Waste Management 29, 883-895.
[48] Manaf, L.A., Samah, M.A.A.,Zukki, N.I.M., 2009. Municipal solid waste management in Malaysia: Practices and challenges. Waste Management 29, 2902-2906.
[49] Matter, A., Dietschi, M.,Zurbrügg, C., 2013. Improving the informal recycling sector through segregation of waste in the household – The case of Dhaka Bangladesh. Habitat International 38, 150-156.
[50] Pappu, A., Saxena, M.,Asolekar, S.R., 2007. Solid wastes generation in India and their recycling potential in building materials. Building and Environment 42, 2311-2320.
[51] Peng, X., Ou, W., Wang, C., Wang, Z., Huang, Q., Jin, J.,Tan, J., 2014. Occurrence and ecological potential of pharmaceuticals and personal care products in groundwater and reservoirs in the vicinity of municipal landfills in China. Science of The Total Environment 490, 889-898.
[52] Pokhrel, D.,Viraraghavan, T., 2005. Municipal solid waste management in Nepal: practices and challenges. Waste Management 25, 555-562.
[53] Rasul, M.G., Faisal, I.,Khan, M.M.K., 2006. Environmental pollution generated from process industries in Bangladesh. International journal of environment and pollution 28, 144-161.
[54] Rathi, S., 2006. Alternative approaches for better municipal solid waste management in Mumbai, India. Waste Management 26, 1192-1200.
[55] Ritchie, J.,Spencer, L., 2002. Qualitative data analysis for applied policy research. The qualitative researcher's companion, 305-329.
[56] SCIENCEALERT. 2014. *Big kudos! British grocery store is using its food waste to generate energy* [Online]. Australia: ScienceAlert Pty Ltd. Available: http://www.sciencealert.com/news/20142407-25914.html.
[57] Sharholy, M., Ahmad, K., Mahmood, G.,Trivedi, R., 2008. Municipal solid waste management in Indian cities–A review. Waste management 28, 459-467.

[58] Sharholy, M., Ahmad, K., Vaishya, R.,Gupta, R., 2007. Municipal solid waste characteristics and management in Allahabad, India. Waste Management 27, 490-496.
[59] Shekdar, A.V., 2009. Sustainable solid waste management: an integrated approach for Asian countries. Waste Management 29, 1438-1448.
[60] SMS Rahman, S.S., Kashif Mahmud, 2009. Study of Solid Waste Management and its Impact on Climate Change: A Case Study of Dhaka City in Bangladesh. Bangladesh Environment Network JAPAN (BENJapan), 229-231.
[61] Sufian, M.A.,Bala, B.K., 2006. Modelling of electrical energy recovery from urban solid waste system: The case of Dhaka city. Renewable Energy 31, 1573-1580.
[62] Talyan, V., Dahiya, R.,Sreekrishnan, T., 2008. State of municipal solid waste management in Delhi, the capital of India. Waste Management 28, 1276-1287.
[63] TB, Y. 1996. *Sustainability of solid waste management system of Dhaka City Corporation.* . M. Sc. Thesis, Bangladesh University of Engineering and Technology.
[64] Troschinetz, A.M.,Mihelcic, J.R., 2009. Sustainable recycling of municipal solid waste in developing countries. Waste Management 29, 915-923.
[65] UDENRIGSMINISTERIET, 2014. THE WASTE SECTOR IN BANGLADESH, A short presentation on waste generation and management. MINISTRY OF FOREIGN AFFAIRS OF DENMARK.
[66] USEPA, 2010. Methane and Nitrous Oxide Emissions From Natural Sources. U.S. Environmental Protection Agency, Washington, DC, USA.
[67] Visvanathan, C., 2006. Clean Development Mechanisms (CDM) in Solid Waste Management. Asian Institute of Technology (AIT), Bangkok, Thailand.
[68] Wei, L.,Liu, Y., 2012. Present Status of e-waste Disposal and Recycling in China. Procedia Environmental Sciences 16, 506-514.
[69] Weng, Y.-C.,Fujiwara, T., 2011. Examining the effectiveness of municipal solid waste management systems: an integrated cost–benefit analysis perspective with a financial cost modeling in Taiwan. Waste management 31, 1393-1406.
[70] Yousuf, T.B.,Rahman, M., 2007. Monitoring quantity and characteristics of municipal solid waste in Dhaka City. Environmental monitoring and assessment 135, 3-11.
[71] Yousuf, T.B.,Rahman, M.M., 2009. Transforming an open dump into a sanitary landfill: a development effort in waste management. Journal of material cycles and waste management 11, 277-283.
[72] Zhen-Shan, L., Lei, Y., Xiao-Yan, Q.,Yu-Mei, S., 2009. Municipal solid waste management in Beijing City. Waste management 29, 2596-2599.
[73] Zurbrugg, C., 2002. Urban solid waste management in low-income countries of Asia how to cope with the garbage crisis. Presented for: Scientific Committee on Problems of the Environment (SCOPE) Urban Solid Waste Management Review Session, Durban, South Africa, 1-13.
[74] Zurbrügg, C., Drescher, S., Rytz, I., Sinha, A.H.M.M.,Enayetullah, I., 2005. Decentralised composting in Bangladesh, a win-win situation for all stakeholders. Resources, Conservation and Recycling 43, 281-292.

American Journal of Engineering Research (AJER) 2016
American Journal of Engineering Research (AJER)
e-ISSN: 2320-0847 p-ISSN : 2320-0936
Volume-5, Issue-2, pp-101-108
www.ajer.org
Research Paper Open Access

Assessment of the Reliability ofFractionator Column of the Kaduna Refinery using Failure Modes Effects and Criticality Analysis (FMECA)

Ibrahim A.[1] and El-Nafaty U. A[2]
[1,2]*Department of Chemical Engineering, Abubakar Tafawa Balewa University, Bauchi State, Nigeria.*

Abstract*—The reliability of a process equipment is the probability that an item will perform a required function under stated condition(s). It is an important issue in any process industry. Failure to assess the reliability of most process equipment had led to huge financial losses. As a result, this research aims at assessing the reliability of the Fractionator column of the Kaduna Refining and Petrochemicals (KRPC), Fluid Catalytic Cracking Unit (FCCU), using the Failure mode, effects and criticality analysis (FMECA). The failure mode effects analysis (FMEA) was firstused to identify failure modes, mechanisms, cause, effects severity of the fractionator column through its fourteen (14) sub-units(fractionator primary condenser, bottoms product cooler, debutanizer oil condenser, main fractionator, main fractionator oil drum, main fractionator reflux drum, heavy naphtha exchanger, heavy cycle oil exchanger, bottoms exchanger, BFW heater, steam generator, stripper reboiler, debutanizer reboiler, top reflux pumps). Both quantitative and qualitative criticality analyses (CA) were used to determine the effectiveness and reliability of the unit (Fractionator column). For the qualitative analysis, items risk priority number (RPN) were computed and it was found that, six (6) of the sub-units (feed/ main fractionator bottoms exchanger, main fractionator reflux drum, main fractionator bottoms pumps, feed/ heavy naphtha exchanger, main fractionator, and main fractionator bottoms/BFW heater) had their RPN>300, with feed/ main fractionator bottoms exchanger having the highest RPN of 460. For the quantitative analysis, items criticality number (Cr) were computed and it was found that most of the sub-units had their Cr>0.002. In addition, the results of the criticality matrix showed that, fifteen (15) out of the twenty nine (29) failure modes identifiedwere above or closely below the criticality line. Therefore, the effectiveness and reliability of the unit is low. As such, sub-units with RPN>300 and failure modes above or closely below the criticality line were recommended for replacement or predictive maintenance.*

Keywords*—FCCU; Fractionator column; reliability; FMEA/FMECA; risk priority number, criticality number; and criticality matrix.*

I. INTRODUCTION

The negligence of most process industries not assessing the reliability of their process equipment had led to huge financial losses across the globe[1]; this is as a result of their process equipment failure. In Nigeria today, the failure rate of FCCU is high resulting to huge financial losses[2]. FCCU is one of the most important conversion processes used in petroleum refineries. It is widely used to convert high-boiling, high-molecular weight hydrocarbon fractions of petroleum crude oils to more valuable gasoline, olefinic gases, and other products. The feedstock to an FCC is usually heavy gas oil (HVGO) from atmospheric distillation or vacuum distillation. It has an initial boiling point of at least 340 °C at atmospheric pressure and an average molecular weight ranging between 200 to 600. The cracking is done in the presence of a finely divided catalyst which is maintained in an aerated or fluidized state at a temperature and pressure of 700 °C and 2.4bar respectively[3]. The objective of the Fractionator unit is to distilled into FCC end products of cracked naphtha, fuel oil and off gas. The failure of the this unit may lead to accumulation of cracked product from the reactor – regeneration unit, which may lead to shutdown of the entire units. As such, the reliability analysis of the unit is of great importance. Therefore, the basic input for finding the optimal maintenance tasks comes from Failure mode, effects and criticality analysis (FMECA) of the equipment [4]. FMECA is a step-by-step approach for identifying all possible failures in a design, manufacturing or assembly process, product or service [5]. It identifies and carries out corrective actions to address the most serious concerns.

Information gained by performing FMECA can be used as a basis for troubleshooting activities, maintenance, manual development and design of effective built-in test techniques[6].The analysis is characterized as consisting of two sub-analyses, the first being the failure modes and effects analysis (FMEA), and the second, the criticality analysis (CA).The method is widely used and accepted throughout the military and commercial industries [7].This tool was used by Ibrahim, A. et'al[8], 2015 to assess the reliability of a Reactor – regenerator unit. Their result showed that the reliability of the unit was found to be low. Similarly, Thangamani, G. et'al[9], 1995used this tool to assess the reliability of a FCCU. Also, Flecher, P[10]. 2012 used this tool to assess the risk of Sinopec X'ian branch FCCU. His result showed that reactor-regenerator systems have the highest potential hazard. In addition, Mahendra, P[4]. 2012 apply FMECA for ensuring reliability of process equipment. At the end of his work, highly critical systems and failure modes were identified and that the duration for which the equipment is out of work is reduced significantly. Similarly, Masoud. H. et'al[11] 2011 in their research "The application of FMEA in the oil industry in Iran: The case of four litre oil canning process of Sepahan Oil Company". The aim of their research was to show how FMEA could be applied to improve the quality of products at Sepahan Oil Company.However, after implementation of the improvement actions from FMEA, the can scrap percentage was reduced from 50000 to 5000 ppm and the percentage of the oil waste was reduced from 1 to 0.08%. Therefore, the use of FMECA to assess the reliability of FCCU will help to minimize huge financial loses as a result of equipment failure.

II. Methodology

FMEA was used to identify potential failure modes, failure mechanism, failure effects, detection method, compensation provision and severity of the reactor-regeneration unit. The FMEA data were generated from the failure logbooks, operating manuals, equipment maintenance manuals and questionnaires. After FMEA analysis, both quantitative and qualitative criticality analysis (FMECA) were performed. According to Ibrahim, A. et'al[8], 2015, Keller, P[12]. 2014, and RAC[13] 2005 equations (1), (2), (3) and (4) were used for the quantitative criticality analysis, while according to Puthillath, B. et'al[14] 2012, Yelmaz, M[15]. 2009, Sydney Water [16]2010 and Sultan, L.L[6]. 2011 equation (5) was used for the qualitative analysis.

$$Cr = \alpha * \beta * \lambda_i * t \quad (1)$$

Where,

α is the failure effect probability

$$\alpha = \frac{\lambda_i}{\bar{\lambda}} \quad (2)$$

$$\bar{\lambda} = \sum_{i=1,2,3\ldots}^{n} \lambda_i \quad (3)$$

β is the failure mode ratio

λ_i is the failure rate

$$\lambda_i = \frac{Occurrence}{Operating\ time} \quad (4)$$

t is the operating time

$$RPN = D * O * S \quad (5)$$

Where,

D is the detection

O is the occurrence

S is the severity

A criticality matrix was then computed from the plot of criticality number and severity using MS-Excel spread sheet. This was used to identify critical items which were then ranked according to their level of criticality.

III. Results and Discussion

The result of FMEA for the Fractionator is shown in Table 1. It generally indicates the potential failure modes, failure mechanism, failure effects, detection method, compensation provision and severity of the sub-units (fractionator primary condenser, bottoms product cooler, debutanizer oil condenser, main fractionator, main fractionator oil drum, main fractionator reflux drum, heavy naphtha exchanger, heavy cycle oil exchanger, bottoms exchanger, BFW heater, steam generator, stripper reboiler, debutanizer reboiler, top reflux pumps) under the fractionator. The fourteen (14) sub-units under study had twenty seven (27) failure modes, twenty seven (27) failure mechanism and twenty seven(27) failure effects. The detection method involve either the use of alarming systems, flowsensors or inspections. The compensation provision used were either Supervisory Control And Data Acquisition (SCADA) indicators, redudant systems or operation overide. The severity of the twenty one (21) failure effects of the sub-units is above average, between four (4) to nine (9). That is, froma

failure which may cause minor injury, minor property damage, or minor system damage which will result in delay or loss of sub-unit (marginal), to a failure which may cause death or lack of ability to carry out operation without warning (catastrophic). This values and description of the failures above were in conformity with the RAC[13], 2005 and Technical manual[17], 2006. Table 2 represents the qualitative FMECA for the fractionator unit. From the Table, six (6) sub-units (main fractionator, main fractionator reflux drum, heavy naphtha exchanger, main fractionator bottom exchanger, main fractionator bottoms/BFW heater and main fractionator bottom pumps) have their RPN greater than 300 these sub-units are critical and have low reliabilities. Eleven (11) of the sub-units (fractionator primary condenser, bottoms product cooler, debutanizer oil condenser, main fractionator oil drum, heavy cycle oil exchanger, steam generator, stripper reboiler, debutanizer reboiler, top reflux pumps, LCO product pump and heavy naphtha pump) have their RPN less than 200. These sub-units are said to be less critical and have moderate reliabilities. Ibrahim, A. et'al[8] 2015 and Puthillath, B. et'al[14] 2012 used these methods of RPN to categorize items.

Table 1: A FMEA sheet for Fractionator

	FAILURE MODE EFFECT ANALYSIS (FMEA)						
	STUDY AREA: Area 3 (KRPC)						
	SYSTEM : Fractionator						
	OBJECTIVE: To distilled into the FCC end products of cracked naphtha, fuel oil and off gas						
ITEM ID	FUNCTIONAL ID	POTENTIAL FAILURE MODE(S)	FAILURE MECHANISM	FAILURE EFFECTS	DETECTION METHOD	COMPENSATION PROVISION	SEVERITY
A01	fractionator primary condenser	ineffective overhead product cooling	tube blockage	low gasoline yield	alarm system	SCADA Indicator	3
		electric motor failure	motor winding open	over heating	alarm system	SCADA Indicator	8
A03	fractionator bottoms product cooler	improper product cooling	tube blockage	hot product sent to tank	alarm system	SCADA Indicator	7
		electric motor or fan failure	motor winding open	over heating	alarm system	SCADA Indicator	4
A05	debutanizer oil condenser	improper product cooling	tube blockage	hot product sent to tank	alarm system	SCADA Indicator	8
		electric motor or fan failure	motor winding open	over heating	alarm system	SCADA Indicator	4
C01	main fractionator	flooding of the column	tray collaps	improper seperation of product	alarm system	level indicator	2
		poor distillation	tray collaps	more of bottom product	alarm system	level indicator	5
D03	main fractionator oil drum	high level in seperator	P04 blockage	lost of product to drain to lower level	alarm system	level indicator	9
D04	main fractionator reflux drum	bad reflux in main fractionator	upstream blockage	improper seperation of product	alarm system	level indicator	9
		low level	P03 cavitation	high C01 over head temperature	alarm system	level indicator	8
E02A/B	feed/ heavy naphtha exchanger	ineffective heat transfer	tube blockage	low H02 outlet temperature	alarm temperature sensor	SCADA Indicator	5
		leakage	tube rupture	low outlet temperature	alarm temperature sensor	SCADA Indicator	5
		accumulated dirt	filament blockage	lube oil flow restriction	alarm temperature sensor	SCADA Indicator	7
		loss of vacuum	tube rupture	compressor might trip off	alarm temperature sensor	SCADA Indicator	6
E04	feed/ heavy cycle oil exchanger	ineffective heat transfer	tube blockage	low H02 outlet temperature	alarm temperature sensor	SCADA Indicator	5
		leakage	tube rupture	low outlet temperature	alarm temperature sensor	SCADA Indicator	5
E05	feed/ main fractionator bottoms exchanger	ineffective heat transfer	tube blockage	low H02 outlet temperature	alarm temperature sensor	SCADA Indicator	5
		leakage	tube rupture	low outlet temperature	alarm temperature sensor	SCADA Indicator	8
E07	main fractionator bottoms/BFW heater	improper heat recovery	tube blockage	low or no steam generation	alarm temperature sensor	SCADA Indicator	3
		poor BFW line-up	tube coking	low outlet temperature	alarm temperature sensor	SCADA Indicator	8
E08	main fractionator bottoms steam generator	improper heat recovery	tube blockage	bad cooling of slurry and no steam generation	alarm temperature sensor	SCADA Indicator	4
E11	stripper reboiler	bad or no heat transfer	tube blockage or leakage	ineffective reboiling	alarm temperature sensor	SCADA Indicator	2
E12	debutanizer reboiler	ineffective reboiling	tube blockage	poor seperation of gasoline/LPG	alarm temperature sensor	SCADA Indicator	5
P03A/B	main fractionator top reflux pumps	low level in reflux drum	improper column refluxing	poor seperation of product	flow sensor	Redundant System	2
		low suction head pressure	suction strainer dirty	poor discharged head pressure	flow sensor	Redundant System	8
		leakage	tube rupture	insufficient over head reflux	flow sensor	Redundant System	3

Table 2: A qualitative FMECA for Fractionator

	QUALITATIVE FAILURE MODES EFFECTS AND CRITICALITY ANALYSIS (FMECA)					
	STUDY AREA: Area 3 (KRPC)					
	SYSTEM : Fractionator					
	OBJECTIVE: To distilled into the FCC end products of cracked naphtha, fuel oil and off gas					
ITEM ID	**FUNCTIONAL ID**	**SEVERITY**	**OCCURRENCE**	**DETECTION**	**RPN1**	**RPN2**
A01	fractionator primary condenser	3	2	2	12	212
		8	5	5	200	
A03	fractionator bottoms product cooler	7	2	8	112	192
		4	4	5	80	
A05	debutanizer oil condenser	8	2	8	128	208
		4	4	5	80	
C01	main fractionator	2	8	3	48	328
		8	5	7	280	
D03	main fractionator oil drum	9	6	3	162	162
D04	main fractionator reflux drum	9	6	3	162	442
		8	5	7	280	
E02A/B	feed/ heavy naphtha exchanger	5	2	7	70	381
		5	3	7	105	
		7	1	8	56	
		6	5	5	150	
E04	feed/ heavy cycle oil exchanger	5	3	6	90	170
		5	2	8	80	
E05	feed/ main fractionator bottoms exchanger	5	9	4	180	460
		8	5	7	280	
E07	main fractionator bottoms/BFW heater	3	1	8	24	304
		8	5	7	280	
E08	main fractionator bottoms steam generator	4	6	7	168	168
E11	stripper reboiler	2	3	7	42	42
E12	debutanizer reboiler	5	3	8	120	120
P03A/B	main fractionator top reflux pumps	2	3	1	6	184
		8	5	4	160	
		3	2	3	18	
P05A/B	main fractionator heavy naphtha pumps	3	2	3	18	178
		8	5	4	160	
P09A/B	main fractionator bottoms pumps	8	5	7	280	424
		9	8	2	144	
P10A/B	main fractionator bottoms LCO product pumps	3	1	2	6	294
		8	5	6	240	
		8	3	2	48	

Table 3 shows the prioritized items for corrective action based on the fractionator RPN. Item with the highest RPN showed item to be considered first for either replacement, repair or maintenance. This is to ensured safety and reliability of the unit. The feed/ main fractionator bottoms exchanger has the highest RPN of 460 this means highest priority for corrective action, the order follows up to stripper reboiler with the least RPN value of 42. This means least priority for corrective action.In terms of selection criteria for maintenance program, Puthillath, B. et'al[14] 2012 also adopted this system of item ranking.

Table 3: A prioritized item ranking for fractionator

	ITEM RANKING QUALITATIVE (FMECA)	
	STUDY AREA: Area 3 (KRPC)	
	SYSTEM : Fractionator	
ITEM ID	FUNCTIONAL ID	ITEM RPN
E05	feed/ main fractionator bottoms exchanger	460
D04	main fractionator reflux drum	442
P09A/B	main fractionator bottoms pumps	424
E02A/B	feed/ heavy naphtha exchanger	381
C01	main fractionator	328
E07	main fractionator bottoms/BFW heater	304
P10A/B	main fractionator bottoms LCO product pumps	294
A01	fractionator primary condenser	212
A05	debutanizer oil condenser	208
A03	fractionator bottoms product cooler	192
P03A/B	main fractionator top reflux pumps	184
P05A/B	main fractionator heavy naphtha pumps	178
E04	feed/ heavy cycle oil exchanger	170
E08	main fractionator bottoms steam generator	168
D03	main fractionator oil drum	162
E12	debutanizer reboiler	120
E11	stripper reboiler	42

Table 4 depict the quantitative FMECA for fractionator unit.The data(item failure rates, failure mode ratio, maintainability, and item criticality number) where computed for the fourteen (14) sub-units(fractionator primary condenser, bottoms product cooler, debutanizer oil condenser, main fractionator, main fractionator oil drum, main fractionator reflux drum, heavy naphtha exchanger, heavy cycle oil exchanger, bottoms exchanger, BFW heater, steam generator, stripper reboiler, debutanizer reboiler, top reflux pumps). The criticality number (Cr) showed the level of risk and reliability of each of the sub-unit.The higher the criticality number (Cr) the more risk involve and the lower the reliability of the item. All the sub-units with the exception of heavy cycle oil exchanger have their Cr > 0.003. Similar data were obtained by RAC[13], 2005 and Technical Manual[17], 2006 in assessing the reliability of their defence equipment.

Table 4: A quantitative FMECA sheet for Fractionator

			QUANTITATIVE FAILURE MODES EFFECTS AND CRITICALITY ANALYSIS (FMECA)					
			STUDY AREA: Area 3 (KRPC)					
			SYSTEM : Fractionator					
			OBJECTIVE: To distilled into the FCC end products of cracked naphtha, fuel oil and off gas					
FUNCTIONAL ID	Operating time (hr	OCCURRENCE	Failure rate λ (/hr	Item failure rate	Failure effect probability	Failure mode ratio α	Failure mode criticality number	Item criticality number
fractionator primary condenser	17280	2	1.15741E-07	4.05093E-07	1	0.29	0.00058	0.00413
	17280	5	2.89352E-07		1	0.71	0.00355	
fractionator bottoms product cooler	17280	2	1.15741E-07	3.47222E-07	1	0.33	0.00066	0.00334
	17280	4	2.31481E-07		1	0.67	0.00268	
debutanizer oil condenser	17280	2	1.15741E-07	3.47222E-07	1	0.33	0.00066	0.00334
	17280	4	2.31481E-07		1	0.67	0.00268	
main fractionator	17280	8	4.62963E-07	7.52315E-07	1	0.62	0.00496	0.00686
	17280	5	2.89352E-07		1	0.38	0.0019	
main fractionator oil drum	17280	6	3.47222E-07	3.47222E-07	1	1	0.006	0.006
main fractionator reflux drum	17280	6	3.47222E-07	6.36574E-07	1	0.55	0.0033	0.00555
	17280	5	2.89352E-07		1	0.45	0.00225	
feed/ heavy naphtha exchanger	17280	2	1.15741E-07	6.36574E-07	1	0.18	0.00036	0.00352
	17280	3	1.73611E-07		1	0.27	0.00081	
	17280	1	5.78704E-08		1	0.1	0.0001	
	17280	5	2.89352E-07		1	0.45	0.00225	
feed/ heavy cycle oil exchanger	17280	3	1.73611E-07	2.89352E-07	1	0.6	0.0018	0.0026
	17280	2	1.15741E-07		1	0.4	0.0008	
feed/ main fractionator bottoms exchanger	17280	9	5.20833E-07	8.10185E-07	1	0.64	0.00576	0.00756
	17280	5	2.89352E-07		1	0.36	0.0018	
main fractionator bottoms/BFW heater	17280	1	5.78704E-08	3.47222E-07	1	0.17	0.00017	0.00432
	17280	5	2.89352E-07		1	0.83	0.00415	
main fractionator bottoms steam generator	17280	6	3.47222E-07	3.47222E-07	1	1	0.006	0.006
stripper reboiler	17280	3	1.73611E-07	1.73611E-07	1	1	0.003	0.003
debutanizer reboiler	17280	3	1.73611E-07	1.73611E-07	1	1	0.003	0.003
main fractionator top reflux pumps	17280	3	1.73611E-07	5.78704E-07	1	0.3	0.0009	0.0038
	17280	5	2.89352E-07		1	0.5	0.0025	
	17280	2	1.15741E-07		1	0.2	0.0004	
main fractionator heavy naphtha pumps	17280	2	1.15741E-07	4.05093E-07	1	0.29	0.00058	0.00413
	17280	5	2.89352E-07		1	0.71	0.00355	
main fractionator bottoms pumps	17280	5	2.89352E-07	7.52315E-07	1	0.38	0.0019	0.00686
	17280	8	4.62963E-07		1	0.62	0.00496	
main fractionator bottoms LCO product pun	17280	1	5.78704E-08	5.20833E-07	1	0.11	0.00011	0.0039
	17280	5	2.89352E-07		1	0.56	0.0028	
	17280	3	1.73611E-07		1	0.33	0.00099	

Table 5 is the quantitative item ranking for the Fractionator unit. Items were ranked according to their level of criticality number. The main fractionator bottoms exchanger have the highest criticality number of 0.00756 while theheavy cyle oil exchanger has the least criticality number of 0.0026. However, in terms of maintenance, or repair or replacement, sub-units with the highest criticality number would be considered first.

Table 5: A quantitative FMECA item ranking for Fractionator

	ITEM RANKING QUANTITATIVE (FMECA)				
	STUDY AREA: Area 3 (KRPC)				
	SYSTEM : Fractionator				
Item ID	Functional ID	Operating time (hr)	failure rate λ (/hr)	Failure effect probability β	Item criticality number
E05	feed/ main fractionator bottoms exchanger	17280	8.10185E-07	1	0.00756
C01	main fractionator	17280	7.52315E-07	1	0.00686
P09A/B	main fractionator bottoms pumps	17280	7.52315E-07	1	0.00686
D03	main fractionator oil drum	17280	3.47222E-07	1	0.006
E08	main fractionator bottoms steam generator	17280	3.47222E-07	1	0.006
D04	main fractionator reflux drum	17280	6.36574E-07	1	0.00555
E07	main fractionator bottoms/BFW heater	17280	3.47222E-07	1	0.00432
A01	fractionator primary condenser	17280	4.05093E-07	1	0.00413
P05A/B	main fractionator heavy naphtha pumps	17280	4.05093E-07	1	0.00413
P10A/B	main fractionator bottoms LCO product pumps	17280	5.20833E-07	1	0.0039
P03A/B	main fractionator top reflux pumps	17280	5.78704E-07	1	0.0038
E02A/B	feed/ heavy naphtha exchanger	17280	6.36574E-07	1	0.00352
A03	fractionator bottoms product cooler	17280	3.47222E-07	1	0.00334
A05	debutanizer oil condenser	17280	3.47222E-07	1	0.00334
E11	stripper reboiler	17280	1.73611E-07	1	0.003
E12	debutanizer reboiler	17280	1.73611E-07	1	0.003
E04	feed/ heavy cycle oil exchanger	17280	2.89352E-07	1	0.0026

Figure 1 is the criticality matrix for the fractionator. From the figure,the plot of criticality number against severity was used to identify those critical failure modes related to the sub-units. Also, fifteen (15) out of the twenty nine (29) failure modes identified were above or closely below the criticality line while fourteen (14) values of the failure modes were below the criticality line. Those values above and closely below the criticality line showed how critical those failure modes were with respect to the unit (Fractionator). However, it means that the reliability of those sub-units is low, therefore, preventive maintenance is recommended. Ibrahim, A. et'al[8] 2015 and Rooney, et'al[18]1988 also recommended preventive maintenance for high risk, because it may eventually results in substential reduction in production periods.

Table 6: A criticality matrix for fractionator

ITEM ID	SEVERITY	Criticality number
A01	3	0.00058
	8	0.00355
A03	7	0.00066
	4	0.00268
A05	8	0.00066
	4	0.00268
C01	2	0.00496
	8	0.0019
D03	9	0.006
D04	9	0.0033
	8	0.00225
E02A/B	5	0.00036
	5	0.00081
	7	0.0001
	6	0.00225
E04	5	0.0018
	5	0.0008
E05	5	0.00576
	8	0.0018
E07	3	0.00017
	8	0.00415
E08	4	0.006
E11	2	0.003
E12	5	0.003
P03A/B	2	0.0009
	8	0.0025
	3	0.0004
P05A/B	3	0.00058
	8	0.00355
P09A/B	8	0.0019
	9	0.00496
P10A/B	3	0.00011
	8	0.0028
	8	0.00099

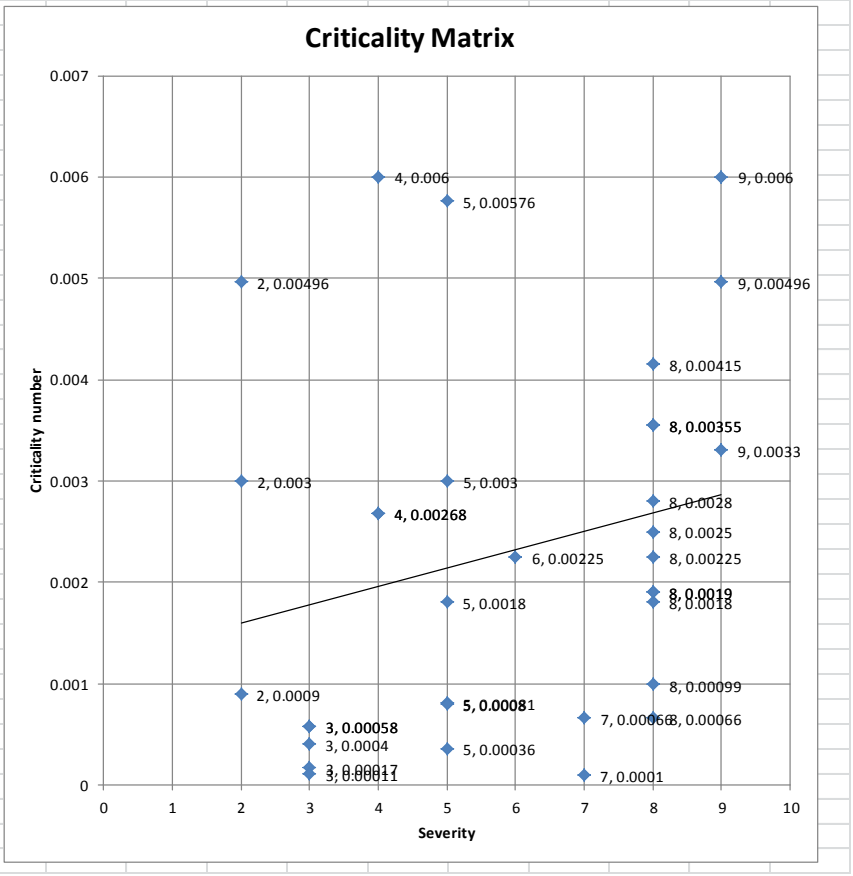

Figure 1: A criticality matrix for fractionator

IV. Conclusion

The performance behavior of fractionator unit via its sub-units (fractionator primary condenser, bottoms product cooler, debutanizer oil condenser, main fractionator, main fractionator oil drum, main fractionator reflux drum, heavy naphtha exchanger, heavy cycle oil exchanger, bottoms exchanger, BFW heater, steam generator, stripper reboiler, debutanizer reboiler, top reflux pumps) was assessed using FMECA as the reliability assessment tool.

Fromthe qualitative analysis used, the reliability of the fractionator was found to be low.This is because nine (9) sub-units (main fractionator, main fractionator reflux drum, heavy naphtha exchanger, main fractionator bottom exchanger, main fractionator bottoms/BFW heater and main fractionator bottom pumps, fractionator primary condenser, bottoms product cooler, and debutanizer oil condenser) of the fractionator unit have their RPN greater than 200, these sub-units are critical and have low reliabilities.Also, from the quantitative analysis, all the sub-units with the exception of heavy cycle oil exchanger have their Cr > 0.003.This means low reliability of the fractionator.

From the analysis of the criticality matrix, most of the values of the failure modes were either above or very close to the criticality line, as such, it can be concluded that the reliability of the fractionator unit is low. As such, preventive maintenance is recommended.

The use of FMECA to assess the reliability of fractionator unit,will help to reduce financial losses as a result of equipment damage, injury to personnel and above all loss of life.

Reference

[1] Judith, H. 2011. The 100 Largest Losses. Marsh Energy Practice.
[2] Hamisu, M. 2011. Not Quit Good for Oil Industry. Daily Trust Retrieved December.
[3] Hendrix Group. 2011. Petroleum Refining Corrosion. Bakers Landing, Houston, Texas.
[4] Mahendra, P. 2012. Applying FMECA for Ensuring Mission Reliability of Equipment. Institute for Defense Study and Analysis (IDSA) India.
[5] Malay, N., Kumar, P. and Mishra, A. 2012. Failure Mode Effect and Criticality Analysis. International Journal of Scientific and Engineering Research, 3(1).
[6] Sultan, L.L. and Huq, L.J. 2011. Risk analysis method: FMEA/FMECA in the organization. International Journal of Basic & Applied Sciences. 11(05).
[7] Rausand, M. and Haugen, S. 2003. Preliminary Hazard Analysis. Risk Assessment Section 9.6. Rams Group.
[8] Ibrahim, A. and El-Nafaty, U. A. (2015). Reliability Analysis of Reactor-Regenerator unit of the Kaduna Refinery using Failure Modes Effect and Criticality Analysis (FMECA). International Journal of Advance Technology in Engineering and Science (IJATES).3(7), 100-109.
[9] Thangamani, G., Narendran, T.T. & Subramanian, R. 1995. Assessment of availability of a fluid catalytic cracking unit through simulation. Journal of Reliability Engineering and Safety, 47, 207-220.
[10] Flecher, P. 2012. Study of the FCCU Risk Assessment of Sinopec Xi'an Branch. A Research Thesis.
[11] Masoud, H. , Arash, S. and Natraj, R.2011. The application of FMEA in the oil industry in Iran: The Case of four litre oil canning process of sepahan oil company. African Journal of Business Management. 5(8), 3019-3027.
[12] Keller, P. 2014. Criticality Analysis. QA publisher, LLC.
[13] Reliability Information Analysis Center (RAC). 2005. Failure Modes Effect and Criticality Analysis. Department of Defense, USA.
[14] Puthillath, B and Sasikumar, R. 2012. Selection of maintenance strategy of process equipment using FMECA. Intenational Journal of Engineering and Innovative Technology (IJEIT).
[15] Yelmaz, M.2009. Failure Mode Effect and Criticality Analysis Presentation.
[16] Sydney Water. 2010. Failure Modes Effect and Criticality Analysis Procedure.
[17] FMECA technical manual. 2006. FMECA for Command, Control, Communication, Computer Intelligence and Reconnaissance (C41SR) facilities. Department of the Army, Washington D.C.
[18] Roney, J. J., Turner, J. H. and Arendt, J. S. (1988). Preliminary hazards analysis of a fluid catalytic cracking unit complex. Journal of Loss Prevention in Process Industry 1, 96-103.

American Journal of Engineering Research (AJER) 2016
American Journal of Engineering Research (AJER)
e-ISSN: 2320-0847 p-ISSN : 2320-0936
Volume-5, Issue-2, pp-109-119
www.ajer.org
Research Paper Open Access

An Experimental Investigation of Galvanic Anode Specifications for Suitable Cathodic Corrosion Protection of Low Carbon Steel in Kaduna Metropolitan Soil

T.N. Guma, S.U. Mohammed and A.J. Tanimu
Department of Mechanical Engineering,
Nigerian Defence Academy, Kaduna,
Kaduna State, Nigeria

Abstract: *The paper stresses corrosion risks from huge underground engineering steel structures within the metropolitan area of Kaduna-a top city in Nigeria. Cathodic protection (CP) is examined as an effective, economical and durable method of preventing corrosion of such structures if suitably designed-installed. Variables that can cause wide differences and difficulties in CP designs such as material make, surface area and nature of structure, corrosivity level of environment, etc, are recognized. Some supplementary information that accounts for complexity of such variables which can be used to optimize CP design of the structures was sought experimentally. Relative performances by zinc, pure magnesium and magnesium alloy as common and cheap galvanic anodes were investigated in a laboratory CP of polished bare low carbon steel specimens in soil of surveyed resistivity spectrum 31.9-152.9 ohm-m from the area. Specimens were exposed with and without CP by the anodes at ambient temperature up to 40 days in various samples of the soil. Levels of specimen protections were determined by analysis of obtained information on their corrosion rates and polarized potentials relative to the un-protected ones at 8-day intervals. The analysis indicated that; corrosion of the structures can be optimally reduced to negligible rates by polarizing them to -0.85V versus $Cu/CuSO_4$ electrode with the anodes, pure magnesium is comparatively the best of the anodes for CP of the structures in terms of economy and effectiveness followed by magnesium alloy, and a unit surface area of the anodes can protect up to nearly 1200 units of the structure with the -0.85V protective potential depending on the anode type.*

Key words*: Underground engineering assets, variation in soil corrosivity level and risks, Kaduna metropolitan area, steel structures, cathodic protection, some supplementary design information*

I. INTRODUCTION

One of the biggest challenges facing our aging infrastructures is material loss and deterioration by electrochemical reactions that cause corrosion [1]. High liability and costs can arise due to corrosive actions of soils that underground engineering structures are in associated contact with. Study by the Federal Highway Administration of United States showed that the total direct cost of corrosion in the United States alone was $279 billion per year, which is about 3.2 percent of the nation's present gross domestic product (GDP). The study also showed that the major contribution to this value was from corrosion occurring in the ground. These included drinking water and sewer systems, highway bridges, oil and gas and other fluid transmission pipelines [2 and 3]. Corrosion attacks are frequently responsible for most material failures or limitations by causing them to lose their cherished strength, ductility and other mechanical properties. The problem is especially to steel structures and the extent depends on the corrosivity level of the environment. The frequent collapse of critical underground engineering structures such as pipelines due to corrosion is a serious concern to engineers, governments and the general populace. The adverse effects are colossal loss of lives and properties. Unprotected pipelines, buildings, and other engineering structures erected on corrosive soils usually have shorter life span [4, 5, and 6]. Therefore, when construction of a new buried or submerged system is being planned, the corrosivity of the environment should be considered as one of the factors in the design of the system. If corrosion is not considered, the service life of the system may be severely overestimated and public safety may be at risk [2]. The critical material of construction with regard to corrosion in soil environment is carbon steel. Low carbon steel is the most widely used engineering material but has the least corrosion resistance and accounts to about 90% of all steels used for structural works because of its good fabrication and formability properties as well as

availability in various structural sizes and shapes at relatively cheaper prices compared to other structural materials [7 and 8].

Kaduna is one of the top cities in the ranking of population, industrialization, military garrison and administrative importance in Nigeria. The city is located on the southern end of the high plains of Northern Nigeria, gridded by Latitude 100 40IN and 100 60IN and Longitude 70 10IE and 70 35IE [9]. It is a noted centre for refining crude oil, automobile manufacturing, producing weapons, brewing and bottling, textile manufacturing, sand-casting, metal forging, civil engineering construction works, agricultural processing, metalworking, electric power distributing, warehousing, machinery manufacturing, steel working, treating water, etc [10]. One of the three refineries in Nigeria is located in the metropolitan area of the city. The refinery has a production capacity of about 110,000 barrels per stream day. A number of pipelines transport large quantities of crude oil, natural gas, petroleum products in the process of feeding the refinery with raw stock and distributing its products to some away locations. To keep pace with the growing levels of industrialization, military garrison, population and social needs; underground engineering structures such as drinking water and sewer municipal conduits, foundations of highway bridges and buildings, hydraulic tunnels, reservoirs for drinking water, storage facilities for oil and gas, pedestrian underpasses, military installations, containers for burying harmful industrial wastes, electric power transmission and communication facilities, etc have inevitably continued to be constructed in the city metropolis as more beneficial technological means of developments. Site surveys by Tanimu [10] showed that most of the structures were made of steel or consisted of steel components and designed with corrosion consideration. Some of them were subjected to various levels of corrosion attributable to lapses, accessibility difficulties, and costs in maintenance. Changing some of the structures can be very time consuming and expensive procedure while their corrosion problems can be technically corrected or not corrected, and incur loses with or without awareness. Given the implications of failures from such important structures and the role that external corrosion can play in their failures, it is apparent that proper corrosion control can have a major impact on safety, environmental preservation and economics of their operation or services [6 and 10].

The commonly used parameters for evaluating corrosion potential of soil are resistivity, pH, sulfate content, chloride content, Redox potential and sulfide content. Soils usually have a pH range of 5-8. In this range, pH is generally not considered to be a dominant variable affecting corrosion rates. More acidic soils represent serious corrosion risk to common structural materials such as steel, cast iron and zinc coatings. Soil resistivity is historically a broad indicator of soil corrosivity. Soil corrosivity resistivity generally decreases with increasing moisture content and the concentration of chemical species. Soil corrosivity is inversely related to soil resistivity so that low soil resistivity indicates high probability of corrosion potential. Soil resistivity is typically indicative of soil corrosivity in alkaline soils and is useful as a guide in acid soils. Although a high soil resistivity alone will not guarantee absence of serious corrosion, electrical resistivity is effective, suitable and most important parameter for assessment of soil corrosivity/aggressiveness level [6 and 11]. Soil corrosivity level can vary widely from one geographical area or location to another so engineering principle demands that specific corrosivity levels at the locations should be used in optimal protective design of underground structures. Guma *et a*l [6] reported that the soil resistivity of Kaduna metropolitan area varies within the extremes of about 31.9 Ohm-m at the depth of 0.5m to152.9 Ohm-m at the depth of 4.5m with overall mean value of 72.13481 Ohm-m, standard deviation of 33.78109 Ohm-m and coefficient of variation 46.83%. Translated into corrosivity, the report represented a stochastically variable soil corrosivity spectrum that is mildly corrosive on average and generally varies downwards underground from aggressive at depths of less than about 0.5m to slightly corrosive around 4.5m [6].

In order for corrosion to occur, four components must be active. These components are the anode, cathode, electrolyte and metallic path [12]. Cathodic protection is an electrical method of preventing corrosion of metallic structures which are in electrolytes such as soil or water. The technique was first used in 1824 by Sir Humphrey Davy and described in a series of papers presented to the Royal society in London [1 and 12]. It is second only to the use of protective coatings as a mean of corrosion control. Cathodic protection is usually technically feasible and a standard procedure for many external surfaces of underground or underwater structures such as pipelines, ship hulls and interiors, lock gates and dams, water treatment facilities, well casings, trash racks and screens, bridge decks, steel pilings, the interiors of underground storage tanks that contain electrolytes such as water or acid; offshore steel structures such as platforms and oil rigs, waterfront structures such as sheet pilings or bearing piles, and concrete structures exposed to seawater. In practical applications, structures commonly provided with cathodic protection are constructed of iron or steel including stainless steel and the electrolytes are often soil and water. Other metals commonly provided with cathodic protection include lead sheathed cables, copper and aluminum piping, galvanized steel, and cast iron. The problems presented in attempting to provide cathodic protection for existing bare structures are much more difficult than those on coated structures. The major difficulty arises because of the much greater magnitude of anode size or current required [13].

Cathodic protection is achieved by applying counter-corrosion current through the use of sacrificial (galvanic) anodes or impressed current with inert anodes to the structure to be protected. When enough current is applied, the whole structure will be at one potential; thus anode and cathode sites will not exist and the entire structure will be well protected. Little current will lead to ineffective protection. High current will lead to disbondment of any applied coatings, hydrogen embrittlement, more power consumption and higher cost. Installation also demands that the potential of the structure to be protected should be kept less than the protection potential. Sacrificial anode materials used in CP are required to be capable of providing sufficient current to adequately protect a structure, to be self-regulating in terms of potential, to have high driving voltage difference between the operating voltage of the anode and the polarized structure they are protecting over their lifetimes, to consistently have a high capacity to deliver electric current per unit mass of material consumed, not to passivate, and to be easy of manufacturing in bulk available quantities and adequate mechanical properties . CP designs can differ widely for different locations or environments due to variations in corrosivity levels, material make of the structure to be protected, surface area and nature of the structure, type and size of anode used or amount of protective current applied, and degree of interference by stray currents in the environment [14 and 15]. Proper CP can therefore require pertinent preliminary studies in specific environments to reveal abnormal conditions not suspected that can be used to improve design [16 and 17]. The aims of the paper are:

i. To create public awareness of much underground steel structural assets or component parts within the metropolitan area of Kaduna and highlight potential corrosion risks, hazards and liabilities from them.
ii. To examine some basic supplementary criteria that can be used to augment cathodic protection adequacy of such assets with zinc, pure magnesium, and magnesium alloy as relatively common, cheap and available galvanic anodes world over.
iii. To contribute to the total research efforts towards control of structural steel work corrosion in the area to the barest level.

1.1Galvanic anodes in cathodic protection

Advantages of cathodic protection using galvanic or sacrificial anodes are; no external power source is required, ease of installation and relatively low installation costs, unlikely cathodic interference in other structures so popular for protection in congested and complex locations, Low maintenance systems, self-regulation, relatively low risk of overprotection and relatively uniform potential distributions. Disadvantages include: limited current and power output, high-corrosivity environments or large structures may require excessive number of anodes, anodes may have to be replaced frequently under high current demand and anodes can increase structural weight if directly attached to a structure. Numerous materials may be used as galvanic anodes, but only few can economically satisfy all the parameters required for practical applications in view of limitations imposed by electrochemical dissolution rate and/or mechanical durability [18]. A side effect of improperly performed cathodic protection may be production of molecular hydrogen, leading to its absorption in the protected metal and subsequent hydrogen embrittlement; which can cause some metals such as high strength steel to become brittle and crack following exposure to hydrogen [1]. There are three main metals used as galvanic anodes for buried structures such as pipes and tanks. These are pure magnesium, magnesium alloy, and pure zinc. Galvanic anodes are designed and selected to have a more active voltage (technically a more negative electrochemical potential) than the metal to be protected. Magnesium and zinc anodes are commercially available in all sizes and shapes such as blocks, rods, plates or extruded ribbon. Each anode type has relative performance advantages in specific aqueous environments [19].

The design of galvanic anode CP system requires consideration many factors such as the type of structure, resistivity of the electrolyte typically soil or water it will operate in, the type of coating and the desired service life. The primary calculation is how much anode material will be just enough to completely mitigate corrosion of the structure in a specific environment. Too little material will provide protection for a while, but need to be replaced regularly. Too much material would provide protection at an unnecessary cost. The mass in kg for design life in years in which one year is equal to 8760 hour is given by equation 1 [19]:

$$\text{Mass} = \frac{Current\ \ Required\ \ x\ Design\ \ Life\ x\ 8760}{Utilization\ \ \ Factor\ \ x\ Anode\ \ Capacity} \qquad (1)$$

The utilization factor (UF) of the anode is a constant value, depending on the shape of the anode and how it is attached, which signifies how much of the anode can be consumed, before it ceases to be effective. A value of 0.8 indicates that 80% of the anode can be consumed before it should be replaced. A long slender stand-off anode installed on legs to keep the anode away from the structure has a UF value of 0.9, whereas the UF of a short, flush mounted anode is 0.8. Anode capacity is an indication of how much material is consumed as current flows over time [19].

II. MATERIALS AND METHODOLOGY

2.1 Materials

The materials used for the tests were available and easily obtained from reputable commercial sources in Kaduna, Nigeria. They were.

i. A flat low carbon steel sheet of about 3000mm by 5000mm and 3mm-thickness.
ii. 40 litres of distilled water.
iii. 12 litres of 0.8M Analar grade sulphuric acid (H_2SO_4).
iv. Five soil samples of respective average resistivity 31.9, 43.69, 68.3, 90.75 and 152.9 ohm-metre harvested from previously surveyed different underground locations within the metropolitan area of Kaduna by Guma *et al* [6], and
v. Enough number of zinc, pure magnesium and magnesium alloy galvanic anodes of cylindrical shapes, 300 cm^2 surface areas and 0.5Kg masses.

2.2 Test Procedure

The percentage elemental weight composition of the procured low carbon steel sheet was analyzed at 10 locations using suitable mechanically sawn off pieces at the locations and the Japanese-made Shimadzu-PDA-7000 optical emission spectrometer metal analyzer. The analysis confirmed that the sheet was indeed low carbon steel with average percentage elemental weight composition shown in Table 1:

Table 1: Average elemental weight composition of the procured steel

Element	C	Mn	Si	S	Cr	Cu	Fe
Composition [%]	0.02	0.26	0.014	0.009	0.017	0.013	99.6

The three procured anode materials were also each analyzed using the analyzer. The analyses showed on average; 99.95% purity level of the zinc, 99.99% purity level of the pure magnesium anodes and 6.01% Al, 2.98% Zn, 0.15% Mn and 90.84% Mg composition for the magnesium alloy anodes. Steel specimens in form of pieces each 100 by 100mm and 3mm thick were sawn off from the procured and confirmed low carbon steel sheet and used for corrosion rate and potentiostatic polarization studies in parallel experiments. The sheet were used because they were light-weight and flat and considered more suitable for proper cleaning and detection of small changes in their masses for the test.

A preliminary test was conducted on optimum amount of water and acid to be added to 3.1Kg of each harvested soil sample to account for losses due to evaporation from the sample during laboratory experimentation. Daily measurements taken with a pH meter and speedy moisture tester showed that 0.18 litres of water and 2ml of the Analar grade sulphuric acid when sprinkled daily on the samples in plastic containers did not cause average variation of more than ±6.9% moisture content and ±2.3% pH of the samples' predetermined average field conditions of 10% moisture content and Ph 5.8 respectively. This preliminary test method and information were applied to keep acidity and moisture content levels of each test soil sample of about 3.1Kg by mass fairly maintained. Soil samples were collected in impermeable covered plastic containers, conveyed on a motor bike within one hour to the laboratory and used immediately thereafter for the tests. Specimens were exposed at room temperatures in samples of the soil contained in plastic containers of about 0.35m-diameter and 0.3m-depth in the laboratory. The containers were wrapped with waterproofs that were perforated with similar holes so as to further reduce moisture evaporation from the soil samples during the experimentation time whilst ensuring natural aeration of the soil samples. One anode was used for one steel specimen in different containers.

Corrosion rate experiment

In order to establish the optimum CP potential for lowest corrosion rate, potentiostatic weight loss measurements were made and used to determine corrosion rate of each specimen under various exposure durations and soil resistivity. Before each experiment, surfaces of specimens were polished to average surface finishes of 1µm with 220, 500, 800 mesh grinding, washed by brushing with plastic brush and running tap water, cleaned with distilled water, wiped with tissue paper, oven-dried at 110^OC using an electrical oven and kept in desiccators. Just before exposure to the soil, specimens were removed from the desiccators, weighed to the nearest 0.1 milligram using a very accurate digital electronic scale with capability of weighing as low as 0.01 milligram and the weight of each noted as W_1.To study the effect of variation of resistivity spectrum of the metropolitan soil on corrosion rates of the test steel, five specimens of the steel were each separately fully buried for 40 days in soil samples of resistivities 31.9, 43.69, 68.3, 90.7 and 152.9 ohm-m contained in five separate containers without protection and allowed to corrode freely at 25^OC ambient temperature. Each specimen was

removed at the same time after the 40th day; washed with running tap water and bristle brush to remove any corrosion products that formed on the surface of the specimen and then immersed in 10% hydrochloric acid containing chemical inhibitor (thiohanstoff) for 30 seconds, then washed by tap and then distilled water, dried with clean tissue, rinsed in ethanol and heat-dried in an electrical oven at a temperature of about 110^{O}C for 10minutes. Thereafter the specimens were kept in desiccators to cool and then weighted to obtain the weight each as (W_2). The weight loss of each specimen was obtained as $W= W_1-W_2$ and converted into corrosion penetration rate (CPR), in terms of mm/yr. The experiment was carried out in accordance with the procedures used by Schwerdtfeger [20], Mahato *et al* [21] and Rashid [22]. The CPR of each specimen was evaluated as [7 and 22]:

$$CPR = \frac{8.76W}{DAT} \qquad (2)$$

Where: W = weight loss in milligrams, D = density in g/cm^3, A= area in cm^2, and T = exposure time of the steel specimen in hours.

Soil of resistivities 31.9, 90.7 and 152.9 Ohm-m essentially fall in the ranges of aggressive, slight, and progressively less corrosivities respectively [6]. Soil samples of resistivities 31.9, 90.7, and 152.9 Ohm-m from the metropolitan area, were used to study the effect of variation in exposure duration on unprotected and protected specimens exposed to the soil. Five specimens were buried in soil samples of each resistivity for various durations up to 40 days without protection. One specimen was removed from each soil sample at 8-day intervals, and had its CPR determined by equation 2 according to the foregoing procedure. Thereafter, 45 specimens were used to study the effect 8-day interval variation on the corrosion rate of protected specimens. A rubber-covered stranded copper wire was soldered to one end of each of the specimens for electrical connection to the anodes. 15 of the 45 specimens were submerged in separate plastic containers each containing soil sample of resistivity 31.9 Ohm-m. Five of the 15 specimens were each connected to a zinc anode, five each to a magnesium alloy anode, and five each to a pure magnesium anode with each anode buried 10cm away from the specimen in the soil in the respective containers. This was similarly done with the 90.7 Ohm-m, and then 152.9 Ohm-m resistivity soil samples. One protected specimen by each anode was removed at 8-day intervals up to 40 days from the soil samples for each case of 31.9, 90.7, and 152.9 Ohm-m resistivity and had its CPR determined by equation 2 after similar cleaning and weight loss by the earlier used procedure.

Potential measurement

Various sizes of prepared specimens of the steel were used for the potential measurement. For the corrosion rate, the same mass and specimen exposure area (300cm^2) were used. Specimens were immersed in turn in test soil of given resistivity in a similar procedure to the foregoing section after being connected to a specified anode with the same size of copper wire. The tube saturated $Cu/CuSO_4$ was placed within 2mm from the specimen and electrically connected to it whilst the $Cu/CuSO_4$ electrode was connected to the negative terminal of the voltmeter type E7000 and the positive terminal of the voltmeter to the specimen. Specimen potentials were recorded at intervals of eight days using the voltmeter and $Cu/CuSO_4$ electrode as the reference electrode. After removing the specimens, the soldered wire connection of the specimens were carefully removed by applying heat from a soldering iron and the last bits of solder were removed by scrapping with a soft metal tool. Cleaning and weighing of specimen before the tests and after polarization were as explained in the foregoing section. After wards the specimen sizes were increased relative to that of one anode in the same procedure and the corresponding protective potentials noted.

III. RESULTS AND DISCUSSIONS

The test results of the study are presented in Figures 1-10.

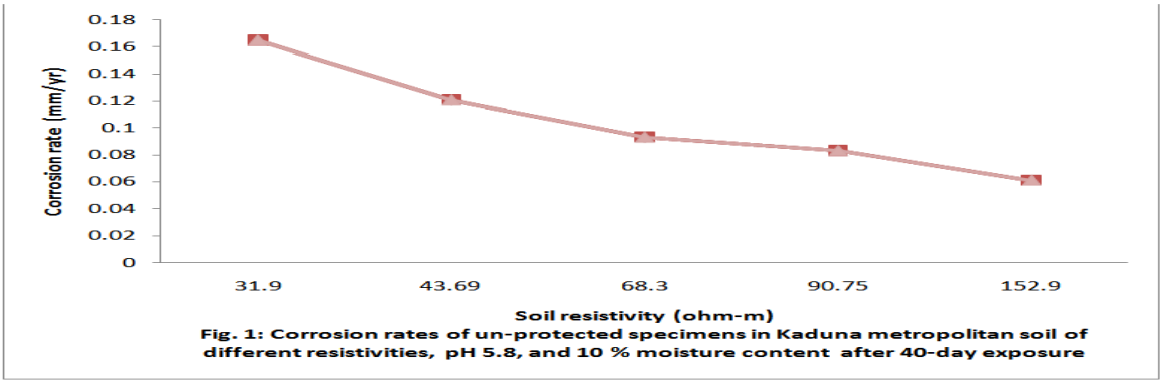

Fig. 1: Corrosion rates of un-protected specimens in Kaduna metropolitan soil of different resistivities, pH 5.8, and 10 % moisture content after 40-day exposure

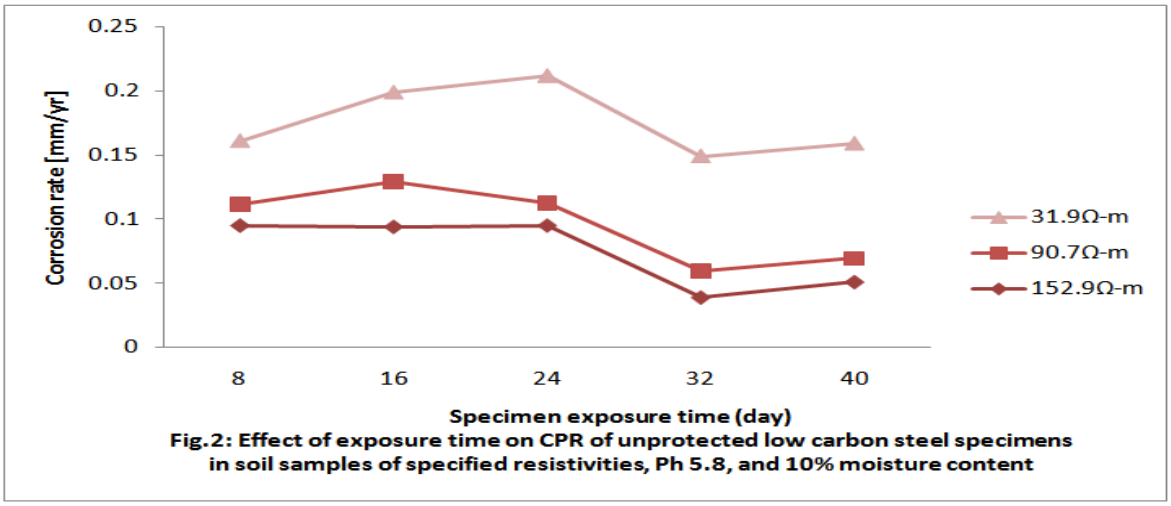

Fig.2: Effect of exposure time on CPR of unprotected low carbon steel specimens in soil samples of specified resistivities, Ph 5.8, and 10% moisture content

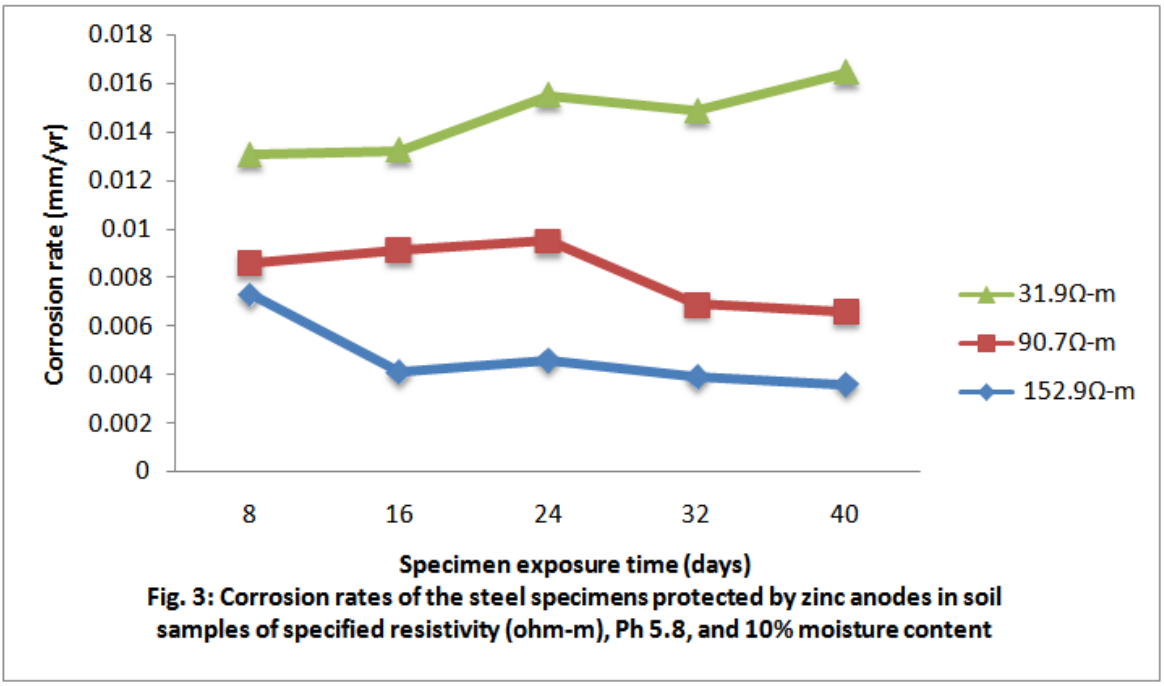

Fig. 3: Corrosion rates of the steel specimens protected by zinc anodes in soil samples of specified resistivity (ohm-m), Ph 5.8, and 10% moisture content

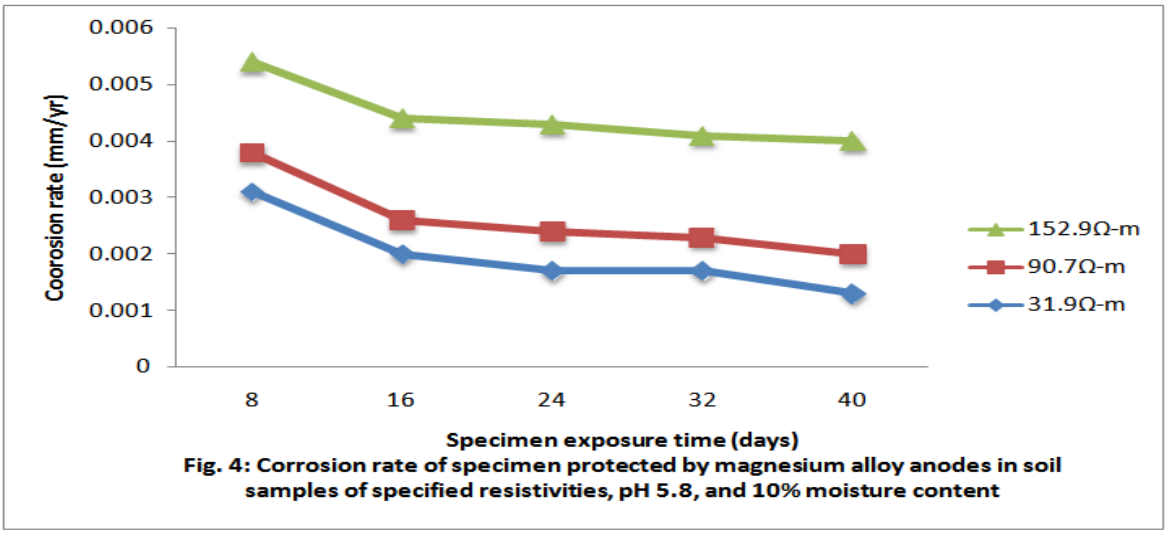

Fig. 4: Corrosion rate of specimen protected by magnesium alloy anodes in soil samples of specified resistivities, pH 5.8, and 10% moisture content

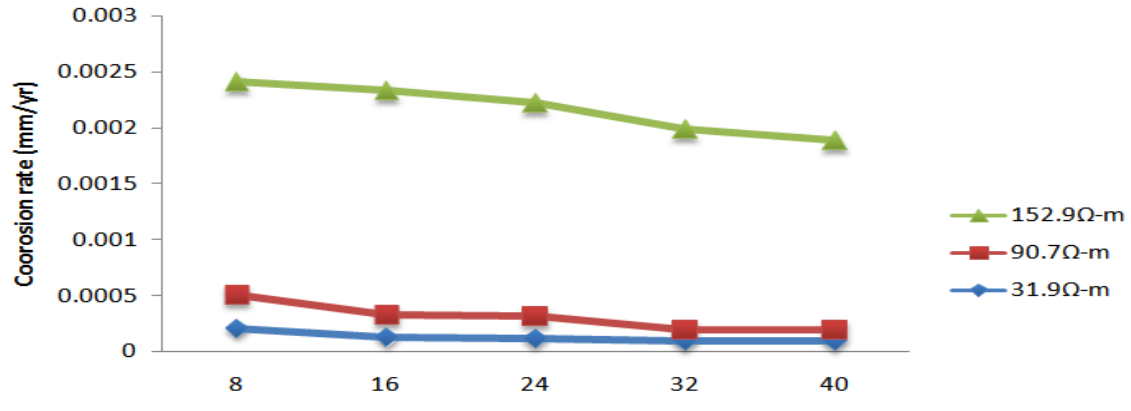

Fig. 5: Corrosion rate of specimen protected by pure magnesium anodes in soil samples of specified resistivities, pH 5.8, and 10% moisture content

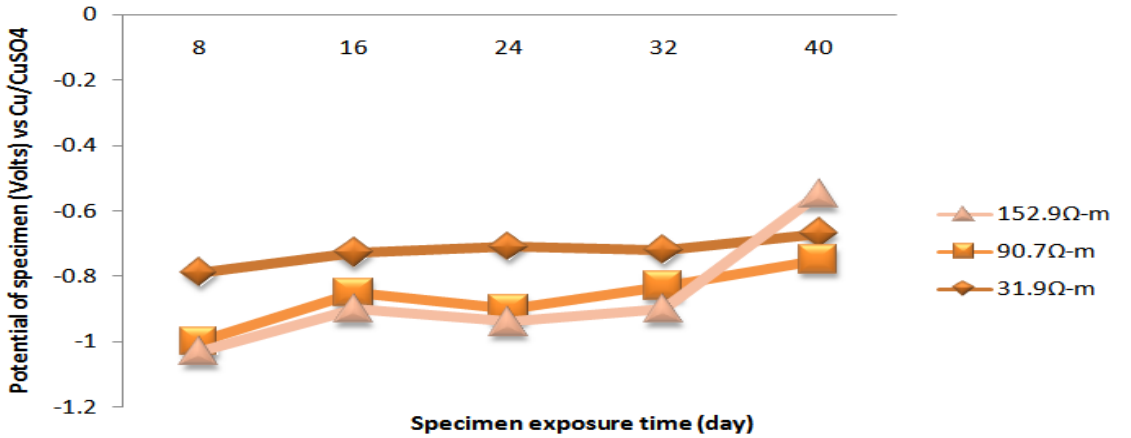

Fig.6: Polarized potential of specimen protected by zinc anodes in soil samples of specified resistivities, Ph 5.8, and 10% moisture content

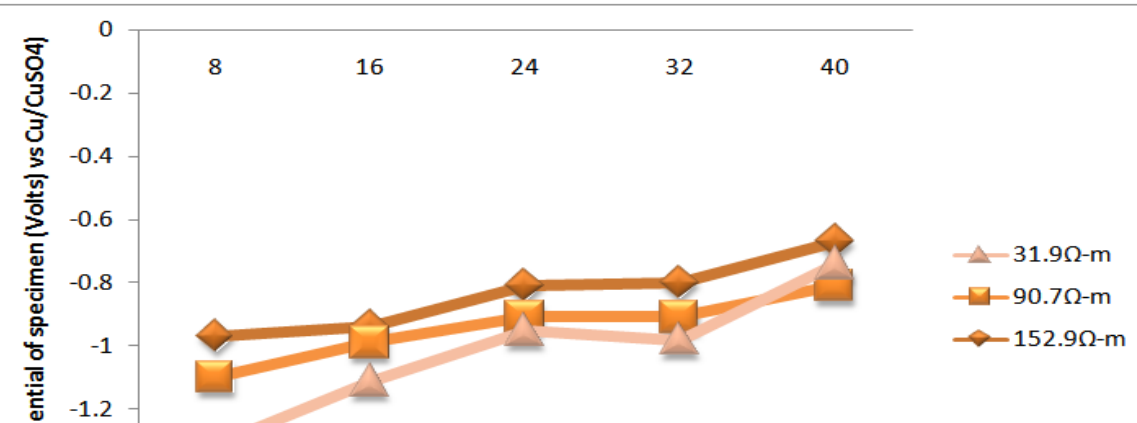

Fig.7: Polarized potential of specimen protected by magnesium alloy anodes in soil samples of specified resistivities, Ph 5.8, and 10% moisture content

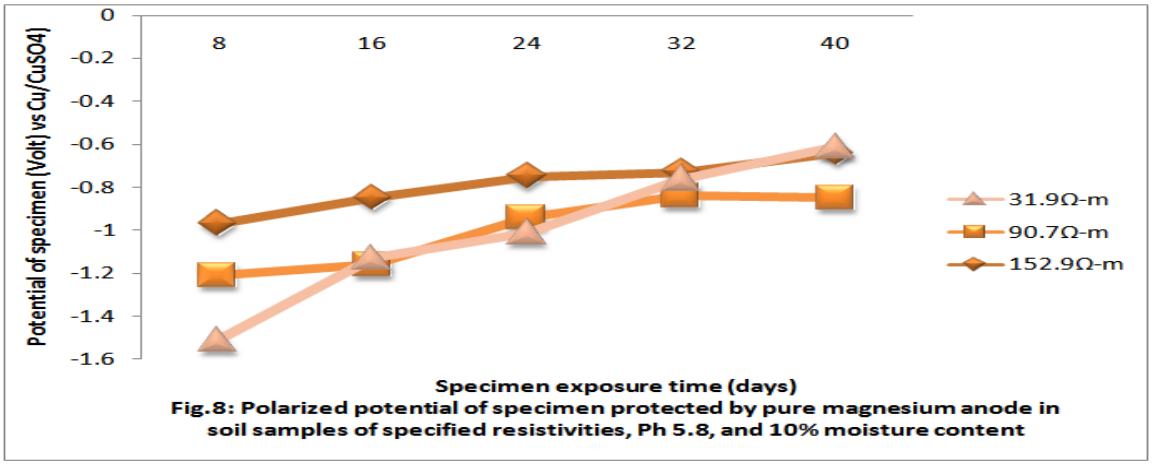

Fig.8: Polarized potential of specimen protected by pure magnesium anode in soil samples of specified resistivities, Ph 5.8, and 10% moisture content

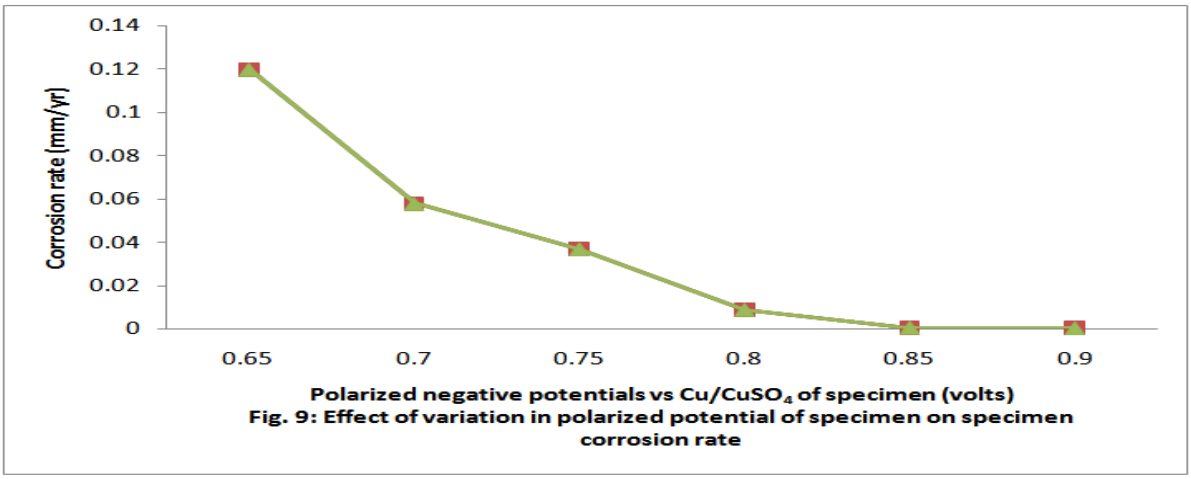

Fig. 9: Effect of variation in polarized potential of specimen on specimen corrosion rate

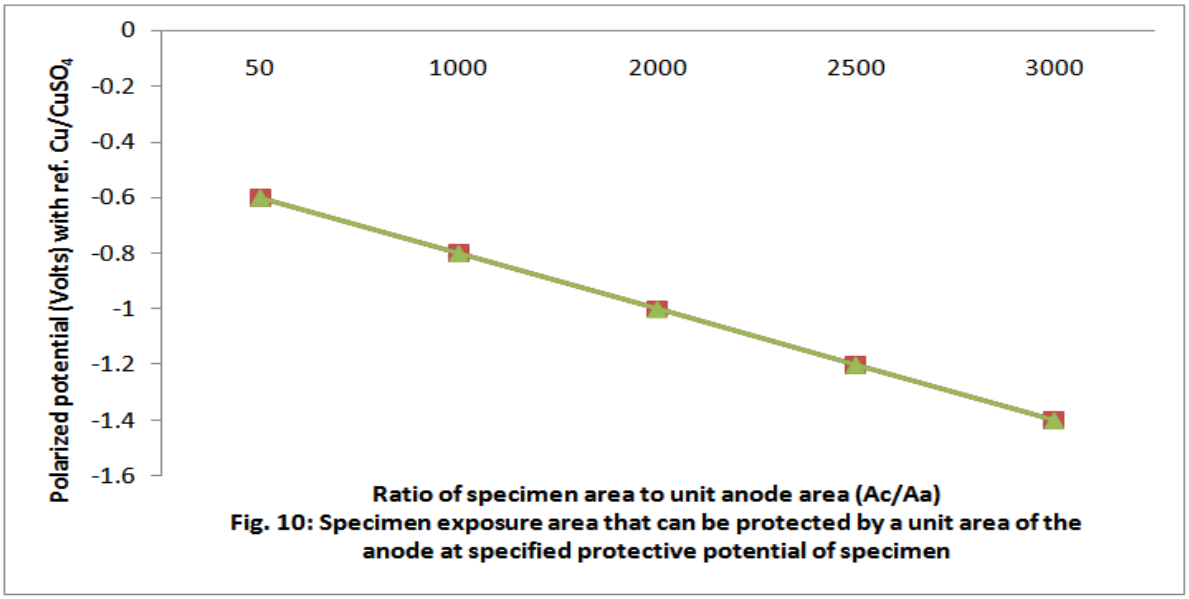

Fig. 10: Specimen exposure area that can be protected by a unit area of the anode at specified protective potential of specimen

Fig. 1 shows corrosion rates of unprotected specimens submerged in different-resistivity samples of the metropolitan soil after 40 days. From the figure it can be observed that corrosion rates of the specimens range from 0.061 to 0.165mm/yr for the entire resistivity spectrum of the soil. The highest rate of 0.165mm/yr occurred in soil sample of resistivity 31.9 Ohm-m. This value decreases with increase in resistivity to about 0.061mm/yr in soil sample of resistivity 152.9 Ohm-m. According to John Tarilonye Afa and Felix Opuama Ngobia [23], John Howard [24] and Guma *et al* [6]; soil resistivity is inversely related to corrosivity. It is thus clear that this trend of resistivity-corrosivity relationship is also attested by results for the metropolitan soil.

Fig. 2 on the other hand shows effects of exposure duration on corrosion rates of unprotected specimens submerged in different-resistivity samples of the soil for various durations up to 40 days. From the figure, it is apparent that corrosion rates of the specimens increased with exposure duration up to about the 24th day and thereafter decrease minimally to about 0.159, 0,069 and 0.051 Ohm-m in soil samples of resistivities 31.9 Ohm-m, 90.7 Ohm-m and 152.9 Ohm-m respectively. Several previous studies showed that corrosion rate generally decrease with time due to corrosion product formation and resulting in various levels of passivation of the corrosion [25]. The decrease in corrosion rates after the 24th day can thus be attributed to passivation according to Callister [7].

Fig. 3-5 show effects of exposure time on corrosion rates of specimens protected by the zinc, magnesium alloy and pure magnesium anodes in the test soil samples of 31.9, 90.7 and 152.9 Ohm-m resistivities. From the figures, it can be clearly observed that specimens protected by the zinc anode had highest corrosion rates while those by pure magnesium anode had the least rates in the soil samples for the same exposure durations. This indicates that pure magnesium anode is most suitable for the metropolitan soil because its protection spans the soil resistivity spectrum with relatively smaller corrosion rates compared to the zinc and magnesium alloy anodes. The corrosion rates generally turned to decrease to more or less constant values towards the 40th day of exposure except for specimens protected by the zinc anode in soil sample of resistivity 152.9 Ohm-m which increased with exposure duration as can be observed from Figures 3-5. The corrosion rates for each case of protection by the anodes are however minimal compared to those of the unprotected specimens as can be observed in Figures 3-5 in tandem with Figure2. This shows that each of the three anodes can provide protection to the study steel, the level of which however depends on the anode size and prevailing resisistivity. For the same size of anode, pure magnesium alloy anode exhibits outstanding protection performance in all the soil samples. Zinc anode exhibits relatively lowest protection performance in the 31.9 Ohm-m resistivity soil while pure magnesium the lowest in the 152.9 Ohm-m resistivity soil.

Fig. 6-8 shows effects of exposure duration on the polarized potentials of protected specimens by the anodes in the soil samples. For each figure and soil resistivity, the potentials increased steadily to higher values with increase in exposure duration as can be observed. This indicates that the specimens were protected. Loto and Popoola [1] observed similar trend of behavior for mild steel specimens protected by zinc and aluminum anodes in sea water and sulphuric acid. Scantlebury *et al* [26] studied corrosion of mild steel in marine environments under cathodic protection. His electrochemical studies at the two protection potential namely: -780 and -1100mV were examined by different techniques. DC polarization experiments was carried out for mild steel in natural sea water and 18.5g/L NaCl solution to evolve corrosion current density. He concluded that mild steel does not corrode under the protection potentials, viz., -780 and -1100mV. It can thus be observed the polarized potentials presented in Figures 6-8 more or less fall in this range so indicate reasonable protection of the specimens. It can however be observed that the pure magnesium anode proved more effective as sacrificial anode for the test steel because the polarized potential of the steel by it has the widest range of about -1.6 to -0.8 compared to those of the other anodes. The bigger the anode or its area, more electrons are supplied to protect the cathode and the longer time it takes for replacement. The potentials of pure magnesium, magnesium alloy (6%Al, 3%Zn and 0.15%Mn), zinc, and low carbon steel with respect to $Cu/CuSO_4$ in a neutral Ph environment are: -1.75V, -1.6V, -1.1V and -0.2 to -0.8V respectively [27]. This also shows that pure magnesium has the most negative potential, so is most suitable of the three anodes for delivering higher current per unit mass where needed such as high-resistivity soils. The differences in the protective performances can thus be attributed to their capacities to deliver protective current per unit mass. Moreover In high-resistivity environments, corrosion rates are controlled largely by electrolytic resistance rather than by polarization alone [20].

Fig. 9 shows the effects of polarized potential of specimens by the anodes on corrosion rates. From the figure, it very clear that corrosion rate of specimens decreased from about 0.12mm/yr at the -0.65 potential to negligible rate at the -0.85V potential and zero rate as potentials became more negative with respect to $Cu/CuSO_4$**.** According to Zuhair [27] and Collins [28] a CP potential reading with respect to $Cu/CuSO_4$ of between -0.5 to -0.6 represents intense corrosion, -0.6 to -0.7 corrosion, -0.7 to -0.8 slow corrosion, -0.8 to -0.9 cathodic protection, -0.9 to -1.1 overprotection and -1.1 to -1.4 severe overprotection in soil environments. Also, previous work in low resistivity environments by Schwerdtfeger [20] and other investigators has shown that corrosion can be reduced to a negligible degree by polarizing a steel structure to -0.85 volts (protective potential) with reference to a copper-copper sulphate electrode. However, this required protective potential tends to shift to more negative value from the -0.85V as soil corrosivity level drastically increases. For example, the protective potential of -1.1 to -1.4V has been reported by Zuhair [27] to be more satisfactory for Saudi's Aramco highly corrosive. For steel in anaerobic electrolyte of nearly neutral pH, a commonly accepted protection potential is -0.85V; when exposed to sulphate-reducing bacteria a potential of -0.95V with reference to copper/copper sulphate electrode would be required. These show that if the environment is particularly different in nature such as corrosivity level, the potential may change significantly [16].

From these it is clear that the test protective criteria of -0.85V for the Kaduna metropolitan area also meet the general criteria used by engineers for CP of steel structures for soils of usual corrosivity.

Fig. 10 shows effect of varying the surface area of the cathode relative to a unit surface area of the anode on the least negative protective potential of the cathode in the soil. From the figure it is indicative that at the optimum protective potential of -0.85V, a unit area of anodes can protect up to about 1200 unit area of the specimen. Tai-Ming Tsai [25] studied the performance of aluminum alloys used as sacrificial anodes for protection of steel in seawater. His results showed that steel can be protected under area ratio up to 4000-5000 with -0.85V protective potential [25]. This shows that less surface area of a steel structure in the metropolitan soil can be protected compared to the sea water environment. One reason attributable to this is that the resistivity of the sea water was lower than about31.9 Ohm-m for the soil.

IV. SUMMARY AND CONCLUSION

Cathodic protection is one of the most effective and economical methods of durably preventing corrosion of engineering systems or structures in aqueous environments if properly designed installed and maintained. One important requirement of CP is that it should be applied in the most economical way. Proper CP design therefore requires careful study with regard to complexity of variables that affect it such as environmental corrosivity, type of material to be protected, nature and surface area of the material, type and size of anode to be used or amount of current to be applied so as to establish conditions for optimal mitigation of corrosion in specific environments or localities. The paper sought laboratory information on relative merits of zinc, magnesium alloy and pure magnesium as cheap and locally available galvanic anodes for suitable CP of underground engineering steel structures in the metropolitan area of Kaduna-a top city in Nigeria. Obtained information show that the -0.85V protective potential generally accepted by the engineering community as adequate for CP of bare steel in soil environments is also met for the metropolitan soil. Corrosion of underground engineering steel structures in the soil can therefore be reduced to negligible rate by polarizing them to the protective potential using the anodes. A unit surface area of the anodes can protect up to nearly 1200 units of the structure with the -0.85V protective potential depending on the anode type. The pure magnesium has been found to be most suitable out of the three anodes for CP of the structures in term of economical size and outstanding effectiveness that spans resistivity spectrum of the soil.

REFERENCES

[1] C.A. Loto and A.P.I. Popoola. Effect of anode and size variations on the cathodic protection of mild steel in sea water and sulphuric acid. *Internationbal journal of the physical sciences 6(12),* 18 June, 2011, 2861-2868

[2] Underground Structures (n.d). The Great Soviet Encyclopedia, 3rd edition (1970-1979). Retrieved from: http://encyclopedia2:thefreedictionary.com/Undegroud + Structures (23/05/2015).

[3] Cooper Testing Labs Inc Geotechnical and Corrosion Testing. Corrosion Testing, Issue 7, January, 2004.

[4] A.S. Ekine and G.O Emujakpone. Investigation of corrosion of buried oil pipeline by the electrical geophysical methods. *Journal of applied science and environmental management, 14(1),* 2010, 63-65.

[5] Oyedele Kayode Festus, Meshida Ebenizer, A. and Obidike, C.C. Assessment of coastal soil resistivity using resistivity tomography at Lekki, Lagos. *International journal of science and advanced technology, 2(6),* 2012, 77-81.

[6] TN. Guma, SU. Mohammed and AJ. Tanimu. A field survey of soil corrosivity level of Kaduna metropolitan area through electrical resistivity method. *International journal of scientific engineering and research, 3(12),* 2015.

[7] Callister, W.D. Material science and engineering: An introduction, 5th edition. John wiley and sons inc, 2004, pp. 357-601.

[8] Basim O. Hassan, Huda D. Abdul Kader and Marwa F. Abdul-Jabbar. Experimental study on carbon steel corrosion and its inhibition using sodium benzoate under different operating conditions. *Iraqi journal of chemical and petroleum engineering 12(3),* 2011, 11-24.

[9] Ndububa Christopher, Jidauna Godwill Geofrey, Averik Peter Danjuma, Oyatayo Taofik Kehinde, Abaje Iliya Bitrus and Ali Andesikuteb Yakubu. Characterization of sprawling in Kaduna metropolitan area. *American journal of environmental protection, 3(3),* 2014, 131-137.

[10] T.N. Guma, and C.I.C. Oguchi. Field test assessment of corrosivity of river Kaduna to mild steel. *PeCop journal of science engineering and technology 4(1&2),* 2011, 40-50.

[11] Ahmed. J. Tanimu (2015). Experimental Assessment of Suitable Anode Specification for Cathodic Protection of Low Carbon Steel in Very Corrosive Acidic Soil Environment. B.Eng Research Project, Unpublished, Department of Mechanical Engineering, Nigerian Defence Academy, Kaduna, Nigeria.

[12] Marwah S. Hashim, Dr Khearia A. Mohammed A. and Dr Nawal Jasim Hamadi. Modelling and control of impressed current (iccp) system. *Iraqi journal of electrical and electronic engineering 10(2),* 2014, 80-88.

[13] James B. Bushman, P.E. Corrosion and cathodic protection theory. Bushman & Associates, Inc. Corrosion Consultants, P.O. Box 425 Medina, Ohio 44256 USA, 2015, 769-2197.

[14] Peabody, A.W. 2001. Control of pipeline corrosion, 2nd edition, R.L Bianchetti Ed. NACE International.

[15] Iseru Ebike, Fagbemi Emmanuel, Awolola Kayode and Akpovwovwo Teddy. Mitigating external corrosion failures in buried petroleum pipelines in Nigeria: a review. *International journal of ecological science and environmental engineering, 1(2),* 2014, 67-72.

[16] PE Francis Cathodic Protection. www.npl.co.uk/.../cathodic (25/7/2015).

[17] S.S. Leeds and R.A. Cottis. The effect of surface films on cathodic protection. A paper submitted for publication to the journal of corrosion science and engineering, UMIST, 9(3), 2004.

[18] Ahmed A Atshan, Basim O Hasan and Mohammed H. Ali. Effect of anode type and position on the cathodic protection of carbon steel in sea water. I*nternational journal of current engineering and technology* 2013, 2017-2024.

[19] Galvanic Anode. Wikipedia enwikipedia.org/wiki/Galvanic anode, 21/03/2015.

[20] W.J. Schwerdtfeger. Current and potential relations for the cathodic protection of steel in a high resistivity environment. *Journal of research of the national bureau of standards-c. engineering and instrumentation 63(1),* 1959, 37-45.
[21] B.K. Mahato, C.Y. Cha, and U.W. Shemlit, Corrosion sciences, 20, 1980, 421-441.
[22] K.T. Rashid. Effect of mixing speed and solution temperature on cathodic protection current density of carbon steel using magnesium as sacrificial anode. *Engineering and technology journal 28(8),* 2009, 1640-1653.
[23] John Tarilonye Afa and Felix Opuama Ngobia. Soil characteristics and substation earthing in Bayelsa state. *European science sournal, 9(9*), 2013, pp. 81-89.
[24] John Howard. WEB Extra: Soil resistivity testing and grounding system design-part 1 of 2, osp magazine. practical communications inc 1320, tower road, Schaumberg, 2015
[25] Tai-Ming Tsai. Protection of steel using aluminum sacrificial anodes in artificial sea water. *Journal of marine science and technology, 4(1)*, 1996, 17-21.
[26] Scantlebury, J.D, Dae Kyeong Kim, Srinivasan Murajidharan, Tae Hyun Ha, Jeong Hyo Bae, Yoon Cheol Ha and Hyun Geo Lee. Electrochemical studies on the alternating current corrosion of mild steel under cathodic protection condition in marine environments, *Electrochimica acta, 51*, 2006, 5259-5267.
[27] Dr. Zuhair M. Gasem. Cathodic protection ME 472-061 corrosion engineering 1 ME, KFUPM. www.scibd.com/doc/131766374/cthodic-protection (05/10/2014).
[28] Charles C Collins. A study of cathodic protection of underground metal structures and cathodic protection survey of pipelines on campus of Montana State College. A thesis submitted to the graduate faculty in partial fulfillment of the requirements for the degree of Master of Science in electrical engineering, Montana State University, 1957.

American Journal of Engineering Research (AJER) 2016
American Journal of Engineering Research (AJER)
e-ISSN: 2320-0847 p-ISSN : 2320-0936
Volume-5, Issue-2, pp-120-124
www.ajer.org
Research Paper Open Access

Elimination of Fluoride Ions from Water of Wells and Tyikomiyne Sources by The Hydroxyapatite Phosphocalcic, Talssint (Eastern Morocco)

H. Taouil[1]*, S. Ibn Ahmed[1], E. H. Rifi[1], Y. ASFERS[1],
[(1)]*Laboratoire des Matériaux, d'Electrochimie et d'Environnement.*
Université Ibn Tofail. Département de Chimie, B.P. 133, 14000 Kenitra, Maroc.

Abstract: *Two sources and five wells Tyikomiyne area, Talssint region on the eastern coast of Morocco were analyzed for fluoride ion. In all the wells studied, fluoride contents exceed the standard set by the WHO (1.5 mg/L), probably due to the geological nature of the terrain traversed. Thus, our work aims more specifically on the treatment of water from these wells containing fluoride using support apatite. The results obtained show that the apatite is suitable to obtain a better performance of the elimination of the fluoride ion.*
Keywords: *Elimination, Fluoride ions, Water, Talssint region, Morocco.*

I. Introduction

Groundwater is a very important part of the hydraulic heritage. They have compared to surface water clear advantages in terms of coverage of needs. In Marrakech, groundwater plays an important role in the development of irrigation and drinking and industrial water, whether in urban or rural centers [1-3]. In Tyikomiyne area (Figure 1), using the waters of springs and wells for drinking and irrigation, but the geological nature of the soil in the region likely cause contamination of these waters by fluoride ions, which can migrate and reach groundwater, accumulate in the food chain and pose risks to human health.

Interest in contamination of groundwater, aquifers of water and soil by fluoride ions from natural rocks is increasingly increased. This is because of the adverse effect this has on the human health. That is why it is considered a major environmental problem and removal of this pollutant is becoming increasingly important. Thus the study of the quality of water Tiykomiyne well physicochemistry water Tyikomiyne wells and evaluation of the water quality of the river Tislit-Talssint was recently reported by our group [4- 7]. In this work, we analyzed the fluoride ion content of the water wells and sources Tyikomiyne then we do the treatment of water from these wells and springs containing fluoride using an apatite support.

Figure 1 Study area location in the watershed of the river Guir.

The center of Talssint belongs to the south side of the High Atlas, it is the Guir Basin (Figure 2), which contains numerous discrete groundwater and deep aquifers whose recognition remains to be done [8]. The center of Talsint is the capital of the rural district of Talsint, caïdat under the same name and the circle of Beni-Tadjit, part of the province of figuig, eastern region of Morocco[8]. Our study concerns among the wells and sources of Tyikomiyne area Talssint region which, to our knowledge, has been no prior academic study and is limited by the village Ezzaouia the south, Affia area to the north, the regional road RP601 to 'Beni-Tadjit west and east Jbal Alaajra**.** Thus two sources and five wells have been retained on the study area (Figure 2):

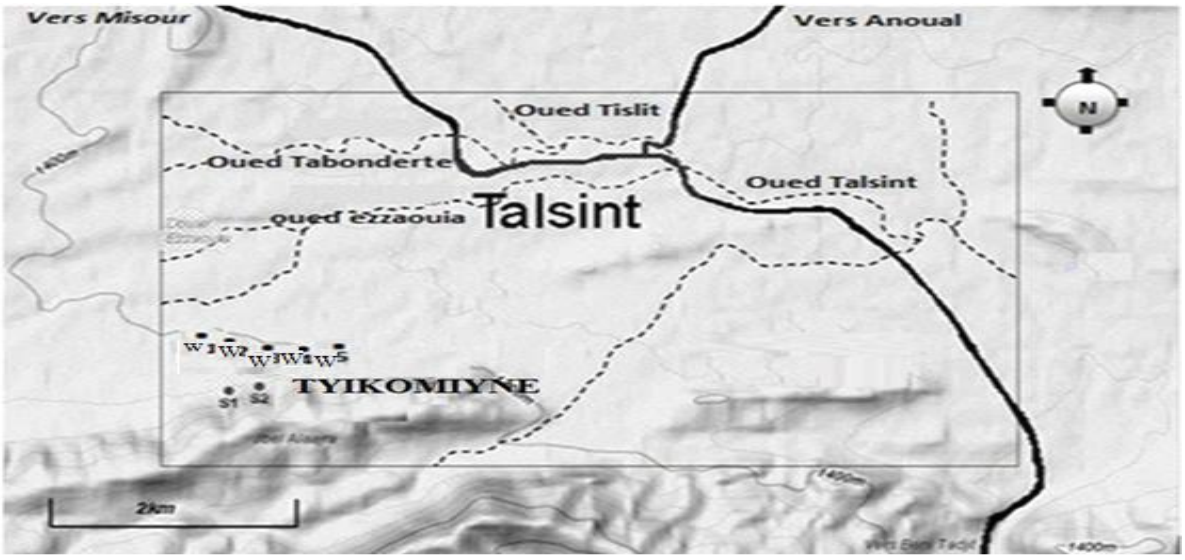

Figure 2. Location of wells and sources that are considered from left to right:
Faryat (W1), El Masjid (W2), Hadi (W3), Hilla (W4), Deppiz (W5), Annakhla (S1), Aghram (S2),

The region is characterized by pre-Saharan and Saharan environments. Temperatures are high in summer and very cold in winter. The average minimums of the coldest month (January) is -5 ° C and maxima of the hottest month (July) 47 ° C. The average annual rainfall was around 244.9 mm for the period 1983/2007 and 500 mm for the period 2008/2010, , With important interannual variations, with extremes of 61 mm in 1998/99 and 684.5 mm in 2009/2010 [8].

II. Expérimental

2.1 Materials used

In the field of radioactive waste, apatite phosphosilicates whose composition is close to that of natural apatite, confined in their wombs of radioactive elements [9]. The apatite phosphates belong to a large family of biomaterials applied in dentistry and Otorhinolaryngology [10-12]. And other studies have shown that the importance of these materials is their ability to set a large number of metal species in aqueous solution diluted with a great performance[13]. For our part, the hydroxyapatite calcium phosphate was used as extractant matrix fluoride in our water treatment of the five wells and two sources. Its chemical formula is: Ca_{10} (PO 4)$_6$ (OH)$_2$.

The calcium phosphate hydroxyapatite of formula Ca10 (PO4) 6 (OH) 2 belong to the crystallographic family of apatites, isomorphic compounds having the same hexagonal structure. This compound is the calcium phosphate most commonly used as a biomaterial. The main uses of hydroxyapatite in the medical sector are:

- Coatings for prostheses.
- For the development of bone substitutes (types of calcium phosphate ceramics, types, ionic cements ...).

His interest results from its perfect biocompatibility and bioactivity[14]. The hydroxyapatite calcium phosphate crystallises in the hexagonal system (space group = $P_{6\ 3/m}$) with the following crystallographic parameters [15] :

a = 9,418 Å, c = 6,881 Å, b = 120°.

Hydroxyapatite the solubility equilibrium is generalized in the form:

$$Ca_{10}(PO_4)_6(OH)_2 \rightleftharpoons 10\ Ca^{2+} + 6\ PO_4^{3-} + 2\ OH^-$$

2. 2. Extraction Technique and Method of Analysis

We used an extraction technique based on: glass electrode, thermometer, magnetic stirrer and pH meter (Figure 3).

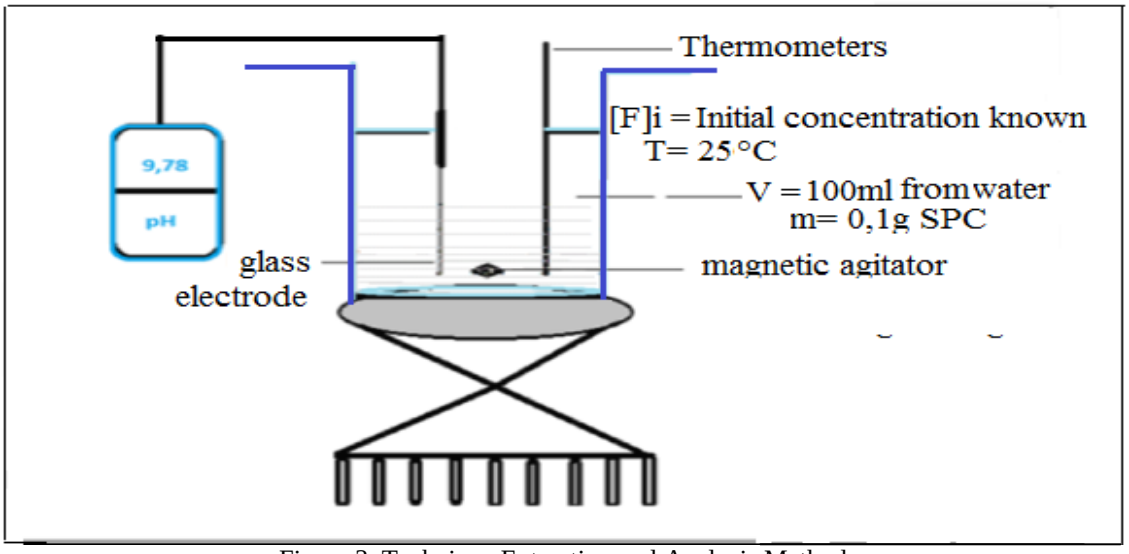

Figure 3. Technique Extraction and Analysis Method

Each support phosphate 0.1g sample mass is placed in a cell thermostated at room temperature, containing 100 ml of water to be analyzed; and these waters are initial known concentrations of fluoride ion. Each cell is provided with a control thermometer with a combined glass electrode and a magnetic stirrer. The initial pH is adjusted by the first pH meter. To promote better contact between the support and the pollutant fluoride to remove the samples are stirred at room temperature for 4 hours. When the extraction equilibrium is attained, the loaded carrier is separated from the fluoride supernatant solution by filtration.
So Fluoride was assayed by ion chromatography at the National Center of Scientific and Technical Research (CNRST).
The extraction yield is given by the following relationship:

$$R = \frac{(C_i - C_f)\ 100}{C_i}$$

Ci: Initial concentration of fluoride in water studied.
Cf: Concentration of fluoride, to the extraction balance.

III. Results

The addition of small amounts of fluoride is necessary to significantly reduce dental caries. However, its excessive accumulation in the body causes fluorosis, dental and musculoskeletal essentially reached [16]. The comparison of the levels of fluoride ion, recorded in the waters of the well studied and those set by the World Health Organization, shows that these waters are contaminated by this element which creates a risk for the dental health of populations in the region [16].

The results of treatment with fluoride ions Hydroxyapatite calcium phosphate are given in Table 1:

	$[F^-]_i$	$[F^-]_f$	pH_i	pH_f	R%
Well 1	2.09	0.12	8.17	9.78	94.25
Well 2	1.76	0.19	8.10	9.62	89.20
Well 3	1.70	0.30	8.04	9.41	82.35
Well 4	1.75	0.47	7.52	8.85	73.14
Well 5	2.08	0.19	8.12	9.63	90.86
Source 1	1.44	0.33	8.00	8.95	77.08
Source 2	1.52	0.27	7.06	9.47	82.23

Table 1. Treatment of fluoride ions by hydroxyapatite calcium phosphate

Thus we simultaneously plot the histogram of fluoride ion concentrations according to the study sites before and after the extraction of a portion and the histogram of the initial pH (pHi: pH before extraction) and final pH (pHf: pH after extraction) on the other (figure 4).

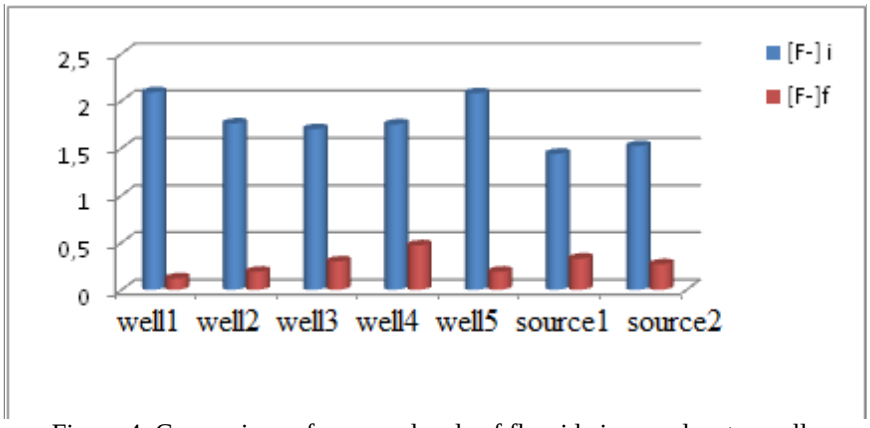

Figure 4: Comparison of average levels of fluoride ions and water wells Tyikomiyne of sources before and after extraction.

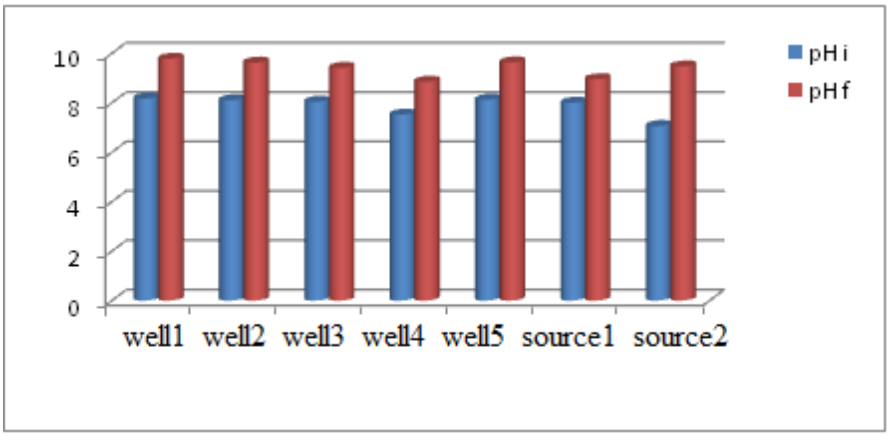

Figure 5: Water pH Comparisons wells and Tyikomiyne sources before and after extraction.

According to Figures 4 and 5 it is seen that for water puits1for example, the initial amount of fluoride is about 2.09 mg / l, and the remaining amount after extraction, is around 0.12 mg / l, other hand, the initial pH is of the order of 8.17 while the final pH is about 9.78. It is noted that in all the wells and springs investigated, the concentrations of fluoride ion decrease after extraction, while the final pH increases. Increasing the pH is essentially due to the release of hydroxide ions OH- dropped by the phosphate carrier.

The balance sheet anion exchange between the support and the phosphate of fluoridated water sample is as follows:

$$F^-(\text{liquid}) + OH^-(\text{solid}) \longrightarrow F^-(\text{solid}) + OH^-(\text{liquid})$$

The OH- dropped by the support hydroxide is released into the solution at the end of the reaction, while the fluoride ion F- is consumed by the calcium phosphate carrier. Then we plotted the ion extraction yield histogram fluorides based on plants studied (Figure 6).

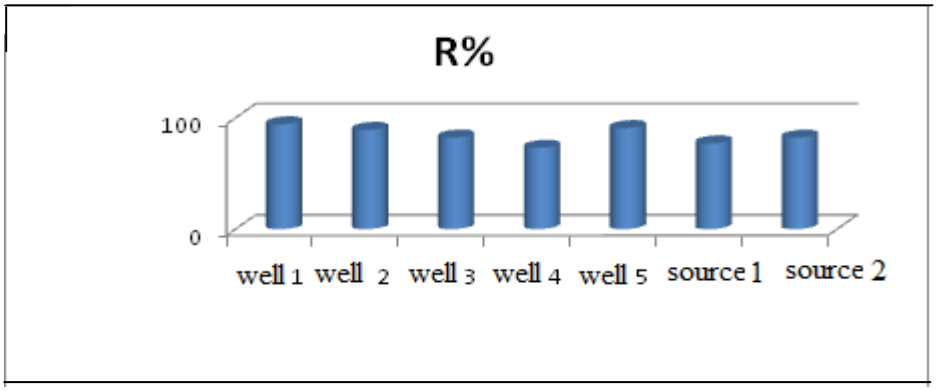

Figure 6: Performance for fluoride ion extraction according the studied stations

Assay results of figure 6 show that the maximum yield has been obtained at the well1 , is of the order of 94.25. While the minimum yield was obtained at the well 4 which is of the order of 73.14. These results suggest that the apatite is suitable for a better performance of the elimination of the fluoride ion.

IV. Conclusion

The extraction of fluoride ion by hydroxyapatite $Ca_{10}(PO4)_6OH_2$ was studied. The results obtained in this study show that:

In all water wells and studied sources of Tyikomiyne area Talssint region, the fluoride ion concentrations decrease after extraction and the pH of the supernatant solution increases during extraction due to the release of the OH- ions in the apatite support. So the extraction equilibrium is effected by anion exchange: OH- ions forming the solid support are substituted with F- ions contained in the water sample to be analyzed.

V. Acknowledgements

Thanks are due to the National Centre of Scientific and Technical Research (CNRST)-Morocco.

Références

[1] Ali Ait Boughrous (2007) Biodiversité, écologie et qualité des eaux souterraines de deux régions arides du Maroc: le Tafilalet et la région de Marrakech, *Thèse de Doctorat*, Université Cadi Ayyad, Marrakech, Maroc.

[2] M. El Adnani, A. Ait Boughrous, A. Nejmeddine, M. Yacoubi Khebiza et A. El Gharmali, Impact of the mining wastes on the physicochemical characteristics of water and the structure of the zooncenoses of the wells in the area of Marrakesh, Morocco. *Environmental Technology*, 28 (2007) 71-82.

[3] F. Boukhoubza, A. Ait Boughrous, M. Yacoubi-Khebiza, A. Jail, L. Hassani, L. Loukili-Idrissi et A. Nejmeddine, Impact du stockage des effluents d'huileries (margines) sur la qualité physico-chimique et biologique des eaux souterraines au sud de Marrakech (Maroc), *Environmental Technology*, 29 (2008) 959-974.

[4] H. Taouil, S. Ibn Ahmed, A. El Assyry, N. Hajjaji, A. Srhiri, F. Elomari, A. Daagare, Manganese, nickel, lead, chromium and cadmium in the watershed Guir, impact on the quality of wells water in Tiykomiyne (Eastern Morocco), *Int. J.Agric. Policy. Res.*, 1(5) (2013) 150-155

[5] H. Taouil, S. Ibn Ahmed, A. El Assyry, N. Hajjaji, A. Srhiri,Physicochimie de l'eau des puits Tyikomiyne, région de Talssint (Maroc Oriental), *Sciencelib Editions Mersenne*, Vol 5, N° 130511 (2013)

[6] H. Taouil, S. Ibn Ahmed, N. Hajjaji, A. Srhiri, A. El Assyry, F. El Omari, Etude d'impact du fluor des eaux de certaines sources et puits utilisés comme sources d'eau potable en milieu rural dans la région de talssint (Maroc Oriental), *Sciencelib Editions Mersenne*, Vol 5, N° 130401 (2013)

[7] H. Taouil, S. Ibn Ahmed, A. El Assyry, N. Hajjaji, A. Srhiri, Water quality evaluation of the riverTislit-Talsint (East Morocco**), *J. Mater. Environ. Sci.***, 4(4) (2013) 502-509

[8] ONEP (*Office National de l'Eau Potable*), Direction Régionale de l'Oriental ; étude d'assainissement du centre de Talsint et quartiers périphériques (province de Figuig). Rapport provisoire, Aout 2007.

[9] J.C. ELLIOT, Structure and chemistry of the apatites and others Calcium Orthophosphates, *Studies in Inorganic Chemistry* 18, *Elsevier* (1994)

[10] L. HENCH, *J. Am. Ceram. Soc.* 74, 1487 (1991)

[11] R. Z. Legros, Monographs in Oral Science, vol 15, H.M.Meyers Edidors, Sa Fransisco (1991)

[12] Jean-Philippe Lafon, Eric Champion, Didier Bernache-Assollant, Raymonde Gibert, Anne-Marie Danna, *Journal of Thermal Analysis and Calorimetry*, 72(3) (2003) 1127-1134

[13] L. Chafki, E.H. Rifi, S. Ibn Ahmed. Traitement des solutions de cadmium par des supports phosphocalciques. *ScienceLib Editions Mersenne*, Vol 3, N° 110804 (2011)

[14] A. Oglivie, R. M. Frank, E. P. Benque, M. Gineste, M. Heughebaert, J. Hemmerle, The biocompatibility of hydroxyapatite implanted in the human periodontum, *J. Periodont. Res.*, 22 (1987) 270-283

[15] M. I. Kay, R. A. Young, A. S. Posner, Crystal structure of hydroxyapatite, *Nature*, 204 (1964) 1050-1052

[16] H. Taouil, S. Ibn Ahmed, N. Hajjaji, A. Srhiri, A. El Assyry, F. El Omar. Etude d'impact du fluor des eaux de certaines sources et puits utilisés comme sources d'eau potable en milieu rural dans la région de Talssint (Maroc oriental) ScienceLib, Volume 5, (2013) N ° 130401 ISSN 2111-4706

American Journal of Engineering Research (AJER) 2016
American Journal of Engineering Research (AJER)
e-ISSN: 2320-0847 p-ISSN : 2320-0936
Volume-5, Issue-2, pp-125-135
www.ajer.org
Research Paper Open Access

Development of A Cost Effective 2.5kva Uninterruptible Power Supply System

Olanrewaju Lateef Kadir[1], Okechi Onuoha[2], Nnaemeka Chiemezie Onuekwusi[3], Ufuoma Onochoja[4], Chikwelu Nonso Udezue[5]
[1,2,4,5](Projects Development Institute (PRODA), Nigeria)
[3](Federal University of Technology, Owerri (FUTO), Nigeria)

ABSTRACT : *This paper is on the detailed development of a cost effective Uninterruptible Power Supply (UPS) system for domestic use. The UPS serves as a standby / backup power supply unit for power supply from the main commercial supply line. In this paper, an easy to implement block diagram showing all the important units of the UPS system is given. Detailed design showing all calculations and considerations were also included in this work. Also, a simple cost analysis showing the cost of producing this system from the scratch and also the cost of a similar product in Nigeria is also shown.*
The UPS consists of charge a controlling section, an inverting section, an automatic change-over / switching section a transformation and a load section. The battery is charged through a rectifier. The rectified DC output was achieved using a bridge rectifier and a voltage regulator. The change-over was done by an electric relay whose function is to establish connection between the load and either the mains or the batteries.
Keywords - *zener diode; automatic change over; oscillator; national grid; low reluctance; battery bank*

I. INTRODUCTION

The importance of electrical power supply cannot be over-emphasized. It provides lightings during the day to indoor areas and to entire surrounding at night. The tasks of generating and distributing uninterruptible power in developing countries seem to be impossible to solve by their governments. As a result, individuals, business centers, companies are trying to solve this problem on their own. One of the methods used in solving this is the use of mechanical generating plant which is usually called generator. The use of generators as alternatives has limitations. These limitations include: high cost of operation and maintenance; it causes a lot of environmental pollution; it produces a lot of noise; and most mechanical generators are bulky.
Another method used in solving the problem is the uninterruptible power supply (UPS). The UPS derives its power from energy stored in a battery. The UPS is a better alternative than the generator in terms of noise, environmental pollution and size.
The aim of this article is develop an easy to operate 2.5kVA uninterruptible power supply that will generate power from battery. UPS is an electronic system or circuit that changes direct current (DC) stored in a battery to alternating current (AC). It is used to supply continuous power to the load connected to its output socket. The battery(s) will be charged by a rectifier circuit which consists of a transformer, a bridge rectifier, a filter and a voltage regulator. In view of erratic power, the UPS serves as a main to the household appliances or load connected to it.
The article contains four sections. After this introductory section, section two explains the individual functions of all the components of the circuit and how they operate. This section also discusses the circuit design calculations and description. Testing and performance evaluation are presented in section three and conclusions and recommendations are drawn in section four.

II. DESIGN METHODOLOGY

1.1 Block Diagram of an uninterruptible Power Supply

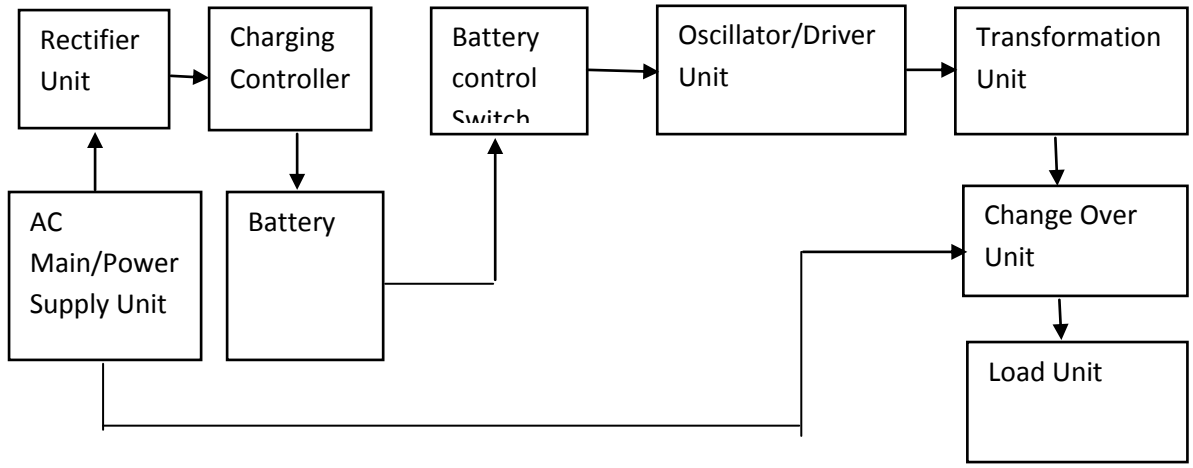

Fig. 1.1: Block Diagram of an Uninterruptible Power Supply

Figure 1.1 shows the block diagram of a UPS. This diagram was used in the design calculation.

1.2 Load Unit

The load unit is the output unit of the UPS. This is where all the electrical power consuming appliances are connected to the UPS. This unit makes use of a socket outlet. A voltmeter may be included in the output to display the output voltage.

1.3 Change-Over Unit

At the changeover unit is a relay switch (RL_1) that was incorporated at the output of the UPS to switch the source of power supply to the output from either the battery or the supply mains (national grid).

1.4 Transformation Unit

In this section of the design, a 24/240V step-up transformer (T_1) was used. The transformer has a centre tap which was connected to the positive terminal of the battery. Figure 1.2 shows the circuit diagram for the 24/220V transformation unit together with the driver, changeover and load units.

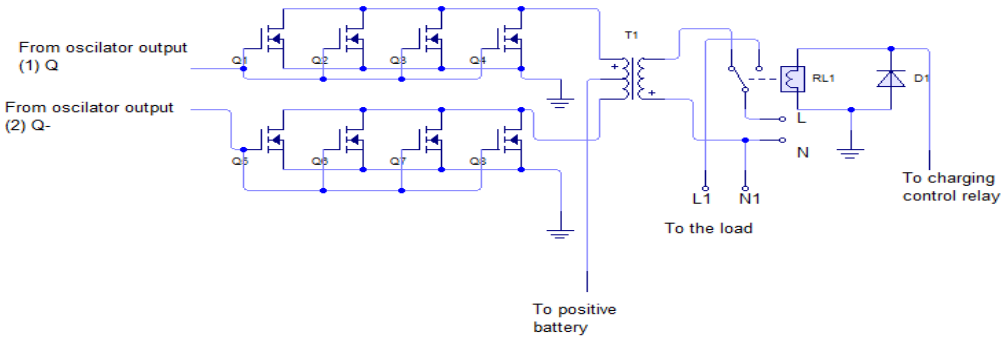

Fig. 1.2: Circuit Diagram for a 24/240V Transformation/Change-over/Load Unit

1.4.1 Determination of the number of turns of coil on each side of T_1 windings

Power rating of T_1 was 2.5kVA. The volt per turn is given by

$$E_t = 4.44\, fB_{max} A = \frac{V_p}{N_p} = \frac{V_s}{N_s} \qquad (1.1)$$

Where
E_t is volt per turn, f is the frequency in *Hertz*, B_{max}, is the maximum flux density in *tesla*, A is the lamination core area in m^2, V_p (in volt) is the primary side voltage, N_p is the number of turns on the primary side, V_s (in volt) is the secondary side voltage, N_s is the number of turns on the secondary side.
The size of the transformer core must be determined based on the transformer total power. The area of the core should at least have the value according to the equation 1.2. Therefore the area of lamination of transformer T_1 is given as

$$A = \sqrt{power \ \ (Watt \ )} cm^{\ 2} \qquad (1.2)$$

$$A = \sqrt{power \ \ (Watt \ )} \times 10^{\ -4} m^{\ 2} \qquad (1.3)$$

$$A = \sqrt{IV \ \cos \ \theta} \times 10^{\ -4} m^{\ 2} \qquad (1.4)$$

Where
$Cos\theta$ is the power factor.
Choosing a power factor of 0.8 and maximum flux density of lamination to be 1.2 Tesla, the volt per turn is obtained using equations 3.1 and 3.4.

$$E_{\ t} = 1.1913 \ \ volt \ \ / \ turn$$

The expected output voltage of T_1 is 240V.
Secondary voltage V_s of T_1 is 240V
The number of turns in the secondary winding (N_s) is obtained using equations 1.5

$$N_{\ s} = \frac{V_{\ s}}{E_{\ t}} turns \qquad (1.5)$$

$$N_{\ s} \approx 202 \ \ turns$$

Also, the numbers of turns in the primary winding (N_p) is given as in equation 1.6

$$N_{\ p} = \frac{V_{\ p}}{E_{\ t}} turns \qquad (1.6)$$

$$N_{\ p} \approx 20 \ turns$$

1.4.2 Coil Gauge Required for T_1

Recall,

$$Power \ \ (VA \ ) = IV \qquad (1.7)$$

Power rating of T_1 is 2500VA, assuming 90% efficiency. Then the input rating is given by

$$P_i = \frac{P_{out}}{eff} \qquad (1.8)$$

Where P_i is the input power, P_{out} is the output power and eff is the efficiency.

Voltage on the secondary side is 240V, thus, current I_s in the secondary side of T_1 is

$$I_{\ s} = \frac{P_{out}}{V_{\ s}}$$

$$I_{\ s} = 10 \ .42 \ \ Amperes$$

From the America Wire Gauge (AWG), Gauge 11 will be sufficient for the secondary coil.
Voltage on the primary side is 24V, thus primary current, I_p

$$I_p = \frac{P_i}{V_p}$$

$$I_p = 115.7 \; Amperes$$

From AWG, Gauge 1 will be sufficient for primary side.

1.5 Oscillator Unit

The oscillator unit makes use of an IC (CD4047) configured in a-stable multi-vibrator for pulse generation of 50Hz duration. This is shown in Figure 1.3

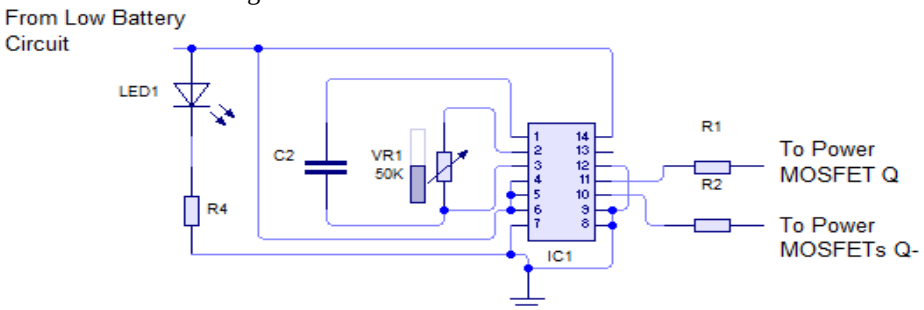

Fig. 1.3: Oscillator Circuit

The configuration is such that pins 4, 5, 6 and 14 were connected to V_{cc} while pins 7, 8, 9 and 12 were connected to the ground. The VR_1, and C_2 network will determine the frequency of oscillator which is 50Hz. Pin 10 and pin 11 are the output (Q) and complementary output (Q-) respectively and this results in the separation of signal into two separate channels. Each channel was connected to the gates of two separate power MOSFETs channel. Each channel of the MOSFETs was then connected to the ends of the primary side of T_1.
The IC is to be provided with a constant voltage from the battery through a voltage regulator IC 7812.
The LED_1 is to indicate when the inverter is working. R_1 and R_2 serve as limiting resistor to limit the current entering the gates of the MOSFETs.
The period T of the oscillator is given by

$$T = 4.4VR_1C_2(\sec\ s) \qquad (1.10)$$

and

$$T = \frac{1}{f}$$

$$f = \frac{1}{4.4VR_1C_2}$$

Where
f is frequency which in this case is *50Hz*. Choosing C_2 to be *100nf*, VR_1 was obtained to be equal to *45.5k Ω* from equation 1.10
From the manufacturer data sheet, when the voltage at pin 14 is 12V, the voltage and current output at pin 10 and pin 11 of IC 4047CD are 5.6V and 50mA.

$$R_1 = \frac{V_{out} - V_{GS}}{I_{max}} \qquad (1.11)$$

Where V_{out} at pin 10 and pin 11 of IC 4047CD are *5.6V*, V_{GS} = *0* and I_{max}=*50mA*. From equation 1.11, $R_1 = R_2 = 100\Omega$

$$V_{cc1} = V_{LED\ 1} + I_{LED\ 1}R_4 \qquad (1.12)$$

Where V_{cc1}=12V (from R_{g1}), V_{LED1}=2V and I_{LED1}=10mA (from manufacturer specification). From equation 1.12 R4 was computed to be 1kΩ

1.6 Driver Unit

This section makes use of power MOSFETs IRFP250N. The MOSFETs has a maximum current (I_M) and voltage of 30A and 200V respectively. Each output of the oscillator was connected to each channel of the MOSFETs which resulted in the channels being alternatively ON and OFF. The required number of power MOSFETs, N_m, was obtained using equation 1.8.

$$N_m = \frac{I_p}{I_m} \qquad (1.13)$$

Hence 4 MOSFETs can safely handle the expected primary current but 6 MOSFETs was recommended for higher reliability.

1.7 Battery Control Switch Unit

This unit is used to disconnect the battery from the inverting section whenever there is power supply from the national grid. This unit makes use of relay switch.

1.8 Charging Controller

The charging controller is used to protect the battery from over drainage and over charging. The charging controller consists of low battery voltage trip unit and charging control unit.

1.8.1 Low Battery Control Circuit

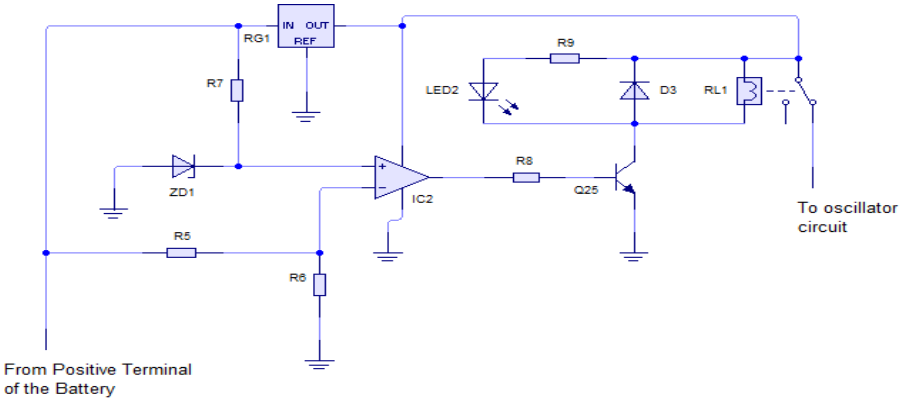

Fig. 1.4: Low Battery Voltage Trip Circuit

The low battery voltage trip is required to disconnect the battery from the output when its voltage has dropped to certain level. This is to ensure that the battery is not over drained by the UPS. Figure 2.4 shows the circuit diagram for low voltage battery trip.
This unit makes use of LM324 comparator (IC_2) and zener diode Z_{D1}
Pin 1 is the output terminal.
Pin 2 is the non-inverting terminal.
Pin 3 is the inverting terminal.
Pin 2 of the op-amp is set to a constant voltage of +10V by Z_{D1}, while pin 3 is set to 9V through potential divider formed by R_5 and R_6.
As the battery voltage is discharging, the voltage at pin 3 will be reducing. When the voltage at pin 3 becomes lower than the voltage at pin 2, it results to a high voltage at pin 1 which will bias the transistor Q_{25} through resistor R_8. This triggers the relay connected to it thereby disconnecting the battery from oscillator.
At pin 2, the inverting terminal,

$$V_{R6} = \frac{R_6 \times V_{cc2}}{R_5 + R_6} \qquad (1.14)$$

Where
V_{cc2} is the battery voltage

V_{R6} is the voltage across the inverting terminal set to 9V by potential divider formed by resistor R_5 and R_6.
Using equation 3.14, $R_5 = R_6 = 1k\Omega$
At pin 3 (non-inverting terminal), the zener diode $Z_{D1,}$ is set to a voltage of 10V.

$$V_{cc\,2} = R_7 I_{ZD\,1} + V_{ZD\,1} \qquad (1.15)$$

Where V_{ZD1} is the zener diode voltage, 10V and I_{ZD1} is the zener diode current, 10mA. R_7 is obtained to be $1k\Omega$
The transistor C1815 (Q_{25}) has the following specifications from the data sheet.
I_{cmax} = 0.5A, V_{BEmax} = 5V, β = 100
Output voltage of the op-amp = $0.9 \times V_{cc\,3}$
Where V_{cc3} is the voltage regulator's output voltage supplied to power the op-amp.
Output at pin 1 = $0.9 \times 12 = 10.8V$
Thus, $V_{BB} = 0.9V_{cc\,3} \times 10.8$

$$R_8 = \frac{V_{BB} - V_{BE}}{I_B} \qquad (1.16)$$

and

$$I_B = \frac{I_C}{\beta} \qquad (1.17)$$

For LED_2

$$R_9 = \frac{V_{CC\,1} - V_{LED}}{I_{LED}} \qquad (1.18)$$

Where $V_{cc1} = 12V$, $V_{LED2} = 2V$ *and* $I_{LED2} = 10mA$. From equations 1.16, 1.17 and 1.18, R_8 *and* R_9 are obtained to be $2k\Omega$ *and* $1k\Omega$ respectively
Diode D_3 is IN4007. It has a peak voltage of 50V and a maximum current of 7A; it can safely protect the relay from inverse voltage.

1.8.2 Charging Controller Unit

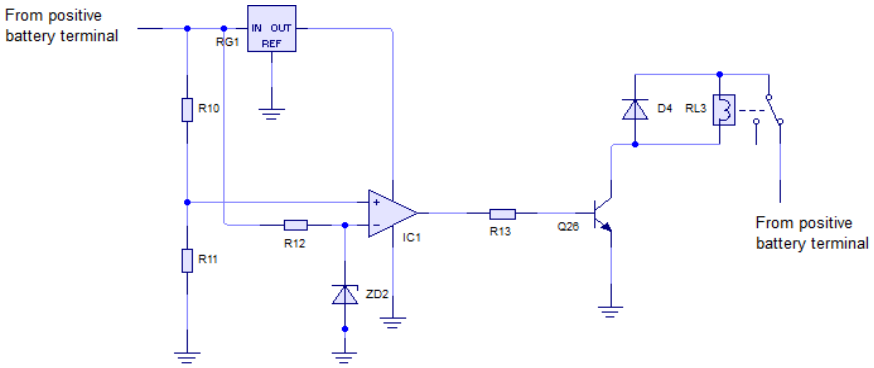

Fig. 1.5: Charging controller circuit

This stage is designed to prevent the battery from overvoltage charging. Figure 1.5 shows the circuit diagram for charging controller unit. Two fully charged batteries were connected in series giving a total voltage of 24V. IC_3 was used as a comparator in the charging controller unit. The inverting terminal was fixed at a constant voltage of 12V through zener diode Z_{D2}.

Thus,

$$R_{12} = \frac{V_{CC\,2} - V_{ZD\,2}}{I_{ZD\,2}} \qquad (1.19)$$

Where V_{cc2} is the batteries voltage, $V_{ZD2} = 12V$, $I_{ZD2} = 10mA$. R_{12} is obtained to be $1.2k\Omega$
Once the batteries are fully charged, the voltage across the non-inverting terminal is higher than that of the inverting terminal, this will triggers the transistor Q_{26} connected to it. This disconnects the batteries from the charging source. The charging source is reconnected when the voltage at the inverting terminal is higher than the voltage at the non-inverting terminal. The non-inverting terminal is therefore set to 14V through potential divider formed by R_{10} and R_{11}.
Then,

$$R_{11} = \frac{R_{10} V_{OP^+}}{V_{CC\ 2} - V_{OP^+}} \qquad (1.20)$$

Where V_{cc2} is the batteries voltage, $V_{op}^+ = 14V$ and $R_{10} = 1k\Omega$. A resistor of $1k\Omega$ is obtained for R_{11}. Transistor Q_{26} (IC1815) has the following specifications: $I_{cmax} = 0.5A$, $V_{BEmax} = 0.7V$, $\beta = 100$

$$R_{13} = \frac{V_{BB} - V_{BE}}{I_B} \qquad (1.21)$$

$$I_B = \frac{I_C}{\beta} \qquad (1.22)$$

$$V_{BB} = V_{CC\ 1} \times 0.9$$

A resistance of $2k\Omega$ is obtained for R_{13}
D_4 is a IN4007 diode with the following specification: Peak inverse voltage of 50V, and maximum current of 7A. The diodes were used as protector for the relays against the inverse voltage.

1.9 Rectifier Circuit

The rectifier circuit consists of transformer T_2, capacitor C_1 and a voltage regulator as shown in Figure 1.6

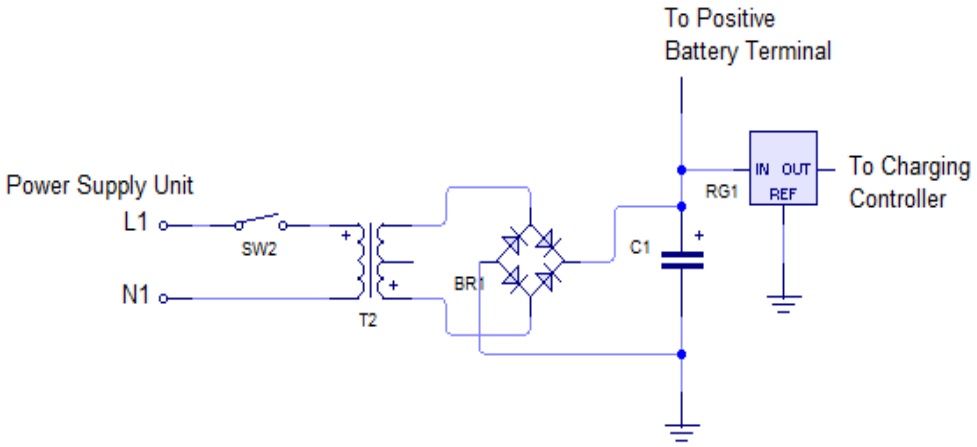

Fig. 1.6: Rectifier Circuit

T_2 is rated at 220/30V and the bridge rectifier consists of four diodes, D1 – D4 (IN4007). The diodes are used to convert the ac voltage available at the secondary of the power supply circuit to dc voltage. They have a peak inverse voltage of 100V, and a maximum current of 30Amperes which can safely handle 30V T_2. Capacitor C_1 is used to filter the ripples in the rectified voltage. The value of the capacitor depends on the load current and the degree of smoothing required. The capacitor is selected based on equation 1.23.

$$I_c = C\frac{dv_c}{dt} \qquad (1.23)$$

Where
C is the Capacitance of capacitor in Farad, dv_c is the ripples voltage (2V) produced by the rectifier and dt is the time between peaks of the input waveform.

$$t = \frac{1}{f} = \frac{1}{50} = 0.02 \text{ sec onds}$$

Where f is the frequency in Hertz.
The secondary current I_c of transformer T_2 is 6Amperes. From equation 1.23, C is obtained to be 6000μF
The voltage regulator, R_{G2} is 7815 IC with maximum output voltage of 15V. The output of the rectifier circuit is connected to the batteries for charging.

1.10 Power Supply/ AC Mains Unit

The power supply unit represent the input from the national grid. This unit is used to provide charging to the battery from the national supply grid. The AC input is rectified to the required output voltage to charge the battery through the rectifier circuit or unit. The UPS is made easy such that the supply from the national mains goes directly to the output when the supply main is available. A changeover is incorporated in the output to switch between supply from battery and supply mains from national grid without any noticeable interruption.

1.11 Battery Bank

A battery is an electrochemical device that converts electrical energy to chemical energy during charging and chemical energy back to electrical energy during discharging. A battery bank is needed in UPS design to store the energy when there is power supply from the national grid. Deep cycle battery type are recommended in UPS design because they are specifically designed for charge and discharge for a longer time. The battery should be large enough to store large amount of energy. Many sizes of batteries are available in the market, some includes: 12V/100A, 12V/150A and 12V/200A. The batteries can be connected in series to increase their voltage capacity or connected in parallel to increase their current capacity. The batteries used for this UPS are connected in series to produce 24V output.
Figure 1.7 shows the complete circuit diagram of the 2.5kVA UPS.

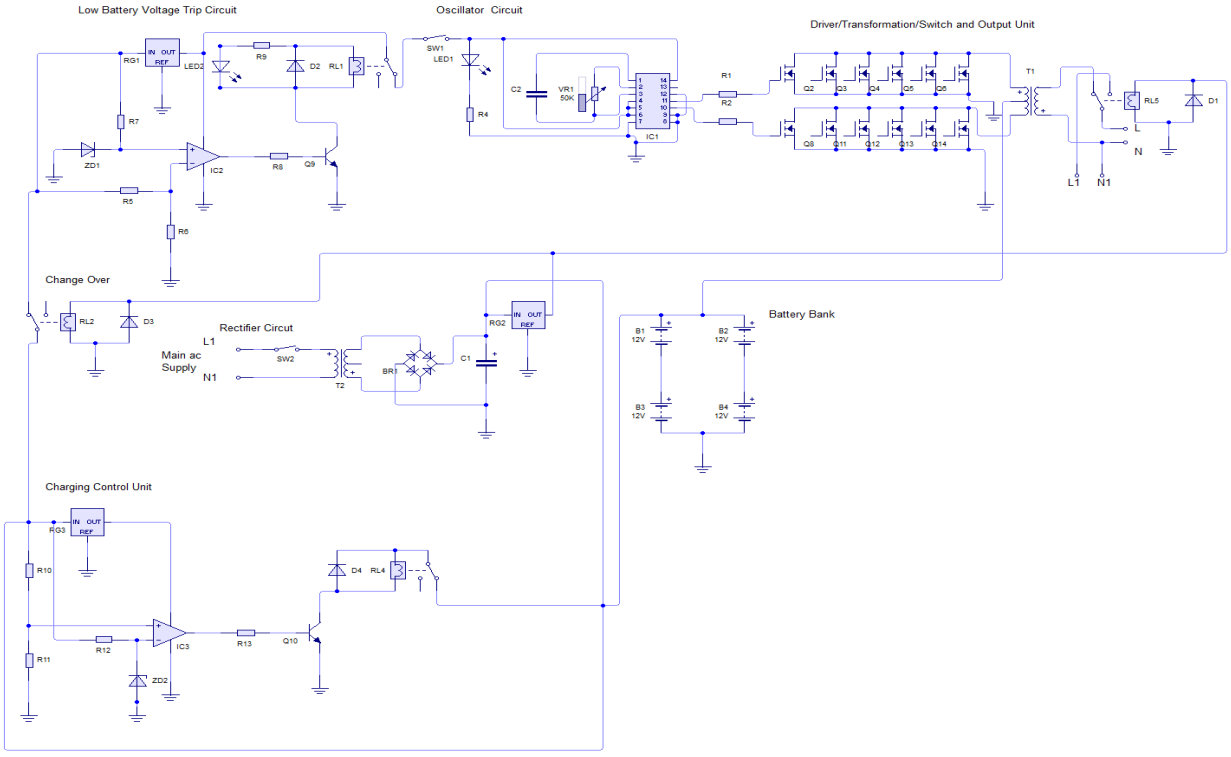

Fig. 1.7: Complete Circuit Diagram of Power Inverter

III. PERFORMANCE EVALUATION

The UPS was tested stage by stage. The system output voltage was measured at no load. Table 3.1 shows the expected and measured value.

3.1 Output Voltage Test

Table 2.1: Output Voltage Test

	Expected Output Voltage (V)	Measured Output Voltage	Correlation (%)	Remarks
From Battery (Inverter Mode)	240	243.2	98.77	Satisfactory
From Commercial Main Supply	220	220	100	Satisfactory

3.2 Over-Drain Test

This test was carried out to prevent the batteries from too much draining i.e. to stop discharging when the voltage dropped to certain level. The system was powered ON and the oscillator output voltage was measured at different battery voltage. The result is as shown in Table 2.2.

Table 2.2: Over-drain Test

S/N	Battery Voltage (V)	Oscillator Output (V)	System Output (V)	Remarks
1	24	5.6	243.2	Satisfactory
2	22	5.6	223.5	Satisfactory
3	20	5.6	201.6	Satisfactory
4	18	5.6	182.4	Satisfactory
5	17	0.03	0	Satisfactory

3.3 Charging Test

This test was carried out in order to ensure that the charging current provided from the charging source does not overcharge the batteries. The results of the test is as shown in Table 2.3.

Table 2.3: Charging Test

S/N	Battery Voltage (V)	Indicator	
1	18	ON	The results obtained from the test were satisfactory.
2	20	ON	
3	22	ON	
4	24	ON	
5	26	OFF	

34 Output Power/Load Test

The duration of supply from the UPS when there is no supply from the national grid is a function of total power connected to its output or load unit and power rating or capacity of the battery. The battery capacity is 24V, 200Ampere hour (24V/200Ah). The UPS was tested with 1000W halogen bulbs. The discharge duration is as shown in Table 2.4.

Table 3.4: Output Power/Load Test

Power (Watt)	Output Voltage (V)	Duration (Hour)
1000	240	4hrs, 25 minutes
2000	240	2hrs, 15 minutes

3.5 Cost Implication

The development of this UPS is also cost effective. Table 2.5 shows the rough estimates of cost of different components used in the development of the UPS.

Table 2.5: Cost of Components of the Power Inverter

Components	Cost (₦)
Transformer T_1	25000
Transformer T_2	4500
Diodes and LED	500
Voltage regulators	500
Resistors	500
Capacitors	500
Relay switches	2000
FETs	2000
Integrated circuits and sockets	1500
Casing	5500
Sockets and plug	800
Switches	500
Meters	600
Connecting wires	4000
Miscellaneous	5000
TOTAL COST	**53400**

It will be observed that the total cost of the UPS (₦53,400) is less than the selling price of a similar UPS here in Nigeria. The least cost of a similar UPS system here in Nigeria costs at least ₦80,000. The cost of the UPS designed in this work will reduce significantly if the UPS is to be massively produced.

IV. CONCLUSIONS

From the tests carried out on the UPS, it can be resolved that the main objective has been achieved. The system's output voltage on NO LOAD was 243.2V when the battery voltage was 24V. From Table 3.2, the batteries stopped discharging when the voltage across them dropped below 18V. From Table 3.3, the charging stopped when the voltage of the series connected batteries was more than 24V, thereby facilitating a reliable and efficient use of the batteries. The UPS load/output test also showed that the UPS can carry 2000W (2500VA) successfully. Though the output voltage was seen reducing as more loads were connected, the duration of supply from the UPS depends on the power of the connected loads and the battery capacity. The duration can be increased by increasing the battery capacity.

REFERENCES

[1] Robert Boylestad, Louis Nashlsky "Electronic Devices and Circuit Theory, Seventh Edition, Prentice Hall, Upper Saddle River, New Jersey, 2003

[2] North Star Battery Operation Manual, 2009

[3] www.fairchildsemi.com

[4] Theraja B. L. and Theraja A. K. "A textbook of Electrical Technology", Vol 1, 21st Edition, S Chand & Company Limited, 2005.

[5] Paul Horowitz, "The Art of Electronics", Second Edition, Cambridge University Press, 2009

[6] David I. J and Nelms R. M, "Basic Engineering Circuit Design Analysis, Eight Edition, Published by John Winley and Sons, Inc, 2006

[7] www.epanorama.net

American Journal of Engineering Research (AJER) 2016
American Journal of Engineering Research (AJER)
e-ISSN: 2320-0847 p-ISSN : 2320-0936
Volume-5, Issue-2, pp-136-144
www.ajer.org
Research Paper Open Access

The Evaluation of Urban Landscape upon Japanese Representative LRT Cities Using Visual Engineering

Jia Chen, Mamoru Takamatsu
(Faculty of Engineering, University of Toyama, Gofuku3190, Toyama city,930-8555 Japan)

ABSTRACT : *Light Rail Transit (LRT)is also considered the key to achieving a compact city in the future, and is being actively introduced to many cities in recent Japan. By with introducing the LRT system, it becomes very necessary to research the evaluation of urban landscape along the LRT line in order to improve landscape and urban planning as well as to provide a more attractive city for citizens and visitors. In this study, visual engineering and psychophysical measurement method was used to analyze people's subjective responses for urban landscape. We selected two Japanese representative LRT cities (Hiroshima and Toyama)as models, and the appearance of daytime and nighttime landscapes were evaluated on the basis of actual photographs by using the semantic differential method. From the results, the chief findings are showed as follows:1) overall evaluation of the nightscapes was better than that of the daytime landscapes. 2) Landscape lighting played the important role in the charming nightscape.3) Three dimensions were produced by factor analysis. The first seemed to relate to how inspiring the urban landscape was, and it was termed the factor of "activity". The second dimension related to how comfortable the exterior of the landscape was, and it was called the factor of "Pleasantness". The third was termed the factor of "regularity".*

Keywords-*LRT, urban planning, visual engineering, urban landscape, SD method, factor analysis*

I. INTRODUCTION

In June 2004, the landscape act was enacted as the first comprehensive act on landscape in Japan. The purpose of this act is to build a beautiful and dignified land, create an attractive and comfortable living environment and realize vibrant communities with distinct personalities by taking comprehensive measures to develop good urban and rural landscapes such as formulating landscape plans, in order to improve the quality of life of the people of Japan and contribute to the growth of the national economy and sound development of society. [1][2]

In particular, the urban landscape is an important component of the landscape actand has great significance in the construction of a comfortable, livable, and ecologically friendly city. Urban landscape also contributes to the cityscape in terms of visual quality. Within dense built environments, it creates a sense of openness and more attractive places to live for citizens and visitors. As the rapid development in most Japanese cities, urban landscape has become an important part of their urban planning. Well designed and managed urban landscape can improve citizens' quality of life, it is more efficient to evaluate the urban landscape forthe future city planning.[3]

Therefore, there are many studies on the evaluation of urban landscape such as:

Prof. Higuchi, Dr. Tamagawa et al.(1988)[4]analyzed the identifiableness of urban landscape, to research how nightscapes differ from daytime landscapes and find how we can make identifiable nightscapes.

Dr.Ahn Hyun, Dr. Kimetetal. (2007) [5]the survey was also carried out for the analysis of people's subjective responses to the images of urban night streetscapes. For analysis of the result of the survey, the SPSS10.0 statistical program was used along with statistical techniques, such as frequency analysis, correlation analysis, and variance analysis.

Prof.Kawasaki, Dr.Tsuchidaet al.(2008) [6]researched the relation between a whole image and a part of the image for urban landscapes from high points in the center of Kanazawa city, one of Japan's most traditional cities. The results of the SD method were analyzed with factor analysis, and four factors were extracted mainly. It was found that all whole pictures evidence the strong impact on the image of each factor compared with the parts.

Prof. Nakamura, et al.(2010) [7] Chofu area in Shimonoseki city was taken up as an example of the analysis, and the landscape is evaluated based on an actual photograph. "Image held in landscape and image of points the region" was analyzed.SD scaled questionnaire is taken in the experiment and multivariate analysis, and self-organizing neural network(SOM) were used as methods of the data analysis.

Prof. Matsumoto, Dr. Kacha etal. (2015) [8] studied on the evaluation of impression in streetscapes in Algeria and Japan. It was the semantic evaluation of the visual attributes of dataset of streetscape images. It focuses on the emotional impressions of the participants who evaluated the visual richness of the dataset.

On the other hand, urban transportation systems are being reviewed in countries around the world against a backdrop of chronic traffic congestion, exhaust air pollution and a rapidly aging society. Light Rail Transit (LRT) system is also considered the key to achieving a compact city design in the future, and is increasingly being adopted to many cities in Japan. By with introducing the LRT system, urban landscape around the LRT route is being play an important role in developing strategies for urban renewal. It becomes very necessary to research the evaluation of urban landscape along the LRT line in order to improve landscape and urban design as well as to provide a more attractive city for citizens and visitors.

In present study, we used visual engineering and psychophysical measurement method to analyze people's subjective responses for urban landscape. Two Japanese representative LRT cities were chosen as samples, Hiroshima city and Toyama city, which were successful introduction LRT systems in 2005 and 2006(Figure.1).The appearance of the daytime and nighttime urban landscapes along the LRT lines were evaluated on the basis of actual photographs by using the semantic differential method. Through by factor analysis, this study tried to analyze the effects and influence of urban landscape and described the characteristics of urban landscape along the LRT lines. It is expect to provide the basic data to create more beautiful and attractive urban landscape of the LRT city in the future.

(a)Toyama Port-ram-line (b)Hiroshima Green-mover-line

Figure.1LRTsystemin Japan

II. EXPERIMENTAL

2.1 Semantic Differential (SD) method

Semantic Differential (SD) technique is a typical method in performing landscape image evaluation test, was developed by C.E.Os good [9][10]. Impression evaluation by SD method, for a given impression measure, is an evaluation method for numerical select the degree to which subjects felt. This method, it is possible to quantify the evaluation value for each evaluation item, and that is also possible to comparative analysis between a pluralities of target. The analysis of the evaluation data of the SD method, we used the factor analysis method. This analysis made it possible to grasp the overall impression to the target from the impression words that are similar to adjectives. The evaluation is digitalized for each evaluation item, and comparative analysis becomes possible among multiple object. In determining impression evaluation words used in this experiment, 25 persons of subject were asked to freely write the impression toward sample pictures.

Table 1Judgment standards of adjectives[11][12]

[1]	Not to use adjectives that are used as special meaning by specialists, or adjectives that change the meaning depending on the knowledge of a subject.
[2]	To use a variety of words without concentrating on similar words.
[3]	To add words that are not connected to the sense of value, without leaning to adjectives related to value.
[4]	To avoid words that are easily judged on the purpose of surveying.
[5]	To use soft, sensory and intuitive adjectives.
[6]	To avoid obscure words.
[7]	To make the adjectives can be used in precedent studies as much as possible.

In the questionnaire, based on the after-mentioned judgment standards of Table1,20 contrastive adjectives were selected as suitable for evaluation the impression of Toyama and Hiroshima urban landscapes among 287 items of written impression words, including two overall indicators of the adjectives were adopted. Also, for the evaluation by a quantification theory, seven-grade system［+3, +2, +1, 0, -1, -2, -3］was usedin evaluation sheet of SD method. (Fig.2)[13][14]

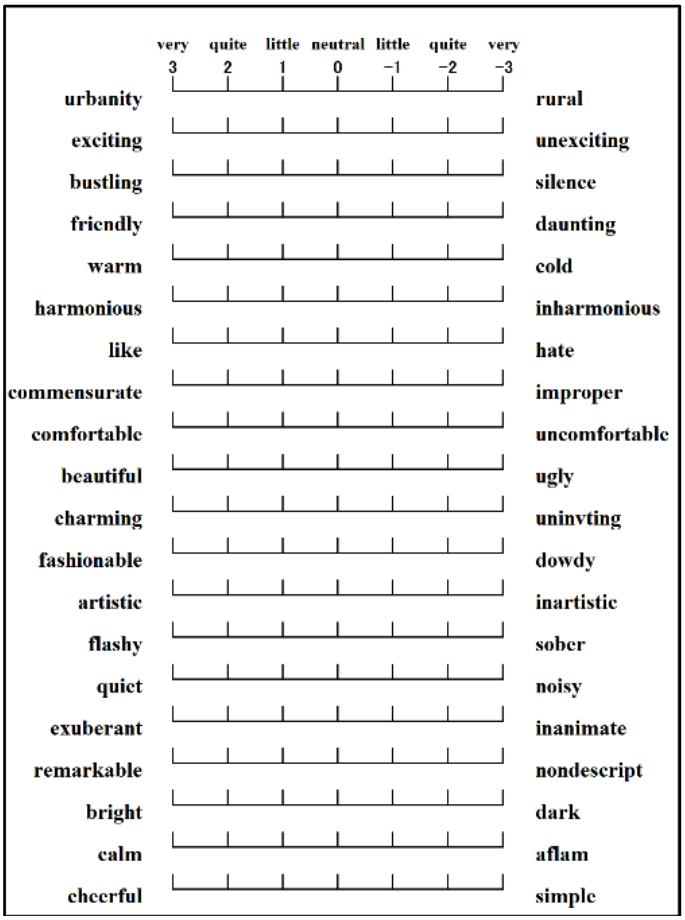

Figure.2Evaluation sheet of SD method

2.2 Selection of experimental samples

Hiroshima city is the capital of Hiroshima Prefecture, and the largest city in the Chugoku region of western Honshu, the largest island of Japan. Hiroshima is best known as the first city in history to be targeted by a nuclear weapon when the United States Army Air Forces (USAAF) dropped an atomic bomb on the city on August 6, 1945, near the end of World War II. Hiroshima city having a population of 1,170,000 is a city in Japan with the most users of the streetcar. The network of LRT system is 35.1km,55 million users took in 2009.

Toyama city, which introduced the Japan's first full-scale LRT system in the spring 2006, located on the coast of the Sea of Japan in the Chubu region on central Honshu, about 250 km north of the city of Nagoya and 380 km northwest of Tokyo. Historically, the modern city was incorporated on April 1, 1889, withdrawing from Kaminiikaw a district. As of 2014, the city had an estimated population of 337,324.Toyama LRT line passed through the center of Toyama city, such as ring water's park, Toyama castle, Toyama glass art museum access etc.[15]

According to the characteristics of the cities, we selected a total of 40 places from 2typical(historical and commercial)of the urban landscapes along the Hiroshima LRT and the Toyama LRT line as well as those have been widely recognized by the citizens and visitors. The urban landscape photography samples were be selected an observation point that can understand the whole pictures and characteristics of the landscapes.[16]

(a)Photographic equipment as the shooting conditions digital camera (Canon Eos Kiss X5), lens focal length 35mm equivalent and 28mm equivalent, dedicated tripod.

(b)Take photos' date and time to be selected in the good weather of summer, during 10:00 to 15:00, and after sunset 19:30 to 21:30.

(c)Shoot position in the LRT wayside road centerline supplementary near and then, the height from the

ground to the center of the camera lens is set to 1500 mm.

(d)Photography quality can be maintained at high quality pixels, the alignment condition of the four or more points. Our vision and visual angle also taken into consideration, and conscious so that it becomes a natural scenery samples as possible.[17][18]

According the above-described criteria were taken photographic samples. In reading all the photos have taken a personal computer, we have created daytime samples 40 pieces, nighttime samples40 pieces of a total of 80 points of the experimental observation for the urban landscape with LRT route. Actually used somedaytime samples are shown in Fig.3

a. Hiroshima Peace Memorial Parkb. Hiroshima Castle c. MAZDA Zoom-Zoom Stadiumd. Itsukushima Shinto Shrine

e. Toyama Ring Water's Park f. Toyama Castle g. Toyama Glass Art Museum h. Toyama Electrical Building

Figure.3Example of daytime sample photos

2.3 Experiment method

We did all of experiment under the conditions of a dark room. The distance of the subject's anterior 4 m place the screen (W2.4m × H1.8m) for presenting the landscape sample, using a projector, and is presented in a random one by one slide experimental landscape samples on the entire surface of the screen.

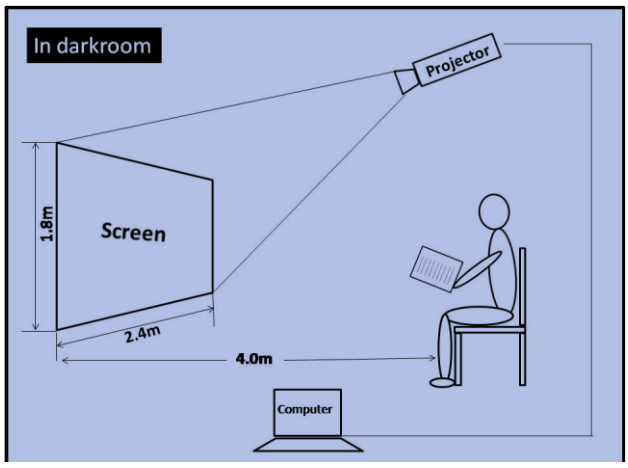

Figure.4Image of experimental

Subject observed the presentation of the landscape sample in one minute, thereafter, evaluates the impression felt the scene sample data sheet using the SD method of psychological techniques. In order to prevent accidental filling, etc., it is assumed that fill one by one for one scene sample.[19]

The configuration of the subject are25 students (17 males, 8 females) of the faculty of engineeringwith 21.9 average age, both are familiar to the SD method. In addition, psychological subject, namely in consideration of feeling and physical condition etc., in order to measure and reduce the error as much, experiments were performed while taking a break at fixed intervals.[20]

III. RESULTS AND DISCUSSION

3.1 Experiment results

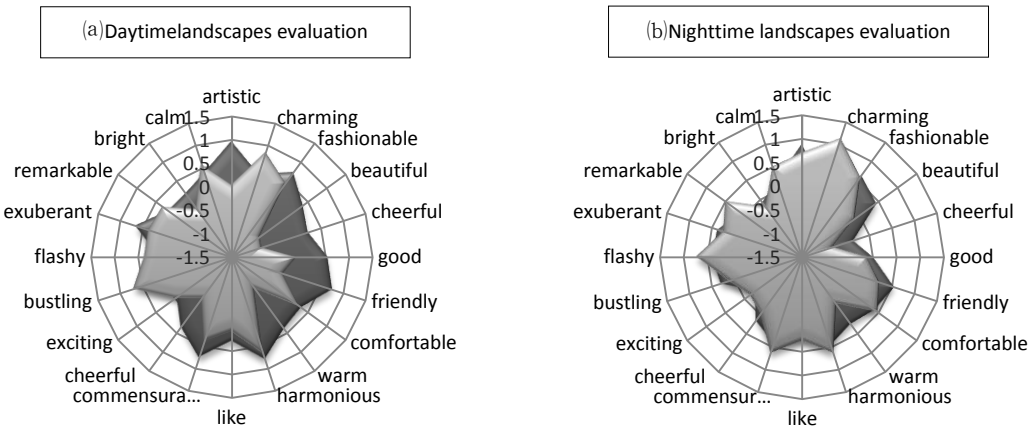

Figure.5Average result for all samples(■Hiroshima■Toyama)

We showed average impression evaluation result of all samples in Fig.5. For all landscape samples, it is intended that the average value of all image evaluation results of the displayed on the polar coordinates. In each figure, placing the adjective of positive impression in the circumferential direction. The radially taking an evaluation value, the evaluation value of each adjective enough to be located outside the circle indicating that is high. The parameter is "■Hiroshima" and "■Toyama".

First, Fig.5 (a) showed the average value in daytime, it can be said that shows the respective landscape evaluation trend "Hiroshima" and" Toyama". The variation of the daytime urban landscape evaluation value is large, compared with "Hiroshima", the area surrounded by the closed curve in the order of "Toyama" is larger. That is, in the evaluation of the daytime landscape samples showed that the image evaluation of the "Toyama" is above it in the overall the "Hiroshima". Specifically, the difference was remarkable in adjectives such as(artistic), (beautiful), (cheerful), (good), (friendly)and (warm).

Then, in Fig.5 (b) showed the average value at night both "Toyama" and "Hiroshima", different from the previous result, higher overall trend compared image evaluation is that of the daytime urban landscapes can be seen. The difference was obviously in adjectives such as (charming), (friendly), (harmonious), (commensurate), (flashy) and (calm).In particular, the evaluation of "Toyama" such as (cheerful), (warm), (exciting) and (bright)value that has been shown very low.

3.2 Factor analysis

Toyama and Hiroshima city totally 80 pieces samples of experimental data that used in this experiment, in order to more quantitatively assess the results, we were subjected to factor analysis. By the analysis to better interpret the landscape sample results factor analysis, on the basis of the results obtained from the subjects and subjected to factor analysis with respect to average data of an image evaluation of each adjective pair in the landscape sample it was showed in Table 2.

With performing the factor analysis, principal component analysis was performed for firstly determining the number of factors. The Eigen values of the factor for the correlation matrix between each adjective pair is 1.0 values or more factors are three extraction cumulative for the contribution rate was 79.14%, in consideration of the possibility of semantic interpretation is the number of three factors was conducted factor analysis.

Table 2. Result of factor analysis

Axis	Label	Adjectives Name	Factor 1	Factor 2	Factor 3
1st Axis	Activity	Urbanity Rural	0.901043	0.207936	0.105482
		Exciting Unexciting	0.825898	0.418232	0.260493
		Bustling Silence	0.798481	0.294507	0.348639
		Flashy Sober	0.738077	0.550268	0.128313

		Exuberant Inanimate	0.697234	0.376081	0.532197
		Remarkable Nondescript	0.664421	0.540431	0.230119
		Bright Dark	0.644894	0.437176	0.161598
		Calm Aflame	0.615687	0.480708	0.107348
2nd Axis	Pleasantness	Good Bad	0.254288	0.857552	0.282212
		Friendly Daunting	0.379473	0.838978	-0.07758
		Comfortable Uncomfortable	0.526019	0.786869	0.159778
		Warm Cold	0.505595	0.761755	0.126943
		Harmonious Inharmonious	0.277914	0.736685	0.555638
		Like Hate	0.235191	0.680509	0.577099
		Commensurate Improper	0.110587	0.635546	0.482484
		Beautiful Ugly	0.488222	0.624323	0.498644
3rd Axis	Regularity	Charming Uninviting	0.226523	0.554423	0.869139
		Fashionable Dowdy	0.511379	0.091644	0.742833
		Artistic Inartistic	0.319054	0.563368	0.696762
		Cheerful Simple	0.148995	0.289834	0.644631
Contribution Rate (%)			39.14%	28.11%	11.89%
Cumulative Contribution Rate(%)			39.14%	67.25%	79.14%

As a result, it shows the contribution rate after varix rotation until the resulting second factor and the factor loadings of each adjective pair in Table 2, Factor loadings indicates the influence factors on each evaluation item, factor of interpretation which went in load factors.

Results of factor analysis, three factors were deposited roughly, was estimated meanings representing each factor from the factor loadings adjective pairs in each factor. (Table 2)

1. The first factor was39.14%contribution rate and it was high factor loadings of urbanity, exciting, bustling, flashy, exuberant, remarkable, bright and calm. Then, it was interpreted as Activity factor.

2. The second factor was 28.11% contribution rate, high factor loadings of good, friendly, comfortable, warm, harmonious, like, commensurate and beautiful. From these features, it was named Pleasantness factor.

3. The third factor is 11.89% contribution rate at high factor loadings of charming, fashionable, artistic and cheerful, it was termed Regularity factor.

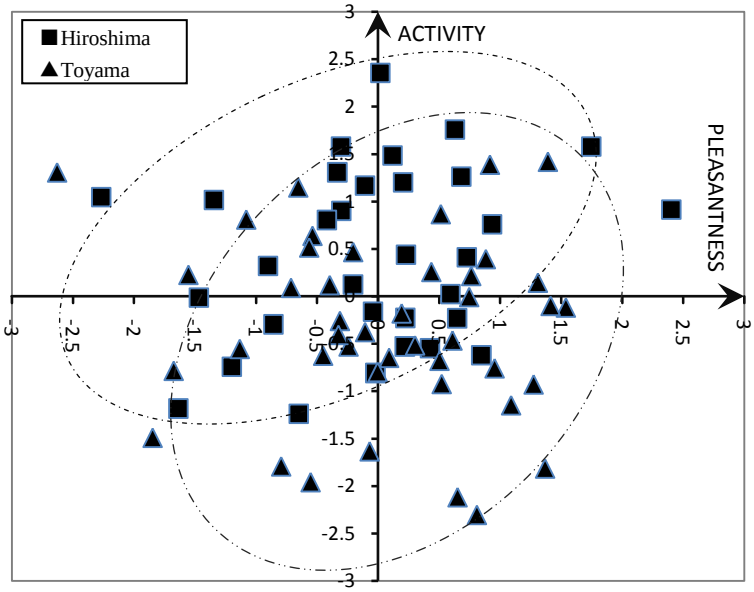

Figure.6Factor analysis points evaluation for all samples
(Activity factor to Pleasantness factor)

Based on the factor analysis results, it showed two graphs plotted together factors score of each sample (Fig.6) and (Fig.7). InFig.6, the horizontal axis is first factor［Activity］, and the vertical axis is one that took the ［Pleasantness］.The parameters are the two stages of the points indicated by "■Hiroshima" and "▲Toyama". InFig.7,the horizontal axis is second factor［Pleasantness］, and the vertical axis is the third factor［Regularity］. The parameters are the two stages of the points indicated by "◆Hiroshima" and "●Toyama".

From Fig.6,［Activity］in the night time landscape as a whole tendency, and［Pleasantness］means that has been shown to be higher than the day time landscape. In particular, in the［Activity］of the vertical axis, they tend to factor score can be greatly increased in the nighttime landscape was seen. This difference is mainly is due appropriate landscape lighting effects at night, as compared to it more lively than daytime landscape, it is believed that because gave a certain impression of vitality.

Specifically, particularly high landscape sample of evaluation in the［Activity］of the vertical axis, Urban place, ANA hotel and Mazda zoom-zoom Stadium etc., neither of which are nighttime urban landscape. Day and night of Hiroshima castle, day and night of Toyama castle, which are very low factor score The main cause of such negative evaluation is due to the "vibrant and lively" of the commercial and tourist facilities scenery, historical landscape, such as Itsukushima Shinto Shrine and Toyama castle is an all-quiet is calm. It is considered to be because the relatively susceptible to impression.

Also inFig.7, the［Regularity］of the horizontal axis, daytime and night landscape of high evaluation such asToyama ring water's park, day and night of Koshinokuni cultural center, Toyama castle it is a night scene. On the other hand, evaluation low landscape, JR Toyama Station, there was a daytime scenery and night view of the CIC building. From the above, a high valuation landscape, a lot of green, lighting tended to stand out landscape and beautifully lit up the Toyama Castle unique landscapes such as an LED illumination, such as maintenance has been Toyama ring waters' park. On the other hand, low landscape of the valuation, the commercial ones, are in the city, such as station building, include the landscape to receive the mundane impression. Further, the main cause of negative evaluation in night view of the CIC building may be due to fluorescent mercury lamp has been used to light up. As a feature of the fluorescent mercury lamp illuminance for low color rendering property but can be secured, the landscape can be mentioned disadvantages would appear dimensionally such as gray color. In addition, JR Toyama Station, it is believed to inhibit the [Evaluation] of the landscape due to the impact of the wire such that has been spread around in large utility pole and sky before station building.

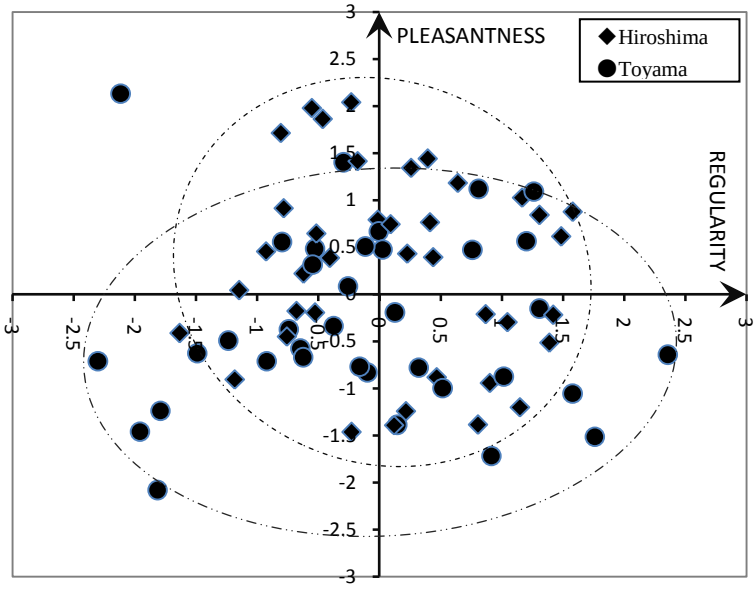

Figure.7Factor analysis points evaluation for all samples
(Pleasantness factor to Regularity factor)

From the results of the factor analysis, in the commercial landscape, daytime landscapes although more of Toyama is highly rated, it is reversed when it comes to nighttime landscapes, that of Hiroshima evaluation is higher. This evaluation value over the nighttime landscape from daytime landscape both two cities are rising, but is due to better Hiroshima landscape is large rise width of the evaluation. The landscapes of Hiroshima, such as Mazda stadium and peace memorial park are many place such as illumination and light up have been made

effective, in such a landscape sample "exciting" , "flashy" , "bright" and "beautiful" evaluation value adjective pairs such as are rising. However, The urban landscape of Toyama excluding the place where illumination such as Toyama ring water park have been made, is not observed areas the evaluation value is increased greatly. Consequently, it is considered that the difference between the evaluation value in the daytime and nighttime occur.

In addition, in the historical landscapes, the same with commercial landscapes, from daytime to nighttime landscape on the overall evaluation values between the two cities is increased and the difference of the evaluation value is shortened, but Hiroshima both daytime and nighttime towards the wayside of the landscape it became a result of the evaluation is higher than that of Toyama. The reasons is by Hiroshima wayside of landscape to the ingenuity, such as using the illumination light to match the appearance of the building, although a high evaluation value at daytime landscape also maintains at night scene, Some landscapes of Toyama LRT wayside, light-up were not performed, the evaluation value has become a generally low value.

The urban landscapes of Toyama LRT, since although daytime commercial urban landscapes obtained a good evaluation, but evaluation in the others were below that of Hiroshima LRT. It may be desirable to go conducted to improve the light-up and urban design in the future.

IV. CONCLUSION

As mentioned above, the overall image evaluation of the night urban landscape was better than that of the daytime along the LRT lines. We found that the appropriate light-up was more important in improving the image of the urban landscape and activating the citizen's life at night. The importance of nighttime urban landscape along the LRT line has been recognized again. In order to produce a beautiful attractive urban landscape, the role of the landscape lighting are very important, rather than merely applying illumination, I considered there is a need to be done with an understanding of the landscape of the characteristics and purposes.

From factor analysis, three dimensions were produced by factor analysis. The first seemed to relate to how inspiring the urban landscape was, and it was termed the factor of "activity". The second dimension related to how comfortable the exterior of the urban landscape was, and it was called the factor of "pleasantness". The third dimension related to how harmonious the urban landscape , and it was termed the factor of "regularity".

By comparing the image evaluation of Toyama and Hiroshima of urban landscape along the LRT line, only the daytime commercial landscape in Toyama LRT wayside is good for evaluation, the obtained became the evaluation below the urban landscape along the line of landscape Hiroshima in other. With the March 2015 opening of the Shinkansen, Toyama LRT line running through the center of Toyama currently in service, the number of user increases are being expected. In order to produce a beautiful attractive urban landscape, we considered there is a need to be done light-up and urban design go made improvements that may be desirable around Toyama LRT line in the future.

Finally, this experiment was limited to subjects before and after 20s students, it is considered that it is necessary to measure in consideration of the age of the subject in the future.

V. ACKNOWLEGEMENTS

I would like to express my gratitude to Associate Professor Mamoru Takamatsu, visual and auditory information processing lab, department of intellectual information systems engineering, faculty of engineering of Toyama university, for his constant guidance through the present study, who teaching me the experimental procedures and usage of all suggestions devices.

In addition, I wish to thank all the member of Associate Professor Takamatsu visual and auditory information processing laboratory.

REFERENCES

[1] J.Chen and M.Takamatsu, Research on the characteristics and evaluation of nightscape along the LRTline, *Journal of Engineering Research and Application*, 5(11), 2015, 108-114.

[2] J. Chen, H. Sawa, L. Ma, M. Takamatsu, and Y. Nakashima, Basic study on the features of scene viewed from centram-train window, *Proc. 43th Journal of the Color Science Association of Japan Meeting*, Kyoto, Japan, 2012, 148-149.

[3] J. Chen, L. Ma, S. Wang, Y. Nakashima and M. Takamatsu,Evaluation of landscape lighting for urban nightscape in a snowy region, *Proc. 5th CJKLighting Conference*, Tokyo, Japan, 2012, 283-286.

[4] T. Higuchi, H. TamagawaandK. Akema, A comparative study on the identifiableness of cityscape between in daytime and at night,*Architectural Institute of Japan*, *388*, 1988, 79-85.

[5] T. H. Ahn, W. Kim, T. J. Kim and H. K. Moon, Subjective images of nightscapes in downtown Seoul, *Proc. 18th ILUMINATInternationalConference*, Seoul, Korea, 2007, 11-20.

[6] Y. Kawasaki, Y.TsuchidaandY.Shimokawa, Psychological evaluation between a whole image and a part of the image for views from high points in the center of Kanazawa, *J. Environ.Eng., AIJ, 73(627)*, 2008, 669-677.

[7] H. Nakamura, H.Y. Wang and T. Tsuchida, Landscape analysis of historical town using Kanseiengineering,*Proc. 26th Fuzzy System Symposium*, Hiroshima, Japan, 2010, 31-36.

[8] L. Kacha, N. Matsumotoand A. Mansouri, Study on the evaluation of impression in streetscapes in Algeria and Japan using

Kansei engineering, *J. Archit. Plan., AIJ, 80(712)*, 2015, 1357-1363.
[9] C. E. Osgood, Semantic differential technique in comparative study of cultures, *American Anthropologist, 66(3)*, 1964, 171-200.
[10] C. E. Osgood, Study on the generality of affective meaning systems, Amer.Psychology, 17, 1964, 10-28
[11] Y. Nakamura, Impression of the urban landscape,*Journal of the Illuminating Engineering Society,74(3)*, 1999, 143-148.
[12] T. Kumamoto, K. Ohta, Selection of impression word for Impression-based retrieval, *Transaction of Information Processing Society of Japan, 44(7)*, 2003, 1808-1811.
[13] M. Zhang, Y. Nakashima and M. Takamatsu, Research on illumination of historical buildings by the color temperature, *International Journal of Computer Science and Network Security,10(8)*, 2010, 27-33.
[14] L. Ma, Y. Nakashima and M. Takamatsu,Study on the optimum color temperature for the illumination of Japanese stylegarden, *The Institute of Electrical Engineering of Japan, A133(11)*, 2013, 558-564.
[15] Y. Nakashima and M. Takamatsu, Evaluation on color rendering effect of landscape lighting,*The Illuminating Engineering Institute of Japan, 87(2)*, 2003, 128-132.
[16] T. Tsuchida, Kansei engineering study for streetscape zoning using self-organization maps, *International Journal of Affective Engineering, 12(3)*, 2013, 365-373.
[17] M. Nagamachi, Kansei affective engineering, CRC Press Taylor and Francis Group, Boca Raton, USA,2011
[18] T. Nakama and Y. Kinoshita, A Kansei analysis of the streetscape in Kyoto - an application of the Kansei structure visualization technique, *Proceedings of the International Conference on Kansei Engineering and Emotion Research*, Kyoto, Japan, 2010, 314-323
[19] C. Linares and A. F. Page, Differential semantics as a Kansei engineering tool for analyzing the emotional impressions which determinethe choice of neighborhoods, The case of Valencia, Spain, Landscape and Urban Planning, *87(13)*, 2008, 247-257.
[20] S. Sakai, T. Sato,T. Ishida and H. Aran, Impression of Cityscape and its Comparison between Kyoto and Bangkok,*Journal of the Color Science Association of Japan Special Issue 37th Annual Meeting*, Japan, 2006, 180-181.

American Journal of Engineering Research (AJER) 2016
American Journal of Engineering Research (AJER)
e-ISSN: 2320-0847 p-ISSN : 2320-0936
Volume-5, Issue-2, pp-145-150
www.ajer.org
Research Paper Open Access

Augmented Reality, an Emerging Technology and its View Management Problem.

Nehal Agrawal
Department of Computer Engineering Mukesh Patel School of Technology Management and Engineering, NMIMS, Mumbai, India

Abstract: *This paper talks about the emerging augmented reality technology, which has become popular in recent times due to availability of smartphones. Augmented reality applications need to annotate real world objects with information. Labelling is the most intuitive technique to achieve this goal. But labelling sometimes causes overlapping and occlusion amongst labels and objects. This causes ambiguity. This paper reviews two interactive system of view management to address the problems.*

Keywords: *Augmented reality, Virtual reality, View management, Point of interest (POI), Annotation, Label, Layout.*

I. Introduction

Augmented reality is a technology through which a user's real world view can be altered by superimposing computer generated virtual texts and images on the users viewing screen in real time. It is an emerging technology and has found applications in various fields such as medicine, tourism, defense, arts etc. This technology has gained popularity in recent times due to the availability of smartphones which contain the required hardware to support augmented reality.

Most applications make use of labels to provide digital information to the user in context of their real time environment. These labels annotate real world buildings and places with textual information. The digital information is registered based on geographical locations (Point of interest) with corresponding GPS position. These POI's are projected on the screen with the help of labels.

As the number of POI's in the frame increase, number of labels increase. This often leads to labels occluding important real world objects and other labels. As a result, the view of the user is hampered. Furthermore, augmented reality environments are dynamic, due to which the labels must be coherent with the frame. Jumping labels are undesirable. They distract the user and hamper the view.

The decision of where to place the labels so that readability is increased and the view of the user is not hampered, is the problem of view management. View management refers to the layout decisions that determine spatial relationships among the 2D annotations in the view plane. Researchers have come up with several techniques to solve the problem of view management.

In this paper, we discuss two techniques. First, Image-Driven View Management [1]. Second, Dynamic Labeling Management [2].

II. Augmented Reality- The concept

a. Definition

Augmented reality technology consist of the following building blocks [3]:

Real world.

Real time.

Computer Graphics.

Seamless integration of the graphics in real world.

An AR enabled device.

Keeping these building blocks in mind, a formal definition of augmented reality is:

Augmented Reality (AR) is a real-time device mediated perception of a real-world environment that is closely or seamlessly integrated with computer generated sensory objects [3].

It is important to understand the difference between virtual reality and augmented reality. They both form the part of mixed reality. In virtual reality, real world objects augment the virtual environment and in augmented reality, virtual objects augment the real time environment.

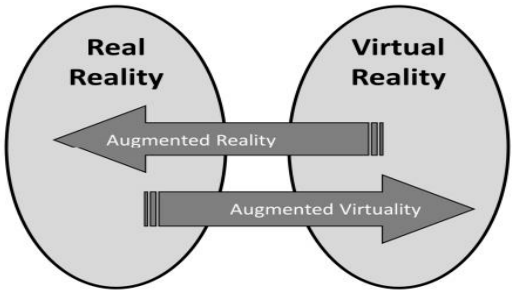

Figure 1 Conceptual model of the relationships between the Real (Physical) Reality and Virtual Reality.

b. Classification

Based on the five natural powers of human sense of sight, taste, hearing, touch and smell. Augmented reality can be classified as

Visual augmented reality. (Sight)

Haptic augmented reality. (Touch)

Gustatory augmented reality. (Taste)

Olfactory augmented reality. (Smell)

Audio augmented reality. (Hearing)

The classifications of AR are evolving. The main types of AR in the context of their conceptual evolution are

Marker augmented reality. (Recognition based AR)

An AR marker is an image or a view of real-world objects that provides a unique pattern that can be captured by an AR camera and recognized by AR software [3].

The AR software recognizes the marker and calculates the correct position for placement of the graphic. This graphic is then embedded in real time near the marker.

Marker less augmented reality. (Location based AR)

In marker less AR, objects in real world are tracked without the use of markers. . It places graphics in real time based on the position (the latitude, longitude and altitude) of the AR object in the real world environment. [3]

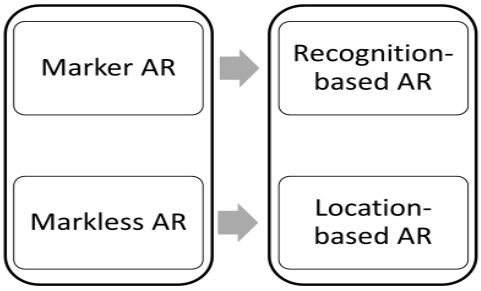

Figure 2 The evolution of the conceptual model of Augmented Reality.

III. View Management in AR

View management refers to the layout decisions that determine spatial relationships among the 2D annotations in the view plane.[1] Researchers have come up with several techniques to solve the problem of view management. In this paper, we discuss two such techniques.

a. Image-Driven View Management

Image driven view management technique takes into consideration the layout (point based placement or labeling) of a label along with its representation (visual style) to increase readability. It makes use of the pixel based approach for placement of labels and considers an extensive list of aspects for placing labels based on the real time content. [1]

This technique focuses on unambiguity, aesthetics, readability and frame-coherence of labels. It is a hybrid technique that combines a layout algorithm with adaptive rendering. The approach adopted analyses the image to determine the placement of labels. It takes care of the following [1]

1. Labels should not overlap important real world objects.

2. Labels should be rendered in a way that they easily relate to their corresponding POI's.

3. Labels should be readable over the background.

3. Labels should be coherent to the frame.

i. Image Based Layout

The layout technique uses information from the image to determine position of the labels. The goal is to avoid occluding important real world objects.

To identify important areas in the image, saliency algorithm is used along with edge analysis. Saliency algorithm produces an intensity image (saliency map) where the grey levels represents the importance of information in the image. The edge analysis produces an edge map. Taken together, the salient information and the edge information encode the pixel positions where labels should be placed.

To implement optimization, Greedy algorithm is used. Greedy algorithm sequentially optimizes each label and evaluates the objective function of each. The minimum value among the candidate positions is selected as the position of the label. The algorithm sorts out the labels from left to right and in depth from closest to farthest. It iterates for each label, for different positions in the space and minimizes the objective function. [1]

To handle image motion and dynamic content in the image, the layout algorithm is executed at low frequency after initially placing all labels. To avoid jumping labels, each label is locally tested for changes of the saliency or edges information and re-computation is avoided as needed.

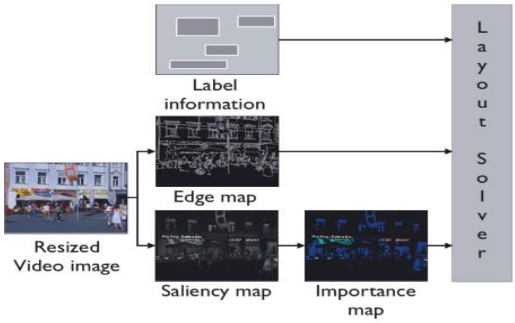

Figure 3 Image analysis for our layout algorithm: the image is resized, saliency map and edges map are computed. A threshold is applied to the saliency image.

ii. Adaptive Representation

Leader lines

When moving labels further away from their anchor position, leader lines are required to link them. Users must be able to distinguish the leader line from the background for which the contrast between the colour of the line and the surrounding pixels should be high. The contrast is achieved by following the process of computing an average of the lightness of the pixels surrounding the leader line and modifying the colour of the leader line to yield a contrast. [1]

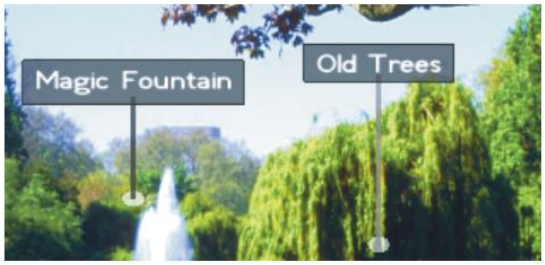

Figure 4 Colour of leader lines are adapted to background.

Anchor

Anchor points help the user in identifying the real position of the POI (if the POI is in front or behind the object present in the view). The inner radius of the anchor encode the distance. If a POI is close to the user, the ring will be a full disk, if the POI is far from the user, the ring will converge to a circle. The opacity is modulated by encoding its value in function of the distance to the viewer. Hence, close POIs are opaque, while distant POI are transparent. To determine the radius, distance of the POIs are rescaled from the user's viewpoint to a normalized range. [1]

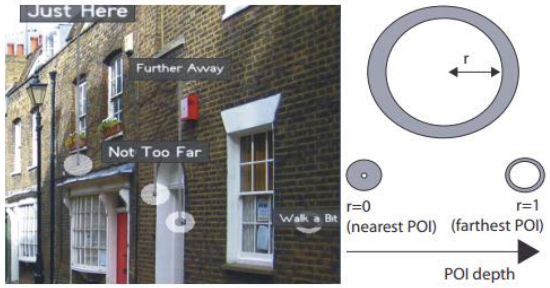

Figure 5 Anchor Ring concept and example with POIs at different distance.

Background and text

When the label overlays a dark or bright area of a video image, the readability is impaired. Hence active rendering styles for the labels is adopted. A separated technique, which works in HLS (hue, saturation and lightness) colour space and allows to adapt lightness or saturation of a label background or of its content is adopted.[1]

Three approaches can be used

1. Global approach: It computes the average lightness over the entire image and modifies the lightness of the label background to have a contrast difference above a certain threshold.

2. Local approach: considers only the computation of the average lightness in the neighbourhood of each label's background, and contrast modifications are applied separately for each label.

3. Salient relative approach: considers the average lightness of the salient regions, so the labels can be more prominent with respect to the saliency information on the image.[1]

iii. Context and Temporal coherence (Consistency)

To achieve temporal coherence, label movement caused by jitter introduced by unsteadily holding the device is minimized. Label movement is also avoided there are only small dynamic changes in the scene. An inertial sensor is used to determine the yaw magnitude of the current rotational camera motion.[1]

The Algorithm avoids placement of labels on detailed features or visually prominent elements (people, cars, visual signs, and complex facades) and places labels in uniform areas (sky, ground area, grass). For urban facades, labels are generally moved between windows and reliably avoid overlaying shop signs. The saliency map computation is also efficient for filtering highly repetitive textures. The edge map computation generates a

large number of lines for complex scenes with trees or complex building structures. Therefore a small weight factor for the edges map is used in the objective function.

b. Dynamic Labelling Management

In dynamic labelling management, layout decision of the labels are based on users' desired constraints. The goal of this technique is to place label efficiently to avoid ambiguity. Occlusion problem are solved in two directions:[2]

Labels are rearranged to explore more available positions.

Information filtering is used to reduce number of labels. Irrelevant information for the user is eliminated.

This technique combines three sub-techniques:[2]

View driven filtering technique to reduce number of labels.

Adaptive labelling technique to optimize placement.

Fast label searching to instantly respond to user's inquiry.

Hence this technique integrates label placement algorithm and information filtering.

i. View Driven Label Filtering

Properties of an object can be categorized as Objective and subjective. The filtering function helps determine the elimination of labels. View driven filtering technique has the following characteristics [2]

Level of details for objects vary with their distance from viewer. Details consist of colour, size and contents shown on them. Example if the text of a label is "Reserve Bank of India" can be abbreviated to "RBI" when the viewer moves away from it.

Hardware automatically clips the object outside the view frustum but their labels have to be clipped manually.

To indicate the priority of objects, system strengthens the contrast of label display. Label size become larger as priority increases. Other factors that influence the priority are distance from user, object size and user focused.

Objects with same feature are bounded into a single group such that only one label is needed for all objects in the group.[2]

Objective properties:[2]

Label context: Stores the text associated with the label (different text for different distance level)

Group index: Indicates the group to which this object belongs.

Position: Stores the bounding box of the projection of each object on the 2D screen.

Size: Stores the minimal and maximum size of the visible label.

Transparency: Property used to improve label display if overlapping cannot be avoided.

Subjective properties:[2]

Priority: Each object is assigned a priority that helps in filtering.

Focus region: This property represents the user-focused region which helps in filtering labels outside of the region.

Filtering technique reduces the data redundancy and display efficiency is enhanced.

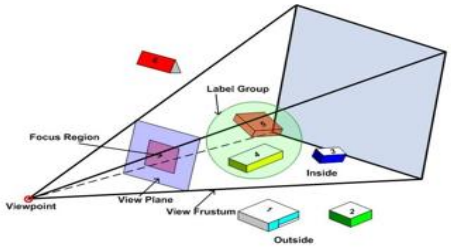

Figure 6 Only objects/groups of objects that lie inside the focus region are labelled.

ii. Adaptive Label Placement

This system calculates the bounding box of the projection for each object and then determines a rational area to place the corresponding label. There are two placement schemes

Internal labelling: Places label inside the bounding box.

External labelling; Places label outside the bounding box. An arrow is used to connect the label and associated object.[2]

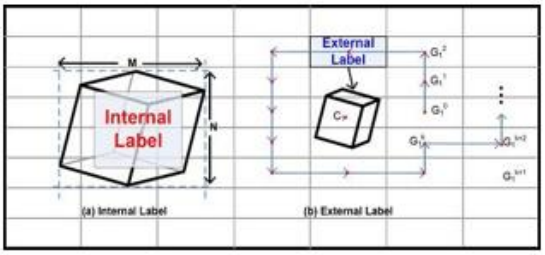

Figure 7 Internal and External labelling.

iii. Label Searching

Labels give users extra information related to the environment but excessive information usually make users confused even if all labels are well displayed. Hence this system supports fast label searching. The interface of label searching is an input box. Users may input some keywords and the system will use a coloured arrow to show the direction of the inquired label.[2]

iv. Dynamic Labelling

Users can navigate the environment with the assistance of dynamic labelling and structured label searching facility.[2]

IV. Conclusion

Augmented reality annotates real world with valuable information for the user. Placement of this information on the view screen of user must be monitored such that the view is enhanced and not hampered. This is taken care of by the view management techniques talked about in the paper. The first technique combines a layout algorithm with adaptive rendering. The second technique integrates label placement with label filtering. Both take care of dynamic label placement. All these features make these algorithms effective.

References

[1] Raphael Grasset, Tobias Langlotz, Denis Kalkofen, Markus Tatzgern and Dieter Schmalstieg "Image-Driven View Management for Augmented Reality Browsers", Graz University of Technology.

[2] Fan Zhang and Hanqiu Sun "Dynamic Labeling Management in Virtual and Augmented Environments", Dept. of Computer Science and Engineering The Chinese University of Hong Kong, Hong Kong.

[3] Vladimir Geroimenko "Augmented Reality Technology and Art: The Analysis and Visualization of Evolving Conceptual Models, School of Art and Media", Plymouth University, Plymouth, UK.

American Journal of Engineering Research (AJER) 2016
American Journal of Engineering Research (AJER)
e-ISSN: 2320-0847 p-ISSN : 2320-0936
Volume-5, Issue-2, pp-151-156
www.ajer.org
Research Paper Open Access

Application of Virtual Reality in a Learning Experience

Victor U. Obrist[1] and Eustaquio A. Martínez (tutor)[2]
Polytechnic School – U.N.E.[12]
Ciudad del Este, Paraguay[12]

ABSTRACT: *The project is an application that allows users to interact in a virtual environment via a web interface, in which models are in three dimensions to simulate different activities. The application focuses on education with virtual reality technology, enriching the student's perception through the interaction with objects in an artificial world, facilitating their learning. A website was designed for this purpose, on which the application can be executed directly in the web browser with the help of a plugin or downloaded and run as a native application. The user navigates in the virtual environment containing a three-dimensional replica of one of the laboratories of the Polytechnic School N.U.E.. The tests consisted of running the model and laboratory simulations. The results obtained from forms show that the use of virtual reality is valid, accepted and helps understanding the context of the simulations.*

Keywords: *Virtual Reality, Simulation, Computer Graphics, Education, Learning.*

I. INTRODUCTION

New information and communication technologies are emerging with the modern times, one of them is the Virtual Reality, which is widely used in areas of research, simulation, among others that deal with the use of computers for displaying information and give users new ways to make the most of it. Using this advantage, Virtual Reality is gaining ground in education, getting students to interact and even manipulate information, having rich teaching and enabling the understanding of any area with ease, even the most technical.

1.1 Problematic

Most universities and vocational training centers in the developing countries do not have equipment necessary for the education of future professionals, whichwith luck will have few opportunities to see and operate cutting-edge equipment in the workplace. One option would be to get donations and assemble laboratories to house the equipment, which would generate infrastructure and security costs, plus the possibility that they may suffer some damage. Another option would be to mount a "virtual laboratory", which could simulate many types of laboratories according to the needs, all in one location, with the assurance that if equipment is damaged in the virtual laboratory, can be replaced or fixed in the moment of the event, requiring only restarting that specific simulation.

A divergence of this kind of laboratory would use the Internet as a means of dissemination of the class, since having a location for simulation, you are tied to schedules, leading the student to have to wait when is available for use outside school hours.

The implementation of the system using Internet solve this problem, being able to even have classes in homes, students attend the simulation with the "virtual" presence of the teacher, and if they have questions outside of class time, could access it to better investigate , without having to wait for use.

With the creation of these simulation and studies centers, teaching of abstract matters would be benefit, since the manipulation of parameters could be perceived in a better way, changes involving them and their importance in the studied model. Both students and teachers have at their disposal a powerful tool in education, particularly in vocational subjects in technical field.

1.2 Virtual Reality

Defining Virtual Reality (VR, or simply VR Virtual Reality English), is difficult. There are probably as many definitions as there are researchers, as its recent and rapid evolution has not allowed a clear definition. Thus, it not is surprising that the virtual reality turns out to be relative to different people and in different situations.Some definitions to follow:

- **Virtual reality** is the experience of telepresence, where telepresence is the sense of presence using a means of communication.
- **Virtual reality** is a way by which human visualize, manipulate and interact with computers and extremely complex data.
- **Virtual reality** is three-dimensional interactive environments and simulations that reproduce real situations.
- **Virtual reality** is a highly interactive environment where users participate with the use of a computer in a virtually real world. The user is immersed so completely that this reality, artificial origin, three-dimensional computer simulation, that appears to be real.
- **Virtual reality** is an interactive three-dimensional computer simulation in which the user feels inserted into an artificial environment, and they perceived as real incentives based on sensory organs [1].

That is why the term "Virtual Reality" is usually associated with almost everything that has to do with three-dimensional images generated by computer and the user interaction with the graphical environment. This implies the existence of a complex electronic system to project 3D visual space and to send and receive signals with information about the user's actions, whom, with a system of this type, you can feel like you are immersed in a "virtual world".

The aim of Virtual Reality is to create an experience that makes the user feel immersed in a seemingly actual virtual world; to do this; he uses 3D graphics and sound that surrounds the scenes shown. It uses virtual reality view of an observer, the user, who moves into the virtual world using suitable devices, such as glasses or electronic gloves.

Virtual Reality exploits every image reproduction techniques and extends them, using them in the environment in which the user can examine, manipulate and interact with the exhibits. A virtual world is a mathematical model that describes a "three-dimensional space" within this "space" are contained objects that can represent anything from a simple geometric entity, such as a cube or a sphere, to a complex shape, such as it can be an architectural development, a new physical state of matter or the model of a genetic structure. It is ultimately a step beyond what would be the interactive, dynamic and real-time computer simulation [2].

II. VIRTUAL REALITY IN EDUCATION

The techniques of virtual reality (multisensory digital simulation) appear in the eyes of many experts as the definitive means of computer input in the processes of education and training. In this sense, education is one of the most promising areas of social use for the dissemination of this emerging medium of communication and digital simulation, which can be considered a perfected form of multimedia.

Interactive multi-sensory techniques, such as virtual reality, offer extraordinary possibilities in this regard. In fact virtual reality, coupled with advanced telecommunications network, allows to imagine a teaching environment in which it is possible to experience the presence of the teacher and other fellow students and exchange opinions and materials with them as if we were together without none of the participants have to move from where it previously found at the beginning of the class. In this new context, the traditional role of the teacher changes, no longer a mere transmitter of knowledge more or less valid, to become the instructor about students learning with the help of technology, which is what provides interactive resources learning [3].

Techniques related to virtual reality are very suitable for training in all disciplines and trades requiring skill, because they facilitate the realization of practices in all situations (including, especially, those that may be hazardous in the physical world).

A basic architecture for the development of an almost unlimited variety of virtual labs developed. In them, scientists in many different disciplines are able to penetrate into previously unreachable horizons thanks to the possibility of being there: within a molecule, in the midst of a violent storm or in a distant galaxy [4].

Several applications use virtual reality as a tool. Within the field of education, they are from virtual labs to virtual classrooms for behavioral studies. Here are two projects using virtual reality in some way or another are mentioned.

2.1 AULA Nesplora

AULA is an assessment test that uses virtual reality to help diagnose the disorder Attention Deficit / Hyperactivity Disorder (ADHD) [5].

The AULA system analyzes the behavior of the child in a virtual school class. The test is initially perceived as a game, where you must perform a different task while typical distractions of a classroom are presented.

2.2 Labster. Virtual Biological Laboratory

Labster [6] is an international company dedicated to developing online tools for teaching science globally. Its main product is an easily scalable platform for online teaching of life sciences, which has been shown to significantly increase learning over traditional methods as well as substantially reduce costs [6].

The Labster platform is a 3D virtual learning environment based on a Virtual Laboratory. It includes 3D animations molecules, questionnaires and support theory that invites the student to an immersive multimedia experience.

III. METHODOLOGY

3.1 Architecture

This work is proposed, the development and implementation of an application that uses virtual reality technology as a support tool in teaching using a web interface. To achieve this objective a website with the following structure is created:

- **Main Page:** Contains a welcome and brief introduction about the page. Moreover they are available the download version of the application for different operating systems (Windows, Linux and Mac) the link to the application and a list of contact.
- **Application:** A page where the application of virtual reality lies with instructions to use it.
- **Simulation forms:** Contains questions about the simulations and the application itself. Used to collect data from the usability, performance and compliance objectives.
- **SQLite database:** Stores data entered into forms for further processing.

In order to provide portability, the application has a run mode online (online), which uses a supported Web browser with the Unity WebPlayer plugin. Both application forms run on the user's Web browser an internet connection being necessary (see Fig. 1).

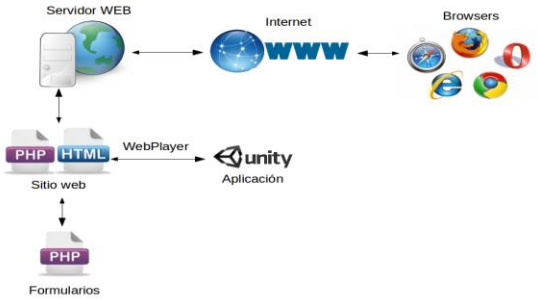

Figure 1. Online Architecture

It also has an offline mode (offline), in which you need to download the application from the website, by operating system and architecture. Once downloaded and unzipped, it runs as a native application on the operating system, using Internet only for forms (see Fig. 2).

The application development, started with 3D modeling of the laboratory building based on photos of itself using Blender 3D, once the modeling process is completed, it began the texturing of the model with photos taken as a reference. The photos were treatment and adjusted to extract textures and add them to the model. The texturing task and adjustment was made with GIMP software. Finally, textured model was imported into the Unity 3D application for coding events, create executables and Web version of the proposal, using the programming language C#.

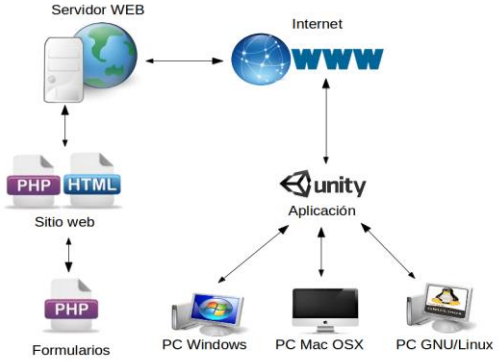

Figure 2. Offline Architecture

3.2 Population

The population established close professional authors and students from the Polytechnic School – National University of the East - Paraguay first grade courses Systems Engineering, totaling 80 participants. Of this group, 20 were professionals and 60 students.

IV. TESTS AND RESULTS

4.1 Tests

The application went through a stage of testing to determine the efficiency and accuracy of the data shown by the simulations. Manually problems arose, they experienced varying the parameters according to the problems and the results are verified, having algorithm settings to their tN.U.E.. Tests were performed for Windows and GNU-Linux, both 64-bit, as they lacked the equipment for use architectures. Once this stage testing the public began.

The website address, www.vuob.info/simvr spread through social networks, email, where the use of the application was entirely made by the user, without any assistance in addition to the existing instructions in the Web page.

Besides disseminating professionals, tests were conducted on the campus of the Polytechnic School - N.U.E., one of the computer labs modeling land with groups of students from the Engineering Systems with the help of Professor of matter Physics. First, demonstration and use of the application proceeded, which was connected to the website from internet, showing the use of the same with a real connection. Then the students used the application running simulators prepared in the same, with the support of the teacher and authors in case of doubt. Finally, via web forms for later analysis they were filled.

The teacher and students showed great interest in incorporating the application in teaching methodology.

4.2 Results

The results obtained with the application are presented. They were extracted from the database and represent the values of the latter form with respect to application. Each of the issues under study is detailed.

*4.2.1 Degree of Realism***:** The model used in the application is a representation of the laboratory building of the Polytechnic School - N.U.E., being of great importance its resemblance to the actual building, as this aspect is one of the pillars of virtual reality. To do textures from photos were used. According to the results, the impact was positive, as in Fig. 3 shows that 47.5% of participants responded with the highest note of the evaluation.

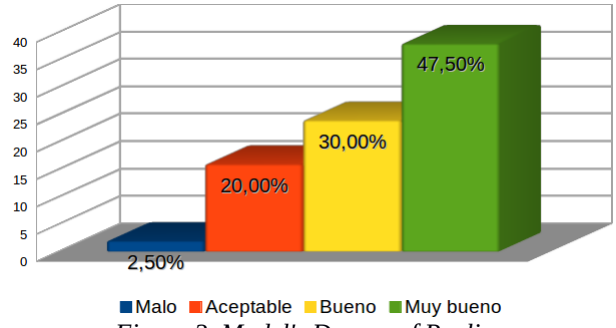

Figure 3. Model's Degree of Realism

*4.2.2 Receipt of Virtual Reality technology:*The responsiveness of the user was studied with respect to applications using virtual reality. As shown in Fig. 4, 95% of the respondents said that they favor the use of this technology in applications.

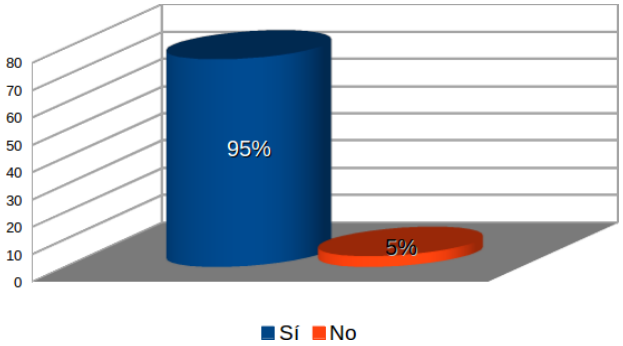

Figure 4. Receipt of Virtual Reality

*4.2.3 Learning using Virtual Reality:*The results on whether the virtual reality technology helped to some extent to the user better understand the content presented in the simulations are shown below. As shown, 90% of respondents say that this technology provided some help in understanding the content (see Fig. 5).

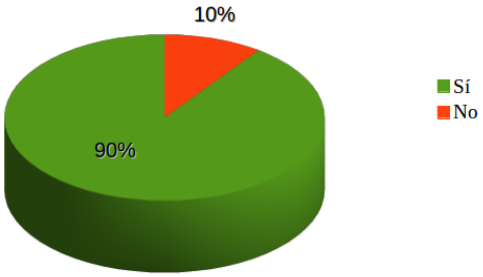

Figure 5. Learning using Virtual Reality

*4.2.4 User Experience with the Application:*Among the features of virtual reality is, the similarity of the movements people make in a virtual environment compared to those made in real life, facilitating their adaptation and immersion. Fig. 6 shows that the application was well received and had more positive than negative with respect to its usability.

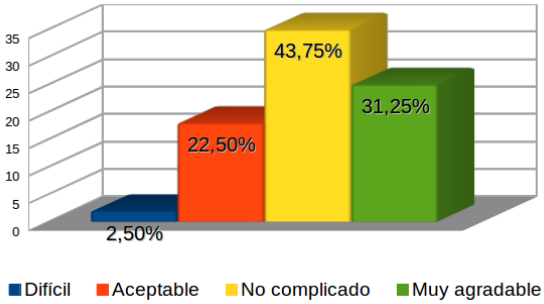

Figure 6. User Experience

*4.2.5 Response Speed Enforcement:*For the virtual reality experience to be effective, it must respond to real-time user actions. Below it is shown in Fig. 7 the response provided by the application as perceived by the user. It is noted, which is in line with expectations, as a normal or quick response provides better immersion in the virtual model.

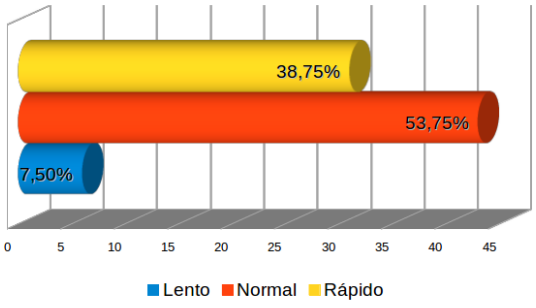

Figure 7.Speed application response

*4.2.6 Portability:*A study mode, the user is asked about his operating system, to demonstrate the application portability. As can be seen in Fig. 8, the majority of users use Windows (88.75 %), including its variants: Windows XP, Windows Vista, Windows 7, and Windows 8; It is one of the most used systems globally. But it's not the only one, a small but significant percentage of users with GNU / Linux operating system represented by 10 \% of the total and another group which is the 1.25 \% who used the Mac OSX operating system is observed, which demonstrates the application portability.

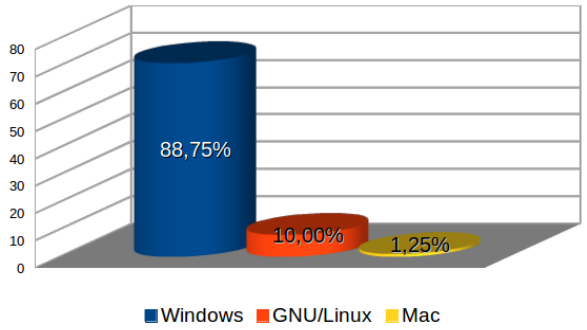

Figure 8. Application's Portability

V. CONCLUSIONS AND FUTURE WORK.

The application development performed in this work succeed to meet this objective, which was to develop and implement a system that allows a user to interact with virtual scenarios in a learning environment.

5.1 Brief review of work

A multiplatform application, both web and desktop for Windows, GNU / Linux and Mac OSX operating systems, was developed, allowing people to interact in virtual scenarios that serve as tool in learning different subjects.

A 3D model of the laboratory building of the Polytechnic School was created, using Blender application. For physical appearance, pictures were taken then treated with the Gimp software. The model was exported to Unity with two simulations of Physics' phenomena, the oblique shot and uniform motion were created. The application was exported to several platforms by the Unity software.

In order to show the feasibility of the proposal, several tests with students of the institution and outside it were made. In the same presents very satisfactory results on the use of virtual reality technology in conjunction with teaching.

5.2 Major Achievements

This work demonstrates the use of virtual reality in the learning environment. Considering the tests, the main achievements were achieved:

- Using virtual reality technology in a web and platform environment.
- Representation with a high degree of fidelity of the laboratory building of the Polytechnic School U.N.E.
- Running simulations of physical phenomena and positive feedback of results by students.
- Provide a support tool in the teaching-learning process.

5.3 Future Work

In view of the possibilities with the use of virtual reality, open to research the following:

- Development and implementation of a multi-user module, enabling users to use avatars thereby enhancing virtual experience.
- Application development for mobile platforms (Android, iOS, Windows Phone 8.1), extending architectures executing it.
- A comparison of the level of learning using the traditional method and using the application virtual reality.

REFERENCES

[1] I. SantelicesMalfanti, J.C. Parra Márquez, R. García Alvarado, "*Introducción práctica a la realidad virtual*". Eds. Universidad del Bío-Bío (2001)
[2] J. Martínez, J.R. Hilera, S. Otón. "*Aplicación de la Realidad Virtual en la enseñanza a través de Internet*". http://pendientedemigracion.ucm.es/info/multidoc/multidoc/revista/num8/hilera-oton.html
[3] D. Levis. "*Realidad Virtual y educación*". http://www.diegolevis.com.ar/secciones/Articulos/master_eduvirtual.pdf
[4] Realidad Virtual como método de entrenamiento. "*Realidad Virtual*", http://entrenamientovr.wordpress.com/realidad-virtual/
[5] AULA. "*AULA*", http://www.aulanesplora.com/
[6] Labster. "*Virtual Lab for Teaching Life Science*".http://www.labster.com

American Journal of Engineering Research (AJER) 2016
American Journal of Engineering Research (AJER)
e-ISSN: 2320-0847 p-ISSN : 2320-0936
Volume-5, Issue-2, pp-157-165
www.ajer.org
Research Paper Open Access

Thermodynamics of adsorption/desorption of cellulases NS 50013 on /from Avicel PH 101 and Protobind 1000

Khurram Shahzad Baig
Department of Chemical Engineering, Ryerson University, Toronto, ON M5B 2K3

Abstract: *Insight from thermodynamic parameters of enthalpy (ΔH), entropy (ΔS) and Gibbs free energy (ΔG) was used to predict conditions for desorption of cellulases from wheat straw. The analogues of the cellulose and lignin components of wheat straw used were Avicel PH 101 and Protobind 1000, respectively. The ΔH_a for adsorption on Avicelat pH 5 was -16.10kJmol^{-1}, ΔS_a was -50.10 Jmol^{-1}K^{-1} which indicated an increase in order due to adsorption and ΔG_a was negative only from 298K to 323K. Results of adsorption on Protobind 1000 were pretty much the inverse over the same range of temperature, proving the great affinity of cellulases for lignin. Over 298K to 333K, desorption from Avicel resulted in a ΔH_dincrease from 17.50 to 26.20 kJmol^{-1}, and a ΔS_dincrease from 46.89 to 75.65Jmol^{-1}K^{-1}when pH increased from 6 to 9indicating an enthalpy-driven, non-spontaneous desorption. For Protobind, the positive ΔH_d (9.65 to 6.90 kJmol^{-1}) with small positive ΔS_d (21.70 to 9.03 Jmol^{-1}K^{-1}) indicated that disorder was less than that of Avicel. For both the substrates ΔG_d decreased with rise in temperature in given temperature range. The minimum $\Delta G_d$of Avicel than that of Protobind proved that it was more difficult to desorb cellulases from Protobind.For bioethanol producing industries, using lignocellulosic material (e.g., wheat straw) where cellulose is embedded in lignin, removal of lignin is recommend along with adsorption/hydrolysis to be conducted at 323 K and desorption from used material at 333 K and pH 9.*

Keywords: *Adsorption, Avicel PH 101, Cellulases, Desorption, Protobind 1000, Thermodynamics*

I. Introduction

Lignocellulosic materials are used as a source of cellulose for production of bioethanol. These materials consist of lignin, cellulose and hemicellulose, which are interweaved in the cell walls. Cellulose and hemicellulose in the lignocellulosic materials release glucose and xylose that can in turn be fermented to bioethanol. Cost-effective liberation of fermentable sugars from lignocellulosic resources is still the largest obstacle to large-scale commercialization of bioethanol Process[1,2]. The main problem associated with the process is presence of lignin whichpreferentially adsorb cellulases instead of celluloseand resist to desorb cellulases(reusability), hence, increase product bioethanol cost [3,5].

The solution to problem is to remove the lignin and expose more cellulose and hemicellulose from lignocellulosic materials. However, due to the cost of some of these pretreatments, health and/or environmental concerns, the potential for economical bioethanol is not promising. For example, when using steam explosion, high temperature and pressure resistant fabrication material for the reactor is required [6-8]. Ammonia fiber expansion (AFEX) needs pressure resistant and corrosion resistant fabrication material for reactors and it may trigger asthma in workers [9]. Similarly, cellulose solvent(concentrated phosphoric acid) and organic solvent-based lignocellulose fractionation (COSLIF), as well as ionic liquids or organosolv processesrequire expensive corrosion resistant fabrication materials and may harm workers [10-12].In our lab we have successfully removed 90 % of lignin by a novel technique which is a sequential use of water and ozone [13]. All reactions occurred at normal temperature and pressure, no expensive material would be required to construct a reactor.In another technique new insoluble substrate was simply added so that cellulases could readsorb on fresh added substrate [14-15]. However a buildup of lignin rich residues would ultimately increase capability of cellulases to adsorb on the substrate reduce the capability of cellulases to desorb from the substrate because of strong binding on lignin. Hence, removal of lignin reduced cost due to loss of cellulases by nonproductive adsorption.

Some methodologies were also evaluatedto try to decreasethe costs of using cellulases in bioethanol production: (i) decreasing cellulases loading by using low lignin or no lignin containing substrates [16,17],(ii) recycling costly cellulases[14],(iii) increasing cellulases performance (activity)by genetic engineering [18], (iv) increasingdesorption with the addition of an agents such as alkaline media [19,20], Tween [21], urea [3], glycerol [22], and Triton X-100 [23] added as diluent in desorption stage.

A change in pH and /or temperature can be utilized to facilitate adsorption/desorption. Otter *et al*. (1984) showeda recovery of up to 65% with 45% of cellulases activity at pH 10 and reported that theenzymes were completely inactive at pH 10.5. The high cost and/or high dosage of desorbent needed made this approach impractical on a large scale.Although some work has been done on the effect of pH oncellulases adsorption [24-26], less attention was given to see the temperature dependence of the adsorption process. The studies to determine the effect of temperature have shown two aspects: i) small data was used to derive results. Some of the researches reported the results of 2 or 3 selected temperature[27-29] which representedonly that narrow area of study but not a general principle. ii) controversial results for the adsorption process were reported. It was stated that cellulases adsorption on lignocellulose was an exothermic, enthalpy-controlled reaction and the amount of cellulases adsorption decreased as the temperature increased [27,30, 31]. On the contrary, Hoshino *et al*. (1992) and Creagh*et al*. (1996)demonstrated that cellulases adsorption on cellulose was an endothermic and entropy-driven reaction [32, 33]. The temperature dependency and thermodynamics of desorption, however, was rarely reported in the literature.Thermodynamics study could indicate feasibility of the adsorption and desorption reactions from the obtained values of the thermodynamic parameters. The van't Hoff equation canbe adapted to represent the adsorption and desorption processes of cellulases to /from adsorbents like Avicel PH 101 and Protobind 1000. It relates the main thermodynamics parameters such as enthalpy (ΔH) and entropy (ΔS) to the equilibrium distribution coefficient (K) of the adsorbed or desorbed species between an aqueous solution and an adsorbent, as shown in Equation 1:

$$\ln K = -\frac{\Delta H}{RT} + \frac{\Delta S}{R} \quad \ldots \quad 1$$

R is the universal gas constant (8.314 $JK^{-1}mol^{-1}$), and T is the absolute temperature.The other thermodynamic parameter Gibbs free energy (ΔG)is given by Equation 2:

$$\Delta G = \Delta H - T\Delta S \quad \ldots \quad 2$$

The objectives of this project were to settle the controversy on temperature dependency of adsorption of cellulases onto lignocellulosic components (cellulose and lignin)and to develop a temperature dependence for desorption. Adsorption, a prerequisite for desorption was conducted at pH 5 only as is currently being done in the fuel ethanol industry [34] because it gave high adsorption of enzymes in the process. Desorption studies were done at pH 6, 7, 8, and9, over the same temperature range(298K to 343K). To the best of my knowledge, the thermodynamic parameters for enzymatic desorption are being reported first time in this study.

II. Material and Methods

2.1 Materials

Avicel PH 101 (analytical grade, 50µm, 100% solids) was purchased from Sigma Aldrich, Canada. Avicel PH 101 was a microcrystallinecellulose,and a celluloseanalog for wheat straw. Protobind 1000 (analytical grade, 98% solids, 2% ash) a lignin analog of wheat straw, was kindly donated by the GreenValueEnterprises LLC,USA. Protobind 1000 was the. Cellulases NS 50013 was a gift from Novozymes, Denmark. It was composed of approximately, EGI 10%,EGII 10%, CBH I 60%, CBHII 15% and β - glucosidase 2%) [35], with an activity of 53 FPU/ml.

2.2 Adsorption of cellulases

5 ml of cellulases solution (citrate buffer solution at pH 5)was added to 100 mg of the cellulose or lignin substrate. Mixing in 10 ml glass tubes was done in an incubator shaker at 100 rpm.After adsorption each tube was centrifuged at 4000 rpm for 4 minutes and the supernatant weredecanted off.The concentration of free unbound cellulases in the supernatant [E_{fa}] was measured by modified Lowry method using Biochrom Libra S50 UV/Vis Spectrophotometer. The concentration of cellulase that remained adsorbed onto a solid substrate was determined as the difference between the total concentration of cellulase initially applied and the concentration of free cellulase in the decanted supernatantsolution. Triplicates were used for each of the 12 contact times and 5 temperatures (298K-343K). The solid residues (thick slurry) remaining after the centrifugation step was immediately used for desorption study.

2.3 Desorption of cellulases

4.9 ml of distilled water with to a pH value varying from 6 to 9 was added to thick slurry from the centrifugation. The reaction mixture was then placed in an incubator for 20 minute temperature varying from 25 to 70^{o}C. Then centrifuged for 4 minutes at 4000 rpm. The concentration of free unbound cellulases here called desorbed cellulases and measured in the decanted supernatant, as before.

III. Results and Discussion

Fig. 1 shows temporal plotsof unbound(free) cellulases present in the supernatant after contact with Avicel PH 101at pH5and temperatures of 298, 313, 323, 333 and 343K.

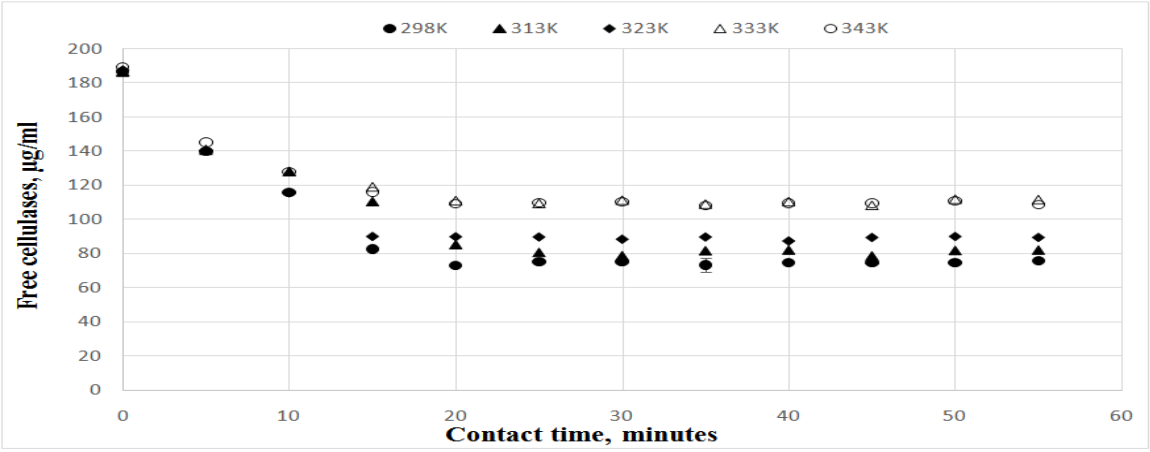

Figure 1: Free cellulases on after contact with Avicel PH 101 at various temperatures at pH 5 also shown with maximum error bar at 95 % probability

Within the first 10 minutes about 60 percent of the initial cellulases were adsorbed on Avicel.Equilibrium was achieved after about 20 minutes for all temperatures. Consequently, a contact time of 30 minutes was chosen for all adsorption studies used for desorption purposes. Since almost one and half times more cellulases were adsorbed at 298K and 313K than at 333K and 343K, 298K was chosen to maximize adsorption prior to desorption studies. When cellulases were placed in contact with Protobind similar trends of adsorption to those of Avicel were obtained. However, equilibrium was reached about after 40 minutes. Consequently a contact time of 45 minutes was chosen for adsorption from lignin. Long adsorption time of cellulases experienced for lignins versus cellulose can be explained by considering:

i) the functional groups taking part in this interaction. Cellulose contains a large number of hydroxyl groups [36] to interact with cellulases. The functional groups of lignin are, carboxylic, carbonyl, aliphatic hydroxyl, and phenolic hydroxyl groups [37-40]. Therefore, cellulases adsorption ability of lignin involved more complex factors other than just the interaction with the hydroxyl groups. More functional groups in lignin offers more attraction to cellulases. When a number of cellulases approaches to lignin molecule, electrostatic repulsion came into play between the cellulases themselves and they need time to rearrange [41, 42].

ii) a repulsion between positively charged amino acids from cellulases and carbonyl from lignin may allow cellulases to rearrange in order to adsorb on lignin and cause delayed adsorption.

iii) Since more cellulases adsorb on lignin than on Avicel, hence it took longer time

Plotting the equilibrium adsorption results for both solid substrates as a van't Hoff relation (Equation 1) linearity of adsorption is observed over the temperature range of 298K ($1/T = 3.35 \times 10^{-3}\ K^{-1}$)to 343K ($1/T = 2.92 \times 10^{-3}\ K^{-1}$) (Fig. 2). The left side of the plot represents higher temperature.

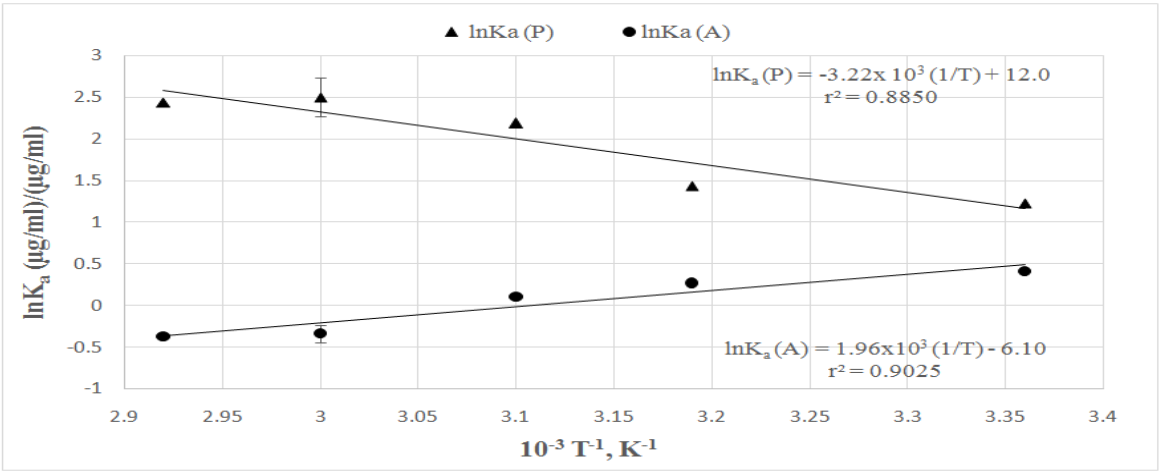

Fig.2: Van't Hoff plots for adsorption on Avicel PH 101 and on Protobind 1000 at pH 5 with maximum error bar at 95% probability

For Avicel, $\ln K_a$ decreased with an increase in temperature, there was a small decrease (10-12 %) in adsorption at 323 K compared to 298 K, and at 343 K the adsorption decreased by 33 %, as was expected from published literature [40, 43-45]. Other research groups reported that some cellulases started denaturing around 323K [19,43,45, 46].The Novozymes cellulases used in this study surpassed this limit by 10 K. On the other hand, Baker's group [47] proved that individual cellulases maintain their activities up to 333K. The observed $\ln K_a$ at lower temperature may be associated to a reduced translational energy androtationalenergy (vibrational energyis negligible) of cellulases and celluloseallowingopposite charges on the cellulose-bindingdomain (CBD) of cellulases and on the Avicelto align themselves. The van't Hoff model gave $\ln K_a = 1.96x10^3$ (1/T) - 6.10. The change in enthalpy (ΔH_a) value obtained from the slope of the equation was found to be-16.1 $kJmol^{-1}$, whichwas expected from the results of cellobiohydrolases I (CBH I) on Avicel [44] who reported -18.2$kJmol^{-1}$ at 288 K to 303 K. The negative ΔH_a of exothermic adsorption means that non-covalent interactions (such as electrostatic, van der Waals, hydrogen bonding, etc.are significant [48-50] between cellulases and Avicel. The ΔS_a value obtained from intercept of the plot was -50 $Jmol^{-1}K^{-1}$. The negative entropy indicated that the mobility of the adsorbed cellulases on the surface of Avicel was restricted. Negative values of ΔS_a were also observed foradsorbed enzymes during other studies [31, 51-52] and for ionic adsorption [53-55]. Another reason for negative ΔS_a value could be unfolding (conformational changes) of cellulases. The unfolding of endoglucanases from *Aspergillus niger* and α-amylase from *Bacillus licheniformis*, DNA ligase and xylanasewere reported where the ΔS value was negative [56-58]. Violet and Meunier (1989) presented the formation of an intermediate compound (X) on the pathway between the natural (N) and the denatured (D) enzyme as (i.e. $N \rightarrow X \rightarrow D$). They noticed that the intermediate state (adsorption of enzymes on substrate) is more ordered structure than the starting state i.e. ΔS_a is negative. According to the second law of thermodynamics, any spontaneous process the overall $\Delta S \geq 0$. Therefore, a negative change in entropy does not contradict the second law, because the adsorption of cellulases on Avicel have a sufficiently large negative ΔH_a (over 320 times of that ofΔS_a) results in a sufficiently large increase in entropy so that the overall change in entropy is positive.

The Gibbs free energy (ΔG_a) value increased from -1170$Jmol^{-1}$to 1080$Jmol^{-1}$ as temperature increased from 298K to 343K.A negative ΔG_a, expected for spontaneous adsorption occurred only from 298 K to 323K.Consequently, only this temperature range is recommended for adsorption of cellulases on Avicel PH 101.For bioethanol producing industries, using wheat straw where cellulose is a component, adsorption can be performedon delignified wheat straw between the temperature range of 298 K to 323 K. Since fermentations are conducted in most of the industries around 313K therefore, adsorption can also be performed at the same temperature for the ease of process.

In the case of Protobind,the experimental data points plotted between 298Kand 343K showed $\ln K_a$ increased with an increase in temperature.The trend line equation (regression equation)was $\ln K_a = -3.22x10^3$ (1/T) + 12.0. Therefore,ΔH_awas26$kJmol^{-1}$, which indicates an endothermic reaction.Theamount of cellulases adsorbed increased from 75% to 94% of the initial cellulases concentration whentemperature increased from 298K to 333K. The ΔS_a for the adsorption of cellulases on Protobind 1000 was positive (100 $jmol^{-1}K^{-1}$) which means that disorder of the system was increased [59].In accordance with the second law of thermodynamics since $\Delta S_a > 0$, the adsorption of cellulases on lignin appears to be an irreversible process.The ΔG_a decreased from -2.90$x10^3$ $Jmol^{-1}$ to -7.40$x10^3$ $Jmol^{-1}$ as temperature increased from 298K to 343K, which becomes the suitable adsorption temperaturerange for Protobind 1000.By choosing 298 K, 20% less cellulase would be adsorb on ligneous component than at 343 K and 30% more cellulases will adsorb [delignified wheat starw].Therefore, a temperature closer to 298 K is recommended for adsorptionpart of bioethanol production process. Reuse of adsorbed enzymes to save cost of enzymatic hydrolysis is important, therefore, entropy and enthalpy of desorbed cellulases from was studied next.

Desorption from Avicel PH 101and from Protobind 1000

Van't Hoff plots were constructed for the desorption of cellulases from Avicel over a temperature range of 298K to 343 K and a pH range of 6 to 9 (Fig. 3) for desorption time 20 minutes (data not shown). The curves were drawn up to $T \leq 333K$ because there appears to be denaturing of cellulases occurring after 333 K [60-61]. The denaturing was similarto what happened for adsorption but was much more pronounced.

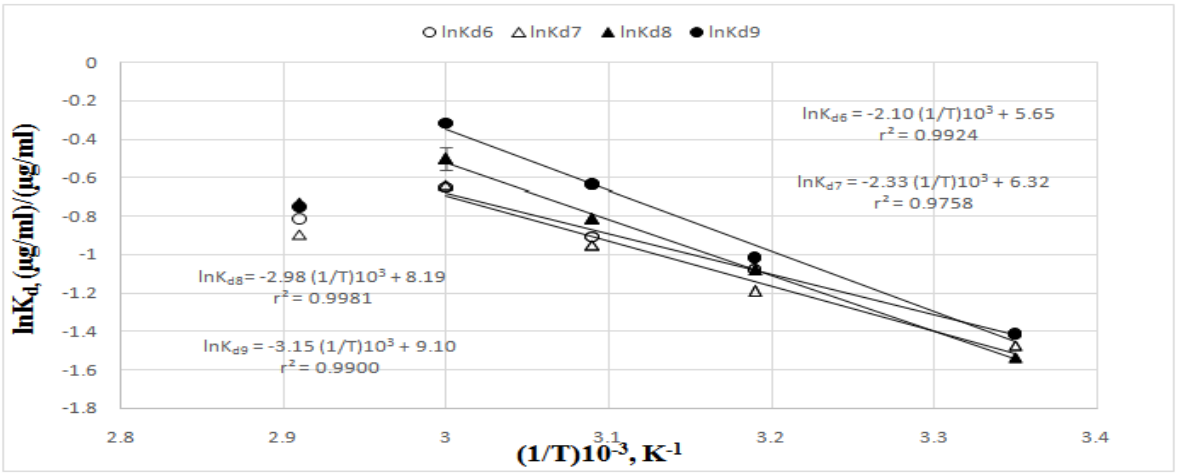

Desorptionregression equations are given below:

$$lnK_{d6} = (-2.10)\frac{1}{T}10^3 + 5.65 \quad \ldots \quad 5$$

$$lnK_{d7} = (-2.33)\frac{1}{T}10^3 + 6.32 \quad \ldots \quad 6$$

$$lnK_{d8} = (-2.98)\frac{1}{T}10^3 + 8.19 \quad \ldots \quad 7$$

$$lnK_{d9} = (-3.15)\frac{1}{T}10^3 + 9.10 \quad \ldots \quad 8$$

Since all slopes of the van't Hoff equationswere negative, all ΔH_d values were positive.There was a slight increasing trend in $\Delta H_d$from pH 6 to pH 9:17.5, 19.4, 24.1, 26.2kJmol^{-1}, respectively.This meant that heat energywas gained by the cellulasesdesorption system,which resulted in the decrease invander Waals interactions and hydrogen bonding between cellulases and cellulose. The ΔH_d values obtained from the last two point 333K to 343K for all pH values were negative as -15.8, -24.6, -21.5, and -41.5kJmol^{-1} respectively. The negative signs of enthalpy usually mean that the heat is being released by the occurring reaction.The changes in entropy, ΔS_d, for all pH values were (46 to 75 Jmol^{-1}K^{-1}) positive. [Entropy of adsorption was ΔS_a was -50]This indicated decreased randomness which favored desorption. At 333K to 343K the ΔS_d was -52, -79, -68, and -127 Jmol^{-1}K^{-1}for pH6 to pH 9 which indicatedfurther decreased desorption. The values of ΔG_d obtained from Equation 2are given in Table 1.

Table 1: ΔG_d obtained for desorption of cellulases from Avicel PH 101 for pH 6 to pH 9 at temperatures 298K to 343K

T K	ΔG_{d6} Jmol^{-1}K^{-1}	ΔG_{d7} Jmol^{-1}K^{-1}	ΔG_{d8} Jmol^{-1}K^{-1}	ΔG_{d9} Jmol^{-1}K^{-1}
298	3.54 x10^3	3.77 x10^3	3.80 x10^3	3.60 x10^3
313	2.84 x10^3	2.98 x10^3	2.80 x10^3	2.48 x10^3
323	2.37 x10^3	2.12 x10^3	2.10 x10^3	1.72 x10^3
333	1.90 x10^3	1.94 x10^3	1.45 x10^3	0.970 x10^3
343	2.31 x10^3	2.52 x10^3	2.05 x10^3	2.10 x10^3

ΔG_d values were all positive and decreased with increase in temperature. Gibbs free energy (ΔG_d) decreased with the increase in temperature which means at pH 9 and 333K the cellulases showed minimum affinity (adsorption interest) for the substrate. The maximum desorption of cellulases was achieved at almost 333K for all pH values. Theoretically,the maximum desorption achieved should be at 343K since high temperature support desorption. The decrease in desorption while moving from 333K to 343K can be attributed to the configurational changes of cellulases which render the cellulases to desorb. The ΔG_d values calculated for temperature 343K were large and positive as compare to the values at 333K represented a less desorption the temperature(last row of Table 1).The positive and large ΔH_d, smallΔS_d value, with positive ΔG_d values indicated that desorption process was favorable for pH ranging from 6 to 9 and the temperature ranging from 298K to 333K only. Beyond T ≥333K, ΔH_d was negative ΔS_d was negative and $\Delta G_d$was very large which resulted in decrease in desorption due to denaturing of cellulases.

Desorption of cellulases NS 500013 from Protobind, in similar conditions as that for, Avicel is shown in Fig. 4. The maximum error barof all individualized experiments is at pH8 and 313K (3.19 x 10^{-3} K^{-1}). Again data for T ≥ 333K showed incompatibility with rest of the data because of very low lnK_d values observed (low desorption from the Protobind surface).

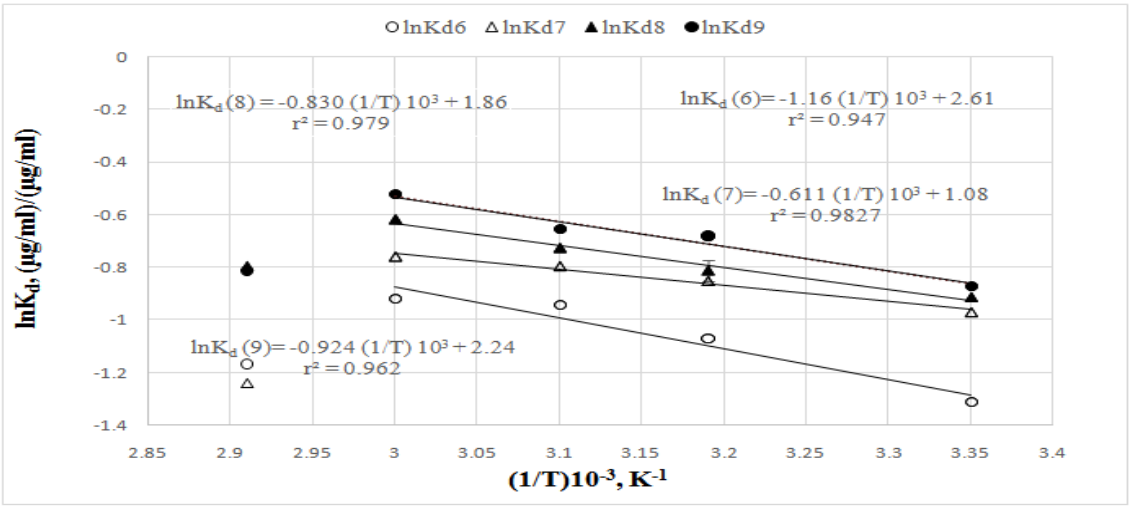

Figure 4: Desorption of Cellulases NS 50013 from Protobind 1000at various pH and temperatures with maximum error bar at 95% probability

The lnK_d increased with an increase in temperature from 298K to 333K and the corresponding regression equations are given below:

$$lnK_{d6} = (-1.16)\frac{1}{T}10^3 + 2.60 \quad \ldots \quad 9$$

$$lnK_{d7} = (-0.610)\frac{1}{T}10^3 + 1.00 \quad \ldots \quad 10$$

$$lnK_{d8} = (-0.830)\frac{1}{T}10^3 + 1.80 \quad \ldots \quad 11$$

$$lnK_{d9} = (-0.920)\frac{1}{T}10^3 + 2.20 \quad \ldots \quad 12$$

As with Avicel, all slopes for desorption from Protobind had negative values, although their values for Protobind were in the range of 0.610Kto 1.160K, 2-4 times less than Avicel at the respective pH values, leading to positiveΔH_dvalues of 9.60, 5.10, 6.90 and 7.70kJmol^{-1}respectively.The positive ΔH_d values indicated that the supplied heat enrgy was consumed in weakening the interactions between cellulases and Protobind. The large negative ΔH values were observed between 333K to 343K andwas attributed to a conformational change in enzymes.The small ΔS_d values of 21.70, 9.00, 15.40, and 18.60 Jmol^{-1}K^{-1} for all desorption from Protobind signify that all reactions are not entropy driven rather enthalpy-driven. This small ΔS_d in case of desorption could be the result of an indirect decrease in entropy due to the influence of water molecules in the vicinity of non-polar cellulases residues which are broken down at higher temperatures. The decrease in the entropy of desorption may be due to the decrease in the conformational flexibility of cellulases [62].The small ΔS_d implying that the cellulases-substrate complex has restricted flexibility (highly ordered), therefore less desorption.For a process that involves a decrease in entropy and a small change in enthalpy, a positive free energy change, ΔG, means that will not occur spontaneously [63]. ΔG_d values calculated for pH 6, 7, 8 and 9 over the range of temperature 298K to 333Kare presented in Table 2. They remainedpositive and almost the same throughout the range of temperature and pH

Table 2: ΔG_d obtained for desorption of cellulases from Protobind 1000 for pH 6 to pH 9 at temperatures 298K to 343 K

T K	pH 6 $Jmol^{-1}K^{-1}$	pH 7 $Jmol^{-1}K^{-1}$	pH 8 $Jmol^{-1}K^{-1}$	pH 9 $Jmol^{-1}K^{-1}$
298	3.18×10^3	2.38×10^3	2.30×10^3	2.14×10^3
313	2.86×10^3	2.25×10^3	2.08×10^3	1.86×10^3
323	2.64×10^3	2.16×10^3	1.93×10^3	1.67×10^3
333	2.40×10^3	2.07×10^3	1.78×10^3	1.48×10^3
343	3.29×10^3	3.47×10^3	2.24×10^3	2.28×10^3

ΔG_d values decreased from 2.40, 2.07, 1.78and 1.48$kJmol^{-1}K^{-1}$as pH increased from pH 6, 7, 8, and 9 at 333K and it also decreased with increase in temperature up to 333K. Minimum energy is required to desorb at pH 9 and 333K. ΔG_d was increased for all pH at 343K. The ΔG_d values calculated for temperature 343K were very large and positive as compare to the values at 333K represented a less desorption the temperature (last row of Table 2).Themaximum energyto desorb cellulases from Protobind was obtained at 343K for all pH values as given in the last row of Table 2.Desorption from the cellulases-substrate complexwas restricted due to unfolding of cellulases.

Positive ΔH_d and small ΔS_d were obtained from the plots for both Avicel and Protobind for desorption of cellulases over a range of temperature from 298 to 333K. Negative ΔH_d and small ΔS_d were obtained for both Avicel and Protobind at 343K. Similarly, ΔG_d decreased moving from pH 6 to pH 9, and further decreased increasingtemperature from 298K to 333K. ΔG_d was minimum at pH 9and 333K for both substrates. For lignocellulosic materials containing both cellulase and lignin desorption of cellulasescan be performed at pH 9 with 333K.

IV. Conclusion

Change in enthalpy for adsorption of cellulases on the surface of the Avicel was observed which decreased with the increase in temperature and indicated an exothermic reaction. A positive ΔH_a value for adsorption of cellulases on Protobind indicated an endothermic reaction. The ΔS_a value for Avicel was negative which means disorder of cellulases-cellulose system was decreased on adsorption. The contribution of entropy to the adsorption of cellulases on Protobind 1000 was opposite to that to the Avicel. Change in free energy of adsorption for Protobind was negative for all temperatures range while ΔG for Avicel change from negative to positive at 323K. It means that the 298K to 323K temperature ranges was spontaneous for adsorption on lignocellulosic materials. Lignocellulosic material may have a positive or negative change in enthalpy for adsorption of cellulases depending upon the composition of the substrate.

The positive ΔH_d for both Avicel and Protobind favored desorption. The positive ΔS_d for both Avicel and Protobind indicated that the increased randomness also favored desorption. A positive and minimum ΔG_d indicated that cellulases have less affinity for substrate at pH9 and 333K where cellulases showed maximum on desorption.

Since wheat straw is a combination of cellulose and lignin, the thermodynamic study offers a strategy for using wheat starw for ethanol production. The negative ΔH_a ,ΔS_a and ΔG_a indicated that maximum temperature for adsorption suitable is 298K to 323K. In depth study showed that maximum adsorption on Avicel was between temperatures 298K to 323K and maximum adsorption on Protobind was on temperature 333K to 343K. To avoid adsorption on lignin (in addition to optimum removal of lignin) low temperatures such as 298K to 323K should be used for adsorption because at these temperature thermodynamic conditions give less support for adsorption on lignin. For desorption of cellulases from wheat straw, the positive ΔH_d, ΔS_d and ΔG_d indicated favored desorption at pH 9 temperatures 323k and 333K.

V. Acknowledgement

Authors would like to express sincere thanks to Dr. Jairo Lora and GreenValueEnterprise LLC for supplying the sample of Protobind 1000 as a gift.

References

[1] L.R. Lynd, M. S. Laser, D. Bransby, B.E. Dale, B. Davison, R. Hamilton, M. Himmel, M. Keller, J.D. McMillan, J. Sheehan, and C.E. Wyman, How biotech can transform biofuels. *Nature Biotechnology 26*,2008, 169–172.

[2] X. Zhang, and P.Y. Zhang, One-step production of biocommodities from lignocellulosic biomass by recombinant cellulolytic Bacillus subtilis: Opportunities and challenges. *Engineering in Life Sciences 10*: 2010, 1-9

[3] M.V. Deshpande, K.E. Eriksson, Reutilization of enzymes for saccharification of lignocellulosic materials,*Enzyme and Microbial Technology 6*, 1984, 338–340.

[4] L.P. Ramos, C. Breuil, and J.N. Saddler, Comparison of steam pretreatment of eucalyptus, aspen, and spruce wood chips and their enzymatic hydrolysis. *Applied Biochemistry and Biotechnology 34*, 1992, 37–47.

[5] H. Palonen, M. Tenkanen, and M. Linder, Dynamic interaction of Trichoderma reesei cellobiohydrolases Cel6A and Cel7A and cellulose at equilibrium and during hydrolysis. *Applied Environmental and Microbiology 65*, 1999, 5229–5233.

[6] M. Heitz,E. Capek-Menard, P.G. Koeberle, J. Gagne, R.P. Chornet, J.D. Taylor, and E. Yu, Fractionation of Populustremuloides at the Pilot Plant Scale: Optimization of Steam Pretreatment Conditions using the STAKE II Technology,*Bioresour. Technol. 35(23)*, 1991

[7] F. Zimbardi, E. Ricci, and G. Braccio, Technoeconomic study on steam explosion application in biomass processing. *Applied Biochemistry Biotechnology, Spring 98-100*, 2002, 89-99.

[8] L.P. Ramos, The chemistry involved in the steam treatment of lignocellulosic materials. Quím. Nova 26(6), 2003.

[9] M.J. Taherzadeh, andK. Karimi, Enzyme based hydrolysis processes for ethanol from lignocellulosic materials: a review. Bioresources 2 (4), 2007, 707-738.

[10] J.S. Rollin, *Synthetic Enzymatic Pathway Conversion of Cellulosic Biomass to Hydrogen. Ph.D Dissertation*, Biological Systems Engineering, Virginia Polytechnic Institute and State University, Blacksburg, VA. USA.2013.

[11] W. Wang, *Nanotechnology applications for biomass pretreatment, functional material fabrication and surface modification. Ph.D. Dissertation*, Chemical Engineering. Michigan State University. USA.2012.

[12] L. Xio, Z. Sun, Z. Shi, F. Xu, and R. Sun, Impact of hot compressed water pre-treatment on the structural changes of woody biomass for bioethanol production. *Bioresources 6 (2)*, 2011, 1576-1598.

[13] K.S. Baig, J. Wu, G. Turcotte, and H.D. Doan, Novel ozonation technique to delignify wheat straw for biofuel production, *Energy and Environment Journal 26.3*, 2015, 303-318

[14] M. Tu, R.P. Chandra, and J.N. Saddler, Evaluating the distribution of cellulases and the recycling of free cellulases during the hydrolysis of lignocellulosic substrates. *Biotechnology Progress 23*, 2007, 398–406

[15] Y.P. Lu, B. Yang, D. Gregg, J.N. Saddler, and S.D. Mansfield, Cellulase adsorption and an evaluation of enzyme recycle during hydrolysis of steam-exploded softwood residues,*Applied Biochemistry and Biotechnology 98*, 2002, 641–654.

[16] R. Kumar, and C. E. Wyman, An improved method to directly estimate cellulase adsorption on biomass solids. *Enzyme Microbial Technology 42(5)*, 2008, 426-433.

[17] N. Sathitsuksanoh, Z. Zhu, N. Templeton, J. Rollin, S. Harvey, and Y-HP. Zhang, Saccharification of a potential bioenergy crop, Phragmites australis (common reed), by lignocellulose fractionation followed by enzymatic hydrolysis at decreased cellulase loadings,*Industrial and Engineering Chemistry Research 48(13)*, 2009, 6441-6447.

[18] E.G. Hibbert, and P.A. Dalby, Directed evolution strategies for improved enzymatic performance. *Microbial Cell Factories 4:29*, 2005

[19] D.E. Otter, P.A. Munro, and R. Geddes, Elution of Trichoderma reesei cellulase from cellulose by pH adjustment with sodium hydroxide. *Biotechnology Letters 6*, 1984, 369–374.

[20] A.C. Rodrigues, A.F. Leitao, S. Moreira, C. Felby, and M. Gama, Recycling of cellulases in lignocellulosic hydrolysates using alkaline elution. *Bioresource Technology 110*, 2012, 526–533.

[21] D., Seo, H. Fujita, and A. Sakoda, Effect of a non-ionic surfactant Tween 20, on adsorption/desorption of saccharification enzymes onto/from lignocelluloses and saccharification rate. *Adsorption 17*, 2011, 813-822.

[22] G. Beldman, M.F. Searle-van Leeuwen, F.M. Rombouts, and A.G.J. Voragen, The cellulases of Trichoderma viride. Purification, characterization and comparison of all detectable endoglucanases, exoglucanases and β-glucosidases, *European Journal of Biochemistry 146*, 1985, 301-308.

[23] Y. Bai, D. Lin, F. Wu, Z. Wang, and B. Xing, Adsorption of Triton X-series surfactants and its role in stabilizing multi-walled carbon nanotube suspensions, *Chemosphere 79*, 2010, 362–367.

[24] T. Reinikainen, O. Teleman, and T.T. Teer, Effects of pH and high ionic strength on the adsorption and activity of native and mutated cellobiohydrolyses I from *Trichoderma reesei*,*Protein 22*, 1995, 392-403.

[25] R. Du, R. Su, X. Li, X. Tantai, Z. Liu, J. Yang, W. Qi, and Z. He, Controlled adsorption of cellulase onto pretreated corncob by pH adjustment,*Cellulose 19*, 2012, 371–380.

[26] N. Weiss, J. Borjesson, L.S. Pedersen, and A. S. Meyer, Enzymatic lignocellulose hydrolysis: Improved cellulase productivity by insoluble solids recycling, Biotechnology *for Biofuels 6 (1)*, 2013, 5.

[27] J. Medve, J. Stahlberg, and F. Tjerneld, Adsorption and synergism of cellobiohydrolase I and II of Trichoderma reesei during hydrolysis of microcrystalline cellulose. *Biotechnology and Boengineering 44(9)*, 1994, 1064-1073.

[28] G. Radeva, I. Valchev, and S. Petrin, Study of the adsorption equilibrium in cellulase-pulp system. *Journal of the University of Chemical Technology and Metallurgy 46(2)*, 2011, 197-202.

[29] Z. Gan, T. Zhang, Y. Liu, and D. Wu, Temperature-triggered enzyme immobilization and release based on cross-linked gelatin nanoparticles. *PLoS ONE 7(10)*, 2012, e47154. doi:10.1371/journal.pone.0047154.

[30] D.W. Kim, and Y.G. Hong, Ionic strength effect on adsorption of cellobiohydrolases I and II on microcrystalline cellulose, *Biotechnology Letters 22*, 2000, 1337–1342.

[31] H. Ooshima, M. Sakata, and Y. Harano, Adsorption of cellulase from *Trichoderma viride* on cellulose. *Biotechnology and Bioengineering 25*, 1983, 3103–3114.

[32] E. Hoshino, E., T. Kanda, Y. Sasaki, and K. Nisizawa, Adsorption mode of exo-cellulases and endo-cellulases from Irpexlacteus (Polyporustulipiferae) on cellulose with different crystallinities. *Journal of Biochemistry 111*,1992, 600–605.

[33] A. L. Creagh, E. Ong, E. Jervis, D.G. Kilburn, and C.A. Haynes, Binding of the cellulose-binding domain of exoglucanaseCex from Cellulomonasfimi to insoluble microcrystalline cellulose is entropically driven,*Proceedings of the National Academy of Sciences. U.S.A. 93*, 1996, 12229–12234.

[34] P.W. Madson, and D. A. Monceaux, Fuel ethanol production. *KATZEN International Inc.* Cincinnati, OH, USA. 2003.

[35] L. Hilden, and G. Johansson, Recent developments on cellulases and carbohydrate-binding modules with cellulose affinity. *Biotechnology Letters 26*, 2004, 1683-1693.

[36] E. Sjostrom, Cellulose Derivative. Wood Chemistry: *Fundamentals and Applications*. 2nd Ed. Academic Press Inc., San Diego, California. 1993. ISBN-10:0-12-647481-8.

[37] A. Berlin, M. Balakshin, N.Gilkes, J. Kadla, V. Maximenko, S. Kubo, and J. Saddler, Inhibition of cellulase, xylanase and beta-glucosidase activities by softwood lignin preparations, *Journal of Biotechnology 125(2)*, 2006, 198-209.

[38] X. J. Pan, Role of functional groups in lignin inhibition of enzymatic hydrolysis of cellulose to glucose. *Journal of Biobased Materials and Bioenergy 2(1)*, 2008, 25-32.

[39] N. Pareek, T. Gillgren, and L. J. Jonsson, Adsorption of proteins involved in hydrolysis of lignocellulose on lignins and hemicelluloses. *Bioresource Technology 148*, 2013, 70-77.

[40] J.L. Rahikainen, R. Martin-Sampedro, H. Heikkinen, S. Rovio, K. Marjamaa, T. Tamminen, O.J. Rojas, and K.Kruus, Inhibitory effect of lignin during cellulose bioconversion: the effect of lignin chemistry on non-productive enzyme adsorption. *Bioresoure Technology 133*, 2013, 270-278.
[41] W. Norde, Adsorption of proteins from solution at the solid-liquid interface. *Advances in Colloid and Interface Science 25(4)*, 1986, 267-340.
[42] S. Nakagame, *The Influence of Lignin on the Enzymatic Hydrolysis of Pretreated Biomass Substrates. Doctoral Dissertation.* The Faculty of Graduate Studies (Forestry). The University of British Columbia, Vancouver, Canada, 2010.
[43] J. Andreaus, H. Azevedo, and A. Cavaco-Paulo, Effects of temperature on the cellulose binding ability of cellulase enzymes, *Journal of Molecular Catalysis B: Enzymatic 7 (1-4)*, 1999, 233–233.
[44] D.W. Kim, Y.H. Jang. C.S. Kim,and N. Lee, Effect of metal ions on the degradation and adsorption of two cellobiohydrolases on microcrystalline cellulose. *Bulletin Korean Chemical Society 22 (7)*, 2001, 716-720.
[45] M. Tu, X. Zhang, M. Paice, P. MacFarlane, and N.J. Saddler, The potential of enzyme recycling during the hydrolysis of a mixed softwood feedstock. Bioresource Technology 100, 2009, 6407–6415.
[46] J. Rahikainen, S. Mikander, K. Marjamaa, T. Tamminen, A. Lappas, L. Viikari, and K. Kruus, Inhibition of enzymatic hydrolysis by residual lignins from softwood-study of enzyme binding and inactivation on lignin-rich surface. *Biotechnology Bioengineering 108*, 2011, 2823–2834.
[47] J.O. Baker, K. Tatsunoto, K. Grohmann, J. Woodward, J. M. Wichert, S.P. Shoemaker, and M.E. Himmel,Thermal denaturation of Trichoderma reesei cellulases studied by differential scanning calorimetry and tryptophan fluorescence, *Applied Biochemistry Biotechnology 34–35*, 1992, 217-231.
[48] A. Ababou, and J.E. Ladbury, Survey of the year 2005: literature on applications of isothermal titration calorimetry. *J Mol Recognit.;20(1)*, 2007, 4–14
[49] M.J. Cliff, L.D. Higgins, R.B.Sessions, J.P. Waltho, and A.R. Clarke, Beyond the EX1 limit: Probing the structure of high-energy states in protein unfolding,*J. Mol. Biol. 336*, 2004, 497–508.
[50] S. Leavitt, and E. Freire, Direct measurement of protein binding energetics by isothermal titration calorimetry,*Curr. Opin. Struct. Biol. 11*, 2011, 560–566
[51] A. B. Borastan, The interaction of carbohydrate-binding modules with insoluble non-crystalline cellulose is enthalpically driven,*Biochem. J. Vol. 385*, 2005, 479–484
[52] B. Saha, J. Saikia, G. Das, Correlating enzyme density, conformation and activity on nanoparticle surface for high functional bio-nanocomposite. Electronic Supplementary Material (ESI) for Analyst. *Journal of The Royal Society of Chemistry 2014*.
[53] W.S.W. Ngah, M.A. K. M. Hanafiah, Adsorption of copper on rubber (Heveabrasiliensis) leaf powder: Kinetic, equilibrium and thermodynamic studies. *Biochemical Engineering Journal, 39*, 2008, 521-530. ISSN: 1369-703X.
[54] V. Padmavathy, Biosorption of nickel (II) ions by baker's yeast: Kinetic, thermodynamic and desorption studies. *Bioresource Technology 99*, 2008, 3100-3109. ISSN: 0960-8524.
[55] H. Ramdane, A. El Rhilassi, M. Mourabet, M. Bennani-Ziatni, A. Elabidi, A. Zinedine, and A. Taitai, Calcium phosphates as adsorbents for the controlled release of carbofuran. *Journal Material and Environmental Sciences 5 (6)*, 2014, 1715-1726
[56] M. Violet, and J.C. Meunier, Kinetic study of the irreversible thermal denaturation of Bacillus licheniformis α-amylase. *Biochemical Journal 263*, 1989, 665–670.
[57] S. D'Amico, C. Gerday, and G. Feller, Activity–stability relationships in extremophilic enzymes, *Journal of Biological Chemistry 278*, 2003, 7891–7896
[58] T. Collins, M.A. Meuwis, C. Gerday, and G. Feller, Activity, stability and flexibility in glycosidases adapted to extreme thermal environments. *J. Mol. Biol. 328*, 2003, 419–428.
[59] P. Saha, and S. Chowdhury, Insight Into Adsorption Thermodynamics. Thermodynamics. Tadashi, M. Ed. Intech Open Science, India. ISBN 978-953-307-544-0. 2011.
[60] E. Dehghanifard, A.J. Jafari, R.R. Kalantary, A.H. Mahvi, M.A. Faramarzi, and A. Esrafili, Biodegradation of 2,4-dinitrophenol with laccase immobilized on nano-porous silica beads. *Iranian Journal of Environmental Health Science & Engineering 10(25)*, 2013.
[61] A. P.M. Tavares, O. Rodríguez, M. Fernández-Fernández, A. Domínguez, D. Moldes, M. A. Sanromán, and E. A. Macedo. Immobilization of laccase on modified silica: stabilization, thermal inactivation and kinetic behaviour in 1-ethyl-3-methylimidazolium ethylsulfate ionic liquid. *Bioresource Technology 131*, 2013, 405–412.
[62] P.L. Privalov, and S. J. Gil, Stability of protein structure and hydrophobic interaction. *Advances in Protein Chemistry39*, 1988,191-234.
[63] M.P. Rout, J.D. Aitchison, M.O. Magnasco, and B.T. Chait, Virtual gating and nuclear transport: the hole picture. *Trends in Cell Biology 13(12)*, 2003, 622-628.

American Journal of Engineering Research (AJER) 2016
American Journal of Engineering Research (AJER)
e-ISSN: 2320-0847 p-ISSN : 2320-0936
Volume-5, Issue-2, pp-166-173
www.ajer.org
Research Paper Open Access

Virtual Sober Companion-Mood Analysis.

[1]Krishna Balasubramanian , [2]Prof. Nikhil Gala
[1]*Bachelors of Technology- Computer Engineering Mukesh Patel School of Technology, Management and Engineering. NMIMS University, Mumbai, India.*
[2]*Department of Electronics and Telecommunications NMIMS University,Mumbai,India.*

Abstract: *The rehabilitation of drug addicts involves a phase of sober companionship where a person who has had a history with the drug but has maintained abstinence for more than three years is asked to accompany the recovering addict during all chores and tasks. The aim is to provide a cheaper alternative to human sober companions by introducing a virtual counterpart. Of the many facets to this application building and patient recovery project, Mood Analysis is the main module that is to be well understood and studied before any step towards making the application. The paper provides a review of all available works related to this domain.*
Keywords: *Smartphone, Operational logs, mood detection, mood enhancement, FitBit, CPS, BCI, POI.*

I. Introduction

There are over 3 million people in India alone hooked on to drugs. Cannabis, heroin, opium and brown sugar hash are the most commonly used drugs in India. However, some evidence indicates that there is an increasing prevalence of meth as well. Drug addiction is a major problem for many families, communities and law enforcement agencies. Massive numbers of addicts are left to be treated by the families as financial costs, available services and lack of appropriate care challenge the country. This is not only the case for drug addicts.
There are over 110 million people in India who smoke cigarettes. Smoking causes lung cancer, pregnancy related problems, pulmonary heart disease and other heart and blood related ailments.
The de-addiction process involves relieving the addict from the urge to pursue the addiction besides detoxification and psychiatric help to cope with the damage done by some drugs. The last phase of the de addiction process involves the addict having a sober companion at all times.
A sober companion or sober coach provides one-on-one assistance to newly recovering drug addicts and alcoholics. The goal is to help the client maintain total abstinence from alcohol and drugs, and to establish healthy routines outside of a residential treatment facility. Sober companion treatment usually lasts for 30 days – often, much longer. The time required to effect a meaningful change varies greatly depending upon the client, his co-occurring disorders, and the family life at home.

Sober Companions are generally hired by celebrities, ex-military and retired sportsmen who resort to drugs besides all the glamour, struggle, pressure and other stresses of life.

In India, majority of the drug addicts are BPL or belong to the middle class and hence cannot afford a paid sober companion. A virtual sober companion who does exactly what the human counter-part does is the solution to the problem.

The major part of work in this domain and the eventual development of the application is the identification of the mood or mental consciousness or state of mind of the user, hence the research papers and approach to research is of finding optimal solutions to mood identification and analysis. An efficient virtual sober companion would also bring about a change in the detected mood and improve the condition of the user.

II. Previous Works in the field

MoodSense Technology: Can Your Smartphone Infer Your Mood? [1]

MoodSense[1] is a smartphone service which aims at inferring the mood of the user based on data that already exists in the smartphone.

An experiment was conducted to identify the usability of the service and make a miniature prototype of the service.
The environment of the said experiment included:
(1) Subjects aged between 20 and 29.
(2) 8 of them were female and 17 were male.
(3) 17 of the users were students but the rest covered a diverse set of occupations including two software engineers, one web editor, one salesman and one teacher.
(4) LiveLab iPhone Logger was used to capture user behaviour using daemons operating in the background. The data was archived nightly to a server over a cell data or Wi-Fi connection.

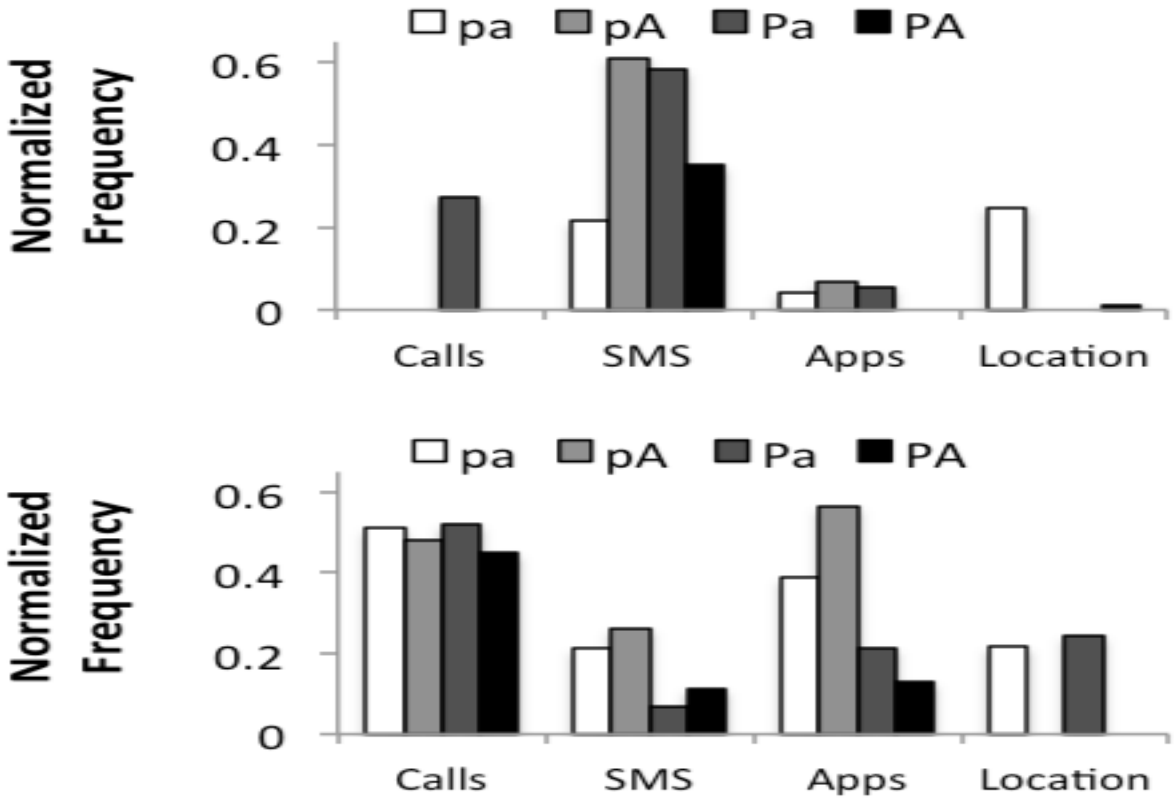

Figure 1: Normalised Frequency of Most Frequent Feature in each category for Two Users.

MoodSense could be essentially built on a model that predicted mood using smartphone usage statistics. The analysis of data collected in the experiment suggested that the model was indeed feasible but flouts various security and privacy norms.Summary, Key points and notes of different sections of the research paper are discussed below.
Gradually, mobile phone sensing has reached beyond the recognition of physically observable human behaviour or environmental context. The activities of an individual can be identified and studied to establish an accurate decision about his or her mood and mental standpoint.This is the basis of the research and it is legitimate as a huge load of data that runs in an individual's smartphone is adequate to analyse and infer mood.
Techniques that allow devices to infer the internal mental state of users are being developed and are opening exciting new opportunities for mobile applications. This is done by various methods. The research work over MoodSense [1] contributed to this new direction as the first demonstration of automatic mood inference using routinely collected phone data (e.g., browser, call, SMS, location history etc.).
A time-series of location estimates for the user is clustered using the DBSCAN clustering algorithm, which allows them to then count user-visits to each location cluster.This technique indicates the dependencies of each parameter which is being calculated.
User mood is represented by the following states: PA – above median pleasure and above median activeness; pA – below median pleasure and above median activeness;Pa–above median pleasure and below median activeness; and finally, pa – below median pleasure and below median activeness.
This application flouts various security norms, privacy norms and patient doctor privileged information.

A new treatment for substance addiction defies the recovery movement.[2]

The medical aspect of drug addiction rehabilitation is of utmost importance and the mental state identification of the user is necessary.An experiment is conducted to identify the moods and mental states of an addict at different times of the day.
The environment of the said experiment is (1)Participants in this study must be heavy addicts.(2)For male alcoholics,the threshold translated to 35 or more standard drinks a week—5 ounces of wine, 12 ounces of beer, or 1.5 shots of hard liquor. For women it was 28 or more drinks a week.
A medical approach was chosen where the brain and its working is mapped using medical equipment and the analysis was studied.
A set of pointers are established to maintain the sanity and mental conditioning of the recovering addict. These pointers are formulated by a panel of renowned psychiatrists.
"Depression does not cause drinking; drinking causes depression."
Also known as drug dependence, drug addiction the disease is not a subjective diagnosis.
It is defined by a set of symptoms: a strong need, or urge, to consume; not being able to stop consumption once started consuming; drug withdrawal symptoms such as nausea, sweating, shakiness, and anxiety; and the need to consume greater amounts of the drug to experience its effects, a phenomenon known in addiction parlance as tolerance.
Pharmaceutical giants like to keep their contributions low-key or steer clear of these applications altogether.
Addiction is common in people with mental health problems. But although substance abuse and mental health disorders like depression and anxiety are closely linked, one does not directly cause the other.
Alcohol or drugs are often used to self-medicate the symptoms of depression or anxiety. Unfortunately, substance abuse causes side effects and in the long run worsens the very symptoms they initially numbed or relieved.
Alcohol and drug abuse can increase underlying risk for mental disorders.Mental disorders are caused by a complex interplay of genetics, the environment, and other outside factors. If you are at risk for a mental disorder, drug or alcohol abuse may push a person over the edge.
Alcohol and drug abuse can make symptoms of a mental health problem worse. Substance abuse may sharply increase symptoms of mental illness or trigger new symptoms. Alcohol and drug abuse also interact with medications such as antidepressants, anti-anxiety pills, and mood stabilisers, making them less effective.
When consumptions is heavy and frequent, the body becomes physically dependent on the drug and goes through withdrawal if consumption is stopped suddenly. The symptoms of drug withdrawal range from mild to severe.
A timely intervention reminding the addict about his current state of mind and his decision of quitting the vice for the well-being of himself and his near and dear. This could be done by a utility pager.
According to reports published in the *Journal of the American Medical Association*: [5]
Roughly 50 percent of individuals with severe mental disorders are affected by substance abuse.
37 percent of alcohol abusers and 53 percent of drug abusers also have at least one serious mental illness.
Of all people diagnosed as mentally ill, 29 percent abuse either alcohol or drugs.
Five steps to a sober lifestyle suggested at the end of the experiment were:
Take care of self. To prevent mood swings and combat cravings, concentrate on eating right and getting plenty of sleep. Exercise is also key: it releases endorphins, relieves stress, and promotes emotional well-being.
Build support network. Positive influences and people who make one feel good about themselves should be in proximity. The more one is invested in other people and the community, the more they have to lose—which will help them stay motivated and on the recovery track.
Develop new activities and interests.Find new hobbies, volunteer activities, or work that gives a sense of meaning and purpose. When doing things which are fulfilling, eventually one will feel better about them self and drug or substance consumption will hold less appeal.
Continue treatment. Chances of staying sober improve if the addict is participating in a support group like Alcoholics Anonymous, have a sponsor, or are involved in therapy or an outpatient treatment program.
Deal with stress in a healthy way. Alcohol abuse is often a misguided attempt to manage stress. Find healthier ways to keep stress level in check, such as exercising, meditating, or practicing breathing exercises or other relaxation techniques.

Happy Hour - Improving Mood With An Emotionally Aware Application.[3]

The aim was to enable a mood enhancing mobile service which not only identified the mood but also brought abut a positive change to it .The factors leading to the development of such an application and the main reasons why it was possible are:

1) On a single device, it is possible to enumerate not only several wireless connectivity interfaces (4G/LTE, Wi-Fi, NFC, Bluetooth) but also various sensors (GPS, accelerometer, gyroscope, proximity/ambient light).

2)CPSs are known as Human-in-the loop Cyber-Physical Systems (HiTLCPSs), where the human becomes an integral part of the control-loop and his nature directly affect the system's actions.

3) Behaviour Change Intervention (BCI) system to improve human physical and mental well-being.
BCIs are therapeutic systems that focus on providing advice, support and relevant information to patients, in order to motivate the correction of prejudicial behaviours.

4)The BCIs suggest a suitable exercise routine to bring about a change in the user's mood.

5)A POI (point of interest) manager is hard-coded into the system where the decisions are to be made.

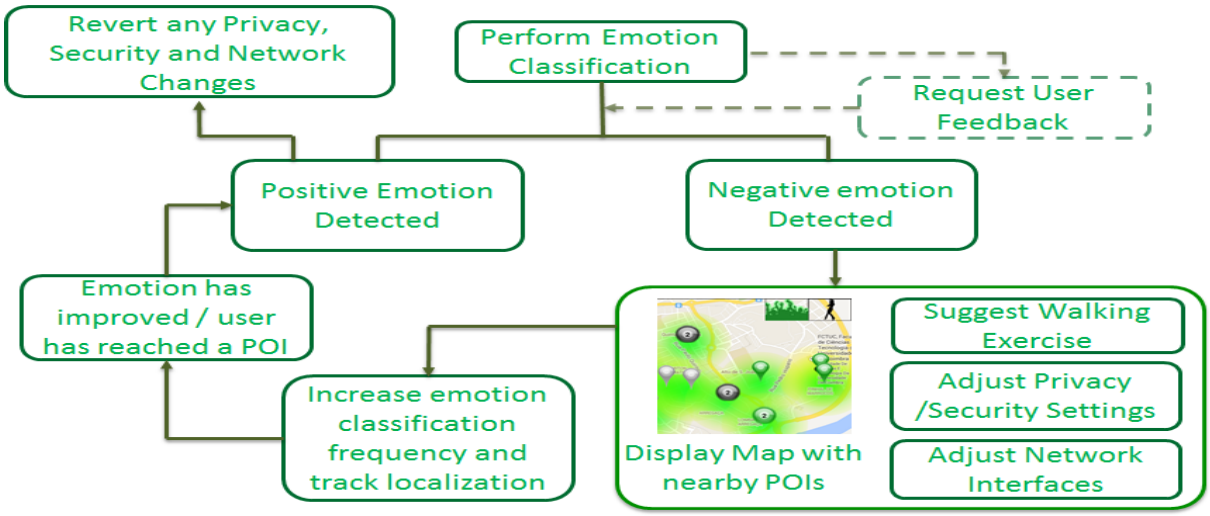

Figure 2: HappyHour application flow .[3]

An experiment was conducted to identify the moods and
The environment of the said experiment is**:**
(1) user mobile phone with the pre installed HAPPY HOUR mobile application.
(2) APK to identify input (pre installed system software in smartphones)

The user is asked to enter his or her emotion and this emotion is then analysed by a set of predefined functions stored in the database of the application. The CPSs suggest a physical exercise to the user which will aid the change of the mood of the user. This physical exertion is suggested to the user to change his or her mood according to a positive hierarchical order pre set by the database and ordered preferences of the application.

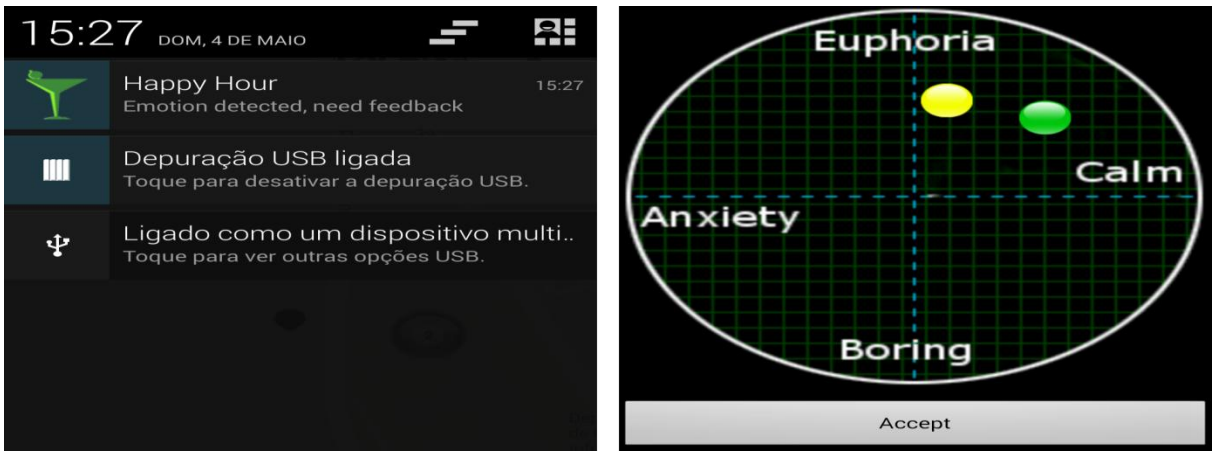

Figure 3: HappyHour Emotional Feedback . [3]

The BCI system plays an important role in identifying the mood and bringing about a positive change in it. It is aimed at improving physical and mental well being.BCIs are therapeutic systems that focus on providing advice, support and relevant information to patients, in order to motivate the correction of prejudicial behaviours. The human in the loop CPSs help in identification of an appropriate user feedback mechanism.

POI manager is a hard coded module which is a major decision making module without which the entire application would be of no use and completely un operational. This is an apt counterpart to the artificial intelligence of some advanced systems.

The POI manager also monitors data and privacy settings from other social networking applications present on the users' phone. This data is monitored and is kept to suitable settings so as to enable accurate collection of data and effective mood analysis.

The various phases of the running of the application are:

1)MONITORING HUMAN EMOTIONS

The core of the emotion-awareness lies in the ability to process different forms of sensing. From the beginning, the objective was not to propose robust methods for emotion detection, but instead, to provide a practical proof-of-concept that shows how emotional information can benefit HiTLCPSs.

2)EMOTIONALLY AWARE RULE SYSTEM

Depending on the emotion classification result and the user's feedback, the HiTL control assumes different decisions. These measures are the responsibility of the "emotionally aware rule system", which is implemented based on sets of actions. Users specify profiles for each emotional state, and actions associated with each profile. These profiles allow the application to automate and specify privacy and networking configurations in accordance to a HiTL paradigm. In particular, if a negative emotional state is detected (e.g. high anxiety or boredom), the default behaviour takes direct measures to improve the user's mood.

3)POINT OF INTEREST INFORMATION

The information provided by the application allows users to identify the best place in a local area to visit. Since every person has their own music tastes and emotional responses, providing detailed information about the environment of each POI might have impact on decision-making process. For in- stance, a person could choose a crowded bar with music if they want to dance, or decide to go visit a more quiet nature park for a relaxing walk, instead. Tracking and aggregating users' emotions and their activity allows HappyHour tocategorise points of interest. The android application allows users to select a destination for their walk through a map.

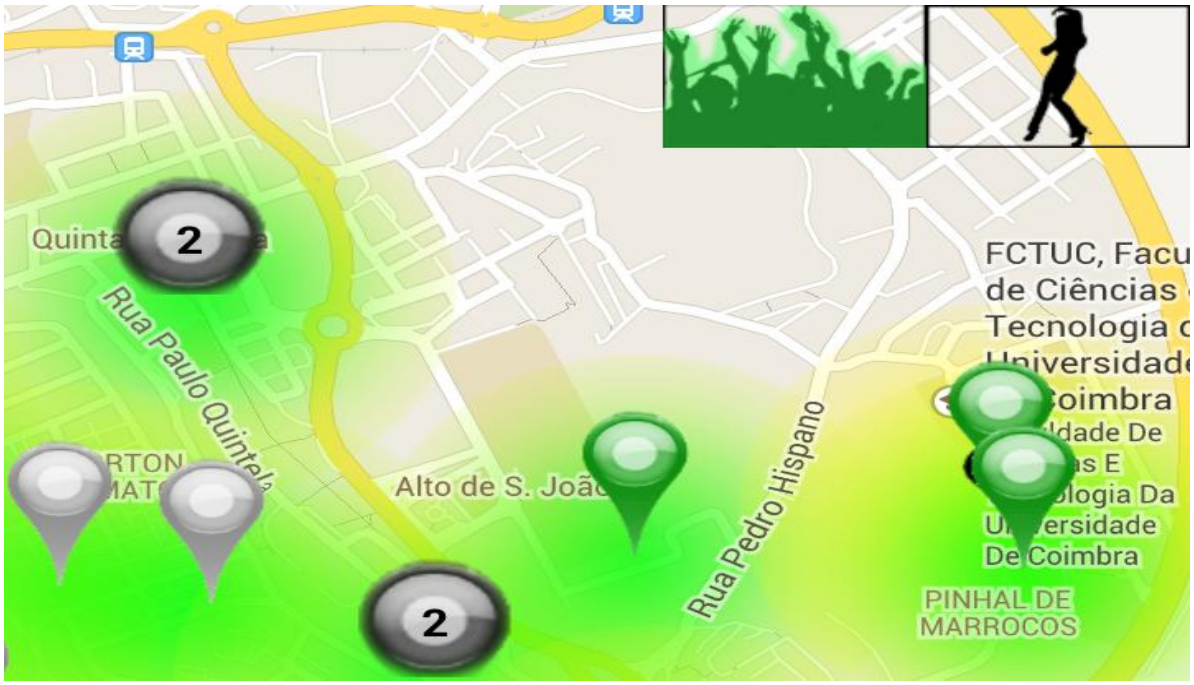

Figure 4: Happy Hour heat maps. [3]

Smartphone-Based Recognition of States and State Changes in Bipolar Disorder Patients.[4]

The study is based on the assumption that a consistent pattern of bad mood cycles can be a symptom to a major mental disorder. The treatment of the mental disorder would lead to the betterment of the mood cycles hence curing the user of any mental illness simultaneously.

The rehab patients, who constitute a major portion of my target audience have mood swings quite in relation to the bipolar behaviour which is a pertinent illness of recovering addicts.
So the basis of the research is the detection of any mental illness by identification of symptoms and treating the mental illness and coaxially ridding the patient of mood swings and other mental disorders. This not only helps in accurate mood detection but also does the work of an efficient mood enhancer by following medically correct procedure of treatment.
Some of the salient features of the technology implemented here are:
1) Self-Assessment of Mental Disorder Symptoms Using Mobile Phones-The mood swing patterns and instance mood readings of the user are matched with a set of pre defined readings and parametric data which are medically recognised.
2) Objective Monitoring of Symptoms of Mental Disorders-The acquired inputs of the user are segregated and compared with a database where it is then combined and related ailments with similar symptoms are identified and recognised.
3) Wearable Technology in Health Care-It refers to its compatibility with FitBit, iWatch, moto-watch and other wearable tech that help in health detection specifically motion , heart rate and gyroscope.
4) Automatic Recognition of Mental State- The data from the phones inbuilt sensors like the speedometer, GPS, gyroscope, photo sensor etc and that of the wearable technology the data is compared with the predefined set of moods and behaviours and the instant mood of the user is established.
Considering the usability of the envisioned system, some important aspects should be highlighted here:
1) The recognition results of a system as outlined here are not meant to automatically trigger medication. There is no danger that a false recognition would trigger potentially dangerous wrong medication.
2) Required reaction times are on a time scale of a few days rather than a single day. In fact, radical change seldom happens from one day to the next.
Initial experiments and several discussions with the medical personnel gave an insight into the relative relevance of different behavioural aspects:
1)Social interaction
2) Physical motion
3)Travel patterns
The mobile usage is used to track the users state of mind by monitoring texts, social networking activity and call logs. The data from these operational parameters are identified and analysed to predict the mood of the user. The mood analysis leads to cross checking of the prescribed mood with a set or symptoms of mental disorders . This makes the diagnosis of any mental disorder easier and the treatment of any psychological disorder or disfigured mood cycle easier and accurate .
Precision and recall graphs are made to analyse the user moods and are an attempt to quantify the users state of mind. The precision and recall graphs are used and constructed for sound and phone modalities.
Precision or *positive predictive value* is the fraction of retrieved instances to that of the instances that are relevant, while *recall* or *sensitivity* is the fraction of relevant instances to that of all that have been retrieved.
Phone modalities are the user logs and operational parameters. The sound modalities are basically the external input t the user in the form of sound example video, music or any other source which can affect the users mood as sound being the medium.
A density based clustering is also done to identify the readings of the phone sound and fusion modalities. Their uniqueness is a key to the precision of this experiment.

(av. # instances)	**Recall** (std)	**Precision** (std)	**total** (std)
PHONE (43)	54.4% (11.4)	37.3% (29)	64.2% (13)
SOUND (43)	61.3% (7.3)	24.2% (31)	69.8% (4.5)
FUSION P + S (43)	**58.4%** (3.2)	**59.0%** (11.3)	**69.3%** (3.5)
ACC (48)	62.9% (7.9)	64.8% (7.8)	71.7% (3.8)
LOC (33)	72.3% (14.5)	76.5% (13.7)	81.7% (6,5)
FUSION A + L (49)	**66.3%** (11.0)	**57.9%** (16.6)	**75.6%** (6.2)
all-in FUSION (49)	**65.8%** (8.8)	**72.0%** (12.2)	**76.4%** (4.1)

Figure 5: Accuracy in% (# of total instances)and Recall Precision for Phone,Sound and Fusion [4]

Patients	PHONE	Rec/Prec	SOUND	Rec/Prec	Fusion	Rec/Prec
p0102	75(46)	64.4/70.1	66(46)	51.2/40.4	73(46)	58.5/68.0
p0201	62(38)	52.5/53.2	68(32)	60.8/62.0	71(38)	58.7/66.4
p0302	71(60)	62.0/63.6	74(60)	64.5/52.0	71(60)	60.7/65.3
p0602	36(35)	33.9/35.0	76(35)	68.5/78.7	65(35)	57.0/48.0
p0902	68(41)	63.7/65.3	71(41)	68.5/68.5	68(41)	62.3/65.5
p1002	65(37)	78.7/69.4	65(37)	54.0/40.8	65(40)	53.3/41.4
Average	**66%**	**61/58**	**70%**	**60/59**	**69%**	**52/55**

Figure 6: Comparison of recognition of different modalities and fusion of all modalities and of all-in fusion [4]

III. Inferences

The MoodSense service application[1] cannot be used since it flouts various security and privacy norms. An alternative method has to be searched for and another method has to be found and decided upon.It was learnt that the MoodSense technology if not for its legality problems would be the ideal application to be used to identify the users' mood and provide effective relief.

An option would be to wait for the privacy norms to be made lenient by google and other norm deciding bodies so that the technology can be implemented and can help various mood detecting applications function effectively.

The mindset of the user and the crests and troughs of addict behaviour was identified by A new treatment for substance addiction defies the recovery movement.[2]. A fruitful set of pointers that would aid in design of a mood enhancing service application was found. The variations that the mental state of a recovering addict goes through during the usage of the application were learned. The mental conditioning to be provided by the application was identified and was helpful in deciding the services that should be provided by the application.

The mood of the user is specifically kept towards a positive gradient in the Happy Hour Application[3]. This is helped and aided by the POI manager where a decision is made to monitor the data flowing in from the other social networking applications. This also suggests any mild physical exertion which will bring about a positive change in the users' mood. The important feature of this application is the user feedback mechanism where the users mood is input and is then analysed rather than being presumed on device usage and history/logs etc which would be inaccurate and inefficient.

The use of the operational data, social interactions and physical motion are parameters whose study provides us with true study of the users mood by Smartphone-Based Recognition of States and State Changes in Bipolar Disorder Patients [4]. The treatment and diagnosis of mental disorders are an accurate method of finding out untapped mod disorders and untapped state of mind which may actually need conditioning and treatment and may prove to be a pivot in the overall treatment of the user.

IV. Conclusion

After a comparative analysis of the previous works in the field of mood inference by smartphones it was concluded that the accurate mood detection could be done by analysing data received by operational logs and related health data from gyroscope, photo sensor and GPS.

The accuracy of this data was established by a number of experiments mentioned above. The integral step towards efficient mood detection would be quantifying the input to a form acceptable for quick processing and swift comparison. The standardisation of the data to enable compact databases and their efficient comparison is also to be taken into consideration during design of the application.

Steps to enhance a detected mood should be verified by medical personnel and then implemented. Each step which detects a state of mind or induces a change to the mood should be certified by a qualified physician or psychiatrist.

V. Acknowledgements

I would like to thank my parents for supporting me in this endeavour. I would also like to thank my friends and family for always being motivational and helpful. I am forever indebted to my mentor Mr.Nikhil Gala without whom this review paper would be not be possible.I would take this opportunity to thank the dean of our college Dr.S Y Mhaiskar for his constant guidance.

References

[1] Robert LiKamWa,Yunxin Liu,Nicholas D. Lane and Lin Zhong, "*can a smartphone detect the mood of the user?*",University of Rice,Microsoft Reasearch Summit,2010.

[2] Susan Seligson and Dr. D. Gatica-Perez, "*A new treatment for substance addiction defies the recovery movement.*", in ISWC 2011.

[3] Pedro Carmona, David Nunes, Duarte Raposo, David Silva , Jorge Sa´ Silva and Carlos Herrera , "*Happy Hour - Improving Mood With An Emotionally Aware Application*," University of Coimbra Department of Informatics Engineering (Quito, Pichincha, Ecuador).

[4] J. Agnes Gru¨nerbl,Amir Muaremi, Venet Osmani, Gernot Bahle, Stefan O¨ hler, Gerhard Tro¨ster, Oscar Mayora,Christian Haring, and Paul Lukowicz, ",*Smartphone-Based Recognition of States and State Changes in Bipolar Disorder Patients*" Ad Hoc Networks, vol. 24, pp. 264–287, 2015.

[5] K. Church, E. Hoggan and N. Oliver, "*A study of mobile mood awareness and communication through MobiMood*", in NordiCHI,2010.

[6] Goaer, Olivier Le; Barbier, Franck; Cariou, Eric and Pierre, Samson, "*Android Executable Modeling: Beyond Android Programming*", in : 27-29 Aug. 2014.

[7] C. D. Batson, L. L. Shaw and K.C. Oleson, "*Differentiating affect, mood and emotion: toward functionally-based conceptual distinctions*", Emotion, Newbury Park, 1992.

[8] T.-D. Tran, C. Herrera, D. Nunes, and J. S. Silva, "*An adaptable frame- work for interoperating between wireless sensor networks and external applications*," in 3rd Conference on Sensor Networks (SensorNets2014), Lisbon, Portugal, January 2014.

[9] N. Lane, E. Miluzzo, H. Lu, D. Peebles, T. Choudhury, and A. Camp- bell, "*A survey of mobile phone sensing*," Communications Magazine, IEEE, vol. 48, no. 9, pp. 140–150, Sept 2010.

American Journal of Engineering Research (AJER) 2016
American Journal of Engineering Research (AJER)
e-ISSN: 2320-0847 p-ISSN : 2320-0936
Volume-5, Issue-2, pp-174-181
www.ajer.org
Research Paper Open Access

Application of Nkwo-Alaike Clay for the Production of Ceramic Wares Using Cullet as Sintering AID

A.S. Ogunro[1], F.I. Apeh[2], O. C. Nwannenna[3]and A. E. Peter[4]
[1,2,3]*Nigerian Building and Road Research Institute, Engineering Materials Research Department, Km. 10, Idiroko Road, P.M.B 1055, Ota Ogun State, Nigeria.*
[4]*Aluminum Smelting Company of Nigeria, Ikot Abasi, Akwa Ibom State.*

ABSTACT : *Nkwo-Alaike clay which was collected from Imo State, South-East Nigeria, was characterized and cullet was added as sintering aid (flux) in order to decrease the firing temperature thereby saving cost of fuel utilization. The cullet collected were milled into powder and batches containing mixture of 10%, 20%, 30% cullet powder with clay were prepared and moulded under 30MPa in order to evaluate the effect of cullet powder on sintering of the ceramic products. The samples produced were gradually fired to 900-1050^{o}C with soaking time of 1hour at 5^{o}C/min. Physical and thermal properties of the samples were investigated, from the results, the composition containing 20% cullet which was fired at1050°C before its maturity had the best mechanical strength (13.80–28.61MPa) and no pinholes or cracks were recorded. The overall result show that, the firing temperature was reduced from1150^{o}C to 1050^{o}C, making it possible to use the Nkwo-Alaike clay with cullet addition for the production of wall or floor tiles at 20% addition.*

Keywords: *cullet, flux, sintering, soaking time, strength, tiles.*

I. INTRODUCTION

Most solid residues generated by both public and private activities are sometimes being disposed in landfills. The availability of glass wastes from the recovery of landfills is expected to increase with the activities of glass producers [1], these needed to be converted for economic purpose, as in ceramic production.

Ceramic products are widely used in homes, as wall and floor tiles, water closet (WC), Jugs, plates, etc. Clay is mostly used as the raw material for their production. They are manufactured using high amount of fluxing agents like, sodium and potassium feldspars, nefeline, talc and ceramics fritz [2]. Ceramic tiles have various characteristics and it can be used in many different places because of its high mechanical resistance and surface hardness [3].

The main constituent of clay is silica (SiO_2) and alumina (Al_2O_3) with the addition of other materials to attain the desire product standard. In this work, waste glass (cullet) powder which contains about 71% silica (SiO_2) was added to clay in various proportions for the production of ceramic tiles in order to determine its effects on the ceramic properties. The production of tiling materials are one of the priorities of the traditional ceramic industry [2]. As a result, several studies related to the substitution of conventional raw materials in tile-making (i.e. clays, sands and feldspars) by other natural resources or industrial wastes were carried out during the last decade [1,3,4].Promising results have been obtained using glass cullet waste [3, 5,11] cathode ray tube (CRT) glass [1, 6], different industrial residues [4] and various volcanic rocks [2].In the work carried out by [1,3,6], the optimal amount of the replacement, that is, cullet or CRT were between 5–10 wt.%.

The crystalline proportion of the final ceramic products may be increased by using glass-ceramic frits [7] or compositions with high crystallization trends [8]. In this case, due to re-crystallization processes during the heat treatment, as the amount of residual amorphous phase decreases while increasing the crystalline proportion will have a positive effect on the mechanical properties of ceramic products [9].The major focus of these studies was to use Nkwo-Alaike clay base with cullet powder as alternative flux.

II. MATERIALS AND METHOD

The materials used for this study include: clay materials and broken bottles (cullet). The clay materials used was collected from Nkwo-Alaike deposit in Imo State; the depth is 2.0m down the threshold and 7m interval from three different points using digger and shovel. The broken bottles used as additive was collected from the immediate environment.

The waste broken bottles collected were washed with Omo-Detergent and water to remove contaminants in them after which they were air dried. Hammer crusher machine was used to crush the air dried bottles before it was disc milled for 5 hours (five hours) to fine powders. The powders were sieved with a 0.8mm mesh size in order to get the finer samples that will be added to the clay samples before pressing.

These materials were prepared and tested in accordance with [10] to determine their suitability for the production of ceramic wares. In carrying out the test, the following were determined; fired linear shrinkage (F.LS),compressive strength (CS), water absorption (WA), bulk density (BD), apparent porosity (AP), thermal shock resistance, refractoriness, moisture content and loss on ignition (LOI), and as well as the chemical analysis.. The detail analyses on the experiments are enumerated below.
The cullet collected were milled into powder and sieved. Hundred percent (100%) of the original materials (Nkwo-Alaike clay) collected was prepared and formed into tiles as a control sample. The clay as a base material was mixed with cullet in various weight fractions of 90:10; 80:20; and 70:30.

A mould pattern or die for the ceramic tile was constructed specially using mild steel plate of the dimensions: length 14cm, width 12cm, depth 5cm, and thickness 1cm of two pieces each. The plates were machined to give the squareness and depth required. After which it was mounted on ceramic tile press to begin the production of the tile samples.

The clay was mixed with the cullet (ceramic mass) in batches as indicated above. The clay and the cullet with 6-8% water content (200ml of water) were homogenized in a Bluebird-Model 12SS clay mixer and the green sample with initial dimension of (5.08cm x 5.08cm) and (2.5cm x 2.5cm) were obtained by pressing; using hydraulic ceramic tile press of 10-50MPa capacity at 30MPa. Four specimens were pressed from each sample mixed in order to study and analyze the effect of cullet addition on the clay, especially, the firing temperature. Table 2.1 shows the mix ratios in percent by weight of the clay sample and cullet used in the research.

Table 2.1: Percent by weight of the clay and cullet

S/N	Specimens	Mix Ratio		
		Clay (%)	Cullet (%)	Water (ml)
1	N	100	0	200
2	N_1	90	10	200
3	N_2	80	20	200
4	N_3	70	30	200

The tiles produced were air dried for 14 days after which they were oven dried at a temperature of 200^0C for 3 days in order to remove the moisture content. The oven-dried tiles were fired in a gas kiln for a period of 8hrs at gradual of 800^oC, 900^oC, $1{,}000^o$Cand $1{,}100^o$ C respectively and as well soaked at 800^oC for 2hours to produce biscuit wares. The Biscuit wares were allowed to cool for 24hours before removing them from the kiln.

2.1 Fired Linear Shrinkage

Test pieces of the ceramic mass were made into standard slabs of 5.08cm x 5.08cm and 2.5cm x 2.5cm. The pieces were marked along a line to be able to determine the shrinkage degree from the original position after the application of heat. The distance between the two ends of the slabs was measured with Vernier Calipers after which, the samples were air dried for 24 hours and oven dried at 110^0C for 24 hours. They were then fired at $1{,}100^0$C for 6 hours. The samples were cooled to room temperature and measurements of the degree of shrinkage were taken. The fired linear shrinkage was calculated using equation (2.1).

$$\text{Fired shrinkage} = \frac{(DL - Fl)}{DL} * 100 \qquad (2.1)$$

where, DL = Dried Length; FL = Fired Length.

2.2 Compressive Strength

Test pieces were prepared to a standard size of 76.2mm cube on a flat surface. They were dried and fired in a Nabertherm (1999) model muffle resistance furnace at $1{,}100^0$Cand the temperature maintained for 6 hours. The pieces were then cooled to 27^oC and then placed on a compressive tester (Testometric M-500-25KN) and load applied axially by turning the land wheel at a uniform rate till failure occurs. The manometer readings were recorded and comprehensive strength (CS) was calculated using equation (2.2);

$$C.S = \frac{Max\ .Load\ \ (KN\ )}{C\ .A(m^{2})} \quad (2.2)$$

where, C A = cross-sectional area; CS = compressive strength.

2.3 Water Absorption Test on the Biscuit Wares

The biscuit wares were trimmed and dressed, then each of them were weighed and then soaked in a bowl of water for 2hours and then removed, wiped with dry foam and weighed in accordance with [10].The water absorption was calculated using formula (2.3).

$$WA = \frac{B - A}{A} * 100 \quad (2.3)$$

where, A= is weight of biscuit ware before soaking (g); B= is weight of biscuit ware after soaking, (g).

2.4 Bulk Density

Samples of the clay materials measuring 60mm x 60mm x 15mm were prepared. The specimens were air dried for 24hours and then oven dried at 110^{0}C, cooled in desiccators and weighed to the accuracy of 0.0018 (Dried weight); after which the specimens were transferred to a beaker and heated for 30 minutes to help get rid of the trapped air. The specimens were cooled and soaked weight (W) taken. The specimen each was then suspended in water using beaker placed on a balance. The suspended weight(s) each piece was taken and the bulk density was calculated using equation (2.4).

$$\text{Bulk Density} = \frac{D_{pw}}{(W - S)} g / cm^{3} \quad (2.4)$$

where, D= Dried weight; W= Soaked weight; S=Density of water.

2.5 Apparent Porosity

Representative of test pieces of the ceramic mass were prepared, samples of cylindrical shape of 1.65 cm diameter were moulded in dry pressing under 30MP and air-dried for 24 hours. The pieces were then oven dried at 110^{0}C for 24hours and then fired at a temperature of $1{,}100^{0}$C, cooled and transferred into desiccators and weighed to nearest 0.01g. The specimens were then transferred into 250ml beaker in empty vacuum desiccators. Water was then introduced into the beaker until the test pieces were completely immersed and allowed to soak in boiled water for 30 minutes, agitated from time to time to assist to release trapped air bubbles. The soaked weight (W) was recorded. The specimens were then weighed suspended in water using beaker placed on balance. This gave suspended weight(S); the apparent porosity was calculated using equation (2.5):

$$\text{Apparent porosity} = \frac{(W - D)}{(W - S)} * 100 \quad (2.5)$$

where, W = Soaked weight; D = Dried weight; S = Suspended weight.

2.6 Thermal Shock Resistance

Test pieces measuring 50mm x 75mm were prepared. The pieces were inserted in a Nabertherm (1999) model muffle resistance furnace, after drying, which has been maintained at regular temperature of 900^{o}C for 10 minutes. There were then removed with a pair of tongs from the furnace one after the other and cooled for 10 minutes. The process continued until test pieces were readily pulled apart in the hands. The numbers of heating and cooling in cycles for each piece were recorded as its thermal shock resistance.

2.7 Refractoriness Value of the Ceramic Mass

The refractoriness of the ceramic mass was determined along with the known Standard (Pyrometric Cone Equivalent, PCE) in which the test pieces were prepared and mounted on a refractory plaque along with some PCE, that is, one whose melting point is slightly above and slightly below that expected of the test cones (ASTM. Designation C24). The plaque was then put inside the furnace and the temperature was raised at a rate of 100^{0}C per minute. The test continued until the tip of the test cone had bent over level with the base to evaluate its refractoriness value.

2.8 Moisture Content Analysis

The ceramic mass were air dried and weighed (W) and then placed in a Nabertherm (1999) model furnace which was heated to a constant temperature of 110°C for 24hrs. The sample was taken out cooled in desiccators and re-weighed (W_1). The loss in weight gives the amount of moisture content (MC) which can be expressed as percentage of initial clay sample. The following expression as is in equation (2.6) was used for the calculation:

$$M.C = \frac{W - W_1}{W} \times 100 \quad (2.6)$$

where, MC= is the moisture content (%); W= is the weight of the sample before drying (g); W_1=is the weight of the sample after drying (g).

2.9 Chemical Analysis

Chemical analyses of the materials were carried out using Atomic Absorption Spectrophotometer (AAS, PG 990 AFG) in order to determine the clay chemical and cullet compositions. Loss on Ignition (LOI) was also carried out on the samples and the results are shown in Tables 3.1-3.2.

2.10 Biscuit Firing

The pressed tiles were fired in a gas kiln for a period of 8hours at gradual temperatures of 800, 900, 1,000 and 1,100°C. It was soaked at 800°C for 2hours to obtain biscuit wares. The Biscuit wares were allowed to cool for 24hours before removing them from the kiln; Table 3.4 shows the result of the biscuit wares.

2.11Glazing

The glazing was carried out using 25g of powder glaze which was milled for 1hour in the ball milling machine after which, 400litres of water was added and mixed to form a homogenous mixture before sieving the mixture with 0.8mm sieve. The biscuit wares were dipped in glaze paste at interval of 10 seconds beginning with the biscuit that has the highest water absorption capacity. The samples were fired in a gas kiln and the glaze mass melted at a temperature of 1,025°C. The samples were removed from the kiln after 12hours of cooling to avoid cracking. The aim of glazing was to make the tile resistant to dirt, stain and water and as well as giving an esthetic look.

III. DISCUSSION OF RESULTS

In this work, Nkwo-Alaike (NA) clay obtained from Imo State and broken bottles (cullet) were characterized. The results of the chemical analyses of the raw materials used are presented in Tables 3.1-3.2. Table 3.1 depicts the chemical composition of the waste glass, containing a relatively large percentage of SiO_2 (71.08%) in the material with 1.05% (Al_2O_3), 0.76% (MgO), 11.19% (CaO), 0.02% (ZnO), 14.52% (Na_2O) and 0.01% (K_2O). The presence of alkaline and alkaline earth oxides in the broken bottles (cullet) composition will act as fluxing agents helping the sintering process of the ceramic products on the addition of the cullet[11].

The percentage composition of silica (SiO_2) present in Nkwo-Alaike clay is 56.7% (see Table 3.2). Silica content above 46.5% indicates free silica (quartz) in the system which will enhance the ceramic properties [11, 12], therefore, silica content in NA will improve ceramic properties of the sample investigated.

The alumina (Al_2O_3) content of NA fell below the recommended value of 26.70% as shown in Table 3.2. For good characteristics clay, the alumina should have a chemical composition of 26.70 % or above [12]. Low percentage of alumina reduces the coefficient of thermal expansion of ceramic products as a result of the reaction between alumina and potassium ion [13].The Fe_2O_3 (1.76%) for the NA clay is slightly higher than the recommended value of 1.60%. Composition of Fe_2O_3 less than 2% in clay will lead to whitish color after firing, while that above 2% will tend to change the colour to brownish or ruby-red as a result of oxidation [14].The percentage of CaO and MgO in the clay sample is within the standard value; 0.3% and 0.2%.respectively. High percentage of CaO and MgO may increase the shrinkage value of the materials when fired.

As observed from the graph (Figure 3.1), L.O.I. increased with increase in temperature for the entire specimen (10%, 20% and 30%) of cullet. At 1,000°C and above, which is the sintering temperature; the loss of mass was constant, indicating that the reaction (dehydration, burning-off of the impurities, etc.) is almost completed. Increasing the amount of cullet in the mixture reduces loss of mass as observed in the research. The values for L.O.I obtained for different batches of the mixtures were within the range as recommended [15].The moisture content of the clay sample is 9.5% which is within the recommended range of 8-10% an indication that a moderate addition of water will be required.

The chart showing the comparative analysis of the physical properties of the clay sample is displayed in Figure 3.5. The average fired linear shrinkage for the samples are within the recommended values of 4–6 % [16, 17] (see Table 3.3). Higher shrinkage value may result in warping or cracking of the ceramic products during firing. 20-30% addition of cullet in NA clay recorded no visible change in the fired linear shrinkage of the mix below 1,000^{o}C. At 1,000^{o}C and above, there was an increase in fired linear shrinkage for samples with 10-30% cullet which may be due to the presence of fluxing oxides (Figure 3.3). Firing at 1,200^{o}C, the fired linear shrinkage went above the recommended maximum limit of 6% which led to cracking of the ceramic products [18].

The apparent porosity (A.P) for NA clay is 27.77% which falls within the standard values of 10–30 % which is the recommended value [15]. With the increase in firing temperature, the value for A.P tended to decrease and this may be attributed to the densification of the samples that occurred at a greater stage of the firing. The apparent porosity of the mix (N1, N2, and N3) was approximately 30% at 800^{o}C and 900^{o}C. At 1,000^{o}C and above, there was a continuous fall in A.P for different cullet percentages added. At 1,200^{o}C, a greater decrease in A.P (A.P < 15%) was recorded at 30% cullet addition due to the burning off of some impurities. On the other hand, low percentage of apparent porosity enhances the entrapping of gases in the ceramic products which may be responsible for large number of pinholes on the glazed tiles (N3) and this phenomenon will adversely affects the life span of the tiles when in use [19].

The average bulk density of the clay is shown in Table 3.3 and this value fall within the recommended values of the range of 1.7–2.1g/cm^3 for ceramic tiles [15]. This shows that the clay can be used for the purpose it was intended for. However, the ceramic mass containing 10-30% cullet present a decrease in bulk density with increasing firing temperature, which may be due to the presence of some impurities, such as, TiO_2, CaO and K_2O.

The compressive strength of NA clay was 27.60MPa and it was within the standard values of 22.9-59MPa [15]. Thus, the NA clay when processed into tiles will have strong resistance to load. The strength characterizations of the blended samples show that, the compressive strength varies from 13.8–27.60MPa with respect to firing temperature (Figure 3.4). For the samples fired at 900^{o}C, there was an initial increase in strength with the addition of the cullet. Firing to 1,050°C witnessed gradual increase in strength for 10%-30% cullet addition.

The thermal shock resistances of the samples were within the acceptable values of 26-30 cycles [20]. This result is a pointer to a better performance of the ceramic products when used for the purpose they were intended for.

As shown in Figure 3.2, a reasonable decrease of water absorption was observed for all samples as the percentage of addition of cullet increases. This decrease was found to be more pronounced on firing at 1,025°C and 1,100°C.This may be due to cohesion between the particles of the mix.

Biscuit firing of mix N1, N2, and N3 came out without crack on the ceramic bodies, while samples N had cracks and pinholes. The cracks may be due to the original nature of virgin material. Blending with cullet showed lower pinholes compared with N. It can be observed from Figure 3.2 that, the blended samples have low water absorption compared with original material. The water absorption experienced a significant reduction over a short range of temperature. It means that the addition of cullet to NA clay will drastically reduce the firing temperature and consequently the time of firing.

Table3.1: Chemical Analysis of the Broken Bottles (Cullet) as compared with Breef (2009)

S/No.	Parameters	Level detected (%)	Level detected(%){BREF,2009}
1.	Siliconoxide (SiO_2)	71.08	71-75
2.	Aluminum oxide (Al_2O_3)	1.05	-
3.	Magnesium oxide (MgO)	0.76	-
4.	Calcium oxide (CaO)	11.19	10-15
5.	Zinc oxide (ZnO)	0.02	-
6.	Sodium dioxide(Na_2O)	14.52	12-16
7.	Potassium oxide (K_2O)	0.01	-

Table 3.2: Chemical Analysis of Nkwo-Alaike Clay

S/No.	Parameter	Chemical Analysis (%)	
		Nkwo-Alaike	*Standard
1	SiO_2	56.7	40-60
2	Al_2O_3	26.55	25-45
3	Fe_2O_3	1.76	1-5
4	MgO	0.30	0.2-1
5	CaO	0.20	0.2-1
6	Na_2O	0.85	<2.0
7	K_2O	0.08	<2.0
8	TiO_2	1.68	<2.0
9	LOI	9.76	5-14

***Grimshaw R.W (1971); Chesti J.H (1973)**

Table3.3: Physical and Thermal Properties of Nkwo-Alaike Clay

Properties	Nkwo-Alaike	*Standard
Fired Linear Shrinkage (%)	4.0	4-6
Apparent Porosity (%)	27.77	10-30
Bulk Density (g/cm^3)	1.72	1.7 – 2.1
Compressive Strength (MPa)	27.60	22.9-59
Thermal Shock Resistance (No of Cycles)	26	20-30
Moisture Content (%)	9.50	8-12.00
Water Absorption (%)	2.64	2.6-2.7

***Grimshaw R.W (1971); Chesti J.H (1973)**

Table 3.4: Biscuit Firing Result

S/N	Test Specimen (Clay : Cullet)	Observations	
		Biscuit Firing	Glaze Firing
1	N (100:0)	Has cracks	-
2	N1(90:10)	Fine	Shiny surface
3	N2(80:20)	Fine	Few pinholes
4	N3(70:30)	Fine	Few pinholes

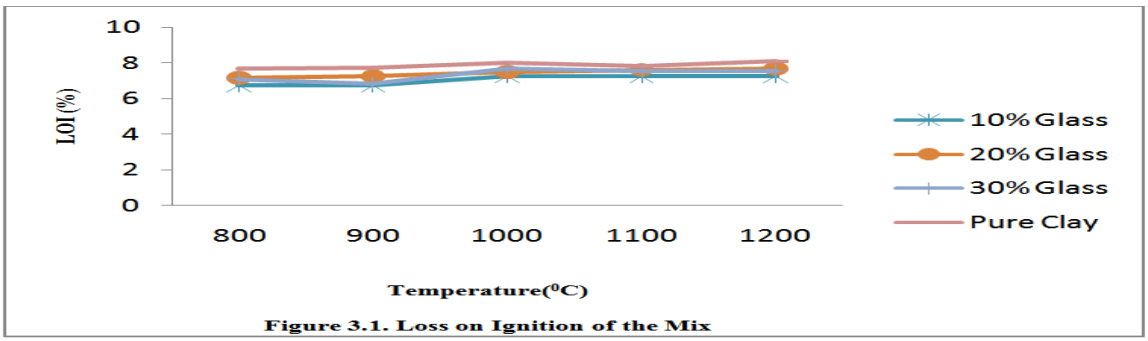

Figure 3.1. Loss on Ignition of the Mix

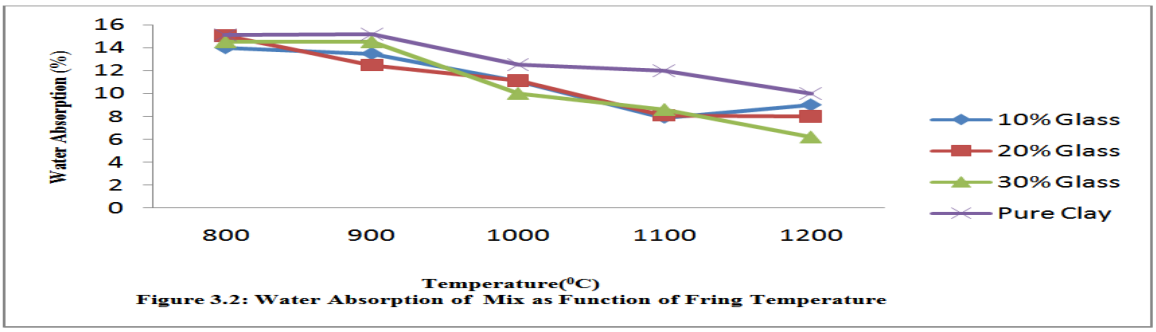

Figure 3.2: Water Absorption of Mix as Function of Fring Temperature

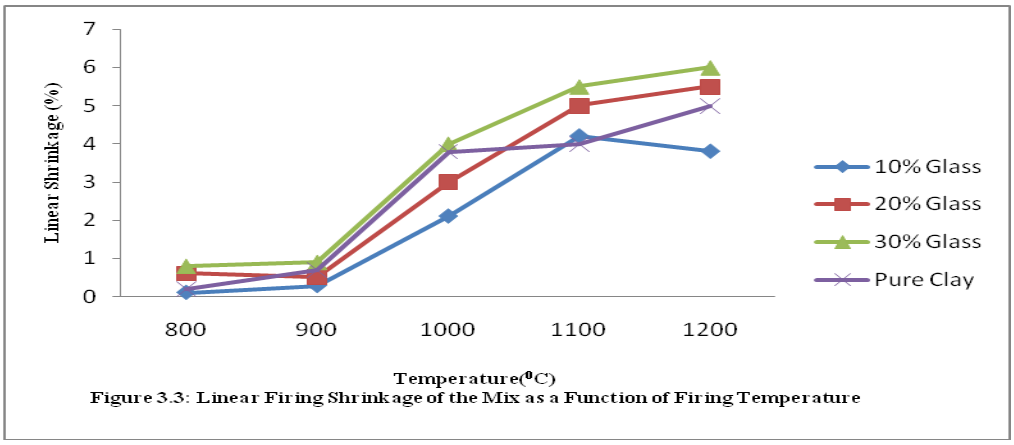

Figure 3.3: Linear Firing Shrinkage of the Mix as a Function of Firing Temperature

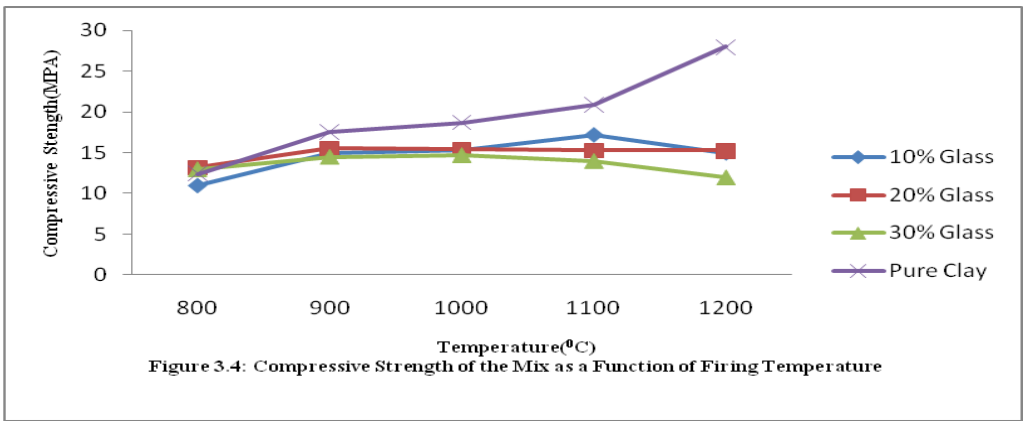

Figure 3.4: Compressive Strength of the Mix as a Function of Firing Temperature

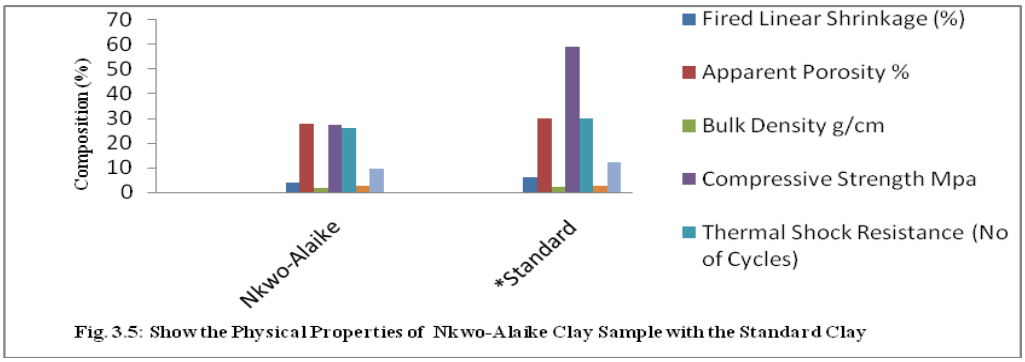

Fig. 3.5: Show the Physical Properties of Nkwo-Alaike Clay Sample with the Standard Clay

***Grimshaw R.W (1971); Chesti J.H (1973)**

IV. CONCLUSION

From the results obtained from all the experiment carried out, it shows that, it is possible to utilize broken bottles (cullet) as alternative raw material (reducing the primary raw material usage) to lower the sintering temperature during the production of ceramic wares. With the addition of cullet which served as fluxing agent during the firing process, the firing shrinkage was curtailed as well. The additions of cullet lower the water absorption of the tiles as observed.

It was established that during firing, cullet accelerate the densification process in the system and this was clearly shown in the results. The addition of cullet to clay for the production of ceramic tiles has economic value, that is, reduction of the firing temperature and time leading to energy savings. There was also an improvement in the physical properties of the ceramic tiles produced. The compressive strength of the samples produced range from 13.68–28.61 MPa and the results obtained generally confirmed that, blending of Nkwo-Alaike with cullet for the production of ceramic tiles will yield good ceramic products.

REFERENCES

[1] Andreola, F., Barbieri, L., Corradi, A., Lancellotti, I. and Manfredini, T. (2002) Utilisation of municipal incinerator grate slag for manufacturing of porcelainized stoneware tiles manufacturing. Journal of the European Ceramic Society, 22, 1457–1462.

[2] Gennaro, R., Cappelletti, P., Cerri, G., Gennaro, M., Dondi, M., Guarini, G., Langella, A. and Naimo D. (2003) Influence of zeolites on the sintering and technological properties of porcelain stoneware tiles. Journal of the European Ceramic Society, 23, 2237–2245.

[3] Tucci, A., Esposito, L., Rastelli, E., Palmonari, C. and Rambaldi, E. (2004) Use of soda-lime scrap-glass as a fluxing agent in a porcelain stoneware tile mix. Journal of the European Ceramic Society**,** 24, 83–92use in Masonry Construction subjected to Chemical Environment".

[4] Torres, P., Fernandes, H.R., Agathopoulos, S., Tulyaganov, D.U. and Ferreira, J.M.F. (2004) Incorporation of granite cutting sludge in industrial porcelain tile formulations. Journal of the European Ceramic Society, 24, 3177–3185.

[5] Bragança, S.R., Licenzi, J., Guerino, K. and Bergmann, C.P. (2006) Recycling of iron foundry sand and glass waste as raw material for production of whiteware. Waste Management & Research, 24, 60–66.

[6] Karamanova, E., Andreola, F., Lancelloti, I., Barbieri, L. and Karamanov, A. (2007) Recycling of CRT waste glass in porcelain stoneware production. In: Proc. of 7th International SGEM Conference 'Modern Management of Mine Producing, Geology and Environmental Protection', June 2007, Albena, Bulgaria (CD), SGEM-Society, Sofia, Bulgaria.

[7] Zanelli, C., Baldi, G., Dondi, M., Ercolani, G., Guarini, G. and Raimondo, M. (2008) Glass ceramic frits for porcelain stoneware bodies: effects on sintering, phase composition and technological properties. Ceramics International, 34: 455–465.

[8] Ergul, S., Akyildiz, M. and Karamanov, A. (2007) Ceramic material from basaltic tuffs. Industrial Ceramics, 37: 75–80.

[9] Hlavac, J. (1983), "The Technology of Glass and Ceramics: an Introduction. Elsevier, Amsterdam".

[10] ASTM, 1989 "Standard Test Methods for Refractories ,Carbon, Graphite Products, Activated Carbon, Vol. 15.1, Pcn1-150189-60,"

[11] Nwannenna, O.C., Ogunro, A. S., Apeh, F. I., (2015) "Comparative Study on the Addition of Cullet to Mowe and Ibamajo Clays for Ceramic Tiles Production" IISTE, Chemical and Material Research, Vol. 7, No. 4, pp 16-25.

[12] Ryan, W.C (1978), Properties of Ceramic Raw Materials, Oxford, Paragon Press, pp.6.

[13] El-Kheshen, A. A (2003), Effect of alumina addition and the properties of glass/ceramic composite, Science direct on Line, Vol.102, issue 5, pp 205-209.

[14] Singer F. and Singer S. (1993) Industrial Ceramic, London Chapman and Hill Limited, Pp. 234, Society Bulletin, 79, 23–29.

[15] Omowumi O.J (2000) "Characterization of some Nigerian clays as Refractory materials for Furnace Lining", NJCM, Vol. 2, No. 3, pp1-4.

[16] Chester, J. H. (1973), "Refractories, Production and Properties", the Iron and Steel Institutes, London, pp. 4-13, 295-315.

[17] Grimshaw, R.W(1971) "The Chemistry and Physics of Clay and Allied Ceramics Materials", 4th Edition Revised New York, Wiley Interscience pp15

[18] Macedo, R.S., Galdino, A.G.S., Morais, C.R.S., Ferreira, H.C. (1996), "Estudo Preliminar De Argilas Do Estado Da Paraíba Parautiliza çãocomo Matéria-Prima EmCerâmica Vermelha: Parte I", Cerâmica, V. 42, N.275, Pp. 259.

[19] Gupta, O.P. (2008), Elements of Fuels, Furnaces and Refractories" 5th edition, second reprint, Khanna Publishers, New Delhi-110006.

[20] De Bussy J. H. (1972), Mineral and Technology, Non-metallic ores silicate Industries and Solid minerals fuels volume 2 Longman Group Limited pp 267 – 290.

American Journal of Engineering Research (AJER) 2016
American Journal of Engineering Research (AJER)
e-ISSN: 2320-0847 p-ISSN : 2320-0936
Volume-5, Issue-2, pp-182-188
www.ajer.org
Research Paper Open Access

Analysis of an Improved SIRS Epidemic Model with Disease Related Death Rate and Emigration Rate

Shivram Sharma[1], V.H. Badshah[1], Vandana Gupta[2]
[1]*School of Studies in Mathematics, Vikram University, Ujjain (M.P.), India*
[2]*Govt. Kalidas Girls' College, Ujjain (M.P.), India*
[1]shivramsharmajnu85@gmail.com,[1]vhbadshah@gmail.com,
[2]drvg1964@gmail.com

Abstract: *In this paper, we consider an SIRS epidemic model with an asymptotically homogeneous transmission function, disease related death rate and emigration rate. We obtain the disease free and endemic equilibrium. We also establish the conditions for the global stability of the equilibriums. An example is also furnished which demonstrates validity of main result.*

Keywords*: SIRS model, Transmission function, Basic reproductive number, disease-free equilibrium, endemic equilibrium, Stability.*
2010 AMS Subject Classification: 34D23; 93A30; 93D20.

I. Introduction

A mathematical model is a description of a system using mathematical concept and language. Mathematical models are used not only in the natural sciences and engineering disciplines but also in the social sciences. The first SIR epidemic model was proposed by Kermack and Mckendrick [23] in the year 1927. The SIRS epidemic model has been studied by many authors (see [1-5], Hethcote [16, 17], Capasso and Serio [9], Mena-Lorca [29]) and the different epidemic models have been proposed and studied in the literature (see Hethcote and Tudar [19], Lie et al. [25, 26], Hethcote et al. [20], Hethcote and Van den Driessche [21], Derrick and Vanden Driessche [12], Berretta and Takeuchi [6, 7], Beretta et al. [8], Ma et al. [27, 28], Ruan and Wang [32],Song and Ma [33], Song et al. [34], D'onofno et al. [13], Xiao and Ruan [35]).

Bilinear and standard incidence rates have been frequently used by many authors [18, 10, 29, 30, 24, 14 and 22]. Disease transmission is a dynamical process driven by the interaction between the susceptible and the infective. The behaviour of the SIRS models are greatly affected by the way in which transmission between infected and the susceptible individuals are modelled. Many models of epidemiology are based on the so called "mass action" assumption for transmission. During the last few decades, such assumptions have faced some questions and consequently a number of realistic transmission functions have become the focus of considerable attention (Capasso and Serio [9], Lie et al. [25, 26], Hethcote et al. [20], Hethcote and Van den Driessche [21], Ruan and Wang [32], Xiao and Ruan [35]). Pathak et al. [31] have considered an SIR epidemic model with an asymptotically homogeneous transmission function.

In this paper we consider an SIRS epidemic model with an asymptotically homogeneous transmission function, disease related death rate and emigration rate. In the next section, we give basic definitions. In the third section, we present the model and derive the disease free equilibrium and the endemic equilibrium. In the fourth section, we prove some theorems for the global stability of the disease free and endemic equilibrium. The fifth section contains an example which demonstrates validity of main result. In the last section, we give conclusion.

II. Preliminaries

Definition 2.1 The incidence in an epidemiological model is the rate at which susceptible become infectious. If the unit time is days, then the incidence is the number of new infection per day.

Definition 2.2 The average number of secondary infections produced by one infected individuals during the mean course of infection (infectious period) in a completely susceptible population is called a basic reproductive number or simply the reproductive number σ .

Definition 2.3 SIRS means the recovered individuals have only temporary immunity after they recovered from infection.

III. The mathematical model

The proposed model is the nonlinear ordinary differential equations:

$$\begin{aligned}
\frac{dX}{dt} &= (A - B) - \frac{\beta XY}{1 + aX + bY} - dX + \delta Z \\
\frac{dY}{dt} &= \frac{\beta XY}{1 + aX + bY} - (\gamma + \alpha + d)Y \qquad (3.1) \\
\frac{dZ}{dt} &= \gamma Y - (\delta + d)Z \\
\frac{dN}{dt} &= (A - B) - dN - \alpha Y
\end{aligned}$$

Where $N(t)$ is the total varying population size as a function of time t, and $X(t), Y(t), Z(t)$ denote the number of individuals who are susceptible, infectious and recovered at time t, respectively and $X(t) + Y(t) + Z(t) = N(t)$, A is the constant immigration rate of the population, B is the emigration rate of the population, d is the natural death rate of the population, β is the transmission coefficient, α is the disease-related death rate constant, γ is the natural recovery rate of the infective individuals, δ is the loss of immunity rate constant, a and b are the parameters which measure the effects of sociological, psychological or other mechanisms. We assume that d, α and δ are nonnegative and that A, B, β, γ and $\delta + d$ are positive.

Where $N = X + Y + Z$. In the absence of disease i.e. $\alpha = 0$ the population size approaches the constant size $\frac{A - B}{d}$. For the asymptotically transmission function the contact number or basic reproduction number is

$$\sigma = \frac{\beta(A - B) - (A - B)a(\gamma + \alpha + d)}{d(\gamma + \alpha + d)}. \qquad (3.2)$$

For the system (3.1) the first octant in XYZ space is positively invariant. Because $\frac{dN}{dt} < 0$ for $N > \frac{A - B}{d}$, all paths in the first octant approach, enter or stay inside the subset $T = \left\{(X, Y, Z) : X + Y + Z \le \frac{A - B}{d}\right\}$. The continuity of the right side of (3.1) and its derivatives implies that unique solutions exits on a maximal time interval. Since solutions approach, enter or stay in T, they are eventually bounded and hence exist for all positive time [11]. We first consider the existence of equilibrium of system (3.1).

For any values of parameter, model (3.1) always has a disease-free equilibrium $P_o = \left(\frac{A - B}{d}, 0, 0\right)$. To find the positive equilibria, set

$$\begin{aligned}
(A - B) - \frac{\beta XY}{1 + aX + bY} - dX + \delta Z &= 0 \\
\frac{\beta XY}{1 + aX + bY} - (\gamma + \alpha + d)Y &= 0 \qquad (3.3) \\
\gamma Y - (\delta + d)Z &= 0 \\
(A - B) - dN - \alpha Y &= 0
\end{aligned}$$

IV. Main results

Theorem 4.1. From the system (3.2) it follows that

(i) if $\sigma \le 1$, then there is no positive equilibrium;

(ii) if $\sigma > 1$, then there is a unique positive equilibrium $P_e = (X_e, Y_e, Z_e)$ of the system (3.1), called the "endemic equilibrium", given by

$$X_e = \frac{(\gamma + \alpha + d)(1 + bY_e)}{\beta - a(\gamma + \alpha + d)}$$

$$Y_e = \frac{(\delta + d)[(A - B)\beta - (\gamma + \alpha + d)\{(A - B)a + d)\}]}{bd(\gamma + \alpha + d)(\delta + d) + [\alpha(\delta + d) + d(\gamma + \alpha + d)][\beta - a(\gamma + \alpha + d)]}$$

$$Z_e = \frac{\gamma Y_e}{\delta + d} \qquad (4.1)$$

$$N_e = \frac{(A - B) - \alpha Y_e}{d}$$

It is clear that the limit set of system (3.1) is on the plane $X + Y + Z = \frac{A - B}{d}$. Thus we focus on the reduced system

$$\frac{dY}{dt} = \frac{d\beta Y}{(d + aA) + (b - a)dY - adZ}\left(\frac{A - B}{d} - Y - Z\right) - (\gamma + \alpha + d)Y \equiv P(Y, Z)$$

$$\frac{dZ}{dt} = \gamma Y - (\delta + d)Z \equiv Q(Y, Z) \qquad (4.2)$$

Theorem 4.2. System (4.2) does not have nontrivial periodic orbits if $(2d + \gamma + \delta + \alpha)(b - a) > a\gamma$.

Proof. Since $Y > 0$ and $Z > 0$. Take a Dulac function

$$D(Y, Z) = \frac{\{d + a(A - B)\} + (b - a)dY - adZ}{d\beta Y}.$$

We have

$$\frac{\partial(DP)}{\partial Y} + \frac{\partial(DQ)}{\partial Z} = -1 - \frac{(\delta + d)\{d + a(A - B)\}}{d\beta Y} - \left[(2d + \gamma + \delta + \alpha)(b - a) - a\gamma\right] < 0$$

if $(2d + \gamma + \delta + \alpha)(b - a) > a\gamma$

In order to study the properties of the disease-free equilibrium P_0 and the endemic equilibrium P_e.

Theorem 4.3. The equilibrium $P_o = \left(\frac{A - B}{d}, 0, 0\right)$ is locally asymptotically stable if $\sigma \le 1$ and P_o is saddle point if $\sigma > 1$.

Proof. The Jacobian of system (3.1) at P_o is

$$J(P_o) = \begin{pmatrix} -d & -\frac{\beta(A - B)}{d + a(A - B)} & \delta \\ 0 & \frac{\beta(A - B)}{d + a(A - B)} - (\gamma + \alpha + d) & 0 \\ 0 & \gamma & -(\delta + d) \end{pmatrix}$$

The characteristic equation is

$$(d+t)(\delta+d+t)\left[\frac{\beta(A-B)}{d+a(A-B)}-(\gamma+\alpha+d)-t\right]=0 \qquad (4.3)$$

The roots of (4.3) are

$$-d,\ -(\delta+d) \text{ and } \frac{\beta(A-B)}{d+a(A-B)}-(\gamma+\alpha+d)$$

The first two roots having negative real parts and third root $\frac{\beta(A-B)}{d+a(A-B)}-(\gamma+\alpha+d)$ will have negative real part if $\sigma \le 1$. Thus all roots of (4.3) have negative real parts so P_o is locally asymptotically stable if $\sigma \le 1$ and the root $\frac{\beta(A-B)}{d+a(A-B)}-(\gamma+\alpha+d)$ will have positive real part if $\sigma > 1$ so P_o is saddle point.

Theorem 4.4. The equilibrium $P_o=\left(\frac{A-B}{d},0,0\right)$ is globally asymptotically stable if $\sigma \le 1$.

Proof. Since the set $T=\left\{(X,Y,Z): X+Y+Z \le \frac{A-B}{d}\right\}$ is attractive and positive invariant.

To prove that all paths in T approach $P_o=\left(\frac{A-B}{d},0,0\right)$ for $\sigma \le 1$, define the Liapunov function $L=Y$ in T with

$$\frac{dL}{dt}=\frac{dY}{dt}=\left[\frac{\beta X}{1+aX+bY}-(\gamma+\alpha+d)\right]Y \le 0. \qquad (4.4)$$

The Lasalle-Liapunov theory [15] implies that all paths in T approach the largest positively invariant subset of the set T where $\frac{dL}{dt}=0$.

Here $\frac{dL}{dt}=0$ only if $Y=0$ or $(X,Y,Z)=P_o$. The positively invariant subset of the plane $Y=0$ is the point P_o so P_o is globally asymptotically stable for $\sigma \le 1$. To study the properties of the endemic equilibrium P_e. Let us define

$$x=\frac{\beta}{\delta+d}Y,\quad y=\frac{\beta}{\delta+d}Z,\quad \tau=(\delta+d)t$$

We obtain

$$\frac{dx}{d\tau}=\frac{px}{1+qx-ry}(K-x-y)-mx,$$
$$\frac{dy}{d\tau}=sx-y, \qquad (4.5)$$

Where

$$p=\frac{d}{d+a(A-B)},\quad q=\frac{(\delta+d)d(b-a)}{\beta\{d+a(A-B)\}},\quad r=\frac{a(\delta+d)d}{\beta\{d+a(A-B)\}},$$
$$K=\frac{(A-B)\beta}{d(\delta+d)},\quad m=\frac{\gamma+\alpha+d}{\delta+d},\quad s=\frac{\gamma}{\delta+d}.$$

For equilibrium point set,

$$\frac{dx}{d\tau} = 0 \text{ and } \frac{dy}{d\tau} = 0$$

We obtain, two equilibrium point $(0,0)$ and (x_e, y_e) where

$$x_e = \frac{Kp - m}{p(1+s) + m(q - rs)}, \quad y_e = sx_e$$

The trivial solution $(0,0)$ of system (4.5) is the disease-free equilibrium P_o of model (3.1) and the unique positive equilibrium (x_e, y_e) of system (4.5) is the endemic equilibrium P_e of model (3.1) if and only if $Kp - m > 0$ and $q - rs > 0$.

Theorem 4.5. Suppose $m - Kp < 0$, then there is a unique endemic equilibrium (x_e, y_e) of model (4.5) which is a stable node.

Proof. The Jacobian of system (4.5) at (x_e, y_e) is

$$J = \begin{pmatrix} \frac{px_e[sx_e(r+q) - (1+Kq)]}{(1+qx_e - rsx_e)^2} & \frac{px_e[(Kq-1) - x_e(r+q)]}{(1+qx_e - rsx_e)^2} \\ s & -1 \end{pmatrix}$$

$$\det J = \frac{px_e[(1+s) + K(q - rs)]}{(1+qx_e - rsx_e)^2}$$

Since $q > rs, \det(J) > 0$ when $m - Kp < 0$ and

$$tr(J) = \frac{[ps(r+q)x_e - p(1+Kq)]x_e - [x_e(rs - q) - 1]^2}{(1+qx_e - rsx_e)^2}$$

The sign of $tr(J)$ is determined by

$S = [ps(r+q)x_e - p(1+Kq)]x_e$. Substituting $x_e = \frac{Kp - m}{p(1+s) + m(q - rs)}$ into S, We have

$$S = \frac{p[-K(p+mq)(q-rs) - (mqs + mq + p + ps)](Kp - m)}{[p(1+s) + m(q-rs)]^2}.$$

Since $q > rs$, $[p(1+s) + m(q-rs)]^2 > 0$ and, $[-K(p+mq)(q-rs) - (mqs + mq + p + ps)] < 0$

hence $S < 0$ if $m - Kp < 0$. However, when $m - Kp < 0$, we have $tr(J) < 0$.

This completes the proof.

Theorem 4.6. The equilibrium $P_e = (X_e, Y_e, Z_e)$ is globally asymptotically stable if $\sigma > 1$.

Proof. The proof can be obtained by theorem 4.5.

V. Example

In this section, we give an example to demonstrate the results obtained in the previous sections.

Example 5.1. We take the parameters of the system as $d = 2.37, a = 3.5, b = 3, A = 6.5, B = 3, \delta = 1.2, \alpha = 0.19, \beta = 10, \gamma = 0.20$. Then $P_O = (1.4768, 0, 0)$ and $\sigma = 0.1819 < 1$. Therefore, by theorem 4.4, P_O is a global asymptotically stable in the first octant.

Now we take the parameter of the system as $d = 0.37, a = 3.5,$

$b = 3,\ A = 6.5,\ B = 3,\ \delta = 1.2,\ \alpha = 0.19,\ \beta = 5,\ \gamma = 0.20.$

Then $P_e = (4.8307, 4.6245, 0.5891)$ and $\sigma = 29.1252 > 1$. Therefore, by theorem 4.6, P_e is a global asymptotically stable in the interior of the first octant.

VI. Conclusion

In this paper, we have considered the rich dynamics SIRS epidemic model with an asymptotically homogeneous transmission function, disease related death rate and emigration rate. We have carried out the global qualitative analysis of a realistic SIRS model. Our main results shows that when $\sigma \leq 1$, the disease-free equilibrium P_O is globally asymptotically stable. When $\sigma > 1$, the endemic equilibrium $P_e = (X_e, Y_e, Z_e)$ exists and is globally asymptotically stable.

References

[1] Anderson, R.M., May, R.M., "Population biology of infectious diseases. I", Nature, 280: 361-367, (1979).

[2] Anderson, R.M., May, R.M., "Population dynamic of micro-parasites and their invertebrate hosts", Phil. Trans. Roy. Soc. London B., 291: 451-524, (1981).

[3] Anderson, R.M., Jackson, H.C., May, R.M., Smith, A.D.M., "Population dynamics of fox rabies in Europe", Nature, 289: 765-777, (1981).

[4] Anderson, R.M., "Transmission dynamics and control of infectious disease agents", In: Anderson R.M., May, R.M. (eds.) Population biology of infectious diseases, New York Heidelberg Berlin, Springer, 149-176, (1982a).

[5] Anderson, R.M., "Directly transmitted viral and bacterial infectious of man", In: Anderson R.M. (eds.) Population dynamics of infectious diseases, London New York: Chapman and Hall, 1-37, (1982b).

[6] Beretta, E., Takeuchi, Y., "Global stability of a SIR epidemic model with time delay", J. Math. Biol., 33: 250-260, (1995).

[7] Beretta, E., Takeuchi, Y., "Convergence results in SIR epidemic model with varying population sizes", Nonlinear Anal., 28: 1909-1921, (1997).

[8] Beretta, E., Hara, T., Ma, W., Takeuchi, Y., "Global asymptotic stability of a SIR epidemic model with distributed time delay", Nonlinear Anal., 47: 4107-4115, (2001).

[9] Capasso, V., Serio, G., "A generalization of the Kermack-McKendrick deterministic epidemic Model", Math. Biosci., 42: 43-61, **(**1978**).**

[10] Chamchod, F. and Britton, N.F., "Analysis of vector bias model on malaria transmission", Bulletin of Mathematical Biology, 73(3): 639-657, (2011).

[11] Coddington, E. A., Levinson, N., "Theory of ordinary differential equation", MaGraw-Hill, New York, (1995).

[12] Derrick, W.R., Van den Driessche, P., "A disease transmission model in nonconstant population", J. Math. Biol., 31: 495-512, (1993).

[13] D'Onofrio, A., Manfredi, P., Salinelli, E., "Bifurcation thresholds in an SIR model with information-dependent vaccination", Mathematical Modelling of Natural Phenomena, 2: 23-38, (2007).

[14] Gabriela, M., Gomes, M., White, L.J. and Medley, G.F., "Reinfection threshold", Journal of Theoretical Biology, 236(1): 111-113, (2005).

[15] Hale, J.K., "Ordinary differential equations", Wiley-Interscience, New York, (1969).

[16] Hethcote, H.W., "Qualitative analysis for communicable disease models", Math. Biosci., 28: 335-356, (1976).

[17] Hethcote, H.W., "Three basic epidemiological models", In: Gross, L., Hallam, T.G., Levin, S.A. (eds.) Applied mathematical ecology, Berlin Heidelberg New York, Springer, 119-144, (1989).

[18] Hethcote, H.W. and Van den Driessche, P., "An SIS epidemic model with variable population size and a delay", Journal of Mathematical Biology, 34(2): 177-194, (1995).

[19] Hethcote, H.W., Tudor, D.W., "Integral equation models for endemic infectious diseases", J. Math. Biology, 9: 37-47, (1980).

[20] Hethcote, H.W., Lewis, M.A., Van den Driessche, P., "An epidemiological model with delay and a nonlinear incidence rate", J. Math. Biology, 27: 49-64, (1989).

[21] Hethcote, H.W., Van den Driessche, P., "Some epidemiological model with nonlinear incidence", J. Math. Biology, 29: 271-287, (1991).

[22] Jiang, Z. and Wei, J., "Stability and Bifurcation Analysis in a delayed SIR model", Chaos solitons and Fractals, 35(3): 609-619, (2008).

[23] Kermack, W.O., McKendrick, A.G., "Contribution to mathematical theory of epidemics", P. Roy. Soc.

Lond. A Mat., 115: 700-721, (1927).
[24] Li, Y.M., Graef, J.R., Wang, L. and Karsai, J., "Global dynamics of a SEIR model with varying total population size", Mathematical Bioscience, 160(2): 191-213, (1999).
[25] Liu, W.M., Hethcote, H.W., Levin, S.A., "Dynamical behaviour of epidemiological models with nonlinear incidence rates", J. Math. Biology, 25: 359-380, (1987).
[26] Liu, W.M., Levin, S.A., Iwasa, Y., "Influence of nonlinear incidence rates upon the behaviour of SIRS epidemiological models", J. Math. Biology, 23: 187-204, (1986).
[27] Ma, W., Song, M., Takeuchi, Y., "Global stability of an SIR epidemic model with time-delay", Appl. Math. Lett., 17: 1141-1145, (2004).
[28] Ma, W., Takeuchi, Y., Hara, T., Beretta, E., "Permanence of an SIR epidemic model with distributed time delays", Tohoku Math. J., 54: 581-591, (2002).
[29] Mena-Lorca, J.M., Hethcote, H.W., "Dynamic models of infectious diseases as regulators of population sizes", J. Math. Biology, 30: 693-716, (1992).
[30] Mishra, B.K. and Saini, D.K., "SEIRS epidemic model with delay for transmission of malicious objects in computer network", Applied Mathematics and Computation, 188(2): 1476-1482, (2007).
[31] Pathak, S., Maiti, A., Samanta, G.P., "Rich dynamics of an SIR epidemic model", Nonlinear Analysis: Modelling and Control, 15(1): 71-81, (2010).
[32] Ruan, S., Wang, W., "Dynamical behaviour of an epidemic model with nonlinear incidence rate", J. Differ. Equations, 188: 135-163, (2003).
[33] Song, M., Ma, W., "Asymptotic properties of a revised SIR epidemic model with density dependent birth rate and tie delay", Dynamic of Continuous, Discrete and Impulsive Systems, 13: 199-208, (2006).
[34] Song, M., Ma, W. Takeuchi, Y., "Permanence of a delayed SIR epidemic model with density dependent birth rate", J. Comput. Appl. Math., 201: 389-394, (2007).
[35] Xiao, D., Ruan, S., "Global analysis of an epidemic model with nonmonotone incidence rate", Math. Biosci. 208: 419-429, (2007).

American Journal of Engineering Research (AJER) 2016
American Journal of Engineering Research (AJER)
e-ISSN: 2320-0847 p-ISSN : 2320-0936
Volume-5, Issue-2, pp-189-198
www.ajer.org
Research Paper Open Access

Single-Phase Nine-Level Inverter with Novel Pulse Width Modulation Scheme for Resistive-Inductive Load

[1]Gerald C. Diyoke, [1]I. K. Onwuka

[1]*Department of Electrical and Electronic Engineering, Michael Okpara University of Agriculture, UmudikeAbia State Nigeria.*

Abstract: *A single-phase nine-level inverter with a novel pulse width modulation (PWM) scheme for R-L load is presented in this paper. Four triangular carrier signals that are identical to each other with an offset that is equivalent to the amplitude of the sinusoidal reference signal were used to generate the PWM signals. The inverter is capable of producing nine levels of output-voltage levels (Vdc, Vdc/4, Vdc/2, 3Vdc/4, 0,−Vdc,−Vdc/4,−Vdc/2, 3Vdc/4) from the dc supply voltage. In this paper the dc supply is obtained from ac supply which is boosted to a higher amplitude of dc voltage using dc to dc converter. In this paper, Matlab/ Simulink software is used for the system simulation. Hence, the output load voltage, current and FFT plots are obtained. This paper is focused on minimizing the number of semiconductors devices, weights, and costs for a higher number of output voltage levels.*

Index Terms: *Boost converter, modulation index, multilevel inverter, pulse width-modulation (PWM), total harmonic distortion (THD).*

I. INTRODUCTION

The Demand for renewable energy consumption has increased significantly over the years because of shortage of fossil fuels, greenhouse effect and the need to reduce pollution of our environments. Among other definitions of renewable energy include any type of energy generated from natural resources that is infinite or constantly renewed. Examples of renewable energy include solar, wind, and hydro-power. Renewable energy, due to its free availability and its clean and renewable character, ranks as the most promising renewable energy resources such asSolar energy, Wind energy that could play a key role in solving the worldwide energy crisis. Among various types of renewable energy sources, solar energy and wind energy have become very popular and demanding due to advancement in power electronics techniques [1]. In this paper, the dc source is obtained from rectified ac voltage source with uncontrolled single phase rectifier circuit configuration. Consequently, the rectified dc voltage is stepped up using boost dc to dc converter circuit. The stepped up dc voltage is fed to a Hybrid multilevel inverter topology.

Uncontrolled rectifier circuits are of different topologies both in single and multiple phasewith different load configurations. Among them include:

1) Half-wave uncontrolled
2) Full bridge uncontrolled
   I) Mid-point configuration
   II) Full bridge configuration

Six major types of dc to dc converters have been investigated [2]. The Boost dc to dc converter otherwise called step-up converter has a dc voltage gain greater than or equal to the input voltage. The operation is in two different modes namely i) continuous current conduction and ii) discontinuous current conduction. In this paper, the selection of circuit elements were made so that the circuit operates in continuous current conduction mode. At this juncture, the Hybrid inverter topology is connected and the first member of this group is three level. The three-level inverter can satisfy specifications through its very high switching, but it could also unfortunately increase switching losses, acoustic noise, and level of interference to other equipment [3]–[5].Improving its output waveform reduces its harmonic content and, hence, also the size of the filter used and the level of electromagnetic interference (EMI) generated by the inverter's switching operation [6].

In recent years, multilevel inverters have become more attractive for researchers and manufacturers due to their advantages over conventional three level PWM inverters. They offer improved output waveforms, smaller filter size and lower EMI, lower Total Harmonic Distortion (THD).

The three common topologies for multilevel inverters are as follows [7]:
1) Diode clamped (neutral clamped)
2) Capacitor clamped (flying capacitors)
3) Cascaded H-bridge inverter

This paper recounts the development of a novel H-bridge single-phase multilevel inverter that has three diode embedded bidirectional switches and a novel pulse width modulated (PWM) scheme.

This paper is structured as: In section I, the concept of multilevel inverter and basic types are enumerated. Section II presents the proposed H-bridge single-phase nine level inverter and its modes of operation. Section III details how the pulse width modulated (PWM) signals are generated. Here in section IV presents in details the Matlab/Simulink simulation results. In section V conclusion is presented.

II. PROPOSED MULTILEVEL INVERTER CONFIGURATION

The proposed single-phase nine-level inverter was developed from the five-level inverter in [8] – [12]. It comprises a single-phase conventional H-bridge inverter, three bidirectional switches, and a capacitor voltage divider formed by C_1, C_2, C_3, and C_4, as shown in Fig. 1. The modified H-bridge topology is significantly advantageous over other topologies, that is, less power switches, power diodes, and less capacitors for inverters of the same number of levels [3].

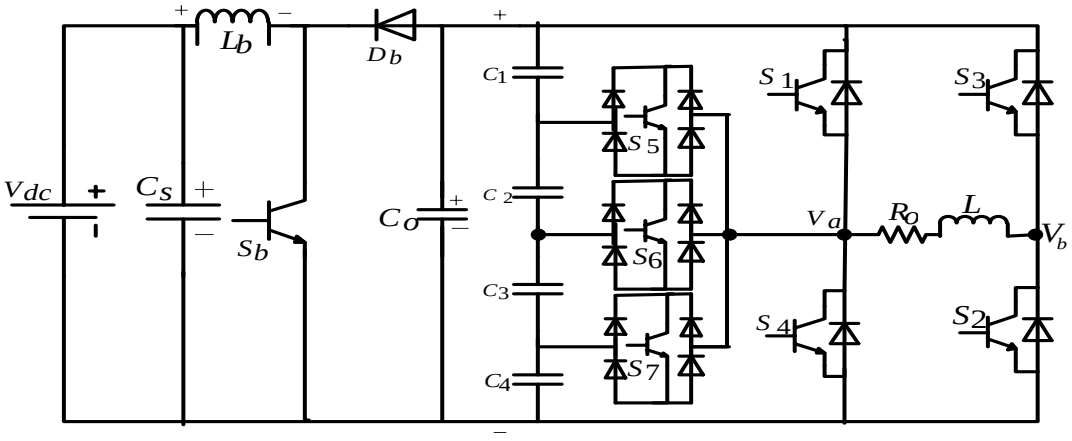

Fig. 1 Proposed single-phase nine-level with R-L load.

A single-phase fully uncontrolled rectifier with a low amplitude was connected to a Boost dc to dc converter with a high duty cycle. The inverter with R-L load was connected to the output voltage of the Boost dc to dc converter which amplifies the inverter input voltage. Proper switching of the inverter can produce nine output voltage levels (Vdc, Vdc/4, Vdc/2, 3Vdc/4, 0, −Vdc, −Vdc/4, −Vdc/2, 3Vdc/4) from the dc supply voltage.

The proposed inverter's operation can be divided into ten switching states, as shown in Fig. 2(a) – (j). The required nine-level of the output voltage were generated as follows.

1) Zero output: This level can be produced by two switching combinations; switches S_2 and S_4 are ON and all other controlled switches are OFF; terminal voltage V_{ab} is short circuited thus the output voltage becomes zero. This action is made possible because V_a and V_b are both connected to zero potential. Fig. 2(a) shows load connection at this stage. Mathematically,
$$V_{ab} = 0 = L\frac{dI_0}{dt} + I_0R_0 \quad (1)$$
2) One-fourth positive output (Vdc/4): The bidirectional switch S_7 is turned ON connecting the load positive terminal, and S_2 ON connecting the load negative terminal to the ground. All other controlled switches are turned OFF. From Fig. 2(b) the applied potential to load is Vdc/4. The mathematical expression is given by equation (2) below.
$$V_{ab} = \frac{V_{dc}}{4} = L\frac{dI_0}{dt} + I_0R_0 \quad (2)$$

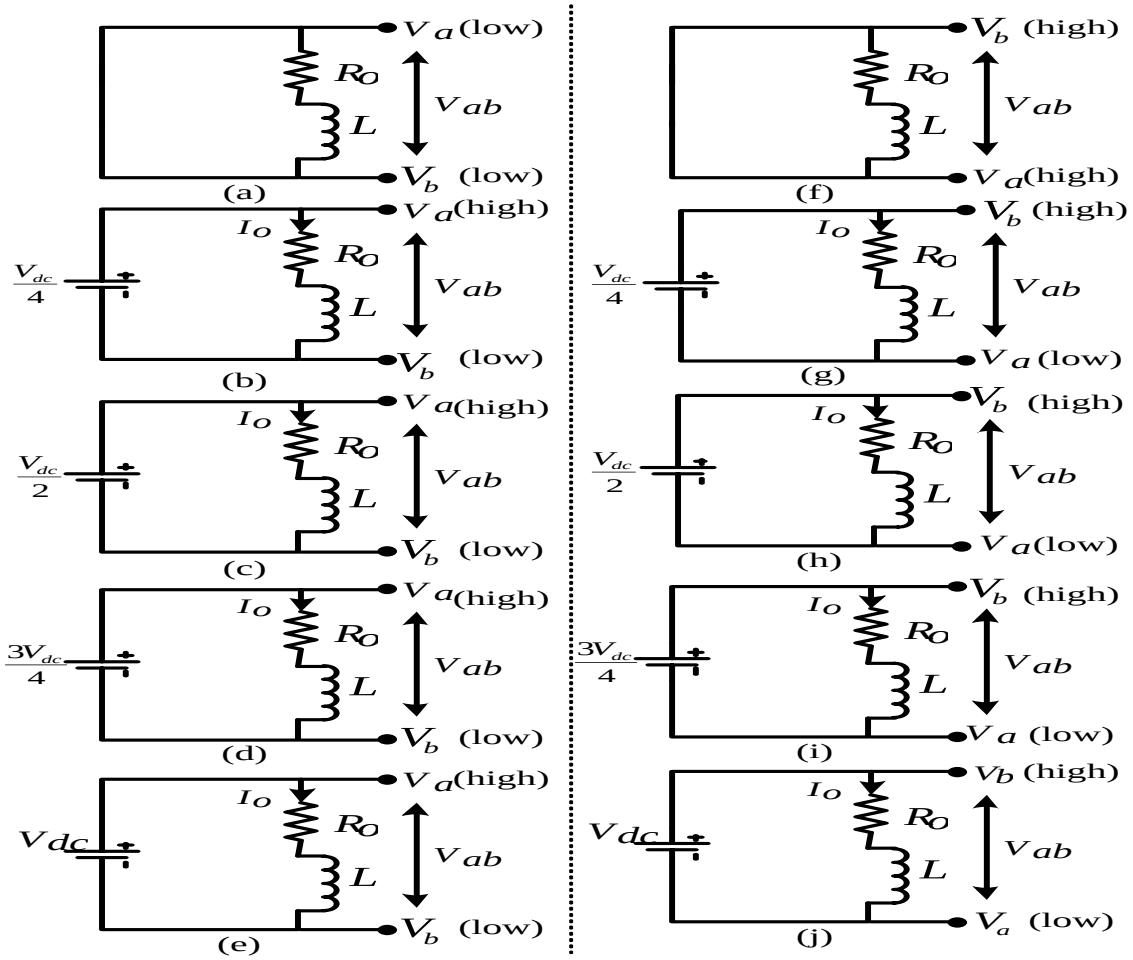

Fig. 2 Output voltage (V_{ab}) under different switching period.

3) One-half positive output(Vdc/2): The bidirectional switch $S_6$is turned ON connecting the load positive terminal, and S_2ON connecting the load negative terminal to the ground. All other controlled switches are turned OFF. From Fig. 2(c) the applied potential to load is Vdc/2. The mathematical expression is given by equation (3) below.

$$V_{ab} = \frac{V_{dc}}{2} = L\frac{dI_0}{dt} + I_0R_0 \quad (3)$$

4) Three-fourth positive output (3Vdc/4): The bidirectional switch $S_5$is turned ON connecting the load positive terminal, and S_2ON connecting the load negative terminal to the ground. All other controlled switches are turned OFF. From Fig. 2(d) the applied potential to load is Vdc/2. The mathematical expression is given by equation (4) below.

$$V_{ab} = \frac{3V_{dc}}{4} = L\frac{dI_0}{dt} + I_0R_0 \quad (4)$$

5) Maximum positive output (V_{dc}): $S_1$is ON, connecting the load positive terminal to V_{dc}, and $S_2$is ON, connecting the load terminal to ground. All other controlled switches are OFF; the voltage applied to the load terminals is V_{dc} as shown in Fig. 2(e). The mathematical expression is given by

$$V_{ab} = V_{dc} = L\frac{dI_0}{dt} + I_0R_0 \quad (5)$$

6) Zero output: This level can be produced by two switching combinations; switches $S_1$and S_3 are ON and all other controlled switches are OFF; terminal voltage $V_{ab}$is short circuited thus the output voltage becomes zero. This action is made possible because $V_a$and V_b are both connected to maximum potential V_{dc}. Fig. 2(f) shows load connection at this stage. Mathematically,

$$V_{ab} = 0 = L\frac{dI_0}{dt} + I_0R_0 \quad (6)$$

7) One-fourth negative output (-Vdc/4): The bidirectional switch $S_5$is turned ON connecting the load positive terminal, and S_3ON connecting the load negative terminal toV_{dc}. All other controlled switches are turned OFF. From Fig. 2(g) the applied potential to load is -V_{dc}/4. The mathematical expression is given by equation (7) below.

$$V_{ba} = -V_{ab} = \frac{-V_{dc}}{4} = L\frac{dI_0}{dt} + I_0R_0 \quad (7)$$

8) One-half negative output (-Vdc/2): The bidirectional switch $S_6$is turned ON connecting the load positive terminal, and S_3ON connecting the load negative terminal to V_{dc}. All other controlled switches are turned OFF. From Fig. 2(h) the applied potential to load is -V_{dc}/2. The mathematical expression is given by equation (8) below.

$$V_{ba} = -V_{ab} = \frac{-V_{dc}}{2} = L\frac{dI_0}{dt} + I_0R_0 \quad (8)$$

9) Three-fourth negative output (-3Vdc/4): The bidirectional switch $S_7$is turned ON connecting the load positive terminal, and S_3ON connecting the load negative terminal to V_{dc}. All other controlled switches are turned OFF. From Fig. 2(i) the applied potential to load is -3V_{dc}/4. The mathematical expression is given by equation (9) below.

$$V_{ba} = -V_{ab} = \frac{-3V_{dc}}{4} = L\frac{dI_0}{dt} + I_0R_0 \quad (9)$$

Table 1:OUTPUT VOLTAGE ACCORDING TO THE SWITCHES' (OFF) 0 – (ON) 1 CONDITION

States	S_1	S_2	S_3	S_4	S_5	S_6	S_7	V_a	V_b	V_{ab}
1	0	1	0	1	0	0	0	0	0	0
2	0	1	0	0	1	0	0	$\frac{V_{dc}}{4}$	0	$\frac{V_{dc}}{4}$
3	0	1	0	0	0	1	0	$\frac{V_{dc}}{2}$	0	$\frac{V_{dc}}{2}$
4	0	1	0	0	0	0	1	$\frac{3V_{dc}}{4}$	0	$\frac{3V_{dc}}{4}$
5	1	1	0	0	0	0	0	V_{dc}	0	V_{dc}
6	1	0	1	0	0	0	0	V_{dc}	V_{dc}	0
7	0	0	1	0	1	0	0	0	$\frac{V_{dc}}{4}$	$\frac{-V_{dc}}{4}$
8	0	0	1	0	0	1	0	0	$\frac{V_{dc}}{2}$	$\frac{-V_{dc}}{2}$
9	0	0	1	0	0	0	1	0	$\frac{3V_{dc}}{4}$	$\frac{-3V_{dc}}{4}$
10	0	0	1	1	0	0	0	0	V_{dc}	$-V_{dc}$

10) Maximum negative output (-Vdc): The bidirectional switch $S_4$is turned ON connecting the load positive terminal, and S_3ON connecting the load negative terminal toV_{dc}. All other controlled switches are turned OFF. From Fig. 2(j) the applied potential to load is -V_{dc}. The mathematical expression is given by equation (10) below.

$$V_{ba} = -V_{ab} = -V_{dc} = L\frac{dI_0}{dt} + I_0R_0 \quad (10)$$

Table I shows the switching combinations that generated the nine output voltage levels (Vdc, Vdc/4, Vdc/2, 3Vdc/4, 0, −Vdc, −Vdc/4, −Vdc/2, 3Vdc/4).

III. PWM MODULATION

A novel PWM modulation strategy was introduced to generate the PWM switching signals. Four carrier signals ($V_{carrier\ 1}$,$V_{carrier\ 2}$,$V_{carrier\ 3}$,and $V_{carrier\ 4}$) were compared with a control signal ($V_{control}$,) in Fig. 5. The carrier signals had the same frequency and amplitude and were in phase with offset value that was equivalent to its amplitude. The carrier signals were each compared with control signal.

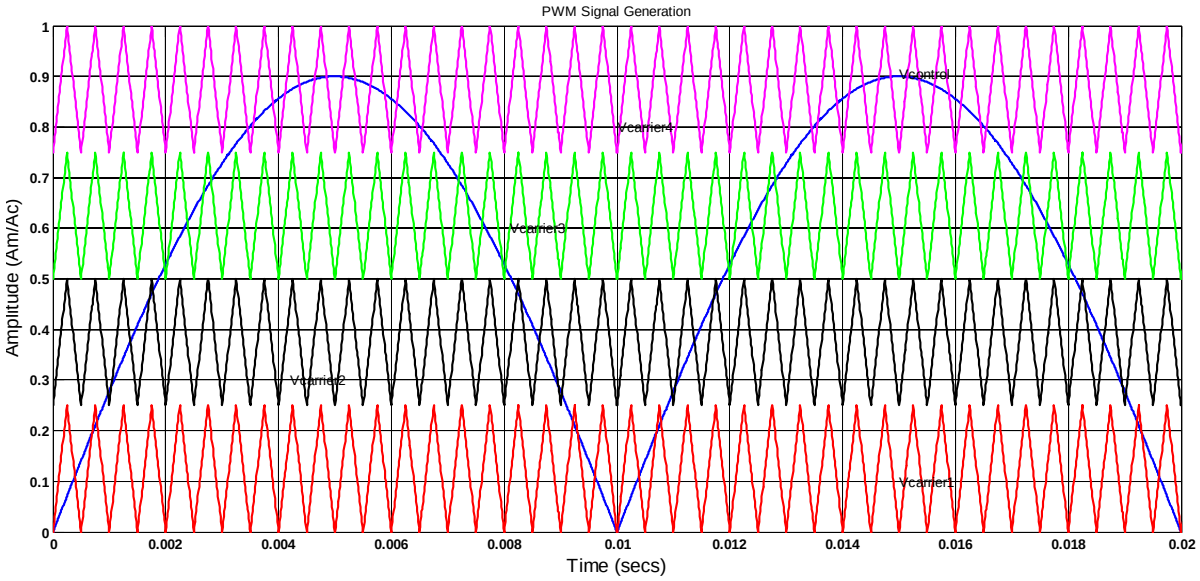

Fig. 5 PWM switching generation.

The general structure of the proposed system is given in given Fig. 6. In this modulation strategy, the fundamental frequency PWM (A) is a square wave signal synchronized with the modulation waveform; A=1 during the positive half cycle of the modulation signal, and A=0 during negative half cycle. Carrier based pulse width modulation (CBPWM) is based on comparison of rectified sinusoidal reference signal, with carrier to determine the voltage level that the inverter should switch to. The base PWM signals (A, B, C, D, E) for hybrid PWM controller are shown in Fig. 7. The hybrid PWM controller is implemented using a simple combinational logic, hence, it can be processed very quickly with less number of logic components.

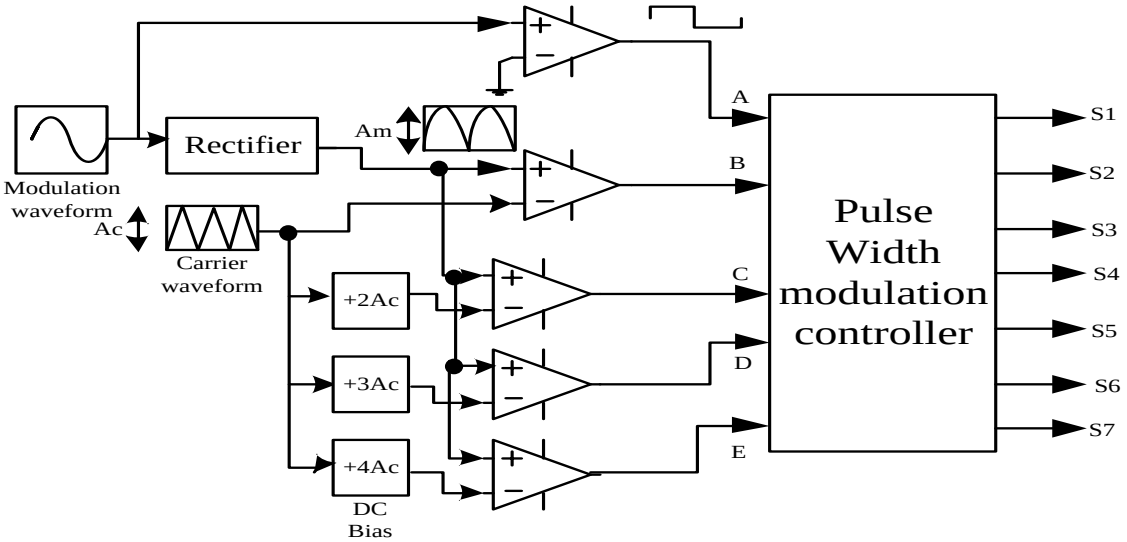

Fig. 6 Scheme of Pulse Width Modulation generator.

The functions of the combinational logic for a nine level hybrid PWM are expressed as

S1=AE+$\bar{A}\bar{B}$; S2=A; S3=$\bar{A}$; S4=A$\bar{B}$+$\bar{A}E$;

S5=AD$\bar{E}$+$\bar{A}B\bar{C}$; S6=C$\bar{D}$; S7=AB$\bar{C}$ + $\bar{A}D\bar{E}$. (11)

The generated signals are displayed in Fig. 8. It is shown that each gate signal is composed of both high and low switching frequency signals per cycle. In the full cycle plot it is observed that the switching signal ofS_1,S_4,S_5, S_6, and S_7 are operated at a high frequency while S_2 and S_3 are operated at fundamental frequency.

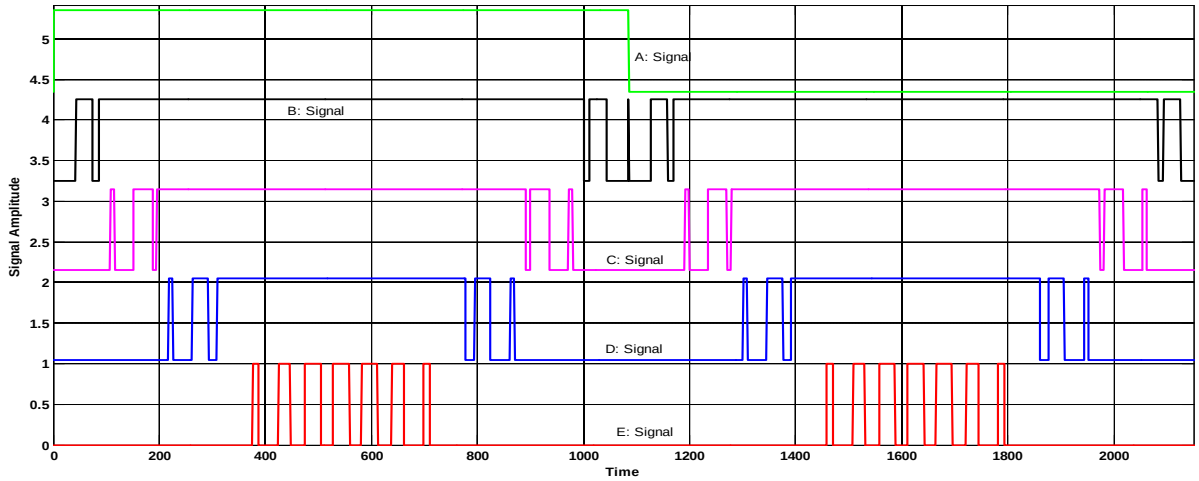

Fig. 7. Base PWM signals for nine-level inverter circuit configuration.

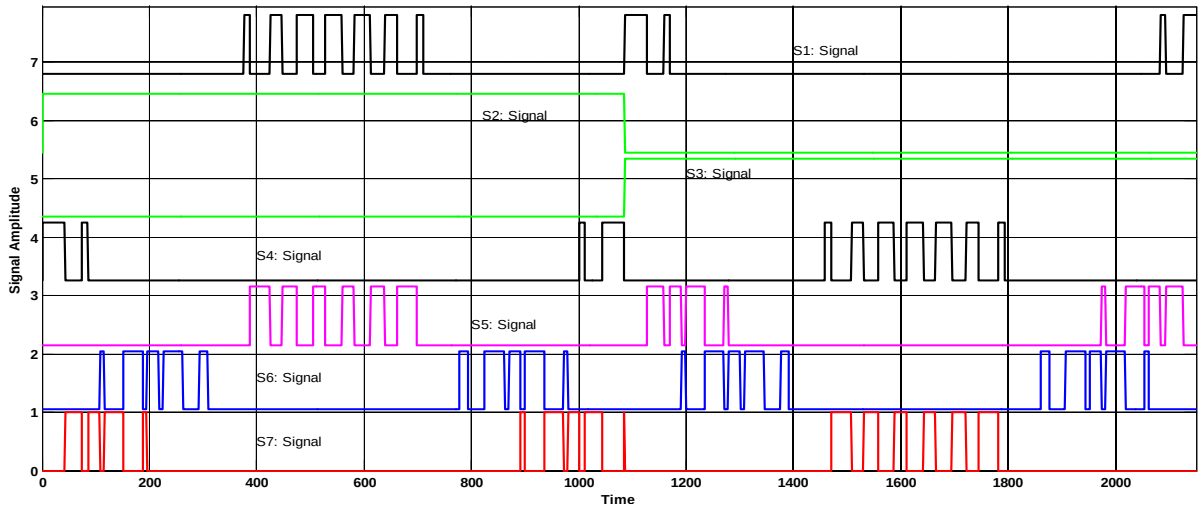

Fig. 8 Switching pattern for the single-phase nine-level inverter

For one cycle of the fundamental frequency, the proposed inverter operated through eight modes. Fig.9 shows the per unit output-voltage signal for one cycle. The eight modes are described as follows:

$$\left.\begin{array}{c} Mode\ 1: 0 < \omega t < \theta_1\ and\ \theta_6 < \omega t < \pi \\ Mode\ 2: \theta_1 < \omega t < \theta_2\ and\ \theta_5 < \omega t < \theta_6 \\ Mode\ 3: \theta_2 < \omega t < \theta_3\ and\ \theta_4 < \omega t < \theta_5 \\ Mode\ 4: \theta_3 < \omega t < \theta_4 \\ Mode\ 5: \pi < \omega t < \theta_7\ and\ \theta_{12} < \omega t < 2\pi \\ Mode\ 6: \theta_7 < \omega t < \theta_8\ and\ \theta_{11} < \omega t < \theta_{12} \\ Mode\ 7: \theta_8 < \omega t < \theta_9\ and\ \theta_{10} < \omega t < \theta_{11} \\ Mode\ 8: \theta_9 < \omega t < \theta_{10} \end{array}\right\} \quad (12)$$

The phase angle depends on modulation index M_a. Theoretically, for a single control (reference) signal and a single carrier signal, the modulation index is defined to be

$$M_a = \frac{A_m}{A_c} \quad (13)$$

While for a single-control signal and a dual carrier signal, the modulation index is defined to be

$$M_a = \frac{A_m}{2A_c} \quad (14)$$

Thus, for a single-control signal and a triple carrier signal, the modulation index is defined to be

$$M_a = \frac{A_m}{3A_c} \quad (15)$$

Since the proposed nine-level PWM inverter utilizes four carrier signals, the modulation index is defined to be

$$M_a = \frac{A_m}{4A_c} \quad (16)$$

Where A_c is the peak to peak value of the carrier signal and A_m is the peak to peak value of the voltage reference signal.

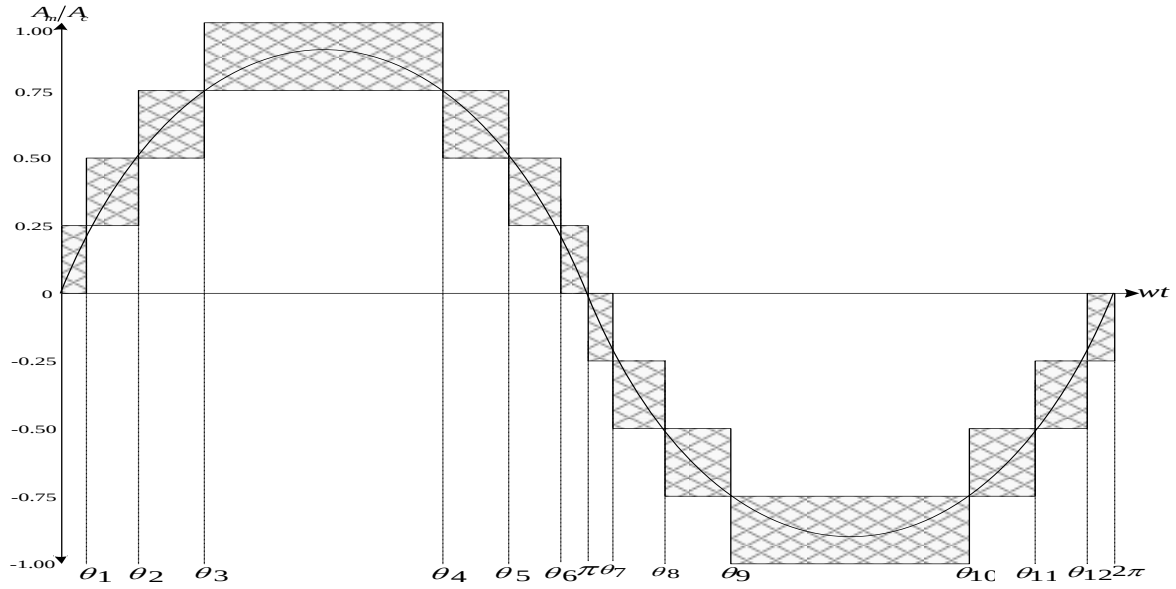

Fig. 9 Nine-level output (V_{ab}) and switching angles.

IV. SIMULATION RESULTS

The single-phase nine-level inverter topology for the proposed modulation strategy uses single reference/control signal and four carrier signals which was modeled and simulated in MATLAB and is shown below. The simulation was carried out with two input signals namely sine and triangular waves with differentamplitudes and frequencies. Seven firing signals were generated as shown in Fig. 10 below.

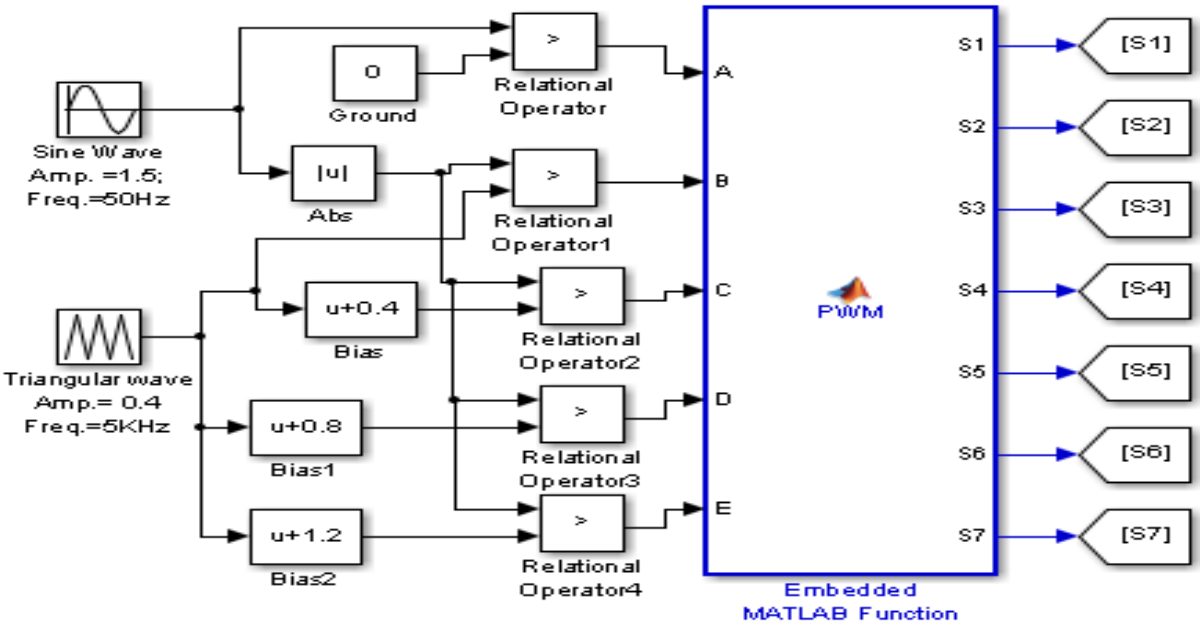

Fig. 10Matlab/Simulink model of firing signals.

Fig. 10 consists of a sine wave generator, triangular wave, rectifier circuit, four offset generator, five comparators, many logic gates (OR, AND, etc.). The logic gates are embedded in Simulink subsystem as shown in the figure above. The signals are generated from the expressions in equation (11).

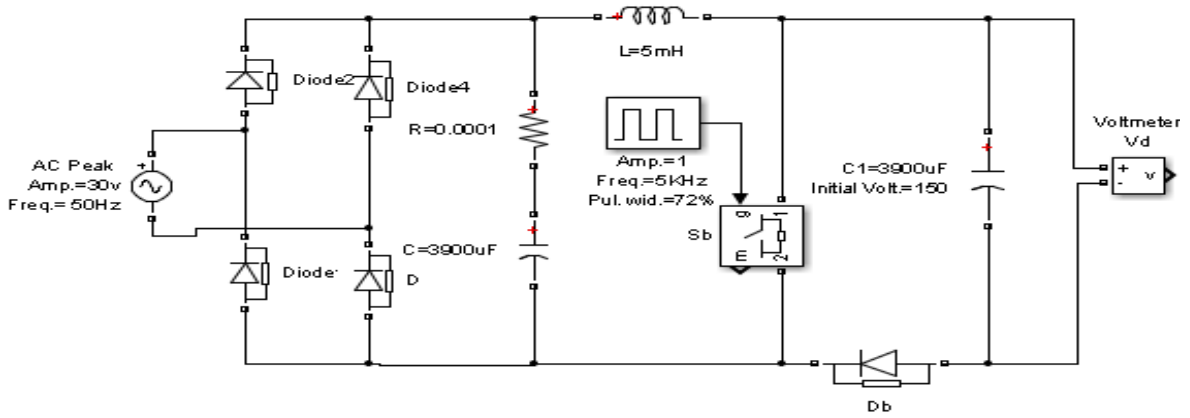

Fig. 11Matlab/Simulink model of AC to DC converter.

Fig. 11 shows Matlab/Simulink model of AC to DC circuit converter. This model is composed ofuncontrolled full wave rectifier circuit with low AC input voltage. The output voltage is filtered with a capacitor value of 3900µF by 100V. This output rectifier voltage is supplied to a Boost DC to DC converter which aids in enhancing the input voltage to the inverter circuit to higher amplitude.

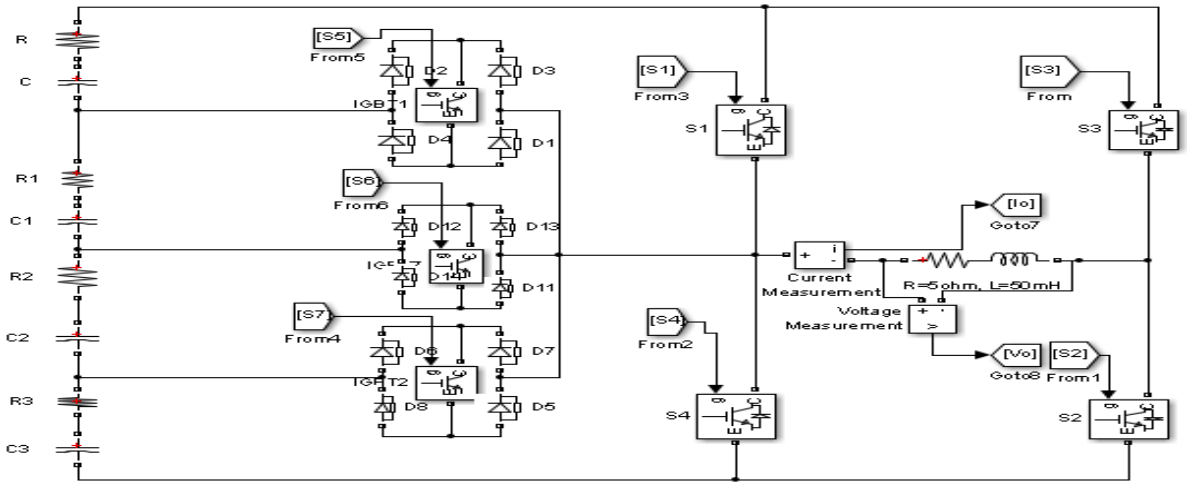

Fig. 12Proposed single-phase nine-level inverter configuration

Fig. 12 shows Matlab/Simulink model for proposed single-phase nine-level inverter topology with resistive-inductive load.The inverter input voltage is connected from Fig. 11 above also, the firing signals are sourced from Fig. 10.

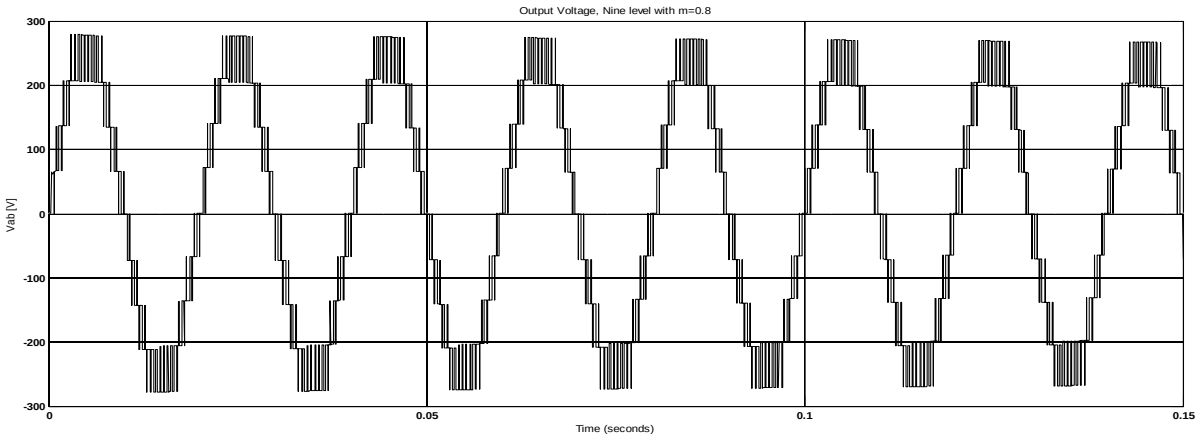

Fig. 13 Inverter Output Voltage

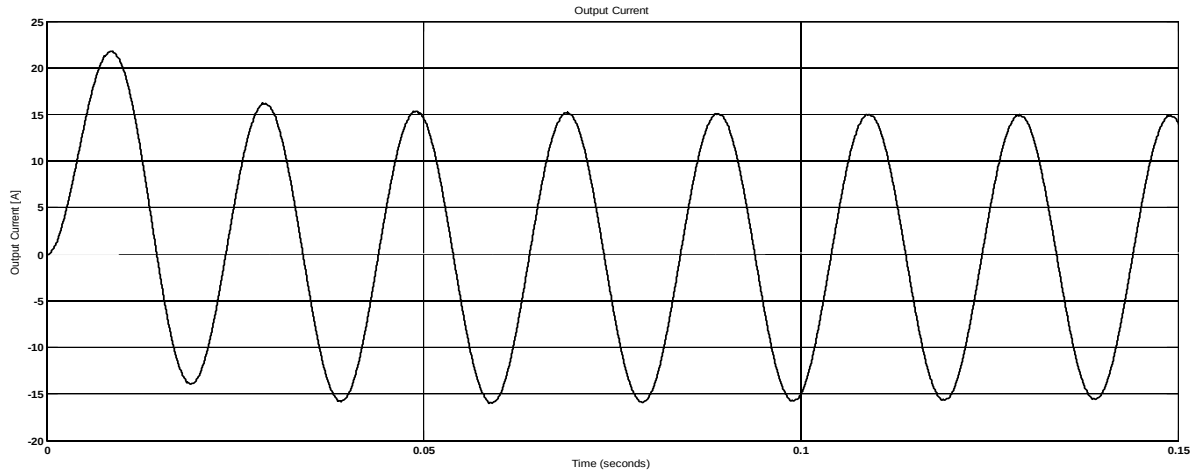

Fig. 14 Inverter Output Current

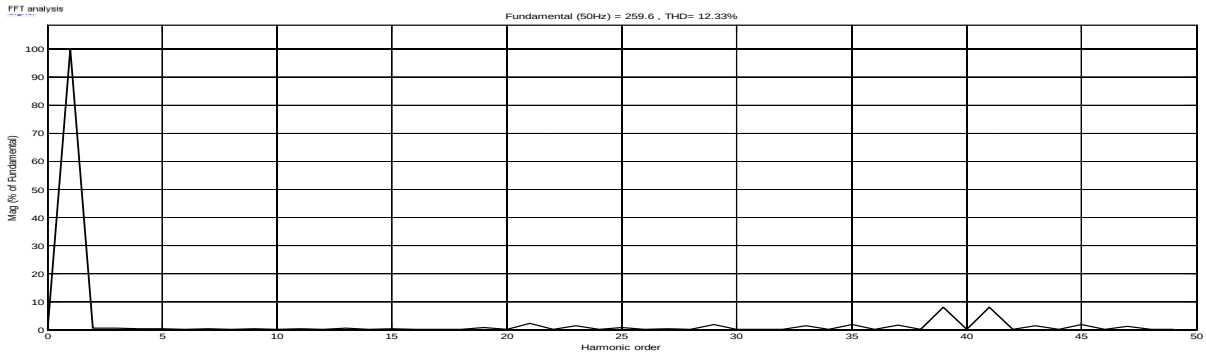

Fig. 15 Output FFT analysis

Fig. 13 shows seven and half cycles of the inverter output voltage of approximately 260VAC at a modulation index of 0.8 under an R-L load. Fig. 14 depicts the inverter output current of a value 15A which lags the output voltage by $72°.34'$ load angle. Thus, the load impedance is approximately 16.48Ω. Fig. 15 shows the FFT spectrum of the output voltage of the nine-level inverter with THD of 12.33%.

V. CONCLUSION

This paper has presented a single-phase nine-level inverter with reduced number of switches. A sine wave reference signal andmultiple carrier triangular signalspulse width modulation method have been proposed. The behaviour of the proposed multilevel inverter was analysed in detail. It is found that this method of modulation scheme gives a reduced number of circuit control components when compared to the same output voltage levelof diode clamped topology. As a result of that, the circuit configuration can be realised with low cost and less weight. Furthermore, it gives a better quality output voltage and THD value. Therefore, theproposed multilevel inverter is recommended for photovoltaic applications.

REFERENCES

[1] R. Anand& A. Nazar Ali, "A Single phase Five level Inverter for Grid Connected Photovoltaic System by employing PID Controller",African Journal of Scientific Research Vol. 6, No. 1 (2011), pp. 306-315.

[2] G. C. Diyoke, "Analysis and Simulation of Buck Switch Mode Dc to DC Power Regulator", International Journal of Technical Research and Applications Vol. 3, Issue 1, pp. 97-103, Jan. – Feb. 2015.

[3] Nasrudi A. Rahim, KrismadinataChaniago and JeyrajSelvaraj, "Single-Phase Seven-Level Grid-Connected Inverter for Photovoltaic System", IEEE *Trans. Ind. Electron.*, vol. 58, no. 6, pp. 2435–2443, June 2011.

[4] Thanuj Kumar Jaja& G. Srinivasa Rao, "A Novel Nine Level Grid-Connected Inverter for Photovoltaic System", International Journal of Modern Engineering Research (IJMER), Vol. 2, Issue 2, pp.154-159, Mar-Apr 2012.

[5] V. Vinoth Kumar & S. Dinakarraj, "Multilevel Inverter for Single-Phase System with Reduced Number of Switches", IOSR Journal of Electrical and Electronics Engineering (IOSR-JEEE), Vol. 4, Issue 3, pp.49-57, Jan. – Feb. 2013.

[6] P. K. Hinga, T. Ohnishi, and T. Suzuki, ― "A new PWM inverter for photovoltaic power generation system," in*Conf. Rec. IEEE Power Electron. Spec. Conf.*, 1994, pp. 391–395.

[7] G. SaniShehu,A. BalaKunya,I. HarunaShanono, andT.Yalcinoz,- A Review of Multilevel Inverter Topology and Control Techniques, Journal of Automation and Control Engineering Vol. 4, No. 3, pp.233-241 June 2016.

[8] G. Ceglia, V. Guzman, C. Sanchez, F. Ibanez, J. Walter, and M. I. Gimanez, ―A new simplified multilevel inverter topology for DC–AC conversion, *IEEE Trans. Power Electron.*, vol. 21, no. 5, pp. 1311–1319, Sep. 2006.

[9] V. G. Agelidis, D. M. Baker, W. B. Lawrence, and C. V. Nayar, ―A multilevel PWMinverter topology for photovoltaic applications, in *Proc. IEEE ISIE*, Guimäes, Portugal, 1997, pp. 589–594.

[10] S. J. Park, F. S. Kang,M.H.Lee, and C. U. Kim, ―Anewsingle-phase five-level PWM inverter employing a deadbeat control scheme,‖ *IEEE Trans. Power Electron.*, vol. 18, no. 3, pp. 831–843, May 2003.

[11] J. Selvaraj and N. A. Rahim, ―Multilevel inverter for grid-connected PV system employing digital PI controller,‖ *IEEE Trans. Ind. Electron.*, vol. 56, no. 1, pp. 149–158, Jan. 2009.

[12] N. A. Rahim and J. Selvaraj, ―Multi-string five-level inverter with novel PWM control scheme for PV application,‖ *IEEE Trans. Ind. Electron.*, vol. 57, no. 6, pp. 2111–2121, Jun. 2010.

American Journal of Engineering Research (AJER) 2016
American Journal of Engineering Research (AJER)
e-ISSN: 2320-0847 p-ISSN : 2320-0936
Volume-5, Issue-2, pp-199-203
www.ajer.org
Research Paper Open Access

A Survey Paper on Real Time Detection & Reporting By Social Networks

Thokal Nisha E., Golekar Sulbha S., Vavhal Priyanka B., Ashish Kumar
Department of CSE, G.H.Raisoni College of Engg. & Management, Ahmednagar, Savitribai Phule Pune University, India,414005.

***ABSTRACT*:** *In today's era social network like Twitter, Facebook, LinkedIn playing very vital role in human behavior & their day to day life. These social networking sites can be used as social sensors such that we can predict or report Real time natural disastrous events likeStorms, fire, traffic jams, riots, heavy rain-falls, earthquakes. And also social events Parties, baseball games, presidential campaign .We have used twitter here for such purpose to have a tendency to investigate the period of time interaction of events like earthquakes in Twitter associate degreed propose a rule to observe tweets and to sight a target event. To sight a target event, we have a tendency to devise a classifier of tweets supported options like the keywords in a very tweet, the amount of words, and their context. This model is provided which might notice the centre of the event location & it will do real time reporting to all active users. The twitter users also act as a sensors and report the event information by making tweet or post. Once our module gets such tweets then it will start analysis and ready to predict real time event & location. Our reporting system also considers amount of tweets generated from same region so that system can check the authenticity of event. We choose earthquake related datasets for training at initial as we found it is very essential and continuously occurring event all over the world. We also can change our module with respect to different data sets of different events.*

***Keywords*:** *Twitter, event detection, social sensing element, location estimation, Earthquake, Hadoop- Data processing, Machine Learning, Probabilistic Model, Earthquake monitoring, Instruments and techniques, Seismological data, Social Media, General or miscellaneous.*

I. INTRODUCTION

Twitter is an online social networking service that enables users to send and read short 180 character messages called "tweets". Registered users can read and writes tweets, but those who are not registered can only read . Users access Twitter through the website interface, SMS or mobile device app[19]. The service rapidly gained worldwide popularity, with more than 100 million users posting 340 million tweets a day in 2012.The service also handled 1.6 billion search quries per day. In 2013, Twitter was one of the ten most visited websites and has been described as "the SMS of the Internet".As of May 2015, Twitter has more than 500 million users, out of which more than 302 millions are active. Twitter is classified as a microblogging service. Microblogging may be a variety of blogging that allows users to send transient text updates or micromedia like images or audio clips[15]. An important characteristic that's common among small blogging services is their period nature. though web log users usually update their blogs once each many days, Twitter users write tweets many times during a single day.In such a way, varied update leads to varied reports associated with events. They embrace social events like parties, baseball games, and presidential campaigns. They additionally embrace black events like storms, fires, traffic jams, riots, significant precipitation, and earthquakes. Actually, Twitter is employed for varied period of time notifications like that necessary for facilitate throughout a large-scale hearth emergency or live traffic updates. The analysis question of our study is, "can we tend to discover such event prevalence in period of time by watching tweets?" This paper presents associate investigation of the period of time nature of Twitter that's designed to determine whether or not we are able to extract valid data from it. we tend to propose an occurrence notification system that monitors tweets and delivers notification promptly victimisation information from the investigation. As an application, we develop an earthquake reporting system using Japanese tweets. Japan has numerous earth- quakes. Twitter users are similarly numerous and geogra- phically dispersed throughout the country. Therefore, it is sometimes possible to detect an earthquake by monitoring tweets. Our system detects an earthquake occurrence and sends an e-mail, possibly before an earthquake actually arrives at a certain location: An earthquake propagates at about 3-7 km/s. For that reason, a person who

is 100 km distant from an earthquake is able to communicate and act for about 20 s before the arrival of an earthquake wave. Moreover, strong earthquakes often cause tsunami, which engender more catastrophic disasters than the earthquakes themselves in distant and near places in relation to the earthquake epicenter, as did the Haiti earthquake in 2010 and the Great Eastern Japan earthquake in 2011. Therefore, prompt notification of earthquake occurrences is extremely important to decrease damage by tsunami. In many cases, it could provide notification of tens of minutes or even hours before a tsunami strikes a coastal area[1].

II. RELATED WORK

2.1 EVENT DETECTION: A survey[1] by Takeshi Sakaki, Makoto Okazaki, Yutaka Matsuo,2013
As described in this paper, we target event detection.We target events such as earthquakes, typhoons, and traffic jams, which are readily apparent upon examination of tweets. These events have several properties.

1.many users experience the event. 2.for that reason, people are induced to tweet about it. 3.so that real-time location estimation is possible. Such events include social events such as large parties, sports events, exhibitions, accidents, and political cam- paigns. They also include natural events such as storms, rain are heavy, tornadoes, typhoons/hurricanes/cyclones, and earthquakes. We designate an event we would like to detect using Twitter as a target event.

In this section, we explain how to detect a target event using Twitter. First, we crawl tweets including keywords related to a target event. From them, we extract tweets that certainly refer to a target event using devices that have been trained with machine learning. Second, we detect a target event and estimate the location from those tweets by treating Twitter users as "social sensors."

2.2 Semantic Analysis of Tweets:

To detect a target event from Twitter, we search from Twitter and find useful tweets. Our method of acquiring useful tweets for target event detection is portrayed in. Tweets might include mention of the target event. For example, users might make tweets such as "Earthquake!" or "Now it is shaking." Consequently, earthquake or shaking might be keywords (which we call query words). However, users might also make tweets such as "I am attending an Earthquake Conference." or "Someone is shaking hands with my boss." Moreover, even if a tweet is referring to the target event, it might not be appropriate as an event report. For instance, a user makes tweets such as "The earthquake yesterday was scary." or "Three earthquakes in four days. Japan scares me." These tweets are truly descriptions of the target event, but they are not real-time reports of the events. Therefore, it is necessary to clarify that a tweet is truly referring to an actual contemporaneous earthquake occur- rence, which is denoted as a positive class. To classify a tweet as a positive class or a negative class, we use a support vector machine [14], which is a widely used machine-learning algorithm. By preparing positive and negative examples as a training set, we can produce a model to classify tweets automatically into positive and negative categories.
We prepare three groups of features for each tweet
statistical features: the number of words in a tweet message, and the position of the query word within a tweet.
keyword features: the words in a tweet.
word context features: the words before and after the query word.
We can give an illustrative example of these features using the following sentence. "I am in Japan, earthquake right now!"
keyword: earthquake
Using the obtained model, we can classify whether a new tweet corresponds to a positive class or a negative class.

2.3 Semantic and Sentiment Analysis:[2] Prof Shivani Desai,Priyank Bhatt,Vraj Solanki,Sep 2014.
This paper aims at surveying a number of such algorithms, methods and techniques to classify any sentence as positive, negative or neutral and also discuss the issues related to each method faced during implementation and execution. The essential issues in sentiment analysis are to identify how sentiments are expressed in texts and whether the expressions indicate positive (favorable) or negative (unfavorable) opinions toward the subject and how efficiently and correctly sentences are classified.

2.4 SYSTEM OVERVIEW

In our model we are focusing on submodules like Tweeter dataset crawling for training purposes. Then Implementing machine learning module and data analysis module on Hadoop framework is very important part. Interactive GUI which gave us real time analysis reports and charts is last part of project where active users will get notifications for such events. We tend to are getting to propose an occurrence notification system. An occurrence watching system monitors tweets and delivers notification promptly mistreatment investigation results. We tend to propose a system that's supported investigation of tweets i.e. real time investigation. during this analysis, in brief, we tend to take 3 steps:

1) We analyze no of tweets associated with target events;

2) We got to style such a probabilistic module to research and extract events from those tweets and predict locations of events with category verifying as positive and negative class.

3) Finally developed coverage system that extracts earthquakes from Twitter and sends a message to registered users.

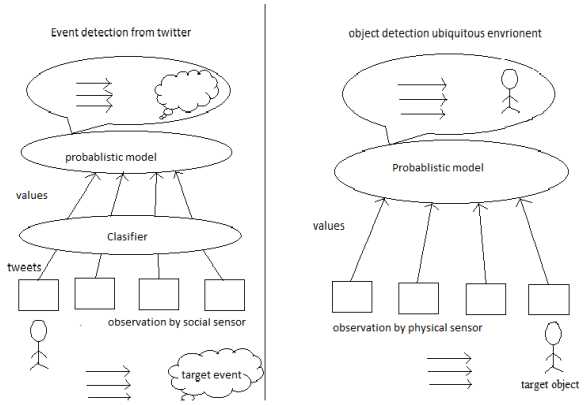

Fig 1:System overview

2.5 IMPLEMENTATION:[3]S.Anand & K.Narayana

This paper presents an investigation of the real-time nature of Twitter that is designed to ascertain whether we can extract valid information from it. We propose an event notification system that monitors tweets and delivers notification promptly using knowledge from the investigation. In this research, we take three steps: first, we crawl numerous tweets related to target events; second, we propose probabilistic models to extract events from those tweets and estimate locations of events; finally, we developed an earthquake reporting system that extracts earthquakes from Twitter and sends a message to registered users.

2.5 METHODS

For event detection and placement estimation, we tend to use probabilistic models. during this section, we tend to 1st describe event detection from time-series information. Then we tend to describe the situation estimation of a target event.

1)Temporal Model

Each tweet has its own post time. once a target event happens, however do the sensors discover the event, we tend to describe the temporal model of event detection. First, we tend to examine the particular information. The several quantities of tweets for a target event: Associate in Nursing earthquake. it's apparent that spikes occur within the variety of tweets. every corresponds to an incident} occurrence. Specifically concerning Associate in Nursing earthquake, quite ten earthquakes occurred throughout the amount.

2) Spatial Model

Each tweet is related to a location. we tend to describe a technique which will estimate the situation of an occasion from device readings. to resolve the matter, many ways of Bayesian filters square measure planned like Kalman filters, multi-hypothesis following, grid-based and topological approaches, and particle filters. For this study, we tend to use particle filters, each of that square measure wide employed in location estimation.

a) Particle Filters

A Particle filter could be a probabilistic approximation algorithmic rule implementing a Bayes filter, and a member of the family of successive Monte Carlo strategies.

b) Consideration of sensing element Geographic Distribution

We should take into account the sensing element geographic distribution to treat readings of social sensors additional. exactly. In location estimation by physical sensors, those sensors area unit situated equally in several cases. we will treat sensing element readings equally in such things. Actually, social sensors aren't placed equally in several cases as a result of social media user's area unit targeted in urban areas. In Japan, most users board capital of Japan. Therefore, we should always incorporate the geographic distribution of social sensors into abstraction models.

c) Techniques to hurry up the method

As represented during this paper, we wish to estimate location of events quickly as shortly as potential as a result of one objective of this analysis is to develop a period earthquake detection system. Therefore, we tend to should decrease the time quality of strategies used for location estimation.

3) Information Diffusion associated with a period Event

Some info associated with an occasion diffuses through Twitter. for instance, if a user detects associate earthquake and makes a tweet regarding the earthquake, then a fan of that user would possibly create tweets that. This characteristic is very important as a result of, in our model, sensors won't be reciprocally freelance, which might have associate unsought result in terms of event detection.For event detection and placement estimation, we tend to use probabilistic models. From time-series information, we 1st describe event detection. Then we tend to describe the placement estimation of a target event. Each tweet has its own post time. once a target event happens, however do the sensors observe the event? we tend to describe the temporal model of event detection. First, we tend to examine the particular information. every corresponds to prevalence occurrence. Specifically relating to associate earthquake, over ten earthquakes occurred throughout the amount.

2.6 PROPOSED WORK:

We are going to design the system called 'CrisisAlertCall' is kind of alarming or reporting system based on Hadoop Framework to process huge amount of tweeter data related with 'Earthquake' like calamities. Actually it is one of much needed project started by seeing hazards to people in Nepal. Recently in July-August 2015 Nepal faced very big natural calamity due to Earthquake. Many people lost their lives. By seeing such huge hazard we are proposing such system which will make reports or alarms to social network users on their accounts or public announcing on web by analyzing huge amount of Tweets, Posts related with. 'CrisisAlertCall' is prepared by not only focusing on Earthquake, but also events like Storm, Heavy Rainfall, Flood etc. can be monitor by us. One of best thing in this project is we are using Hadoop Framework which was not present in existing system. Means we can process very huge data within very short time period.

Our Systems' flow will starts from Tweets crawling. First we collect as many tweets as possible from Tweeter Database or else we crawl the web for Tweets. Then we will process them as Positive or Negative Tweets using Navie Bays Algorithm. So we have to make them sorted as per feeling or sentiment in tweet. In such scenarios we will use sentiment analysis concepts do make type sorting of tweets. Also from such tweets we have detect event and location too. So it is one of big task while developing. As tweeter data gives us locations as time of tweet we can Processed data of Messenger is used for preparing the algorithm, so that next time if such data came for prediction it will processed directly. For processing we will use Navie bays algorithm over Hadoop Map Reduce framework. When real time Tweeter users tweet on web our system detects event & location & does reporting & alarming automatically. 'CrisisAlertCall' is best prototype for Harmful event detection & location tracking for any kind. What just change is we need to change database for training the system & evaluation.

III. CONCLUSION

we have a tendency to investigated the period nature of Twitter, devoting specific attention to event detection. linguistics analyses were applied to tweets to category verify them into a positive and a negative class. we have a tendency to regard every Twitter user as a device, and set the matter as detection of a happening supported sensory observations. Location estimation strategies like particle filtering area unit used to estimate the locations of events. As associate degree application, we have a tendency to developed associate degree earthquake coverage system, that could be a novel approach to advice folks promptly of associate degree earthquake event.

REFERENCES

[1] T. Sakaki, M. Okazaki, and Y. Matsuo, "*Tweet Analysis for Real-Time Event Detection and Earthquake Reporting System Development,*" Proc. Int'l Conf. World Wide Web (WWW '10), pp. 9526, Vol 25 April 2013.

[2] Prof Shivani Desai, Priyank Bhatt(11BIT044), Vraj Solanki(11BIT059) Semantic and Sentiment Analysis,sep2014.

[3] S.Anand, K.Narayan," *Earthquake Reporting System Development by Tweet Analysis*" IJEERT Volume 2, Issue 4, July 2014, PP 96-106 ISSN 2349-4395 (Print) & ISSN 2349-4409

[4] B. Huberman, D. Romero, and F. Wu, "*Social Networks that Matter: Twitter Under the Microscope,"* ArXiv E-Prints, http://arxiv.org/abs/0812.1045, Dec. 2008.

[5] H. Kwak, C. Lee, H. Park, and S. Moon, "*What is Twitter, A Social Network or A News Media?"*Proc. 19th Int'l Conf. World Wide Web (WWW '10), pp. 591-600, 2010.

[6] G.L. Danah Boyd and S. Golder, "*Tweet, Tweet, and Retweet: Conversational Aspects of Retweeting on Twitter,"* Proc. 43rd Hawaii Int'l Conf. System Sciences (HICSS-43), 2010.

[7] Tumasjan, T.O. Sprenger, P.G. Sandner, and I.M. Welpe, *"Predicting Elections with Twitter: What 140 Characters Reveal About Political Sentiment,"* Proc. Fourth Int'l AAAI Conf. Weblogs and Social Media (ICWSM), 2010.

[8] P. Galagan, *"Twitter as a Learning Tool. Really,"* ASTD Learning Circuits, p. 13, 2009.

[9] K. Borau, C. Ullrich, J. Feng, and R. Shen, *"Microblogging for Language Learning: Using Twitter to Train Communicative and Cultural Competence,"* Proc. Eighth Int'l Conf. Advances in Web Based Learning (ICWL '09), pp. 78-87, 2009.
[10] J. Hightower and G. Borriello, *"Location Systems for Ubiquitous Computing,"* Computer, vol. 34, no. 8, pp. 57-66, 2001.
[11] M. Weiser, *"The Computer for the Twenty-First Century,"* Scientific Am., vol. 265, no. 3, pp. 94-104, 1991.
[12] V. Fox, J. Hightower, L. Liao, D. Schulz, and G. Borriello, "*Bayesian Filtering for Location Estimation*," IEEE Pervasive Computing, vol. 2, no. 3, pp. 24-33, July-Sept. 2003.
[13] T. Sakaki, M. Okazaki, and Y. Matsuo, "*Earthquake Shakes Twitter Users: Real-Time Event Detection by Social Sensors*," Proc. 19th Int'l Conf. World Wide Web (WWW '10), pp. 851-860, 2010.
[14] M. Sarah, C. Abdur, H. Gregor, L. Ben, and M. Roger, "*Twitter and the Micro-Messaging Revolution*," technical report, O'Reilly Radar, 2008.
[15] *Microblogging – Wikipedia, the free encyclopedia.*
[16] Java, X. Song, T. Finin, and B. Tseng, "*Why We Twitter: Understanding Microblogging Usage and Communities,"* Proc. Ninth WebKDD and First SNA-KDD Workshop Web Mining and Social Network Analysis (WebKDD/SNA-KDD '07), pp. 56-65, 2007.
[17] *Twitter search for Haiti survivors Channel 4 15 Jan, 2010.*
[18] Krūms, Jānis (January 15, 2009). *"There's a plane in the Hudson. I'm on the ferry going to pick up the people.*
[19] Paul S. Earle*, Daniel C. Bowden, Michelle Guy(ANNALS OF GEOPHYSICS, 54, 6, 2011; doi: 10.4401/ag-5364)"Twitter earthquake detection: earthquake monitoring in a social world".

American Journal of Engineering Research (AJER) 2016
American Journal of Engineering Research (AJER)
e-ISSN: 2320-0847 p-ISSN : 2320-0936
Volume-5, Issue-2, pp-204-209
www.ajer.org
Research Paper Open Access

Design of a PWM for UPS with Pulse Dead Time

Ahmed Majeed Ghadhban
Department of Electrical Power & Machines Engineering, Collage of Engineering/ Diyala University, Diyala, Iraq.

ABSTRACT : *This paper presents a new design of a power width modulator PWM with and without dead time for each PWM pulses based on specific criteria given. In order to study and design a new model of PMW Inverter and to show the effects of dead time on the PWM which was designed and achieved. In this paper, comparison between PWM with &without dead time. The design methodology comprises of the calculations and results analysis. P-Spice simulator was used as a tool to verify the results. The effectiveness of the proposed technique was confirmed. All the waveforms voltage, current, and power achieved and discussed.*
Keywords – *PWM, Modeling, power electronics design, Harmonics elimination, and inverters.*

I. INTRODUCTION

One of the main problems encountered in open-loop pulse width modulation inverter (PWM) drives is the nonlinear voltage gain caused by the non ideal characteristics of the power inverter. The most important nonlinearity is introduced by the necessary blanking time to avoid the so-called shoot through of the dc link. To guarantee that both switches in an inverter leg never conduct simultaneously a small time delay is added to the gate signal of the turning-on device.

This delay, added to the device's finite turn-on and turn-off times, introduces a load dependent magnitude and phase error in the output voltage. Since the delay occurs in every PWM carrier cycle the magnitude of the error grows in inverse proportion to the output fundamental frequency, introducing a serious waveform distortion and fundamental voltage drop The voltage distortion increases with switching frequency introducing harmonic components that, if not compensated, may cause instabilities as well as additional losses in the machine being driven[1].

The output voltage distortion is the finite voltage drop across the switches during the on state the dead time necessary to prevent the short circuit of the power supply in pulse width modulated (PWM) voltage inverters results in output voltage deviations. Although individually small, when accumulated over an operating cycle, the voltage deviations are sufficient to distort the applied PWM signal [2].

The top and bottom switch has to be "complementary", i.e. if the top switch is closed (on), the bottom must be off, and vice-versa. In practical, a dead time as showed below is required to avoid "shoot-through" faults as showed in Fig.(1)[3].

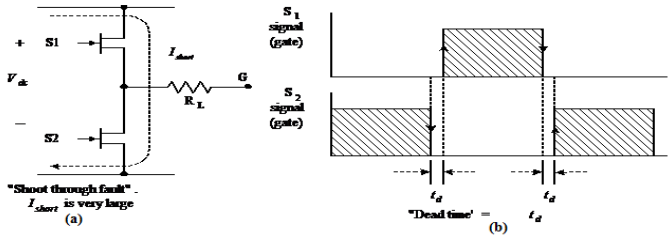

Fig.1 a) Shoot through fault, b) Dead time waveform

Based on various circuit topologies and modulation strategies have been reported for better utilization of multilevel voltage source inverters. Multilevel topologies are classified in to three categories: diode clamped inverters, flying capacitor inverters and cascaded inverters. The topologies have an equal number of main switches[4].

The diode clamped inverter uses a single dc bus that is subdivided in to number of voltage levels by a series string of capacitors. A matrix of semiconductor switches and diodes allows each phase leg output to be switched to any of these voltage levels. The main drawback of diode clamped inverter is the unbalanced dc link capacitor. It restricts the application of diode clamped inverter to five or less number of levels. Flying capacitor inverter requires the most number of capacitors [5-6].

Finally, in this paper design of a power width modulator PWM with dead time for each PWM pulses based on specific criteria given. In order to analyse the effects of dead time insertion to PWM inverter, and To know how to design rectifiers for electronic devices (UPS). All techniques for the analysis and design of rectifiers through simulation were achieved[7].

II. PULSE WIDTH MODULATION

Fig.(2) shows the PWM is the most popular method for producing a controlled output for inverters. They are quite popular in industrial applications[8-9].

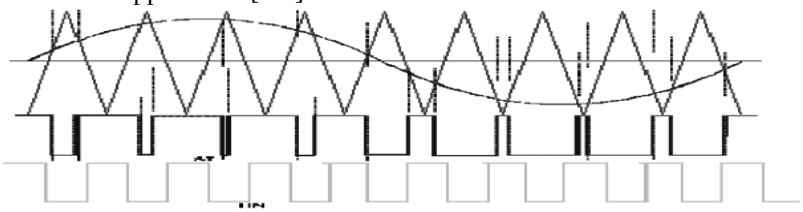

Fig.2 (sine modulated, unmodulated signal)

III. METHODOLOGY

The Methodology of this paper consist of five main stages. As following :
Stage1: design of inverter concept based on theories study.
Stage 2: simulation of the inverter circuit by PSPICE simulator.
Stage3: design & development of the switching pulse based on simulation and calculation.
Stage4: development of single phase inverter, fine, tuning, and testing.
Stage 5: Input data get results monitoring and conclusion.

IV. DESIGN and CONSIDERATIONS

Two designs was considered in this paper the power width modulator PWM with and without dead time with specific criteria as shown:
1) Input voltage: 24V Battery bank
2) Output voltage: 240Vrms + 5%
3) Output power: 500 W
4) Voltage THD < 5%

The amplitude of the PWM of the fundamental frequency output is controlled by ma . This is significant for an unregulated DC voltage because the value of ma can be adjusted to compensate the variations in the DC voltage, thus producing a constant amplitude output. When ma is greater than 1 or over modulation, the amplitude of the output increases with ma , but not linear.

$Mf = f_{carrier} / f_{ref}$. (1)

Where;
fcarrier = ftri =Triangular carrier waveform frequency.
freference = fsin = Fundamental waveform frequency.

$Ma = V_{m,ref} / V_{m,carrier}$ (2)

Where;
Vm,reference = Vm,sin = Peak amplitude of reference waveform.
Vm,carrier = Peak amplitude of triangular carrier waveform.

V. SIMULATION RESULTS

A. PWM inverter without dead time

Figure(3) shows the Circuit diagram of PWM inverter with dead time. Consist of four switches and two comparators with R load.

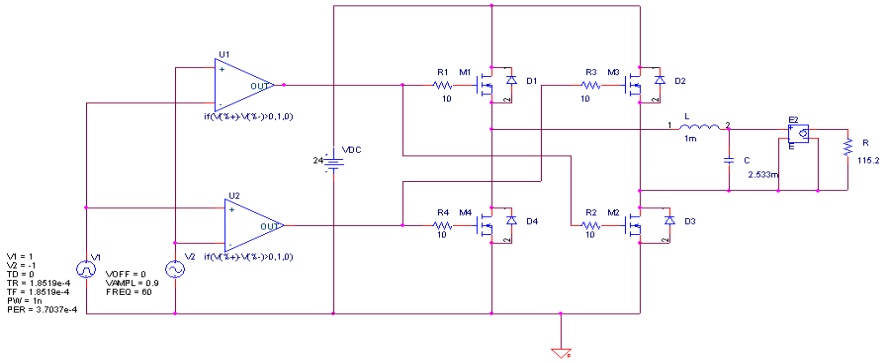

Fig.3 Circuit diagram of PWM inverter without dead time.

Fig. (4) shows the voltage output waveform. From the reading shown that the voltage output is 341.698V. The result shown meet the requirement for the design specification where the design need 240V_{rms} voltage output.

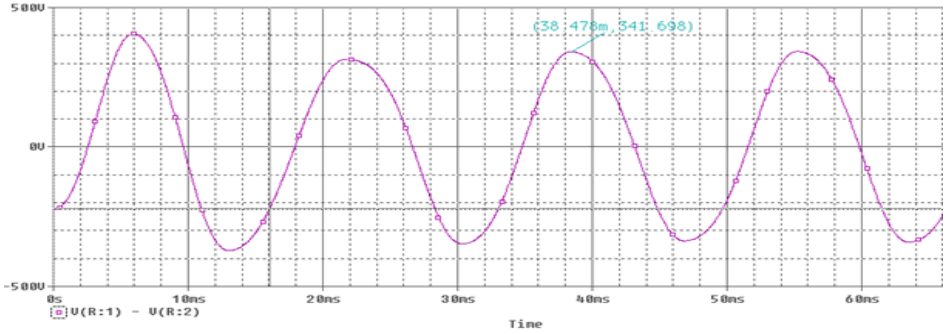

Fig.4 Inverter output voltage.

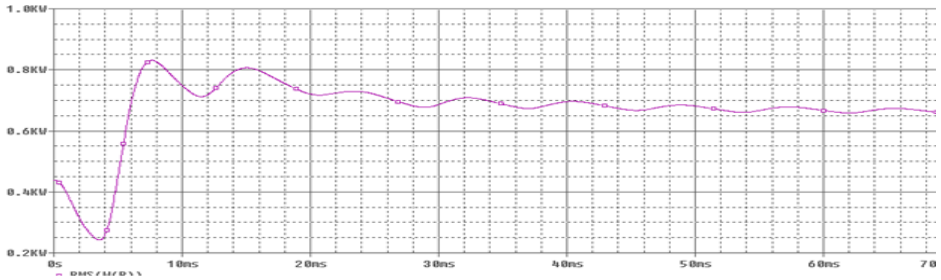

Fig. 5 Power output.

The power is going to stabilize around 650W. The time for the graph cannot be increased anymore because convergence will occurred. After checking with the voltage output, the V_{rms} value is 251. 458 as shown in Fig.(5). By using the formula for the power,

$P=V_{rms}^2/R$ (3)

The calculated power is 550W and this met the requirement for the power output. Fig.(5) shows the waveform for the PWM output. Waveform for the output V_{rms} value as shown in the Fig.(6)

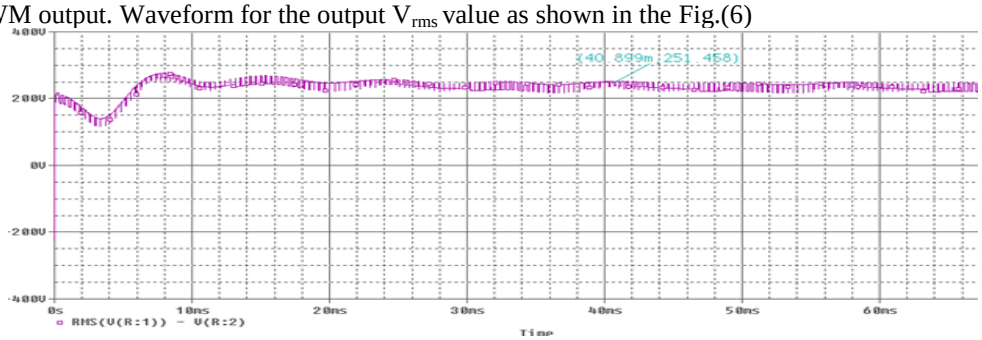

Fig.6 Waveform for the output V_{rms} value.

Fig. (7&8) shows the switches pulses. Two switches work at time.

Fig. 7 S1&S3 pluses

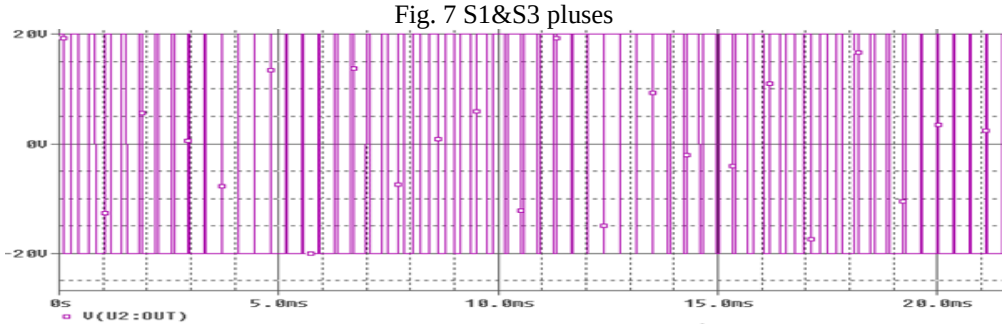

Fig.8 S2&S4 pluses

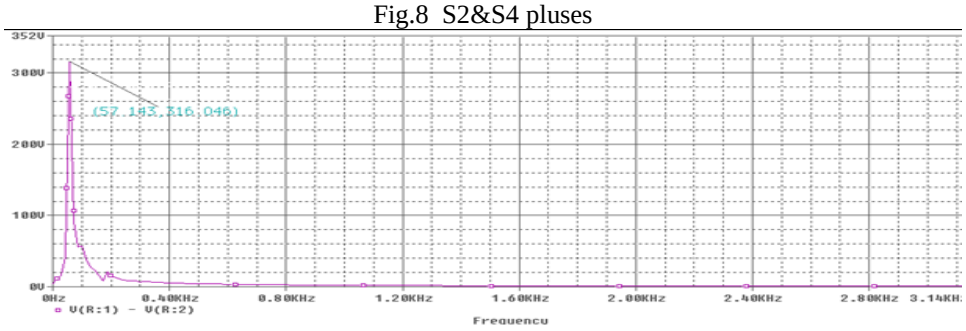

Fig.9 Harmonic frequency.

In Fig.(9) , the Fourier series for the voltage output is shown. To find the first harmonic frequency, the formula used is

$f=kM_Rf_m$ (4)

Where

k is the number of the harmonic will occur, M_R is the modulation ratio and f_m is the modulating frequency. The first harmonics will occur at frequency, 2.7kHz and from the waveform there are no harmonics at that frequency. So we can conclude that the total harmonic for this circuit is below than 5 percent.

B. PWM inverter with dead time

Figure(10) Circuit diagram of PWM inverter with dead time. This design analyzes the effects of dead time insertion to PWM inverter. The dead time between switching pulse for both set of MOSFET (M1, M2 and M3, M4) is 1µs. dead times must be inserted before turning on the switch to avoid simultaneous conduction and shoot-through problems.

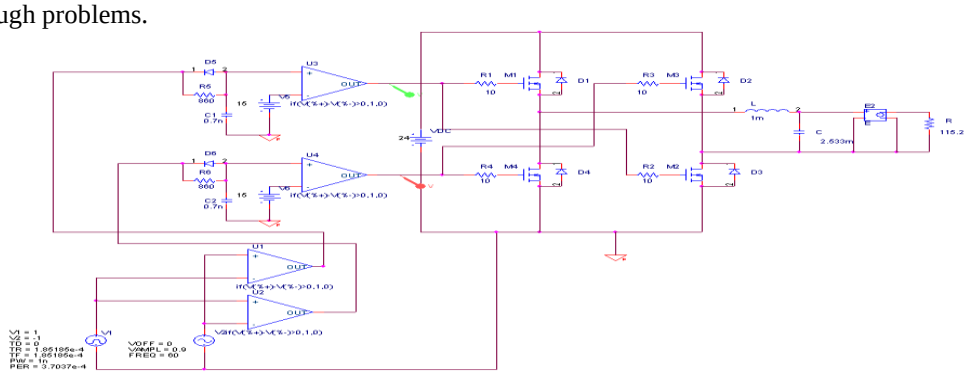

Fig.10 Modified PMW Inverter Circuit for Dead Time Insertion

Fig. (10) shows the modified inverter circuit for dead time 1μs insertion. The switching pulse is connected to R-C circuit. The output from the R-C circuit is then compared once again to get the desired switching pulse with dead time insertion. Here, the values of R and C are adjusted to get the desired 1μs.

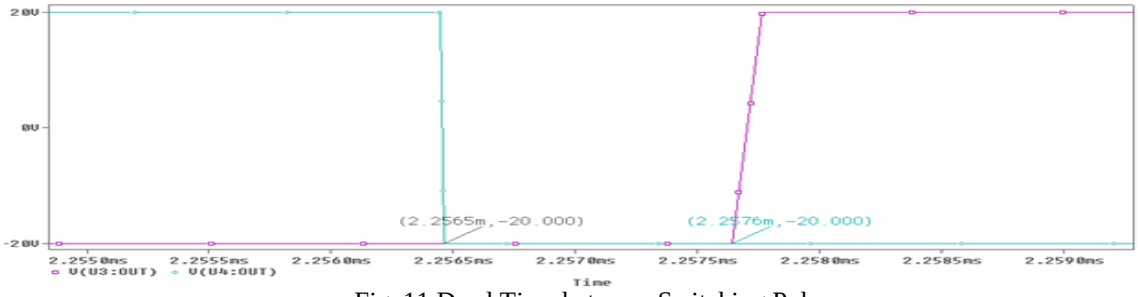

Fig. 11 Dead Time between Switching Pulse.

Fig. (11) shows the switching pulse results for both set of MOSFET switch (M1, M2 and M3, M4). From the result, the dead time is equal to 2.2576ms-2.2565ms = 1.1μs ≈ 1μs.

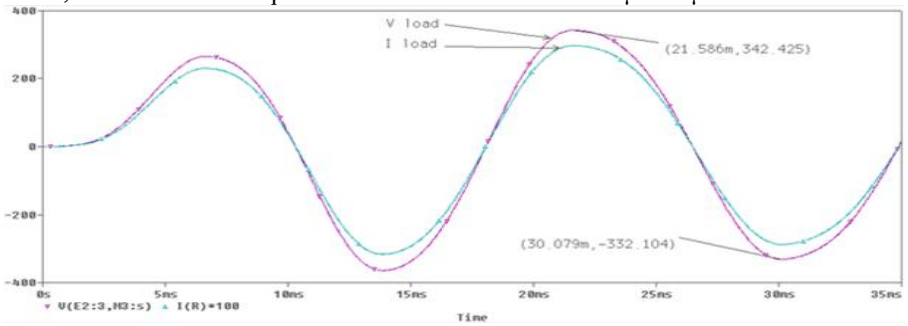

Fig.12Voltage and Current Output at the Load

Fig. (12) shows the voltage and current waveform at the output of the inverter. The output current has been multiplied by 100 for better seen. Due to the convergence problem, the transient simulation only can be running until 35ms which here, we can see that the voltage and current waveform is getting to stabilize and they are in phase.

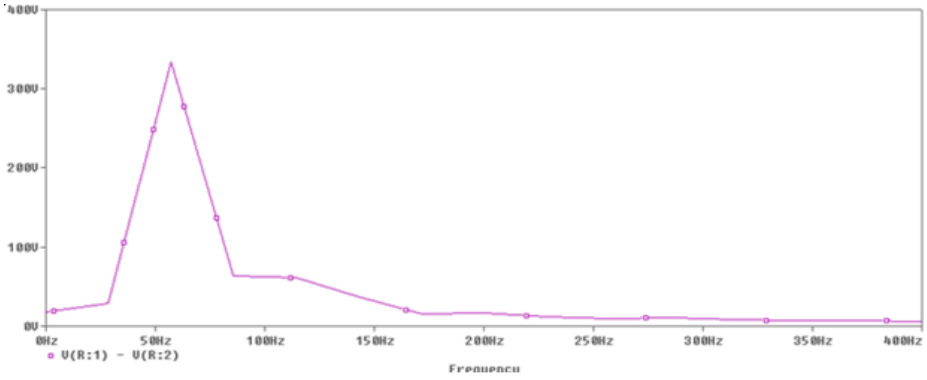

Fig. 13 Fourier series of the Output Voltage without Dead Time Insertion.

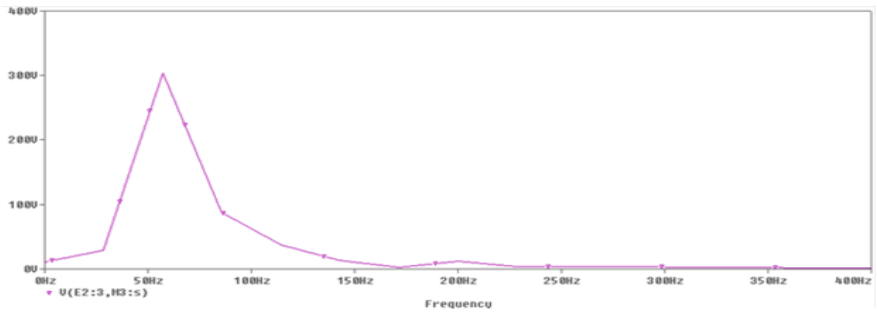

Fig. 14 Fourier series of the output voltage with dead time insertion.

Fig. (13 & 14) shows the harmonic contents of the output voltage with and without dead time insertion respectively. Form both figures; the first dominant harmonic is not present anymore because of the filter insertion at the output of inverter. Although it is a bit difficult to compare between both figures due to both figures having very low harmonic contents, it still can be seen that Fourier waveform of output voltage with dead time insertion has a slightly better result than the output voltage without dead time insertion.

VI. CONCLUSION

In this paper describes the principle of sampling PWM is based on the comparison real time of sine wave waveform (reference waveform) with a triangular carrier waveform. A high frequency triangular carrier waveform Vc is compared with a sinusoidal reference waveform Vr of the desired frequency. The PWM signal is high when the magnitude of the sinusoidal wave is higher than the triangular wave otherwise it is low. The results were proved that the inverter could produce voltage and current waveform purely. And the output voltage for PWM with dead time insertion, it has a lightly better result in term of harmonic contents although when compared with output voltage for PWM without dead time insertion, both waveforms have very low harmonic contents. Thus, the output waveform of a PWM inverter is generally improved by using a high ratio between the carrier frequency and the output fundamental frequency.

REFERENCE

[1] J.Rodriguez, J.S.Lai, an F.Z.peng, "multilevel inverter: A survey of topologies, controls, and applications," IEEE Trans. Ind. Electron., Vol.49, no 4, pp. 724-738. Aug.2002.

[2] B.P.Mcgrath, D.G.Holmes, and T.Meynard, " Reduced PWM harmonic distortion for multilevel inverters operating over a wide modulation range," IEEE Trans. Power Electron., Vol.21, no.4, pp.941-949, Jul.2006.

[3] B.S.Jin, W.K.Lee, T.J.Kim, D.W.Kang, and D.S.Hyun, " A Study on the multicarrier PWM methods for voltage balancing of flying capacitor in the flying capacitor multilevel inverter, " in proc.IEEE Ind. Electron.Conf.Nov.2005, pp.721-726.

[4] J.Hamman and F.S.van Der merwe, "Voltage harmonics generated by voltage fed inverters using PWM natural sampling," IEEE Trans. Power Electron., Vol PE-3, no.3, pp.297-302, Jul.1988.

[5] A Nabae, I Takahashi and H Akagi. „A Neutral Point-clamped PWM Inverter". IEEE Transactions on Ind Application, vol IA-17, September/October 1981, pp 518-523.

[6] H. I. Hussein "On -Line UPS with Low Frequency Transformer for Isolation" Iraq Journal for Electrical and Electronics Engineering, Vol.10.no.2, pp: 100-106, 2014.

[7] H. I. Hussein, "Harmonics Elimination PWM (HEPWM)". International Journal of Engineering Research and General Science, Vol.2.no.2.pp: 172-181. 2014.

[8] M.I Jahmeerbacus, M.K Oolun, M.K.S Oyjaudah, "A Dual-Stage PWM DC to AC Inverter with Reduced Harmonic Distortion and Switching Losses" Science and Technology-Research Journal,Vol 5, pp 79-91, 2000.

[9] R Senthilkumar, M Singaaravelu, " design of single phase inverter using dsPIC30F4013" International Journal Engineering Research & Technology, Vol2, pp. 6500-6506, 2012.

American Journal of Engineering Research (AJER) 2016
American Journal of Engineering Research (AJER)
e-ISSN: 2320-0847 p-ISSN : 2320-0936
Volume-5, Issue-2, pp-210-214
www.ajer.org
Research Paper Open Access

Development of Android Address Book Using Oracle Database

[1]Gbadamosi Luqman and [2]Akanbi Lukman
[1]*Computer Science Department, Lagos State Polytechnic, Lagos State, Nigeria*
[2]*Research Scholar, Embeddedkits Technology, Osun State , Osogbo, Nigeria*

ABSTRACT : *Address book is a database that stores essential information like name, contact number, address, e-mail id etc of our friends, family and other important people. There has been a major challenge among computer scientist and other able individual when creating SQL oracle database and managing files on mobile devices. Present address book applications are not user friendly and there is a need for user to use interactive application. Most individual cannot afford to buy exorbitant price of android address book develop by software development company which cannot be customized to user requirement. This brings to the development of an address book application using SQL LITE database. This will be develop and deploy on any phone with android operating system. The app being cross platform can be used on various Linux operating system such android OS, The result of the application developed is interactive, user friendly, user can store many contact, change Background, Text Fomat, Colour, Theme and more. The application was deployed on mobile phone (android). It was tested on Samsung phone. The .APK application can be installed on any mobile phone operating on Linux operating system. The application is implemented successfully*
Keywords: *Address Book, Android, SQL, .APK, Mobile, Linux*

I. INTRODUCTION

Android is an open source software assemble of an operating system, middleware and key applications for mobile devices introduced by Google capable of running multiple application programs. Android platform is produced to make new and innovative mobile application program for the developers to make full use of all functions connected to handset internet(Ahmad et al, 2012).

Android also supports GPS, Video Camera, compass, and3d-accelerometer and provides rich APIs for map and location functions. Users can flexibly access, control and process the free Google map and implement location based mobile service in his mobile systems at low cost. Android platform will not only promote the technology (including the platform itself) of innovation, but also help to reduce development costs, and enable developers to form their mobile systems with unique characteristics(Almahdi,2011).

II. REVIEW OF RELATED WORKS

The most recent released versions of Android are:

- (Burns , 2010), which revamped the user interface and introduced HTML5 and Exchange ActiveSync 2.5 support.
- (Georggi, 2004), which introduced speed improvements with JIT optimization and the Chrome V8 JavaScript engine, and added Wi-Fi hotspot tethering and
- (Garfinkel, 2010), which refined the user interface, improved the soft keyboard and copy/paste features, and added support for Near Field Communication.
- (Hoffman, 2007), a tablet-oriented release which supports larger screen devices and introduces many new user interface features, and supports multicore processors and hardware acceleration for graphics. Hoffman et al. (2012) also proposed "TaintDroid", an efficient, system-wide dynamic taint tracking and analysis system capable of simultaneously tracking multiple sources of sensitive data

III. SYSTEM ANALYSIS, DESIGN AND DEVELOPMENT

The stages of development involve the following stages

Stage 1: Android: Android is an operating system based on Linux kernel and it is designed primarily for touch screen mobile devices such as smart phones and tablet computers. It is popular with technology and open nature has encouraged a large community of developers to work on it.

Stage 2: SQLITE*:* SQLITE is an in-process library that implements a self-contained, transactional SQL database engine. It is a compact library with all features enabled. SQLITE stores the entire database as a single cross-platform file on a host machine. It implements this simple design by locking the entire database files during writing. It is a popular choice for storing the user information within the application and it is stored in the client side.

Stage 3: Development Tools: Eclipse and Android SDK Tools are Integrated Development Environment (IDE) for designing and developing the Java based application.

Stage 4: Eclipse*:* Eclipse is the Multi-Language Integrated Development Environment (IDE) which comprises a base workspace with extensible plug-in systems. The applications are mostly developed using Java and other languages can be used by adding plug-ins.

Stage 5: Android SDK Tools: Android Software Development Kit (SDK) which is a set of development tools. They include the tools like debugger, libraries, emulator, tutorials, documentation and sample codes. Eclipse and Net beans supports Android Development via plug-in. The older tools and platforms are downloaded at any point of requirement. Android Application are packaged file system with .APK file extension which holds the .dex and resource files etc

IV. SYSTEM IMPLEMENTATION

The implementation of the address book application for android using SQL LITE database includes the following

4.1 Development of the Flowchart

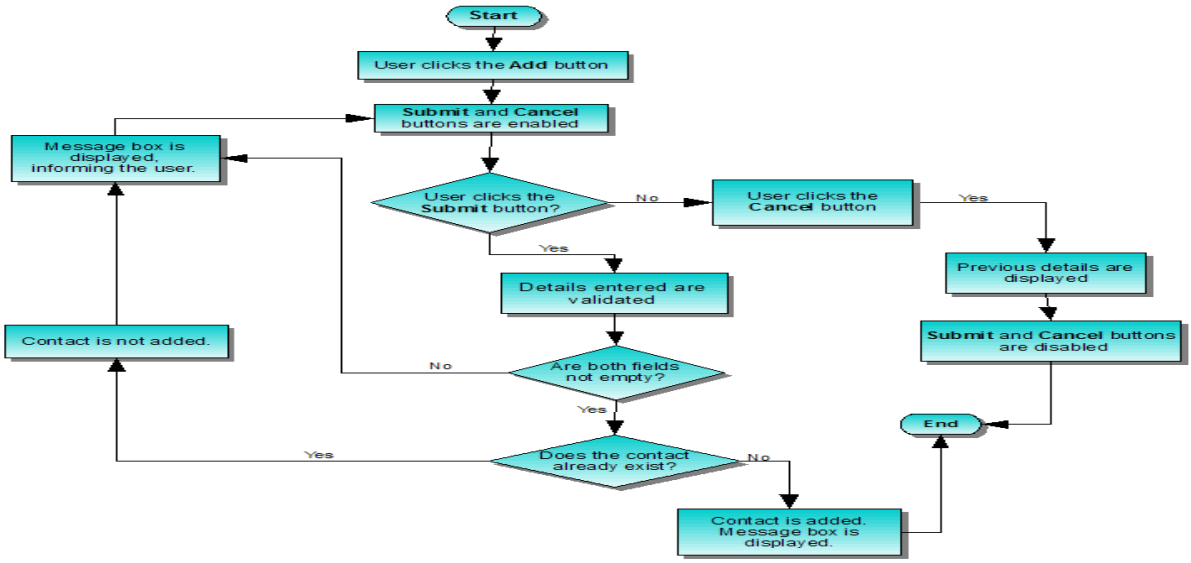

Figure 1.1: Developed Address Book Flowchart

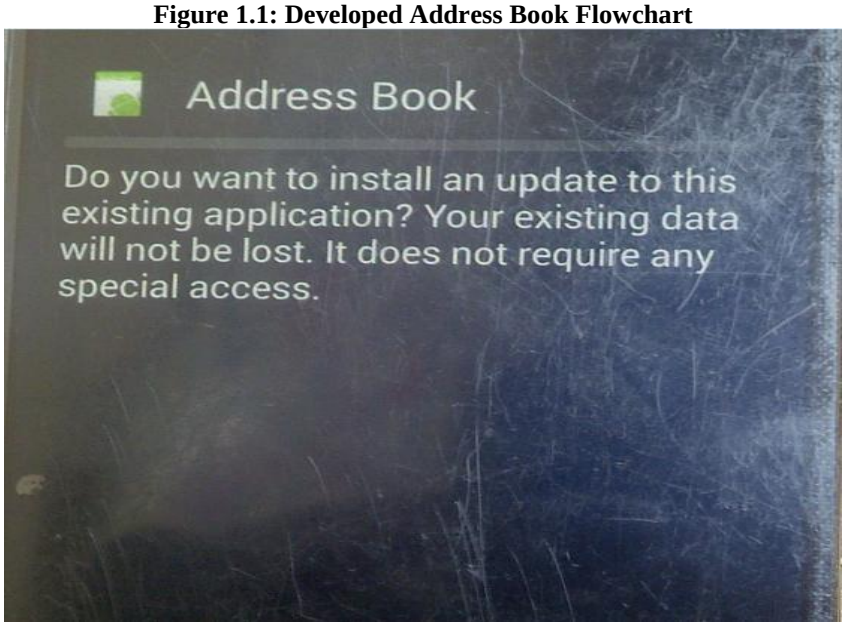

Figure 1.2: Installation Procedure

4.2 DISCUSSION OF THE INPUT USED

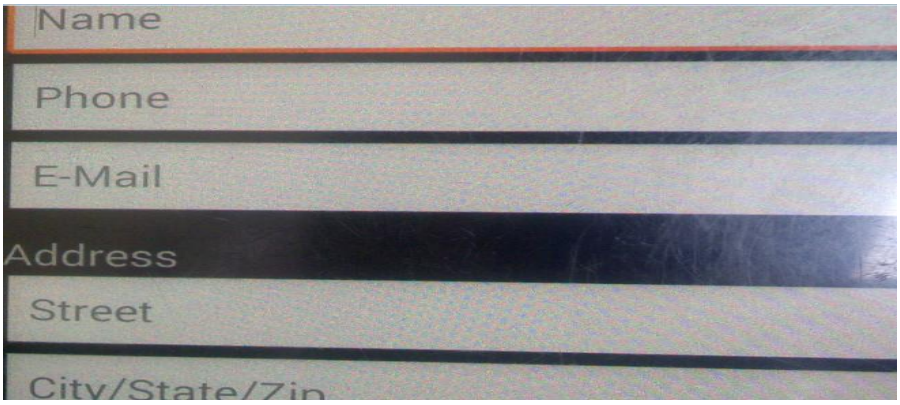

Figure 1.3: Login Information

The input requirements are the information enter into the Sql lite database of the android address book. The detail information of the contact person is entered into the field. Figure 1.3 is the form to fill in the contact information and Figure 1.4 save the contact information into the SQL LITE database for easy retrieval

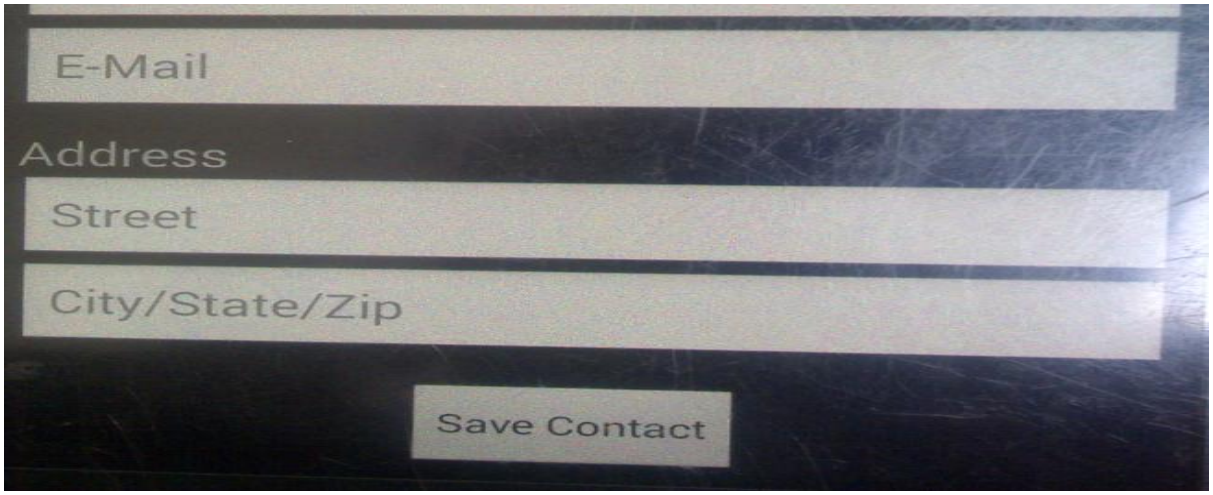

Figure 1.5: Save Contact

4.3 DISCUSSION OF THE OUTPUT OBTAINED

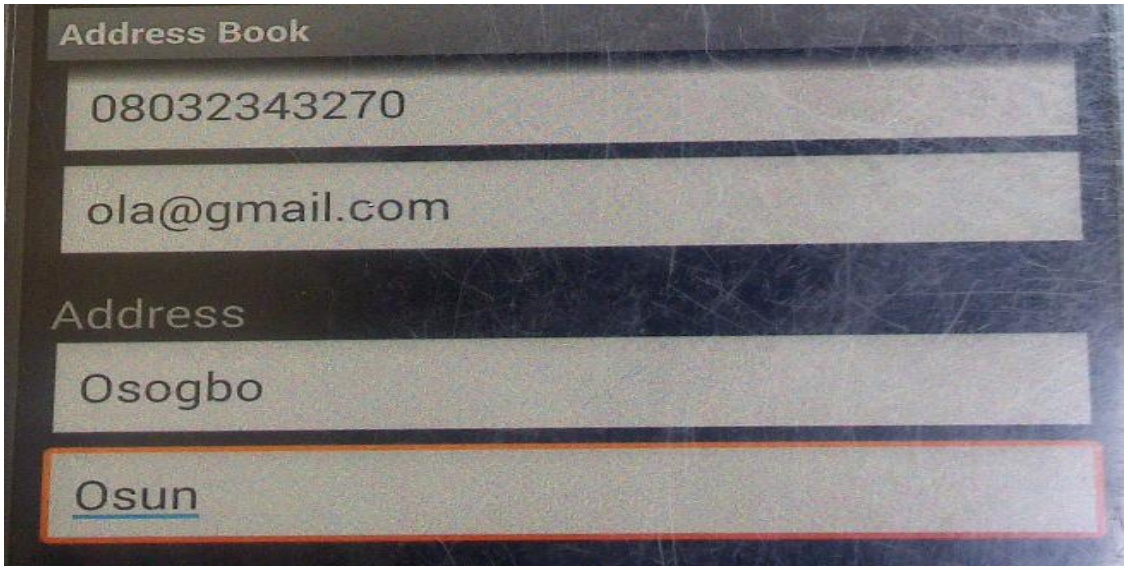

Figure 1.6 :Saved information

Figure 1.7: Result Output

Figure 1.6 and 1.7 are the output information that will be displayed after saving the contact to each field. As the mobile phone user click on any of the name, the information that is already saved in the SQL LITE database will be displayed for easy retrieval

4.4 MAKING USE OF THE PROGRAM

The program will be used and deploy to any phone with linux operating system. Linux operating system user will make use of the address book application for the following

i. Storing of user contact with unlimited space
ii. Adding pictures and audio files
iii. Set passwords to prevent unwanted access
iv. Customizing the entries (font size, color, line numbers, background color)
v. Calendar

V. CONCLUSION

This paper implementation of oracle sql lite database in android programming to create an address book application is implemented successfully and the application was deployed on android phone for testing. Android is a software stack for mobile devices that includes an operating system, middleware, The Android SDK provides the tools and libraries necessary to begin developing applications that run on Android-powered devices. Android provides full support for SQLite databases. Databases created will be accessible by name to any class in the application, but not outside the application

VI. RECOMMENDATION

This paper is recommended to be used by anybody with Linux operating system (android) to keep its personal contact, change themes, fonts and more. It can easily be used by anybody without computer knowledge and user needs not to be train because of its user interactivity.

Incorporating GPS into the application so that the contact of the person can be retrieved incase the phone is stolen. Present design focused on .APK extension of Linux operating system phone (android), therefore future application can be develop in order to be deployed on windows phone(e.g IPHONE).

REFERENCE

[1] **Ahmad Haris Abdul Halim, MaizatulAkmar Ismail and Sri Devi Ravana,(2012)** Integration between Location Based Service (LBS) and Online Analytical Processing (OLAP): Semantic Approach, Journal of Information Systems, Research & Practices, Vol.1(1) Open Hanset Alliance, http://www.openhandsetalliance.com/.

[2] **Almahdi Mohammed Ahmed1 (2011),** Azuraliza Abu Bakar2, Abdul Razak Hamdan3 Dynamic Data Discretization Technique based on Frequency and K-Nearest Neighbour algorithm, 2009 2nd Conference on Data Mining and Optimization, 27-28 October 2009, Selangor, Malaysia

[3] **Burns R. Symbian (2010)** [Internet]. Symbian Signed. Available from:http://developer.symbian.org/ wiki/index.php/Category:Symbian_Signed

[4] **Georggi,(2004)** A General Architecture in Support of Interactive, Multimedia, Location-Based

[5] **Garfinkel S. 2010**. How Android security stacks up. [Internet]. Available from: http://www.technologyreview.com/communications/24944/page2/ Mobile Applications in IEEE Communications Magazine November 2006 Xiaotao Wu and Henning Schulzrinne, Location-based Services in Internet Telephony ieee in 2004

[6] **Hales, W. (2013).** Bridging the Gap Between the Web and Mobile Web. Unite State Of America: O' Reilley Media Inc.

[7] **Hoffman D. 2007**. Blackjacking security threats to BlackBerry devices, PDAs and cellphones in the enterprise. Indianapolis (IN): Wiley.

[8] **Hypponen M. 2006**. Malware goes mobile. [Internet] Sci Am: 70–77. Available from: http://www.cs.virginia.edu/~robins/Malware_Goes_Mobile.pdf.net/

American Journal of Engineering Research (AJER) 2016
American Journal of Engineering Research (AJER)
e-ISSN: 2320-0847 p-ISSN : 2320-0936
Volume-5, Issue-2, pp-215-221
www.ajer.org
Research Paper Open Access

Lift & Drag Reductions on Iced Wings during Take Off and Landing with Unmanned Aerial Vehicles

Ian R. McAndrew FRAeS, PhD
(Department of Graduate Studies, College of Aeronautics, Embry Riddle Aeronautical University, USA)

ABSTRACT: *This research paper addresses an novel problemthat has not been addressed in detail for many decades. Ice formation on aircraft has procedures and protocols to deal with expected and actual problems. Complex modern aircraft are equipped with a variety of techniques to remove Ice formation on an aircraft, especially the wings. The introduction of Unmanned Aerial Vehicles has added an old problem, that of low speed and the lack of power to overcome losses in lift through ice formation. In this research the different types of Ice formation, how they combine and affect Lift and Drag are also addresses in theory and application. Furthermore, practical design and operational recommendations are made for take-off and landing.*

Keywords *–Aerodynamics, Lift and Drag, Ice formation and Unmanned Aerial Vehicles.*

I. INTRODUCTION

Ice formation on wing prior to take-off can be serious and fatal. There are many examples of where aircraft have crashed whilst trying to take-off in icy conditions and fortunately in the modern commercial world this is now a very remote possibility, although it is still surprisingly an occurrence. Any domestic airport that experiences below freezing conditions will have protocols and equipment to deal with ice formation and weather conditions. Runways need to be cleaned and any ice on an aircraft removed; especially from the wings. If not the lift is reduced and drag increased [1].

Ice management is divided into two parts: ice removal and ice prevention. The former can be achieved by many means provided it does not damage the aircraft with a mechanical intervention. While the latter needs the assistance of chemicals and the ones initially developed are no longer used due to the polluting effects in the water table at the airports. The modern chemicals need to be used, sprayed, in a dedicated area where over use is captured and not drained into the environment. If you have ever been delayed on a flight you will know this spraying is done on an industrial scale and prevents ice formation for up to 30 minutes. Any delays and the aircraft will need to return to be re-sprayed [2]. In figure 1, below, it shows a typical spray application on an aircraft to prevent ice formation; mainly on the wings upper surface but also the leading edge. It is worth pointing out here that there are international regulations and procedures for commercial aircraft to follow in these conditions and it is unlikely that one would take-off without. Unlike small General Aviation, GA, where this may be in the owner's manual and ignored or not understood, an all too frequent happening in various parts of the world.

Figure 1, Ice prevention spray prior to take off.

Figure 2, below shows the distribution of aircraft crashes that occurred in USA from 2006 – 2010 [3]. There were 30 in total, divided into three classifications of aircraft. There were on 2 in this period for what could be classified commercial aircraft, over 50 seats, and are represented by part 121.2. Part 135.6 is for an aircraft over 7 seats and that accounted for 5 crashes [3]. The remainder, 23, can be summarized as small, GA, with 6 or fewer seats. Each represents a crash with at least one fatality. Clearly, smaller aircraft are more at risk and a higher probability of such an event.

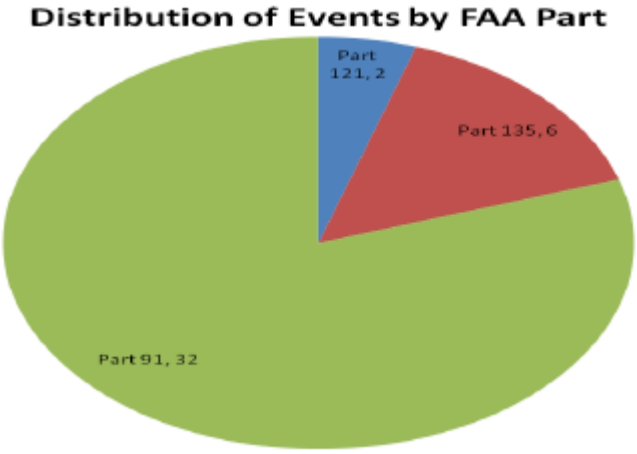

Figure 2, accident by type of aircraft, 2006-2010 in USA

Ice formation is, and will remain an important risk to aircraft at all stages of flight, but especially when taking off and landing. The management of this is critical. In this paper the following section will discuss what we mean by ice formation and the reasons how it affects flight.

II. ICE FORMATION AND INFLUENCES

Leading edge ice is the most critical formation on an aircraft, it will reduce life and increase drag according to thickness. During critical stages of flight, e.g., take-off, it will inhibit the available movement capabilities and stability. As discussed above, there are many recorded incidents of this happening. In figure 3, below, is an example of extreme buildup of leading edge ice on a wing. This would be classified as a serious build-up of ice for any aircraft. This ice has been formed when the aircraft is static and can be from it facing the wind direction to spray on this face due to its parked position. Visual inspection before take-off can identify and actions taken to remove prior to flight [4]. In flight there are two additional reasons. First, RIM ice forms as a wedge on the leading edge at temperatures below -20^0C when water droplets freeze as they strike the wing and freeze rapidly *in situ*.Secondly, Glazed ice, occurs from 0^0C to -20^0C when super cooled droplets strike the leading edge and from as they pass over the leading edge and upper surface. Depending on the altitude, flight path and weather conditions this may occur and re occur. Many aircraft have systems to heat or prevent both types of ice build-up. Those aircraft that fly where this is very comments, turbo-prop, have an additional feature.

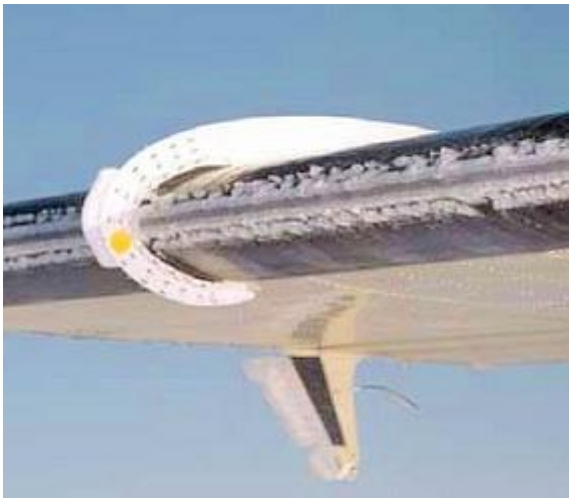

Figure 3, leading edge ice on a wing.

When leading edge ice forms and the aircraft cannot develop enough energy from the engines or mechanically to distribute heat is problematic there are alternative solutions. Figure 4 is an example where the leading edge is rubber that can be inflated with compressed air to expand. The expansion results in the ice being stretched, cracked, and falls away. They are very successful and can remove all ice within seconds of being deployed, a feature that heat cannot emulate as the time will be much longer. It does have disadvantages, maintenance is high and usable life is shorter than conventional material.

Figure 4, rubber leading edge for ice removal.

Ice on the top surface of a wing reduces, Figure 5 below, the maximum lift and the Angle of Attack, α, at the separationpoint. Thus stall starts earlier. This is less than desirable, it is not as serious in comparison to leading edge ice formation. Indeed, it is possible to fly safely with ice if no major or sudden movements whilst ice removal techniques are deployed [5]. If none available a gently slow decent to warmer air is needed Ice forming on a wings upper surface is, as shown, usually smooth enough to only marginally reduce lift in level flight, providing airspeed is not too slow, lift will be sufficient for level flight is possible. Any consequences from increased drag will not considered until later. UAV struggle to gain speed to increase lift unlike most other aircraft.

Figure 5, upper surface ice in flight.

Of course, ice is a problem all over the structure. Figure 6 below, shows Super cooled Large Droplet, SLD, conditions, similar to clear ice. Droplet size in this case is large and extends to unprotected parts. It forms ice significantly faster than normal icing conditions. This is a greater concern with lower altitude flying (historically for unmanned vehicles). It is also as applicable for all parts of the structure and especially leading edges. This was a principal concern for long ocean flights, their only solution was to fly lower, although the increased density of air resulted in increased drag and fuel concerns and was seen as a major concern in the early days. Indeed, drag and low altitude have to be part of any low speed and low altitude flight design.Flights will always involve operating in environments where ice will be a problem and can never be removed. It can be managed and even allowed for in flight planning if the theory is fully understood.

Figure 6, nose ice formation.

III. LIFT AND DRAG ON A WING

Lift and drag are linked. As drag increases the lift needs to increase to maintain level flight. Alternatively, increasing lift will always result in an increase of drag. Figure 7, below, shows the relationship of lift and drag as airspeed increases. More importantly, total drag can be used to maximize efficiency for fuel consumption. Anything that reduces the lift and increases the drag will reduce the endurance. Figure 8 introduces the relationships as ice is formed on a wing [6].

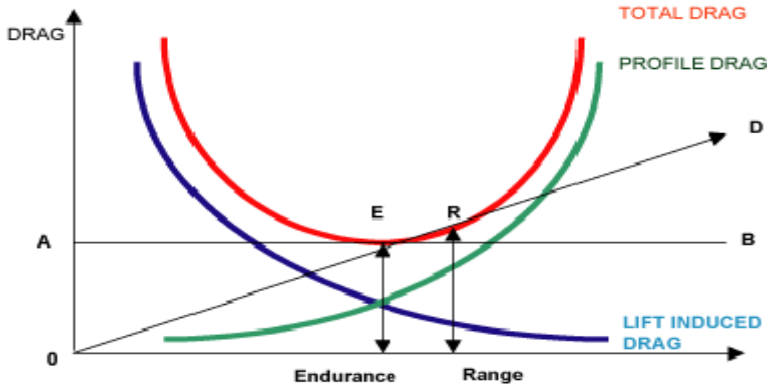

Figure 7, drag v. lift as airspeed increases.

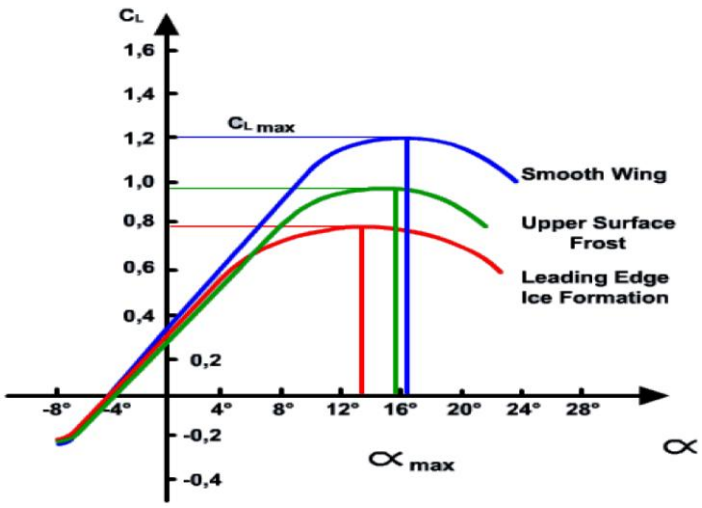

Figure 8, Lift variations under different configurations.

Figure 8, above clearly shows the three classic cases of: a smooth wing, leading edge ice and upper wing ice. A comparison needs to be made with the total lift and the maximum point (where stall occurs). Upper wing ice reduces a little and brings on the point of stall earlier. The leading edge further reduces the lift and stall point. A stall point lowering means rapid or medium movements of the nose up or down will result in the aircraft stalling.

IV. WIND TUNNEL DATA

Figure 9, below, is of a standard airfoil (constant wing section) in the wind tunnel. To simulate ice on a leading edge or upper surface sand paper is attached. If you vary the roughness of the grain you can match different ice thicknesses. Lift and drag are measured in Newton's, N, and the result shows how the Angle of Attach, α, is increased [7]. This is for a constant speed that in this case represented a typical take-off or landing speed for an Unmanned Aerial Vehicle. The wing has no high lift features or parameters and shows a standard configuration. As the research is concentrated on take-off and landing influences these differences will be ignored for the current research.

Figure 9, airfoil section in wind tunnel.

Table1, Lift v. Angle of Attack for the three principal profiles of smooth, upper and leading edge ice formation.

Angle of attack, in degrees	**-4**	**0**	**+4**	**+8**	**+12**	**+16**
Lift (smooth), N	-3	8	21	33	37	30
Lift (upper surface), N	-6	5	16	26	30	26
Angle of attack, in degrees			**+4**	**+8**	**+9.5**	**+11**
Lift (leading edge), N			11	21	24	22

Table 2, Drag v. Angle of Attack for the three principal profiles

Angle of attack, in degrees	**-4**	**0**	**+4**	**+8**	**+12**	**+16**
Drag (smooth), N	5	2	3.5	6.5	11	17
Drag (upper surface), N	6	5	8	13	17.5	24
Angle of attack, in degrees	**-4**	**0**	**+4**	**+8**		
Drag (leading edge), N	7.5	8	14.5	24		

Tables 1 & 2 show the lift and drag influences from the experiment and show the changes and where the stall point occurs for the lift and the bottom out point for the drag [8]. These on their own are classic and closely follow the expected results from figure 8 above. The important part is for take-off and landing. What these allow is for a comparison to be made with the theoretical glide path for landing. Knowing the maximum Angle of Attack allows for take-off to be accommodated if the UAV is taking off from a remote landing with no assistance [9]. The glide ratio can be determined by using this data to configure a Lilienthal Diagram for the three wing configurations addressed here: smooth, upper surface ice and leading edge ice.

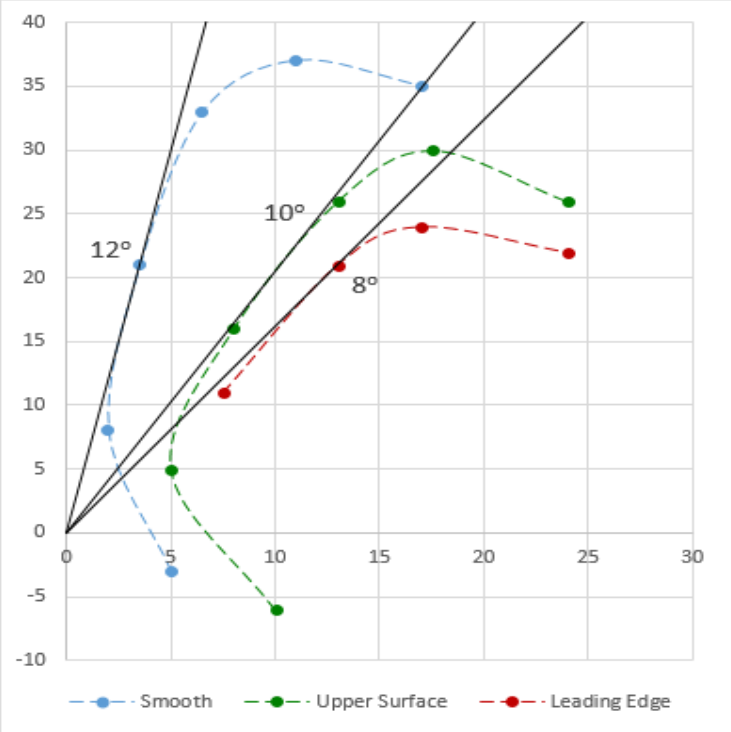

Figure 10, Lilienthal Diagram for the three wing configurations.

This, even more than the take-off, shows a greater influence. The three lines (curves) are for the Co-efficient of lift and drag at each recorded Angle of Attack. Note the (0, 0) points on the graph. The blue line represents the smooth wing. The ideal glide angle is represented by 12^0 (tangent from (0, 0) that means the optimum glide path is this value. If greater than that value there is a risk to stall on approach. For a wing with ice on the upper surface the value reduces to 10^0 and with a leading edge ice even lower at 8^0[10]. Thus, leading edge ice means a very slow angle to land, longer approach, and if this, for any reason, increases there will be stall. If descending from 20,000ft the difference can be as much as 50% more for the leading edge approach. It may be acceptable in emergencies, for typical landings it will congest the sky even more. With an UAV it is generally not possible to detect leading edge ice as the pilot is remote, they are low-tech and have no warning systems. It can be argued the default landing pattern for all UAV should be based of parameters where it is assumed as the worst case

V. CONCLUSION

This research has addressed a problem facing all flights, that of ice formation. The theory has been explained and practical applications. When applied to UAV there are unique problem and situations. The data shows that theory is close to practice, but not completely. Using the drag and lift values the glide paths were determined using a Lilienthal Diagram. What this shows is that with leading ice the glide path should be considerable increased and should always unless it is known for a fact that no ice is present.

Until UAV can operate (have the same array of safety and operational features) according to typical aircraft, and have the systems to ensure safe situations then the default situation must be assumed. UAV designs should be required to determine these situations before being allowed to fly beyond the line of sight or over populated areas that pose a risk to the public.

VI. ACKNOWLEDGEMENTS

Thanks and appreciation are expressed and extended to my Dean, Dr K Witcher, for his support and encouragement in the time to finish this seminal study that has lead in various directions with several publications at conferences and in Peer Reviewed Journals.

REFERENCES

[1] National Transportation Safety Board, "Accident Synopses", Aviation Accident Database and Synopses, [online database], URL: http://www.ntsb.gov/aviationquery/index.aspx, [cited June 5, 2011]

[2] Federal Aviation Administration, "Aviation Safety Reporting System", ASRS Database Online, URL: http://akama.arc.nasa.gov/ASRSDBOnline/QueryWizard_Filter.aspx, [cited June 5, 2011]3Steven D. Green: "A study of U.S. Inflight Icing Accidents, 1978 to 2002", AIAA 2006 – 82, 44th AIAA Aerospace Science Meeting and Exhibition – January 2006, Reno, Nevada.

[3] David R. Gingras, Billy P. Barnhart, et al.: "Envelope Protection for In-Flight Ice Contamination", NASA/TM – 2010-216072. AIAA – 2009 – 1458, [online database] URL: http://gltrs.grc.nasa.gov/reports/2010/TM-2010-216072.pdf,[cited July 15, 2011]

[4] Federal Aviation Regulation: Aeronautical Information Manual, U.S Department of Transportation. Aviation Supplies & Academics, Inc. Newcastle, WA 98059-3153

[5] McAndrew IR, Navarro E and Witcher K. (2015). Drogue deflections in low speed unmanned aerial refueling. International Journal of research in Aeronautical Engineering & Mechanical Engineering, IJRAME. 3(1): 119-127.

[6] J. Bertin& R. Cummings: Aerodynamics for Engineers (Prentice Hall, 5th ed. June 28, 2008)

[7] I. R. McAndrew, K Witcher (2013). Design Considerations and Requirements for In-flight Refueling of Unmanned Vehicles. J Aeronaut Aerospace Eng. 2: 108. doi:10.4172/2168-9792.1000108.

[8] J. D. Anderson. Introduction to flight (McGraw Hill, 6th Ed. New York 2005).

[9] McAndrew, I. R., Witcher, K. & Navarro, E. (2015). UNMANNED AERIAL VEHICLEMATERIAL SELECTION AND ITS INFLUENCE ON DRAG AT LOW SPEED, International Journal of Unmanned Systems Engineering, 2nd World Congress on Unmanned Systems Engineering, Granada, Spain, 30th -31st July

[10] Ison, D., McAndrew, I., Weiland, L., & Moran, K. (2013, July). AIR TRAFFIC MANAGEMENT PRINCIPLE BASED DEVELOPMENT OF AN AIRPORT ARRIVAL DELAY PREDICTION MODEL. The Second International Conference on Interdisciplinary Science for Innovative Air Traffic Management on Applied Mathematics and Operations Research for ATM. Toulouse, France.

American Journal of Engineering Research (AJER) 2016
American Journal of Engineering Research (AJER)
e-ISSN: 2320-0847 p-ISSN : 2320-0936
Volume-5, Issue-2, pp-222-228
www.ajer.org
Research Paper Open Access

Development of an Animal Drawn Hydraulic Boom Sprayer

Anibude, E.C; Jahun, R.F and Abubakar, M.S.
Department of Agricultural Engineering, Bayero University, Kano.-Nigeria,

Abstract: *The pest attack on crop is a serious problem in the Northern Nigeria. The small/medium scale farmers spray in a season using manually operated knapsack sprayers which are laborious, time consuming and posses narrow swath width. And the tractor mounted boom sprayers are too expensive for these farmers. The prototype of an animal drawn hydraulic boom sprayer was developed considering the agronomical and functional requirement for application of chemicals on field crops. The major components include; 100 litres spray tank capacity, mainframe, operator seat, 3Hp petrol engine, piston pump, Boom, ten flat fan nozzles, wheel and axle shaft. The petrol engine was used as the power source for operating the piston pump during spraying and pair of bullocks was used for hauling purpose. Application rate of 260 L/ha was achieved, theoretical field capacity of 1.16 ha/hr, effective field capacity of 1.04 ha/hr and 89.6% field efficiency. Comparing the results with what was obtained using the manually operated knapsacks sprayer represents 62% and 37% increase in effective field capacity and field efficiency respectively.*

Significance: *The finding of the research study presented in this paper could be used to reduce the drudgery faced when using knapsack sprayers and boost agricultural mechanization during the application of liquid chemical on field crops.*

Keywords: *Boom sprayers, field crops, animal traction.*

I. INTRODUCTION

Chemicals are widely used for controlling disease, insects and weeds in the crops. They are able to save a crop from pest attack only when applied on time. They need to be applied on plants and soil in the form of spray, dust or mist and granule. The chemicals are costly, therefore equipment for uniform and effective application is essential (Bindrah and Singh, 1980).The primary aim of crop protection equipment (sprayers) is the reduction in the population of developmental stage of pest which is directly responsible for damage within individual fields and is most efficient when the chemical is applied economically on a scale dictated by the area occupied by the pest and the urgency with which the pest population has to be controlled taking the environment into consideration (Mathews, 1992). The use of mechanical power in Agriculture has been increased due to use of more tractors. Even though the tractor operated boom sprayers is available for spraying but due to low ground clearance, the crop may damage during spraying. Even though draught animal power is in decreasing trend, Northern – Nigerian farmers still predominantly use the bullocks for agricultural purpose. The small/medium farmers are maintaining a pair of bullocks for carrying out field operation. Animal drawn sprayers have been used where farmers have draught animals such as oxen. Mathews (1992) reported an animal drawn sprayer constructed in central Africa, which has the tank, boom and pump mounted on a suitable wheeled frame. The sprayer can be operated even when conditions are too wet to allow the passage of a tractor, and the animal does not damage the crop. The pump is driven by means of a chain drive from one of the wheels on a frame. When this is used, the pump has to be operated from a few yards to builds up sufficient pressure at the nozzle before spraying starts, if wheel slip occurs, spray pressure will decrease. Singh *et al* (2009), Developed and evaluated a bullock drawn sprayer. The sprayer was developed considering the agronomical and functional requirement for application of chemicals on soybean and other field crops. A commercially available pressure vessel of 9498cm^3 was adopted to maintain the required fluid pressure during spraying in the field. Two reciprocating pumps of 127cm^3 swept volumes were provided to create working pressure range of 300-350 kPa inside the pressure vessel at 94-100rpm. The unit was tested for spraying of chemical in the laboratory and on field with pair of bullocks. During laboratory test, the uniformity coefficient of droplets ranged from 2.2 to 2.7 and was within the acceptable level of 4.0 for all the six nozzles. In field testing, the average discharge of six nozzles varied from 481.6 to 529ml/min with average boom discharge of 3.03 l/min at pressure of 343 $\pm$ 2.5 kPa. Effective field capacity and power requirement to operate the sprayer was 0.56 ha/hr and 0.68kW respectively. Kalikar et al. [2013] carried out performance evaluation of bullock cart mounted engine operated sprayer. The engine of 4Hp was used as power source for operating the sprayer and the bullocks were used for hauling purpose. The sprayer

units consist of 9 hollow cone nozzles adjustable according to row spacing of crop. During performance evaluation, the field capacity of the sprayer was 1.89 ha/hr and average speed of bullocks cart during spraying operation in cotton crop was 2.8 Kmph. The draft measurement for spraying operation was found to be 804.42N. Mohan, S. [2012] developed an engine operated sprayer, and it was conceptualized that a long pipe attached to pump make it versatile and a small diesel engine can run the pump and make tractor free for other farm operations. Accordingly, a 250 liters plastic tank was fixed on the frame having tires attached on two sides and hook for towing with tractor. An ASPEE-HTP triplex plunger pump was used and operated with 5.5hp 3600 rpm Greaves diesel engine. Veerangouda *et al.*[2010] did performance evaluation on three types of sprayers namely bullock drawn traction sprayer, bullock drawn engine operated sprayer and local cart mounted engine operated sprayer for cotton crop. The bullock drawn traction sprayer is capable to cover 6 rows at a stretch with an average field capacity of 0.66 ha/hr with a power output of 0.68KW. The average quantity of chemical solution sprayed per ha was 441.80 l/ha. The bullock drawn engine operated sprayer is capable to cover 6 rows at a stretch for cotton crop with an average quantity of 585.92 l/ha at an operating pressure of 20kg/cm^2. The average travel speed of unit is 2.84kmph with an average draft of 76.67kg. The field capacity of bullock drawn engine sprayer is 1.19 ha/hr with a power out put of 0.60kw. The field capacity of local cart mounted engine sprayer is 0.66 ha/hr with power output 0.72kw. Among three sprayers tested, the bullock drawn engine operated sprayer worked satisfactorily.

In order to cover large area and to avoid labour scarcity the animal drawn hydraulic boom sprayer has been developed for field crops at Agricultural Engineering Department, Bayero University, Kano. The animal drawn boom sprayer has been tested and its performance evaluation has been carried out during the year 2015.

II. MATERIALS AND METHODS

2.1 Design Consideration: Boom length, draught requirement and source, operating pressure, number of nozzle/nozzle spacing, ridge height, width and spacing were taken into consideration during the prototype sprayer development.

2.2 Selection Of Materials

The criteria for materials selection for the various components of the prototype sprayer was based on their availability of the materials in the local market or the environment, suitability of the materials for the working conditions in services and the cost of the materials (Khurmi and Gupta, 2007).

Table 2.1 shows the materials selected for the main components.

S/N	Components	Materials Selected
1	Main frame	Mild steel angle iron
2	Tank	Galvanized sheet
3	Spray boom	Mild steel square pipe
4	Traction wheel	Mild steel flat bar
5	Axle shaft	Carbon steel round bar
6	Nozzles	Plastic
7	Belts	Rubber
8	Draft pole	Galvanized steel pipe
9	Operator seat	Mild steel angle iron
10	Engine seat	Mild steel angle iron

2.3 Establishment of Design Parameters and Components

2.3.1 Size of Frame: The size of the main frame in terms of length, width and height was established with respect to ridge size, number of ridges per swath and stability of the implement. The size of the frame members were selected base on strength, rigidity and weight limitations for the comfort of the draught animal.

2.3.2 Minimum Permitted Weight of Bull: The minimum permitted weight of bull for draught was chosen as 1500N (Goe and Mcdowell, 1980). This implies that, for a pair of bulls (assuming the same weight) will be twice the minimum permitted weight. That is;

Wt = Wp x 2

Wp = Minimum permitted weight

Wt = total weight of bulls.

2.3.3 Tank: The tank was designed by considering the shape, volume capacity and weight.

Shape of the tank: The shape of tank was chosen to be cylindrical based on the fact that cylindrical shape fits in tightly into the tank holder on the main frame. Figure 3.1 shows the tank shape.

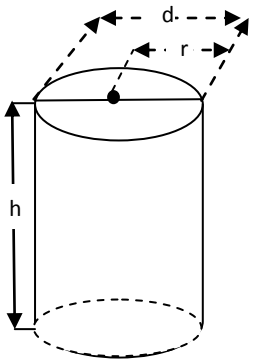

Figure 1: Diagram showing the shape of the tank

Tank capacity: The tank capacity was determined using the following mathematical expression as given by Spiegel (1968);

$C_t = \pi r^2 h$ ..... (1)

Where;
C_t = tank capacity
π = constant (pie)
r = tank radius
h= tank height

Total volume of tank material

Total volume of materials used for the tank is given as

$$Vtm = (2\pi r2 + 2\pi rh) \times thickness\ of\ the\ material \ldots (2)$$

Weight of the Tank Material

Tank weight was determined by considering the density of the tank material (galvanized sheet metal). Thus;

$W_t = V_{tm} \times \rho_t$

Where,
W_t = weight of empty tank
ρ_t = density of tank material.

2.3.4 Boom Size: The Boom size in terms of length was established based on field capacity, speed and time using the expression given by Mathews (1992) thus;

$$L = \frac{A}{t \times S} \ldots\ldots\ldots\ldots\ldots\ldots\ldots\ldots\ldots\ldots\ldots (3)$$

Where,
A = Area to be covered (ha)
S = Spraying speed (Km/hr)
T = Time taken to cover an area (hr)
L = Length of boom.

2.3.5 Pump Selection: The pump was selected based on the pressure required to be maintained at the nozzle, type of spray materials to be sprayed and the volume of spray liquid to be delivered per unit time (l/min) (Kaul and Suleiman, 1990).

2.3.6 Determination of Pump Output: The pump output in liter/minute was determined in accordance with Kaul and Suleiman (1990) thus;

$$Pump\ output = \frac{S \times AR \times V}{600} \ldots\ldots\ldots\ldots (4)$$

Where,
S = Swath width = boom length (m)
AR = Application rate (L/ha)
V = Velocity = spraying speed (km/hr)

2.3.7 Nozzles and Nozzles Spacing: It is important to select nozzles that develop the desired spray pattern. The following points mentioned by Kaul and Suleiman (1990) were carefully considered during the selection of the appropriate nozzles.

a. The type of spray operation.
b. Approximate pressure to be used for spraying
c. Nozzle spacing.
d. Type of spray pattern
e. Approximate speed of travel.

2.3.8 Determination of nozzle flow rate: The nozzles throughput in litre/minute was determined in accordance with Kaul and Suleiman (1990)

$$\text{Nozzle throughput} = \frac{PO \times NS}{BL} \ldots\ldots (5)$$

Where,
PO = Pump Output (L/min)
NS = Nozzle spacing (meters)
BL = Boom Length (meters)

2.3.9 Description of the Machine/ operation: The prototype sprayer is made basically of the main frame, spray tank, pump/prime mover, traction wheel, boom, nozzles and flexible rubber hose. The main frame is mounted on the axle shaft with two traction wheel and carries the spray tank, pump/prime mover and boom assembly. The spray tank is connected to the nozzles with the aid of distributing flexible rubber hose via the pump. At the rear end of the frame, is bolted the boom on the boom riser which carries the nozzles. The chemical in the spray tank flows by the gravity to the pump and sends the chemical with a pressure monitored on the pressure gauge to the nozzles. The prime mover (engine) which is the power source gives power to the pump with the aid of v-belt and pulleys. A pair of bullocks is used as draught for pulling the prototype while the spraying operations are on-going.

Plate 1: Assembled Prototype Sprayer

Plate 2: Assembled Prototype Sprayer

2.3.10 Determination of Application Rate: The spray liquid application rate was determined using the mathematical expression as given by Kaul and Suleiman (1990).

$$Ap = \frac{V_t}{A_t} \ldots\ldots\ldots\ldots\ldots\ldots\ldots\ldots\ldots (6)$$

Where,
A_p = Application rate (L/ha)
V_t = Total volume of effective spray (L)
A_t = Total Area treated (ha)

2.3.11 Nozzle Discharge rate: Nozzle discharge test was done to know the amount of liquid discharge from each nozzle and to check the variation between the discharge rates of each nozzle. Liquid was pumped at the same time interval and discharge was collected from each nozzle at the same time by tithing big white polythen leathers on each nozzle. After 60 secs the valves were closed and each liquid collected from the nozzle was measured with the aid of graduated measuring cylinder. Coefficient of variation was used to analyze the discharge rate within the nozzle (plate 3)

Plate 3: Measurement of Nozzle Flow Rate

2.3.12 Field Discharge and Time: All relevant field times used for the performance analysis were recorded during the test. The sprayer tank was field with a known quantity of spray liquid. The sprayer was then run until all the designated portion of the field was sprayed. The time and amount of spray liquid were noted. The spraying was done in three replicated. The data collected was employed to determine the effective field capacity, theoretical field capacity and field efficiency.

Plate 4: Prototype Being Tested On the Field

III. RESULT AND DISCUSSION

Table 1: Performance Parameters of the Prototype Sprayer

	S/N	Parameters	Value
Functional	1	Number of nozzle and spacing, mm	10 × 500
	2	Swath width, m	5.3
	3	Mean pressure, bar	2
	4	Discharge rate, ml/min/nozzle	730 – 960
Performance	5	Quantity of solution sprayed, l	65
	6	Effective time, (min)	12.89
	7	Lost time, min	2.07
	8	Total time, min	14.96
	9	Field size or Area treated, ha	0.25
	10	Forward speed, km/hr	2.19
	11	Field capacity, h/hr	1.04
	12	Field efficiency, %	89.6

Table 2. Discharge rate of individual nozzle

Test	Discharge, ml/min										Mean Discharge ml/min		C.V%
	N1	N2	N3	N4	N5	N6	N7	N8	N9	N10			
1	700	800	750	950	800	850	950	700	750	750	800	8.0	
2	780	800	850	950	800	850	950	800	700	750	823	8.23	
3	750	850	800	100	800	850	950	700	750	750	820	8.20	
Average	740	816	800	960	800	850	950	730	730	750	814	8.14	9.93%

N1, N2 ...N10 are ten flat fan nozzles fitted on the boom of sprayer at 500 mm spacing used for spraying of pesticides on field crops.

The field size, test duration, spray pressure, swath, discharge, speed of operation, field capacity and other relevant information are given in Table 1. The average discharge rate of 814 ml/min was observed at an operating pressure of 2 bars at the forward speed of 2.19 km/hr. The operating pressure was maintained constant by locking the throttle lever. During spraying operation, the quantity of pesticide solution sprayed was 65 litres on 0.25 hectares of land which gave an application rate of 260 L/ha. The field capacity of 1.04 ha/hr was calculated with field efficiency of 89.6%. During field trials, it was observed that uniformity in spraying was achieved as the bullock power was utilized only for traction purpose. Comparing the application rate of the prototype sprayer with that of the conventional knapsack sprayer, as given by Malik *et. al* (2012), shows that the 260 l/ha application rate of the prototype sprayer compared with 200 l/ha from the knapsack sprayer represents a 23% increase in application rate. Also that the 1.04 ha/hr field capacity and 89.6% field efficiency of the prototype sprayer compared with 0.4 ha/day and 56% from the knapsack sprayer represents a 62% and 37% increase in field capacity and efficiency.

During the discharge rate test of individual nozzle Table 2, the average discharge of nozzles varied from 960 to 730 ml/min with the average boom discharge of 8.14 L/min at a pressure of 2 bars. The discharge rate decreased for the nozzles mounted at both ends of boom as compared to nozzle mounted in the middle of boom. It was due to increase in frictional force during flow of liquid to reach both ends of the boom. The coefficient of variation for the average of nozzle discharges was 9.93%, which showed that the variation in discharges of the nozzle was particularly good when it is less than 10% for field operation (Norbdy, 1978) and (Gomez and Gomez, 1984)

IV. Conclusion And Recommendations

4.1 Conclusion

The animal drawn hydraulic boom sprayer with piston pump maintained the nozzle pressure of 2 bar during the spraying of chemical on field crops at average speed of 2.19 km/hr with a pair of bullocks. The average discharge of the ten nozzles varied from 730 to 960 ml/min with boom discharge of 8.14 L/min at nozzle height of 500 mm from the plant canopy. The maximum difference in discharge rates among the nozzles was 9.93%, and within the limit of 10% for the field test. Effective field capacity, application rate and field efficiency were 1.04 ha/hr, 260 l/ha and 89.6% respectively. Results obtained from the prototype sprayer revealed that field capacity, application rate and field efficiency represents an increase of 62%, 23% and 37% respectively when compared with knapsack sprayer. The prototype sprayer applied the pesticide behind the operator, which minimized the chances of exposure of chemical to the man and animals.

4.2 Recommendations

In course of field test, it was observed that the volume of solution during spraying wasn't proportional to the speed of animal thereby resulting in under-dosing. And if the animal stops moving for sometime spraying is constant resulting in over-dosing some areas.

To further improve on the developed sprayer, the following suggestions are recommended for future development.

a. In-cooperation of a control switch or valve that will aid in stopping the spraying whenever animal is stopped or during turning.
b. A better nozzle body should be used for better discharge efficiency and reduction of leakage.
c. The material used in the construction of the tank should be changed to plastic to prevent corrosion, while tank capacity should be increased to reduce number of refilling.
d. Width of the wheel should be increased to improve balance, while pneumatic tires should be used to improve upon traction.

References

[1]. Aaron, K. (1994) Chemical Application Management, Farm Business Management. Illinois Publication Pp 31-51.
[2]. Bindrah, O.S. and H. Singh (1980).Pesticide Application Equipment. Oxford and IBH Publishing Co., India, 464pp.
[3]. Goe, M.R. and R.E. McDowell (1980). Animal Traction: Guidelines to utilization. Ithaca, NewYork, Cornell University International Agriculture Minco No. 81.
[4]. Gomez K. A and Gomez A.A (1984). Statistical procedure for Agricultural Research. Second Edition. Pub. John Wiley and Sons Inc. New York.
[5]. Kalikar, Vinayakumar, Prakash, K.V., Veerengouda, M. and Sushilendra (2013). Performance evaluation of bullock cart mounted engine operated sprayer. Internat. J. Agric. Engg., 6(1): 101-104.
[6]. Kaul, R.N. and Egbo, C.O, (1985). Introduction to Agricultural Mechanization, MacMillian Intermediate Agricultural Series. Pg. 106.
[7]. Kaul, R.N. and M.L. Suleiman (1990).Introduction to crop protection machinery. ABUCONS(Nig.) ,Ltd. Book Series, A.B.U., Press, Zaria, Nigeria, 100pp.
[8]. Malik, R.K, Pundir, A., Dar, S.R., Singh S.K., Gopal R., Shankar, P.R., Singh,
[9]. N. and Jat, M.L. (2012): Sprayers and spraying techniques. A manual, CSISA, IRRI and CIMMYT. 20pp.
[10]. Matthews, G.A. (1992). Pesticide Application Methods. Longman Scientific and Technical, New York, 2nd Edition, 405pp.
[11]. Mohan S.S.(2012), Engine operated sprayer. VPO Sadhra, District S.B.S. Nagar, Nawanshahar, Punjab.
[12]. Nordby A. (1978), Dyseposision pa spredebommer dyschlyde arbeidstrykk – vaeskedordeling. N.J.F. seminar, akersproyterog a Kersprlyting, AS, NHL. Norge.Pp25-35.
[13]. Singh R.C., Singh V.V., and U.C. Dubey (2009).Development and performance evaluation of a bullock drawn sprayer. Journal of Agricultural engineering vol. 46(3), pp11-14.
[14]. Spiegel, Murray R. (1968), Mathematical handbook of formulas and tables; Schaum's outline series in mathematics. McGraw- hill book company.pp24-26.
[15]. Veerangouda, M., K.V. Prakash, Jajiwan, R. and G. Neelakantayya (2010). "Performance Evaluation of Bullock drawn Sprayers for Cotton Crop." Karnataka Journal of Agricultural Science, 23(5): pp756 – 761

American Journal of Engineering Research (AJER) 2016
American Journal of Engineering Research (AJER)
e-ISSN: 2320-0847 p-ISSN : 2320-0936
Volume-5, Issue-2, pp-229-236
www.ajer.org
Research Paper Open Access

Design and Simulation of Dc-Dc Voltage Converters Using Matlab/Simulink

[1]Marvin Barivure Sigalo, [2]Lewis T. Osikibo
Center for Electrical Power System Research (CEPSR)
Department of Electrical Engineering
Rivers State University of Science and Technology
Port Harcourt Rivers State Nigeria

Abstract: *The design of power electronic converter circuit with the use of closed loop scheme needs modeling and then simulating the converter using the modeled equations. This can easily be done with the help of state equations and MATLAB/SIMULINK as a tool for simulation of those state equations. An attempt has been made in this paper to simulate all basic non-isolated power converters. So that these models can be readily used for any close loop design (say using PI, fuzzy, or sliding mode control etc.).*

Index Terms—*Switching converters, MATLAB/SIMULINK, system modeling, cascade control, subsystems*

I. INTRODUCTION

Controller design for any system needs knowledge about system behavior. Usually this involves a mathematical description of the relation among inputs to the process, state variables, and output. This description in the form of mathematical equations which describe behavior of the system (process) is called model of the system. This paper describes an efficient method to learn, analyze and simulation of power electronic converters, using system level nonlinear, and switched state- space models. The MATLAB/SIMULINK software package can be advantageously used to simulate power converters. This study aims at development of the models for all basic converters and studying its open loop response, so these models can be used in case of design of any close loop scheme. Also as a complete exercise a closed scheme case has been studied using cascaded control for a boost converter.

II. SIMULINK MODEL CONSTRUCTION OF DC-DC SWITCHING CONVERTER

System modeling is probably the most important phase in any form of system control design work. The choice of a circuit model depends upon the objectives of the simulation. If the goal is to predict the behavior of a circuit before it is built. A good system model provides a designer with valuable information about the system dynamics. Due to the difficulty involved in solving general nonlinear equations, all the governing equations will be put together in block diagram form and then simulated using Matlab's Simulink program. Simulink will solve these nonlinear equations numerically, and provide a simulated response of the system dynamics.

A. Modeling Procedure

To obtain a nonlinear model for power electronic circuits, one needs to apply Kirchhoff's circuit laws. To avoid the use of complex mathematics, the electrical and semiconductor devices must be represented as ideal components (zero ON voltages, zero OFF currents, zero switching times). Therefore, auxiliary binary variables can be used to determine the state of the switches. It must be ensure that the equations obtained by the use of Kirchhoff's laws should include all the permissible states due to power semiconductor devices being ON or OFF.

The steps to obtain a system-level modeling and simulation of power electronic converters are listed below.

1) Determine the state variables of the power circuit in order to write its switched state-space model, e.g., inductor current and capacitor voltage.

2) Assign integer variables to the power semiconductor (or to each switching cell) ON and OFF states.

3) Determine the conditions governing the states of the power semiconductors or the switching cell.

4) Assume the main operating modes of the converter (continuous or discontinuous conduction or both) or the modes needed to describe all the possible circuit operational modes. Then, apply Kirchhoff's laws and combine all the required stages into a switched state-space model, which is the desired system-level model.

5) Write this model in the integral form, or transform the differential form to include the semiconductors logical variables in the control vector: the converter will be represented by a set of nonlinear differential equations.

6) Implement the derived equations with "SIMULINK" blocks (open loop system simulation is then possible to check the obtained model).

7) Use the obtained switched space-state model to design linear or nonlinear controllers for the power converter.

8) Perform closed-loop simulations and evaluate converter performance.

9) The algorithm for solving the differential equations and the step size should be chosen before running any simulation. The two last steps are to obtain closed-loop simulations [2].

Fig 2 Open-loop modeling of Buck DC-DC converters

III. SIMULATION OPEN-LOOP MODELING OF DC-DC CONVERTERS

A. Buck Converter Modeling

The buck converter with ideal switching devices will be considered here which is operating with the switching period of T and duty cycle D Fig. 1, [1]. The state equations corresponding to the converter in continuous conduction mode (CCM) can be easily understood by applying Kirchhoff's voltage law on the loop containing the inductor and Kirchhoff's current law on the node with the capacitor branch connected to it. When the ideal switch is ON, the dynamics of the inductor current $i_L(t)$ and the capacitor voltage $v_C(t)$ are given by,

$$\begin{cases} \dfrac{di_L}{dt} = \dfrac{1}{L}(V_{in} - v_o) \\ \dfrac{dv_o}{dt} = \dfrac{1}{C}(i_L - \dfrac{v_o}{R}) \end{cases}, \quad 0 < t < dT, \quad Q:ON$$

and when the switch is OFF are presented by,

$$\begin{cases} \dfrac{di_L}{dt} = \dfrac{1}{L}(-v_o) \\ \dfrac{dv_o}{dt} = \dfrac{1}{C}(i_L - \dfrac{v_o}{R}) \end{cases}, \quad dT < t < T, \quad Q:OFF$$

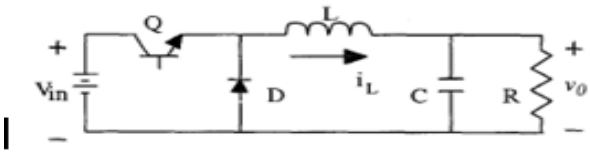

Fig.1 DC-DC Buck Converter

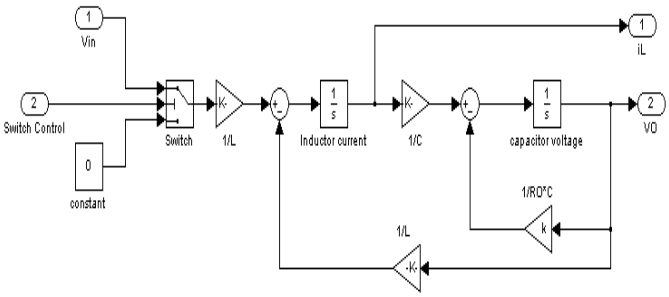

These equations are implemented in Simulink as shown in Fig. 2 using multipliers, summing blocks, and gain blocks, and subsequently fed into two integrators to obtain the states $i_L(t)$ and $v_C(t)$ [2][3] [4].

B. Boost Converter Modeling

The boost converter of Fig. 3 with a switching period of T and a duty cycle of D is given. Again, assuming continuous conduction mode of operation, the state space equations when the main switch is ON are shown by, [1].

$$\begin{cases} \dfrac{di_L}{dt} = \dfrac{1}{L}(V_{in}) \\ \dfrac{dv_o}{dt} = \dfrac{1}{C}(-\dfrac{v_o}{R}) \end{cases}, \quad 0 < t < dT, \quad Q:ON$$

and when the switch is OFF

$$\begin{cases} \dfrac{di_L}{dt} = \dfrac{1}{L}(V_{in} - v_o) \\ \dfrac{dv_o}{dt} = \dfrac{1}{C}(i_L - \dfrac{v_o}{R}) \end{cases}, \quad dT < t < T, \quad Q:OFF$$

Fig. 4 shows These equations in Simulink using multipliers, summing blocks, and gain blocks, and subsequently fed into two integrators to obtain the states $i_L(t)$ and $v_C(t)$, [2][3][4]

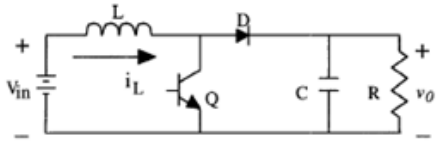

Fig. 3 DC-DC Boost Converter

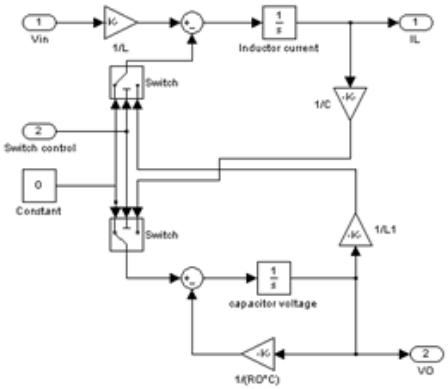

Fig. 4 Open-loop modeling of Boost DC-DC converters

C. Buck-Boost Converter Modeling

In Fig. 5 a DC-DC buck-boost converter is shown. The switching period is T and the duty cycle is D. Assuming continuous conduction mode of operation, when the switch is ON, the state space equations are given by, [1]

$$\begin{cases} \dfrac{di_L}{dt} = \dfrac{1}{L}(V_{in}) \\ \dfrac{dv_o}{dt} = \dfrac{1}{C}(-\dfrac{v_o}{R}) \end{cases}, \quad 0 < t < dT, \quad Q:ON$$

and when the switch is OFF

$$\begin{cases} \dfrac{di_L}{dt} = \dfrac{1}{L}(v_o) \\ \dfrac{dv_o}{dt} = \dfrac{1}{C}(-i_L - \dfrac{v_o}{R}) \end{cases}, \quad dT < t < T, \quad Q:OFF$$

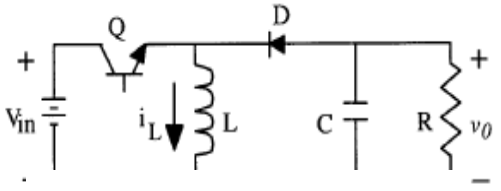

Fig. 5 DC-DC Buck-Boost Converter

These equations are implemented in Simulink as shown in Fig. 6 using multipliers, summing blocks, and gain blocks, and subsequently fed into two integrators to obtain the states $i_L(t)$ and $v_C(t)$, [2] [3] [4].

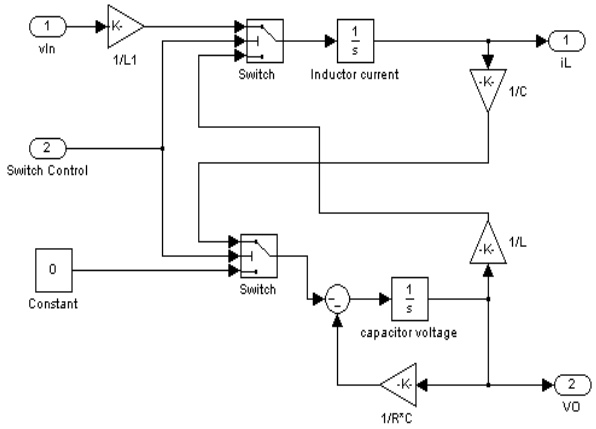

Fig. 6 Open-loop of Buck-Boost DC-DC Converters

The Cuk converter of Fig. 7 with switching period of T and duty cycle of D is considered. During the continuous conduction mode of operation, the state space equations are as follows, [1]

$$\begin{cases} \dfrac{di_{L1}}{dt} = \dfrac{1}{L_1}(v_{in}) \\ \dfrac{dv_c}{dt} = \dfrac{1}{C_2}(-i_{L2}) \\ \dfrac{di_{L2}}{dt} = \dfrac{1}{L_2}(-v_o + v_c) \\ \dfrac{dv_o}{dt} = \dfrac{1}{C_1}(i_{L2} - \dfrac{v_o}{R}) \end{cases} , \quad 0 < t < dT \quad , \quad Q:ON$$

When the switch is OFF the state space equations are represented by

$$\begin{cases} \dfrac{di_{L1}}{dt} = \dfrac{1}{L_1}(v_{in} - v_o) \\ \dfrac{dv_c}{dt} = \dfrac{1}{C_2}(i_{L1}) \\ \dfrac{di_{L2}}{dt} = \dfrac{1}{L_2}(-v_o) \\ \dfrac{dv_o}{dt} = \dfrac{1}{C_1}(i_{L2} - \dfrac{v_o}{R}) \end{cases} , \quad dT < t < T \quad , \quad Q:OFF$$

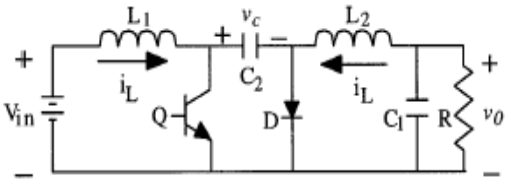

Fig.7 DC-DC Cuk converter

These equations are implemented in Simulink as shown in Fig. 8 using multipliers, summing blocks, and gain blocks, and subsequently fed into two integrators to obtain the states and , [2] [3] [4]

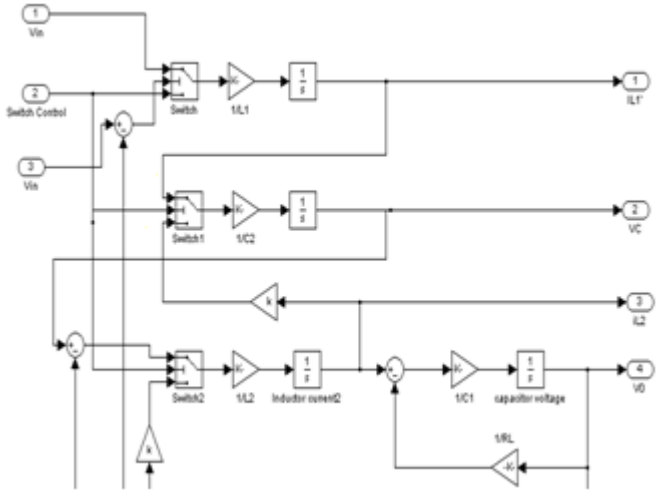

Fig. 8 Open-loop modeling of Cuk DC-DC converters

E. Subsystems

Each of the power electronic models represents subsystems within the simulation environment. These blocks have been developed so they can be interconnected in a consistent and simple manner for the construction of complex systems. The subsystems are masked, meaning that the user interface displays only the complete subsystem, and user prompts gather parameters for the entire subsystem. Relevant parameters can be set by double-clicking a mouse or pointer on each subsystem block, then entering the appropriate values in the resulting dialogue window [4].

To facilitate the subsequent simulation analysis and feedback controller verification, the pulse-width-modulation signal to control the ideal switch can also be built into the masked subsystem Fig. 9(a) and Fig. 9(b). For each converter to verity it's working in open loop configuration trigger pulses have been derived using a repeating sequence generator and duty cycle block. Function block compares the duty cycle and saw tooth from repeating sequence- derived trigger pulses are connected as an input to the switch control. Hence inputs for the masked subsystem are duty ratio and input voltage, and the outputs are chosen to be inductor current, capacitor voltage, and output voltage. When double-clicking the pointer on the masked subsystem, one enters parameter values of the switching converter circuit in a dialogue window. The intuitive signal flow interface in SIMULINK makes this mathematical model and its corresponding masked subsystem very easy to create.

IV. SIMULATION CLOSED-LOOP OF DC-DC CONVERTERS USING CASCADED CONTROL

The simulation model for cascaded control of DC-DC switching converters is build using the above-mentioned steps is as shown in Fig. 10. The DC-DC buck, boost, buck-boost, and Cuk converters was previously designed, and simulated on digital computer using Matlab package with the parameters given in Table 1, and Table 2. Inductor current and capacitor voltage for open loop simulation of all converters are as shown in Fig.11 (a, b, c, and d).

Table 1 Buck, Boost, and Buck-Boost converters parameters

V_{in}	L	C	R	f	V_o
24, 10, 24V Respectively	69 mH	220 μF	13 Ω	100 KHz	12, 20, -24V Respectively

Table 2 Cuk converter parameters

V_{in}	L_1	L_2	C_1	C_2	f	R	V_o
24 V	69 mH	19 mH	47 μF	220 μF	100 KHz	15 Ω	31.8 V

Results of Closed loop using a cascaded control scheme for a boost converter is shown in Fig. 12(a). Here the output voltage rises up to 21.3V (6.5%) for the step variation of load from 10Ω to 13Ω (30%). The output voltage resumes its reference value (of 20V) within 15ms after the transient variation of load. As per fig 12(b), for a step change at the input voltage from 10V to18 V (80%) (at 0.5 Sec instant), a satisfactory performance is obtained in the output voltage which has a rise up to 22.8V (14%), but it is quickly dropped to its set value

(20V) within 16 ms. Simulation results verify that the control scheme in this section gives stable operation of the power supply. The output voltage and inductor current can return to the steady state even when it is affected by line and load variation.

V. CONCLUSIONS

This paper analysis nonlinear, switched, state-space models for buck, boost, buck-boost, and Cuk converters. The simulation environment MATLAB/SIMULINK is quite suitable to design the modeling circuit, and to learn the dynamic behavior of different converter structures in open loop. The simulation model in MATLAB/SIMULINK for the boost converter is build for close loop. The simulation results obtained, show that the output voltage and inductor current can return to steady state even when it is affected by input voltage and load variation, with a very small over shoot and settling time.

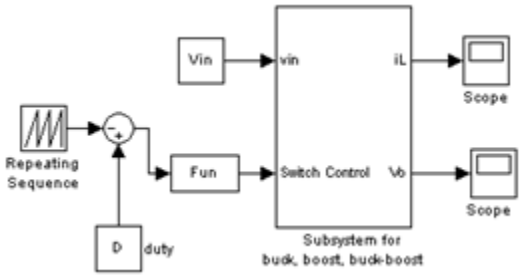

Fig. 9(b) Subsystem for Cuk converters

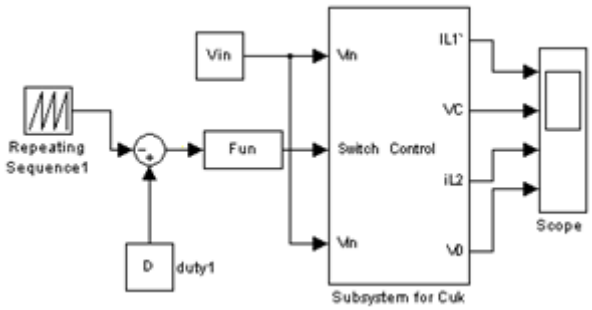

Fig. 9(a) Subsystem for Buck, Boost and Buck-Boost converters

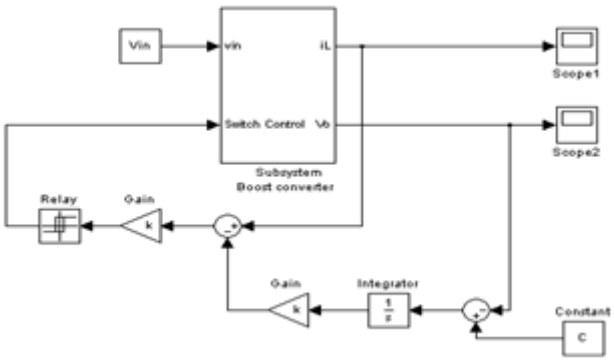

Fig.10 Simulink block diagram representing close loop Scheme of Boost converter using cascaded control

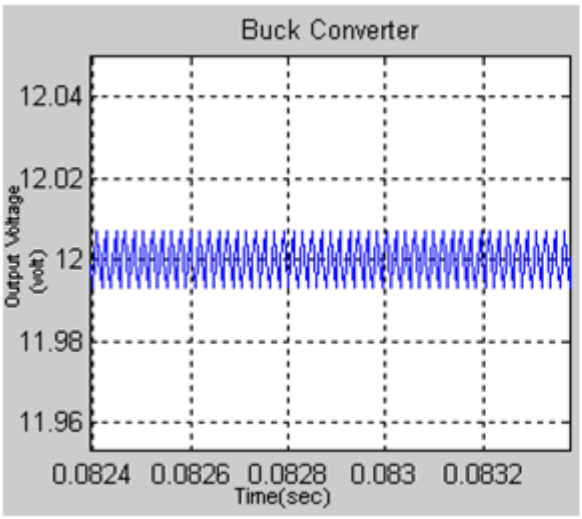

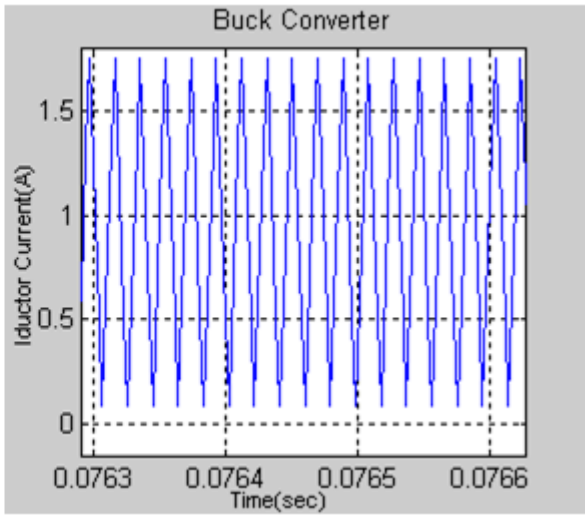

Ripple (peak-to-peak = 0.11%) (a)

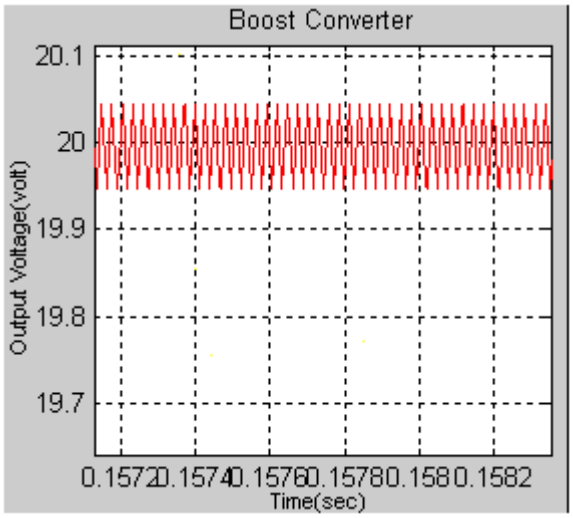

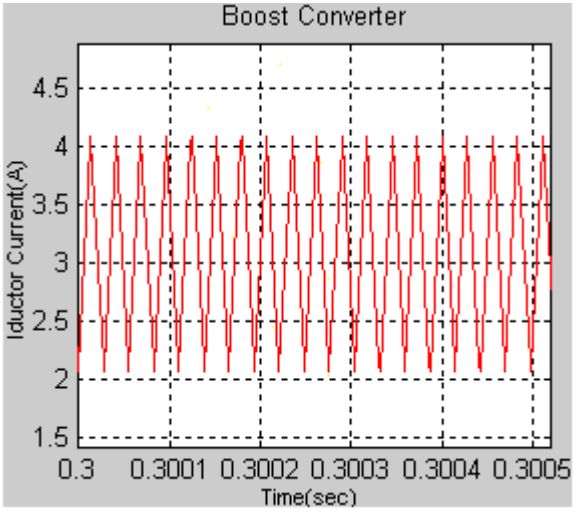

Ripple (peak-to-peak = 0.43%) (b)

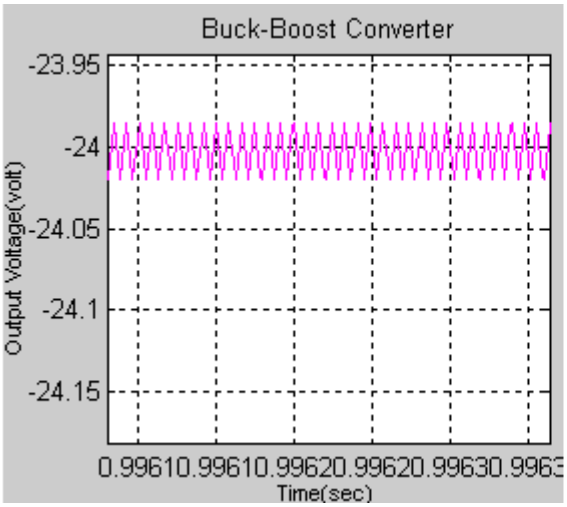

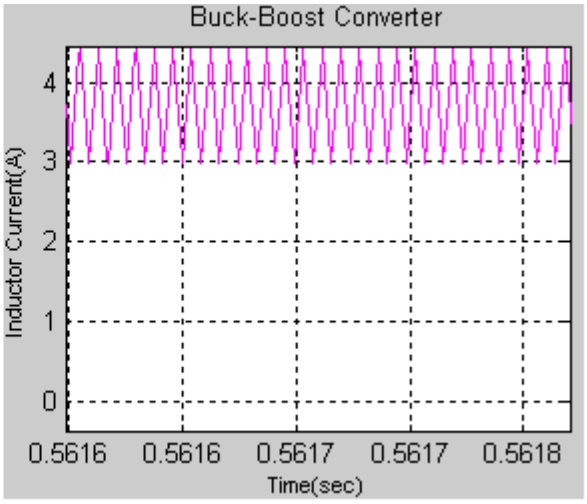

Ripple (peak-to-peak = 0.12%) (c)

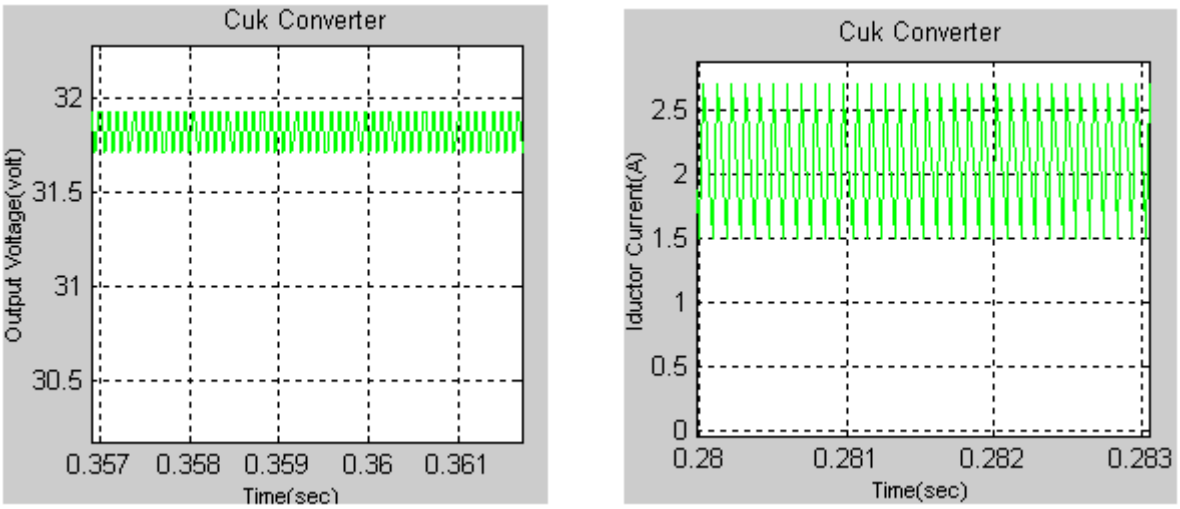

Ripple (peak-to-peak = 1.96%) (d)

Fig. 11 Output voltage and inductor cu rrent Open-loop for (a) Buck (b) Boost (c) Buck-Boost (d) Cuk Converters

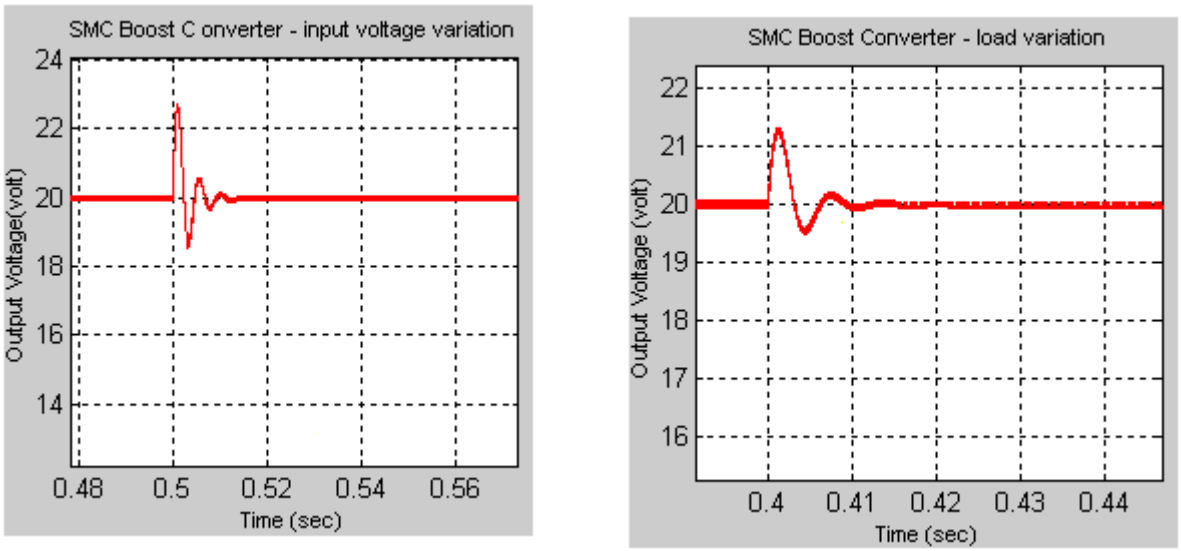

(a) (b)

Fig. 12 Output voltage of SMC Boost Converter when (a) load variation (b) input voltage variation

References

[1]. J.Mahdavi, A.Emadi, H.A.Toliyat, Application of State Space Averaging Method to Sliding Mode Control of PWM DC/DC Converters, IEEE Industry Applications Society October 1997.

[2]. Vitor Femao Pires, Jose Fernando A. Silva, Teaching Nonlinear Modeling, Simulation, and Control of Electronic Power Converters Using MATLAB/SIMULINK, IEEE Transactions on Education, vol. 45, no. 3, August 2002.

[3]. Juing-Huei Su, Jiann-Jong Chen, Dong-Shiuh Wu, Learning Feedback Controller Design of Switching Converters Via MATLAB/SIMULINK, IEEE Transactions on Education, vol. 45, November 2002.

[4]. Daniel Logue, Philip. T. Krein, Simulation of Electric Machinery and Power Electronics Interfacing Using MATLAB/SIMULINK, in 7th Workshop Computer in Power Electronics, 2000,pp. 34-39.

[5]. N. Mohan, T. Undeland, W. Robbins, Power Electronics Converters, Applications and Design, ISBN 9814-12-692-6.

American Journal of Engineering Research (AJER) 2016
American Journal of Engineering Research (AJER)
e-ISSN: 2320-0847 p-ISSN : 2320-0936
Volume-5, Issue-2, pp-237-240
www.ajer.org
Research Paper Open Access

OLAP Mining Rules: Association of OLAP with Data Mining

Naseema Shaik[1], Dr. Wali Ullah[2], Dr. G. Pradeepni[3]
[1](Research Scholar, Department of Computer Science, KL University, INDIA)
[2] (Assistant Processor, Department of Computer Science, Jazan University, KSA)
[3](Associate Professor, Department of Computer Science, KL University, INDIA)

Abstract: *Data mining and OLAP are powerful decision support tools. The usage of both systems will differ. OLAP systems concentrate on the efficiency of building OLAP cubes. Here No specific algorithms are going to be implement. On the other hand, statistical analyses are traditionally developed for two-way relational databases, and have not been generalized to the multi-dimensional OLAP data structure. Combining both OLAP and data mining may provide excellent solutions. In large data warehouse environments, many different types of analysis can occur. There may also apply more advanced analytical operations on data. Two major types of such analysis are OLAP (On-Line Analytic Processing) and data mining. Rather than having a separate OLAP or data mining engine, OLAP mining rules has integrated OLAP and data mining capabilities directly into the database server. This paper provides a brief introduction to these technologies, and more detail can be found in these products' respective documentation.*

Keywords: *Data mining, OLAP systems, OLAP cubes, Association rules, OLAP mining.*

I. INTRODUCTION

The OLAP and data mining (OLAP mining) is a mechanism which integrates on-line analytical processing (OLAP) with data mining so that mining can be performed in different portions of databases or data warehouses and at different levels of abstraction at user's finger tips. With rapid developments of data warehouse and OLAP technologies in database industry, it is promising to develop OLAP mining mechanisms. With our years of research into data mining, an OLAP-based data mining system, DBMiner, has been developed, where OLAP mining is not only for data characterization but also for other data mining functions, including association, classification, prediction, clustering, and sequencing. Such integration increases the flexibility of mining and helps users find desired knowledge. In this paper, we introduce the concept of OLAP mining and discuss how OLAP mining should be implemented in a data mining system by using association rules.

II. OLAP AND DATA MINING ARE USED TO SOLVE DIFFERENT KINDS OF ANALYTIC PROBLEMS

OLAP summarizes data and makes forecasts. For example, OLAP answers questions like "What are the average sales of policies, by area and by year?" where as Data mining discovers hidden patterns in data. Data mining operates at a detail level instead of a summary level. Data mining answers questions like "Who is likely to buy policies in the next six months, and what are the characteristics of these likely buyers?" OLAP and data mining can complement each other. For example, OLAP might pinpoint problems with sales of policies in a certain area. Data mining could then be used to gain insight about the behavior of individual customers in the region. Finally, after data mining predicts something like a 5% increase in sales, OLAP can be used to track the net income.

III. OLAP MINING OVERVIEW & ARCHITECTURE

"Online Analytical Processing Provides you with a very good view of what is happening, but cannot predict what will happen in the future or why it is happening where as Data Mining is a combination of discovering techniques and prediction techniques [1]."

The architecture which proposes in this paper fulfills several important, and often interrelated, goals:

1. **Modularity**: All modules, which adhere to a predefined interface, can interact seamlessly Interoperability. The system has to work with a wide array of databases and storage models. The integration of multiple database systems based on wrapper modules needs to be supported.
2. **Scalability:** OLAP requires consistent reporting performance, independent of the size of the underlying database or its dimensionality.
3. **Extendibility:** We want to add additional modules without rebuilding the system [2].

The data mining and OLAP are powerful tools to support decision making. However, people use them separately for years: OLAP systems focus on efficiency to build cubes OLAP, and applied to any algorithms for mining statistical data, on the other hand, developed a traditional statistical analysis for two-way relational databases, and have not been circulated to the structure of the multi-dimensional data OLAP. May combine data mining and OLAP to provide excellent solutions. OLAP is completely different from its predecessor, for an online transaction processing (OLTP) systems. OLTP focuses on the automation of data collection procedure. Keeping detailed data, consistent and modern, is the most important condition for the application of OLTP.

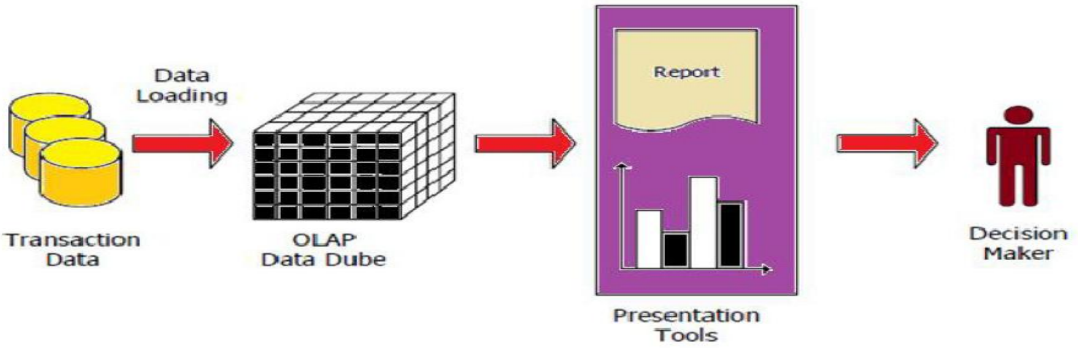

Fig1: OLAP Architecture

Component-based OLAP systems offer a number of benefits both to the user and the developer. The user can choose from different suppliers and combine different query optimization strategies and query evaluation algorithms [3]. Extensible OLAP systems offer a major benefit to developers, as well. We will show how to decompose an OLAP system into functional units, which can communicate using a "software bus". We propose a data model based on sets and vectors for the communication.

A number of approaches exist to the storage of data in data warehouses. [4] Contrasts the performance of value based (ROLAP) and multidimensional (MOLAP) implementations. The data-structures used include grid-files [5], B*-trees, R*-trees [1], X-trees, HB-trees [6], Gist [7], arrays and sets-based data-structures.

OLAP systems have a structured architecture based on the following essential components:

1. Database - the data source used for OLAP analysis. As database can use a relational database to ensure our multidimensional storage facilities, a multidimensional database, a data warehouse, etc.

2. OLAP server - the one that manages multidimensional data structure and at the same time a link between the database and OLAP customer.

3. OLAP customer - are those that provide data mining applications but also supports the generation of results

(Graphs, reports, etc.). There are several options in OLAP data could be stored and processed. Thus, depending on the method of organizing and storing data, there may be three options [2]:

4. Client Files - data is stored locally on a client computer as files are organized, on which operations can be applied to analyze the processing and transformation. This organization of data has some drawbacks of which we can enumerate: the amount that can be processed is indulged reduced time to processing information is quite high, the data shows a poor security, lack of advanced multidimensional analysis.

5. Relational databases - this arrangement is used when the data comes as a relational DBMS and data warehouse is a repository be implemented virtually or using a relational model.

6. Databases multidimensional - in this case, the data are organized into a data warehouse on a dedicated server, which is called multidimensional server.

The figure below shows the architecture of OLAP systems, which vary depending on how data storage and processing of their type, but generally on how one can identify three levels of data: the data sources, OLAP server and the presentation of data or interface user.

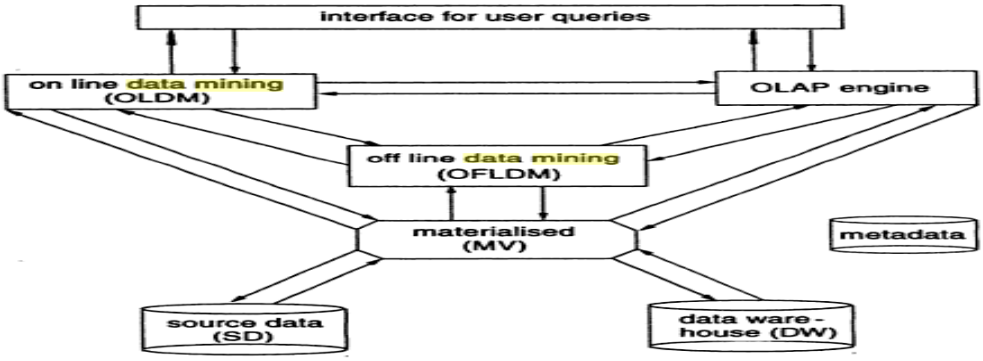

Fig 2: An Integrated view of OLAP Mining Architecture

Some researchers began to generalize some data mining concepts on OLAP cubes in recent years. These works include the cube grade problem the constrained gradient analysis, and data-driven OLAP cube exploration [8]. We will review these studies briefly in this section.

It is a generalized version of association rule. Two important concepts in association rule are support and confidence. Let us take the market basket example. Support is the fraction of transactions that contains a certain item (bread and butter), and confidence is that the proportion of transactions that contains another item B given that these transactions contain A which declare that the association rule can also be viewed as the change of the count aggregates when imposing another constraint, or in OLAP terminology, making a drill-down operation on an existing cube cell. They think other aggregates like sum, average, max, and min can be studied in addition to the count. Also, other OLAP operations, like roll-up and one-dimension mutation can be incorporated [9]. They argued that the cube grade could support the "what if" analysis better, and they introduced two query languages to retrieve the cube grade sets.

IV. IMPLEMENTATION OF OLAP MINING BY ASSOCIATION

Association rule mining finds interesting relationships in data. The goal of associative rule data mining is to find all associative rules that have high confidence (Strong Rules) in the data set. In meteorological application, association mining used to find the relationship between the weather elements and natural events, weather and disaster prediction [8], and multi-station atmospheric data analysis [10].

Table below illustrates some useful rules extracted from New York weather data ordered by confidence.

Associations rules for New York City weather data

#	Rule	Conf.
1	[RH=mid Temp=warm Wind=Moderate] ==> [Rain=no rain]	0.99
2	[RH=high Temp=warm] ==> [Rain=no rain]	0.99
3	[Temp=warm Wind=Moderate] ==> [Rain=no rain]	0.99
4	[month = 2]==> [temp = cold]	0.96
5	[month = 1] ==> [temp = cold]	0.96
6	[month = 12] ==> [temp = cold]	0.95
7	[Wind=Light] ==> [Rain=no rain]	0.91
8	[Wind=light Temp=cold rain]==>[RH=moderate]	0.91
9	[Rain= Heavy Rain]==>[Temp = cold]	0.88
10	[Temp = cold]==>[Wind = Moderate]	0.74
11	[RH= low Wind = Moderate Temp=warm] ==> [Rain=Light Rain]	0.65
12	[Wind = Moderate] --> [RH = mid]	0.60

Rules #1, #2, #3, #7 and #11, can be used to predict rainfall. For example from rule #1 we understand that there is no rain tomorrow if today is warm (temperature between 16 °C and 23 °C), wind speed is moderate (13-30 km/h) and relative humidity is mid (between 56.5 - 76.0). Also Rule #11 could be used for rain prediction, it means that if the relative humidity today is low (below 36), wind speed is moderate and temperature is warm then, rain tomorrow maybe light (< 2.5 millimeters per hour). Rules #4, #5 and #6 provide with better understanding for Gaza city weather. These rules give us an indication that cold season includes December, January and February.

V. CONCLUSION

OLAP Mining does not provide any formal or standard technique to be modeled. Each vendor defines their own approach regarding the needs of respective end users. However, there is a general model used on Data Warehouses called Star schema but it cannot model all the appropriate conceptual issues and problems like information loss is very often. A similar approach, which overpasses the information loss problem of the Star schema, is the Snowflake schema also a common database model for Data Warehousing but as most of computer scientists claim it is a logical view rather a conceptual view of the database model.

REFERENCES

[1] Cop pock D. S. "Data Mining and Modeling: So you have a Model, Now What?" DM Review Magazine, Feb 03.
[2] Salton, G. and McGill, M. Introduction to Modern Information Retrieval, McGraw-Hill Book Company, New York 1983.
[3] Lungu I., Bâra A., Sisteme informatice executive, Editura Ase, Bucureşti, 2007.
[4] Central Intelligence Agency, "CIA World Fact book 2011," Mobile Reference. 2010.
[5] Li X., Plale N., Vijayakumar R., Ramachandran S., Graves H., "Conover. Real-time storm detection and weather forecast activation through data mining and events processing, "To appear Earth Science Informatics, H.A. Babaie, Ed., Springer. 2008.
[6] Berkhin P., "Survey of clustering data mining techniques, Accrue Software, San Jose", CA, Tech. Rep., 2002.
[7] Dong-Jun S., Breidenbach, J. P., "Real-Time Correction of Spatially Nonuniform Bias in Radar Rainfall Data Using Rain Gauge Measurements," Journal of Hydrometeorology, vol. 3, no. 2, pp. 93- 111. 2002.
[8] R. Kimball. The Data Warehouse Toolkit: Practical Techniques for Building.Dimensional Datawarehouses. John Wiley & Sons, Inc., 1996.
[9] J. Widom. Research problems in data warehousing. In Conference on Information and Knowledge Management, 1995.
[10] Nandagopal S., Karthik S.Arunachalam V."Mining of Meteorological Data Using Modified Apriori Algorithm," European Journal of Scientific Research, No.2, pp.295-308. 2010.

American Journal of Engineering Research (AJER) 2016
American Journal of Engineering Research (AJER)
e-ISSN: 2320-0847 p-ISSN : 2320-0936
Volume-5, Issue-2, pp-241-247
www.ajer.org
Research Paper Open Access

Analysis of Attacks in Cognitive Radio Networks

Manjurul H. Khan[1], P.C. Barman[2]
[1] *ICT Department-System, Janata Bank Limited, Head Office, Dhaka, Bangladesh.*
[2] *Department of Information & Communication Engineering, Islamic University, Kushtia, Bangladesh.*

***ABSTRACT*:** *Cognitive Radio (CR) is a promising technology for next-generation wireless networks in order to efficiently utilize the limited spectrum resources and satisfy the rapidly increasing demand for wireless applications and services. It solves the spectrum scarcity problem by allocating the spectrum dynamically to unlicensed users. It uses the free spectrum bands which are not being used by the licensed users without causing interference to the incumbent transmission. So, spectrum sensing is the essential mechanism on which the entire communication depends. Cognitive radio networks introduce new classes of security threats and challenges, such as licensed user emulation attacks in spectrum sensing and misbehaviours in the common control channel transactions, which degrade the overall network operation and performance. So that it causes the crucial threat in the cognitive radio network. In this paper, our objectives are to give the various security issues in cognitive radio networks and advantage and disadvantage of security mechanisms with the existing techniques to mitigate it.*

Keywords- *Cognitive Radio, Spectrum Sensing, Primary User, Secondary User, Malicious User.*

I. INTRODUCTION

Cognitive Radio (CR) is an enabling technology to effectively address the spectrum scarcity and it will significantly enhance the spectrum utilization of future wireless communications systems. In a CR network, the Secondary (or unlicensed) User (SU) is allowed to opportunistically access the spectrum "holes" that are not occupied by the Primary (or licensed) User (PU). Generally, the SUs constantly observe the spectrum bands by performing spectrum sensing. Once a spectrum "hole" is discovered, an SU could temporarily transmit on this part of the spectrum. Upon the presence of a PU in this part of the spectrum, however, the SU has to switch to another available spectrum band by performing spectrum handoff, avoiding interference with the PU transmission. The development of CR technology leads to the new communications paradigm called Dynamic Spectrum Access (DSA), which relaxes the traditional fixed spectrum assignment policy and allows a CR networks to temporally "borrow" a part of the spectrum from the primary network. As a consequence, the scarce spectrum resources are shared, in a highly efficient and resilient fashion, between the primary network and the CR network.

Organization of this paper is as follows: section II gives a brief overview of Cognitive radio core functions. Details of threats and attack categories are given in section III. In section IV and V, we give a defence mechanism and detection mechanism respectively in CRNs as well as advantage and disadvantage of mechanism. Finally, section VI concludes the paper with our future work.

II. COGNITIVE RADIO CORE FUNCTIONS

There are four fundamental functions which the CRN device must perform, as shown in Figure 1 and as stated below [1,2]

1) Spectrum sensing identifies the parts of the accessible spectrum and senses the presence of the PU operating in the licensed band.
2) Spectrum management determines the best channel to establish communication.
3) Spectrum sharing sets up a coordination access among users on the selected channel.
4) Spectrum mobility vacates the channel in case the PU is detected.

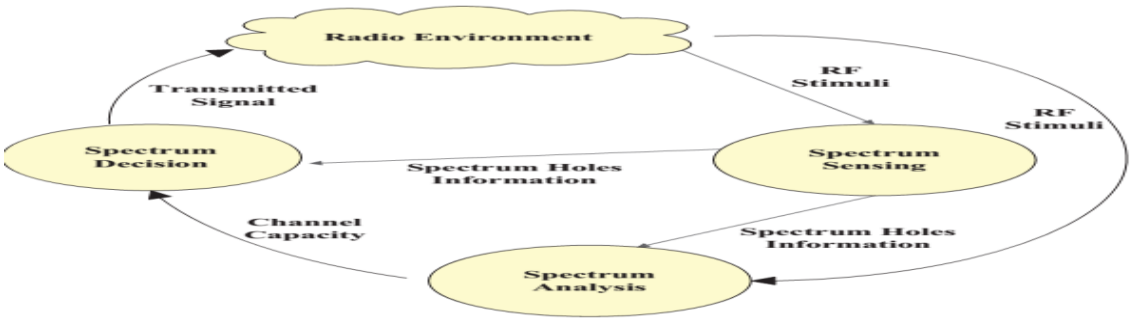

Figure 1. Cognitive Cycle [3].

III. CATEGORIES OF THREATS AND ATTACKS

3.1 Analysis of Access Point

CR facilitates in secondary usage of licensed band by dynamically spectrum allocation manner. Therefore, secondary user (SU) must sense the spectrum accurately to avoid interference with the PU. With this, the CR management experiences different kinds of anomalous behaviour from the other Access points (Aps) [4].Which represent in table 1.

Table1. Analysis of access Point

Types of Access Point	Definition
Misbehaving Access Point	It does not obey any rules for sensing, recognizing and managing the spectrum.
Malicious Access Point	It aims to vandalize the networks by falsely reporting the spectrum sensing results to SUs in order to cause interference between PU and SUs.
Cheat Access Point	It aims to increase its utility function by decreasing profit of other SUs.
Selfish Access Point	It occupies the channel for longer time to make profit to itself only.

3.2 Overviews of the attacks occurring at different CR functions

Spectrum sensing, Spectrum management, Spectrum sharing and Spectrum mobility are performed in CR functions. Overviews of the attacks occurring at different CR functions are figure out in Table 2.

Table 2.Overview of the attacks occurring at different CR functions

Attack Name	CR function	Description
Forgery & Data tamper	Spectrum Sensing	Spectrum Management system makes wrong decision by receiving the attackers sensing information.
Overlapping		An attacker impacts other networks by transmission to a specific network.
Denial of Service		An adversary user decreases the availability of the spectrum bandwidth by blocking the communication, through creating noise spectrum signals which cause interference with PU.
Lion or Jamming message		An attacker transmits high signalling power to disturb the or the secondary user which results forcing the cognitive user to hop to different channel to utilise.
Spectrum Sensing Data Falsification(SSDF)		In collaborative spectrum sensing, a collaboration technique used among CR nodes to generate and utilise a common spectrum allocation for the exchange of information about available channels. However adversary node gives false observations information to other users.

Eaves dropping	Spectrum Sharing	Weaknesses within the layer due to the poor authentication and no existing encryption mechanisms.
Denial of Service & masquerade		Repetition of the frequent packets that result in Overcrowding the channel which is being busy to be utilised by legitimated users.
Selfish Behaviour or selfish masquerade attack		an attacker does not follow the normal communication process for maximising their throughput, saving energy or gaining unfair beneficial access of using spectrums through injecting frequent anomalous behaviour.
Key depletion		An attacker attempts to break the cipher by repetition of the session key.
Forgery Attack		Lack of authentication mechanism leads to the occurrence of modification and forgery on MAC CR Frames which result in the launch of DoS attacks.
Biased Utility	Spectrum Management	An attacker tries to reduce the bandwidth of other SUs in order to obtain more bandwidth by changing the spectrum parameters.
False feedback		An attacker secretes the incidence of the PU in order to disturb the information sensing of other SUs.
Routing information jamming	Spectrum Mobility	A malicious node causes a targeted node to initiate spectrum handoff before the routing information is exchanged.

3.3 Attack Scenario on Protocol Layer

We categorize the various attacks depending on their behaviour shown towards the five layers of the protocol stack [5] as shown in Table 3.

Table 3.Attack scenario on Protocol Layer

Types of attacks	Definition	Protocol Layer
PUEA	The physical layer attack is classified as a primary user emulation attack (PUEA), where the malicious user (MU) mimics the primary user's signal characteristics, thereby causing SUs to erroneously identify the attacker as the primary user.	Physical Layer
Jamming	Jamming is when the jammer sends a continuous packet of data into the channel, making the SU to never sense the channel as idle.	
Objective function attack(OFA)	The objective function attack (OFA) is when the MU may try to change the parameters of utility resource, so that the CR node fails to adapt correctly.	
Common control data attack(CCDA)	Common control data attack (CCDA) is a major risk which disrupts the transmission by preventing the elements of the channel from sharing information about the spectrum usage and also provides all the information to the attacker.	
spectrum sensing data falsification (SSDF)	Here the attacker falsifies the fusion centre decision by sending wrong spectrum sensing result.	Link Layer
Control channel saturation Denial-of-service (DoS)	When the attacker saturates the control channel by reserving it.	
Selfish channel negotiation(SCN)	Where the malicious node provides wrong channel information, so that other nodes change their route.	
Wormhole attack	An attacker builds bogus route information and tunnels the	Network

	packet to another location. This creates routing loops and wastes energy.	Layer
Sink hole attack	Here, the attacker advertises itself as the best route to a specific destination and lures the neighbour nodes to use this route and forward their packets so as to drop those packets.	
Hello flood attack	When the attacker sends a broadcast message to all the nodes in a network with enough power to convince them that, it is the closest neighbour of those nodes.	
Lion attack	The attacker launches PUEA and forces the CR nodes to perform frequency hopping among channels in order to disrupt TCP.	Transport Layer
Jellyfish attack	Jellyfish attack is performed on the network layer but it affects the performance of the transport layer, especially the TCP protocol.	
Cognitive radio virus attack	The cognitive radio network is vulnerable to viruses that can effect radio function and learning Policy of the radio is changed or not allowed to be updated, providing the attacker unfair spectrum access.	Applicati-on Layer
Logic Error Attack	Those attacks corresponding to all the layers may have an adverse effect on the application layer.	
Buffer Overflow attack		

IV. DEFENCE MECHANISM IN CRNs [6]

A number of researchers have made efforts to address the security requirements and provide secure communication among SUs by applying different security mechanisms, such as authentication and authorisation access by different techniques, within a CRN.

4.1 Digital Signature

In[7,8,9] proposed different protection systems based on applying a digital signatures for protecting the network from DoS attacks and providing secure communication. Their approaches involve the activities of a CA, PUs, and both PUs' and SUs' base stations. However, the main differences of these mechanisms are that the BSs are connected to the CA using wire links in[10], while in[11] the approach, an asymmetric key scheme instead of a CA is mainly used.

Advantage:

i.Low complexity and using the basic architectures of symmetric and asymmetric key infrastructures.

Disadvantage:

i.It has not been simulated and tested to proof the security. It also does not work in Ad-hoc environment due to being based on centralised entities.

4.2 Certificate Authority

Another effective traditional approach-based CA on the application layer for achieving the same purpose of authentication is presented in [12,13].The proposed method uses both EAP-TTLS(for establishing a secure connection) and EAP-SIM (for authenticating the user) algorithms.

Advantage:

i.Effective security mechanism due to identifying and verifying the user and the server respectively.

Disadvantage:

i.Requires a third-party to verify the user identity. Also the mechanism has not been simulated and tested to ensure security against malicious behaviours.

4.3 Trust Values

Trust values technique procedures are proposed in [14,15] to address and analysis the issues within CRNs. Based on this, the trust value will be calculated, which leads to the decision that will either allow the current user to utilise the available licensed channel or not.

Advantage:

i.It is an additional procedure that can be built on the top of other security techniques to increase the level of the protection and detection in term of secure communication.

Disadvantage:
i.Requires a third party procedure is to provide previous information of a node. Moreover, when a new node joins the network, the CA will not be able to provide reference for that particular user. Hence the mechanism does not operate in strong fixed level of the authentication for all cognitive users equally.

4.4 User Identification

User identification process generating by using specific port. Here, each user has a fixed port.

Advantage:
i. Low complexity by generating two virtual ports for secure transmission: the first is for control traffic information and another is for data transmission which is blocked by default unless the user has been authenticated.
Disadvantage:
i. It requires a third party to provide information like user preferences.

4.5 Deadlock

In [16] the author proposed a new method, called Deadlock, which utilizes device dependent radio metrics as a fingerprint. It uses non-parametric Bayesian classification to model the feature space of a single device as a multi variable Gaussian distribution with unknown parameters, and feature space of multiple devices as an infinite Gaussian mixture. Collapsed Gibb's sampling algorithm is applied to get samples from the posterior distribution, and active devices found out. Then the MAC addresses are collected.
Advantage:
i. One physical device sharing only one ID as a result it is free from any attack.
Disadvantage:
i.If more than one physical device is sharing the same ID, then PUE attack is identified.

4.6 Modifying the modulation scheme

The use of frequency hopping and direct sequence spread spectrum techniques can make it more difficult to launch effective denial of service attacks. The attacks may still degrade service quality.
Advantage:
i. It is very effective scheme for overlapping secondary user attack.
Disadvantage:
i. It needs a third party to complete the task.

V. DETECTION MECHANISM IN CRNs

5.1 Puzzle Punishment & COOPON Activity

Selfish behaviour detection techniques for the CCC are proposed in [17,18] where a puzzle punishment model is applied for bad behaviour activities in a situation where a receiver is asked for a new hidden channel that has not been included previously. Thus, the sender would be a suspicious case. Therefore, the receiver applies the puzzle punishment to detect whether the sender is a selfish node or not. If the sender node solves the puzzle, they will be considered as a legitimate user and communication will be resumed normally; otherwise, the communication will be disconnected.
Cooperative neighbouring cognitive radio Nodes (COOPON) is applied among a group of neighbouring users to detect selfish nodes who broadcast fake channel lists. Consequently, neighbouring users can detect the selfish users by comparing the transmitted channel list of the target user with their lists.
Advantage:
i. Applied in both CCC and data channel which decreases the potential of misbehaviour in different stages of the network.
Disadvantage:
i. Focuses only on detecting selfish behaviour and does not provide the complete secure communication between sender and receiver.

5.2 Timing parameter

In timing parameter works proposed in [19] MAC Layer. When the negotiation phase is taking place, the node, which receives a request, sets up timing parameters for controlling the time interval. This forces the sender to transmit data without getting a higher rate. If the sender does not obey and sends packets more frequently, the receiver node takes action against the sender. Then the receiver node analyses the sender's misbehaviour and broadcasts the information over the current network.

Advantage:
i.Detecting misbehaving nodes during the negotiation phase. It helps to maintain the channel from getting saturated.
Disadvantage:
i.Theoretical and has not been simulated and tested to provide the detection scheme results.
ii.Weak against eavesdropping and forgery attacks especially once the FCL is not hidden which is exploited to launch Jamming attacks.

5.3 Anomalous Spectrum Usage Attacks

In [20] presented a cross-layer technique for CRNs for detecting ASUAs. Collecting the information on both the physical and network layers provides an awareness of the current spectrum. It operates against the PUE and jamming attacks to provide successful access to the spectrum.
Advantage:
i.Combining both physical and network layers for detecting malicious users give a better achievement instead of selecting only a layer.
Disadvantage:
i.Focuses only on the detection approach and does not consider a significant protection scheme against both jamming and PUE attacks mobility.

5.4 Pinokio

A method of detection of Byzantines called Pinokio. Pinokio uses a Misbehavior Detection System (MDS) that maintains a profile of the networks normal behavior based on training data. The MDS detects misbehavior by monitoring the bit rate behaviour. By protocol, the bit rate should change periodically and be adjusted by a node contiguously, the bit rates between two nodes should show some reciprocity, and the usage of a low bit rate should occur over a narrow channel. Nodes not exhibiting these characteristics are not acting in a manner conducive to spectrum efficiency, and so are suspect.[21]
Advantage:
i. It uses training data, which is very effective in MAC layer.
Disadvantage:
i. Sometimes bit rate behaviour is not fair.

VI. CONCLUSION

The awareness, reliability and adaptability nature of CR networks make it more precious to be deployed successfully in near future. Along with this realization, it has also opened the door for lots of threats, especially in security because of the presence of malicious nodes, who want to vandalize the entire communication networks. Cognitive radio is a promising concept which uses the available spectrum more efficiently through opportunistic spectrum deployment. As security has a significant priority in CR networks, the security threats that face CRN were discussed. We were also discussed protection mechanism and detection mechanism respectively in CRNs as well as advantage and disadvantage of mechanism. For future work, the physical layer will more efficient in terms of detection of this MU, because this is the primary layer whose information is to pass to the upper layers.

REFERENCES

[1] Baldini, G., Sturman, T., Biswas, A., Leschhorn, R., Godor, G., and Street, M., (2012)"Security Aspects in Software Defined Radio and Cognitive Radio Networks: A Survey and A Way Ahead," Communications Surveys & Tutorials, IEEE, vol. 14, no, 2. pp. 355-379.
[2] Domenico, A., Strinati, E., Benedetto, M., (2012) "A Survey on MAC Strategies for Cognitive Radio Networks," Communications Surveys &Tutorials, IEEE, vol. 14, no. 1, pp. 21-44.
[3] S. Haykin, "Cognitive radio: brain empowered wireless communications," IEEE Journal on Selected Areas in Communications, pp. 201–220, February 2005.
[4] Arkoulis, S.; Kazatzopoulos, L.; Delakouridis, C.; Marias, G.F.,"Cognitive Spectrum and Its Security Issues," Next Generation Mobile Applications, Services and Technologies, 2008. NGMAST '08.The Second International Conference on , vol., no., pp.565,570, 16-19 Sept. 2008.
[5] Wassim El-Hajj; HaiderSafa; MohsenGuizani, "Survey of Security issues in Cognitive Radio Network," journal of internet technology,volume 12, 2011.
[6] A.Wajdi,M.Ali&A. S. Ghazanfar "Spectrum Sharing Security and Attacks in CRNs: a Review"Luton, United Kingdom,(IJACSA)International Journal of Advanced Computer Science and Applications,Vol. 5, No. 1, 2014.
[7] Sanyal, S., Bhadauria, R. and Ghosh, C., (2009) "Secure communication in cognitive radio networks," in Computers and Devices for Communication. CODEC. 4th International Conference on, pp. 1-4.
[8] Parvin, S., and Hussain, F.. (2011), "Digital signature-based secure communication in cognitive radio networks," in Broadband and Wireless Computing, Communication and Applications (BWCCA), 2011 International Conference on, pp. 230-235.

[9] Mathur, C., Subbalakshmi, K., (2007), “Digital signatures for centralised DSA networks”Consumer Communications & Networking Conference, CCNC. 4th IEEE.
[10] Parvin, S., andHussain, F.. (2011), "Digital signature-based secure communication in cognitive radio networks," in Broadband and Wireless Computing, Communication and Applications (BWCCA), 2011 International Conference on, pp. 230-235.
[11] Mathur, C., Subbalakshmi, K., (2007), “Digital signatures for centralised DSA networks”Consumer Communications & Networking Conference, CCNC. 4th IEEE.
[12] Zhu, L., Mao, H., (2010) "Research on authentication mechanism of cognitive radio networks based on certification authority," in Computational Intelligence and Software Engineering (CiSE), 2010 International Conference on, 2010, pp. 1-5., 101.
[13] Zhu, L., Mao, H., (2011), "An Efficient Authentication Mechanism for Cognitive Radio Networks," Power and Energy Engineering Conference (APPEEC), 2011 Asia-Pacific, pp.1-5, 25-28 March 2011.
[14] Parvin, S., Han, S., Tian, B., Hussain, F., (2010), "Trust-based authentication for secure communication in cognitive radio networks,"in Embedded and Ubiquitous Computing (EUC), IEEE/IFIP 8th International Conference, pp. 589-596.
[15] Parvin, S., Hussain, F., (2012) "Trust-based Security for Community based Cognitive Radio Networks",. 26th IEEE International Conference on Advanced Information Networking and Applications, pp. 518-525.
[16] Nguyen, N.T.; RongZheng; Zhu Han, "On Identifying Primary User Emulation Attacks in Cognitive Radio Systems Using Nonparametric Bayesian Classification," Signal Processing, IEEE Transactions on , vol.60, no.3, pp.1432,1445, March 2012.
[17] Wu, H., and Bai, B., (2011) "An improved security mechanism in cognitive radio networks," in Internet Computing & Information Services (ICICIS), 2011 International Conference, pp. 353-356.
[18] Jo, M., Han, L., Kim, D., In, H.P., (2013) "Selfish attacks and detection in cognitive radio Ad-Hoc networks," Network, IEEE , vol.27, no.3, pp.46,50.
[19] Shaukat, R., Khan, S., Ahmed, A., (2008) "Augmented security in IEEE 802.22 MAC layerprotocol,"in Wireless Communications, Networking& Mobile Computing,. '08. 4th International Conference, pp 1-4.
[20] Sorrells, C; Potier, P; Qian, L; Li, X., (2011) "Anomalous spectrum usage attack detection in cognitive radio wireless networks," in Technologies for Homeland Security (HST), 2011 IEEE International Conference, 2011, pp. 384-389.
[21] M.Padmadas,Dr.N.Krishnan&V.NellaiNayaki, "Analysis of Attacks in Cognitive Radio Networks”,international Journal of Advanced Research in Computer and Communication Engineering ,Vol. 4, Issue 8, August 2015.

American Journal of Engineering Research (AJER) 2016
American Journal of Engineering Research (AJER)
e-ISSN: 2320-0847 p-ISSN : 2320-0936
Volume-5, Issue-2, pp-248-253
www.ajer.org
Research Paper Open Access

The performance evaluation of an algorithm for fingerprint biometric recognition

Virtyt Lesha
Department of electronics and telecommunications/Polytechnic University of Tirana/Albania

ABSTRACT: *In this article we have treated the performance of an algorithm designed to achieve the biometric identification through fingerprints. The paper consists in providing the design steps of this algorithm consisting of transformations that are currently being introduced in the system images. The algorithm used is in itself a database that holds a certain number of fingerprint images which are chosen to be included in the database in question. After the introduction of the database, the system is ready to perform the fingerprint identification. This process comprises a series of sub-processes that make up this algorithm. One of the performance parameters of the algorithm is the execution time needed to carry out the identification of various fingerprints. We have used 200 different traces of fingers and we have entered them in the database. Then, for each finger traces we have calculated the time of the execution of milliseconds needed to recognize the fingerprints. This execution time is set in relation to an arbitrary identification number ranging from 1 to 200 and so we have reflected the exponential regression trend-line together with the coefficient of determination. This coefficient has also led to the identification of the limits of this paper.*

Keywords: *algorithm, fingerprint, execution, biometric, regression*

I. INTRODUCTION

The personal identification consists in accompanying a particular individual with a corresponding identity. He plays an important role in our society, [1] where questions relating to the identity of an individual are performed millions of times a day by financial services organizations, health care, in electronic commerce, in telecommunications, government agencies, etc. With a more rapid development of information technology, people are becoming more and more connected with electronics. As a result, the ability to achieve accurate identification of individuals has become critical [2].

A diversity of varieties of systems requires personal and sustainable authentication schemes in order to confirm and identify the identity of persons seeking certain services. The aim of these schemes or systems is to ensure that services are accessible to legitimate users. Examples of these systems include secure access among different buildings, computer systems, mobile phones, ATM, etc [3]. In the lack of robust authentication systems, these systems are imminent. Consequently, the use of biometric parameters was born as a need to confront these threats.

II. METHODOLOGY

The methodology used in this study consists of two aspects. The first is the fingerprint identification algorithm and the second is the performance of this algorithm discussed in terms of execution time of the algorithm in conjunction with different fingerprints that are part of the database.

When a trace finger is added to the database of the application, the algorithm is executed 2 times: the first time for image input and a second time for the image rotated at an suitable angle (22.5 / 2 grade) so that the process becomes as varied in rotation. The rotation of the image is realized through using Matlab program using "`imrotate`" function. [4]

When an image of the fingerprint is added to the database, there is only one core point. On the other hand, when an input image is selected to perform the compliance of the fingerprint, then it will activate a series of fingerprint core and align points shall be carried out for each of them. Finally, it will be taken into consideration only the candidate with the smallest distance.[5] For example, we have 3 images in the database, *img1*, *img2* and *img3* where, each of them is characterized only by a core point and therefore will have 3 points each of their core is associated with an image present in the database. If we select an image for fingerprint compliance (should be "ImgNew") we will find a number of core points (let it be their number N). For each of these N

points nucleus (candidates) we will find the fingerprint images closest that is present in the database. Finally, we will obtain N distances (as the number of candidates of the core points).[6]
With respect to the second aspect, it consists of taking 200 samples consisting of the execution of the user's fingerprint identification process in milliseconds. After defining these samples they will be placed in front of the identification number of each finger trace. The identification number of such traces placed arbitrarily from 1 to 200. So we have created a graph where the x-axis shows the number of identification and the y-axis gives the execution time in milliseconds. Furthermore, on this relationship we have built the exponential regression which expresses the trend of the relationship in question. Also we have shown the respective coefficient of determination [7].

III. THE RESULTS

The rating of pixel-wise orientation field estimation is accelerated more by re-using estimates of the sums. The sum of the elements of a block centered on pixel (I, J) can be used for the calculation of the amount of elements centered on pixel blocks-in (I, J + 1). [8]This can be obtained in the following manner:

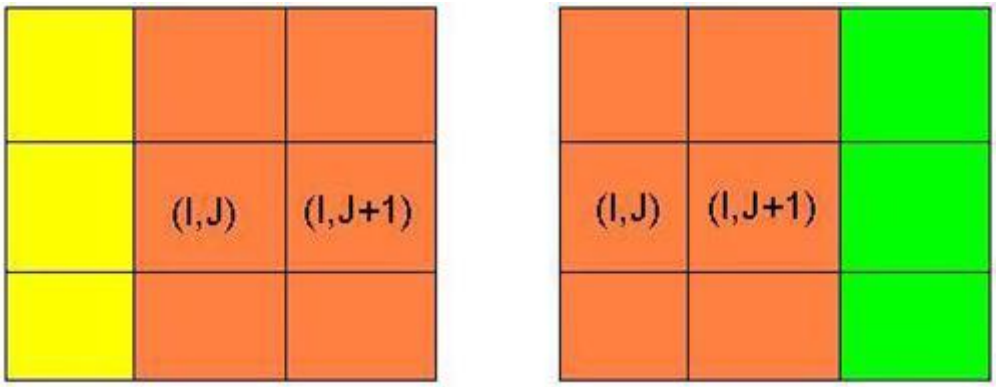

Fig. 1 – The explanation of the pixel-wise field estimation evaluation

Once the sum of values centered on pixel-in (I, J) is calculated (the amount of pixels and yellow pixels orange in the figure to the left), in order to score the sum of centered upon the pixel-in (I, J + 1), we simply learn from previous amount and add the yellow area green area (see figure right); in this way it is possible to maintain a series of calculations. [9] In other words:

$$SUM\ (I, J) = yellow + orange \quad (1)$$

$$SUM\ (I, J+1) = SUM\ (I, J) - yellow + orange \quad (2)$$

Now let's give the necessary steps for establishing the core point in the process of the fingerprint's identification. Initially, for an input image, we improve the fingerprint in order to have a better quality image. [10] In the figure below we have shown an image trace the finger at the entrance to the system.

Fig. 2 – The image of the fingerprint at the entrance of the system\

Below we have presented the enhanced fingerprint.

Fig.3 – The image of the enhanced fingerprint

After this operation, the image is segmented and separated from the background image of the fingerprint. This can be accomplished using a simple block-wise variance, background since usually it is characterized by a small variance. [11] The image originally is digitalized (using command imclose in Matlab), then eroded (using command imerode), so as to avoid holes in the image of the fingerprint and the unwanted effects outside its boundaries (between the fingerprint and background). [12] Image segmentation is repeated several times until the desired conditions are met. This is done so as to avoid adverse effects between the fingerprint and background.[13] Condition for which we are concerned is selected in this way:
The improved image is divided into blocks with specified size (typically 32x32 or 64x64). The whole image is filtered with a complex filter. Let be the maximum value of the image Cf_max the filtered current area of interest (which had previously been estimated by some initial parameters). For each block in the relative maximum we recalculate Cf_rel.[14] Finally, we consider a matrix logic F the elements of which (I, J) are equivalent to 1 if (I, J) is a block and this value is equal to or greater than the limit value (typically 0.65 * Cf_max in our simulations); F (I, J) is equal to 0 in all other cases (for example if F (I, J) is not a relative maximum block or a relative maximum block smaller than the limit value). If the number of non-zero elements of the matrix F is the logical limit value, then the image segmentation parameters re-calculated and the entire process is repeated once again.[15]

In the figure below we have presented the segmented image

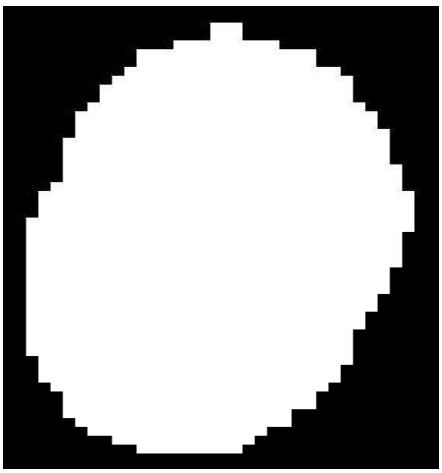

Fig.4 - The image is segmented, closed and eroded (erosion or binary close)

The next step consists of performing the calculation of the fast pixel-wise orientation field. The figure below illustrates this step in case of a finger traces involved in the system.

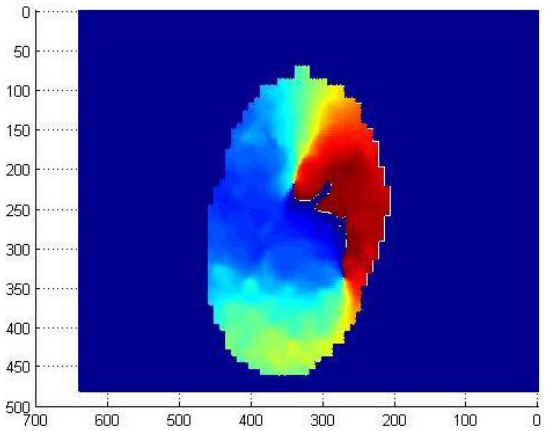

Fig.5 – The evaluation of pixel-wise orientation field in the area of interest

Further we use the field of orientation to provide a logical matrix where pixel-I (I, J) is set to 1 if the angle of orientation is less than or equal to $\pi / 2$.

Figure 6 – The logical matrix is at the local area of the little orientation that is less or equal to $\pi/2$.

Then we have calculated the output filter to improve the image of the fingerprint. In fact, it is not necessary that it be re-counted but we have used the recalculated the image in Figure 3.

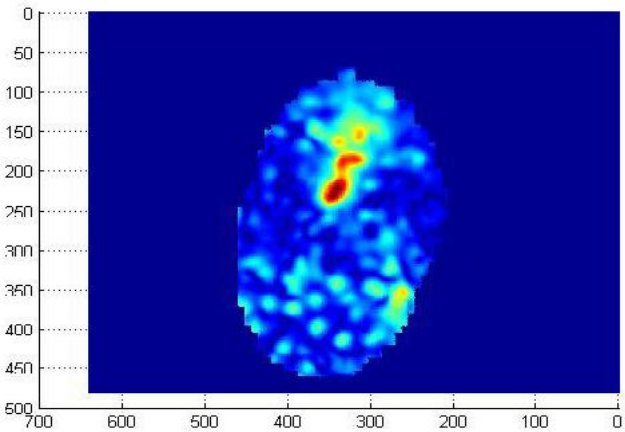

Fig.7 – The output of the complex filter of the enhanced image of the fingerprint

Then we have found the maximum value of the output complex filter where image pixels are placed at logical 1. [16]Finally all calculated points are subdivided into sub-groups of points that are close to each other. For each sub-group we will have a number of candidates and we consider only the sub-group with a number of candidates greater than or equal to 3. [17] For each of these sub-groups we have taken into account the group with the biggest coordinate. In this sub-group we have taken into account the core point with the biggest x-axis coordinate.

Fig.8– The image of the fingerprint and the corresponding core point

At this point we will give the results of simulation in Matlab of the performance of the algorithm used to achieve the identification of the fingerprint.[18]
Below we have shown the chart showing the dependency between the identification number of the ingerprint and time in milli-seconds of execution of identification process for each of the 200 fingerprints to consider.[19]

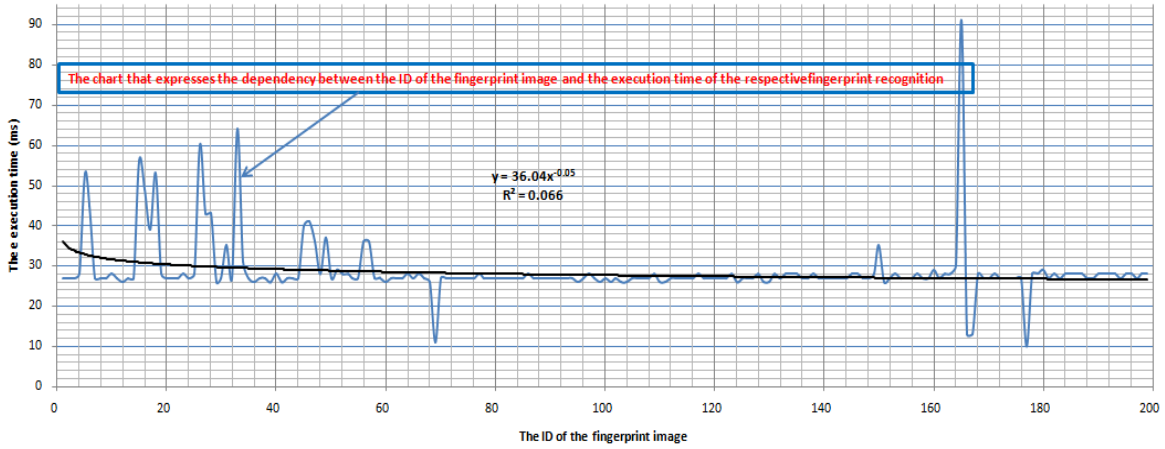

Fig.9 – The chart which expresses the dependency between the number of identification of the fingerprint and time in milli-seconds of execution of the identification for each of the 200 fingerprints

The trend-line is an exponential curve with the following equation:

$$y = 36.04 * x^{-0.5} \quad (3)$$

On the other hand, the coefficient of determination is $R^2 = 0.066$ which means that the dependency of the parameters from each other is in the range 6.6% and the rest remains to be studied and lies in the limitation status of this study.[20]

IV. CONCLUSIONS

In this article we gave the results of the performance of an algorithm designed for the identification of fingerprints. Initially, we have shown an introduction that discusses the problems of the present days on the threats that led to the development of biometric identification and authentication techniques.[21]
Secondly, we have treated the design methodology and performance analysis algorithm simulated in Matlab. This discussion consisted of two aspects: the description of the steps of the process of identification, the transformations incurred by the image of the input fingerprint and performance that perform the algorithm in terms of time of execution of identification of each image's track fingertips.[22]
Finally, we have interpreted the results of the simulations performed in Matlab to identify the finger trace from a database of 200 ones. Also, we have taken 200 samples to trace different user fingerprints together with relevant performance in the process of identifying each of them. This relationship has undergone exponential regression and the respective equation is filed for this regression. The coefficient of determination is 0.066 and it is indicates a 6.6% dependency on the parameters which highlights the limits of this article. [23]

REFERENCES

1. Friston, K. Statistical Parametric Mapping On-line at: *http://www.fil.ion.ucl.ac.uk/spm/ course/note02/* Through discussion of practical aspects of fMRI analysis including pre-processing, statistical methods, and experimental design. Based around SPM analysis software capabilities.
2. Hyvarinen, A. Karhunen, J. and Oja, E. *Independent Component Analysis*, John Wiley and Sons, Inc. New York, 2001. Fundamental, comprehensive, yet readable book on independent component analysis. Also provides a good review of principal component analysis.
3. Shiavi, R *Introduction to Applied Statistical Signal Analysis*, (2nd ed), Academic Press, San Diego, CA, 1999. Emphasizes spectral analysis of signals buried in noise. Excellent coverage of Fourier analysis, and autoregressive methods. Good introduction to statistical signal processing concepts.
4. Hubbard B.B. *The World According to Wavelets* (2nd ed.) A.K. Peters, Ltd. Natick, MA, 1998. Very readable introductory book on wavelengths including an excellent section on the foyer transformed. Can be read by a non-signal processing friend.
5. Strang, G and Nguyen, T. *Wavelets and Filter Banks*, Wellesley-Cambridge Press, Wellesley, MA, 1997. Thorough coverage of wavelet filter banks including extensive mathematical background.
6. Sonka, M., Hlavac V., and Boyle R. Image processing, analysis, and machine vision. Chapman and Hall Computing, London, 1993. A good description of edge-based and other segmentation methods.
7. Boashash, B. *Time-Frequency Signal Analysis*, Longman Cheshire Pty Ltd., 1992. Early chapters provide a very useful introduction to time–frequency analysis followed by a number of medical applications.
8. Ingle, V.K. and Proakis, J. G. *Digital Signal Processing with MATLAB*, Brooks/Cole, Inc. Pacific Grove, CA, 2000. Excellent treatment of classical signal processing methods including the Fourier transform and both FIR and IIR digital filters. Brief, but informative section on adaptive filtering.
9. Bruce, E. N. *Biomedical Signal Processing and Signal Modeling*, John Wiley and Sons, New York, 2001. Rigorous treatment with more of an emphasis on linear systems than signal processing. Introduces nonlinear concepts such as chaos.
10. Jackson, J. E. A User's Guide to Principal Components, John Wiley and Sons, New York, 1991. Classic book providing everything you ever want to know about principal component analysis.
11. Boudreaux-Bartels, G. F. and Murry, R. Time-frequency signal representations for biomedical signals. In: *The Biomedical Engineering Handbook*. J. Bronzino (ed.) CRC Press, Boca Raton, Florida and IEEE Press, Piscataway, N.J., 1995. This article presents an exhaustive, or very nearly so, compilation of Cohen's class of time-frequency distributions.
12. Akansu, A. N. and Haddad, R. A., *Multiresolution Signal Decomposition*: *Transforms, subbands, wavelets*. Academic Press, San Diego CA, 1992. A modern classic that presents, among other things, some of the underlying theoretical aspects of wavelet analysis.
13. Boashash, B. and Black, P.J. An efficient real-time implementation of the Wigner-Ville Distribution, *IEEE Trans. Acoust. Speech Sig. Proc.* ASSP-35:1611–1618, 1987. Practical information on calculating the Wigner-Ville distribution.
14. Haykin, S. *Adaptive Filter Theory* (2nd ed.), Prentice-Hall, Inc., Englewood Cliffs, N.J., 1991. The definitive text on adaptive filters including Weiner filters and gradientbased algorithms.
15. Marple, S.L. *Digital Spectral Analysis with Applications*, Prentice-Hall, Englewood Cliffs, NJ, 1987. Classic text on modern spectral analysis methods. In-depth, rigorous treatment of Fourier transform, parametric modeling methods (including AR and ARMA), and eigenanalysis-based techniques.
16. Kak, A.C and Slaney M. *Principles of Computerized Tomographic Imaging*. IEEE Press, New York, 1988. Thorough, understandable treatment of algorithms for reconstruction of tomographic images including both parallel and fan-beam geometry. Also includes techniques used in reflection tomography as occurs in ultrasound imaging.
17. Rao, R.M. and Bopardikar, *A.S. Wavelet Transforms*: *Introduction to Theory and Applications*, Addison Wesley, Inc., Reading, MA, 1998. Good development of wavelet analysis including both the continuous and discreet wavelet transforms.
18. Stearns, S.D. and David, R.A *Signal Processing Algorithms in MATLAB*, Prentice Hall, Upper Saddle River, NJ, 1996. Good treatment of the classical Fourier transform and digital filters. Also covers the LMS adaptive filter algorithm. Disk enclosed.
19. Cohen, L. Time-frequency distributions—A review. *Proc. IEEE* 77:941–981, 1989. Classic review article on the various time-frequency methods in Cohen's class of time–frequency distributions.
20. Cichicki, A and Amari S. *Adaptive Bilnd Signal and Image Processing*: *Learning Algorithms and Applications*, John Wiley and Sons, Inc. New York, 2002. Rigorous, somewhat dense, treatment of a wide range of principal component and independent component approaches. Includes disk.
21. Johnson, D.D. Applied Multivariate Methods for Data Analysis, Brooks/Cole, Pacific Grove, CA, 1988. Careful, detailed coverage of multivariate methods including principal components analysis.
22. Ferrara, E. and Widrow, B. Fetal Electrocardiogram enhancement by time-sequenced adaptive filtering. *IEEE Trans. Biomed. Engr.* BME-29:458–459, 1982. Early application of adaptive noise cancellation to a biomedical engineering problem by one of the founders of the field.

American Journal of Engineering Research (AJER) 2016
American Journal of Engineering Research (AJER)
e-ISSN: 2320-0847 p-ISSN : 2320-0936
Volume-5, Issue-2, pp-254-264
www.ajer.org
Research Paper Open Access

Secure and Reliable Sharing of Multi-Owner Data for Dynamic Groups in the Cloud

B.Nalini[1], Prof.Dr.D.J.Pete[2]
[1](Electronics and Telecommunications, Datta Meghe College of Engineering/ University of Mumbai, India)
[2](Electronics, Datta Meghe College of Engineering/ University of Mumbai, India)

ABSTRACT : Cloud computing is an emerging computing paradigm in which resources of the computing infrastructure are provided as services over the internet. It provides an economical and efficient solution for sharing group resource among cloud users. Data sharing in a multi-owner manner while preserving data and identity privacy from an untrusted cloud is still a challenging issue because of dynamic nature of multi-owner group. The solution of this issue is addressed in recently best efficient scheme MONA: secure multi-owner data sharing for dynamic groups in the cloud but it has some limitations. In this paper we are further extending the basic MONA by adding the reliability by increasing the number of group managers dynamically and also we are using efficient revocation for dynamic groups by leveraging group signature and dynamic broadcast encryption techniques and for overall security HMAC_SHA1 algorithm. Meanwhile, the storage overhead and encryption computation cost are independent with the number of revoked user**s.**

Keywords -Cloud computing, data sharing, dynamic groups, identity privacy, multi-owner.

I. INTRODUCTION

Cloud computing is a general term for anything that involves delivering hosted services, scalable services like data sharing, accessing etc., over the web on demand basis. It uses the web and central remote servers to maintain data and applications. In cloud computing, the cloud service providers (CSPs), such as Amazon, are able to deliver various services to cloud users with the help of powerful datacenters. By the migration of local data management systems into cloud servers, users can enjoy high-quality services and save significant investments on their local infrastructures. Cloud computing allows consumers and businesses to use applications without installation and access their personal files at any computer with web access. This technology allows for much more efficient computing by centralizing storage, memory, processing and bandwidth. Cloud computing is broken down into three segments: "application" "storage" and "connectivity". Each segment serves a different purpose and offers different products for businesses and individuals around the world.

Cloud computing is one of the greatest platform which provides storage of data in very lower cost and available for all time over the internet. Cloud computing is Internet-based computing, whereby shared resources, software and information are provided to computers and devices on demand. Several trends are opening up the era of Cloud Computing, which is an Internet-based development and use of computer technology. Cloud Computing means more than simply saving on IT implementation costs. One of the most fundamental services offered by cloud providers is data storage. A company allows its staffs in the same group or department to store and share files in the cloud. By utilizing the cloud, the staffs can be completely released from the troublesome local data storage and maintenance. However, it also poses a significant risk to the confidentiality of those stored files. Specifically, the cloud servers managed by cloud providers are not fully trusted by users while the data files stored in the cloud may be sensitive and confidential. To preserve data privacy, a basic solution is to encrypt data files, and then upload the encrypted data into the cloud. Unfortunately, designing an efficient and secure data sharing scheme for groups in the cloud is not an easy task due to the following challenging issues.

First, identity privacy is one of the most significant obstacles for the wide deployment of cloud computing. Without the guarantee of identity privacy, users may be unwilling to join in cloud computing systems because their real identities could be easily disclosed to cloud providers and attackers. On the other hand, unconditional identity privacy may incur the abuse of privacy. For example, a misbehaved staff can deceive others in the company by sharing false files without being traceable. Therefore, traceability, which enables the group manager (e.g., a company manager) to reveal the real identity of a user, is also highly desirable.

Second, multiple-owner manner is highly recommended that any member in a group should be able to fully enjoy the data storing and sharing services provided by the cloud. Compared with the single-owner manner [3], where only the group manager can store and modify data in the cloud, the multiple-owner manner is more flexible in practical applications. More concretely, each user in the group is able to not only read data, but also modify his/her part of data in the entire data file shared by the company.

Third, groups are normally dynamic in practice, e.g., new staff participation and current employee revocation in a company. The changes of membership make secure data sharing extremely difficult. On one hand, the anonymous system challenges new granted users to learn the content of data files stored before their participation, because it is impossible for new granted users to contact with anonymous data owners, and obtain the corresponding decryption keys. On the other hand, an efficient membership revocation mechanism without updating the secret keys of the remaining users is also desired to minimize the complexity of key management.

Several security schemes for data sharing on untrusted servers have been proposed [8], [9], and [10]. In these approaches, data owners store the encrypted data files in untrusted storage and distribute the corresponding decryption keys only to authorized users. Thus, unauthorized users as well as storage servers cannot learn the content of the data files because they have no knowledge of the decryption keys. However, the complexities of user participation and revocation in these schemes are linearly increasing with the number of data owners and the number of revoked users, respectively. By setting a group with a single attribute, Lu et al. [5] proposed a secure provenance scheme based on the cipher text-policy attribute-based encryption technique, which allows any member in a group to share data with others. However, the issue of user revocation is not addressed in their scheme. Yu et al. [4] presented a scalable and fine-grained data access control scheme in cloud computing based on the key policy attribute based encryption (KP-ABE) technique [7]. This scheme unfortunately, the single owner manner hinders the adoption of their scheme into the case, where any user is granted to store and share data.

The solution of the above challenges presented in recently best efficient scheme Mona, a secure multi-owner data sharing scheme for dynamic groups in the cloud. The main contributions of Mona:

1. In Mona, any user in the group can securely share data with others by the untrusted cloud
2. It is able to support dynamic groups efficiently. Specifically, new granted users can directly decrypt data files uploaded before their participation without contacting with data owners. User revocation can be easily achieved through a novel revocation list without updating the secret keys of the remaining users. The size and computation overhead of encryption are constant and independent with the number of revoked users.
3. It provided secure and privacy-preserving access control to users, which guarantees any member in a group to anonymously utilize the cloud resource. Moreover, the real identities of data owners can be revealed by the group manager when disputes occur.

But it has some limitations. We further extending the basic MONA by adding the reliability as well as improving the scalability by increasing the number of group managers dynamically.

The remainder of this paper is organized as follows: Section II overviews the related work. In Section III, we describe the system model and our design goals. In Section IV, we presented some modules and algorithm used in implementation of the system. In Section V, shows some results of our implemented system. Finally, we conclude the paper in Section VI.

II. RELATED WORK

M. Armbrust et al. [2] presented a security one of the most often-cited objections to cloud computing; analysts and skeptical companies ask "who would trust their essential data, out there‟ somewhere?" There are also requirements for auditability, in the sense of Sarbanes-Oxley azon spying on the contents of virtual machine memory; it's easy to imagine a hard disk being disposed of without being wiped, or a permissions bug making data visible improperly. There's an obvious defense, namely user-level encryption of storage. This is already common for high-value data outside the cloud, and both tools and expertise are readily available. This approach was successfully used by TC3, a healthcare company with access to sensitive patient records and healthcare claims, when moving their HIPAA-compliant application to AWS. Similarly, auditability could be added as an additional layer beyond the reach of the virtualized guest OS, providing facilities arguably more secure than those built into the applications themselves and centralizing the software responsibilities related to confidentiality and auditability into a single logical layer. Such a new feature reinforces the Cloud Computing perspective of changing our focus from specific hardware to the virtualized capabilities being provided

S. Kamara et al. [3] proposed a security for customers to store and share their sensitive data in the cryptographic cloud storage. It provides a basic encryption and decryption for providing the security. However, the revocation operation is a sure performance killer in the cryptographic access control system. To optimize the revocation procedure, they present a new efficient revocation scheme which is efficient, secure, and unassisted. In this scheme, the original data are first divided into a number of slices, and then published to the cloud storage. When a revocation occurs, the data owner needs only to retrieve one slice, and re-encrypt and republish it. Thus, the revocation process is accelerated by affecting only one slice instead of the whole data.

They have applied the efficient revocation scheme to the cipher text-policy attribute-based encryption based cryptographic cloud storage. The security analysis shows that the scheme is computationally secure.

In [4] Yu et al. presented a scalable and fine-grained data access control scheme in cloud computing based on the KP-ABE technique. The data owner uses a random key to encrypt a file, where the random key is further encrypted with a set of attributes using KP-ABE. Then, the group manager assigns an access structure and the corresponding secret key to authorized users, such that a user can only decrypt a cipher-text if and only if the data file attributes satisfy the access structure. To achieve user revocation, the manager delegate's tasks of data file re-encryption and user secret key update to cloud servers. However, the single-owner manner may hinder the implementation of applications with the scenario, where any member in a group should be allowed to store and share data files with others.

Lu et al. [5] proposed a secure provenance scheme, which is built upon group signatures and cipher-text-policy attribute based encryption techniques. Particularly, the system in their scheme is set with a single attribute. Each user obtains two keys after the registration: a group signature key and an attribute key. Thus, any user is able to encrypt a data file using attribute based encryption and others in the group can decrypt the encrypted data using their attribute keys. Meanwhile, the user signs encrypted data with her group signature key for privacy preserving and traceability. However, user revocation is not supported in their scheme.

Ateniese et al. [6] leveraged proxy reencryptions to secure distributed storage. Specifically, the data owner encrypts blocks of content with unique and symmetric content keys, which are further encrypted under a master public key. For access control, the server uses proxy cryptography to directly re-encrypt the appropriate content key(s) from the master public key to a granted user's public key. Unfortunately, a collusion attack between the un-trusted server and any revoked malicious user can be launched, which enables them to learn the decryption keys of all the encrypted blocks.

In [9], Kallahalla et al. proposed a cryptographic storage system that enables secure file sharing on untrusted servers, named Plutus. By dividing files into file groups and encrypting each file group with a unique file-block key, the data owner can share the file groups with others through delivering the corresponding lockbox key, where the lockbox key is used to encrypt the file-block keys. However, it brings about a heavy key distribution overhead for large-scale file sharing. Additionally, the file-block key needs to be updated and distributed again for a user revocation.

E. Goh et al. [10] presented a SiRiUS, a secure file system designed to be layered over insecure network and P2P file systems such as NFS, CIFS, Ocean Store, and Yahoo! Briefcase. SiRiUS assumes the network storage is untrusted and provides its own read-write cryptographic access control for file level sharing. Key management and revocation is simple with minimal out-of-band communication. File system freshness guarantees are supported by SiRiUS using hash tree constructions. SiRiUS contains a novel method of performing file random access in a cryptographic file system without the use of a block server. Extensions to SiRiUS include large scale group sharing using the NNL key revocation construction. Our implementation of SiRiUS performs Ill relative to the underlying file system despite using cryptographic operations. SiRiUS contains a novel method of performing file random access in a cryptographic file system without the use of a block server. Using cryptographic operations implementation of SiRiUS is also possible. It only uses the own read write cryptographic access control. File level sharing are only done by using cryptographic access.

In [10] files stored on the untrusted server include two parts: file metadata and file data. The file metadata implies the access control information including a series of encrypted key blocks, each of which is Encrypted under the public key of authorized users. Thus, the size of the file metadata is proportional to the number of authorized users. The user revocation in the scheme is an intractable issue especially for large-scale sharing, since the file metadata needs to be updated. In their extension version, the NNL construction [11] is used for efficient key revocation. However, when a new user joins the group, the private key of each user in an NNL system needs to be recomputed, which may limit the application for dynamic groups. Another concern is that the computation overhead of encryption linearly increases with the sharing scale.

D. Boneh et al.[12] focused on a Hierarchical Identity Based Encryption (HIBE) system where the cipher-text consists of just three group elements and decryption requires only two bilinear map computations, regardless of the hierarchy depth. Encryption is as efficient as in other HIBE systems. They prove that the scheme is selective-ID secure in the standard model and fully secure in the random oracle model. The system has a number of applications: it gives very efficient forward secure public key and identity based cryptosystems (with short cipher-texts), it converts the NNL broadcast encryption system into an efficient public key broadcast system, and it provides an efficient mechanism for encrypting to the future. The system also supports limited delegation where users can be given restricted private keys that only allow delegation to bounded depth. The HIBE system can be modified to support sub linear size private keys at the cost of some cipher-text expansion.

A.Fiat et al.[16] proposed a system on multicast communication framework, various types of security threat occurs. As a result construction of secure group communication that protects users from intrusion and eavesdropping are very important. In this Dissertation (First Stage), they propose an efficient key distribution

method for a secure group communication over multicast communication framework. In this method, they use IP multicast mechanism to shortest rekeying time to minimize adverse effect on communication. In addition, they introduce proxy mechanism for replies from group members to the group manager to reduce traffic generated by rekeying. They define a new type of batching technique for rekeying in which new key is generated for both leaving and joining member. The rekeying assumption waits for 30 sec so that number time's key generation will be reduced.

III. SYEM MODEL & DESIGN GOALS

To achieve a secure and reliable multi-owner data sharing for dynamic groups in the cloud, in this paper we are presenting the system model, which keeps the sharing of multi-owner data is secure and reliable. In this method we are further presenting how we are managing the risks like failure of group manager by increasing the number of backup group manager, hanging of group manager in case number of requests more by sharing the workload in multiple group managers. This method claims required efficiency, scalability and most importantly reliability. We combine the group signature and dynamic broadcast encryption techniques. Specially, the group signature scheme enables users to anonymously use the cloud resources, and the dynamic broadcast encryption technique allows data owners to securely share their data files with others including new joining users.

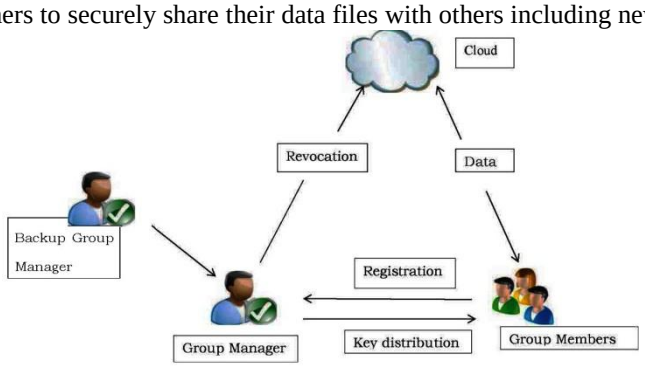

Figure 1: System Model

3.1 System Model

We consider a cloud computing architecture by combining with an example that a company uses a cloud to enable its staffs in the same group or department to share their files. The system model consists of four different entities: the cloud, a group manager (i.e., the company manager), backup group manager and a large number of group members (i.e., the staffs) as illustrated in Figure 1.

3.1.1 Cloud

Cloud is operated by CSPs and provides priced abundant storage services. However, the cloud is not fully trusted by users since the CSPs are very likely to be outside of the cloud users' trusted domain. Similar to [3], [7], we assume that the cloud server is honest but curious. That is, the cloud server will not maliciously delete or modify user data due to the protection of data auditing schemes , but will try to learn the content of the stored data and the identities of cloud users.

3.1.2 Group manager

Group manager takes charge of system parameters generation, user registration, user revocation, and revealing the real identity of a dispute data owner. In the given example, the group manager is acted by the administrator of the company. Therefore, we assume that the group manager is fully trusted by the other parties.

3.1.3 Backup group manager

Backup group manger takes charge all the responsibilities of group manger if group manger unable to perform his duties.

3.1.4 Group members

Group members are a set of registered users they will store their private data into the cloud server and share them with others in the group. In our example, the staffs play the role of group members. Note that, the group membership is dynamically changed, due to the staff resignation and new employee participation in the company.

3.2 Design Goals

We describe the main design goals of the proposed scheme including access control, data confidentiality, anonymity and traceability, and efficiency as follows:

3.2.1 Access Control

The requirement of access control is twofold. First, group members are able to use the cloud resource for data operations. Second, unauthorized users cannot access the cloud resource at any time, and revoked users will be incapable of using the cloud again once they are revoked.

3.2.2 Data Confidentiality

Data confidentiality requires that unauthorized users including the cloud are incapable of learning the content of the stored data. An important and challenging issue for data confidentiality is to maintain its availability for dynamic groups. Specifically, new users should decrypt the data stored in the cloud before their participation, and revoked users are unable to decrypt the data moved into the cloud after the revocation.

3.2.3 Anonymity and Traceability

Anonymity guarantees that group members can access the cloud without revealing the real identity. Although anonymity represents an effective protection for user identity, it also poses a potential inside attack risk to the system. For example, an inside attacker may store and share a mendacious information to derive substantial benefit. Thus, to tackle the inside attack, the group manager should have the ability to reveal the real identities of data owners.

3.2.4 Efficiency

The efficiency is defined as follows: Any group member can store and share data files with others in the group by the cloud. User revocation can be achieved without involving the remaining users. That is, the remaining users do not need to update their private keys or reencryption operations. New granted users can learn all the content data files stored before his participation without contacting with the data owner.

IV. SYSTEM IMPLIMENTATION

4.1 Modules

4.1.1 Cloud Module:

In this module, we create a local Cloud and provide priced abundant storage services. The users can upload their data in the cloud. We develop this module, where the cloud storage can be made secure. However, the cloud is not fully trusted by users since the CSPs are very likely to be outside of the cloud users' trusted domain. Similar to we assume that the cloud server is honest but curious. That is, the cloud server will not maliciously delete or modify user data due to the protection of data auditing schemes, but will try to learn the content of the stored data and the identities of cloud users.

4.1.2 Group Manager Module:

Group manager takes charge of followings,

1. Key generation,

2. User registration,

3. User revocation, and

4. Revealing the real identity of a dispute data owner.

Therefore, we assume that the group manager is fully trusted by the other parties. The Group manager is the admin. The group manager has the logs of each and every process in the cloud. The group manager is responsible for user registration and also user revocation too.

4.1.3 Group Member Module:

Group members are a set of registered users that will store their private data into the cloud server and Share them with others in the group. Note that, the group membership is dynamically changed, due to the staff resignation and new employee participation in the company. The group member has the ownership of changing the files in the group. Whoever in the group can view the files which are uploaded in their group and also modify it.

4.1.4 File Security Module:

- Encrypting the data file.
- File stored in the cloud can be deleted by either the group manager or the data owner (i.e., the member who uploaded the file into the server).

4.1.5 Group Signature Module:

A group signature scheme allows any member of the group to sign messages while keeping the identity secret from verifiers. Besides, the designated group manager can reveal the identity of the signature's originator when a dispute occurs, which is denoted as traceability.

4.1.6 User Revocation Module:

User revocation is performed by the group manager via a public available revocation list (RL), based on which group members can encrypt their data files and ensure the confidentiality against the revoked users.
We used HMAC_SHA-1 algorithm to implement the System for secure sharing of data between the group members.

4.2 HMAC_SHA1_ ALGORITHAM:

A keyed-hash message authentication code (**HMAC**) is an algorithm for applications requiring message authentication. Message authentication is achieved via the construction of a message authentication code (MAC). MACs based on cryptographic hash functions are known as HMACs. The purpose of a MAC is to authenticate both the source of a message and its integrity without the use of any additional mechanisms. HMACs have two functionally distinct parameters, a message input and a secret key known only to the message originator and intended receiver(s). Additional applications of keyed hash functions include their use in challenge-response identification protocols for computing responses, which are a function of both a secret key and a challenge message. An HMAC function is used by the message sender to produce a value (the MAC) that is formed by condensing the secret key and the message input. The MAC is typically sent to the message receiver along with the message. The receiver computes the MAC on the received message using the same key and HMAC function as was used by the sender, and compares the result computed with the received MAC. If the two values match, the message has been correctly received, and the receiver is assured that the sender is a member of the community of users that share the key. The HMAC specification in this standard is a generalization of HMAC as specified in Internet RFC 2104, HMAC, Keyed-Hashing for Message Authentication, and ANSI X9.71, Keyed Hash Message Authentication Code. Authenticate packets with HMAC using message digest algorithm (The default is SHA1). HMAC is commonly used message authentication algorithm (MAC) that uses a data sharing, a secure hash algorithm, and a key, to produce a digital signature.

HMAC involves hash algorithms in combination with the secret key. HMAC can be used with any of the iterative hash functions and MD5, SHA-1 and SHA256 are such examples and the resulting MAC functions are referred as HMAC-MD5, HMAC-SHA-1 and HMAC-SHA256. Security 18 of HMAC depends on the underlying hash function, the size of the output and the quality of the secret key. HMAC-SHA1 does not suffer from a collision attack in the same way as SHA-1 because in the beginning of the HMAC-SHA1 the message to hash is based on the secret key not known by the attacker. To compute HMAC the following calculation is performed.

$$\mathrm{HMAC}(K, m) = H\big((K \oplus \mathrm{opad}) \parallel H(K \oplus \mathrm{ipad}) \parallel m\big) \quad (1)$$

Where

H is a cryptographic hash function,
K stands for the secret key and if the key is shorter than the block size it is then padded with zeroes or if the key is longer than the block it is then truncated.
m is the message to be authenticated,
|| denotes concatenation,
⊕ denotes exclusive or (XOR),
opad is the outer padding (0x5c5c5c…5c5c, one-block-long hexadecimal constant),

and **ipad** is the inner padding (0x363636…3636, one-block-long hexadecimal constant).

Figure.2shows the principle of HMAC-SHA1. HMAC functions can be used in several ways. The secret key known by the HMAC clients can be given as a parameter or the key is not known by the sender and receiver but instead, the key is hidden and the user can choose the key by giving it as a parameter. Alternative way is to keep the key totally hidden and the HMAC function takes the message as a parameter and then uses the hidden secret key in the HMAC operation.

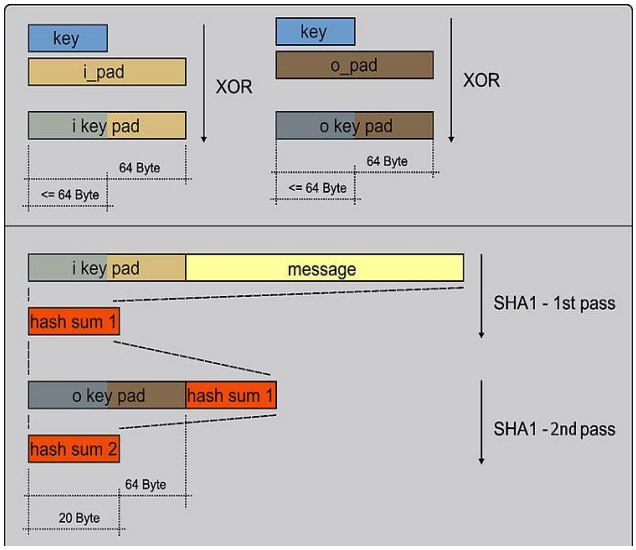

Figure2.HMAC SHA-1

HMAC SPECIFICATION
To compute a MAC over the data 'text' using the HMAC function, the following operation is performed:

$MAC(text)t = HMAC(K, text)t = H((K_0 \oplus opad) \| H((K_0 \oplus ipad) \| text))t$ (2)

A step by step process in the HMAC algorithm is illustrated below.
Step 1: If the length of K = B: set K_0 = K. Go to step 4.
Step 2: If the length of K > B: hash K to obtain an L byte string, then append (B-L) zeros to create a B-byte string K0 (i.e., K_0= H(K) || 00...00). Go to step 4.
Step 3: If the length of K < B: append zeros to the end of K to create a B-byte string K0 (e.g., if K is 20 bytes in length and B = 64, then K will be appended with 44 zero bytes 0x00).
Step 4: Exclusive-OrK_0 with ipad to produce a B-byte string: $K_0 \oplus$ipad.
Step 5: Append the stream of data 'text' to the string resulting from step 4: ($K_0 \oplus$ipad) || text.
Step 6: Apply H to the stream generated in step 5: H($K_0 \oplus$ipad) || text).
Step 7: Exclusive-Or K_0 with opad: $K_0 \oplus$opad.
Step 8: Append the result from step 6 to step 7: ($K_0 \oplus$opad) || H(($K_0 \oplus$ipad) || text).
Step 9: Apply H to the result from step 8: H($K_0 \oplus$opad)|| H(($K_0 \oplus$ipad) || text)).
Step 10: Select the leftmost t bytes of the result of step 9 as the MAC.

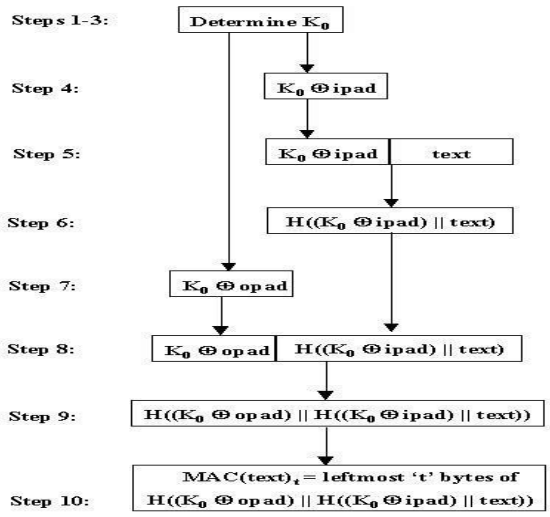

Figure3 Illustration the of HMAC construction

V. RESULTS

This Project is implemented using Java as programming language. Net beans usedas integrated development environment (IDE) for coding. Xamp server for combining Apache application server and MySQL for database purposes. The database stores the list of group members registered and also the revocation list.The group manger generate group key and distribute to all his group members. All group members upload their data and download data from the cloud which was uploaded by the other group member also modify their part of data and uploaded again in the cloud. Every group member can upload into the cloud and download from the cloud without revealing their real identity instead they use group signature. The following are screenshot of scheme.

Cloud is operated by Cloud Service Provider (csp) s and provides priced abundant storage services. However, the cloud is not fully trusted by users since the CSPs are very likely to be outside of the cloud users' trusted domain. Similar to [3], [7], we assume that the cloud server is honest but curious. That is, the cloud server will not maliciously delete or modify user data due to the protection of data auditing schemes, but will try to learn the content of the stored data and the identities of cloud users. The below Figure 4 shows the csp module the csp can view the dataupload in cloud and downloaded from cloud in encrypted form and data owner identity also encrypted form.

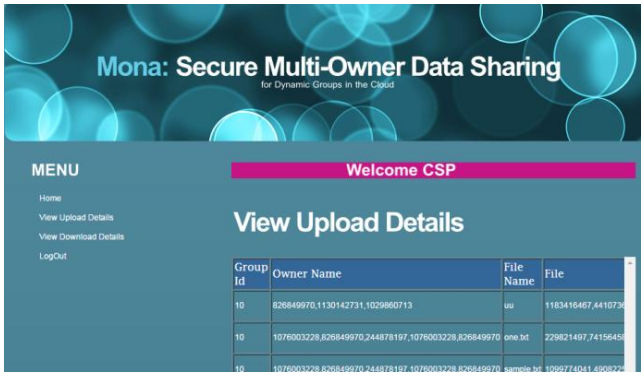

Figure 4 Upload Details of Data in Encrypted Form

Group manager takes charge of key generation, user registration, user revocation, and revealing the real identity of a dispute data owner. In the given example, the group manager is acted by the administrator of the company. Therefore, we assume that the group manager is fully trusted by the other parties. The following figs gives some key duties of group manager as follows Figure 5 Group manager home page it gives the all the details of group members in that group.

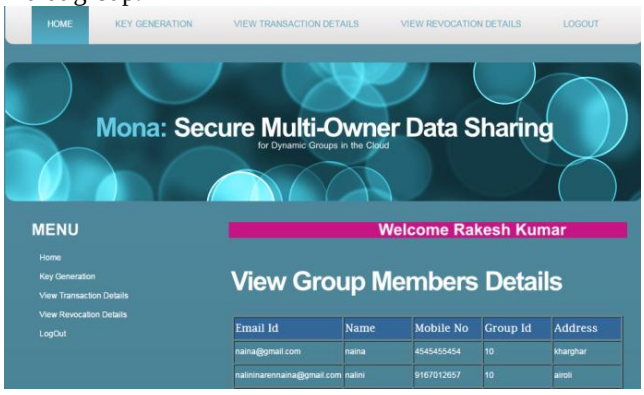

Figure 5 Group Manager Home page

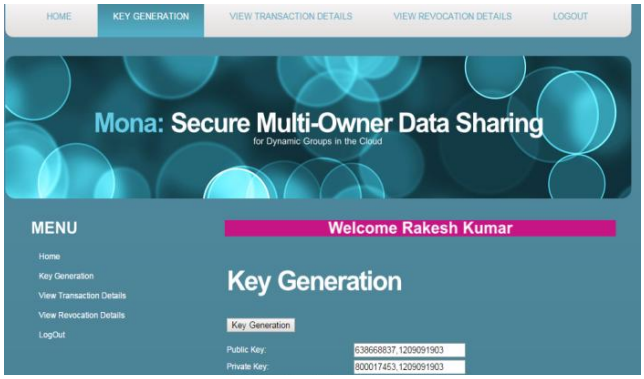

Figure 6 Key Generation

The Figure 6 gives the generation of private and public keys and distributes those keys to group members of the group. The group members can upload their files using public key distributed by group members. Group members can download using private key distributed to them.

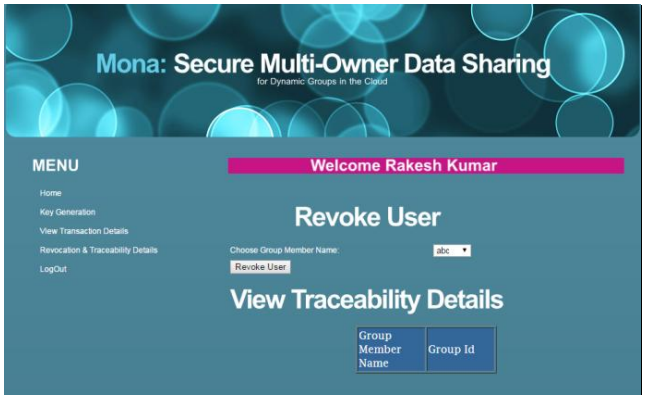

Figure 7 User Revocation

Figure 7 shows the revocation and traceability of the group member. The revoked user can't log into the system. If any disputes occurs among the group members on data ownership group manager will reveal the real identity of the group member i.e. traceability.

Groupmemersare the registered users in the group Figure 8 shows group members registration form the user will register in the group by filling the required information in the fields.

Figure 8 Group Member Registration Form

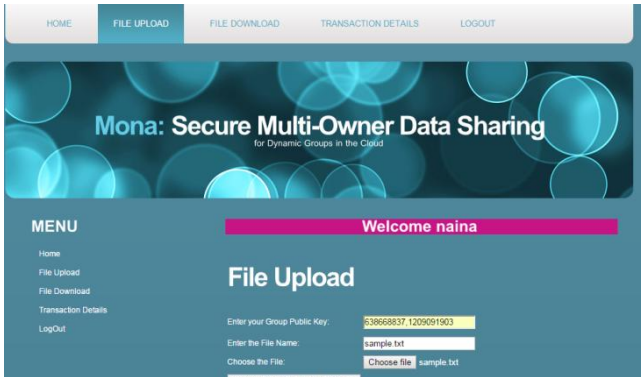

Figure 9 File Upload

Group membersupload theirlocal data files into cloud using group signature. Theychoose theirfile from local system and click on encrypt & upload with signature button. The uploaded content stored in cloud in an encrypted form.

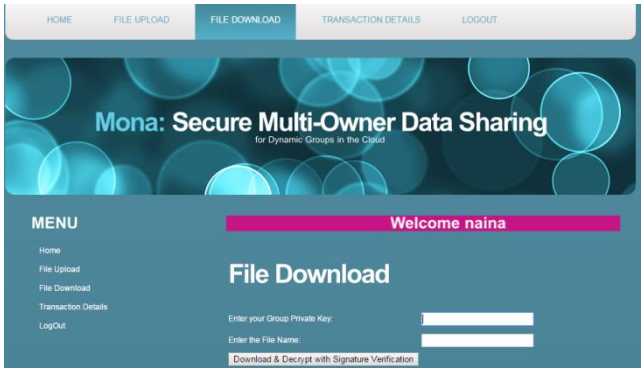

Figure 10 File Download

Figure 10 shows the file downing activity of the .group members download file from cloud with group private key. The downloaded content available in decrypted form in our local system. If they want to do modifications and upload they can do.

VI. CONCLUSION

Cloud computing is very attractive environment for business world in term of providing required services in a very cost effective way. This project focuses on problem of secure data sharing scheme for dynamic groups in an untrusted cloud. In this scheme, a user is able to share data with others in the group without revealing identity privacy to the cloud. In this scheme, we are further presenting how we are managing the risks like failure of group manager by increasing the number of backup group manager, hanging of group manager in case number of requests more by sharing the workload in multiple group managers. This method claims required efficiency, scalability and most importantly reliability.

REFERENCES

[1] Xuefeng Liu, Yuqing Zhang, Boyang Wang, Jingbo Yan "Mona:Secure Multi-owner Data Sharing for Dynamic Groups in the Cloud," Trans. IEEE Parallel and Distributed Systems, vol 24,No 6,June 2013.

[2] M. Armbrust, A. Fox, R. Griffith, A.D. Joseph, R.H. Katz, A. Konwinski, G. Lee, D.A. Patterson, A. Rabkin, I. Stoica, and M. Zaharia, "A View of Cloud Computing," Comm. ACM, vol. 53, no. 4, pp. 50-58, Apr. 2010.

[3] S. Kamara and K. Lauter, "Cryptographic Cloud Storage," Proc. Int'l Conf. Financial Cryptography and Data Security (FC), pp. 136-149, Jan. 2010.

[4] S. Yu, C. Wang, K. Ren, and W. Lou, "Achieving Secure, Scalable, and Fine-Grained Data Access Control in Cloud Computing," Proc. IEEE INFOCOM, pp. 534-542, 2010.

[5] R. Lu, X. Lin, X. Liang, and X. Shen, "Secure Provenance: The Essential of Bread and Butter of Data Forensics in Cloud Computing," Proc. ACM Symp. Information, Computer and Comm. Security, pp. 282-292, 2010.

[6] B. Waters, "Ciphertext-Policy Attribute-Based Encryption: An Expressive, Efficient, and Provably Secure Realization," Proc. Int'l Conf. Practice and Theory in Public Key Cryptography Conf. Public Key Cryptography, http://eprint.iacr.org/2008/290.pdf, 2008.

[7] V. Goyal, O. Pandey, A. Sahai, and B. Waters, "Attribute-Based Encryption for Fine-Grained Access Control of Encrypted Data," Proc. ACM Conf. Computer and Comm. Security (CCS), pp. 89-98, 2006.

[8] G. Ateniese, K. Fu, M. Green, and S. Hohenberger, "Improved Proxy Re-Encryption Schemes with Applications to Secure Distributed Storage," Proc. Network and Distributed Systems Security Symp. (NDSS), pp. 29-43, 2005.

[9] M. Kallahalla, E. Riedel, R. Swaminathan, Q. Wang, and K. Fu, "Plutus: Scalable Secure File Sharing on Untrusted Storage," Proc. USENIX Conf. File and Storage Technologies, pp. 29-42, 2003.
[10] E. Goh, H. Shacham, N. Modadugu, and D. Boneh, "Sirius: Securing Remote Untrusted Storage," Proc. Network and Distributed Systems Security Symp. (NDSS), pp. 131-145, 2003.
[11] D. Naor, M. Naor, and J.B. Lotspiech, "Revocation and Tracing Schemes for Stateless Receivers," Proc. Ann. Int'l Cryptology Conf. Advances in Cryptology (CRYPTO), pp. 41-62, 2001.
[12] D. Boneh, B. Lynn, and H. Shacham, "Short Signature from the Weil Pairing," Proc. Int'l Conf. Theory and Application of Cryptology and Information Security: Advances in Cryptology, pp. 514-532, 2001.
[13] D. Boneh and M. Franklin, "Identity-Based Encryption from the Weil Pairing," Proc. Int'l Cryptology Conf.Advances in Cryptology(CRYPTO), pp. 213-229, 2001.
[14] C. Delerablee, P. Paillier, and D. Pointcheval, "Fully CollusionSecure Dynamic Broadcast Encryption with Constant-Size Ciphertexts or Decryption Keys," Proc. First Int'l Conf. Pairing-Based Cryptography, pp. 39-59, 2007.
[15] D. Boneh, X. Boyen, and E. Goh, "Hierarchical Identity Based Encryption with Constant Size Ciphertext," Proc. Ann. Int'l Conf. Theory and Applications of Cryptographic Techniques (EUROCRYPT),pp. 440-456, 2005.
[16] A. Fiat and M. Naor, "Broadcast Encryption," Proc. Int'l Cryptology Conf. Advances in Cryptology (CRYPTO), pp. 480-491, 1993.